

Visible Light Photoredox Catalyzed Deoxygenations and Polymer-tagged Photocatalysts

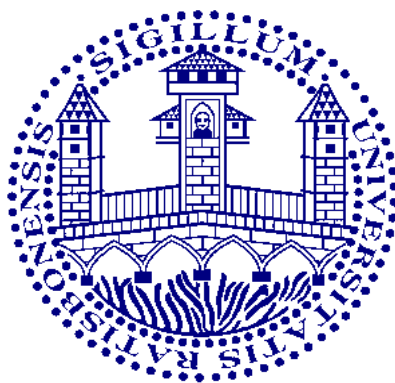
Dissertation

Zur Erlangung des Doktorgrades

Dr. rer. nat.

an der Fakultät für Chemie und Pharmazie

der Universität Regensburg



vorgelegt von

Daniel Rackl

aus Neumarkt i. d. OPf.

Regensburg 2015

Diese Arbeit wurde angeleitet von:

Prof. Dr. Oliver Reiser

Promotionsgesuch eingereicht am:

16.07.2015

Promotionskolloquium am:

14.09.2015

Prüfungsausschuss:

Vorsitz: PD Dr. Sabine Amslinger

1. Gutachter: Prof. Dr. Oliver Reiser
2. Gutachter: Prof. Dr. Axel Jacobi v. Wangelin
3. Gutachter: Prof. Dr. Robert Wolf

Der experimentelle Teil der vorliegenden Arbeit wurde in der Zeit von Oktober 2011 bis April 2015 unter der Leitung von Prof. Dr. Oliver Reiser am Lehrstuhl für Organische Chemie der Universität Regensburg angefertigt.

Herrn Prof. Dr. Oliver Reiser möchte ich herzlich für die Themenstellung, die anregenden Diskussionen und seine stete Unterstützung während der Durchführung dieser Arbeit danken.

Meiner Familie

„Es kommt nicht darauf an, mit dem Kopf durch die Wand zu rennen, sondern mit den Augen die Tür zu finden.“

-Werner von Siemens

Table of Contents

A Zusammenfassung	1
B Summary	2
C Introduction	3
1 Photophysics of Photocatalysts	5
2 Notable Literature Examples of Photoredox Chemistry	10
3 Literature	15
D Photochemical Deoxygenations	18
1 Defunctionalative Deoxygenations	18
1.1 Introduction	18
1.2 Preliminary studies with toluate and diarylphosphinate esters	25
1.3 Substituted benzoates as activation groups	29
1.4 Optimization and control experiments	32
1.5 Mechanistical aspects	33
1.6 Influence of water	35
1.7 Substrate scope	36
1.8 Selective monobenzylation	39
1.9 Further expansion of the substrate scope	42
1.10 <i>In situ</i> benzylation and up-scaling	44

1.11 Conclusion.....	45
2 Deoxygenative Cyclizations	46
2.1 Introduction.....	46
2.2 Preliminary studies with unactivated benzoates.....	48
2.3 Preliminary studies with activated benzoates	50
2.4 Intramolecular trapping	53
2.5 Substrate synthesis.....	57
2.6 Substrate scope and mechanistic considerations.....	61
2.7 Conclusion and outlook	65
3 Experimental Part.....	66
3.1 General information.....	66
3.2 Synthesis of toluate and phosphinate esters	67
3.3 Synthesis of the acid anhydride.....	72
3.4 Synthesis of benzoate esters	73
3.5 Photochemical defunctionalitive deoxygenations	87
3.6 Synthesis of unactivated substrates for intramolecular cyclizations.....	94
3.7 Synthesis of monosubstituted diol compounds	96
3.8 Synthesis of 3,5-bis(trifluoromethyl)benzoate esters for cyclizations	98
3.9 Photochemical deoxygenative cyclizations.....	110
3.10 NMR spectra of new compounds	116
4 Literature.....	134
 E Polymer-tagged Photocatalysts.....	 140
1 Introduction	140
1.1 Inorganic semi-conductors	141

1.2 Surface plasmonic resonators	149
1.3 Organic semi-conductors	151
1.4 Organic dyes and sensitizers	157
1.5 Transition metal complexes	162
1.6 Summary	169
2 Bis-Cyclometalated Iridium(III) Complexes	170
2.1 Introduction.....	170
2.2 Ligand synthesis	171
2.3 Catalyst synthesis	174
2.4 Application in photochemical reactions	175
2.5 Streamlined ligand synthesis	178
3 Tris-Cyclometalated Iridium(III) Complexes	180
3.1 Preliminary studies.....	180
3.2 On-complex modifications	182
3.3 Recycling strategy	184
3.4 Application in photochemical batch reactions	186
3.5 Setup for photoreaction in continuous flow	189
3.6 Application in photochemical flow reactions.....	191
4 Conclusion and Outlook.....	193
5 Experimental Part.....	194
5.1 General information.....	194
5.2 Synthesis of biscyclometalated iridium(III) complexes	195
5.3 Photoreactions in a batch setup with $[\text{Ir}(\text{ppy})_2(\text{PIB-dtb-bpy})](\text{BArF})$	202
5.4 Synthesis of triscyclometalated iridium(III) complexes	205
5.5 Photoreactions in a batch setup with $\text{Ir}(\text{ppy})_2(\text{PIB-ppy})$	210
5.6 Photoreactions in continuous flow	214

5.7 GC-FID analysis.....	218
5.8 NMR spectra of new compounds	219
6 Literature.....	232
F List of Abbreviations	242
G Curriculum Vitae	246
H Acknowledgements.....	249
I Declaration.....	251

A Zusammenfassung

Diese Arbeit beginnt mit einer kurzen Einführung in die Photoredox Katalyse mit sichtbarem Licht. Dazu werden zunächst die zugrunde liegenden photo-physikalischen Prozesse beschrieben und anschließend exemplarisch zwei zukunftsweisende, kürzlich publizierte Arbeiten auf dem Gebiet beschrieben.

Im Kapitel „Photochemical Deoxygenations“ werden Forschungsergebnisse über photochemische C–O Bindungsspaltungen beschrieben. Anfängliche Studien mit Phosphonatestern als Aktivierungsgruppe für die C–O Bindung führen schließlich zur Verwendung von 3,5-Bis(tri-fluormethyl)benzoaten als aktivierende Einheit. Nach Optimierung der Reaktionsbedingungen und Diskussion des Reaktionsmechanismus wird die Substratbreite der Reaktion erkundet und ihre Limitierungen aufgezeigt. Anschließend werden Möglichkeiten zur *in situ* Aktivierung von Alkoholen entwickelt und die Durchführung der Reaktionen in einem kontinuierlichen Verfahren beschrieben. Im folgenden Abschnitt wird die entwickelte Methodik zur Ausbildung neuer C–C Bindungen genutzt. Nachdem Möglichkeiten unaktivierte Alkohole für intramolekulare Zyklisierungen sowie aktivierte Alkohole für intermolekulare Bindungsschließungen ausgeschöpft werden, wird gezeigt, dass intramolekulare Zyklisierungen mit aktivierten Alkoholen sehr wohl durchgeführt werden können und zu chiralen Tetrahydrofuranen führen. Die Substratsynthese und anschließende Photoreaktionen mit ihrem Reaktionsmechanismus werden abschließend diskutiert.

Das Kapitel „Polymer-tagged Photocatalysts“ befasst sich mit der Immobilisierung von Iridium-basierten Photokatalysatoren über homogen lösliche Polymere und deren Recycling. Studien über zweifach zyklometallierte Iridiumkomplexe bringen ein leicht wiederverwendbares Derivat des häufig eingesetzten Katalysators $[\text{Ir}(\text{ppy})_2(\text{dtb-bpy})]^+$ hervor. Dessen Verwendung in der decarboxylativen Synthese von Isoquinolinonen mit sichtbarem Licht wird untersucht. Anschließend werden Optimierungen des Katalysatordesigns und der Synthese beschrieben. Im zweiten Teil wird ein dreifach zyklometallierter Iridiumkomplex synthetisiert und mehrmals sehr erfolgreich bei Photoredoxreaktionen im Batchverfahren wiederverwendet. Abschließend wird eine automatische, kontinuierlich-ablaufende Wiedergewinnung und -verwendung des Katalysators in einem Mikroreaktorverfahren entwickelt.

B Summary

This thesis starts with a brief introduction to visible light mediated photoredox catalysis. Therefore underlying photo-physical processes are presented followed by showcasing of two very recent, trendsetting publications in the area.

Within the chapter “Photochemical Deoxygenations” research results concerning photochemical C–O bond scission reactions are detailed. Preliminary studies with phosphate esters as activation groups for C–O bonds led to the employment of 3,5-bis(trifluoromethyl)benzoates as activating unit. After optimization of the reaction conditions and discussion of the reaction mechanism the substrate scope and limitations of the process are shown. Subsequently experiments towards an *in situ* activation of alcohols followed by performance of the photochemical reaction step in continuous flow are described. The following section deals with the expansion of the developed photochemical C–O bond fragmentation reactions towards the formation of new C–C bonds. After efforts to use unactivated alcohol derivatives in intramolecular cyclizations and activated alcohol derivatives in intermolecular bond formations prove to be unfruitful, intramolecular cyclizations from activated benzoates leading to chiral tetrahydrofuran derivatives are realized. The synthesis of suitable substrates and their photochemical performance is evaluated.

The chapter “Polymer-tagged Photocatalysts” deals with the immobilization of iridium-based photocatalysts with homogeneously soluble polymers and their recycling. Studies with biscyclometalated iridium complexes result in an easily recyclable derivative of $[\text{Ir}(\text{ppy})_2(\text{dtb-bpy})]^+$. Its application in the decarboxylative synthesis of isoquinolinones with visible light is investigated. Optimization of the catalyst design and streamlining of the synthesis are shown. In the second part of the chapter a triscyclometalated iridium complex is synthesized and repeatedly used for photoredox reactions in a batch process. Experiments towards automatic catalyst recovery and reuse in a continuously operating microreactor setup for photoreactions complete the investigations with polymer-tagged photocatalysts.

C Introduction

Sunlight is the solely fully sustainable energy source available to mankind. As much as 89 PWh of energy reach the earth surface *every hour*, corresponding to more than the *annual* world energy consumption (56 PWh, 2013).^{1,2} Technologies to use and store this energy directly and *via* secondary processes (wind, waves) are highly developed and contribute more and more to reduce the global dependence on fossil fuels. The transformation of solar energy into electrical energy is well studied and resultant devices, i.e. solar cells, are used by a continuous rising percentage of private households for daily power generation.³ The artificial storage of the solar energy as chemical energy however is comparably underdeveloped.

A classic area of chemistry deals with the direct excitation of molecules to achieve reactivity. A drawback of this so-called photochemistry is the lack of absorbance of most organic molecules in the visible range of the light spectrum. Hard UV light has to be used to achieve reactivity. This is adversary as most of the sunlight that reaches the earth surface is in the visible range, only a very small portion is highly energetic UV light (Figure 1).

Figure 1. Spectrum of the sunlight reaching earth.⁴

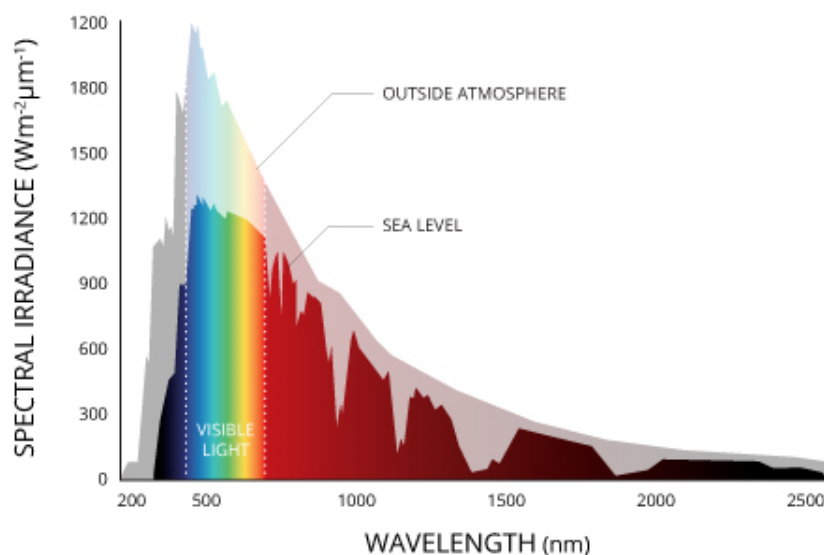


Figure reproduced with courtesy of Fondriest Environmental, Inc.

To make use of light in chemical transformations, catalysts have to be employed which absorb visible light and make it accessible to reactants, either in form of an energy or an electron transfer.⁵ In this way, a harmful and potentially unselective UV-irradiation of the

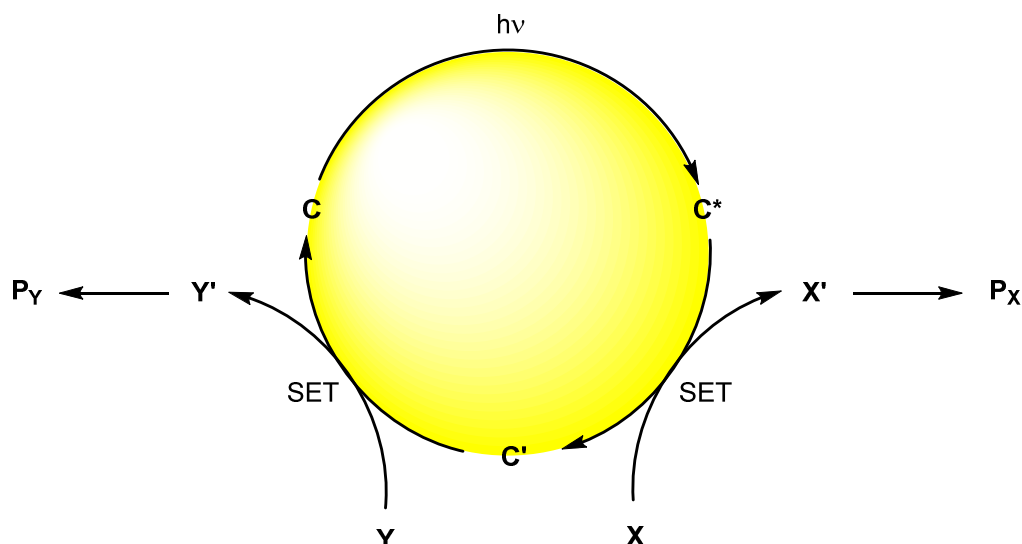
substrate molecules is elegantly circumvented, while at the same time enabling that reactions can be carried out in normal lab glassware with simple visible light LED lamps. The idea to use such long-waved light for chemical reactions was already advertised by Giacomo Ciamician over 100 years ago but only emerged as a powerful synthetic tool within the last decade.^{6–10}

Countless organic transformations which previously required harsh reaction conditions, toxic reagents, or were completely unprecedented, could be elegantly realized with this technique. As catalysts for these transformations, inorganic semi-conductors,^{11,12} organic dyes,^{13–15} and transition-metal complexes^{16,17} can be employed. While semi-conductors typically offer high stabilities, organic dyes are comparably low-priced, organic transition metal complexes are most versatile for a broad range of reaction classes. Whereas also copper,^{18–22} chromium²³ and other non-noble metal complexes have been utilized as photoredoxcatalysts,²⁴ the most commonly employed transition metal complexes are based on pricey ruthenium or iridium. The following sections will briefly explain the underlying physical processes and show selected examples of photoredox reactions.

1 Photophysics of Photocatalysts

The purpose of a photocatalyst is to absorb light and use the gained energy to promote a chemical reaction. The underlying general process is depicted in Scheme 1.⁵ Photocatalyst **C** absorbs light and is promoted to excited state **C***. A suitable reagent **X** can react with excited **C***, in a so-called quenching process, generating chemically modified **X'** and **C'**. Within the regime of photoredox chemistry this modification is always the transfer of a single electron (SET = single electron transfer).^{*} To regenerate **C** and close the catalytic cycle (depicted in yellow), **C'** has to react with another agent **Y**, resulting in the formation of **Y'** and **C**. This is also a redox step. Subsequent follow-up reactions of reactive intermediates **X'** and **Y'** generate products **P_X** and **P_Y**. Ideally, both **P_X** and **P_Y** are synthetically valuable, however, processes where only one of the products is of interest are investigated as well.

Scheme 1. General reaction scheme of a photoredox reaction.

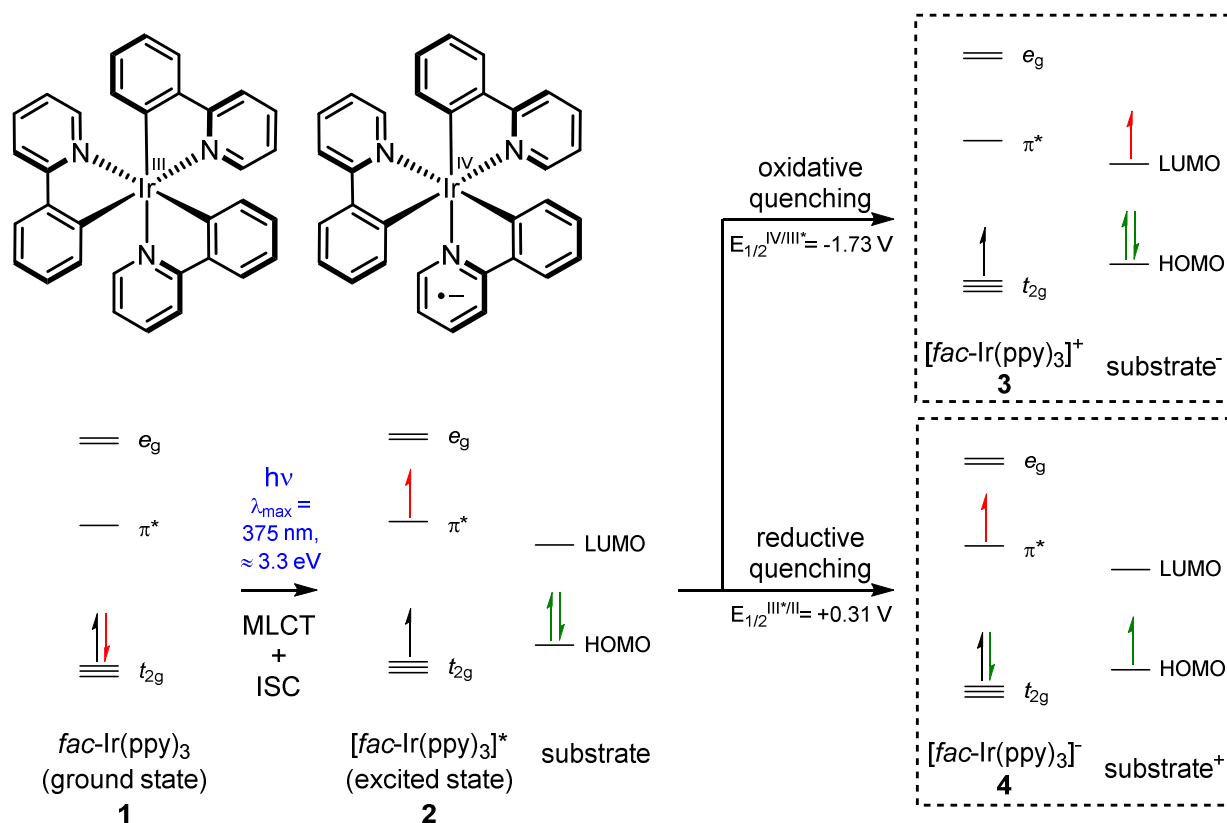


To understand how a photocatalyst operates, it is crucial to take a closer look at the involved photophysical processes. A simplified molecular orbital description is depicted in Scheme 2. *fac*-Ir(ppy)₃ (**1**) serves as an prototypical example of a photoredox catalyst in following considerations. Through absorption of visible light by *fac*-Ir(ppy)₃ (**1**), an electron of its metal-centered *t_{2g}* orbital is excited into a ligand-centered π^* orbital (MLCT = metal to ligand charge transfer). The metal center is thus formally oxidized from Ir³⁺ to Ir⁴⁺ and the ligand consequently reduced. Initially generated singlet MLCT state (not depicted) undergoes fast inter system crossing (ICS) to lower-lying triplet MLCT state **2**. As the decay to ground state

^{*} **C*** might also transfer its excitation energy to reagent **X** instead of causing a single electron transfer. This would directly give back photocatalyst **C** in its ground state and excited **X*** which can then undergo follow-up reactions. This process is called photosensitization.

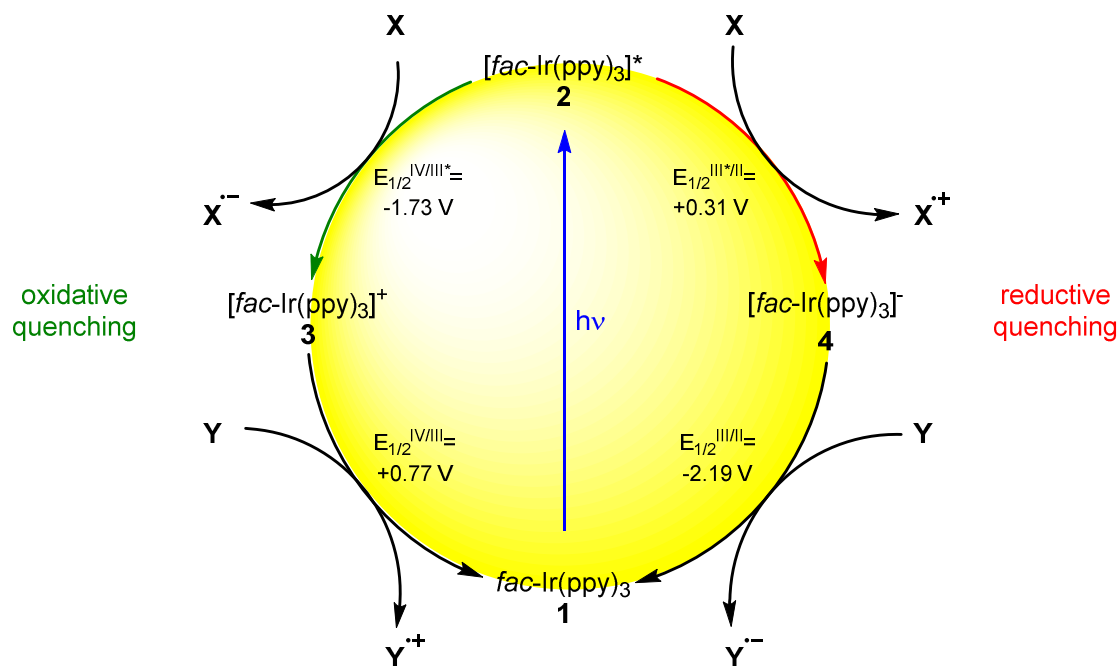
fac-Ir(ppy)₃ (**1**) is spin-forbidden, [*fac*-Ir(ppy)₃]^{*} (**2**) now has a comparably high life time of 1900 ns.^{†,25} Excited triplet MLCT state **2** is now both, a better reductant and a better oxidant than ground state **1**. This can be exploited in a reaction of the excited state photocatalyst **2** with a substrate molecule. When the photocatalyst acts as a reductant, it reduces the substrate molecule by donating a single electron into the lowest unoccupied molecular orbital (LUMO) of the substrate (Scheme 2, upper box). As the photocatalyst *fac*-Ir(ppy)₃ (**1**) itself is oxidized in this process, this is called oxidative quenching. The analogous process where an electron of the highest occupied molecular orbital (HOMO) of the substrate populates a partially occupied *t*_{2g} of the photocatalyst is called reductive quenching (lower box). These intermolecular electron transfer processes are characterized by their respective standard reduction potentials E_{1/2}.

[†] Within this time frame it can now react with a substrate molecule. The longer the life time, the higher the probability to undergo chemical reactions. The life time is thus a key attribute of every photocatalyst.

Scheme 2. Generation of the active triplet species and subsequent quenching of *fac*-Ir(ppy)₃ (**1**).

As these electrochemical half reactions don't give back photocatalyst *fac*-Ir(ppy)₃ (**1**) in its neutral ground state, yet another half reaction is required to achieve this. In case of oxidatively quenched [*fac*-Ir(ppy)₃]⁺ (**3**) a reduction step is necessary to close the catalytic cycle (Scheme 3, left cycle). Likewise, for reductively quenched [*fac*-Ir(ppy)₃]⁻ (**4**) an oxidation step regenerates original photocatalyst *fac*-Ir(ppy)₃ (**1**) (right cycle). Oxidatively quenched [*fac*-Ir(ppy)₃]⁺ (**3**) is a relatively potent oxidant with $E_{1/2}^{\text{IV/III}^*} = +0.77 \text{ V}$, while reductively quenched [*fac*-Ir(ppy)₃]⁻ (**4**) is an incredibly powerful reductant with $E_{1/2}^{\text{III}^*/\text{II}} = -2.19 \text{ V}$. Reduction potentials for all corresponding half reaction steps are given in Scheme 3.

Scheme 3. Photoredox reaction pathways of *fac*-Ir(ppy)₃ (**1**). Oxidative quenching cycle on the left side, reductive quenching cycle on the right.



Depending on what reduction potential is required for a certain chemical transformation, different photoredox catalysts can be employed. A summary of reduction potentials, excited state life times, as well as excitation and emission wavelengths / energies of commonly used photoredox catalysts is given in Table 1.

Table 1. Photophysical properties of commonly used photoredox catalysts.^a

Entry	Photo-catalyst	$E_{1/2}$ (C ⁺ /C ⁻) [V]	$E_{1/2}$ (C ⁻ /C ⁺) [V]	$E_{1/2}$ (C ⁺ /C) [V]	$E_{1/2}$ (C/C ⁻) [V]	Life time τ [ns]	Excitation λ_{\max} [nm]	Excitation ΔE [eV]	Emission λ_{\max} [nm]	Emission ΔE [eV]	Ref.
1	Eosin Y	-1.11	0.83	0.78	-1.06	-	639	1.94	656	1.89	13
2	9-mesityl-10-methyl-acridinium	-	2.06	-	-0.49	2 d ^b	430	2.88	523	2.37	26,27
3	Ru(bpm) ₃ ²⁺	-0.21	0.99	1.69	-0.91	131 ^c	454	2.73	639 ^c	1.94 ^c	28
4	Ru(bpz) ₃ ²⁺	-0.26	1.45	1.86	-0.8	740	443	2.8	591	2.1	29
5	Ru(bpy) ₃ ²⁺	-0.81	0.77	1.29	-1.33	1100	452	2.74	615	2.02	30,31
6	Ru(phen) ₃ ²⁺	-0.87	0.82	1.26	-1.36	500	422	2.94	610 ^d	2.03	30,32
7	[Ir(dF(CF ₃)ppy) ₂ (dtb-bpy)] ⁺	-0.89	1.21	1.69	-1.37	2300	380	3.26	470	2.64	33
8	[Ir(ppy) ₂ (dtb-bpy)] ⁺	-0.96	0.66	1.21	-1.51	557	-	-	581	2.13	33,34
9	Cu(dap) ₂ ⁺	-1.43	-	0.62	-	270	-	-	670 ^e	1.85	18
10	<i>fac</i> -Ir(ppy) ₃	-1.73	0.31	0.77	-2.19	1900	375	3.31	494 ^f	2.51	25

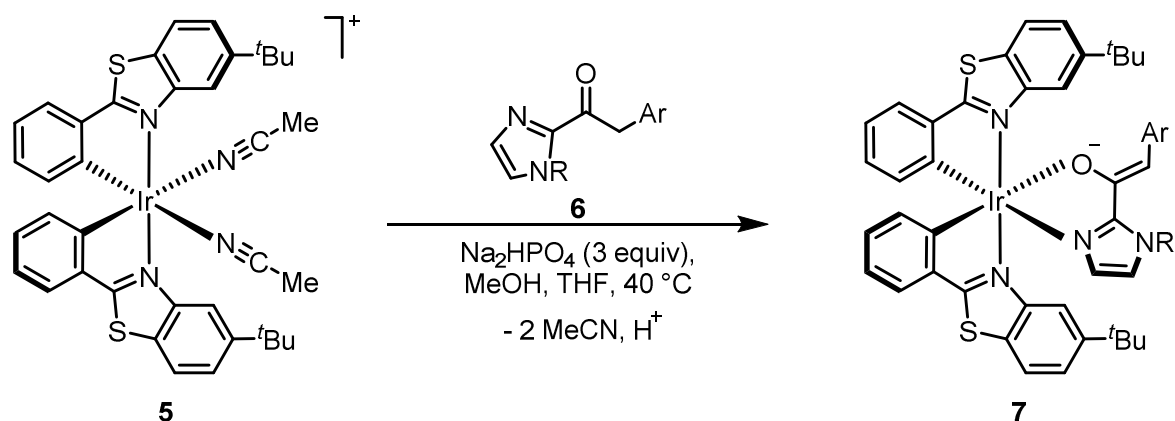
^aAll potentials are relative to the saturated calomel electrode. Data has been obtained in acetonitrile at room temperature. ^bDetermined at 203 K. ^cDetermined in propylene carbonate. ^dDetermined in aqueous media. ^eDetermined in DCM. ^fDetermined in ethanol / methanol 1:1 glass.

2 Notable Literature Examples of Photoredox Chemistry

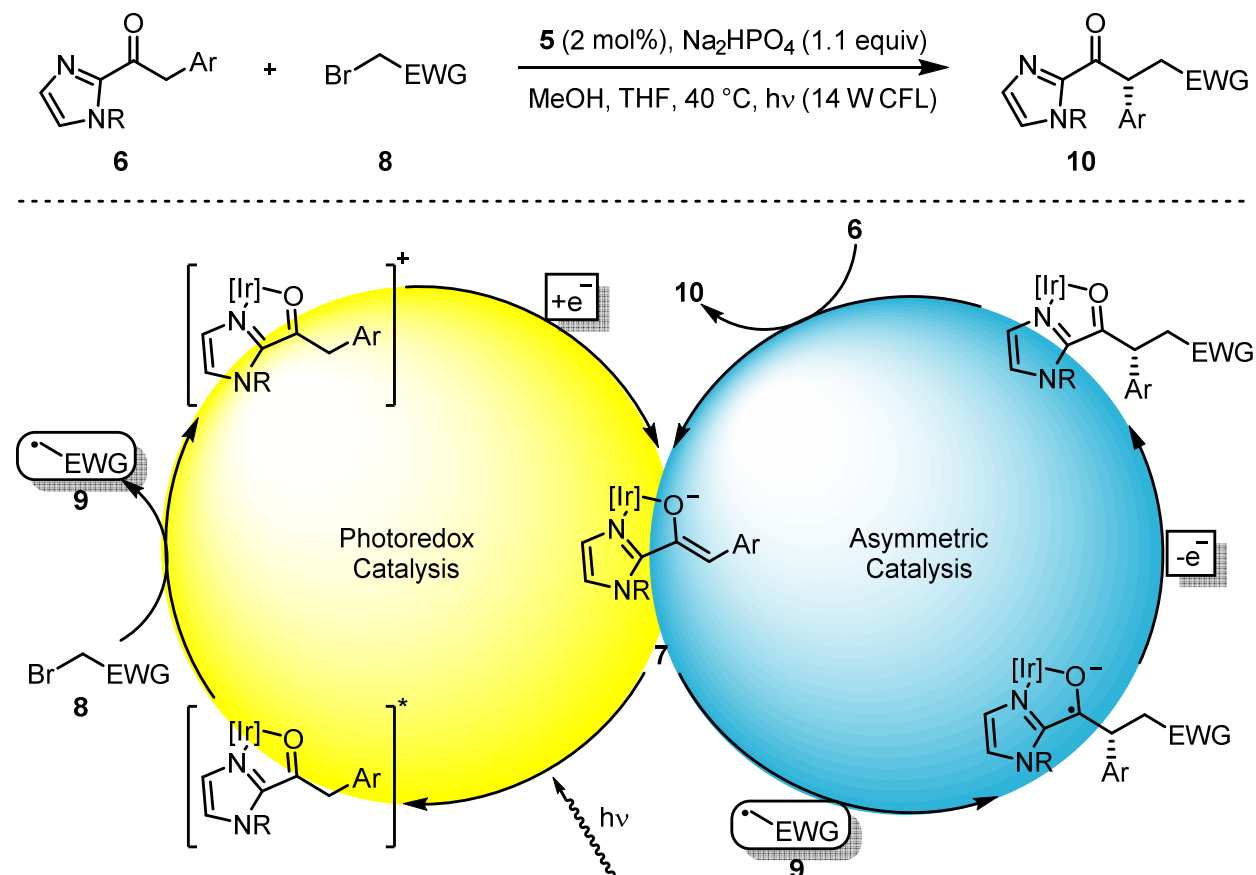
While there has been tremendous progress in the field in the last years, leading to a multitude of marvelous chemical transformations, this section will only discuss two of the very latest developments in order to showcase the vast possibilities that photoredox chemistry offers. To gain a broader overview of this research area, the interested reader is redirected to more extensive reviews.^{8,15,16,35,36}

Asymmetry-inducing reactions are generally highly valuable. However, such examples remained rare in the field of photochemistry. Through the combination of photoredox catalysis with a second catalytic mode, the realization of enantioselective reactions was possible.³⁷ Therefore photoredox catalysts were paired with an asymmetric co-catalyst. Chiral secondary amines,^{12,38–41} chiral *N*-heterocyclic carbenes,⁴² chiral Brønsted acids,⁴³ chiral Lewis acids,⁴⁴ as well as chiral thioureas⁴⁵ have been used for this purpose.

Very recently, Eric Meggers *et al.* described a single catalyst that combines both, the (pro-)photocatalyst and an asymmetry-inducing co-catalyst, in a single molecule **5** (Scheme 4).^{46,47} In the presence of substrate **6**, the active form of the chiral catalyst **7** is generated *in situ* under the reaction conditions. In order to facilitate the required ligand scrambling, a slightly increased reaction temperature of 40 °C proved to be beneficial. Enolate complex **7** has a much higher excited state reduction potential ($E_{1/2}^{IV/III^*} = -1.74$ V) than its cationic precursor complex **5** ($E_{1/2}^{IV/III^*} > -0.71$ V), meaning that it is a very potent reduction agent. Indeed, visible-light excited **7** proved to be able to reduce benzyl and phenacyl bromides **8** (Scheme 5, left side). The thus generated electron-deficient radical **9** is then attacked by the electron-rich, prochiral 2-acyl imidazole moiety of chiral **7** (right side) in an asymmetric fashion. After back electron transfer to regenerate the neutral photocatalyst, the chiral, α -alkylated product **10** is liberated through displacement with a new substrate molecule (**6**).

Scheme 4. Generation of the active photoredox catalyst **7** under the reaction conditions.

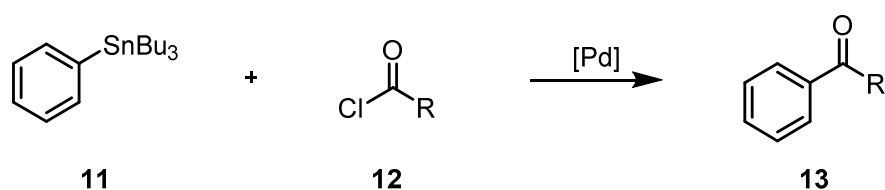
This overall process enables the enantioselective α -alkylation of 2-acyl imidazoles **6** with benzyl and phenacyl bromides **8** in excellent yields and enantioselectivities (both up to 99%). The elegant combination of two catalytic modes in one, structurally simple complex may serve as a blueprint for efficient synthesis of chiral molecules in the future.

Scheme 5. Photoinduced enantioselective alkylation of 2-acyl imidazoles with precatalyst **5**.

The second process that shall be highlighted in this section to demonstrate the broad utility of photoredox chemistry, is the synthesis of ketones *via* decarboxylative arylation of α -oxo acids.⁴⁸ The carbonyl group plays a pivotal role in organic chemistry, both acting as an

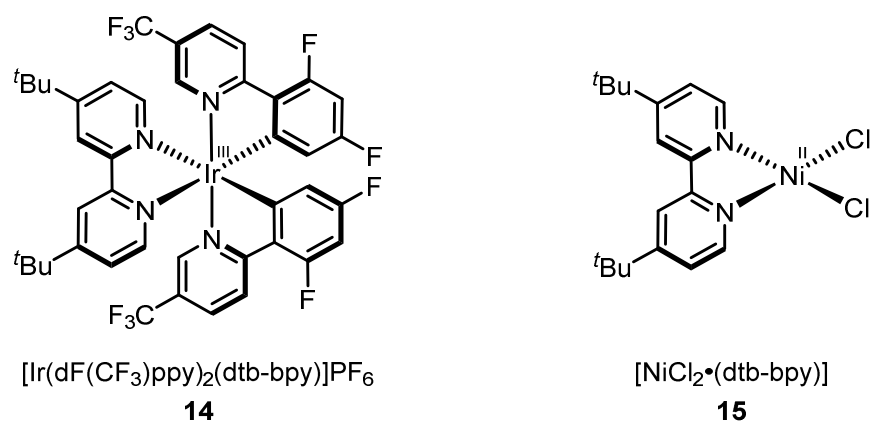
electrophile enabling new bond formations and as target structural unit in many products ranging from pharmaceuticals to materials.⁴⁹ Consequently, countless synthetic methods have been developed in the past to introduce the carbonyl motif into the target compound. A common method to synthesize aryl ketones is the Stille coupling of an acyl chloride **12** with an aryl stannane **11** (Scheme 6).⁵⁰ Obvious drawbacks from this methods are the employment of corrosive acid chlorides as well as stoichiometric amounts of highly toxic organo-tin compounds.

Scheme 6. The Stille cross-coupling represents a common method for the synthesis of ketones.

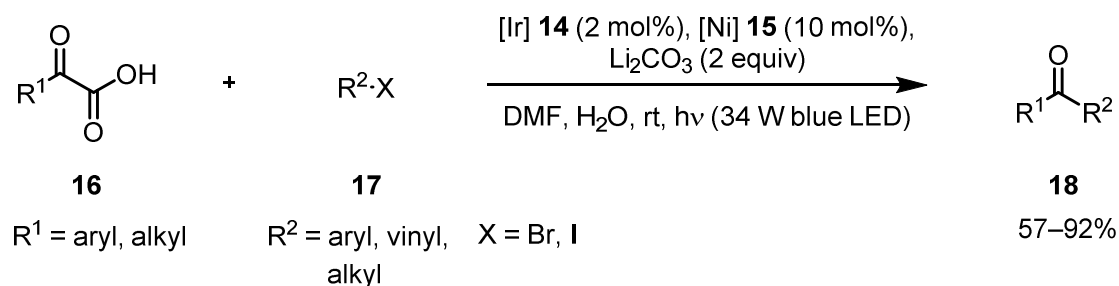


MacMillan *et al.* developed a cross-coupling protocol where both of those disadvantages could be eluded employing a combination of visible light photoredox catalysis and nickel catalysis.⁴⁸ The two employed catalysts for this process are depicted in Figure 2.

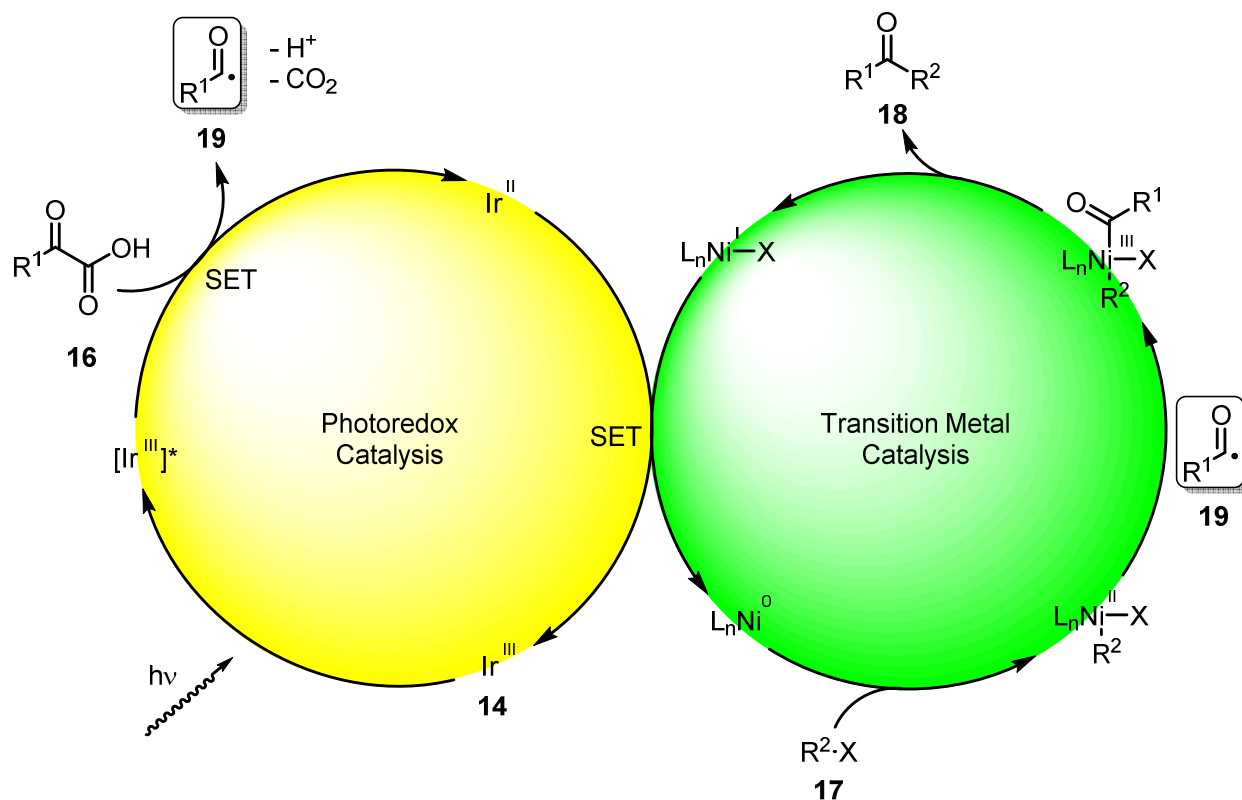
Figure 2. Catalyst combination employed in the photochemical ketone synthesis by MacMillan *et al.*



The substrate scope for this photocatalytic cross coupling reaction is very broad: on the one hand aryl, vinyl, or even secondary alkyl halides can be employed while on the other hand both aryl and alkyl α -keto acids are suitable (Scheme 7).

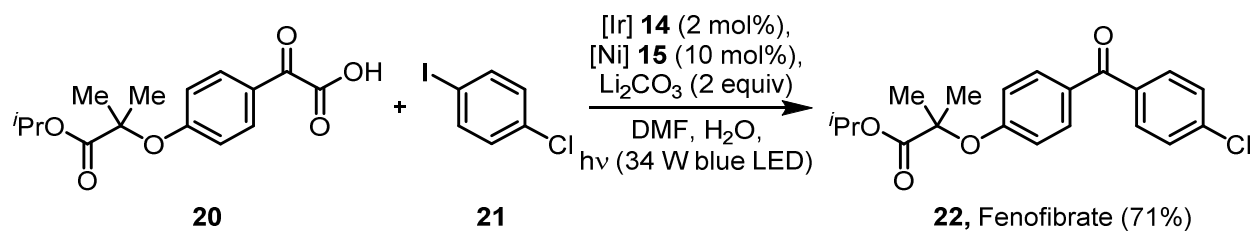
Scheme 7. Visible light mediated coupling of α -keto acids **16** with organohalides **17**.

The proposed mechanism of this reaction is shown in Scheme 8. Irradiation of photocatalyst **14** by a high-powered 34 W blue LED generates highly oxidizing $[Ir^{3+}]^*$ (left side). It can oxidize the deprotonated α -oxo acid **16**, which then quickly extrudes carbon dioxide, generating acyl radical **19**. The transition metal catalytic cycle (depicted in green) is initiated by oxidative addition of organohalide **17**. The resulting electrophilic Ni^{2+} complex is then trapped by acyl radical **19** to give an acylated Ni^{3+} complex. Reductive elimination liberates ketone product **18** and a Ni^+ , which can subsequently regenerate the cationic photocatalyst **14** and the catalytically active Ni^0 species *via* a single electron transfer (SET).

Scheme 8. Mechanism of the decarboxylative arylation of α -keto acids **13**.

The broad utility of this process was demonstrated in the efficient synthesis the cholesterol-modulating drug Fenofibrate **22** (Scheme 9).

Scheme 9. Synthesis of a cholesterol-modulating pharmaceutical by decarboxylative arylation.



3 Literature

- (1) BP Statistical Review of World Energy 2014 <http://www.bp.com/content/dam/bp/pdf/Energy-economics/statistical-review-2014/BP-statistical-review-of-world-energy-2014-full-report.pdf>.
- (2) World energy consumption http://en.wikipedia.org/wiki/World_energy_consumption.
- (3) Bundesverband Solarwirtschaft e.V. (BSW-Solar). Statistische Zahlen der deutschen Solarstrombranche
http://www.solarwirtschaft.de/fileadmin/media/pdf/2013_2_BSW_Solar_Faktenblatt_Photovoltaik.pdf.
- (4) Christopher, N. Solar Radiation & Photosynthetically Active Radiation
<http://www.fondriest.com/environmental-measurements/parameters/weather/photosynthetically-active-radiation/>.
- (5) Dick, B. Photophysics of Photocatalysts A. In *Chemical Photocatalysis*; König, B., Ed.; De Gruyter: Berlin, 2013; pp 19–44.
- (6) Giacomo Ciamician. The Photochemistry of the Future. *Science* **1912**, *36*, 385–394.
- (7) Giacomo Ciamician. Sur Les Actions Chimique De La Lumière. *Bull. Soc. Chim. Fr.* **1908**, *4*, i.
- (8) Prier, C. K.; Rankic, D. A.; MacMillan, D. W. C. Visible Light Photoredox Catalysis with Transition Metal Complexes: Applications in Organic Synthesis. *Chem. Rev.* **2013**, *113*, 5322–5363.
- (9) Zeitler, K. Photoredox Catalysis with Visible Light. *Angew. Chem. Int. Ed.* **2009**, *48*, 9785–9789.
- (10) Narayanam, J. M. R.; Stephenson, C. R. J. Visible Light Photoredox Catalysis: Applications in Organic Synthesis. *Chem. Soc. Rev.* **2011**, *40*, 102–113.
- (11) Chen, X.; Mao, S. S. Titanium Dioxide Nanomaterials: Synthesis, Properties, Modifications and Applications. *Chem. Rev.* **2007**, *107*, 2891–2959.
- (12) Cherevatskaya, M.; Neumann, M.; Földner, S.; Harlander, C.; Kümmel, S.; Dankesreiter, S.; Pfützner, A.; Zeitler, K.; König, B. Visible-Light-Promoted Stereoselective Alkylation by Combining Heterogeneous Photocatalysis with Organocatalysis. *Angew. Chem. Int. Ed.* **2012**, *51*, 4062–4066.
- (13) Neumann, M.; Földner, S.; König, B.; Zeitler, K. Metal-Free, Cooperative Asymmetric Organophotoredox Catalysis with Visible Light. *Angew. Chem. Int. Ed.* **2011**, *50*, 951–954.
- (14) Ghosh, I.; Ghosh, T.; Bardagi, J. I.; König, B. Reduction of Aryl Halides by Consecutive Visible Light-Induced Electron Transfer Processes. *Science* **2014**, *346*, 725–728.
- (15) Nicewicz, D. A.; Nguyen, T. M. Recent Applications of Organic Dyes as Photoredox Catalysts in Organic Synthesis. *ACS Catal.* **2014**, *4*, 355–360.
- (16) Teplý, F. Photoredox Catalysis by [Ru(bpy)₃]²⁺ to Trigger Transformations of Organic Molecules. Organic Synthesis Using Visible-Light Photocatalysis and Its 20th Century Roots. *Collect. Czechoslov. Chem. Commun.* **2011**, *76*, 859–917.
- (17) Koike, T.; Akita, M. Visible-Light Radical Reaction Designed by Ru- and Ir-Based Photoredox Catalysis. *Inorg. Chem. Front.* **2014**, *1*, 562–576.

- (18) Kern, J.-M.; Sauvage, J.-P. Photoassisted C-C Coupling via Electron Transfer to Benzylic Halides by a Bis(di-Imine) Copper(I) Complex. *J. Chem. Soc., Chem. Commun.* **1987**, 546–548.
- (19) Paria, S.; Pirtsch, M.; Kais, V.; Reiser, O. Visible-Light-Induced Intermolecular Atom-Transfer Radical Addition of Benzyl Halides to Olefins: Facile Synthesis of Tetrahydroquinolines. *Synthesis* **2013**, *45*, 2689–2698.
- (20) Pirtsch, M.; Paria, S.; Matsuno, T.; Isobe, H.; Reiser, O. [Cu(dap)₂Cl] as an Efficient Visible-Light-Driven Photoredox Catalyst in Carbon-Carbon Bond-Forming Reactions. *Chem. Eur. J.* **2012**, *18*, 7336–7340.
- (21) Majek, M.; Jacobi von Wangelin, A. Ambient-Light-Mediated Copper-Catalyzed C-C and C-N Bond Formation. *Angew. Chem. Int. Ed.* **2013**, *52*, 5919–5921.
- (22) Bagal, D. B.; Kachkovskyi, G.; Knorn, M.; Rawner, T.; Bhanage, B. M.; Reiser, O. Trifluoromethylchlorosulfonylation of Alkenes: Evidence for an Inner-Sphere Mechanism by a Copper Phenanthroline Photoredox Catalyst. *Angew. Chem. Int. Ed.* **2015**, *54*, 6999–7002.
- (23) Stevenson, S. M.; Shores, M. P.; Ferreira, E. M. Photooxidizing Chromium Catalysts for Promoting Radical Cation. *Angew. Chem. Int. Ed.* **2015**, *54*, 6506–6510.
- (24) Kachkovskyi, G.; Kais, V.; Kohls, P.; Paria, S.; Pirtsch, M.; Rackl, D.; Seo, H.; Reiser, O. Homogeneous Visible Light-Mediated Transition Metal Photoredox Catalysis Other than Ruthenium and Iridium. In *Chemical Photocatalysis*; König, B., Ed.; De Gruyter: Berlin, 2013; pp 139–150.
- (25) Flamigni, L.; Barbieri, A.; Sabatini, C.; Ventura, B.; Barigelletti, F. Photochemistry and Photophysics of Coordination Compounds: Iridium. *Top. Curr. Chem.* **2007**, 143–203.
- (26) Kotani, H.; Ohkubo, K.; Fukuzumi, S. Photocatalytic Oxygenation of Anthracenes and Olefins with Dioxxygen via Selective Radical Coupling Using 9-Mesityl-10-Methylacridinium Ion as an Effective Electron-Transfer Photocatalyst. *J. Am. Chem. Soc.* **2004**, *126*, 15999–16006.
- (27) Zeller, M. A.; Riener, M.; Nicewicz, D. A. Butyrolactone Synthesis via Polar Radical Crossover Cycloaddition Reactions: Diastereoselective Syntheses of Methylenolactocin and Protolichesterinic Acid. *Org. Lett.* **2014**, *16*, 4810–4813.
- (28) Rillema, D. P.; Allen, G.; Meyer, T. J.; Conrad, D. Redox Properties of ruthenium(II) Tris Chelate Complexes Containing the Ligands 2, 2'-Bipyrazine, 2, 2'-Bipyridine, and 2, 2'-Bipyrimidine. *Inorg. Chem.* **1983**, *22*, 1617–1622.
- (29) Crutchley, R. J.; Lever, a. B. P. Ruthenium(II) Tris(bipyrazyl) Dication-A New Photocatalyst. *J. Am. Chem. Soc.* **1980**, 7129–7131.
- (30) Kalyanasundaram, K. Photophysics, Photochemistry and Solar Energy Conversion with tris(bipyridyl)ruthenium(II) and Its Analogues. *Coord. Chem. Rev.* **1982**, *46*, 159–244.
- (31) Juris, A.; Balzani, V. 211. Characterization of the Excited State Properties of Some New Photosensitizers of the Ruthenium (Polypyridine) Family. *Helv. Chim. Acta* **1981**, *64*, 2175.
- (32) Young, R. C.; Meyer, T. J.; Whitten, D. G. Electron Transfer Quenching of Excited States of Metal Complexes. *J. Am. Chem. Soc.* **1976**, *98*, 286–287.
- (33) Lowry, M. S.; Goldsmith, J. I.; Slinker, J. D.; Rohl, R.; Pascal, R. A.; Malliaras, G. G.; Bernhard, S. Single-Layer Electroluminescent Devices and Photoinduced Hydrogen Production from an Ionic Iridium(III) Complex. *Chem. Mater.* **2005**, *17*, 5712–5719.
-

- (34) Slinker, J. D.; Gorodetsky, A. A.; Lowry, M. S.; Wang, J.; Parker, S.; Rohl, R.; Bernhard, S.; Malliaras, G. G. Efficient Yellow Electroluminescence from a Single Layer of a Cyclometalated Iridium Complex. *J. Am. Chem. Soc.* **2004**, *126*, 2763–2767.
- (35) Schultz, D. M.; Yoon, T. P. Solar Synthesis: Prospects in Visible Light Photocatalysis. *Science* **2014**, *343*, 985.
- (36) Paria, S.; Reiser, O. Copper in Photocatalysis. *ChemCatChem* **2014**, 2477–2483.
- (37) Hopkinson, M. N.; Sahoo, B.; Li, J. L.; Glorius, F. Dual Catalysis Sees the Light: Combining Photoredox with Organo-, Acid, and Transition-Metal Catalysis. *Chem. Eur. J.* **2014**, 3874–3886.
- (38) Nicewicz, D. A.; MacMillan, D. W. C. Merging Photoredox Catalysis with Organocatalysis: The Direct Asymmetric Alkylation of Aldehydes. *Science* **2008**, *322*, 77–80.
- (39) Nagib, D. A.; Scott, M. E.; MacMillan, D. W. C. Enantioselective Alpha-Trifluoromethylation of Aldehydes via Photoredox Organocatalysis. *J. Am. Chem. Soc.* **2009**, *131*, 10875–10877.
- (40) Shih, H. W.; Vander Wal, M. N.; Grange, R. L.; MacMillan, D. W. C. Enantioselective Alpha-Benzoylation of Aldehydes via Photoredox Organocatalysis. *J. Am. Chem. Soc.* **2010**, *132*, 13600–13603.
- (41) Neumann, M.; Földner, S.; König, B.; Zeitler, K. Metal-Free, Cooperative Asymmetric Organophotoredox Catalysis with Visible Light. *Angew. Chem. Int. Ed.* **2011**, *50*, 951–954.
- (42) DiRocco, D. A.; Rovis, T. Catalytic Asymmetric α -Acylation of Tertiary Amines Mediated by a Dual Catalysis Mode: N-Heterocyclic Carbene and Photoredox Catalysis. *J. Am. Chem. Soc.* **2012**, *134*, 8094–8097.
- (43) Tarantino, K. T.; Liu, P.; Knowles, R. R. Catalytic Ketyl-Olefin Cyclizations Enabled by Proton-Coupled Electron Transfer. *J. Am. Chem. Soc.* **2013**, *135*, 10022.
- (44) Du, J.; Skubi, K. L.; Schultz, D. M. A Dual-Catalysis Approach to Enantioselective [2+2] Photocycloadditions Using Visible Light. *Science* **2014**, *344*, 392–396.
- (45) Bergonzini, G.; Schindler, C. S.; Wallentin, C.-J.; Jacobsen, E. N.; Stephenson, C. R. J. Photoredox Activation and Anion Binding Catalysis in the Dual Catalytic Enantioselective Synthesis of Beta-Amino Esters. *Chem. Sci.* **2014**, *5*, 1–60.
- (46) Huo, H.; Shen, X.; Wang, C.; Zhang, L.; Röse, P.; Chen, L.-A.; Harms, K.; Marsch, M.; Hilt, G.; Meggers, E. Asymmetric Photoredox Transition-Metal Catalysis Activated by Visible Light. *Nature* **2014**, *515*, 100–103.
- (47) Wang, C.; Zheng, Y.; Huo, H.; Röse, P.; Zhang, L.; Harms, K.; Hilt, G.; Meggers, E. Merger of Visible Light Induced Oxidation and Enantioselective Alkylation with a Chiral Iridium Catalyst. *Chem. Eur. J.* **2015**, *21*, 7355–7359.
- (48) Chu, L.; Lipshultz, J. M.; MacMillan, D. W. C. Merging Photoredox and Nickel Catalysis: The Direct Synthesis of Ketones by the Decarboxylative Arylation of Alpha-Oxo Acids. *Angew. Chem. Int. Ed.* **2015**, *21*, 7355–7359.
- (49) Carey, F. A.; Sundberg, R. J. *Advanced Organic Chemistry*; Springer: New York, 2007.
- (50) Stille, J. K. The Palladium-Catalyzed Cross-Coupling Reactions of Organotin Reagents with Organic Electrophiles. *Angew. Chem.* **1986**, *25*, 508–524.
-

D Photochemical Deoxygenations[‡]

1 Defunctionalative Deoxygenations

1.1 Introduction

The dwindling supply of hydrocarbons from fossil resources calls for the usage of renewable resources for the synthesis of fine chemicals in the future.¹ This strategy suffers from the relative high degree of functionalization of typical feedstock materials, which is often not desired in the target fine chemicals and leads to compatibility issues in further chemical transformations. Carbon – oxygen single bonds are common structural elements in natural materials. For example the very simple natural product α -D-glucose (**1**) contains six oxygen atoms, leading to a much higher molecular complexity than its des-*O*-analog cyclohexane (**2**, Figure 1).

Figure 1. Highly hydroxylated α -D-glucose (**1**) in comparison with simple cyclohexane (**2**).



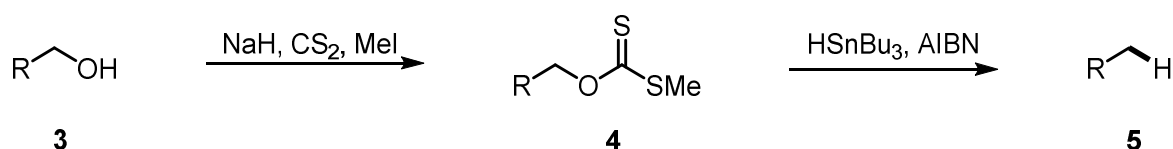
A (partial) reduction to non-functionalized carbon – hydrogen bonds would decrease complexity and increase compatibility of those materials in chemical manipulations in accordance with well-established oil-based protocols developed in the chemical industry during the last century.²

A classical route to achieve such a deoxygenation is the Barton-McCombie reaction (Scheme 1).³ This radical deoxygenation protocol relies on prior formation of methyl xanthate **4** as the actual radical precursor. Triggered by the decomposition of radical starter AIBN, tributyltin hydride initiates the radical fragmentation of xanthate **4** and provides a hydrogen

[‡] This chapter is partially based on D. Rackl, V. Kais, P. Kreitmeier, O. Reiser, *Bellstein J. Org. Chem.* **2014**, *10*, 2157–2165. Appropriate copyrights have been obtained where necessary.

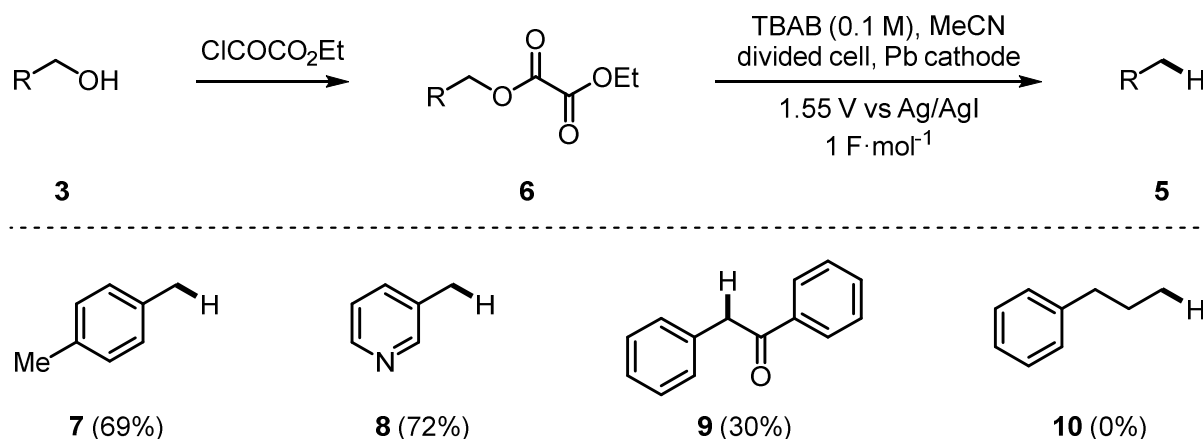
atom source for trapping of the intermediary carbon-centered radical to give deoxygenated **5**. While generally giving deoxygenated products **5** in high yield, this method unfortunately requires over-stoichiometric amounts of highly noxious chemicals. Especially organotin compounds are of great concern as their employment typically disqualifies the method for application in the pharmaceutical industry. Nowadays several improved protocols are available circumventing the usage of stannanes through replacement with *e.g.* silanes.⁴ Nevertheless, the issues related with the formation of xanthates **4** remain.

Scheme 1. Barton-McCombie deoxygenation sequence.



Radical deoxygenations can also be carried out electrochemically, using electrons instead of organic reagents as terminal reductant. Utley *et al.* showed that ethyl oxalate esters **6** can be used for this purpose (Scheme 2).⁵⁻⁷ After prior installation of the ethyl oxalate as activation group, **6** was subjected to electrolysis conditions. Ethyl oxalate esters **6** exhibit a reduction potential of about -1.2 V vs Ag/AgI (corresponds to -1.3 V vs SCE) and were thus treated with a slightly higher current of 1.55 V vs Ag/AgI to achieve preparative, electrochemical reduction. After consumption of 1 F·mol⁻¹ the current was switched off and deoxygenated products **5** could be isolated. This methodology is however limited: only benzylic and allylic alcohol derivatives could be defunctionalized using such an ethyl oxalate activation group.

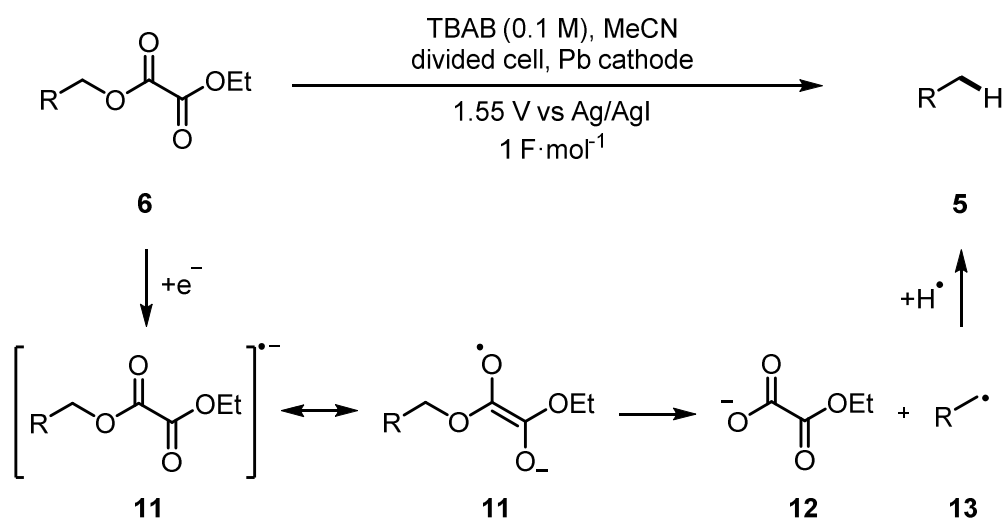
Scheme 2. Electrochemical deoxygenations *via* ethyl oxalates **6** with substrate scope.



The mechanism of this electrochemical deoxygenation is depicted in Scheme 3. First, an electron is injected into the oxalate moiety of **6** through the lead cathode. The so generated radical anion **11** undergoes bond mesolysis, leading to ethyl oxalate anion **12** and carbon-centered radical **13**, which can then abstract a hydrogen atom from the solvent to obtain **5**.

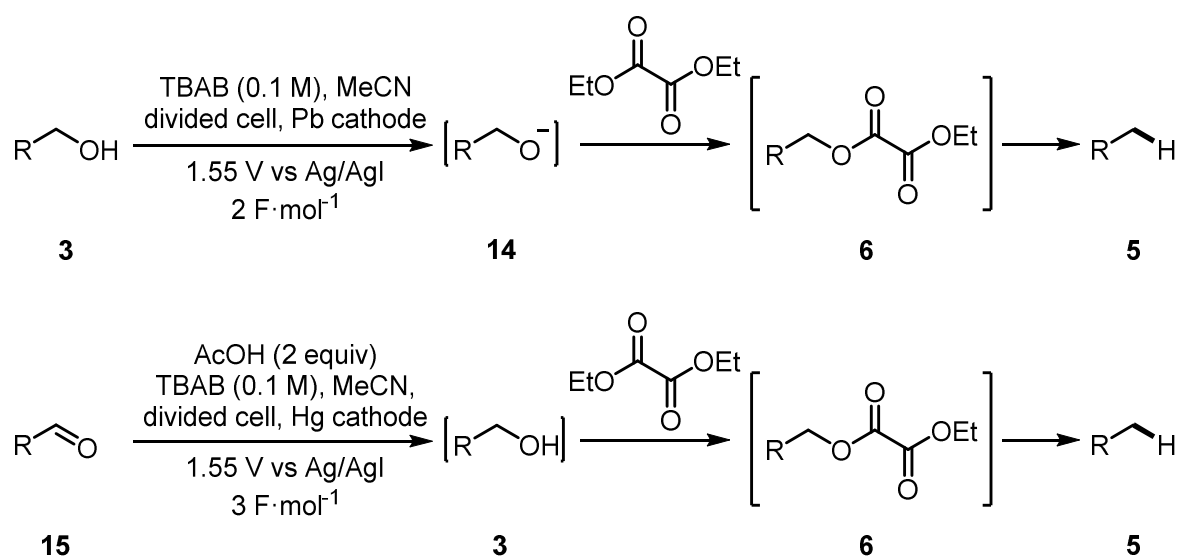
The authors proposed that the stability of **13** is crucial for the reaction. In cases where the radical was not located in either a benzylic or an allylic position, no deoxygenated product **5** could be observed.

Scheme 3. Mechanism of the electrochemical deoxygenation by Utleby *et al.*

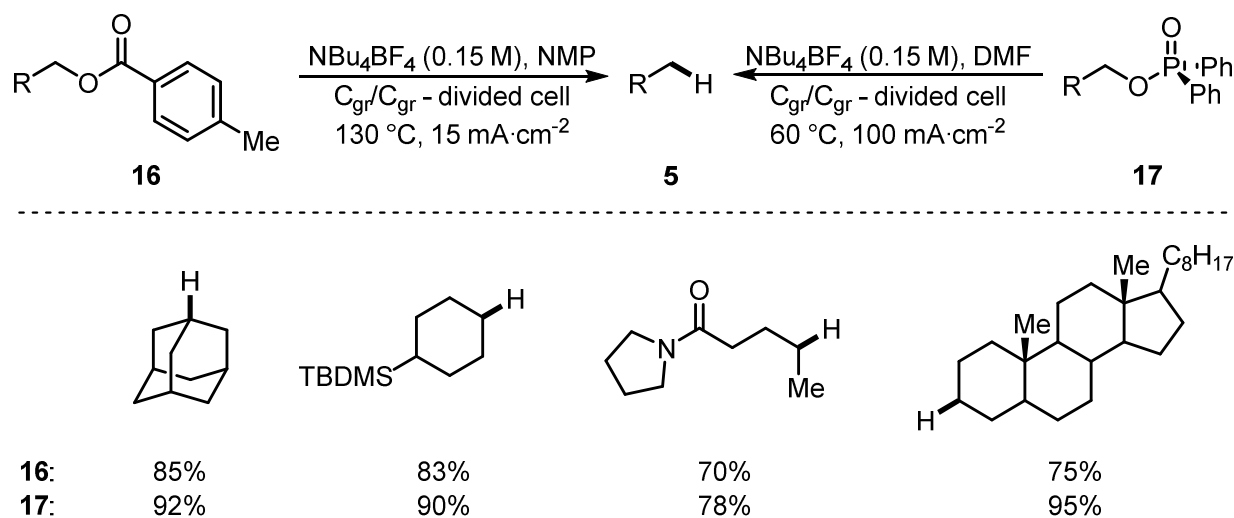


The deoxygenation sequence was streamlined by *in situ* formation of the required oxalate ester, superseding a separate acylation step (Scheme 4, upper part). Therefore, unactivated alcohol **3** was electrolyzed in the presence diethyl oxalate. This process generated alkoxide **14** *in situ*, which could undergo transesterification with diethyl oxalate to form oxalate-activated **6**. Further electrolysis then gave deoxygenated compound **5** as described above. In addition, the deoxygenation sequence could also be started from carbonyl compound **15** which was directly reduced to alcohol **3** under the reaction conditions (Scheme 4, lower part).[§]

[§] Viktor Kais developed a photochemical deoxygenation protocol for ethyloxalate esters in his dissertation.^{85,86}

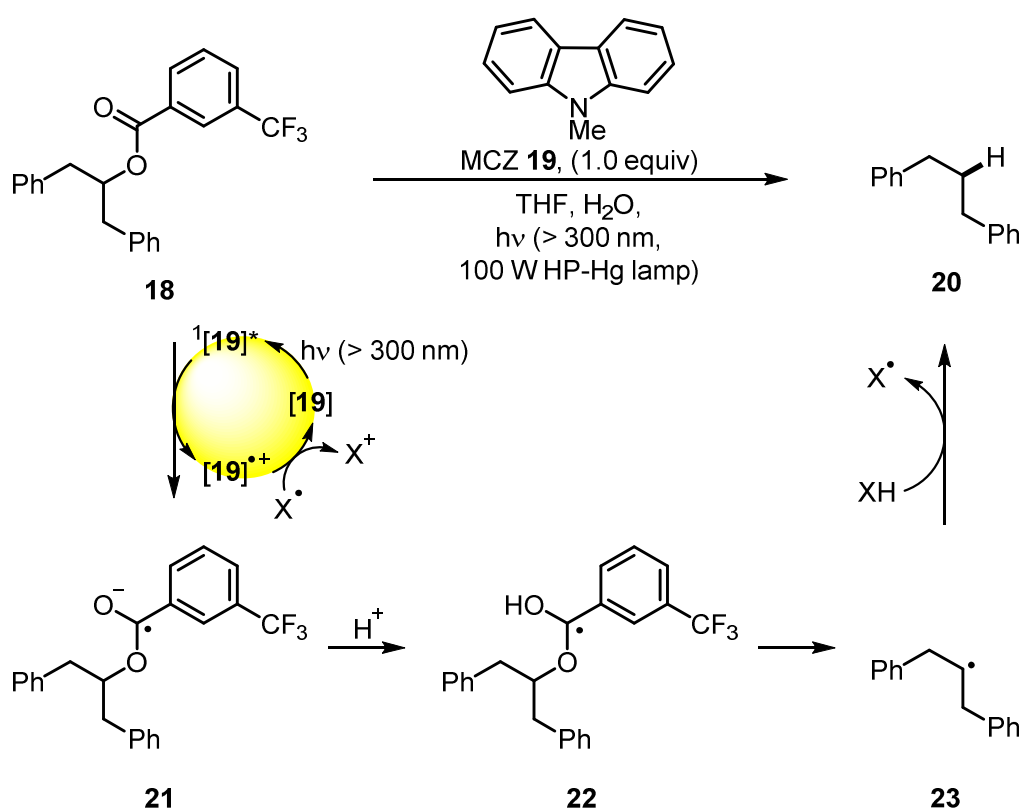
Scheme 4. Streamlining of electrochemical deoxygenations with ethyl oxalates.

To broaden the substrate scope of electrochemical deoxygenations, Lam and Markó moved away from ethyl oxalate as activation group towards toluates **16** and diphenylphosphinates **17** (Scheme 5).^{8,9} Toluatoate ester **16** showed a reversible reduction at -2.4 V vs Ag/AgCl, diphenylphosphinate ester **13** at -2.5 V vs Ag/AgCl. Elevated temperatures were crucial for the deoxygenation reactions to proceed. Even though much higher potentials and harsher reaction conditions were needed to reduce those substances compared to ethyl oxalates, the deoxygenation of hydroxyl functions in unactivated positions was feasible. The results of diphenylphosphinate esters **17** are generally superior to toluates **16**, as the electrolysis can be carried out at milder temperature giving uniformly higher product yields.

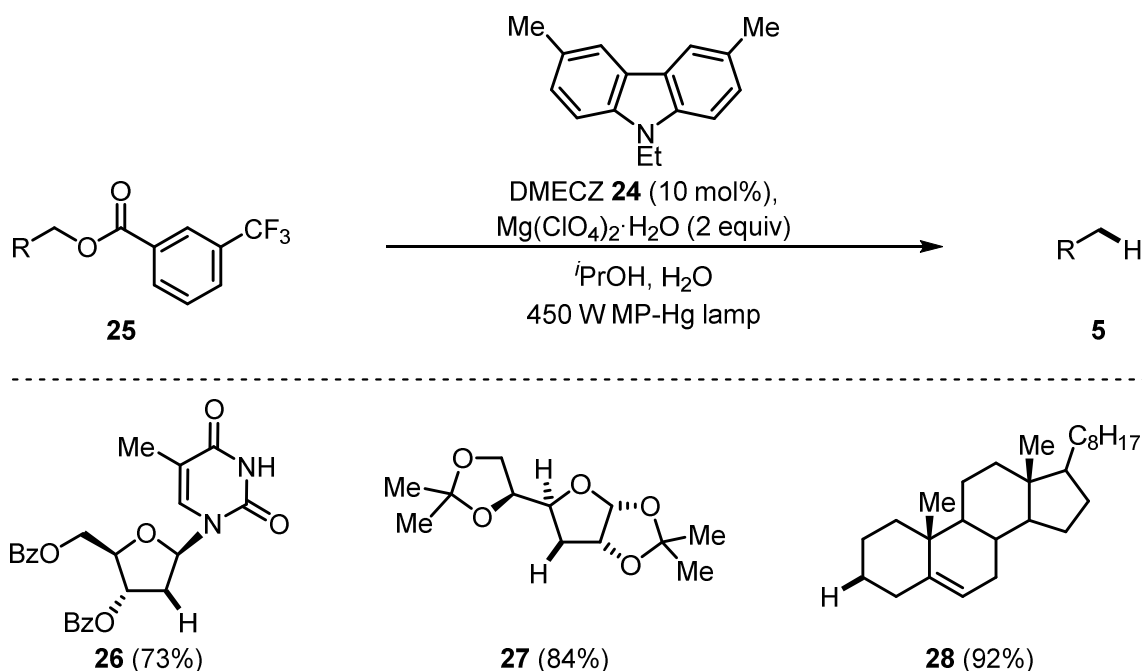
Scheme 5. Electrochemical deoxygenations with toluates **16** and diphenylphosphinates **17**.

Radical deoxygenations have not only been carried out electrochemically but also in a photochemical fashion. Saito *et al.* developed a process where secondary alcohols were activated as 3-trifluoromethyl benzoates like **18** (Scheme 6).¹⁰ The excited singlet state of photosensitizer MCZ (**19**) is postulated to inject an electron in the benzoate moiety of **18** to get radical anion **21** which is then rapidly protonated to **22** in the presence of water. C–O bond fragmentation gives unstabilized carbon-centered radical **23**, which abstracts a hydrogen atom from a solvent molecule to give deoxygenated product **20**. The oxidized form of photosensitizer [**19**]⁺⁺ presumably is reduced to regenerate the ground-state photosensitizer **19**, as **19** can partially be recovered after the irradiation procedure.

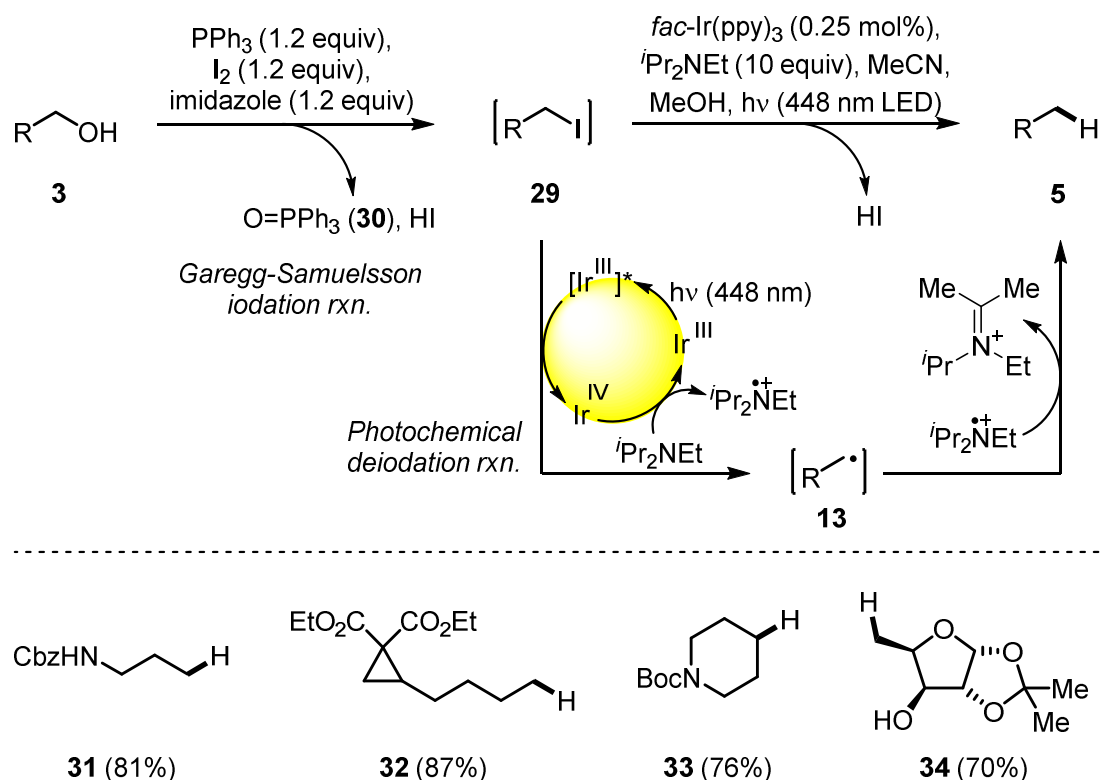
Scheme 6. Photochemical deoxygenation as developed by Saito *et al.*



This promising photochemical deoxygenation protocol was later improved by Rizzo *et al.*¹¹ By using sterically more demanding photosensitizer DMECZ (**24**) instead of MCZ (**19**), side reactions of the photosensitizer could be suppressed (Scheme 7). It was now possible to use the sensitizer in a sub-stoichiometric amount of only 10 mol%. With optimized reaction conditions deoxygenations of a variety of secondary alcohols was possible.^{12–16} However, a severe drawback of this method is that high intensity UV lamps in specialized reaction setups have to be used.

Scheme 7. Improved photocatalyst DMECZ (**24**) and selected deoxygenation examples.

To achieve deoxygenations with benign visible light, Stephenson *et al.* developed an indirect procedure where the to-be-cleaved hydroxyl group in **3** was transformed into an alkyl iodide **29** by a Garegg–Samuelsson reaction (Scheme 8).^{17,18} The actual photochemical reduction was then carried out with alkyl iodides **29** in a subsequent reaction step.¹⁹ Photocatalyst *fac*-Ir(ppy)₃ was irradiated with a blue LED. The catalysts excited state is highly reducing (-1.73 V vs SCE)²⁰ and therefore able to reduce alkyl halides bonds (*e.g.* *sec*-butyl iodide: -1.59 V vs SCE).²¹ The so generated carbon-centered radical **13** can then abstract a hydrogen atom from either the solvent or from the amine radical cation to give the deoxygenated compound **5**. This protocol allows the formal deoxygenation of a broad range of unactivated primary and secondary alcohols in good yield. Tertiary alcohols however can't be deoxygenated as the Garegg–Samuelsson reaction fails to deliver the required iodides. The actual activation, namely the conversion of a hydroxyl group into an iodide, is an undesirable reaction as its atom economy is very poor and redox-inefficient. For every molecule of deoxygenated material one molecule of triphenylphosphine oxide (**30**) is generated and one equivalent of iodine is reduced.

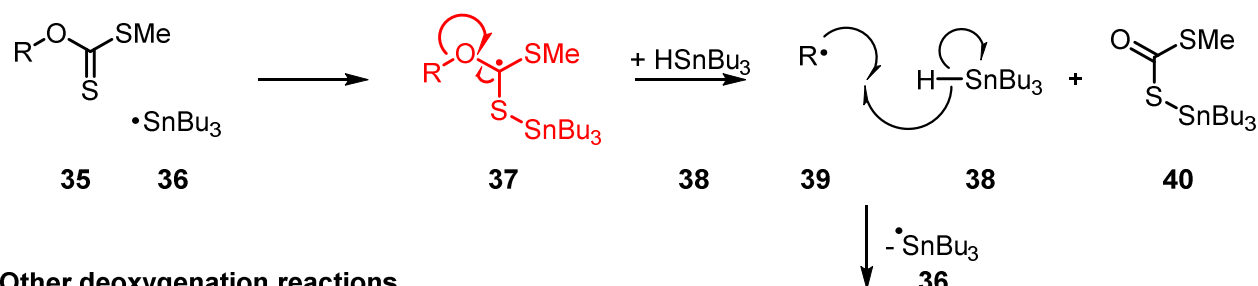
Scheme 8. Garegg–Samuelsson iodation / visible light mediated deiodation sequence.

In all those presented deoxygenation methods an activation of the hydroxyl group is necessary, either *via* conversion to the corresponding halide or formation of an ester derivative, partially using very problematic reagents. This inevitably generates stoichiometric amounts of unwanted by-products and is hence problematic for establishing a sustainable deoxygenation protocol that allows the recycling and reuse of the reagents involved. However, such a sustainable deoxygenation method would be highly desirable. In this work, redox-economic deoxygenation methods in which formation of radicals can be achieved under benign visible light photoredox catalysis were therefore investigated.

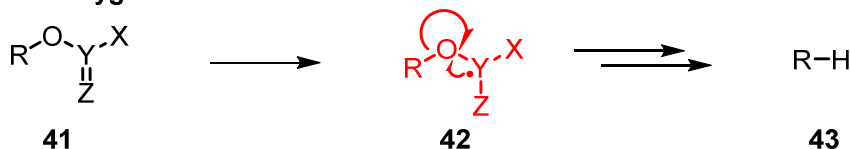
1.2 Preliminary studies with toluate and diarylphosphinate esters

For most of the available radical deoxygenation methods, an analogy of their mechanism can be drawn to the mechanism of the classical Barton-McCombie reaction (Scheme 9). It is always key, to generate a radical adjacent to the C–O bond which is supposed to be cleaved, as depicted for the Barton-McCombie reaction (37) and for a prototypical radical deoxygenation reaction (42). Intermediates of this type can be found in all previously presented radical C–O bond scission process, either *via* ethyl oxalates, toluates, diphenylphosphinates, or *N*-phthalimidoyl oxalates (*vide infra*). For a photochemical deoxygenation process it is therefore also necessary to arrive at such an intermediate.

Barton-McCombie reaction

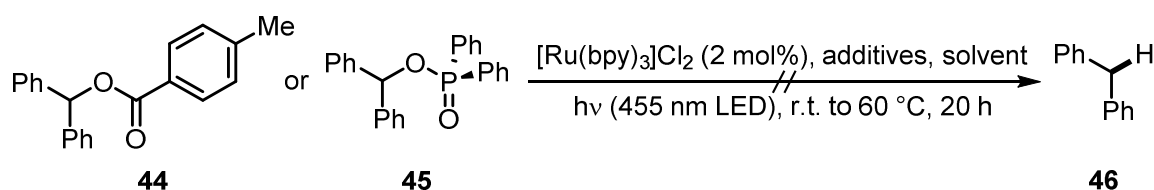


Other deoxygenation reactions



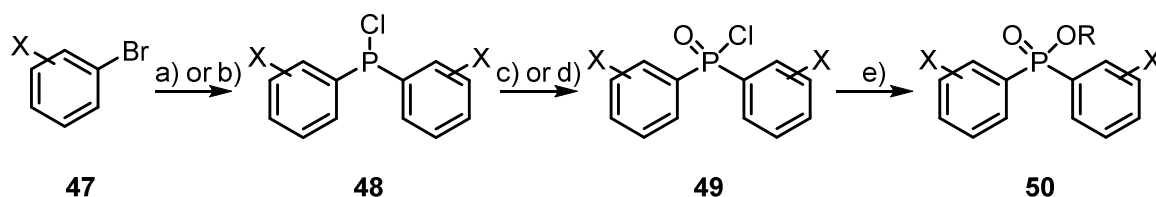
Scheme 9. Prototypical radical deoxygenation in comparison with the Barton-McCombie reaction.

As toluates and especially diphenylphosphinates proved to be good activation groups for hydroxyl functions in electrochemical experiments,^{8,9} first investigations aimed to use such compounds in visible light photoredox catalyzed reactions. Initial screening reactions with *p*-methylbenzoate ester **44** and unsubstituted diphenylphosphinate ester **45** with $[\text{Ru}(\text{bpy})_3]\text{Cl}_2$ in different solvent systems with various Lewis acid additives were however unsuccessful (Scheme 10). Also, the addition of Hantzsch ester as potential hydrogen atom source, Hünig's base as sacrificial electron donor, as well as increased reaction temperatures did not lead to the formation of deoxygenated product **46**. Cyclic voltametric measurements quickly revealed that the reduction potentials of *p*-methylbenzoate ester **44** and diphenylphosphinate ester **45** are -2.29 V and -2.43 V vs. SCE in DMF respectively and therefore not in a region that would be considered accessible by the reductive quenching pathway of $\text{Ru}(\text{bpy})_3\text{Cl}_2$ (-1.33 V vs. SCE) or even *fac*- $\text{Ir}(\text{ppy})_3$ (-2.19 V vs. SCE).

Scheme 10. Initial deoxygenation attempts with toluate **44** and diphenylphosphinate ester **45**.

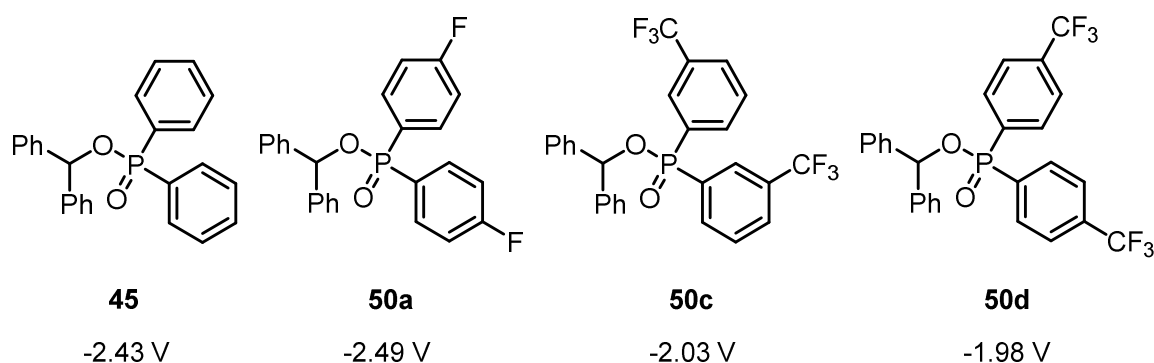
Additives: HCO_2H , Pr_2NEt , Hantzsch ester, LiBF_4 , $\text{Mg}(\text{ClO}_4)_2$, and multiple combinations thereof. Solvent systems: MeCN, DMF, $\text{PrOH}:\text{H}_2\text{O}$ (10:1, v/v).

To shift the reduction potentials into lower regions and thus make the substrates more accessible to common photocatalysts, it was decided to synthesize fluoro- and trifluoromethyl-substituted derivatives **50** of diphenylphosphinate esters **45**.¹⁰ They were synthesized starting from fluoro- and trifluoromethyl-substituted bromobenzenes **47** (Scheme 11).²² Grignard formation or halogen lithium exchange followed by treatment with Et_2NPCl_2 and subsequent deamidation with HCl gave corresponding chlorobisphenylphosphines **48** which were then oxidized to their bisphenylphosphinic chloride **49** by O_2 or O_3 .^{23–25} Treatment of these compounds with diphenylmethanol (**51**) and imidazole gave diarylphosphinate esters **50**.

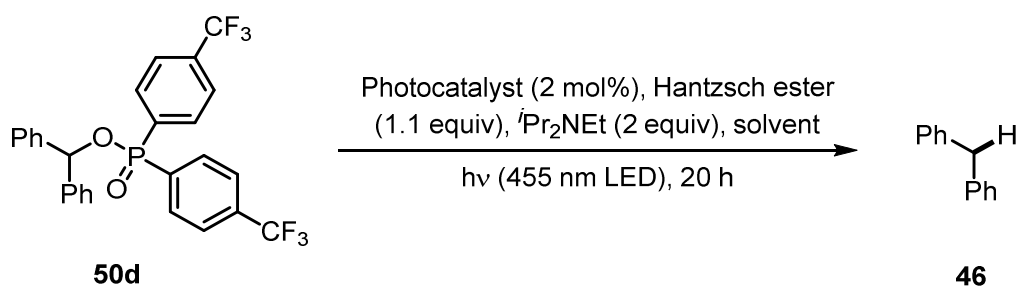
Scheme 11. Synthesis of substituted derivatives of diphenylphosphinate esters **45**.

X = 4-F, 2,3,4,5,6-(F)₅, 3-(CF₃), 4-(CF₃), 3,5-(CF₃)₂. Reagents and conditions: a) 1. $n\text{BuLi}$ (1.0 equiv), Et_2O , 5 °C, 4 h; 2. Et_2NPCl_2 (0.5 equiv), rt, 14 h; 3. HCl in Et_2O (1.25 equiv), -78 °C to rt, 1 h, 44 – 54%; b) 1. Mg (1.6 equiv), THF, rt, 45 min; 2. Et_2NPCl_2 (0.43 equiv), 0 °C to rt, 19 h; 3.) HCl in Et_2O (1.25 equiv), -78 °C to rt, 1 h, 58 – 80%; c) O_2 , benzene, rt, 5 h, 53 – 100%. d) O_3 , DCM, -78 °C, 5 min, quantitative; e) Ph_2CHOH (**51**, 0.83 equiv), imidazole (2.5 equiv), Et_2O , DCM, 0 °C to rt, on, 0 – 53%.

An overview of the successfully synthesized derivatives **50** along with their corresponding reduction potentials is given in Figure 2. The synthesis of pentafluoro- (**50b**) and 3,5-bis(trifluoromethyl)-substituted derivatives (**50e**) unfortunately failed at the stage of the formation of the phosphinate ester. However, from the synthesized compounds **50a**, **50c**, and **50d** certain trends can be seen: the introduction of a single fluoro substituent in para position had a detrimental influence on the reduction potential of the compound by slightly raising it. However, installation of a trifluoromethyl group in either meta or para position significantly lowered the reduction potential and thus made such substrates more accessible to visible light photoredox catalysis.

Figure 2. Synthesized diarylphosphinate esters and their reduction potentials vs SCE in DMF.

Indeed, when the derivative with the lowest reduction potential and therefore most promising substrate **50d** was subjected to photochemical reaction conditions, visible light mediated deoxygenation occurred (Table 1). As temperature played a crucial role in the deoxygenation of diphenylphosphinate esters under electrochemical conditions, the temperature dependence of the reaction was investigated first. A local maximum of product yield was observed at 40 °C (entry 2). Switching the solvent to either DCM or MeCN decreased the yield (entry 6 and 7). The influence of the photocatalyst was screened next. As $[\text{Cu}(\text{dap})_2]^+$ exhibits a higher reduction potential ($E_{1/2}(\text{Cu}^{2+}/\text{Cu}^{+}) = -1.43 \text{ V}$) in its excited state than reductively quenched $[\text{Ru}(\text{bpy})_3]^{2+}$ ($E_{1/2}(\text{Ru}^{2+}/\text{Ru}^{+}) = -1.33 \text{ V}$), higher yields would be expected using this catalyst in the deoxygenation reaction. This assumption however did not hold as $[\text{Cu}(\text{dap})_2]^+$ gave only 7% of deoxygenated product **46** (entry 8). The even stronger reducing photocatalyst $[\text{Ir}(\text{ppy})_2(\text{dtb-bpy})]^+$ ($E_{1/2}(\text{Ir}^{3+}/\text{Ir}^{2+}) = -1.51 \text{ V}$) produced the best deoxygenation results in this preliminary screening (entry 9).

Table 1. Visible light mediated deoxygenation of diarylphosphinate ester **50d**.

Entry	Photocatalyst	Temp. [°C]	Solvent	Yield [%] ^a
1	[Ru(bpy) ₃]Cl ₂	rt	DMF	27
2	[Ru(bpy) ₃]Cl ₂	40	DMF	32
3	[Ru(bpy) ₃]Cl ₂	60	DMF	25
4	[Ru(bpy) ₃]Cl ₂	80	DMF	27
5	[Ru(bpy) ₃]Cl ₂	100	DMF	14
6	[Ru(bpy) ₃]Cl ₂	40	DCM	16
7	[Ru(bpy) ₃]Cl ₂	40	MeCN	21
8	[Cu(dap) ₂]Cl	40	DMF	7
9	[Ir(ppy) ₂ (dtb-bpy)](PF ₆)	40	DMF	42

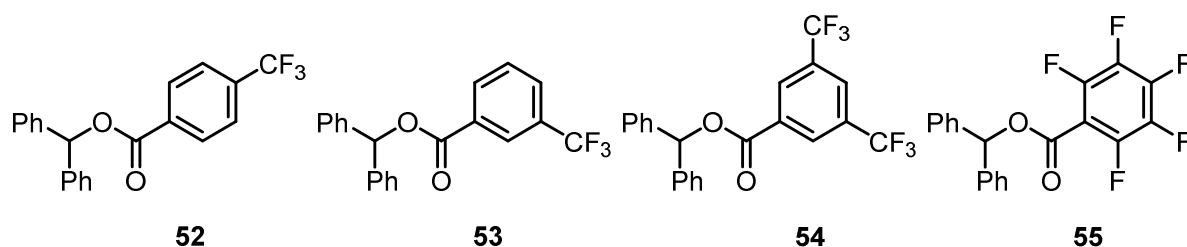
^aDetermined by GC-FID with naphthalene as internal standard.

Those initial results showed that through introduction of suitable substituents in the activating group, the reduction potentials could be adjusted and thus enabled photochemical transformations that were not possible before. Unfortunately, the synthesis of trifluoromethyl-substituted diarylphosphine esters is very tedious, fault-prone, and involves noxious reagents. The employment of diarylphosphine esters in photochemical deoxygenations was therefore not investigated any further, even though promising initial photochemical results were obtained.

1.3 Substituted benzoates as activation groups

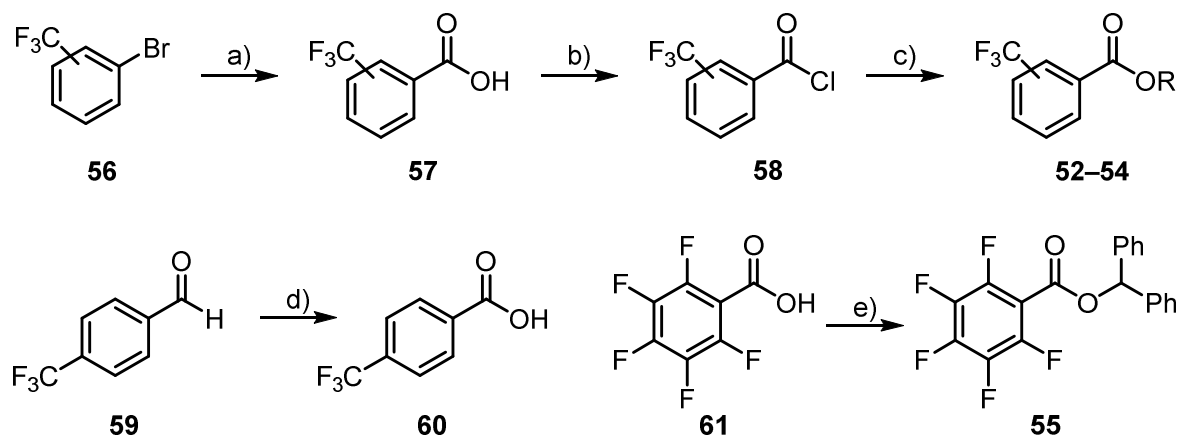
A simpler activating group for hydroxyl functions than diarylphosphinate was needed, which still offered reduction potentials that are in range of common photocatalysts. Simple toluates served this purpose in the case of electrochemical deoxygenations, but their high reduction potential prevents their application in visible light mediated reactions. As was shown in the previous chapter, reduction potentials can be advantageously affected by the introduction of trifluoromethyl groups. Therefore, the same strategy to lower the reduction potentials was applied to benzoate esters. Again, a set of fluoro- and trifluoromethyl- substituted derivatives of benzoate esters was synthesized (Figure 3).

Figure 3. Synthesized fluoro- and trifluoromethyl- substituted benzoate esters **52** – **55**.



Aryl halides **56** were converted to their Grignard compounds through Knochel Grignard exchange and treated with CO_2 (g) to give the corresponding benzoic acids **57** (Scheme 12).^{26,27} 4-(trifluoromethyl)benzoic acid **60** was prepared through oxidation of aldehyde **59** with H_2O_2 .²⁸ DMF-catalyzed formation of the acid chlorides **58** (either *in situ* or isolated) and reaction with alcohols gave trifluoromethyl-substituted benzoate esters **52** – **54** in good to excellent yields. Pentafluoro-substituted benzoate **55** was prepared *via* a DCC-mediated coupling reaction.

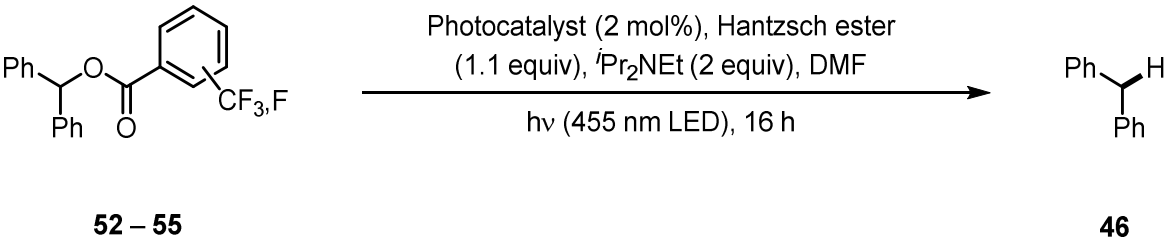
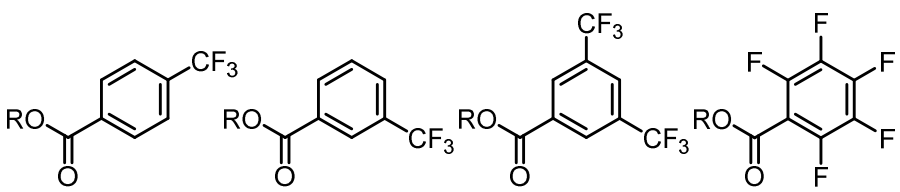
Scheme 12. Synthetic route to fluoro- and trifluoromethyl- substituted benzoate esters.



R = Ph₂CH. Reagents and conditions: a) 1. ⁱPrMgBr (1.1 equiv), THF, -10 °C to 0 °C, 30 min; 2. CO₂ (g), -40 °C to rt; 3. 1M HCl, 0 °C, 30 min, 9 – 89%; b) SOCl₂ (2.2 equiv), DMF (0.08 equiv): 79% or used *in situ* without isolation; c) Ph₂CHOH (**51**, 1 equiv), Et₃N (7 equiv), 4-DMAP (0.05 equiv), DCM, 0 °C, 10 min, 63 – 92%; d) H₂O₂ (30%), reflux, 18 h, 72 %; e) Ph₂CHOH (**51**, 1 equiv), DCC (1.2 equiv), 4-DMAP (0.1 equiv), DCM, 0 °C to rt, on, 63%.

Trifluoromethyl- and pentafluoro- substituted benzoate esters **52** to **55** were subsequently subjected to photochemical deoxygenation conditions (Table 2). Experiments were carried out with either [Ru(bpy)₃]²⁺ or [Ir(ppy)₂(dtb-bpy)]⁺ as photocatalyst, Hantzsch ester **24** as hydrogen atom donor, and ⁱPr₂NEt as sacrificial electron donor in DMF. In comparison to earlier experiments with toluate ester **44** (where no conversion occurred), all investigated substituted benzoate esters gave deoxygenation product **46** in poor to excellent yield after irradiation with a 455 nm LED for 16 h at 40 °C.

Table 2. Trifluoromethyl- and perfluoro- substituted benzoate esters **52** to **55** under photoreductive conditions. Corresponding reduction potentials are given vs SCE in DMF.^a

					
52 – 55		46			
					
		52	53	54	55
		-1.90 V	-1.98 V	-1.73 V	-1.80 V
Photocatalyst					
[Ru(bpy) ₃] ²⁺	5%	8%	10%	n.d.	
[Ir(ppy) ₂ (dtb-bpy)] ⁺	18%	20%	85%	19%	

R = Ph₂CH. ^aYields determined by GC-FID with dodecane as int. standard.

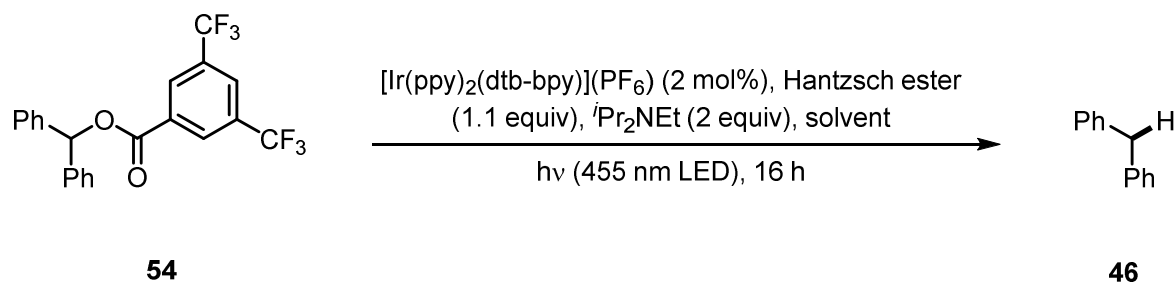
As can be judged from these results, [Ir(ppy)₂(dtb-bpy)]⁺ was again the better catalyst for the photochemical deoxygenation reaction of substituted benzoate esters **52** – **55**, as it was already in the case of phosphinate esters **50a** – **50d**. By far the best benzoate derivative was 3,5-bis(trifluoromethyl)benzoate **54**, it led to more than four times higher deoxygenation

yield after the same reaction time period. These experimental results are in agreement with the measured reduction potentials. The 3,5-bis(trifluoromethyl) substitution pattern resulted in the most favorable shift to a value of -1.73 V vs. SCE in DMF and also gave the best preparative results in photochemical reactions.

1.4 Optimization and control experiments

To optimize the reaction conditions, different solvent systems and reaction temperatures were screened (Table 3). Gratifyingly, toxic DMF could be replaced with more benign acetonitrile without appreciable decreasing the yield (entry 2). The reaction also proceeded in less polar solvents (entry 3 – 4), albeit yields were significantly lower. When the reaction was performed at ambient temperature **46** was only formed in 41% yield after 16 h of irradiation (entry 5). Control experiments suggest that the deoxygenation reaction of 3,5-bis(trifluoromethyl) benzoate **54** is indeed a photochemically mediated process (entry 6 – 7): when either the photocatalyst (entry 6) or the light source (entry 7) was omitted, significantly lower yields were obtained. Leaving out Hantzsch ester (entry 8) apparently did not impede the deoxygenation, while carrying out the reaction without Hünig's base lowered the yield (entry 9), nevertheless, **46** was still formed to a significant extent. These results suggest that Hantzsch ester is not necessary as the hydrogen source and / or reductive quencher.

Table 3. Solvent and temperature dependence of deoxygenation reactions with **54**.



Entry	Temperature [°C]	Solvent	Modifications	Yield [%] ^a
1	40	DMF	-	85
2	40	MeCN	-	80
3	40	DCM	-	20
4	40	THF	-	22
5	rt	DMF	-	41
6	40	MeCN	no photocatalyst	7
7	40	MeCN	no light	15
8	40	MeCN	no Hantzsch ester	91
9	40	MeCN	no Pr_2NEt	53

^aDetermined by GC-FID with dodecane internal standard.

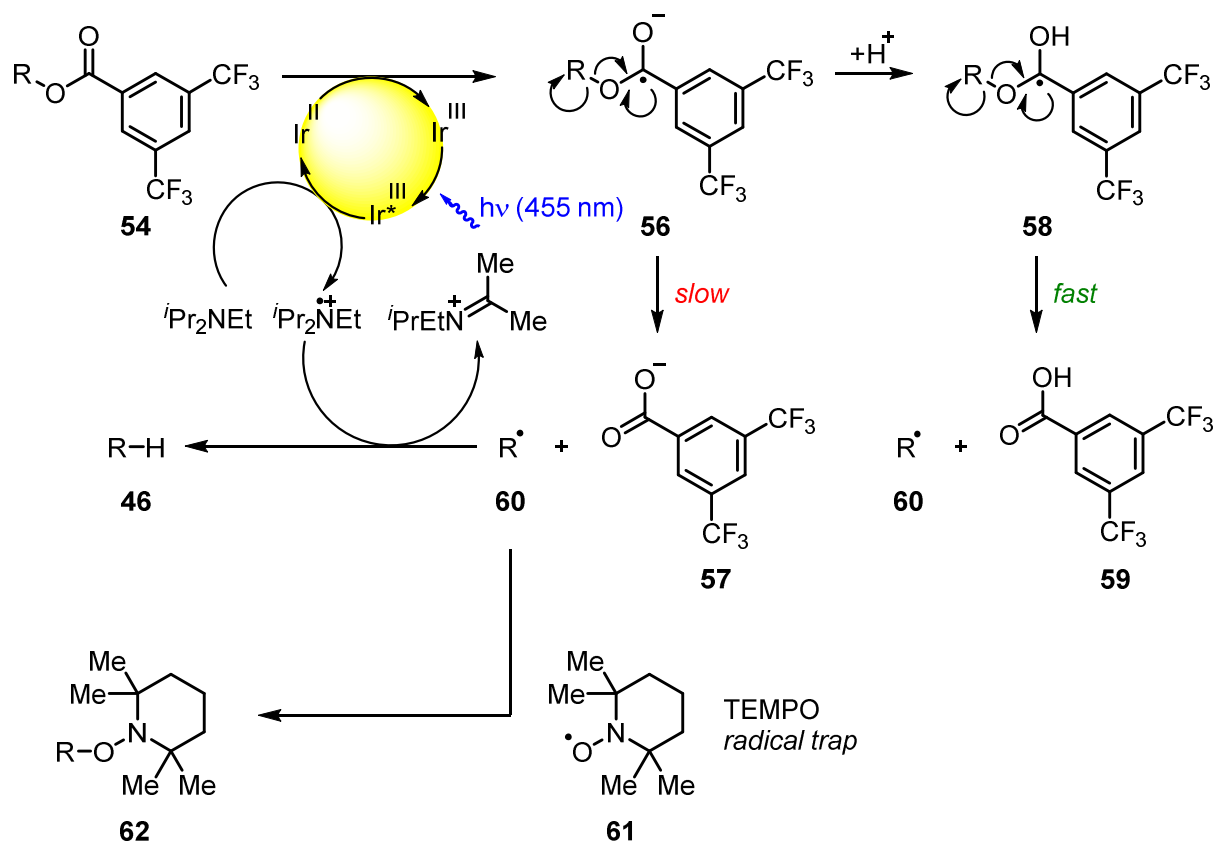
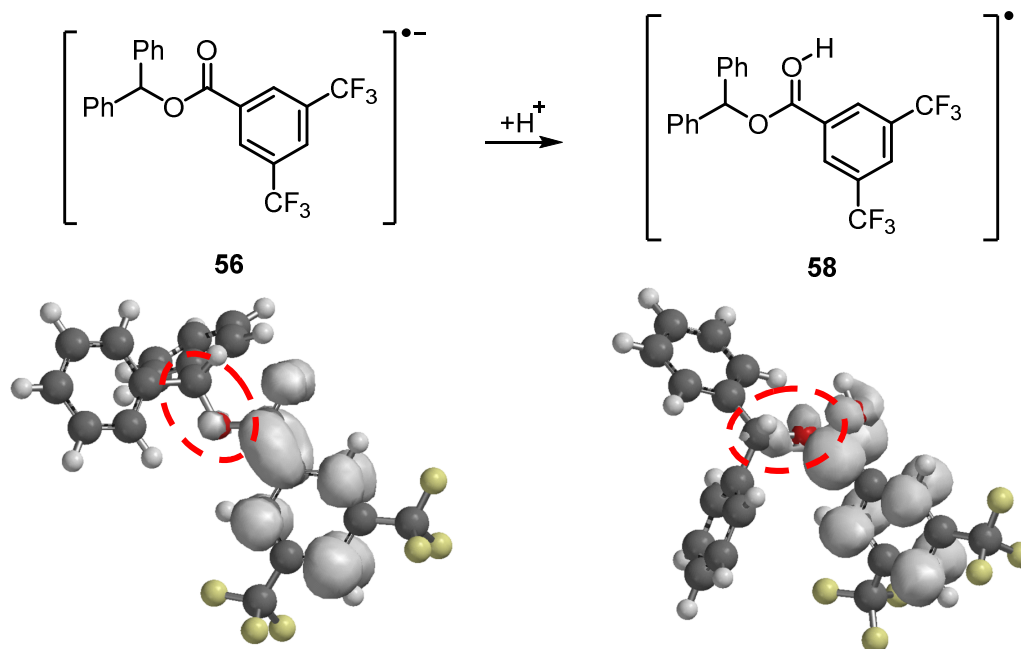
1.5 Mechanical aspects

It was assumed that the mechanism of the deoxygenation reaction involves an electron uptake of the ester moiety in **54** from the reductively quenched photocatalyst $[\text{Ir}]^{2+}$ to give the radical anion **56**, followed by C–O bond mesolysis to produce the carbon-centered radical **60** (Scheme 13). Subsequent hydrogen abstraction should then yield the deoxygenated product **46**. The presence of carbon-centered radical **60** was successfully proven by trapping experiments with TEMPO (2,2,6,6-tetramethylpiperidine 1-oxyl, **61**).^{**} A simple iridium-catalyzed hydrogenation mechanism as an alternative to a photochemical pathway of the reaction could be ruled out; even in the presence of 30 bar H_2 without irradiation under otherwise unchanged reaction conditions no deoxygenation of benzoate **54** could be observed.

Quantum mechanical calculations (B3LYP/6-31G*) for benzhydryl 3,5-bis(trifluoromethyl)benzoate (**54**) revealed that the electron density of the presumed transient radical anion **56** is mainly located at the phenyl moiety of the benzoate – and not in the desired anti-bonding $\sigma^*(\text{C}–\text{O})$ (Scheme 14).^{††} Protonation of the radical anion would lead to neutral radical species **58**, which in the calculations reflects in a shift of electron density towards the to-be-cleaved C–O bond (circled in red). Therefore, a protonation of **56** to **58** would presumably facilitate the deoxygenation step and speed up the overall reaction.

^{**} **62** (R = Ph_2CH) was detected by HRMS when the photochemical deoxygenation reaction was carried out in the presence of 0.9 equiv TEMPO (**61**).

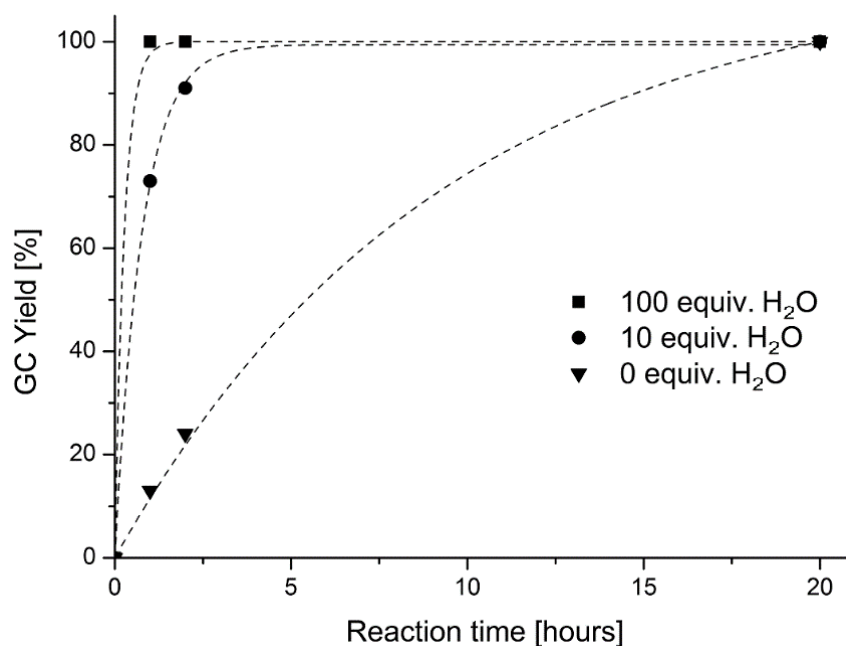
^{††} Calculations were performed by Dr. Peter Kreitmeier.

Scheme 13. Proposed reaction mechanism with and without additional water.**Scheme 14.** Calculated spin densities of the radical anion 56 and its protonated species 58.

1.6 Influence of water

In experiment, such a protonation was envisioned to take place by the addition of the weak acid H_2O . Stronger acids might protonate Hünig's base, thereby limiting the availability of the free electron pair and reducing its propensity to act as sacrificial electron donor. To investigate the proposed rate acceleration, the standard reaction conditions were modified through addition of different amounts of water to the reaction mixture (Figure 4). The deoxygenation without addition of water was relatively slow, 13% of product **46** was observed after a reaction time of one hour. However, when ten equivalents of water were added, already 73% of **46** and with 100 equivalents water full product formation was accomplished after the same reaction time. After irradiation for 20 h full product formation took place in all cases. Therefore, it can be concluded that the addition of water as a weak acid did indeed increase the reaction rate. These experimental results fully back the previously conducted calculations.

Figure 4. Influence of water on the photochemical deoxygenation of **54**.



1.7 Substrate scope

With the newly optimized reaction conditions at hand, different benzylic alcohol derivatives **54** were investigated (Table 4). Uniformly very good isolated yields after short reaction times were achieved in case of dibenzylic alcohol derivatives. Steric bulk (entry 2), as well as a broad range of functional groups with different electronic properties, i.e. an electron donating *p*-methoxy substituent (entry 3), electron withdrawing *p*-nitro substituent (entry 4), ester group containing system (entry 5), chlorinated derivative (entry 6), and electron deficient heteroaromatic system (entry 7), were tolerated well. The corresponding deoxygenated products were obtained in analytical pure form in high yields after filtration through a short plug of silica gel. Noteworthy, no reduction of reducible groups such as nitro (entry 4) or chloro (entry 5) was observed. Moving to monobenzyl alcohols, i.e. replacement of one aromatic group with an alkyl chain, resulted in prolonged reaction times but nevertheless acceptable yields of the deoxygenated products (entry 8 – 9). With α -carbonyl substituted benzylic alcohol derivatives irradiation times could be reduced again and defunctionalized materials were isolated in moderated to good yields (entry 10 – 11). Gratifyingly, the precious activation group bis(trifluoromethyl) benzoic acid **59** could easily be recovered (> 90%) in an acid-base extraction step after the photochemical reaction.

Table 4. Preparative deoxygenation reactions with 3,5-bis(trifluoromethyl)benzoate activation.

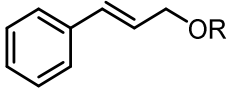
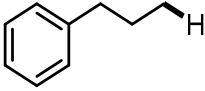
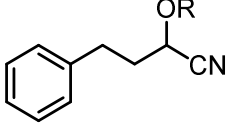
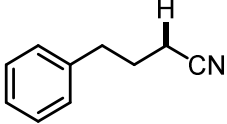
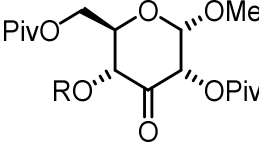
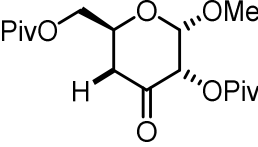
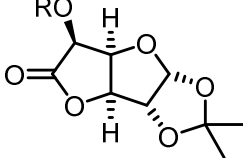
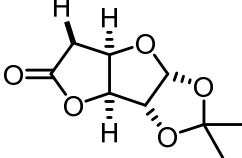
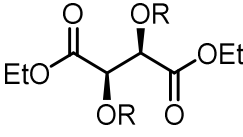
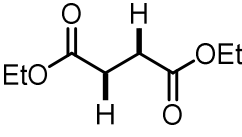
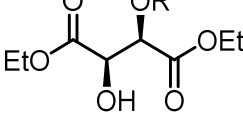
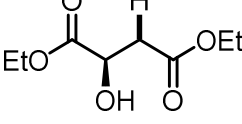
Entry	Substrate	Product	Yield 46 [%] ^a
1			95
2			86
3			87

4		54d		46d	91
5		54e		46e	93
6		54f		46f	92
7		54g		46g	86
8		54h		46h	66 ^{b,c}
9		54i		46i	79 ^c
10		54j		46j	83
11		54k		46k	67

R = Bz(CF₃)₂. ^aIsolated yields of reactions conducted at a 0.2 – 1.0 mmol scale. ^bDetermined by GC-FID with dodecane as internal standard. ^c16 h reaction time.

In addition to benzylic alcohol derivatives, also allylic hydroxyl functions could be deoxygenated with this method (Table 5, entry 1). The deoxygenation product in this case was however a mixture of isomeric β -methylstyrenes and allyl benzene. To obtain a single product, a hydrogenation was performed *in situ* with Pd/C and H₂ to give propylbenzene (**64a**) in quantitative yield. Also 3,5-bis(trifluoromethyl)benzoates of other non-benzylic, α -cyanhydrin (**63b**) and α -hydroxycarbonyl (**63c** – **63f**) compounds turned out to be amenable for the photochemical deoxygenation process.

Table 5. Preparative deoxygenation reactions of non-benzylic benzoates.

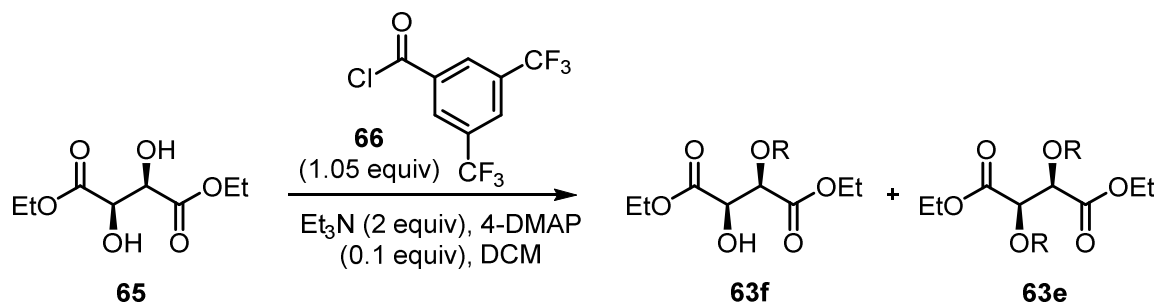
Entry	Substrate	Product	Yield [%] ^a
1			99 ^b
2			86
3			79
4			14 ^c
5			69 ^{d,e}
6			99

R = Bz(CF₃)₂. ^aConditions see Table 4. ^bPd/C and 1 atm H₂ was added after the photochemical deoxygenation; yield determined by GC-FID with an internal standard. ^cParent compound was prone to hydrolysis under reaction conditions. ^d16 h reaction time. ^e¹H-NMR yield.

1.8 Selective monobenzoylation

Especially interesting from a preparative point of view, the mono-deoxygenation of activated diethyl tartrate **63f** to diethyl maleate **64f** could be achieved in excellent yields (Table 5, entry 6). However, to achieve such a mono-deoxygenation a selective mono-benzoylation is necessary. The preparation of mono-benzoate **63f** was not straightforward (Table 6). Reaction of (+)-DET (**65**) with 1.05 equivalents of 3,5-bis(trifluoromethyl)benzoyl chloride (**66**), as were the standard preparation conditions for all prior benzoates, gave only 5% of mono-benzoate **63f** alongside with 45% of bis-benzoate **63e** (entry 1). Modification of the reaction temperature gave almost identical results (entry 2 – 4). Omission of 4-DMAP on the other hand and performance of the reaction at -78 °C was found to give an improved ratio of mono-benzoylation over bis-benzoylation (entry 5 to 8).

Table 6. Benzoylation experiments of (+)-DET (**69**) towards a selective mono-activation.



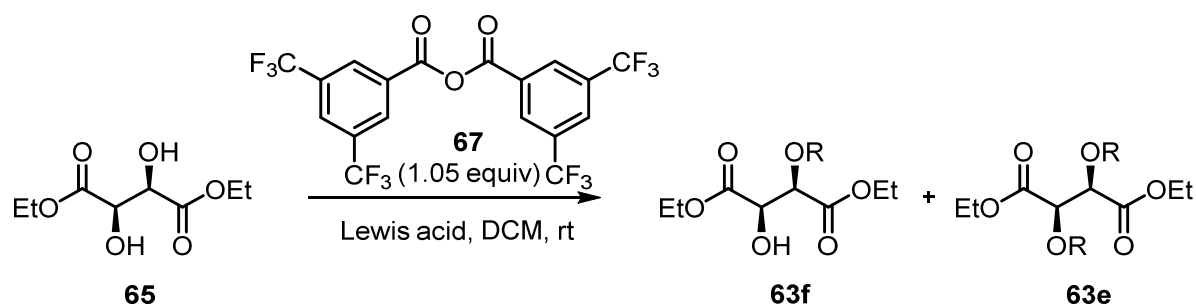
Entry	Scale	Conditions ^a	Monoester 63f : Diester 63e ^b	
1	5 mmol	66 (neat), 0 °C	5% ^c	45% ^c
2	0.5 mmol	66 (0.1 M), -20 °C	17 : 83	
3	0.5 mmol	66 (0.1 M), -40 °C	14 : 86	
4	0.5 mmol	66 (0.1 M), -78 °C	14 : 86	
5	0.5 mmol	66 (0.1 M), rt, no 4-DMAP	38 : 62	
6	0.5 mmol	66 (0.1 M), 0 °C, no 4-DMAP	44 : 56	
7	0.5 mmol	66 (0.1 M), -40 °C, no 4-DMAP	42 : 58	
8	0.5 mmol	66 (0.1 M), -78 °C, no 4-DMAP	47 : 53	

R = Bz(CF₃)₂. ^aTo a solution of **65** (0.1 M) a solution of acid chloride **66** was added dropwise at the indicated temperature and concentration in DCM. ^bDetermined by ¹H-NMR integration. ^cIsolated yield.

Despite the efforts to increase the amount of mono-benzoylation product **63f**, the selectivity remained low with acid chloride **66** as acylation agent. As a less active benzoylation reagent could potentially improve the selectivity, 3,5-bis(trifluoromethyl)benzoic

acid anhydride (**67**) was synthesized for this purpose. Using anhydride **67** without Lewis acid additive, the reaction already favored mono-benzoylation product **63f** (Table 7, entry 1). The presence of a Lewis acid catalyst increased the selectivity of the benzoylation tremendously in favor of **63f** in certain cases. YbCl₃ increased the reaction speed as well as the selectivity (entry 2).^{29,30} While several other, much cheaper, Lewis acids even slowed down the reaction (entry 3 to 7), CuCl₂ again led to high selectivity and even higher conversions (entry 8) compared to YbCl₃. The influence of the most promising Lewis acids YbCl₃ and CuCl₂ was then investigated in more detail. Lowering the amount of YbCl₃ led to longer reaction times, slightly higher conversion rates, and diminished selectivities (entry 9 and 10) while in contrast lowering the amount of CuCl₂ led to decreased conversions but increased selectivities (entry 11). Due to the considerably lower cost of CuCl₂ in comparison to YbCl₃, CuCl₂ was ultimately used for a preparation in a larger scale (entry 12). Surprisingly, the large scale reaction took much longer than the reaction on small scale to reach comparable conversions. The exact nature of this effect is unknown but might be related to the inhomogeneous nature of the reaction (CuCl₂ is not fully soluble in DCM at a loading of 10 mol%). Nevertheless, practical reaction conditions for the synthesis of **63f** were found.

Table 7. Benzoylation of (+)-DET (**65**) with benzoic acid anhydride **67** under Lewis acid catalysis.



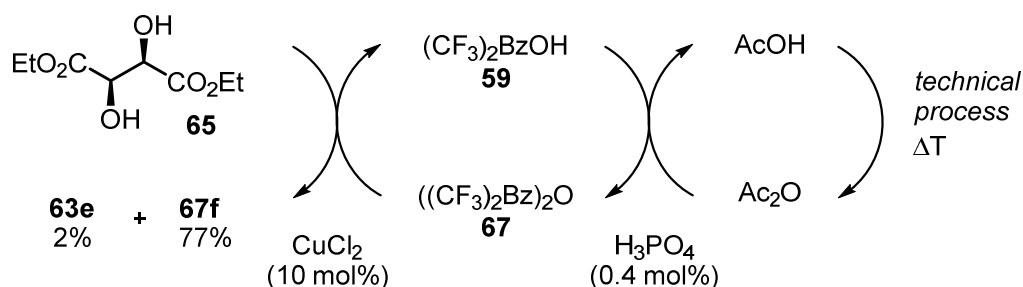
Entry	Lewis acid	Time	Conversion ^a	Monoester 63f : Diester 63e ^b
1	-	68 h	66%	71 : 39
2	YbCl ₃ (10 mol%)	20 h	62%	>95 : 5
3	FeCl ₃ (10 mol%)	2 h	<5%	-
4	ZnCl ₂ (10 mol%)	2 h	<5%	-
5	AlCl ₃ (10 mol%)	2 h	<5%	-
6	TiCl ₄ (10 mol%)	2 h	<5%	-
7	NiCl ₂ (10 mol%)	2 h	<5%	-
8	CuCl ₂ (10 mol%)	68 h	82%	94 : 6 ^b
9	YbCl ₃ (1 mol%)	68 h	80%	93 : 7 ^b
10	YbCl ₃ (0.1 mol%)	140 h	75%	83 : 17 ^b

11	CuCl ₂ (1 mol%)	68 h	56%	>95 : 5 ^b	
12	CuCl ₂ (10 mol%) ^c	7d ^d	81%	77% ^e	2% ^e

R = Bz(CF₃)₂. ^aConversion of **65** on a 0.5 mmol scale. ^b¹H-NMR integration. ^c6 mmol scale. ^dAdditional 7 d under reflux. ^eIsolated yield.

Anhydride **67** was successfully generated from acid **59** by treatment with acetic anhydride on a scale up to 150 g (Scheme 15). Since acetic anhydride can industrially be produced by thermal dehydration of acetic acid,² the overall sequence to the benzoylated starting material **63f** does not require any type of activation reagents such as thionyl chloride or DCC which are often used for ester formation, but ultimately only requires energy in form of heat. After the photochemical deoxygenation, 3,5-bis(trifluoro)benzoic acid **59** is formed, which can be easily recovered in high yield, from which anhydride **67** can be regenerated as described above.

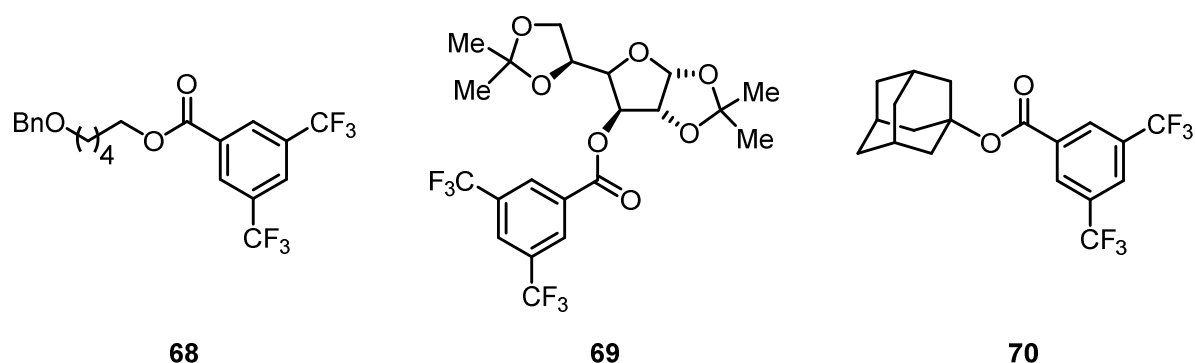
Scheme 15. Net activation agent free preparation of 3,5-bis(trifluoromethyl)benzoates.



1.9 Further expansion of the substrate scope

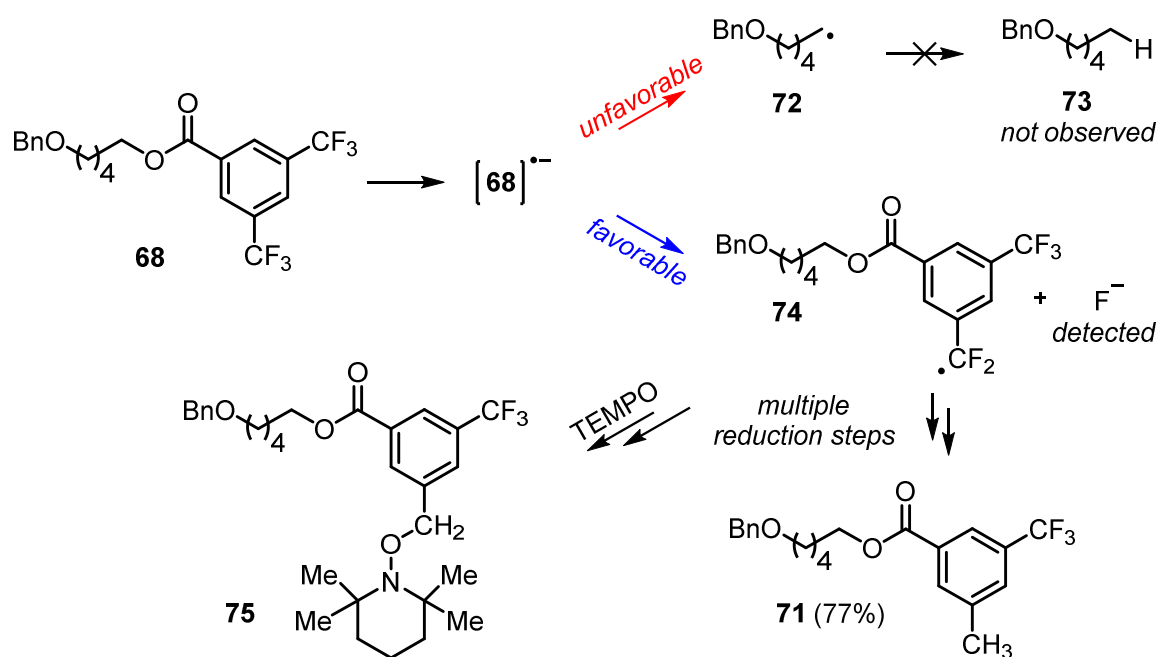
As mentioned before, attempts to deoxygenate simple alkyl substituted alcohols (primary, secondary, and tertiary) under the optimized reaction conditions were not feasible (Figure 5).

Figure 5. Unactivated primary, secondary, and tertiary 3,5-bis(trifluoromethyl)benzoates **68** – **70**.



For example, unactivated 3,5-bis(trifluoromethyl)benzoate **68** gave product **71** where one trifluoromethyl group was completely reduced to a methyl group; no deoxygenated material was observed (Scheme 16). Apparently, electron transfer to the benzoate group still occurs, however, the subsequent C–O bond cleavage does not take place, presumably due to the energetically very unfavorable primary radical intermediate **72** that would result from the desired cleavage of the C–O bond. Instead, carbon – fluorine bond scission, leading to a benzylic radical **74**, is the preferred pathway.

Scheme 16. Reduction of the 3,5-bis(trifluoromethyl)benzoate moiety in case of unactivated **68**.

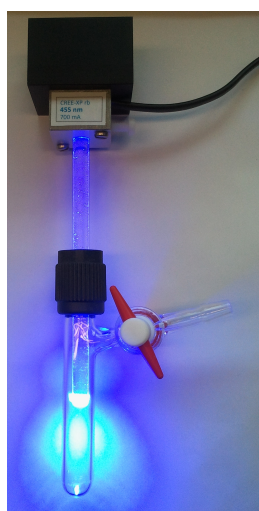
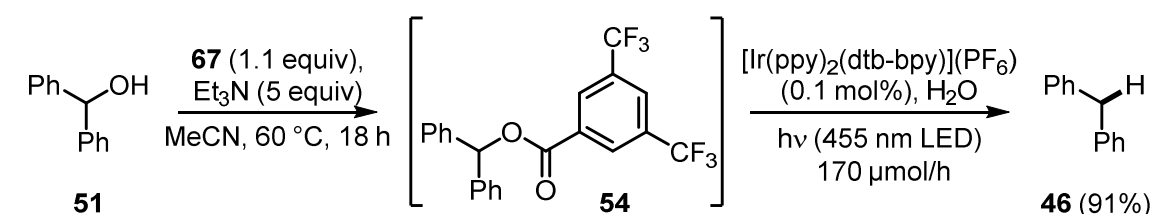


To unambiguously rule out that the methyl group in **71** originates from a substitution process with acetonitrile as the methyl group source, the reaction was carried out in deuterated acetonitrile. No deuterium incorporation was observed which proved that acetonitrile is not responsible for the presence of the methyl group in **71**. Performing the reaction in the presence of stable radical TEMPO (**61**) gave, besides reduction product **71**, adduct **75** which suggests that the methyl group originates from a sequential reduction of the C–F bonds *via* a radical pathway.³¹ In addition, a test for fluoride with $[\text{Fe}(\text{SCN})(\text{H}_2\text{O})_5]^{2+}$ in an evaporated aliquot of the irradiated reaction mixture was positive. Increasing the amount of Hünig's base, which acts as sacrificial electron donor in the initial reduction step of **68**, led to full conversion of the starting material and gave reduction product **71** as the only reaction product in 77% isolated yield. A deoxygenation of hydroxyl functions in unactivated positions therefore appears to be impossible with this method: the crucial carbon-centered radical **72** is not formed in favor of the benzylic radical **74** if no neighboring group (*e.g.* aryl, carbonyl, cyanyl, allyl) is present that could stabilize radical **72**. The defluorination reaction equals the destruction of the activating group. Defluorination product **71** is incapable to be reduced any further under the photochemical reaction conditions. No conversion was observed when isolated **71** was resubjected to the reaction conditions, even after visible light irradiation for seven days.

1.10 *In situ* benzoylation and up-scaling

For larger scale applications it would be desirable to install the activating benzoate group *in situ* rather than in a foregoing reaction step. Also, considering its high price the employment of smaller amounts of iridium-based catalyst would be desirable. Finally, replacing costly *N,N*-diisopropylethylamine with low priced triethylamine can help to minimize the occurring costs. Taking **51** as model substrate, it could be shown that the overall deoxygenation process can be optimized and simplified in this regard by the *in situ* formation of the 3,5-bis(trifluoromethyl)benzoate **54** in MeCN. Acetonitrile is also the ideal solvent for the following photochemical reaction (Scheme 17). Et₃N was used, both as auxiliary base for the benzoylation reaction and also as sacrificial electron donor in the second step. To increase the overall efficiency of photochemical transformations microreactors have been employed earlier in photoredox chemistry.^{32–34} Based on the higher surface-to-volume ratio in the microreactor and improved miscibility, the continuous flow mode typically offers shorter reaction times, higher yields, lower catalyst loadings, and makes upscaling trivial. Full starting material conversion was achieved using only 0.1 mol% of photocatalyst at a flowrate corresponding to a turnover of 170 $\mu\text{mol/h}$ **51**. This sequence yielded 91% of isolated deoxygenation product **46**.

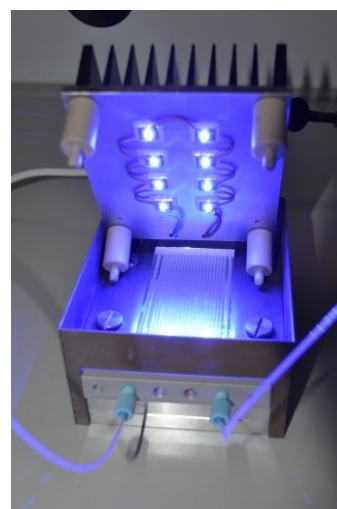
Scheme 17. Optimized conditions for larger scale applications. Comparison with batch conditions.



- **seperate** benzoylation **step**
- **DCM** as solvent for benzoylation
- **costly** **ⁱPr₂NEt** as electron donor
- **high catalyst loading** (2.0 mol%)
- **bad scalability**

Batch Process vs. Continous Flow

- ***in situ*** benzoylation **step**
- **MeCN** as sole solvent
- **cheap** **Et₃N** as electron donor
- **low catalyst loading** (0.1 mol%)
- **ideal scalability**



1.11 Conclusion

In summary, a protocol for the deoxygenation of benzylic alcohols, allylic, α -hydroxycarbonyl, and α -cyanohydrine compounds under visible light photocatalysis was developed using 3,5-bis(trifluoromethyl)benzoic anhydride (**67**) for alcohol activation. 3,5-bis(trifluoromethyl)benzoic acid (**59**) could be recycled and reactivated under redox neutral conditions. Moreover, the *in situ* activation of alcohols with this auxiliary was possible. A continuous process for the deoxygenation of alcohols was developed that ultimately only requires heat, triethylamine as a sacrificial electron donor, and visible light. Despite the relatively expensive activation of alcohols as 3,5-bis(trifluoromethyl)benzoic acid esters, the deoxygenation protocol described here could also become attractive for large-scale applications.

2 Deoxygenative Cyclizations

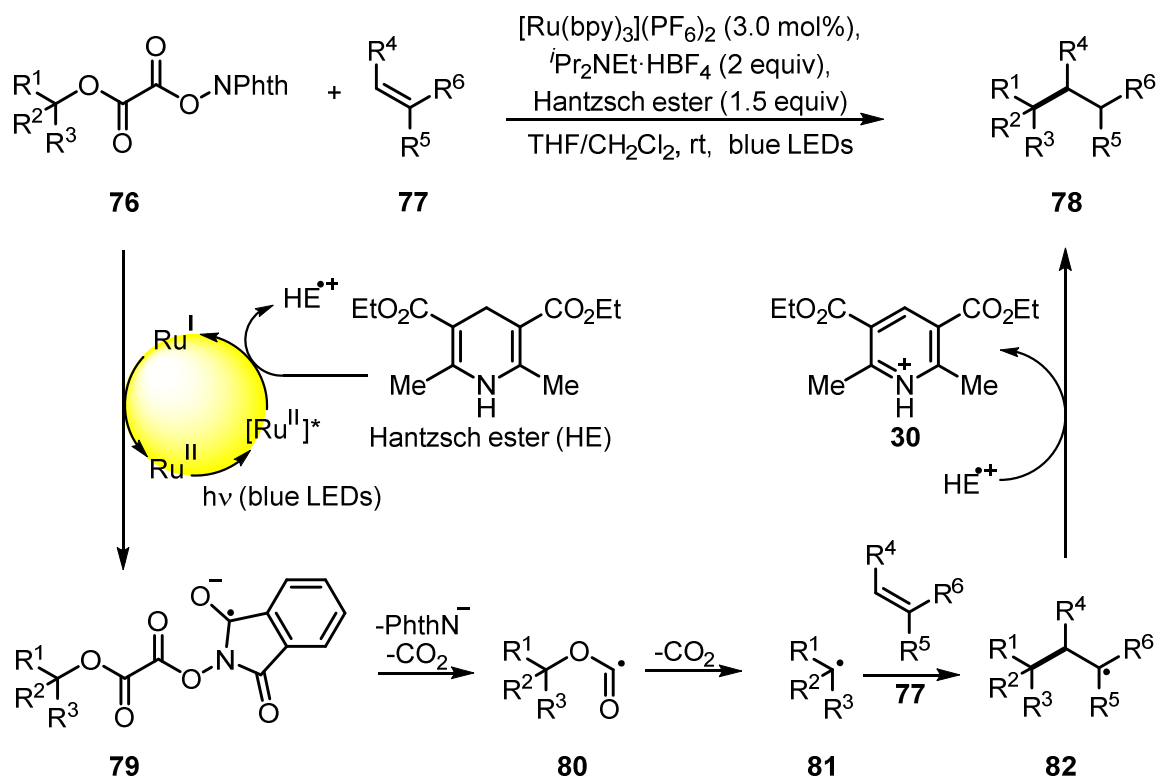
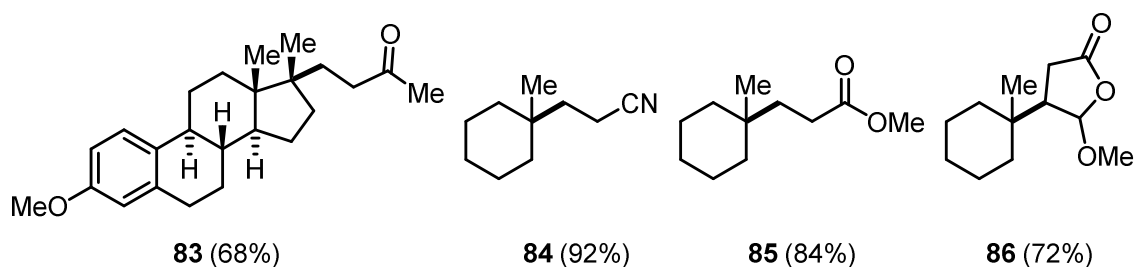
2.1 Introduction

Not only is the simple defunctionalization of hydroxyl compounds *via* carbon-center radicals of synthetic interest but also their direct transformation into another structural unit like new carbon – carbon or carbon – heteroatom bonds.³⁵ This can be achieved by trapping the radicals not with a hydrogen atom donor (*vide supra*) but by using an alternative trapping agent.

When carbon-centered radicals for further functionalization are to be generated from hydroxyl functionalities they are typically formed under Barton-McCombie-like conditions.^{36–43} Recently, Overman *et al.* described a method to produce tertiary carbon-centered radicals **81** from *N*-phthalimidoyl oxalates **76** under visible light irradiation (Scheme 18).⁴⁴ Excited state ruthenium photocatalyst [Ru²⁺]^{*} is reductively quenched by Hantzsch ester (HE). The so-formed Ru⁺ reduces *N*-phthalimidoyl oxalates **7**. Upon N–O bond mesolysis and extrusion of carbon dioxide, the acyl radical **80** remains. Another carbon dioxide ejection then forms a nucleophilic, carbon-centered radical **81** which can be trapped by electron-deficient alkene **77** to form quaternary carbon **82**. Abstraction of a H-atom finally produces target molecule **78**.

This convenient method for the direct construction of quaternary carbon centers exhibits a high diastereoselectivity (> 20:1). Alkene **77** generally attacks from the less hindered side as demonstrated in esterone derivative **83** (Figure 6). This product is also an example for the formation of vicinal quaternary centers. Not only could methyl vinylketone be used as coupling partner but also a variety of other electron-deficient alkenes proved to give quaternary carbon products **84** to **86** in good yield.

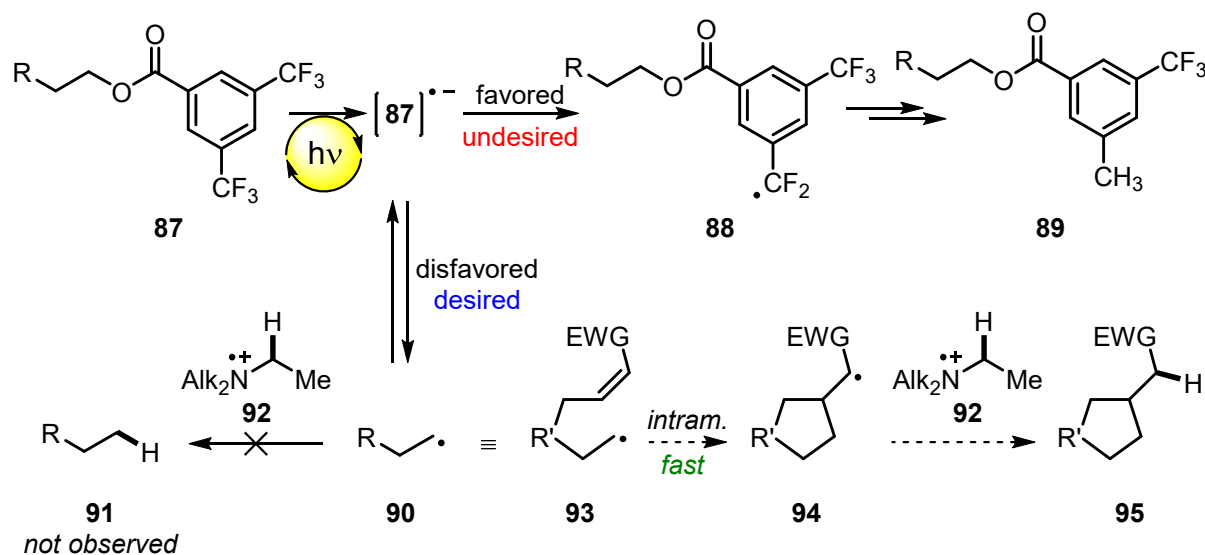
While this technique gives rise to quaternary carbons through C–O bond cleavage, methods to form secondary and tertiary carbon centers through photochemical deoxygenation of a C–O bond are unknown. Such a method would be highly desirable as natural products typically exhibit multiple carbon–oxygen bonds that could be amenable as a synthetic handle to introduce new groups. Visible light photoredox catalysis is often superior to classic chemical transformations (*vide supra*), therefore the formation of secondary and tertiary carbon centers through photochemistry will be investigated in this section.

Scheme 18. Construction of quaternary carbons from tertiary alcohols as invented by Overman *et al.***Figure 6.** Substrate scope of deoxygenations with *N*-phthalimidoyl oxalates.

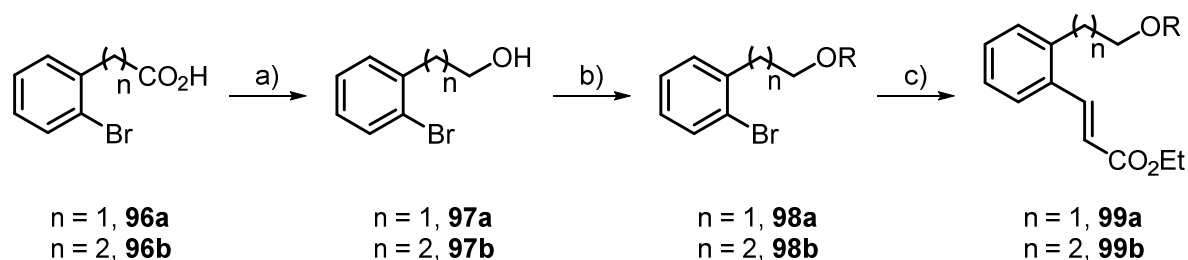
2.2 Preliminary studies with unactivated benzoates

In the previous section of this work it was shown that the substrate scope of visible light mediated deoxygenation *via* 3,5-bis(trifluoromethyl)benzoate activation is limited by the stability of the intermediary carbon-centered radical **90** (Scheme 19). When no radical-stabilizing group was present in the α -position of the carbon-centered radical, also no formation of deoxygenation product **91** was observable (*vide supra*). In sharp contrast to those findings, Saito *et al.* were very well able to deoxygenate even unstabilized alcohols *via* 3-(trifluoromethyl)benzoates using UV light and an organic photosensitizer.¹⁰ Therefore it was speculated that the potentially occurring carbon-centered radical **90** could be trapped in a fast, intramolecular cyclization, as the competing intermolecular hydrogen abstraction from the sacrificial amine radical cation **92** might be too slow and thus an electron back transfer to the catalyst might occur. Cyclized radical intermediate, *e.g.* **94** from an intramolecular 5-*exo-trig* cyclization, could in theory be stabilized by a neighboring electron-withdrawn group and eventually be trapped by a hydrogen atom donor like **92**.

Scheme 19. Strategy to bypass the necessary radical stabilization.

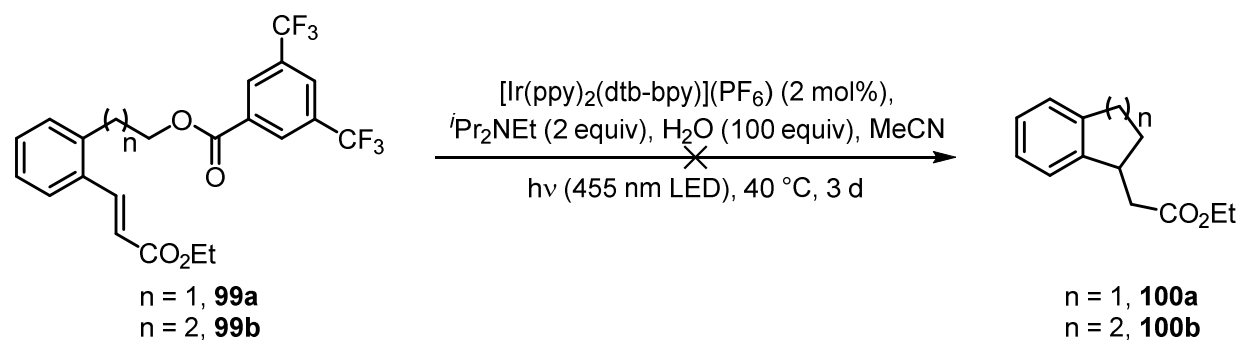


Suitable precursors for a 5-*exo-trig* (**99a**) and a 6-*exo-trig* (**99b**) cyclization were prepared starting from commercial carboxylic acids **96** (Scheme 19). Reduction with lithium aluminum hydride gave alcohols **97** in reasonable yields. After introduction of the activation group in excellent yields, Heck coupling conditions were employed to give α,β -unsaturated esters **99**.

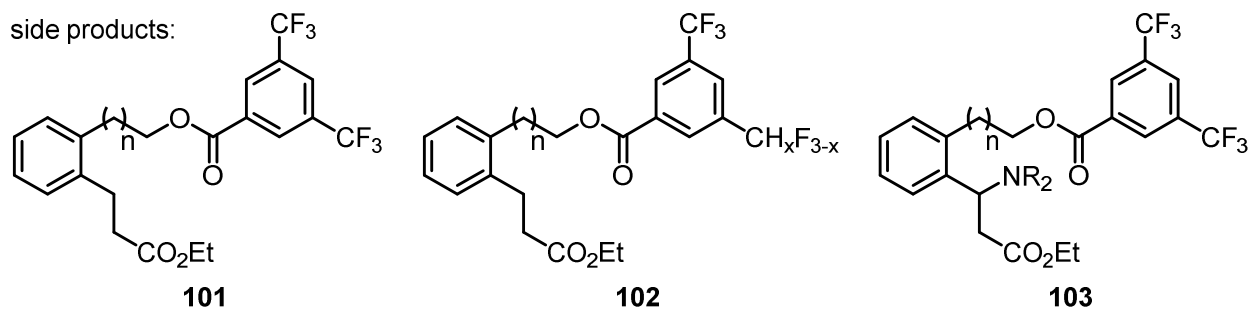
Scheme 20. Preparation of suitable cyclization precursors **99a** and **99b**.

R = Bz(CF₃)₂. Reagents and conditions: a) LAH, THF, rt, 1 h, 61 – 62%; b) (CF₃)₂BzCl, Et₃N, DCM, 0 °C to rt, 2 h, 90 – 99%; c) ethyl acrylate, Pd(OAc)₂, PPh₃, Et₃N, toluene, 100 °C, 16 h, 42 – 44%.

The substrates for intramolecular cyclization **99a** and **99b** were subjected to the previously optimized deoxygenation conditions, however, no formation of cyclized **100a** and **100b** could be observed (Scheme 21). Instead, an inseparable mixture of different products was obtained: reduction of the double bond (**101**),⁴⁵ (partial) defluorination (**102**), and Michael-type addition of amine to the α,β -unsaturated esters (**103**), as well as combinations thereof were formed as judged by mass spectrometry analysis. None of those side products would be formed through carbon-centered radical **90**. A potential broadening of the substrate scope of the deoxygenation method through an intramolecular cyclization possibility of carbon-centered radical **85** was therefore ruled out.

Scheme 21. Attempted deoxygenative cyclization of **99a** and **99b**.

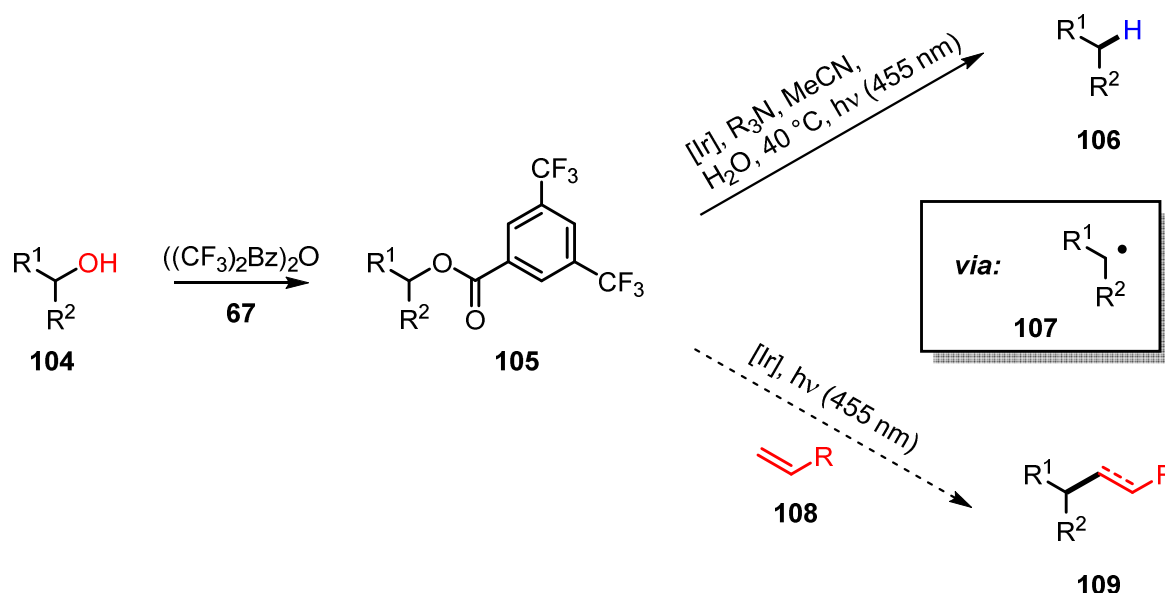
side products:



2.3 Preliminary studies with activated benzoates

As no carbon-centered radicals could be generated from unactivated benzoates, all further investigations were conducted with benzoates in activated positions. It was proven by TEMPO trapping experiments that the photochemical deoxygenation of activated 3,5-bis(trifluoromethyl)benzoates **105** indeed proceeds through a radical intermediate (**107**, Scheme 22). In the presence of an electronically suitable alkene **108**, radical trapping in coherence with the formation of a new C–C bond could theoretically occur. Depending on the exact reaction conditions, this could presumably lead to either reduction or retention of the double bond (**109**).

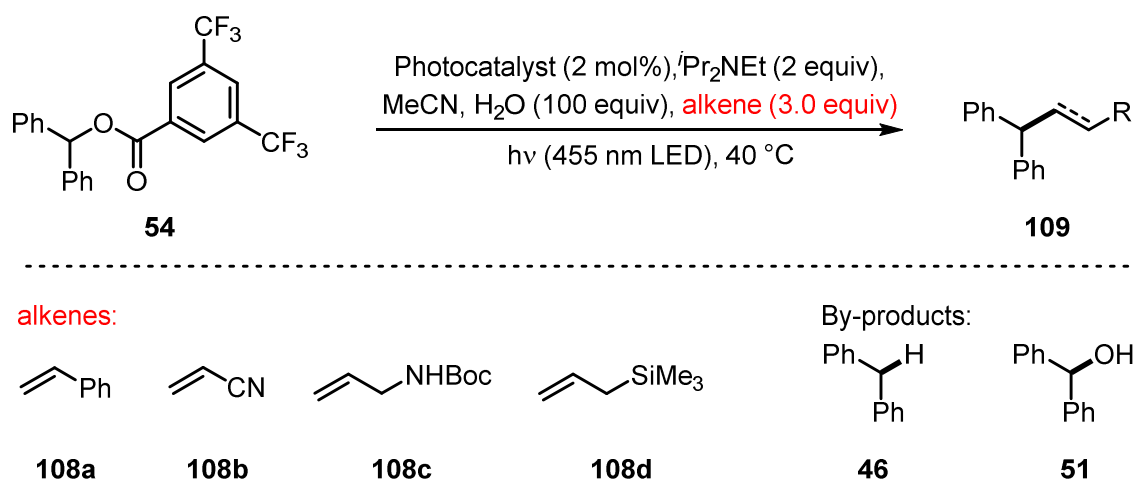
Scheme 22. Intermolecular trapping of intermediary carbon-centered radical **107**.



Utilization of the previously optimized deoxygenation conditions in the presence of an excess of a variety of electronically distinct alkenes gave no trapping product; only defunctionalative deoxygenation was observed (Table 8, entry 1). The hydrogen abstraction process of the transient radical is presumably too fast. To slow down the reaction, water was omitted in the following experiments (entry 2). It was assumed that a slower reaction rate would facilitate the trapping by an alkene. Unfortunately, the only observable effect was that the defunctionalization product was formed significantly slower, which is in agreement with earlier observations. This outcome is also backed by the proposed reaction mechanism: as addition of the weak Brønsted acid water only accelerates the fragmentation of the intermediary radical anion and has no effect on the hydrogen atom abstraction step, no difference in the fate of the carbon-centered radical would be expected. To prevent hydrogen abstraction from the

radical cation of the sacrificial amine further experiments were set up without *N,N*-diisopropylethylamine. Consequently, a simultaneous switch of photocatalyst was required. While reductively quenched $[\text{Ir}(\text{ppy})_2(\text{dtb-bpy})]^+$ was powerful enough ($E_{1/2}(\text{Ir}^{3+}/\text{Ir}^{2+}) = -1.51 \text{ V}$) to inject an electron in **54**, without reductive quenching the excited state photocatalyst is considerably less reducing ($E_{1/2}(\text{Ir}^{4+}/\text{Ir}^{3+*}) = -0.96 \text{ V}$) and thus not able to trigger conversion of **54**. This is different for *fac*- $\text{Ir}(\text{ppy})_3$, even in the absence of a reductive quenching agent its excited state is highly reducing ($E_{1/2}(\text{Ir}^{4+}/\text{Ir}^{3+*}) = -1.73 \text{ V}$). In trapping experiments with the alkenes, *fac*- $\text{Ir}(\text{ppy})_3$ in the absence of water and amine, however, was not capable to generate the coupling product **109** (entry 3). Addition of water to increase the fragmentation rate of the intermediary radical anion was unsuccessful, again no coupling product **109** was isolable (entry 4). These results led to the conclusion that no intermolecular trapping is possible with the examined substrates.

Table 8. Intermolecular radical trapping experiments.



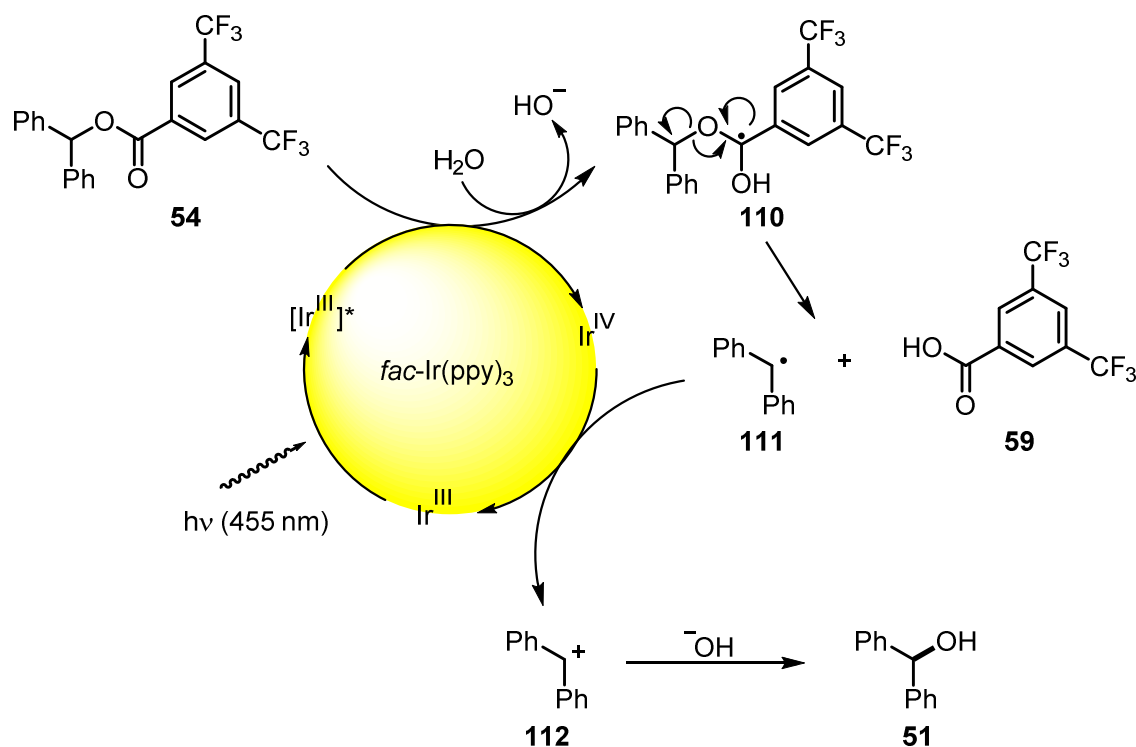
Entry	Alkene	Photocatalyst	Conditions	Yield 109 [%] ^a
1	108a–d	$[\text{Ir}(\text{ppy})_2(\text{dtb-bpy})]\text{PF}_6$	standard	0% ^b
2	108a–d	$[\text{Ir}(\text{ppy})_2(\text{dtb-bpy})]\text{PF}_6$	w/o H_2O	0% ^b
3	108a–d	<i>fac</i> - $\text{Ir}(\text{ppy})_3$	w/o iPr_2NEt , w/o H_2O	0% ^c
4	108a–d	<i>fac</i> - $\text{Ir}(\text{ppy})_3$	w/o iPr_2NEt	0% ^d

^aIsolated yield. ^bFormation of deoxygenation product **46**. ^cNo conversion of starting material **54**. ^dFormation of photo-hydrolyzed material **51** instead.

Interestingly, the formation of diphenylmethanol (**51**) – the formal hydrolysis product of **54** – was observable when a combination of *fac*- $\text{Ir}(\text{ppy})_3$ and water was used (Table 8, entry 4). As the appearance of a hydrolysis product from a benzoate in reaction medium containing water might not seem interesting at first glance, it was however surprising as in all previous

experiments no hydrolysis product was detected. A simple hydrolysis mechanism with an aqueous base was therefore excluded as an explanation for the formation of **51**. Indeed, when the reaction was repeated exactly as before but in the dark, no hydrolysis product **51** was observed. Diphenylmethanol (**51**) is therefore the product of a photo-hydrolysis of **54** (Scheme 23). After formation of carbon-centered radical **111** by reduction of **54** with excited state *fac*-Ir(ppy)₃, the catalytic cycle needs to be closed. As no other electron donor is present, the only reducible species is **111** itself. The resulting carbocation **112** then combines with a hydroxyl ion to give photo-hydrolysis product **51**.

Scheme 23. Mechanism explaining the formation of photo-hydrolysis product **51**.

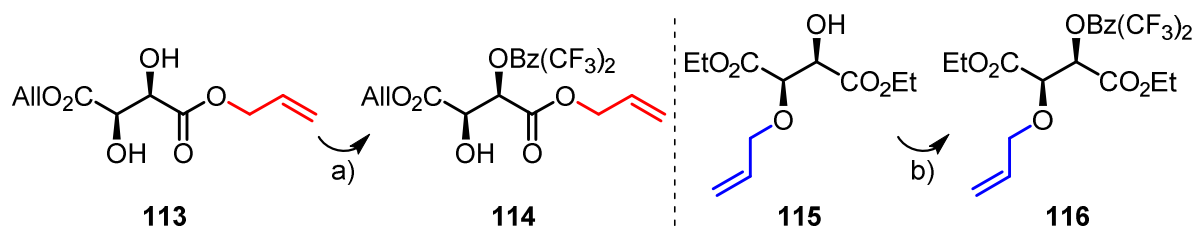


Conducting this reaction with other nucleophiles instead of water could lead to a mild substitution or alkylation protocol. Also, employment of 3,5-bis(trifluoromethyl)benzoic acid **59** as photolabile protection group is conceivable. Photodeprotection would only occur in activated positions as otherwise formation of key intermediate **111** and also **112** would be suppressed.

2.4 Intramolecular trapping

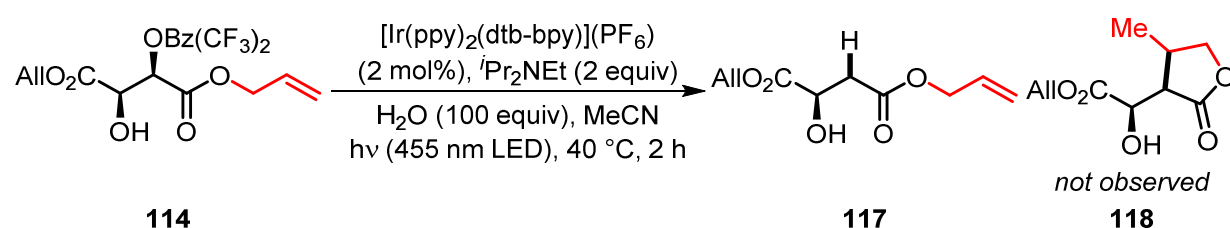
As intermolecular trapping attempts remained fruitless, the next logical step was the investigation of intramolecular processes. For this purpose two different tartrate derivatives were synthesized, as tartrates displayed excellent behavior in earlier deoxygenation reaction and can easily be modified with alkene functionalities (Scheme 24).

Scheme 24. Synthesis of modified tartrate derivatives for deoxygenative cyclizations **114** and **116**.



Reagents and conditions: a) $((\text{CF}_3)_2\text{Bz})_2\text{O}$ (1.1 equiv), CuCl_2 (10 mol%), Pr_2NEt (2.0 equiv), DCM, 0 °C to rt, on, 72%; b) $((\text{CF}_3)_2\text{Bz})_2\text{O}$ (1.1 equiv), Pr_2NEt (2.0 equiv), DCM, rt, 1 h, 53%.

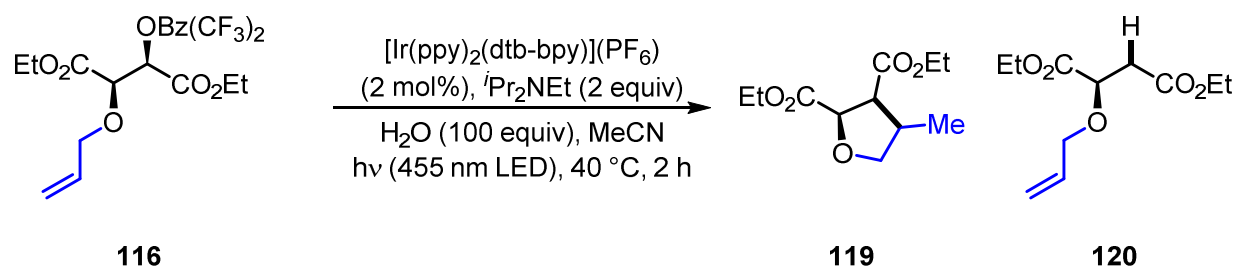
Under the previously optimized deoxygenation conditions no cyclization of **114** was evident (Table 9, entry 1), only defunctionalative deoxygenation product **117** was formed in reasonable yield. Omission of water only slowed the defunctionalization reaction but again no formation of **118** was observed (entry 2). Additionally, a switch of photocatalyst did not lead to a positive result (entry 3 and 4). A carbon-centered radical is clearly formed as deoxygenation occurs, yet no tendency towards an intramolecular cyclization is evident. Presumably inherent (*Z*)-ester geometry inhibits a potential cyclization.⁴⁶

Table 9. Attempts to achieve intramolecular cyclization of **114**.

Entry	Catalyst	Additive(s)	Time	Yield 117 [%] ^a
1	$[\text{Ir(ppy)}_2(\text{dtb-bpy})]\text{PF}_6$	Pr_2NEt (2 equiv) H_2O (100 equiv)	2 h	54
2	$[\text{Ir(ppy)}_2(\text{dtb-bpy})]\text{PF}_6$	Pr_2NEt (2 equiv) -	2 h	- ^b
3	<i>fac</i> - Ir(ppy)_3	Pr_2NEt (2 equiv) -	2 h	27
4	<i>fac</i> - Ir(ppy)_3	- H_2O (100 equiv)	2 h	- ^c

^aIsolated yield. ^bVery slow conversion to **117** as judged by TLC control. ^cNo conversion.

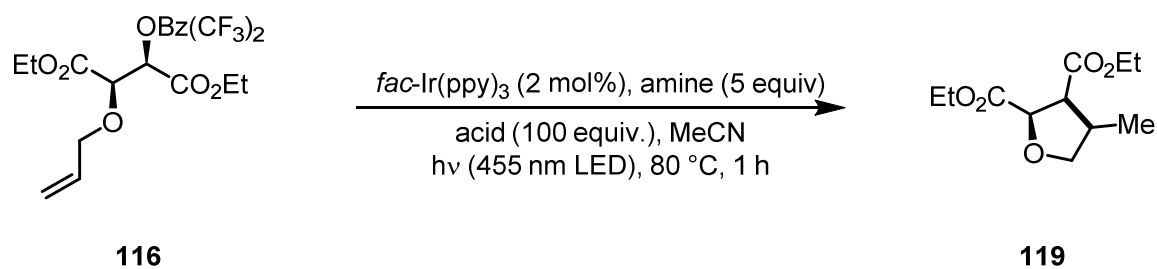
Gratifyingly, employing the 3,5-bis(trifluoromethyl)benzoate activated *O*-allylated tartrate **116** resulted in the formation of tetrahydrofuran **119** in 18% yield (Table 10, entry 1). The formation of a tetrahydropyran *via* a less favorable 6-*endo-trig* cyclization was not observed. It was possible to slightly increase the reaction yield by employing *fac*- Ir(ppy)_3 as photocatalyst in combination with DMF as solvent at higher temperatures and in the absence of a sacrificial amine (entry 4). Unfortunately it turned out that experiments without sacrificial amine took more than three days to reach full conversion, even on a 0.2 mmol scale. Additionally, reproducibility was very poor under those conditions. Different catalysts were screened to improve the situation. Neither $[\text{Ir(ppy)}_2(\text{dtb-bpy})](\text{PF}_6)$, $\text{Ru(bpy)}_3\text{Cl}_2$, nor $\text{Cu(dap)}_2\text{Cl}$ were able to give any cyclization product in contrast to *fac*- Ir(ppy)_3 . Therefore all further optimization experiments were carried out in the presence of 5 equivalents of a sacrificial amine.

Table 10. Attempts to achieve intramolecular cyclization of **116**.

Entry	Catalyst	Additive(s)	Temp.	Time	Yield 119 [%] ^a
1	$[\text{Ir(ppy)}_2(\text{dtb-bpy})]\text{PF}_6$	$i\text{Pr}_2\text{NEt}$ (2 equiv) H_2O (100 equiv)	40 °C	2 h	18 ^b
2	$[\text{Ir(ppy)}_2(\text{dtb-bpy})]\text{PF}_6$	$i\text{Pr}_2\text{NEt}$ (2 equiv) -	40 °C	2 h	- ^c
3	<i>fac</i> - Ir(ppy)_3	- H_2O (100 equiv)	40 °C	2 h	- ^d
4	<i>fac</i> - Ir(ppy)_3	- -	60 °C	3 d	24 ^e

^aIsolated yield. ^bMixture of diastereomers, dr = 11:2:1. ^cVery slow conversion to **119** as judged by TLC control. ^dNo reaction. ^eDMF as solvent. Mixture of diastereomers, dr = 5.3:2.6:1.

Also in the presence of a sacrificial amine was *fac*- Ir(ppy)_3 superior to $[\text{Ir(ppy)}_2(\text{dtb-bpy})](\text{PF}_6)$ (Table 11, entry 1 – 4). The weak acid water led to a higher conversion and a larger portion of cyclization yield. A decrease in reaction temperature led to significantly lower product yields (entry 5 – 7). Higher temperatures presumably enabled benzoate **116** to access a conformation that was more favorable to cyclize. Aliphatic alcohols were less efficient to promote the reaction than water (entry 8 – 11), while the addition of acetic acid resulted in a slightly higher yield (entry 12). When higher amounts of acetic acid were employed, complete suppression of cyclization was evident (entry 13). Comparably expensive $i\text{Pr}_2\text{NEt}$ could be replaced with cheap Et_3N (entry 14 – 15). Finally, innocuous acetonitrile was found to be the ideal solvent of the reaction (entry 16 – 18). The most ideal reaction conditions were obtained in entry 14. Performance on a preparative scale yielded 39% of isolated **119** as an inseparable mixture of diastereomers.

Table 11. Optimization of the deoxygenative cyclization to **115**.

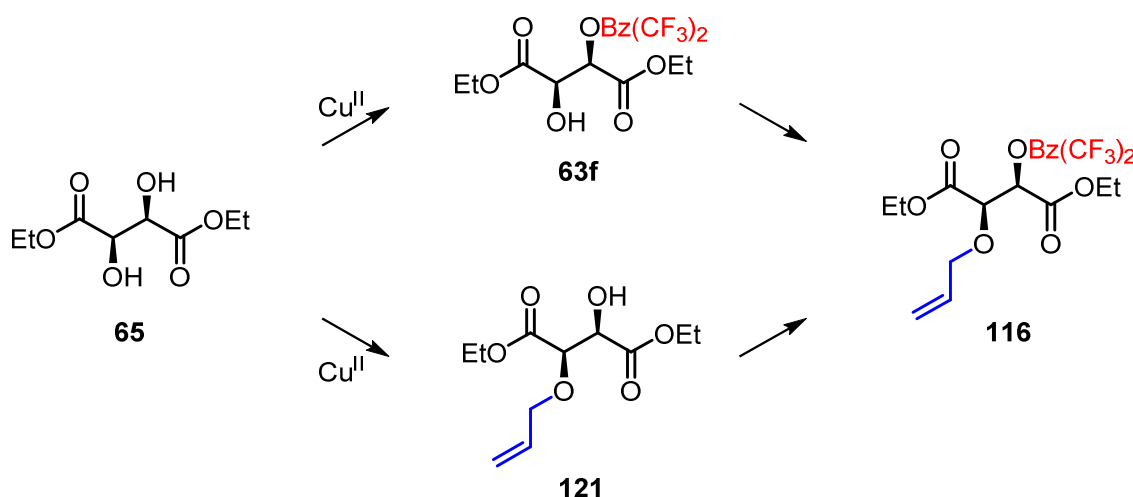
Entry	Solvent	Amine	Acid	Temp. [°C]	Conv. [%] ^a	Yield [%] ^a
1	MeCN	<i>i</i> -Pr ₂ NEt	H ₂ O	80	100	61 ^b
2	MeCN	<i>i</i> -Pr ₂ NEt	-	80	63	20 ^b
3	MeCN	<i>i</i> -Pr ₂ NEt	H ₂ O	80	100	79
4	MeCN	<i>i</i> -Pr ₂ NEt	-	80	100	22
5	MeCN	<i>i</i> -Pr ₂ NEt	H ₂ O	60	100	54
6	MeCN	<i>i</i> -Pr ₂ NEt	H ₂ O	40	100	34
7	MeCN	<i>i</i> -Pr ₂ NEt	H ₂ O	rt	100	14
8	MeCN	<i>i</i> -Pr ₂ NEt	H ₂ O ^c	80	100	56
9	MeCN	<i>i</i> -Pr ₂ NEt	MeOH ^c	80	100	4
10	MeCN	<i>i</i> -Pr ₂ NEt	<i>i</i> -PrOH ^c	80	99	35
11	MeCN	<i>i</i> -Pr ₂ NEt	AcOH ^c	80	100	38
12	MeCN	<i>i</i> -Pr ₂ NEt	HCOOH ^c	80	100	73
13	MeCN	<i>i</i> -Pr ₂ NEt	HCOOH	80	88	0
14	MeCN	Et ₃ N	H ₂ O	80	99	75 (39) ^d
15	MeCN	Bu ₃ N	H ₂ O	80	98	21
16	DMF	Et ₃ N	H ₂ O	80	100	48
17	EtOAc	Et ₃ N	H ₂ O	80	42	10
18	1,2-DCE	Et ₃ N	H ₂ O	80	82	66

^aDetermined by GC–FID with diphenylmethane as internal standard, isolated yield in parenthesis.^b[Ir(ppy)₂(dtb-bpy)]PF₆ as catalyst. ^c10 equiv ^ddr = 6.8:3.3:1.

2.5 Substrate synthesis

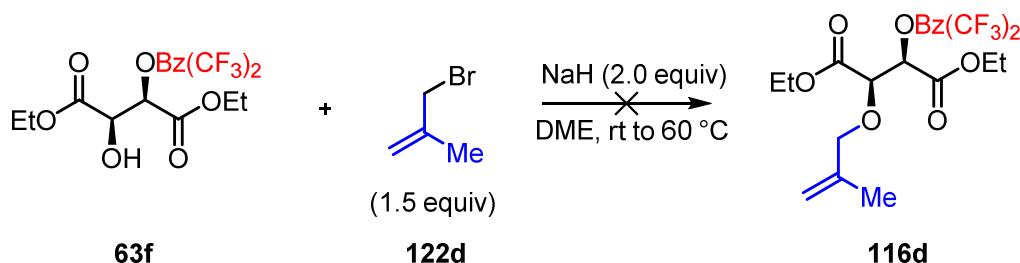
There are two general strategies to obtain allyl substituted tartrates like **116**. Either start with a Cu^{2+} -catalyzed benzoylation followed by an allylation, or *vice versa* (Scheme 25). To minimize the synthetic efforts the first strategy was chosen, as in theory only one allylation step is necessary for each new substrate while in the second strategy two reaction steps are needed for the synthesis of every new substrate.

Scheme 25. Two possible strategies to synthesize cyclizable tartrates of type **116**.



Allylation was envisioned to be realized by quantitative deprotonation of the free hydroxyl function with a base followed by treatment with a substituted allyl bromide as was published for other α -hydroxy esters.⁴⁷ Unfortunately, no allylated product **116d** was formed when **63f** was treated with sodium hydride and allyl bromide **122d** (Scheme 26), instead decomposition of the 3,5-bis(trifluoromethyl)benzoate **63f** occurred. Lowering the amount of NaH to 1.1 equivalents, decreasing the reaction temperature to 0 °C, using different solvents, and employment of Pr_2NEt as a weaker base did not improve the situation.

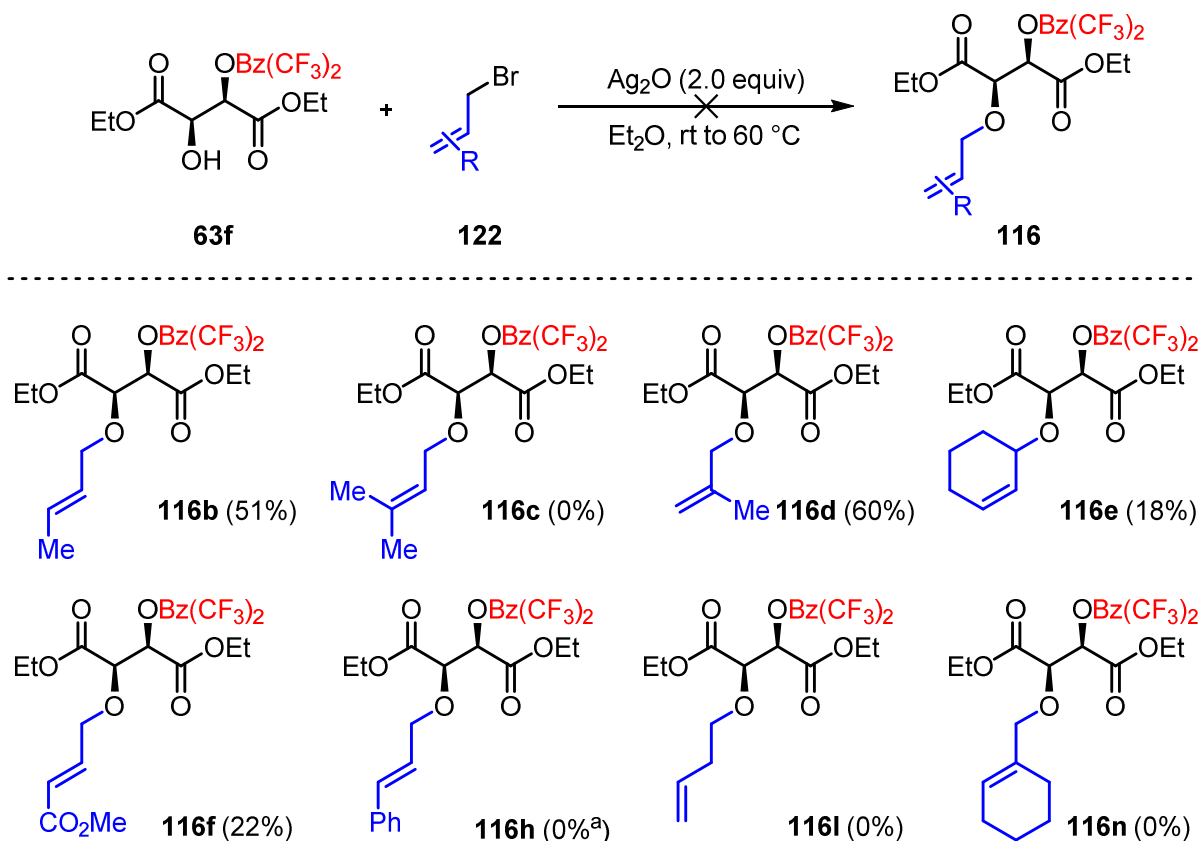
Scheme 26. Failed allylation reaction with NaH as base.



The most commonly encountered allylation method of α -hydroxyl esters in the literature is the usage of over-stoichiometric amounts of Ag_2O in combination with an allyl bromide.⁴⁸ While this reagent combination is certainly not ideal for economic reasons, it generally

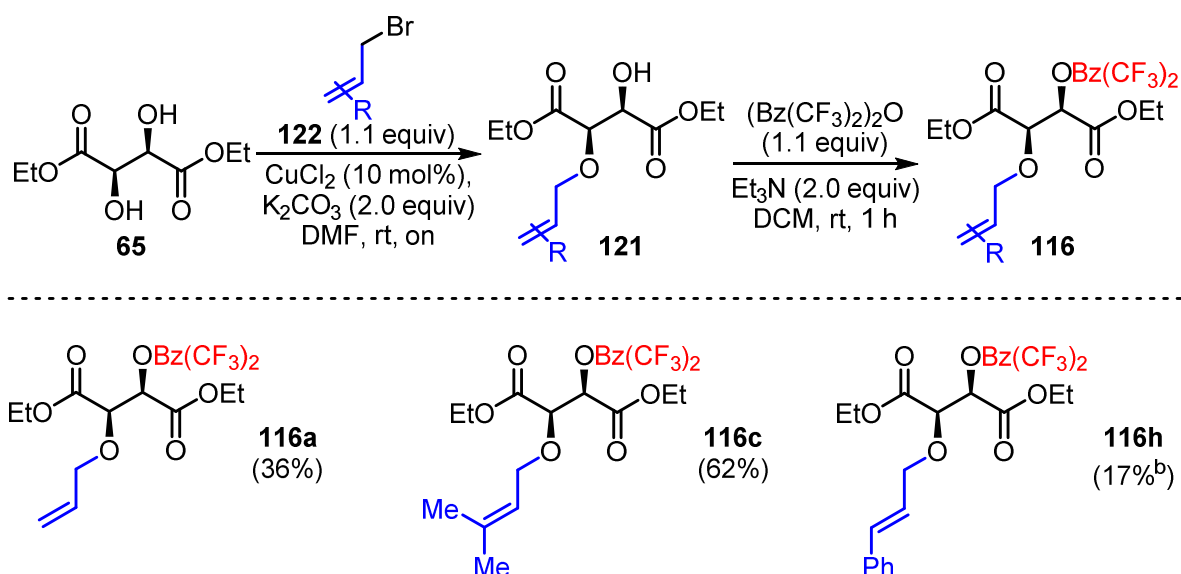
forms allylated compounds in high yields and purities. Applying this Ag^+ -mediated allylation method to 3,5-bis(trifluoromethyl)benzoate **63f** gave access to a set of allylated products in moderate to poor yields (Scheme 26). Other allylated materials could not be synthesized with this procedure.

Scheme 27. Synthesis of allylated tartrates **116** *via* allylations with Ag^+ .



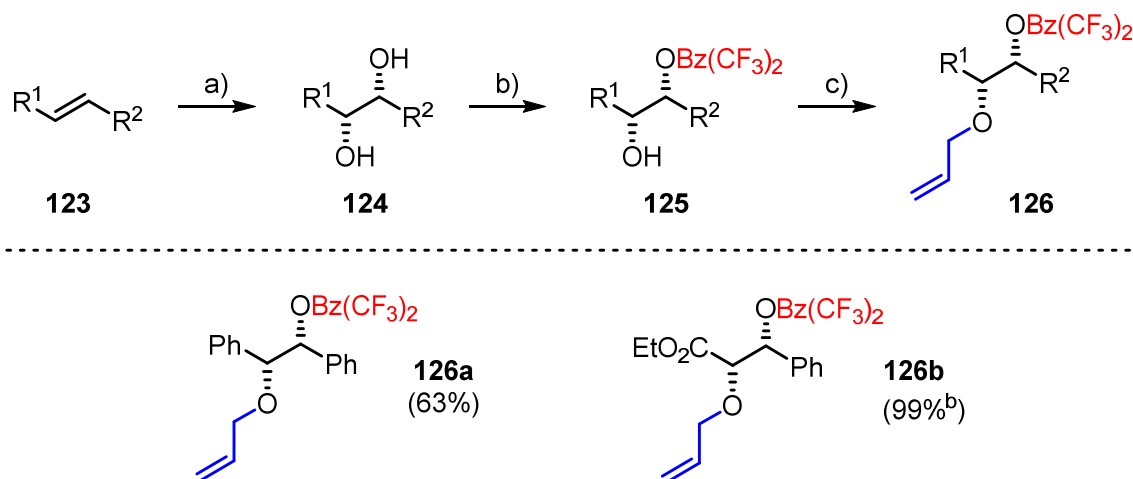
^aCinnamyl chloride was used as allylation agent.

Further allylated and activated tartrates **116** were synthesized *via* a two step procedure starting from (+)-diethyl tartrate (**65**, Scheme 28). Selective mono-allylation was realized through Cu^{2+} -mediated deprotonation of the diol motif in **65**. Subsequent benzylation was achieved with the established conditions using 3,5-bis(trifluoromethyl)benzoyl anhydride (**67**).

Scheme 28. Synthesis of allylated tartrates **116** *via* allylations with Cu^{2+} .^a

^aCombined yield for two steps is given. ^bCinnamyl chloride was used as allylation agent.

Other suitable diol-based substrates could be successfully prepared from alkenes with a Sharpless asymmetric dihydroxylation, Cu^{2+} -mediated mono-benzoylation, and Ag^+ -mediated allylation sequence (Scheme 29).^{††}

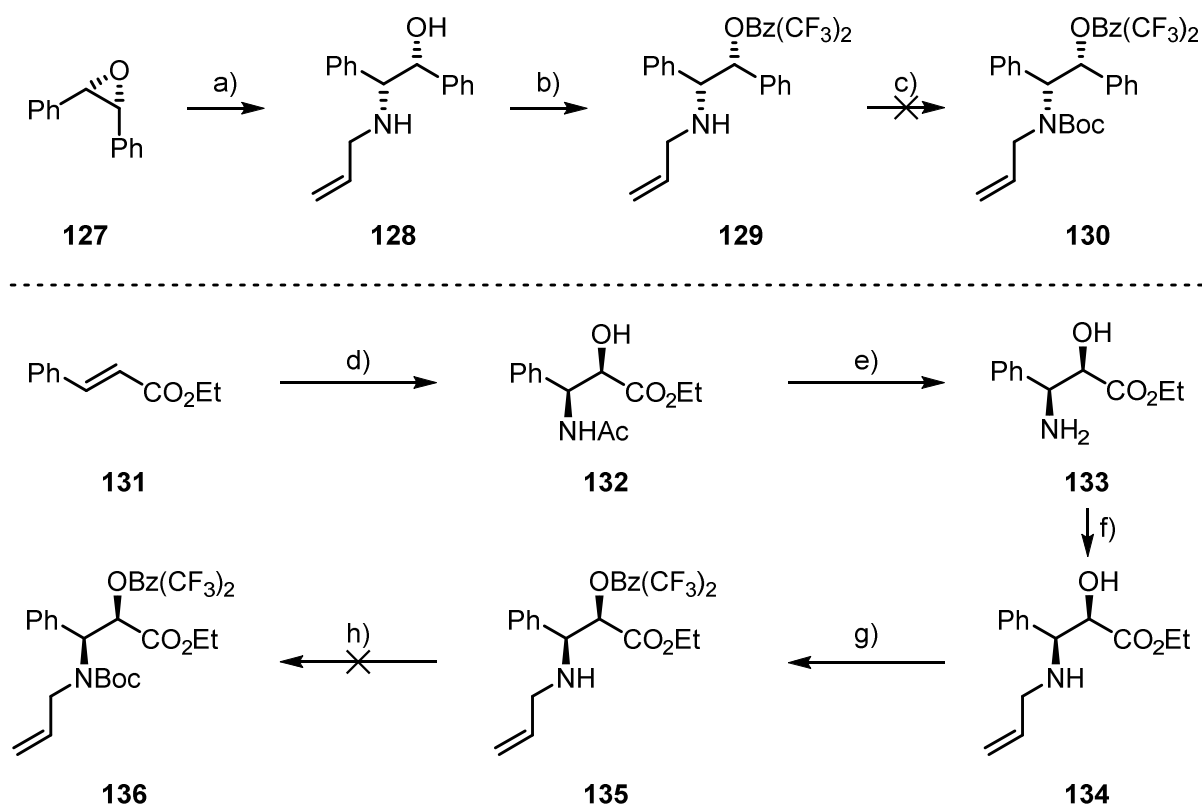
Scheme 29. Synthesis of other diol derivatives **126** *via* Sharpless asymmetric dihydroxylation.^a

^aYields are given only for step c). ^bRelative to corresponding regioisomer of starting material. Reagents and conditions: a) AD-Mix; b) $((\text{CF}_3)_2\text{Bz})_2\text{O}$ (1.1 equiv), CuCl_2 (10 mol%), Et_3N (2.0 equiv), DCM, 0 °C to rt, on; c) allyl bromide (1.5 equiv), Ag_2O (2.0 equiv), Et_2O , rt, 48 h.

^{††} Benzoates **120** were available from earlier electrochemical deoxygenation studies by Sabine Möhle.

It was also envisioned to introduce the cyclizable allyl group not *via* a tether to an oxygen atom but to a nitrogen atom. This would give pyrrolidine- instead of tetrahydrofuran derivatives as photochemical reaction products. A protection group on the bridging nitrogen atom would presumably be required, as otherwise a very electron rich center is available to be oxidized during the photocatalytic transformation. A *tert*-butyloxycarbonyl group is a suitable group, as it can usually be introduced with ease, is stable to the photocatalytic conditions, and can be conveniently removed. Two α -amino alcohols were synthesized for this purpose, one *via* an epoxide-opening with allyl amine and the other by means of a Sharpless aminohydroxylation (Scheme 30). After introduction of the allyl group and benzoate activation, unfortunately Boc-protection failed in both cases. Mixtures of multiple unidentifiable compounds were obtained so that no photochemical pyrrolidine synthesis could be investigated in this work.

Scheme 30. Attempted synthesis of substituted aminoalcohols as cyclization substrates.

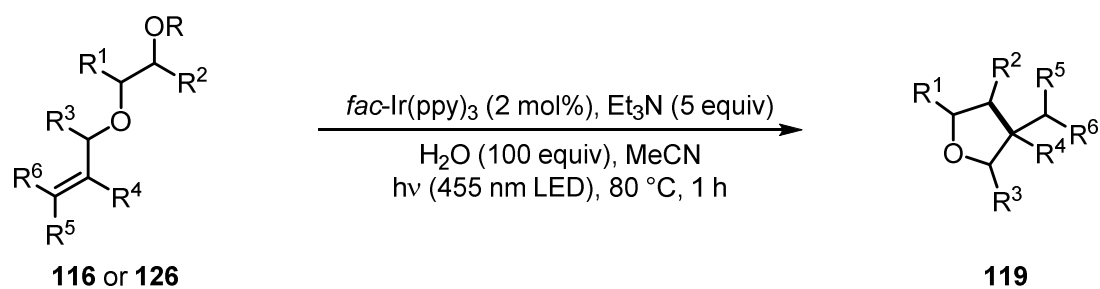


Reagents and conditions: a) AlINH_2 , LiClO_4 , $120\text{ }^\circ\text{C}$, 5 h, 93%; b) $((\text{CF}_3)_2\text{Bz})_2\text{O}$, Et_3N , DCM, rt, on, 22%; c) Boc_2O , DMAP, Et_3N , DCM, rt, on; d) $\text{K}_2\text{OsO}_2(\text{OH})_4$, $(\text{DHQD})_2\text{PHAL}$, AcNHBr , LiOH , H_2O , $t\text{-BuOH}$, $0\text{ }^\circ\text{C}$, on, rt, 2 d, 63%; e) 1. 10% HCl , H_2O , reflux, 4 h; 2. EtOH , CyH , H_2SO_4 , reflux, on; 3. NaHCO_3 , H_2O , 62%; f) AlIBr , Et_3N , THF, rt, 4 d, 74%; g) $((\text{CF}_3)_2\text{Bz})_2\text{O}$, Et_3N , DCM, rt, 20 min, 27%; h) Boc_2O , DMAP, Et_3N , DCM, rt, on.

2.6 Substrate scope and mechanistic considerations

Photochemical cyclization of model compound **116a** gave tetrahydrofuran **119a** in 39% yield as an inseparable mixture of diastereomers (Table 12, entry 1). This result is prototypical for most investigated substrates: generally moderate yields of products **119** as diastereomeric mixtures were obtained. Reduced tetrahydrofuran **119** yields can be rationalized as defunctionalative deoxygenation and / or C–F bond reduction (*vide supra*) are encountered side reactions. The introduction of an additional methyl group in γ -position of the allyl system had only little influence on both, the reaction yield as well as the diastereomeric ratio (entry 2). A further increase of the steric bulk in γ -position with a second methyl group (entry 3) led to a diminished product yield of 31%, while at the same time inversion of the stereochemistry in 3-position could be observed, leading exclusively to all-trans configured tetrahydrofuran derivative **119c**. Methyl substitution in β -position of **116d** again gave a good product yield with excellent diastereomeric induction (entry 4). By employment of cyclohexenyl-substituted **116e**, the synthesis of a cyclohexyl-annulated tetrahydrofuran **119f** was possible in reasonable yield (entry 5). The method did not tolerate α,β -unsaturated esters (entry 6 – 7), only decomposition of the starting material could be observed for **116f**. Acryl-substitution in combination with 3,5-bis(trifluoromethyl)benzoate activation surprisingly led to formation of diethyl succinate (entry 7), the formal double-deoxygenation product.^{§§} Deoxygenation with cinnamyl-containing **116h** resulted in the formation of benzyl substituted tetrahydrofuran **119h** (entry 8), demonstrating that also conjugated alkenes can undergo cyclization under these conditions. When desoxy-substrate **116i** was used simple deoxygenation was more favorable than a 4-*exo-trig* or a 5-*endo-trig* cyclization in accordance with the Baldwin rules (entry 9).⁴⁹ Tetrahydrofuran products were also observed when either both or only one of the ester groups in the tartrate backbone were substituted with phenyl groups (entry 10 and 11), demonstrating a broader applicability of the presented deoxygenative tetrahydrofuran preparation method.

^{§§} When mono-acyl diethyl tartrate was subjected to the reaction conditions only decomposition occurred.

Table 12. Substrate scope of deoxygenative cyclizations with 3,5-bis(trifluoromethyl)benzoates.

Entry	Substrate	Product	Yield and <i>dr</i> ^a
1	 116a	 119a	39% (61:30:9)
2	 116b	 119b	38% (65:21:14)
3	 116c	 119c	31% (>95:5)
4	 116d	 119d	46% (>95:5)
5	 116e	 119e	24% (53:47)
6	 116f	 119f	0% ^b

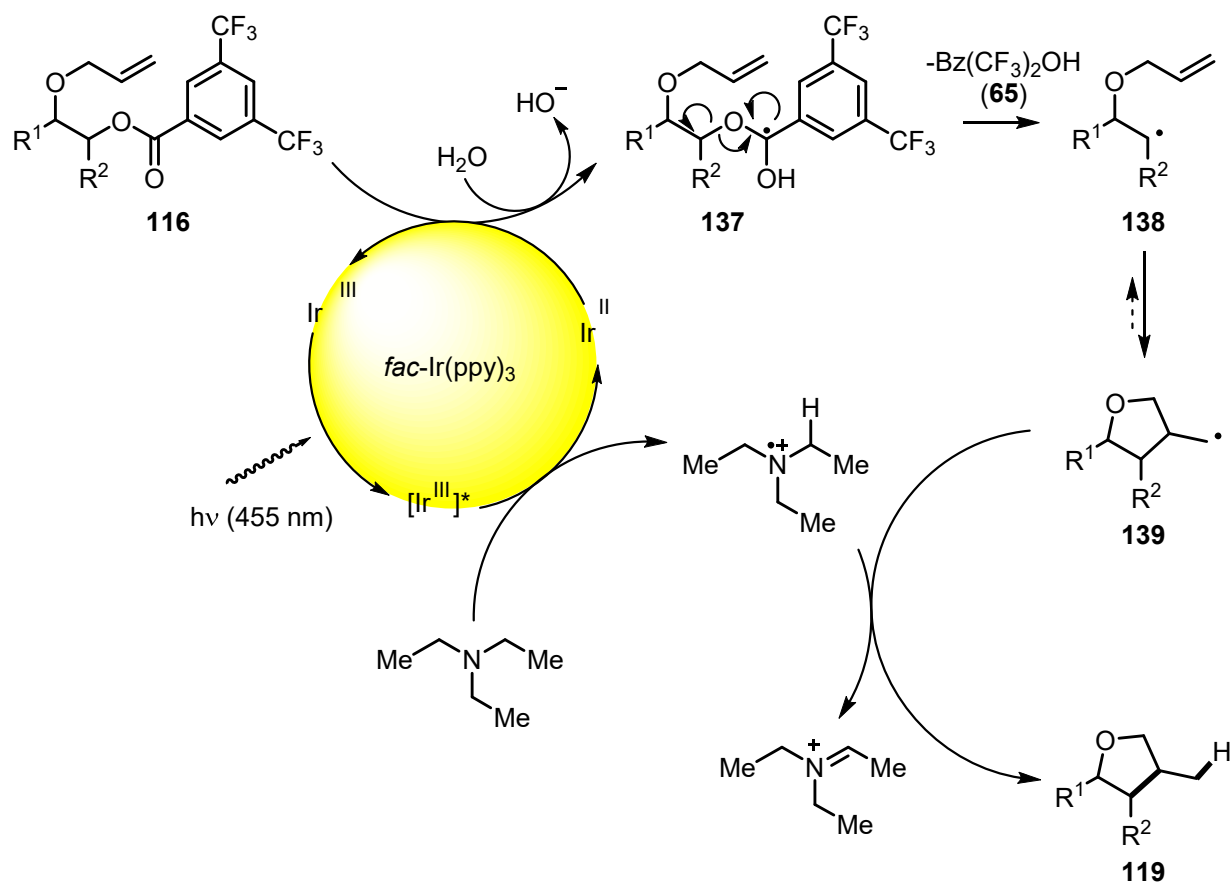
7		116g		119g	49% ^{c,d}
8		116h		119h	48% (78:22)
9		116i		119i	60% ^c
10		126a		119j	42% (49:42:9)
11		126b		119k	57% (67:19:14)

R = Bz(CF₃)₂. ^aIsolated yield, *dr* determined by ¹H-NMR integration ^bDecomposition of starting material. ^cDeoxygenation without cyclization. ^dDiethyl succinate as exclusive reaction product.

The mechanism of the deoxygenative cyclizations is derived from the defunctionalative deoxygenation mechanism (*vide supra*). It likely involves an electron uptake by the activating group from the reductively quenched Ir²⁺ species followed by carbon – oxygen bond fragmentation. This gives rise to a carbon-centered radical **138** which can then either be trapped by hydrogen atom abstraction, leading to undesired simple deoxygenation (not depicted), or in a 5-*exo-trig* fashion to form the tetrahydrofuran core structure (**139**, Scheme 31). The so-formed primary radical **139** stabilizes itself by hydrogen abstraction from a sacrificial amine radical cation. As the steps towards the carbon-centered radicals **138** are identical to the previously proposed mechanism, same substrate limitations apply: only substrates where the occurring carbon-centered radical is stabilized by a neighboring group are able to be converted into tetrahydrofurans. A partial reversibility of the C–C bond formation process of **139** from **138** might explain that higher diastereoselectivities were obtained in case of certain substitution patterns of the allylic group: when carbon-centered radical **139** was tertiary or benzylic, excellent to good diastereocontrol of >95:5 and 78:22 was observed,

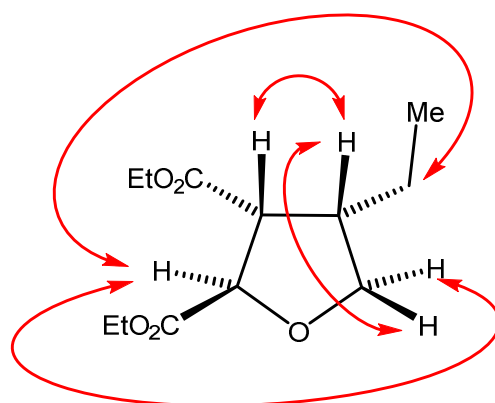
respectively. That micro-reversibility could allow the radical to go to the thermodynamically more favored product instead of the kinetic one.

Scheme 31. Proposed mechanism for photochemical deoxygenative cyclizations of **112**.



The relative stereochemistry of the tetrahydrofuran products was determined by NOE correlations. Key NOE signals for the stereochemical assignment of **119b** are exemplified in Figure 7.

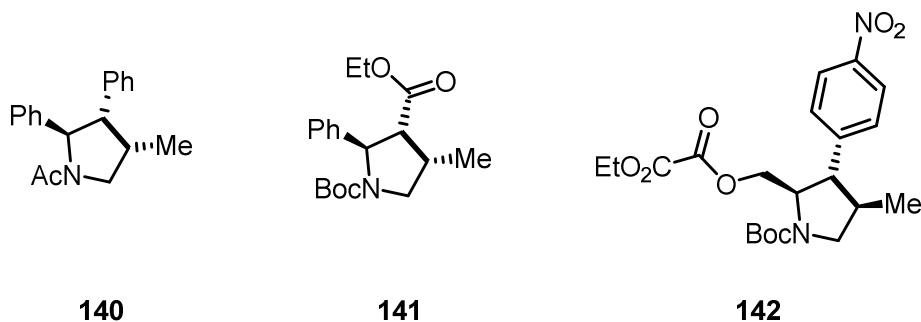
Figure 7. Key NOE correlations for the structural assignment of **119b**.



2.7 Conclusion and outlook

In summary, a protocol for the visible light mediated deoxygenation of mono-allylated diols, followed by an intramolecular 5-*exo-trig* cyclization for the preparation of chiral tetrahydrofuran derivatives, was developed. The method features inexpensive, naturally occurring, chiral starting materials (tartrates) and a sustainable, net halogen-free activation of the hydroxyl group towards radical cyclizations. This was realized by its transformation into recyclable 3,5-bis(trifluoromethyl)benzoate esters. Current experiments in the Reiser group by Eugen Lutsker are underway to extend the scope of the reaction to the synthesis of chiral pyrrolidines. Preliminary results suggest that this process is indeed working, giving optically active, separable pyrrolidines with good stereocontrol in certain instances (Figure 8).

Figure 8. Pyrrolidine synthesized by Eugen Lutsker through deoxygenative cyclization of either 3,5-bis(trifluoromethyl)benzoate or ethyloxalate activated aminoalcohols.

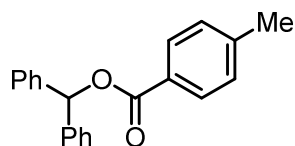


3 Experimental Part

3.1 General information

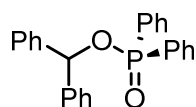
All chemicals were used as received or purified according to Purification of Common Laboratory Chemicals. Glassware was dried in an oven at 110 °C or flame dried and cooled under a dry atmosphere prior to use. All reactions were performed using Schlenk techniques. The blue light irradiation in batch processes was performed using a CREE XLamp XP-E D5-15 LED (λ = 450-465 nm). In micro reactor processes 8 OSRAM OSLO Black Series LD H9GP LEDs (λ = 455±10 nm) were employed. Analytical thin layer chromatography was performed on Merck TLC aluminium sheets silica gel 60 F 254. Reactions were monitored by TLC and visualized by a short wave UV lamp and stained with a solution of potassium permanganate, *p*-anisaldehyde, or Seebach's stain. Column flash chromatography was performed using Merck flash silica gel 60 (0.040-0.063 mm). The melting points were measured on a Büchi SMP-20 apparatus in a silicon oil bath. Values thus obtained were not corrected. ATR-IR spectroscopy was carried out on a Biorad Excalibur FTS 3000 spectrometer, equipped with a Specac Golden Gate Diamond Single Reflection ATR-System. NMR spectra were recorded on Bruker Avance 300 and Bruker Avance 400 spectrometers. Chemical shifts for ^1H NMR were reported as δ , parts per million, relative to the signal of CHCl_3 at 7.26 ppm. Chemical shifts for ^{13}C NMR were reported as δ , parts per million, relative to the center line signal of the CDCl_3 triplet at 77 ppm. Coupling constants J are given in Hertz (Hz). The following notations indicate the multiplicity of the signals: s = singlet, brs = broad singlet, d = doublet, t = triplet, q = quartet, quint = quintet, sept = septet, and m = multiplet. Mass spectra were recorded at the Central Analytical Laboratory at the Department of Chemistry of the University of Regensburg on a Varian MAT 311A, Finnigan MAT 95, Thermoquest Finnigan TSQ 7000 or Agilent Technologies 6540 UHD Accurate-Mass Q-TOF LC/MS. Gas chromatographic analyses were performed on a Fisons Instruments gas chromatograph equipped with a capillary column (30 m \times 250 μm \times 0.25 μm) and a flame ionisation detector. The yields reported are referred to the isolated compounds unless otherwise stated.

3.2 Synthesis of toluate and phosphinate esters



Benzhydryl 4-methylbenzoate (44).

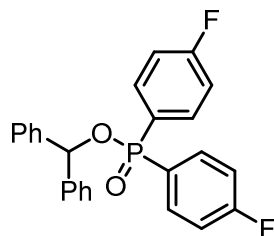
A solution of diphenylmethanol (**51**, 3.68 g, 20.0 mmol, 1.00 equiv) in 120 mL DCM was cooled to -78 °C upon which TMEDA (1.80 mL, 1.39 g, 12.0 mmol, 0.60 equiv) was added, followed by the dropwise addition of 4-methylbenzoyl chloride (3.17 mL, 3.71 g, 24.0 mmol, 1.20 equiv). The reaction was brought to room temperature, stirred for further 30 min, and quenched with 100 mL sat. NH_4Cl (aq). The layers were separated and the aqueous layer was extracted 3x with 100 mL DCM each. The combined organic layers were washed with 100 mL 10% Na_2CO_3 (aq), 100 mL H_2O , and 100 mL brine. After drying over Na_2SO_4 , the solvent was evaporated under reduced pressure to give a white solid which was recrystallized from 30 mL EtOH to give the title compound as white needles. mp: 111 °C; IR (neat): 3029, 1708, 1610, 1494, 1452, 1308, 1266, 1179, 1103, 979, 895, 743, 691 cm^{-1} ; ^1H -NMR (300 MHz, CDCl_3): 8.06 (d, J = 8.3 Hz, 2H), 7.49 – 7.43 (m, 4H), 7.41 – 7.24 (m, 8H), 7.14 (s, 1H), 2.43 (s, 3H); ^{13}C -NMR (75 MHz, CDCl_3): 165.66, 143.90, 140.45, 129.87, 129.19, 128.58, 127.94, 127.52, 127.17, 27.74; HRMS (APCI) m/z calculated for $\text{C}_{21}\text{H}_{19}\text{O}_2$ ($[\text{M}+\text{H}]^+$) 303.1380, found 303.1375.



Benzhydryl diphenylphosphinate (45).

A solution of diphenylmethanol (**51**, 792 mg, 4.30 mmol, 1.00 equiv) in 20 mL Et_2O and 20 mL DCM was cooled to 0 °C, imidazole (878 mg, 12.9 mmol, 3.00 equiv) was added followed by the dropwise addition of diphenylphosphinic chloride (1.00 mL, 1.24 g, 5.20 mmol, 1.20 equiv). The reaction mixture was allowed to reach room temperature and stirred for 2.5 h upon which the formed white precipitate was filtered and dried *in vacuo*. It was dissolved in 50 mL DCM, 50 mL sat. NaHCO_3 (aq) was added, and the suspension stirred for 10 min. The layers were separated and the aqueous layer was extracted 3x with 50 mL DCM each. The combined organic layers were washed with 100 mL water and 100 mL brine, dried over Na_2SO_4 , and evaporated under reduced pressure. The obtained material was purified by flash silica gel column chromatography (hexanes / EtOAc, 3:2) to give 1.28 g (3.32 mmol, 77.2%) of the title compound as a slightly yellow solid. R_f (hexanes : EtOAc, 1:1): 0.41; mp: 121 °C; IR (neat): 3058, 1590, 1493, 1437, 1217, 1113, 987, 879, 691 cm^{-1} ; ^1H -NMR (300 MHz, CDCl_3): 7.78 – 7.65 (m, 4H), 7.51 – 7.41 (m, 2H), 7.39 – 7.18 (m, 14H), 6.49 (d, J = 10.2 Hz, 1H); ^{13}C -NMR (75 MHz, CDCl_3): 140.77, 132.01, 131.98, 131.84, 131.70, 128.37, 128.33,

128.20, 127.85, 127.20, 78.51; HRMS (ESI) m/z calculated for $C_{25}H_{21}O_2P$ ($[M+H]^+$) 385.1352, found 385.1355.



Benzhydryl bis(4-fluorophenyl)phosphinate (50a).

Note: All (sic!) steps towards the final product were performed under N_2 .

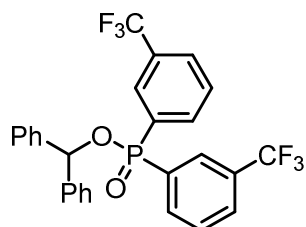
A three-neck-flask equipped with a mechanical stirrer, a reflux condenser, and a dropping funnel was charged with magnesium (3.89 g, 160 mmol, 1.60 equiv). 20 mL THF was added followed by cautious addition of a solution of 1-bromo-4-fluorobenzene (11.0 mL, 17.5 g, 100 mmol, 1.00 equiv) in 100 mL THF in a way that the Grignard formation reaction proceeds under gentle reflux. Upon complete addition the reaction was stirred for 15 min at room temperature and additional 45 min under reflux. An aliquote of the reaction mixture titrated with salicylaldehyde phenylhydrazone through which the concentration of 4-fluorophenyl magnesium bromide was determined to be 0.84 M.⁵⁰

To a solution of 1,1-dichloro-*N,N*-diethylphosphanamine (5.60 mL, 6.69 g, 38.5 mmol, 1.00 equiv) in 35 mL THF at 0 °C a solution of 4-fluorophenyl magnesium bromide (95 mL, 0.84 M in THF, 80 mmol, 2.07 equiv) was slowly added. The reaction mixture was allowed to reach room temperature and stirred over night. Approximately 100 mL THF were distilled off under reduced pressure and 200 mL dry petroleum ether was added to the remainder. The resulting suspension was filtered through a plug of Na_2SO_4 . If necessary, the filtration process was repeated. The solvent was distilled off followed by distillation of the product (bp 80 °C at 0.01 mmHg) to give 4.47 g (15.2 mmol, 39.4%) of *N,N*-diethyl-1,1-bis(4-fluorophenyl)phosphanamine as a colorless oil.

A solution of *N,N*-diethyl-1,1-bis(4-fluorophenyl)phosphanamine (4.47 g, 15.2 mmol, 1.00 equiv) in 100 mL Et_2O at -78 °C was treated with HCl (1.42 M in Et_2O , 12.0 mL, 17.0 mmol, 1.12 equiv) and stirred at room temperature for 1 h. The solvent was evaporated under reduced pressure followed by distillation of the product (bp 60 °C at 0.01 mmHg) to give 3.12 g (12.2 mmol, 80.3%) of chlorobis(4-fluorophenyl)phosphane as a colorless oil.

Through a solution of chlorobis(4-fluorophenyl)phosphane (3.12 g, 12.2 mmol, 1.00 equiv) in 30 mL benzene was bubbled dry O_2 for 5 h, after which the solvent was distilled off to give 3.84 g of a viscous oil containing bis(4-fluorophenyl)phosphinic chloride (~ 33 m%) which was used without further purification.

A solution of diphenylmethanol (**51**, 577 mg, 3.13 mmol, 1.00 equiv) in 20 mL Et₂O and 20 mL DCM was cooled to 0 °C, imidazole (639 mg, 9.39 mmol, 3.00 equiv) was added followed by the dropwise addition of a solution of impure chlorobis(4-fluorophenyl)phosphane (3.84 g) in 10 mL DCM. The reaction mixture was allowed to reach room temperature and stirred for 2 d upon which the formed white precipitate was filtered and dried *in vacuo*. It was dissolved in 50 mL DCM, 50 mL sat. NaHCO₃ (aq) was added, and the suspension stirred for 10 min. The layers were separated and the aqueous layer was extracted 3x with 50 mL DCM each. The combined organic layers were washed with 100 mL water and 100 mL brine, dried over Na₂SO₄, and evaporated under reduced pressure. The obtained material was purified by flash silica gel column chromatography (hexanes / EtOAc, 2:1) to give 506 mg (1.25 mmol, 40%) of the title compound as a slightly yellow solid. *R*_f (hexanes : EtOAc, 2:1): 0.29; mp: 108 °C; IR (neat): 3060, 1590, 1496, 1397, 1301, 1222, 1125, 964, 921, 826, 742, 697, 668 cm⁻¹; ¹H-NMR (400 MHz, CDCl₃): 7.73 – 7.64 (m, 4H), 7.31 – 7.21 (m, 10H), 7.07 – 7.98 (m, 4H), 6.48 (d, *J* = 10.1 Hz, 1H); ¹³C-NMR (101 MHz, CDCl₃): 140.41, 140.37, 134.38, 134.27, 134.15, 128.44, 128.05, 127.18, 115.92, 115.78, 115.71, 115.56, 78.83, 78.78; ¹⁹F-NMR (282 MHz, CDCl₃): -106.51 (d, *J* = 1.2 Hz); ³¹P-NMR (121 MHz, CDCl₃): 30.92; HRMS (ESI) *m/z* calculated for C₂₅H₂₀F₂O₂P ([M+H]⁺) 421.1163, found 421.1160.



Benzhydryl bis(3-trifluoromethyl)phosphinate (50c).

Note: All (sic!) steps towards the final product were performed under N₂.

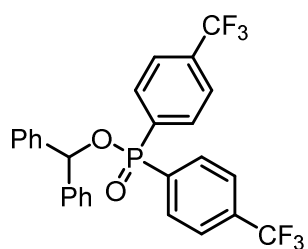
ATTENTION: Direct aryl Grignard formation of any trifluoromethyl-substituted aryl compound can lead to a spontaneous, vigorous explosion! Indirect Grignard formation through Knochel Grignard exchange should be used instead!²⁷

A three-neck-flask equipped with a mechanical stirred, a reflux condenser, and a dropping funnel was charged with magnesium (3.89 g, 160 mmol, 1.60 equiv). 20 mL THF was added followed by cautious addition of a solution of 1-bromo-3-(trifluoromethyl)benzene (14.0 mL, 25.5 g, 100 mmol, 1.00 equiv) in 100 mL THF in a way that the Grignard formation reaction proceeds under gentle reflux. Upon complete addition the reaction was stirred for 1 h at room temperature. An aliquote of the reaction mixture titrated with salicylaldehyde phenylhydrazone through which the concentration of 3-trifluoromethylphenyl magnesium bromide was determined to be 0.81 M.⁵⁰

To a solution of 1,1-dichloro-*N,N*-diethylphosphanamine (4.81 mL, 5.76 g, 33.1 mmol, 1.00 equiv) in 35 mL THF at 0 °C a solution of 3-trifluoromethylphenyl magnesium bromide (95 mL, 0.81 M in THF, 77 mmol, 2.3 equiv) was slowly added. The reaction mixture was allowed to reach room temperature and stirred over night. 120 mL dry petroleum ether was added to the suspension which was then filtered through a plug of Na₂SO₄. The filtrate was cooled to -78 °C and treated with HCl (1.65 M in Et₂O, 50.0 mL, 82.0 mmol, 2.48 equiv) and stirred at room temperature for 1 h. The solvent was evaporated under reduced pressure followed by distillation of the product at 0.01 mmHg to give 6.84 g (19.2 mmol, 58%) of chlorobis(3-(trifluoromethyl)phenyl)phosphane as a colorless oil.

Through a solution of chlorobis(3-(trifluoromethyl)phenyl)phosphane (6.84 g, 19.2 mmol, in 30 mL DCM at -78 °C was bubbled O₃ for 5 min followed by O₂ for 1 h, after which the solvent was distilled off to give a viscous oil containing bis(3-(trifluoromethyl)phenyl)phosphinic chloride (~ 42 m%) which was used without further purification.

A solution of diphenylmethanol (**51**, 162 mg, 0.883 mmol, 1.00 equiv) in 5 mL Et₂O and 5 mL DCM was cooled to 0 °C, imidazole (180 mg, 2.65 mmol, 3.00 equiv) was added followed by the dropwise addition of a solution of impure bis(3-(trifluoromethyl)phenyl)phosphinic chloride (42 m%, 0.936 g, 1.06 mmol, 1.20 equiv) in 5 mL DCM. The reaction mixture was allowed to reach room temperature and stirred for 2 d upon which the formed white precipitate was filtered and dried *in vacuo*. It was dissolved in 5 mL DCM, 5 mL sat. NaHCO₃ (aq) was added, and the suspension stirred for 10 min. The layers were separated and the aqueous layer was extracted 3x with 5 mL DCM each. The combined organic layers were washed with 10 mL water and 10 mL brine, dried over Na₂SO₄, and evaporated under reduced pressure. The obtained material was purified by flash silica gel column chromatography (hexanes / EtOAc, 2:1) to give 219 mg (0.42 mmol, 40%) of the title compound as a white solid. *R*_f (hexanes : EtOAc, 2:1): 0.29; mp: 122 °C; IR (neat): 3072, 2848, 1606, 1493, 1447, 1324, 1118, 1072, 908, 739, 695 cm⁻¹; ¹H-NMR (300 MHz, CDCl₃): 7.98 – 7.84 (m, 4H), 7.73 (d, *J* = 7.8 Hz, 2H), 7.51 (tdt, *J* = 7.7, 3.4, 0.7 Hz, 2H), 7.32 – 7.22 (m, 10 H), 6.57 (d, *J* = 9.6 Hz); ¹³C-NMR (75 MHz, CDCl₃): 139.74, 139.68, 135.00, 134.87, 129.24, 129.06, 128.55, 128.34, 127.19; ¹⁹F-NMR (282 MHz, CDCl₃): -63.37; ³¹P-NMR (121 MHz, CDCl₃): 28.79.

**Benzhydryl bis(4-trifluoromethyl)phosphinate (50d).**

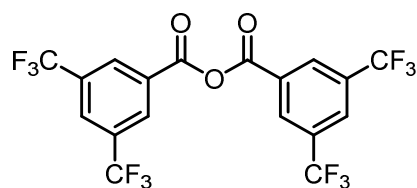
Note: All (sic!) steps towards the final product were performed under N_2 .

A Schlenk flask was charged with magnesium (1-bromo-4-(trifluoromethyl)benzene (4.50 g, 20.0 mmol, 1.00 equiv) and 100 mL Et_2O . The mixture was cooled to 5 °C upon which a solution of $tBuLi$ (1.6 M in hexanes, 12.5 mL, 20 mmol, 1.0 equiv) was added dropwise. The mixture was stirred at 5 °C for 3 h after which 1,1-dichloro-*N,N*-diethylphosphanamine (1.45 mL, 1.74 g, 10.0 mmol, 0.50 equiv) was slowly added. The reaction mixture was allowed to reach room temperature and stirred over night. The solution was cooled to -78 °C and treated with HCl (4.0 M in dioxane, 6.0 mL mL, 24 mmol, 1.2 equiv) and stirred at room temperature for 1 h. 80 mL hexanes was added to the suspension which was then filtered through a plug of Na_2SO_4 . The solvent was evaporated under reduced pressure follow by distillation of the product at 0.01 mmHg to give 1.91 g (5.38 mmol, 54%) of chlorobis(4-(trifluoromethyl)phenyl)phosphane as a colorless oil.

Through a solution of chlorobis(4-(trifluoromethyl)phenyl)phosphane (1.91 g, 5.38 mmol, 1.00 equiv) in 30 mL benzene was bubbled O_2 for 5 h, after which the solvent was distilled off to give 1.76 g (4.73 mmol, 89%) of bis(4-(trifluoromethyl)phenyl)phosphinic chloride as a viscous oil which was used without further purification.

A solution of diphenylmethanol (**51**, 553 mg, 3.00 mmol, 1.00 equiv) in 15 mL Et_2O and 15 mL DCM was cooled to 0 °C, imidazole (613 mg, 9.00 mmol, 3.00 equiv) was added followed by the dropwise addition of a solution of bis(4-(trifluoromethyl)phenyl)phosphinic chloride (1.68 g, 4.50 mmol, 1.50 equiv) in 5 mL DCM. The reaction mixture was allowed to reach room temperature and stirred for 2 d upon which the formed white precipitate was filtered and dried *in vacuo*. It was dissolved in 20 mL DCM, 20 mL sat. $NaHCO_3$ (aq) was added, and the suspension stirred for 10 min. The layers were separated and the aqueous layer was extracted 3x with 20 mL DCM each. The combined organic layers were washed with 20 mL water and 20 mL brine, dried over Na_2SO_4 , and evaporated under reduced pressure. The obtained material was purified by recrystallization from cyclohexane to give 1.25 g (2.40 mmol, 80%) of the title compound as a white solid. mp: 128 °C; IR (neat): 3060, 2847, 1599, 1492, 1446, 1400, 1322, 1123, 1061, 951, 835, 699 cm^{-1} ; 1H -NMR (300 MHz, $CDCl_3$): 7.84 (d, J = 8.2 Hz, 2H), 7.80 (d, J = 8.2 Hz, 2H), 7.61 (dd, J = 8.1, 2.8 Hz, 4H), 7.41 – 7.20 (m, 10H), 6.56 (d, J = 9.55); ^{19}F -NMR (282 MHz, $CDCl_3$): -63.36; ^{31}P -NMR (121 MHz, $CDCl_3$): 28.83.

3.3 Synthesis of the acid anhydride



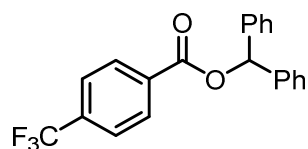
3,5-Bis(trifluoromethyl)benzoic anhydride (67).

A 50 mL three-neck round-bottom flask was equipped with a gas inlet, a dropping funnel, and a 20 cm Vigreux column with a Claisen bridge and a 10 mL round-bottom flask. The flask was charged with 3,5-bis(trifluoromethyl)benzoic acid²⁷ (12.0 g, 46.5 mmol, 1.00 equiv) and phosphoric acid (20 mg, 0.20 mmol, 0.43 mol%) and the dropping funnel was charged with acetic anhydride (8.8 mL, 9.5 g, 93 mmol, 2.0 equiv). The flask was heated to 150 °C in an oil bath and about 6.5 mL of acetic anhydride was added *via* the dropping funnel. The mixture was slowly heated to 190 °C till no more acetic anhydride distilled. About half of the remaining acetic anhydride was added to the reaction mixture *via* the dropping funnel and the mixture was stirred till no more acetic anhydride distilled. The remainder of acetic anhydride was added and again till no more acetic anhydride distilled. Vacuum (20 mbar) was applied and distillation was continued at 190 °C till no more distillate could be collected. The reaction mixture was allowed to cool to 100 °C after which the Vigreux column and the Claisen bridge were replaced with a distillation arch. The crude product was subsequently distilled at 170 °C / 1 mbar into a 50 mL Schlenk flask. Pure product was obtained after recrystallization from toluene / petrol ether as white crystals (9.07 g, 18.2 mmol, 78%). mp: 104 - 105 °C; IR (neat): 3103, 1801, 1749, 1622, 1384, 1286, 1172, 1126, 1052, 100, 915, 888, 843, 753, 726, 698, 681, 642, 613 cm⁻¹; ¹H-NMR (300 MHz, CDCl₃): 8.58 (s, 4H), 8.22 (s, 2H); ¹³C-NMR (400 MHz, CDCl₃): 159.2, 133.1 (q, J = 34), 130.5 (m), 130.4, 128.3 (m), 122.5 (q, J = 273); ¹⁹F-NMR (282 MHz, CDCl₃): -63.6.

3.4 Synthesis of benzoate esters

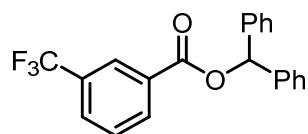
General procedure for the synthesis of benzoate esters *via* the acid chloride (*GPI*)

A 50 mL Schlenk flask equipped with a magnetic stir bar was charged with an alcohol (5.00 mmol, 1.00 equiv), 4-DMAP (31 mg, 0.25 mmol, 0.05 equiv), Et₃N (5.0 ml, 3.5 g, 35 mmol, 7.0 equiv), and DCM (50 mL). The mixture was cooled to 0 °C, then (trifluoromethyl)benzoyl chloride^{27,28} (5.50 mmol, 1.10 equiv) was added dropwise. The reaction mixture was allowed to warm to room temperature, solvent was evaporated under reduced pressure and the residue was purified by flash chromatography.



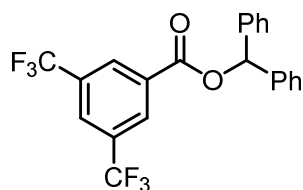
Benzhydryl 4-(trifluoromethyl)benzoate (52).

Following general procedure *GPI* gave 1.12 g (3.13 mmol, 63%) of a white solid after purification on SiO₂ (petrol ether / EtOAc, 50:1 to 25:1). *R*_f(petrol ether): 0.08; mp: 92 °C; IR (neat): 3062, 1722, 1585, 1497, 1455, 1411, 1320, 1268, 1166, 1115, 1065, 1016, 966, 898, 862, 774, 742, 703, 649, 591, 457 cm⁻¹; ¹H-NMR (300 MHz, CDCl₃): 8.26 (d, *J* = 8.5, 2H), 7.74 (d, *J* = 8.5, 2H), 7.45-7.30 (m, 10H), 7.15 (s, 1H); ¹³C-NMR (101 MHz, CDCl₃): 164.4, 139.9, 134.7 (q, *J* = 32.7), 130.2, 128.7, 128.2, 127.2, 125.5 (q, *J* = 3.7), 123.6 (q, *J* = 273), 78.1; ¹⁹F-NMR (282 MHz, CDCl₃): -63.6; HRMS (EI) *m/z* calculated for C₂₁H₁₅F₃O₂ ([M]⁺) 356.1024, found 356.1024.

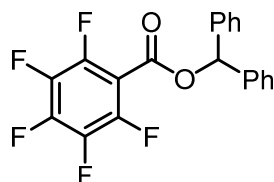


Benzhydryl 3-(trifluoromethyl)benzoate (53).

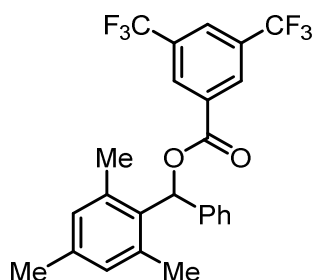
Following general procedure *GPI* gave 1.63 g (4.58 mmol, 92%) of a white solid after purification on SiO₂ (petrol ether / EtOAc, 50:1 to 25:1). *R*_f(petrol ether): 0.13; mp: 73 °C; IR (neat): 3077, 3029, 1725, 1617, 1494, 1455, 1335, 1246, 1169, 1131, 1073, 985, 932, 826, 751, 695, 652, 618, 598, 570, 507, 468, 410 cm⁻¹; ¹H-NMR (300 MHz, CDCl₃): 8.39 (s, 1H), 8.33 (d, *J* = 7.9, 1H), 7.84 (d, *J* = 7.8, 1H), 7.61 (t, *J* = 7.8, 1H), 7.48-7.41 (m, 4H), 7.41-7.28 (m, 6H), 7.16 (s, 1H); ¹³C-NMR (101 MHz, CDCl₃): 164.4, 139.8, 133.0, 131.2 (q, *J* = 32.8), 131.1, 129.7 (q, *J* = 3.7), 129.2, 128.7, 128.2, 127.2, 126.7 (q, *J* = 3.9), 123.7 (q, *J* = 273), 78.1; ¹⁹F-NMR (282 MHz, CDCl₃): -63.3; HRMS (APCI) *m/z* calculated for C₂₁H₁₉F₃NO₂ ([M+NH₄]⁺) 374.1362, found 374.1362.

**Benzhydryl 3,5-bis(trifluoromethyl)benzoate (54).**

Following general procedure *GPI* gave 1.60 g (3.76 mmol, 75%) of a white solid after purification on SiO₂ (petrol ether / EtOAc, 100:1 to 50:1). *R_f* (petrol ether): 0.18; mp: 71 °C; IR (neat): 3110, 3063, 3033, 1732, 1621, 1496, 1456, 1388, 1248, 1173, 1120, 989, 912, 846, 768, 750, 696, 623, 603, 562, 475, 430 cm⁻¹; ¹H-NMR (300 MHz, CDCl₃): 8.56 (s, 2H), 8.09 (s, 1H), 7.45-7.32 (m, 10H), 7.19 (s, 1H); ¹³C-NMR (101 MHz, CDCl₃): 163.1, 139.3, 132.4, 132.3 (q, *J* = 34.3), 129.9 (m), 128.8, 128.4, 127.2, 126.6 (sept, *J* = 3.7), 122.9 (q, *J* = 273), 78.9; ¹⁹F-NMR (282 MHz, CDCl₃): -63.4; HRMS (EI) *m/z* calculated for C₂₂H₁₄F₆O₂ ([M]⁺) 424.0898, found 424.0899.

**Benzhydryl 2,3,4,5,6-pentafluorobenzoate (55).**

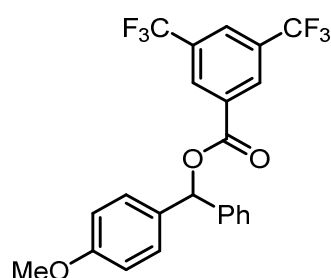
Preparation *via GPI* failed. The title compound was thus synthesized through a DCC/DMAP mediated coupling: A solution of diphenylmethanol (435 mg, 2.36 mmol, 1.00 equiv) and 2,3,4,5,6-pentafluorobenzoic acid^{***} (500 mg, 2.36 mmol, 1.00 equiv) in 20 mL DCM was cooled to 0 °C and treated with 4-DMAP (29 mg, 0.24 mmol, 0.10 equiv) and DCC (587 mg, 2.84 mmol, 1.20 equiv). After stirring for 20 h at room temperature the reaction was quenched by the addition of 20 mL 0.5 M HCl (aq). The layers were separated and the organic phase was washed with 10 mL H₂O, 10 mL sat. NaHCO₃ (aq), 10 mL brine, dried over Na₂SO₄, and evaporated under reduced pressure. The obtained material was purified by flash silica gel column chromatography (hexanes / EtOAc, 20:1) to give 565 mg (1.49 mmol, 63%) of the title compound as a white solid. *R_f* (hexanes / EtOAc, 10:1): 0.60; mp: 93 °C; IR (neat): 3031, 2956, 1737, 1654, 1495, 1454, 1326, 1228, 1106, 992, 960, 924 cm⁻¹; ¹H-NMR (400 MHz, CDCl₃): 7.45 – 7.29 (m, 10H), 7.12 (s, 1H); ¹³C-NMR (101 MHz, CDCl₃): 139.00, 128.70, 128.38, 127.17, 79.76; ¹⁹F-NMR (282 MHz, CDCl₃): -137.44 (m), -148.05 (m), -160.19 (m).

**Mesityl(phenyl)methyl 3,5-bis(trifluoromethyl)benzoate (54b).**

Following general procedure *GPI* using mesityl(phenyl)methanol⁵¹ (438 mg, 1.94 mmol, 1.00 equiv), 3,5-bis(trifluoromethyl)benzoyl chloride (370 μL, 563 mg, 2.04 mmol, 1.05 equiv), 4-DMAP (12 mg, 0.10 mmol, 0.05 equiv), Et₃N (2.0 mL, 1.4 g, 14 mmol, 7.0 equiv),

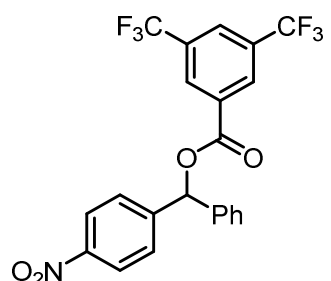
^{***} This material was obtained from Dr. Andreas Kreuzer

and DCM (20 mL) gave 900 mg (1.93 mmol, 99%) of a white solid after purification on SiO₂ (petrol ether / EtOAc, 100:1 to 30:1). *R_f* (petrol ether): 0.41; mp: 75 °C, IR (neat): 2969, 2919, 2869, 1721, 1614, 1495, 1448, 1390, 1354, 108, 1254, 1190 1129, 1036, 957, 951, 911, 854, 807, 760, 725, 695, 622, 599, 531, 497, 439 cm⁻¹; ¹H-NMR (300 MHz, CDCl₃): 8.57 (s, 2H), 8.10 (s, 1H), 7.67 (s, 1H), 7.42-7.29 (m, 3H), 7.22-7.14 (m, 2H), 6.91 (m, 2H); 2.38 (s, 6H), 2.30 (s, 3H). ¹³C-NMR (75 MHz, CDCl₃): 163.4, 138.8, 138.4, 137.7, 132.6, 132.4, 132.1, 132.0, 130.0, 129.9 (m), 128.6, 127.6, 126.5 (m), 125.7, 124.6, 74.8, 21.0, 20.6; ¹⁹F-NMR (282 MHz, CDCl₃): -63.5; HRMS (EI) *m/z* calculated for C₂₅H₂₀F₆O₂ ([M]⁺) 466.1367, found 466.1363.



(4-Methoxyphenyl)(phenyl)methyl 3,5-bis(trifluoromethyl)-benzoate (54c).

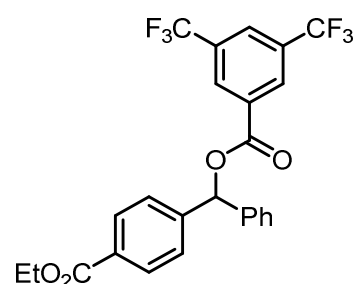
Following general procedure *GPI* using (4-methoxyphenyl)(phenyl)methanol⁵¹ (429 mg, 2.00 mmol, 1.00 equiv), 3,5-bis(trifluoromethyl)benzoyl chloride (381 μL, 581 mg, 2.10 mmol, 1.05 equiv), 4-DMAP (12 mg, 0.10 mmol, 0.05 equiv), Et₃N (2.0 mL, 1.4 g, 14 mmol, 7.0 equiv), and DCM (20 mL) gave 732 mg (1.61 mmol, 81%) of a colorless oil after purification on SiO₂ (petrol ether / EtOAc, 100:1 to 20:1). *R_f* (petrol ether): 0.13; IR (neat): 2840, 2362, 1730, 1613, 1514, 1457, 1388, 1278, 1242, 1175, 1136, 1035, 912, 821, 767, 700, 632, 544, 501 cm⁻¹; ¹H-NMR (300 MHz, CDCl₃): 8.55 (s, 2H), 8.08 (s, 1H), 7.46-7.29 (m, 7H), 7.16 (s, 1H), 6.96-6.88 (m, 2H), 3.81 (s, 3H); ¹³C-NMR (75 MHz, CDCl₃): 163.1, 159.7, 139.5, 132.5, 132.3 (q, *J* = 34.0), 131.4, 129.8 (m), 129.0, 128.7, 128.7, 128.2, 127.0, 126.6 (m), 122.9 (q, *J* = 273), 114.1, 78.6, 55.3; ¹⁹F-NMR (282 MHz, CDCl₃): -63.4; HRMS (EI) *m/z* calculated for C₂₃H₁₆F₆O₃ ([M]⁺) 454.1004, found 454.1003.



(4-Nitrophenyl)(phenyl)methyl 3,5-bis(trifluoromethyl)-benzoate (54d).

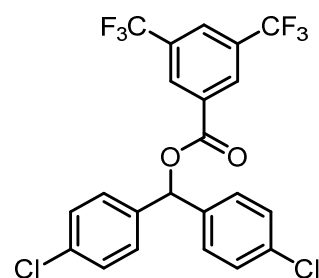
Following general procedure *GPI* using (4-nitrophenyl)(phenyl)methanol⁵² (252 mg, 1.10 mmol, 1.00 equiv), 3,5-bis(trifluoromethyl)benzoyl chloride (218 μL, 333 mg, 1.21 mmol, 1.10 equiv), 4-DMAP (6 mg, 0.05 mmol, 0.05 equiv), Et₃N (1.1 mL, 0.80 g, 7.9 mmol, 7.0 equiv), and DCM (11 mL) gave 528 mg (1.10 mmol, 100%) of a colorless oil after purification on SiO₂ (petrol ether / EtOAc, 30:1). *R_f* (petrol ether / EtOAc, 50:1): 0.19; IR (neat): 3085, 1732, 1609, 1523, 1348, 1227, 1236, 1175, 1127, 974, 912, 845, 765, 742, 697, 613,

574, 516, 461, 440 cm^{-1} ; ^1H -NMR (300 MHz, CDCl_3): 8.54 (s, 2H), 8.30-8.21 (m, 2H), 8.11 (s, 1H), 7.65-7.55 (m, 2H), 7.48-7.35 (m, 5H) 7.22 (s, 1H); ^{13}C -NMR (101 MHz, CDCl_3): 162.9, 147.8, 146.3, 137.9, 132.6 (q, $J = 34.0$), 131.8, 129.9 (m), 129.2, 127.9, 127.4, 127.0 (m), 124.1, 122.8 (q, $J = 273$), 77.8; ^{19}F -NMR (282 MHz, CDCl_3): -63.4; HRMS (EI) m/z calculated for $\text{C}_{22}\text{H}_{13}\text{F}_6\text{NO}_4$ ($[\text{M}+\text{H}]^+$) 470.0822, found 470.0816.



(4-(Ethoxycarbonyl)phenyl)(phenyl)methyl 3,5-bis(trifluoromethyl)benzoate (54e).

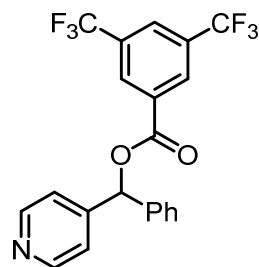
Following general procedure **GPI** using ethyl 4-(hydroxy(phenyl)methyl)benzoate⁵³ (513 mg, 2.00 mmol, 1.00 equiv), 3,5-bis(trifluoromethyl)benzoyl chloride (381 μL , 581 mg, 2.10 mmol, 1.05 equiv), 4-DMAP (12 mg, 0.10 mmol, 0.05 equiv), Et_3N (2.0 mL, 1.4 g, 14 mmol, 7.0 equiv), and DCM (20 mL) gave 954 mg (1.92 mmol, 96%) of a white solid after purification on SiO_2 (petrol ether / EtOAc, 20:1). R_f (petrol ether / EtOAc, 6:1): 0.56; mp: 98 $^\circ\text{C}$; IR (neat): 2984, 1720, 1708, 1615, 1459, 1367, 1273, 1254, 1181, 1130, 1107, 1022, 979, 912, 874, 846, 754, 704, 677, 617, 570, 516, 484, 436 cm^{-1} ; ^1H -NMR (300 MHz, CDCl_3): 8.55 (s, 2H), 8.10 (s, 1H), 8.09-8.03 (m, 2H), 7.53-7.48 (m, 2H), 7.45-7.31 (m, 5H), 7.20 (s, 1H), 4.38 (q, $J = 7.2$, 2H), 1.39 (t, $J = 7.2$, 3H); ^{13}C -NMR (101 MHz, CDCl_3): 166.1, 163.0, 144.0, 138.6, 132.4 (q, $J = 34.0$), 132.2, 130.5, 130.0, 129.8 (m), 128.9, 128.8, 127.4, 126.9, 126.7 (m), 122.8 (q, $J = 273$), 78.4, 61.1, 14.3; ^{19}F -NMR (282 MHz, CDCl_3): -63.5; HRMS (EI) m/z calculated for $\text{C}_{25}\text{H}_{18}\text{F}_6\text{O}_4$ ($[\text{M}]^+$) 496.1109, found 496.1109.



Bis(4-chlorophenyl)methyl 3,5-bis(trifluoromethyl)benzoate (54f).

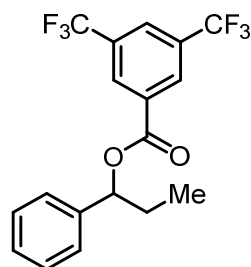
Following general procedure **GPI** using bis(4-chlorophenyl)methanol⁵⁴ (253 mg, 1.00 mmol, 1.00 equiv), 3,5-bis(trifluoromethyl)benzoyl chloride (200 μL , 303 mg, 1.10 mmol, 1.10 equiv), 4-DMAP (6 mg, 0.05 mmol, 0.05 equiv), Et_3N (1.0 mL, 0.7 g, 7.0 mmol, 7.0 equiv), and DCM (10 mL) gave 490 mg (0.99 mmol, 99%) of a white solid after purification on SiO_2 (petrol ether / EtOAc, 20:1). R_f (petrol ether / EtOAc, 6:1): 0.78; mp: 99 $^\circ\text{C}$; IR (neat): 3101, 1729, 1625, 1493, 1346, 1271, 1239, 1185, 1136, 1125, 1091, 994, 912, 830, 799, 771, 705, 581, 530, 498, 443 cm^{-1} ; ^1H -NMR (300 MHz, CDCl_3): 8.51 (s, 2H), 8.10 (s, 1H), 7.42-7.29 (m, 8H), 7.10 (s, 1H); ^{13}C -NMR (75 MHz, CDCl_3): 162.9, 137.3, 134.7, 132.4 (q, $J = 34.0$), 132.0, 129.8 (m), 129.1, 128.6, 126.9

(m), 122.8 (q, $J = 274$), 77.2. ^{19}F -NMR (282 MHz, CDCl_3): -63.4; HRMS (EI) m/z calculated for $\text{C}_{22}\text{H}_{12}\text{Cl}_2\text{F}_6\text{O}_2$ ($[\text{M}]^+$) 492.0119, found 492.0119.



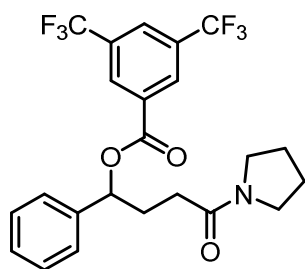
Phenyl(pyridin-4-yl)methyl 3,5-bis(trifluoromethyl)benzoate (54g).

Following general procedure **GPI** using phenyl(pyridin-4-yl)methanol⁵⁵ (370 mg, 2.00 mmol, 1.00 equiv), 3,5-bis(trifluoromethyl)benzoyl chloride (381 μL , 581 mg, 2.10 mmol, 1.05 equiv), 4-DMAP (12 mg, 0.10 mmol, 0.05 equiv), Et_3N (2.0 mL, 1.4 g, 14 mmol, 7.0 equiv), and DCM (20 mL) gave 561 mg (1.32 mmol, 66%) of a white solid after purification on SiO_2 (petrol ether / EtOAc, 4:1). R_f (petrol ether / EtOAc, 4:1): 0.26; mp: 73 $^\circ\text{C}$; IR (neat): 3034, 1730, 1603, 1496, 1458, 1413, 1359, 1273, 1244, 1181, 1124, 999, 914, 847, 792, 771, 756, 699, 654, 620, 597, 478, 438 cm^{-1} ; ^1H -NMR (300 MHz, CDCl_3): 8.64 (d, $J = 5.6$, 2H), 8.55 (s, 2H), 8.11 (s, 1H), 7.46-7.36 (m, 5H), 7.35-7.29 (m, 2H), 7.12 (s, 1H); ^{13}C -NMR (75 MHz, CDCl_3): 162.9, 150.1, 148.2, 137.7, 132.5 (q, $J = 33.8$), 131.8, 129.8 (m), 129.2, 129.1, 128.2, 127.6, 126.9 (sept, $J = 3.7$), 122.8 (q, $J = 274$), 121.5, 77.4; ^{19}F -NMR (282 MHz, CDCl_3): -63.5; HRMS (EI) m/z calculated for $\text{C}_{21}\text{H}_{13}\text{F}_6\text{NO}_2$ ($[\text{M}]^+$) 425.0850, found 425.0847.



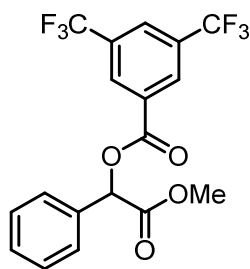
1-Phenylpropyl 3,5-bis(trifluoromethyl)benzoate (54h).

Following general procedure **GPI** using 1-phenylpropan-1-ol (545 mg, 4.00 mmol, 1.00 equiv), 3,5-bis(trifluoromethyl)benzoyl chloride (760 μL , 1.16 g, 4.20 mmol, 1.05 equiv), 4-DMAP (24 mg, 0.20 mmol, 0.05 equiv), Et_3N (4.0 mL, 3.1 g, 28 mmol, 7.0 equiv), and DCM (40 mL) gave 1.23 g (3.27 mmol, 81.7%) of a colorless oil after purification on SiO_2 (petrol ether / EtOAc, 50:1). R_f (petrol ether / EtOAc, 50:1): 0.62; IR (neat): 2974, 2882, 1729, 1624, 1457, 1277, 1244, 1175, 1129, 912, 845, 761, 698, 626, 546, 485, 437 cm^{-1} ; ^1H -NMR (300 MHz, CDCl_3): 8.50 (s, 2H), 8.06 (s, 1H), 7.46-7.28 (m, 5H), 5.95 (t, $J = 7.0$, 1H), 2.24-1.91 (m, 2H), 0.98 (t, $J = 7.4$, 3H); ^{13}C -NMR (101 MHz, CDCl_3): 163.3, 139.6, 132.7, 132.2 (q, $J = 34.0$), 129.7 (m), 128.7, 128.4, 126.7, 126.3 (m), 122.9 (q, $J = 274$), 79.7, 29.2, 10.1; ^{19}F -NMR (376 MHz, CDCl_3): -62.9; HRMS (EI) m/z calculated for $\text{C}_{18}\text{H}_{14}\text{F}_6\text{O}_2$ ($[\text{M}+\text{H}]^+$) 376.0898, found 376.0896.



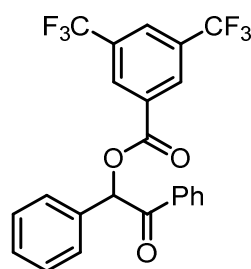
4-Oxo-1-phenyl-4-(pyrrolidin-1-yl)butyl 3,5-bis(trifluoromethyl)benzoate (54i).

Following general procedure *GPI* using 4-hydroxy-4-phenyl-1-(pyrrolidin-1-yl)butan-1-one^{56,57} (467 mg, 2.00 mmol, 1.00 equiv), 3,5-bis(trifluoromethyl)benzoyl chloride (397 μ L, 606 mg, 2.20 mmol, 1.10 equiv), 4-DMAP (12 mg, 0.10 mmol, 0.05 equiv), Et₃N (2.0 mL, 1.6 g, 14 mmol, 7.0 equiv), and DCM (20 mL) gave 899 mg (1.90 mmol, 95%) of a white solid after purification on SiO₂ (petrol ether / EtOAc, 2:1). *R_f* (petrol ether / EtOAc, 2:1): 0.27; mp: 99 °C; IR (neat): 2974, 2878, 1729, 1642, 1444, 1255, 1168, 1035, 1005, 911, 844, 767, 698, 583, 533, 439 cm⁻¹; ¹H-NMR (300 MHz, CDCl₃): 8.49 (s, 2H), 8.06 (s, 1H), 7.49-7.27 (m, 5H), 6.17-6.04 (m, 1H), 3.43 (t, *J* = 7.0, 2H), 3.29 (t, *J* = 6.6, 2H), 2.57-2.20 (m, 4H), 1.97-1.73 (m, 4H); ¹³C-NMR (101 MHz, CDCl₃): 169.9, 163.2, 139.3, 132.6, 132.2 (q, *J* = 34.0), 129.8 (m), 128.7, 128.5, 126.6, 126.4 (sept, *J* = 3.7), 122.9 (q, *J* = 274), 77.9, 46.5, 45.7, 31.1, 30.5, 26.0, 24.3; ¹⁹F-NMR (282 MHz, CDCl₃): -63.4; HRMS (EI) *m/z* calculated for C₂₃H₂₂F₆NO₃ ([*M*+*H*]⁺) 474.1498, found 474.1494.

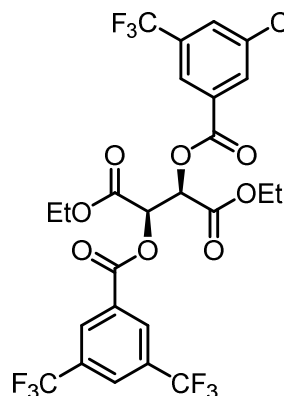


2-Methoxy-2-oxo-1-phenylethyl 3,5-bis(trifluoromethyl)benzoate (54j).

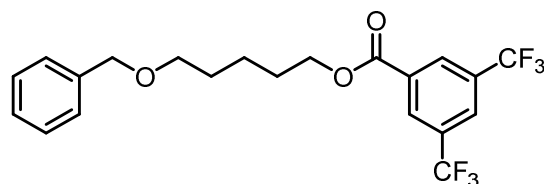
Following general procedure *GPI* using methyl 2-hydroxy-2-phenylacetate (332 mg, 2.00 mmol, 1.00 equiv), 3,5-bis(trifluoromethyl)benzoyl chloride (397 μ L, 606 mg, 2.20 mmol, 1.10 equiv), 4-DMAP (12 mg, 0.10 mmol, 0.05 equiv), Et₃N (2.0 mL, 1.6 g, 14 mmol, 7.0 equiv), and DCM (20 mL) gave 800 mg (1.97 mmol, 98%) of a colorless oil after purification on SiO₂ (petrol ether / EtOAc, 10:1). *R_f* (petrol ether / EtOAc, 6:1): 0.60; IR (neat): 2959, 2361, 1735, 1760, 1624, 1350, 1277, 1240, 1216, 1173, 1130, 1031, 968, 913, 845, 767, 697, 617, 542, 498, 463 cm⁻¹; ¹H-NMR (300 MHz, CDCl₃): 8.54 (s, 2H), 8.10 (s, 1H), 7.61-7.53 (m, 2H), 7.52-7.42 (m, 3H), 6.21 (s, 1H), 3.78 (s, 3H); ¹³C-NMR (75 MHz, CDCl₃): 168.7, 163.4, 133.1, 132.3 (q, *J* = 34.0), 131.4, 130.1 (m), 129.8, 129.1, 127.9, 126.9 (m), 122.8 (q, *J* = 274), 75.8, 53.0; ¹⁹F-NMR (282 MHz, CDCl₃): -63.4; HRMS (EI) *m/z* calculated for C₂₅H₁₈F₆O₄ ([*M*+NH₄]⁺) 424.0978, found 424.0970.

**2-Oxo-1,2-diphenylethyl 3,5-bis(trifluoromethyl)benzoate (54k).**

Following general procedure **GPI** using 2-hydroxy-1,2-diphenylethane (414 mg, 2.00 mmol, 1.00 equiv), 3,5-bis(trifluoromethyl)benzoyl chloride (397 μ L, 606 mg, 2.20 mmol, 1.10 equiv), 4-DMAP (12 mg, 0.10 mmol, 0.05 equiv), Et₃N (2.0 mL, 1.6 g, 14 mmol, 7.0 equiv), and DCM (20 mL) gave 850 mg (1.88 mmol, 98%) of a white solid after purification on SiO₂ (petrol ether / EtOAc, 25:1). *R_f* (petrol ether / EtOAc, 6:1): 0.57; ¹H-NMR (300 MHz, CDCl₃): 8.58 (s, 2H), 8.11 (s, 1H), 8.01 (d, *J* = 7.4, 2H), 7.72-7.50 (m, 3H), 7.50-7.32 (m, 5H), 7.19 (s, 1H); ¹³C-NMR (101 MHz, CDCl₃): 192.7, 163.5, 134.3, 133.8, 132.9, 132.3 (q, *J* = 34.0), 131.7, 130.1 (m), 129.9, 129.5, 129.0, 128.9, 128.8, 126.8 (m), 122.8 (q, *J* = 274), 79.2; ¹⁹F-NMR (282 MHz, CDCl₃): -63.4; HRMS (EI) *m/z* calculated for C₂₅H₁₈F₆O₄ ([M+NH₄]⁺) 470.1185, found 470.1189.

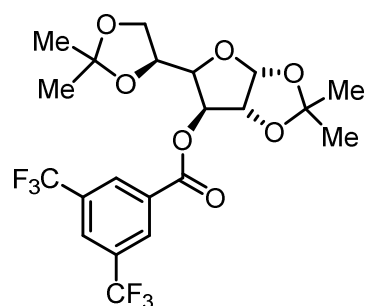
**(2*R*,3*R*)-Diethyl 2,3-bis(3,5-bis(trifluoromethyl)benzoyloxy)succinate (63e).**

Following general procedure **GPI** gave 1.54 g (2.24 mmol, 45% (81% based on 3,5-bis(trifluoromethyl)benzoyl chloride)) of a white solid after purification on SiO₂ (petrol ether / EtOAc, 6:1). *R_f* (petrol ether / EtOAc, 4:1): 0.61; mp: 88 - 90 °C; IR (neat): 2991, 2970, 1760, 1742, 1626, 1459, 1375, 1280, 1219, 1173, 1126, 1057, 938, 905, 847, 802, 767, 695, 680, 525, 492, 436 cm⁻¹; ¹H-NMR (300 MHz, CDCl₃): 8.25 (d, *J* = 1.4, 4H), 8.14 (s, 2H), 6.10 (s, 2H), 4.28 (qd, *J* = 7.2, 1.2, 4H), 1.25 (t, *J* = 7.1, 6H); ¹³C-NMR (75 MHz, CDCl₃): 165.1, 162.6, 132.7 (q, *J* = 34.6), 130.7, 130.0, 127.3, 122.7 (q, *J* = 274), 72.1, 63.0, 14.0; ¹⁹F-NMR (282 MHz, CDCl₃): -63.8; HRMS (EI) *m/z* calculated for C₂₆H₁₉F₁₂O₈ ([M+H]⁺) 687.0883, found 687.0882.

**5-(Benzyloxy)pentyl 3,5-bis(trifluoromethyl)benzoate (68).**

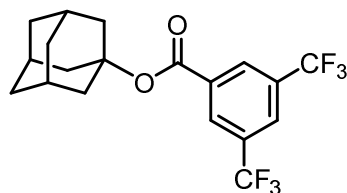
Following general procedure **GPI** using 5-(benzyloxy)pentan-1-ol⁵⁸ (583 mg, 3.00 mmol, 1.00 equiv), 3,5-bis(trifluoromethyl)benzoyl chloride (598 μ L, 912 mg, 3.30 mmol, 1.10 equiv), 4-DMAP (18 mg, 0.15 mmol, 0.05 equiv), Et₃N (3.0 mL, 2.4 g, 21 mmol, 7.0 equiv), and DCM (30 mL) gave 1.26 g (2.91 mmol, 97%) of a colorless oil after purification on SiO₂ (petrol ether

/ EtOAc, 10:1). R_f (petrol ether / EtOAc, 10:1): 0.51; IR (neat): 2941, 2866, 1729, 1621, 1455, 1377, 1277, 1247, 1175, 1134, 965, 912, 844, 770, 734, 698, 614 cm^{-1} ; $^1\text{H-NMR}$ (400 MHz, CDCl_3): 8.48 (s, 2H), 8.06 (s, 1H), 7.38-7.23 (m, 5H), 4.51 (s, 2H), 4.40 (t, $J = 6.7$, 2H), 3.51 (t, $J = 6.3$, 2H), 1.89-1.78 (m, 2H), 1.77-1.65 (m, 2H), 1.60-1.49 (m, 2H); $^{13}\text{C-NMR}$ (101 MHz, CDCl_3): 164.0, 132.6, 132.1 (q, $J = 34.0$), 129.7 (m), 128.4, 127.6, 127.6, 126.3 (m), 122.9 (q, $J = 274$), 73.0, 70.0, 29.4, 28.5, 22.8. $^{19}\text{F-NMR}$ (282 MHz, CDCl_3): -63.4; HRMS (EI) m/z calculated for $\text{C}_{21}\text{H}_{21}\text{F}_6\text{O}_3$ ($[\text{M}+\text{H}]^+$) 435.1389, found 435.1386.



(3a*R*,6*S*,6a*R*)-5-(((*S*)-2,2-dimethyl-1,3-dioxolan-4-yl)-2,2-dimethyltetrahydrofuro[2,3-*d*][1,3]dioxol-6-yl) 3,5-bis(trifluoromethyl)benzoate (69).

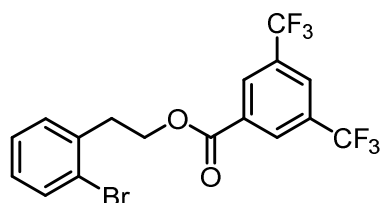
Following general procedure **GPI** using (3a*R*,6*S*,6a*R*)-5-(((*S*)-2,2-dimethyl-1,3-dioxolan-4-yl)-2,2-dimethyltetrahydrofuro[2,3-*d*][1,3]dioxol-6-ol (1.30 g, 5.00 mmol, 1.00 equiv), 3,5-bis(trifluoromethyl)benzoyl chloride (0.91 mL, 1.38 g, 5.00 mmol, 1.00 equiv), 4-DMAP (31 mg, 0.25 mmol, 0.05 equiv), Et_3N (4.9 mL, 3.5 g, 35 mmol, 7.0 equiv), and DCM (50 mL) gave 2.40 g (4.80 mmol, 96%) of a colorless, very viscous oil after purification on SiO_2 (petrol ether / EtOAc, 25:1). R_f (petrol ether / EtOAc, 6:1): 0.65; IR (neat): 2991, 2949, 1738, 1623, 1458, 1375, 1278, 1245, 1131, 1073, 1021, 912, 843, 766, 699 cm^{-1} ; $^1\text{H-NMR}$ (400 MHz, CDCl_3): 8.44 (s, 2H), 8.10 (s, 1H), 5.99 (d, $J = 3.8$ Hz, 1H), 5.55 (d, $J = 1.7$ Hz, 1H), 4.66 (d, $J = 3.8$ Hz, 1H), 4.34 – 4.27 (m, 2H), 4.21 – 4.02 (m, 2H), 1.57 (s, 3H), 1.41 (s, 3H), 1.34 (s, 3H), 1.26 (s, 3H); *Note*: Material thermally decomposed, depicted carbon spectrum is therefore impure. $^{13}\text{C-NMR}$ (75 MHz, CDCl_3): 162.80, 132.45 (q, $J = 34$ Hz), 131.81, 129.77 (m), 126.78 (m), 122.74 (q, $J = 273$ Hz), 112.58, 109.67, 105.15, 83.30, 79.95, 77.94, 72.52, 67.60, 26.87, 26.68, 26.20, 25.02. $^{19}\text{F-NMR}$ (282 MHz, CDCl_3): -63.46; HRMS (ESI) m/z calculated for $\text{C}_{21}\text{H}_{23}\text{F}_6\text{O}_7$ ($[\text{M}+\text{H}]^+$) 501.1342, found 501.1348.



Adamantan-1-yl 3,5-bis(trifluoromethyl)benzoate (70).

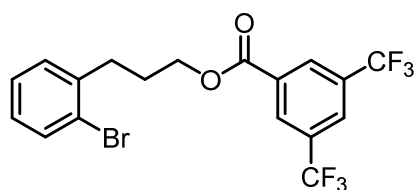
Following general procedure **GPI** using 1-adamantol (761 mg, 5.00 mmol, 1.00 equiv), 3,5-bis(trifluoromethyl)benzoyl chloride (1.38 g, 5.00 mmol, 1.00 equiv), 4-DMAP (31 mg, 0.25 mmol, 0.05 equiv), Et_3N (4.9 mL, 3.6 g, 35 mmol, 7.0 equiv), and DCM (50 mL) gave 1.27 g (3.24 mmol, 65%) of a white solid after purification on SiO_2 (petrol ether / EtOAc, 50:1). R_f (petrol

ether): 0.38; mp: 81 °C; IR (neat): 2914, 2856, 1720, 1624, 1255, 1169, 1129, 1051, 965, 909, 843, 770, 699, 680, 582 cm⁻¹; ¹H-NMR (400 MHz, CDCl₃): 8.41 (s, 2H), 8.02 (s, 1H), 2.28 (s, 9H), 1.73 (s, 6H); ¹³C-NMR (101 MHz, CDCl₃): 162.54, 134.26, 131.91 (q, *J* = 33.9 Hz), 129.58 (m), 125.77 (sept, *J* = 3.8 Hz), 123.00 (q, *J* = 273 Hz), 83.19, 41.32, 36.11, 30.96; ¹⁹F-NMR (282 MHz, CDCl₃): -63.40; HRMS (EI) *m/z* calculated for C₁₉H₁₈F₆O₂ ([M+H]⁺) 392.1211, found 392.1206.



2-Bromophenethyl 3,5-bis(trifluoromethyl)benzoate (98a).

Following general procedure *GPI* using 2-(2-bromophenyl)ethan-1-ol⁵⁹⁻⁶¹ (1.78 g, 8.87 mmol, 1.00 equiv), 3,5-bis(trifluoromethyl)benzoyl chloride (1.77 mL, 2.70 g, 9.78 mmol, 1.10 equiv), Et₃N (2.5 mL, 1.8 g, 17 mmol, 2.0 equiv), and DCM (20 mL) gave 3.51 g (7.96 mmol, 90%) of a colorless oil after purification on SiO₂ (petrol ether / EtOAc, 30:1 to 10:1). *R_f* (petrol ether / EtOAc, 50:1): 0.54; IR (neat): 3067, 2994, 1731, 1621, 1472, 1276, 1243, 1175, 1128, 975, 912, 846, 749, 699 cm⁻¹; ¹H-NMR (300 MHz, CDCl₃): 8.45 (s, 2H), 8.05 (s, 1H), 7.58 (dd, *J* = 7.9, 0.9 Hz, 1H), 7.34 – 7.24 (m, 2H), 7.18 – 7.10 (m, 1H), 4.63 (t, *J* = 6.8 Hz, 2H), 3.28 (t, *J* = 6.8 Hz, 2H); ¹³C-NMR (75 MHz, CDCl₃): 163.80, 136.78, 133.13, 132.30, 132.15 (q, *J* = 34 Hz), 129.81 (m), 128.73, 127.64, 126.36 (m), 124.64, 122.87 (q, *J* = 273 Hz), 65.06, 35.24; HRMS (APCI) *m/z* calculated for C₁₇H₁₂BrF₆O₂ ([M+H]⁺) 440.9919, found 440.9911.



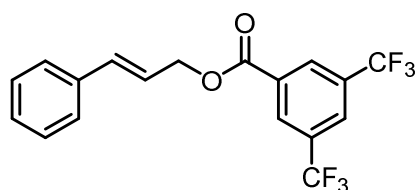
3-(2-Bromophenyl)propyl 3,5-bis(trifluoromethyl)benzoate (98b).

Following general procedure *GPI* using 3-(2-bromophenyl)propan-1-ol⁵⁹⁻⁶¹ (5.12 g, 23.8 mmol, 1.00 equiv), 3,5-bis(trifluoromethyl)benzoyl chloride (5.07 mL, 7.74 g, 28.0 mmol, 1.10 equiv), Et₃N (7.1 mL, 5.1 g, 51 mmol, 2.0 equiv), and DCM (50 mL) gave 10.8 g (23.6 mmol, 99%) of a colorless oil after purification on SiO₂ (petrol ether / EtOAc, 30:1 to 10:1). *R_f* (petrol ether / EtOAc, 50:1): 0.55; IR (neat): 3067, 2961, 1729, 1622, 1456, 1376, 1245, 1174, 1128, 1010, 912, 844, 748, 698, 680, cm⁻¹; ¹H-NMR (400 MHz, CDCl₃): 8.42 (s, 2H), 8.02 (s, 1H), 7.49 (d, *J* = 8.0 Hz, 1H), 7.23 – 7.13 (m, 3H), 7.06 – 6.97 (m, 1H), 4.41 (t, *J* = 6.4 Hz, 2H), 2.89 (t, *J* = 7.4 Hz, 2H), 2.17 – 2.05 (m, 2H); ¹³C-NMR (75 MHz, CDCl₃): 163.90, 140.19, 133.01, 132.42, 132.11 (q, *J* = 34 Hz), 130.38, 129.75 (m), 128.01, 127.61, 126.33 (m), 124.39, 122.89 (q, *J* = 273 Hz), 65.55,

32.77, 28.73; HRMS (APCI) m/z calculated for $C_{18}H_{14}BrF_6O_2$ ($[M+H]^+$) 455.0076, found 455.0071.

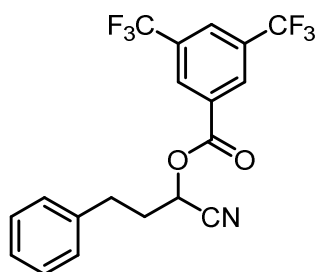
General procedure for the synthesis of benzoate esters *via* the acid anhydride (**GPII**)

A 50 mL Schlenk flask equipped with a magnetic stir bar was charged with an alcohol (2.00 mmol, 1.00 equiv), 3,5-bis(trifluoromethyl)benzoic anhydride (**9**, 1.20 g, 2.40 mmol, 1.20 equiv), Et₃N (0.56 mL, 0.41 g, 4.0 mmol, 2.0 equiv), and DCM (20 mL). The mixture was stirred at room temperature for 2 h. The solvent was evaporated under reduced pressure and the residue was redissolved in 20 mL EtOAc and extracted with 20 mL Na₂CO₃ (aq, 10%) and 20 mL H₂O. The united aqueous phases were acidified with 6 M HCl to give 3,5-bis(trifluoromethyl)benzoic acid (**5**) as a white solid which was filtered and dried *in vacuo*. The organic phase was evaporated and purified by flash chromatography.



Cinnamyl 3,5-bis(trifluoromethyl)benzoate (**63a**).

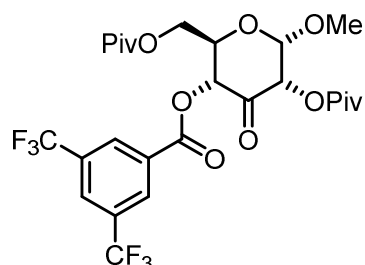
Following general procedure **GPII** using (*E*)-3-phenylprop-2-en-1-ol (671 mg, 5.00 mmol, 1.00 equiv), 3,5-bis(trifluoromethyl)benzoic anhydride (**9**, 2.74 g, 5.50 mmol, 1.10 equiv), Et₃N (1.40 mL, 1.01 g, 10.0 mmol, 2.0 equiv), and DCM (25 mL) gave 0.890 g (3.45 mmol, 69%) of a colorless oil after purification on SiO₂ (petrol ether / EtOAc, 20:1). *R_f* (petrol ether / EtOAc, 10:1): 0.46; IR (neat): 3043, 2953, 1729, 1623, 1450, 1368, 1239, 1174, 1127, 946, 844, 769, 697 cm⁻¹; ¹H-NMR (300 MHz, CDCl₃): 8.52 (s, 2H), 8.07 (s, 1H), 7.47 – 7.41 (m, 2H), 7.39 – 7.27 (m, 3H), 6.78 (d, *J* = 15.8 Hz, 1H), 6.42 (dt, *J* = 15.8, 6.6 Hz, 1H), 5.05 (dd, *J* = 6.6, 0.9 Hz, 2H); ¹³C-NMR (75 MHz, CDCl₃): 163.79, 135.82, 135.78, 132.38, 132.21 (q, *J* = 34 Hz), 129.87 (m), 128.72, 128.46, 126.76, 126.42 (m), 122.06, 66.84; ¹⁹F-NMR (282 MHz, CDCl₃): -63.43; HRMS (CI) *m/z* calculated for C₁₈H₁₂F₆O₂ ([M]⁺) 374.0736, found 347.0723.



1-Cyano-3-phenylpropyl 3,5-bis(trifluoromethyl)benzoate (**63b**).

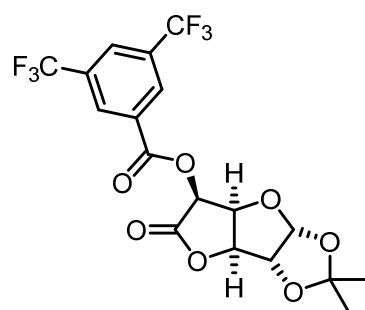
Following general procedure **GPII** using 2-hydroxy-4-phenylbutanenitrile⁶² gave 0.683 g (1.70 mmol, 85%) of a colorless oil after purification on SiO₂ (petrol ether / EtOAc, 10:1). *R_f* (petrol ether / EtOAc, 4:1): 0.82; IR (neat): 2928, 2855, 1743, 1621, 1496, 1456, 1387, 1278, 1235, 1177, 1133, 1030, 993, 911, 845, 761, 732, 697, 681, 650, 486 cm⁻¹; ¹H-NMR (300 MHz, CDCl₃): 8.40 (s, 2H), 8.13 (s, 1H), 7.35-7.15 (m, 5H), 5.59 (t, *J* = 6.8, 1H), 3.05-2.85 (m, 2H), 2.47 (q, *J* = 7.1, 2H); ¹³C-NMR (75 MHz, CDCl₃): 162.3, 138.6, 132.6 (q, *J* = 34.0), 130.3, 130.0 (m),

128.9, 128.3, 127.4 (m), 126.9, 122.6 (q, $J = 274$), 116.1, 66.3, 33.7, 31.0; ^{19}F -NMR (282 MHz, CDCl_3): -63.5; HRMS (ESI) m/z calculated for $\text{C}_{19}\text{H}_{14}\text{F}_6\text{NO}_2$ ($[\text{M}+\text{H}]^+$) 402.0923, found 402.0929.



(2*R*,3*R*,5*S*,6*S*)-6-methoxy-4-oxo-5-(pivaloyloxy)-2-(pivaloxymethyl)tetrahydro-2*H*-pyran-3-yl 3,5-bis(trifluoromethyl)benzoate (63c).

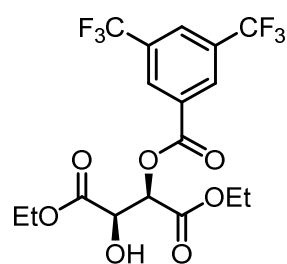
Following general procedure *GPII* using (2*S*,3*S*,5*R*,6*R*)-5-hydroxy-2-methoxy-4-oxo-6-(pivaloyloxymethyl)tetrahydro-2*H*-pyran-3-yl pivalate⁶³ (258 mg, 0.716 mmol, 1.00 equiv), 3,5-bis(trifluoromethyl)benzoic anhydride (**9**, 392 mg, 0.787 mmol, 1.10 equiv), Pr_2NEt (249 μL , 185 mg, 1.43 mmol, 2.0 equiv), and DCM (7 mL) gave 207 mg (0.803 mmol, 76% based on benzoate that was employed and not incorporated in the product) 3,5-bis(trifluoromethyl)benzoic acid (**5**) as a white powder and 309 mg (0.514 mmol, 71.8%) (2*R*,3*R*,5*S*,6*S*)-6-methoxy-4-oxo-5-(pivaloyloxy)-2-(pivaloxymethyl)tetrahydro-2*H*-pyran-3-yl 3,5-bis(trifluoromethyl)benzoate (**63c**) as a white solid after purification on SiO_2 (petrol ether / EtOAc, 6:1 to 3:1). R_f (petrol ether / EtOAc, 4:1): 0.48; mp: 46 $^\circ\text{C}$; IR (neat): 2997, 1734, 1624, 1370, 1278, 1246, 1127, 1055, 1036, 911, 846, 762, 701, 682 cm^{-1} ; ^1H -NMR (300 MHz, CDCl_3): 8.49 (s, 2H), 8.10 (s, 1H), 5.62 (dd, $J = 10.0, 1.0$, 1H), 5.45 (dd, $J = 4.2, 1.0$, 1H), 4.24 (d, $J = 4.2$, 1H), 4.47-4.40 (m, 2H), 4.39-4.32 (m, 1H), 3.52 (s, 3H), 1.27 (s, 9H), 1.24 (s, 9H); ^{13}C -NMR (75 MHz, CDCl_3): 192.8, 177.9, 177.0, 162.2, 132.4 (q, $J = 34.0$), 130.9, 130.1 (d, $J = 3.0$), 127.0 (m), 122.6 (q, $J = 274$), 100.0, 74.4, 73.3, 69.6, 62.2, 56.0, 39.0, 38.9, 27.1, 27.0; ^{19}F -NMR (282 MHz, CDCl_3): -63.5; HRMS (ESI) m/z calculated for $\text{C}_{26}\text{H}_{30}\text{F}_6\text{NaO}_9$ ($[\text{M}+\text{Na}]^+$) 623.1686, found 623.1686.



1,2-*O*-isopropylidene-5-*O*-(3,5-bis(trifluoromethyl)benzoyl)- α -D-xylohexofuranurono-6,3-lactone (63d).

Following general procedure *GPII* using 1,2-*O*-isopropylidene-5-*O*-(3,5-bis(trifluoromethyl)benzoyl)- α -D-xylohexofuranurono-6,3-lactone⁶⁴ (649 mg, 3.00 mmol, 1.00 equiv), 3,5-bis(trifluoromethyl)benzoic anhydride (**9**, 1.50 g, 3.00 mmol, 1.00 equiv), Pr_2NEt (1.05 mL, 775 mg, 6.00 mmol, 2.0 equiv), and DCM (30 mL) gave 432 mg (0.947 mmol, 31.6%) 1,2-*O*-isopropylidene-5-*O*-(3,5-bis(trifluoromethyl)benzoyl)- α -D-xylohexofuranurono-6,3-lactone (**63d**) as a white solid after purification on SiO_2 (petrol

ether / EtOAc 3:1). R_f (petrol ether / EtOAc, 2:1): 0.66; mp: 120-122 °C; IR (neat): 2998, 1823, 1748, 1619, 1380, 1281, 1243, 1177, 1132, 1084, 1028, 912, 844, 818, 769, 700, 682, 507, 438 cm^{-1} ; ^1H -NMR (300 MHz, CDCl_3): 8.54 (s, 2H), 8.12 (s, 1H), 6.07 (d, $J = 3.6$, 1H), 5.78 (d, $J = 4.4$, 1H), 5.20 (dd, $J = 4.3, 3.0$, 1H), 4.99 (d, $J = 3.0$, 1H), 4.90 (d, $J = 3.6$, 1H), 1.52 (s, 3H), 1.36 (s, 3H); ^{13}C -NMR (75 MHz, CDCl_3): 169.0, 162.9, 132.5 (q, $J = 34.0$), 130.5, 130.3 (d, $J = 3.0$), 127.3 (m), 122.6 (q, $J = 273$), 113.8, 107.0, 82.5, 82.4, 76.9, 71.0, 26.9, 26.5; ^{19}F -NMR (282 MHz, CDCl_3): -63.4; HRMS (EI) m/z calculated for $\text{C}_{18}\text{H}_{14}\text{F}_6\text{O}_7$ ($[\text{M}]^+$) 456.0644, found 456.0647.

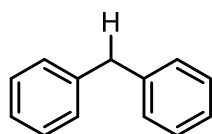
Selective synthesis of monoacylated tartrate**(2R,3R)-diethyl 2-(3,5-bis(trifluoromethyl)benzoyloxy)-3-hydroxysuccinate (63f).**

A 100 mL Schlenk flask equipped with a magnetic stir bar was charged with CuCl_2 (81.3 mg, 0.605 mmol, 0.100 equiv), (2R,3R)-diethyl 2,3-dihydroxysuccinate (**8**, 1.25 g, 6.05 mmol, 1.00 equiv) and DCM (50 mL). A solution of 3,5-bis(trifluoromethyl)benzoic anhydride in DCM (34 mL, 0.18 M, 6.1 mmol, 1.0 equiv) was added and the mixture was stirred at ambient temperature for one week and refluxed for another week. The reaction mixture was transferred to a separation funnel with 150 mL EtOAc, washed twice with 50 mL 10% Na_2CO_3 (aq.), 50 mL water, and 50 mL brine. The combined aqueous phases were boiled up, cooled back to room temperature and acidified with conc. HCl (aq.) upon which the white precipitate was filtered and washed with 50 mL water to give 1.31 g (5.08 mmol, 67% based on benzoate that was employed and not incorporated in the product) 3,5-bis(trifluoromethyl)benzoic acid. The organic phases were dried over Na_2SO_4 , evaporated and the resulting solid was purified on SiO_2 (petrol ether / EtOAc, 6:1 to 2:1) to give 2.07 g (4.63 mmol, 76.5%) (2R,3R)-diethyl 2-(3,5-bis(trifluoromethyl)benzoyloxy)-3-hydroxysuccinate a white solid. R_f (petrol ether / EtOAc, 4:1): 0.34; mp: 98 °C; IR (neat): 3378, 2986, 2944, 1737, 1707, 1627, 1391, 1373, 1280, 1230, 1177, 1124, 1050, 917, 847, 768, 700, 681, 586, 538, 495, 439 cm^{-1} ; ^1H -NMR (300 MHz, CDCl_3): 8.48 (s, 2H), 8.10 (s, 1H), 5.72 (d, $J = 2.3$, 1H), 4.89 (d, $J = 2.0$, 1H), 4.32 (q, $J = 7.1$, 2H), 4.27 (q, $J = 7.1$, 2H), 3.45 (brs, 1H), 1.32 (t, $J = 7.1$, 3H), 1.23 (t, $J = 7.1$, 3H); ^{13}C -NMR (75 MHz, CDCl_3): 170.6, 165.9, 162.8, 132.4 (q, $J = 34.0$), 131.0, 130 (d, $J = 3.0$), 127.1 (m), 122.7 (q, $J = 274$), 74.3, 70.5, 62.9, 62.6, 14.1; ^{19}F -NMR (282 MHz, CDCl_3): -63.5; HRMS (EI) m/z calculated for $\text{C}_{17}\text{H}_{17}\text{F}_6\text{O}_7$ ($[\text{M}+\text{H}]^+$) 447.0873, found 447.0868.

3.5 Photochemical defunctionalitive deoxygenations

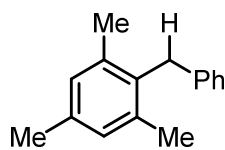
General procedure for defunctionalitive deoxygenations (*GPIII*)

A Schlenk tube was charged with $[\text{Ir}(\text{ppy})_2(\text{dtb-bpy})](\text{PF}_6)^{65,66}$ (3.7 mg, 4.0 μmol , 2.0 mol%), (trifluoromethyl)benzoate ester (0.200 mmol, 1.00 equiv), sealed with a screw-cap and subsequently evacuated and backfilled with N_2 (3x). MeCN (5 ml), Pr_2NEt (70 μL , 52 mg, 0.40 mmol, 2.0 equiv), and degassed water (0.36 mL, 0.36 g, 20 mmol, 100 equiv) was added and the reaction mixture was magnetically stirred until a homogeneous solution was obtained. The reaction mixture was degassed by freeze-pump-thaw (5x) and the screw-cap was replaced with a Teflon sealed inlet for a glass rod, through which irradiation with a 455 nm high power LED took place from above (1 h for every 0.2 mmol of benzoate) while the reaction was magnetically stirred and heated in an aluminum block from below. Afterwards the reaction mixture was diluted with 20 mL Et_2O , washed with 10 mL 10% Na_2CO_3 , 10 mL H_2O , 10 mL brine, and dried over Na_2SO_4 . The combined aqueous phases were acidified with HCl (conc.) upon which (trifluoromethyl)benzoic acid precipitated, which was collected by filtration and washed with water. After evaporation of the organic phase, the product was purified by filtration through a short plug of flash silica gel with a mixture of petrol ether and ethyl acetate.



Diphenylmethane (**46a**).^{67,68}

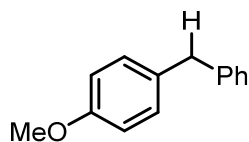
Following general procedure *GPIII* using benzhydryl 3,5-bis(trifluoromethyl)benzoate (**3a**) (424 mg, 1.00 mmol, 1.00 equiv), $[\text{Ir}(\text{ppy})_2(\text{dtb-bpy})](\text{PF}_6)$ (18.3 mg, 20.0 μmol , 2.00 mol%), Pr_2NEt (348 μL , 258 mg, 2.00 mmol, 2.00 equiv), degassed water (1.8 mL, 1.8 g, 0.10 mol, 100 equiv), and MeCN (25 mL) gave 160 mg (0.949 mmol, 95%) of a colorless oil after filtration through SiO_2 with petrol ether. ^1H NMR (300 MHz, CDCl_3): 7.33–7.16 (m, 10H), 4.00 (s, 2H).



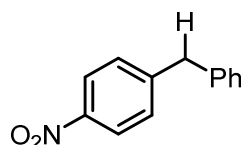
2-Benzyl-1,3,5-trimethylbenzene (**46b**).⁶⁹

Following general procedure *GPIII* gave 38.4 mg (0.182 mmol, 91%) of a colorless oil after filtration through SiO_2 with petrol ether. ^1H -NMR (400

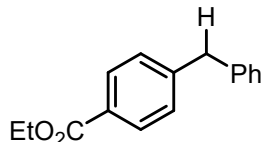
MHz, CDCl₃): 7.29-7.11 (m, 3H), 7.07-6.97 (m, 2H), 6.91 (s, 2H), 4.03 (s, 2H), 2.31 (s, 3H), 2.22 (s, 6H).

**1-Benzyl-4-methoxybenzene (46c).**⁶⁹

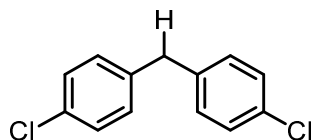
Following general procedure **GP111** gave 34.4 mg (0.174 mmol, 87%) of a colorless oil after filtration through SiO₂ with petrol ether. ¹H-NMR (400 MHz, CDCl₃): 7.32-7.25 (m, 2H), 7.23-7.16 (m, 3H), 7.14-7.08 (m, 2H), 6.85-6.81 (m, 2H), 3.94 (s, 2H), 3.79 (s, 3H).

**1-Benzyl-4-nitrobenzene (46d).**⁷⁰

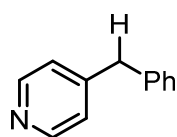
Following general procedure **GP111** gave 38.7 mg (0.181 mmol, 91%) of a yellow oil after purification on SiO₂ (petrol ether / EtOAc, 30:1). ¹H-NMR (300 MHz, CDCl₃): 8.19-8.09 (m, 2H), 7.39-7.14 (7H), 4.08 (s, 2H).

**Ethyl 4-benzylbenzoate (46e).**⁶⁷

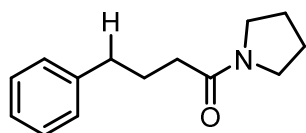
Following general procedure **GP111** gave 44.7 mg (0.186 mmol, 93%) of a colorless oil after filtration through SiO₂ with petrol ether / EtOAc = 50:1. ¹H-NMR (400 MHz, CDCl₃): 7.99-7.94 (m, 2H), 7.33-7.15 (m, 7H), 4.36 (q, *J* = 7.2, 2H), 4.04 (s, 2H), 1.28 (t, *J* = 7.2, 3H).

**Bis(4-chlorophenyl)methane (46f).**⁷¹

Following general procedure **GP111** gave 43.6 mg (0.183 mmol, 92%) of a colorless oil after filtration through SiO₂ with petrol ether. ¹H-NMR (300 MHz, CDCl₃): 7.30-7.22 (m, 4H), 7.13-7.05 (m, 4H), 3.92 (s, 2H).

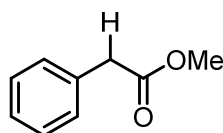
**4-Benzylpyridine (46g).**⁶⁹

Following general procedure **GP111** gave 29.1 mg (0.171 mmol, 86%) of a colorless oil after purification on SiO₂ (petrol ether / EtOAc, 2:1). ¹H-NMR (300 MHz, CDCl₃): 8.51 (s, 2H), 7.38-7.08 (m, 7H), 3.98 (s, 2H).



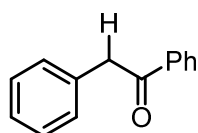
4-Phenyl-1-(pyrrolidin-1-yl)butan-1-one (46i).

Following general procedure **GP111** gave 34.5 mg (0.158 mmol, 79%) of a slightly yellow oil after purification on SiO₂ (petrol ether / EtOAc, 1:1). ¹H-NMR (300 MHz, CDCl₃): 7.30-7.24 (m, 2H), 7.21-7.15 (m, 3H), 3.45 (t, *J* = 7.0, 2H), 3.32 (t, *J* = 6.7, 2H), 2.68 (t, *J* = 7.5, 2H), 2.26 (t, *J* = 7.3, 2H), 2.05-1.77 (m, 6H).



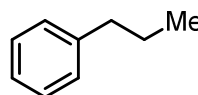
Methyl 2-phenylacetate (46j).⁷²

Following general procedure **GP111** using 2-methoxy-2-oxo-1-phenylethyl 3,5-bis(trifluoromethyl)benzoate (**54j**) (305 mg, 0.750 mmol, 1.00 equiv), [Ir(ppy)₂(dtb-bpy)](PF₆) (13.9 mg, 15.2 μmol, 2.02 mol%), Pr₂NEt (209 μL, 1.50 mmol, 2.00 equiv), degassed water (1.35 mL, 1.35 g, 75.0 mmol, 100 equiv), and MeCN (19 mL) gave 93.7 mg (0.624 mmol, 83%) of a colorless oil after filtration through SiO₂ with petrol ether / EtOAc = 10:1. ¹H-NMR (300 MHz, CDCl₃): 7.41-7.21 (m, 5H), 3.70 (s, 3H), 3.64 (s, 2H).



1,2-Diphenylethanone (46k).⁷³

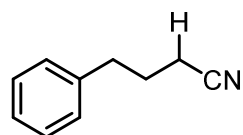
Following general procedure **GP111** gave 26.3 mg (0.134 mmol, 67%) of a colorless oil after filtration through SiO₂ with petrol ether / EtOAc = 25:1. ¹H-NMR (400 MHz, CDCl₃): 8.07-8.00 (m, 2H), 7.60-7.53 (m, 1H), 7.50-7.46 (m, 2H), 7.37-7.31 (m, 2H), 7.30-7.23 (m, 3H), 4.30 (s, 2H).



Propylbenzene (64a).

Following general procedure **GP111** using cinnamyl 3,5-bis(trifluoromethyl)benzoate (74.9 mg, 0.200 mmol, 1.00 equiv) gave a mixture of (Z)-β-methylstyrene, (E)-β-methylstyrene, and allylbenzene (53:21:26) in quantitative yield determined by ¹H-NMR and GC-FID and with an internal standard. 24 mg Pd/C (10%) was added to the reaction mixture,

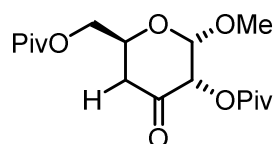
the atmosphere was exchanged to 1 atm of H₂. The mixture was stirred for 20 h at room temperature. GC-FID analysis showed quantitative formation of propylbenzene.



4-phenylbutanenitrile (64b).⁷⁴

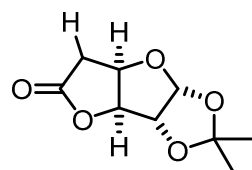
Following general procedure *GP111* gave 24.9 mg (0.171 mmol, 86%) of a colorless oil after filtration through SiO₂ with petrol ether / EtOAc = 6:1.

¹H-NMR (400 MHz, CDCl₃): 7.36-7.28 (m, 2H), 7.26-7.16 (m, 3H), 2.78 (t, *J* = 7.4, 2H), 2.32 (t, *J* = 7.1, 2H), 1.99 (quint, *J* = 7.2, 2H).



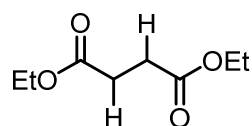
((2*S*,5*S*,6*S*)-6-methoxy-4-oxo-5-(pivaloyloxy)tetrahydro-2H-pyran-2-yl)methyl pivalate (64c).⁶³

Following general procedure *GP111* using (2*R*,3*R*,5*S*,6*S*)-6-methoxy-4-oxo-5-(pivaloyloxy)-2-(pivaloyloxymethyl)tetrahydro-2H-pyran-3-yl 3,5-bis(trifluoromethyl)benzoate (**6b**, 120 mg, 0.200 mmol, 1.00 equiv) gave 54.5 mg (0.158 mmol, 79%) of a white solid after column chromatography on flash silica gel with petrol ether/EtOAc = 3:1. ¹H-NMR (300 MHz, CDCl₃): 5.19 (d, *J* = 4.0, 1H), 5.07 (d, *J* = 4.0, 1H), 4.28-4.07 (m, 3H), 3.37 (s, 3H), 2.64-2.40 (m, 2H), 1.21 (s, 9H), 1.16 (s, 9H).



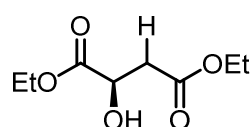
5-Deoxy-1,2-*O*-isopropylidene-α-D-xylo-hexofuranurono-6,3-lactone (64d).⁷⁵

Following general procedure *GP111* using 1,2-*O*-isopropylidene-5-*O*-(3,5-bis(trifluoromethyl)benzoyl)-α-D-xylo-hexofuranurono-6,3-lactone (**63d**, 91.3 mg, 0.200 mmol, 1.00 equiv) gave 5.6 mg (0.028 mmol, 14%) of a colorless oil after column chromatography on flash silica gel with petrol ether/EtOAc = 2:1. ¹H-NMR (300 MHz, CDCl₃): 5.90 (d, *J* = 3.8, 1H), 4.94 (q, *J* = 2.8, 1H), 4.77 (t, *J* = 4.1, 2H), 2.66 (d, *J* = 2.8, 2H), 1.44 (s, 3H), 1.28 (s, 3H).



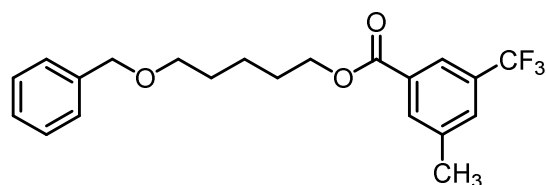
Diethyl succinate (64e).⁶⁸

After following general procedure **GP111** using (2*R*,3*R*)-diethyl 2,3-bis(3,5-bis(trifluoromethyl)benzoyloxy)succinate (**63e**) (686 mg, 1.00 mmol, 1.00 equiv), [Ir(ppy)₂(dtb-bpy)](PF₆) (18.3 mg, 20.0 μmol, 2.00 mol%), Pr₂NEt (1.75 mL, 1.30 g, 10.0 mmol, 10.0 equiv), degassed water (1.8 mL, 1.8 g, 0.10 mol, 100 equiv), and MeCN (25 mL), 1,4-dimethoxybenzene (138 mg, 1.00 mmol, 1.00 equiv) was added to the crude mixture and an aliquot was subjected to ¹H-NMR analysis. The yield of diethyl succinate (**64e**) was determined to be 69%.



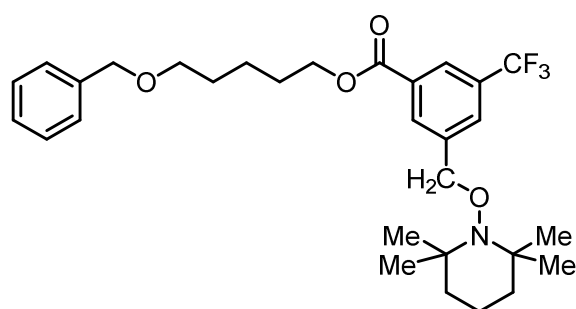
(*R*)-Diethyl 2-hydroxysuccinate (**64f**).⁶⁸

Following general procedure **GP111** using (2*R*,3*R*)-diethyl 2-(3,5-bis(trifluoromethyl)benzoyloxy)-3-hydroxysuccinate (**63f**) (446 mg, 1.00 mmol, 1.00 equiv), [Ir(ppy)₂(dtb-bpy)](PF₆) (18.3 mg, 20.0 μmol, 2.00 mol%), Pr₂NEt (348 μL, 258 mg, 2.00 mmol, 2.00 equiv), degassed water (1.8 mL, 1.8 g, 0.10 mol, 100 equiv), and MeCN (25 mL) gave 188 mg (0.989 mmol, 99%) of a colorless oil after filtration through a short plug of flash silica gel with petrol ether/EtOAc = 1:1. ¹H-NMR (300 MHz, CDCl₃): 4.47 (brs, 1H), 4.34-4.06 (m, 4H), 3.23 (brs, 1H), 2.91-2.73 (m, 2H), 1.30 (t, *J* = 7.2, 3H), 1.26 (t, *J* = 7.2, 3H).



5-(benzyloxy)pentyl 3-methyl-5-(trifluoromethyl)benzoate (**71**).

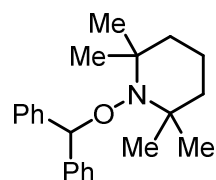
Following general procedure **GP111** using 5-(benzyloxy)pentyl 3,5-bis(trifluoromethyl)-benzoate (**68**) (434 mg, 1.00 mmol, 1.00 equiv), [Ir(ppy)₂(dtb-bpy)](PF₆) (18.3 mg, 20.0 μmol, 2.00 mol%), Pr₂NEt (1.74 mL, 1.29 g, 10.0 mmol, 10.0 equiv), degassed water (1.8 mL, 1.8 g, 0.10 mol, 100 equiv), and MeCN (25 mL) gave 293 mg (0.770 mmol, 77%) of a colorless oil after filtration through SiO₂ with petrol ether. R_f (petrol ether / EtOAc, 6:1): 0.40; IR (neat): 2943, 2860, 1722, 1612, 1455, 1390, 1352, 1247, 1199, 1166, 1123, 973, 855, 769, 734, 694, 614 cm⁻¹; ¹H-NMR (300 MHz, CDCl₃): 8.09 (s, 1H), 8.02 (s, 1H), 7.61 (s, 1H), 7.36-7.23 (m, 5H), 4.51 (s, 2H), 4.35 (t, *J* = 6.7, 2H), 3.51 (t, *J* = 6.4, 2H), 2.47 (s, 3H), 1.86-1.75 (m, 2H), 1.75-1.65 (m, 2H), 1.60-1.48 (m, 2H); ¹³C-NMR (75 MHz, CDCl₃): 165.6, 139.3, 138.5, 133.4, 131.2, 130.7, 130.0 (m), 128.4, 127.7, 127.6, 123.8 (q, *J* = 274), 123.7 (m), 73.0, 70.1, 65.5, 29.4, 28.5, 22.8, 21.3; ¹⁹F-NMR (376 MHz, CDCl₃): -62.7; HRMS (EI) *m/z* calculated for C₂₁H₂₄F₃O₃ ([M+H]⁺) 381.1672, found 381.1668.



5-(benzyloxy)pentyl 3-((2,2,6,6-tetramethylpiperidin-1-yloxy)methyl)-5-(trifluoromethyl)-benzoate (**75**).

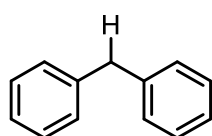
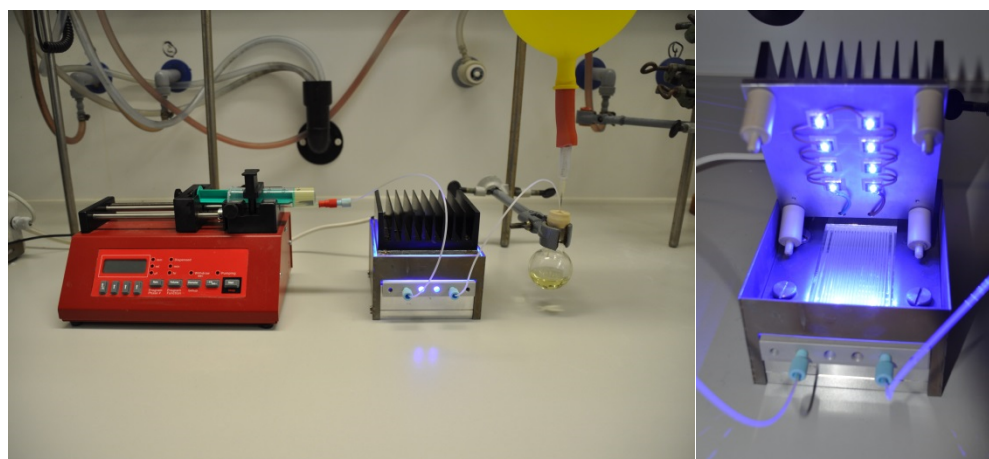
Following general procedure *GP111* using 5-(benzyloxy)pentyl 3,5-bis(trifluoromethyl)benzoate (**68**) (86.9 mg, 0.200 mmol, 1.00 equiv), [Ir(ppy)₂(dtb-bpy)](PF₆) (3.7 mg, 4.0 μmol, 2.00 mol%), Pr₂NEt (348 μL, 258 mg, 2.00 mmol, 10.0 equiv), degassed water (360 μL, 360 mg, 20.0 mmol, 100 equiv), TEMPO (28.2 mg, 0.180 mmol, 0.900 equiv), and MeCN (5 mL) gave 30.1 mg of a colorless oil containing **75** and **71** (3:1, ¹H-NMR integration) after purification on SiO₂ (petrol ether / EtOAc, 100:0 to 10:1). **75**: ¹H-NMR (300 MHz, CDCl₃): 8.22-8.15 (m, 2H), 7.79 (s, 1H), 7.39-7.22 (m, 5H), 4.91 (s, 2H), 4.51 (s, 2H), 4.42-4.30 (m, 2H), 3.56-3.43 (m, 2H), 1.90-1.44 (m, 12H), 1.22 (s, 6H), 1.16 (s, 6H); ¹⁹F-NMR (282 MHz, CDCl₃): -63.1; HRMS (EI) m/z calculated for C₃₀H₄₁F₃NO₄ ([M+H]⁺) 536.2982, found 536.2993.

*Note: The obtained material was not very pure. Peaks of **75** and **71** are superpositioned in the ¹H-NMR spectrum.*



1-(Benzhydryloxy)-2,2,6,6-tetramethylpiperidine (**62**).

Following general procedure *GP111* using benzhydryl 3,5-bis(trifluoromethyl)benzoate (**54a**) (84.9 mg, 0.200 mmol, 1.00 equiv), [Ir(ppy)₂(dtb-bpy)](PF₆) (3.7 mg, 4.0 μmol, 2.00 mol%), Pr₂NEt (348 μL, 258 mg, 2.00 mmol, 10.0 equiv), TEMPO (**61**, 28.2 mg, 0.180 mmol, 0.900 equiv), and MeCN (5 mL) gave a red material after evaporation of the solvent under reduced pressure. The title compound was found in this mixture mainly consisting of deoxygenation product diphenylmethane: HRMS (EI) m/z calculated for C₂₂H₂₂NO ([M+H]⁺) 324.2322, found 324.2322.

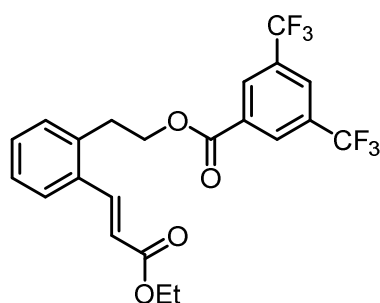
***In situ* acylation and deoxygenations in a microreactor****Diphenylmethane (46).**^{67,68}

A 100 mL Schlenk flask equipped with a magnetic stir bar was charged with diphenylmethanol (**51**, 184 mg, 1.00 mmol, 1.00 equiv) and 3,5-bis(trifluoromethyl)benzoic anhydride (**67**, 548 mg, 1.10 mmol, 1.10 equiv), sealed with a screw-cap and subsequently evacuated and backfilled with N₂ (3x). MeCN (5 mL) and Et₃N (0.70 mL, 0.51 g, 5.0 mmol, 5.0 equiv) were added and the mixture was stirred at 60 °C for 18 h. The reaction mixture was diluted with 16 mL MeCN and 1.8 mL water and [Ir(ppy)₂(dtb-bpy)](PF₆) (0.9 mg, 1 μmol, 0.1 mol%) were added. The reaction mixture was degassed by sparging with N₂ for 30 min and pumped through a micro reactor equipped with 8 LED's at a flowrate of 4.0 mL/h (0.17 mmol/h) *via* a syringe pump. The reaction mixture was evaporated, 20 mL Et₂O was added and the mixture was subsequently washed with 2 x 10 mL 10% Na₂CO₃, 10 mL H₂O, and dried over Na₂SO₄. The combined aqueous phases were acidified with 6 M HCl upon which a white solid precipitated, which was collected by filtration and washed with water to give 3,5-bis(trifluoromethyl)benzoic acid (513 mg, 1.99 mmol, 90%). After evaporation of the organic phase, the obtained oil was purified by filtration through a short plug of SiO₂ with petrol ether to give 153 mg (0.911 mmol, 91%) of diphenylmethane (**4a**) as a colorless oil.

3.6 Synthesis of unactivated substrates for intramolecular cyclizations

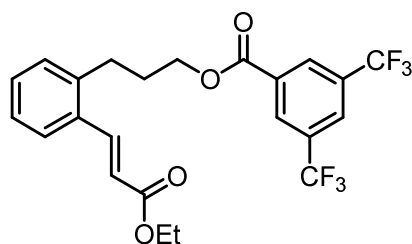
General procedure for Heck reactions (*GPIV*)

A Schlenk flask was charged with aryl halide (1.00 mmol, 1.00 equiv) and toluene (0.1 M). Pd(OAc)₂ (9.0 mg, 40 μmol, 4.0 mol%), triphenylphosphine (21 mg, 80 μmol, 8.0 mol%), ethyl acrylate (164 μL, 150 mg, 1.50 mmol, 1.50 equiv), and Et₃N (418 μL, 303 mg, 3.00 mmol, 3.00 equiv) were added and the reaction mixture was stirred for 5 min at room temperature after which it was refluxed for 16 h. The resulting black suspension was filtered through a plug of celite with the help of DCM. 10 mL H₂O was added to the filtrate and the layers were separated. The aqueous layer was extracted twice with 10 mL DCM each. The combined organic layers were washed with 10 mL H₂O, dried over Na₂SO₄, and evaporated under reduced pressure to give a slightly yellow oil which was purified by flash silica gel chromatography.



(*E*)-2-(3-ethoxy-3-oxoprop-1-en-1-yl)phenethyl 3,5-bis(trifluoromethyl)benzoate (**99a**).

Following general procedure *GPIV* using 3-(2-bromophenyl)propyl 3,5-bis(trifluoromethyl)benzoate (1.32 g, 3.00 mmol, 1.00 equiv), toluene (30 mL). Pd(OAc)₂ (27 mg, 0.12 mmol, 4.0 mol%), triphenylphosphine (63 mg, 0.24 mmol, 8.0 mol%), ethyl acrylate (491 μL, 451 mg, 4.50 mmol, 1.50 equiv), and Et₃N (1.26 mL, 911 mg, 9.00 mmol, 3.00 equiv) gave 610 mg (1.33 mmol, 44%) of a white solid after purification on SiO₂ (petrol ether / EtOAc, 10:1 to 6:1). R_f (petrol ether / EtOAc, 10:1): 0.25; mp: 74 °C; IR (neat): 3003, 2969, 1729, 1713, 1629, 1599, 1485, 1467, 1378, 1312, 1281, 1248, 1162, 1121, 1038, 969, 912, 844, 767, 698, 681 cm⁻¹; ¹H-NMR (300 MHz, CDCl₃): 8.41 (s, 2H), 8.11 (d, *J* = 15.8 Hz, 1H), 8.04 (s, 1H), 7.67 – 7.60 (m, 1H), 7.41 – 7.27 (m, 3H), 6.42 (d, *J* = 15.8, 1H), 4.56 (t, *J* = 7.0 Hz, 2H), 4.24 (q, *J* = 7.2 Hz, 2H), 3.28 (t, *J* = 7.0 Hz, 2H), 1.33 (t, *J* = 7.2 Hz, 3H); ¹³C-NMR (75 MHz, CDCl₃): 166.78, 163.77, 141.18, 136.82, 133.63, 132.21, 132.12 (q, *J* = 34 Hz), 130.73, 130.29, 129.81 (m), 127.64, 126.82, 126.36 (m), 122.85 (q, *J* = 273 Hz), 120.43, 66.13, 60.63, 32.15, 14.26; HRMS (ESI) *m/z* calculated for C₂₂H₁₉F₆O₄ ([M+H]⁺) 461.1177, found 461.1182.



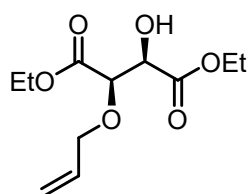
(*E*)-3-(2-(3-ethoxy-3-oxoprop-1-en-1-yl)phenyl)propyl
3,5-bis(trifluoromethyl)benzoate (99b).

Following general procedure *GP IV* using 2-bromophenethyl 3,5-bis(trifluoromethyl)benzoate (455 mg, 1.00 mmol, 1.00 equiv) gave 199 mg (0.419 mmol, 42%) of a colorless oil after purification on SiO₂ (petrol ether / EtOAc, 10:1 to 6:1). *R_f* (petrol ether / EtOAc, 10:1): 0.25; IR (neat): 2979, 2958, 1714, 1634, 1462, 1368, 1313, 1277, 1247, 1172, 1130, 1034, 978, 912, 844, 766, 699, 681, 619 cm⁻¹; ¹H-NMR (300 MHz, CDCl₃): 8.43 (s, 2H), 8.06 (s, 1H), 8.00 (d, *J* = 15.8 Hz, 1H), 7.61 – 7.53 (m, 1H), 7.36 – 7.16 (m, 3H), 6.38 (d, *J* = 15.8 Hz, 1H), 4.42 (t, *J* = 6.4 Hz, 2H), 4.24 (q, *J* = 7.3 Hz, 2H), 2.95 (t, *J* = 7.3 Hz, 2H), 2.19 – 2.06 (m, 2H), 1.32 (t, *J* = 7.3 Hz, 3H); ¹³C-NMR (75 MHz, CDCl₃): 166.87, 163.91, 141.53, 140.36, 133.07, 132.33, 131.89, 130.19, 130.03, 129.77 (m), 126.98, 126.83, 126.35 (m), 119.98, 65.46, 60.56, 29.96, 26.80, 14.30; ¹⁹F-NMR (282 MHz, CDCl₃): -63.39; HRMS (ESI) *m/z* calculated for C₂₃H₂₁F₆O₄ ([*M*+*H*]⁺) 475.1339 found 475.1337.

3.7 Synthesis of monosubstituted diol compounds

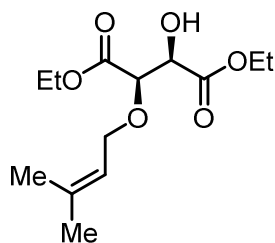
General procedure for the synthesis *via* allylation with copper(II) (*GPV*)

A 25 mL round bottom flask equipped with a magnetic stir bar was charged with dihydroxysuccinate (5.00 mmol, 1.00 equiv), 67.2 mg CuCl₂ (500 μmol, 0.100 equiv), 1.04 g K₂CO₃ (7.50 mmol, 1.50 equiv) and dissolved in DMF (10.0 mL, 0.5 M).⁷⁶ Alkylating reagent (10.0 mmol, 2.00 equiv) was added dropwise at 25 °C. After stirring for three days, the mixture was poured into water (100 mL) and extracted with EtOAc (4 x 100 mL). The organic layers were combined, dried over Na₂SO₄ and evaporated under reduced pressure. The obtained residue was purified by automatic flash silica gel column chromatography.



(2*R*,3*R*)-Diethyl 2-(allyloxy)-3-hydroxysuccinate (121a).³

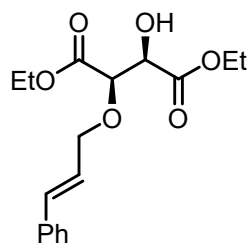
Following general procedure *GPV* using (2*R*,3*R*)-Diethyl 2,3-dihydroxysuccinate (10.3 g, 50.0 mmol, 1.00 equiv), CuCl₂ (672 mg, 5.00 mmol, 0.100 equiv), K₂CO₃ (10.4 g, 75.0 mmol, 15.0 equiv), DMF (100 mL, 0.5 M) and allyl bromide (8.65 mL, 12.1 g, 100 mmol, 2.00 equiv) gave 8.05 g (32.7 mmol, 65%) of (2*R*,3*R*)-diethyl 2-(allyloxy)-3-hydroxysuccinate (**5a**) as a colorless oil after automatic column purification (hexanes / EtOAc 100:0 – 0:100). ¹H NMR (300 MHz, CDCl₃): 5.81 (dddd, *J* = 17.0, 10.3, 6.5, 5.3 Hz, 1H), 5.32 – 5.12 (m, 2H), 4.59 (s, 1H), 4.39 – 4.19 (m, 6H), 3.92 (ddt, *J* = 12.7, 6.6, 1.2 Hz, 1H), 3.08 (bs, 1H), 1.31 (td, *J* = 7.1, 0.9 Hz, 6H).



(2*R*,3*R*)-Diethyl 2-hydroxy-3-((3-methylbut-2-en-1-yl)oxy)succinate (121c).

Following general procedure *GPV* using (2*R*,3*R*)-diethyl 2,3-dihydroxysuccinate (2.06 g, 10.0 mmol, 1.00 equiv), CuCl₂ (134 mg, 1.00 mmol, 0.100 equiv), K₂CO₃ (2.07 g, 15.0 mmol, 1.50 equiv), DMF (20.0 mL, 0.5 M) and 1-bromo-3-methylbut-2-ene (2.31 mL, 2.98 g, 20.0 mmol, 2.00 equiv) gave 1.63 g (5.95 mmol, 60%) of (2*R*,3*R*)-diethyl 2-hydroxy-3-((3-methylbut-2-en-1-yl)oxy)succinate (**5d**) as a colorless oil after automatic column purification (hexanes / EtOAc 100:0 – 0:100). *R_f* (hexanes / EtOAc 1:1) = 0.68; IR (neat): 3675, 3501, 2979, 2910, 2205, 2126, 1976, 1744, 1738, 1450, 1373, 1259, 1199, 1135, 1090, 1017, 861, 781, 697, 605, 437 cm⁻¹; ¹H NMR (300

MHz, CDCl₃): 5.19 (ttd, J = 6.7, 2.8, 1.4 Hz, 1H), 4.51 (dd, J = 9.0, 7.2 Hz, 1H), 4.27 – 4.13 (m, 6H), 4.00 – 3.85 (m, 1H), 3.09 (d, J = 8.4 Hz, 1H), 1.74 – 1.64 (m, 3H), 1.58 (s, 3H), 1.26 (tt, J = 4.2, 2.1 Hz, 6H); ¹³C NMR (75 MHz, CDCl₃): 171.21, 169.67, 138.78, 119.71, 77.63, , 72.39, 67.19, 61.97, 61.43, 25.80, 17.90, 14.21, 14.19; ¹³C NMR (DEPT-135, 75 MHz, CDCl₃): 119.67, 77.59, 72.36, 67.15, 61.94, 61.39, 25.76, 17.86, 14.18, 14.16; HRMS (ESI) m/z calculated for C₁₃H₂₂NaO₆ ([M+Na]⁺) 297.1309, found 297.1308.



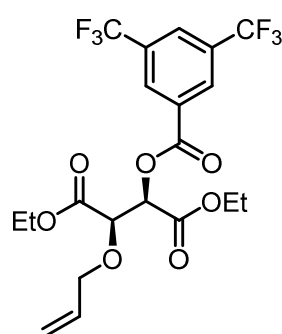
(2*R*,3*R*)-Diethyl 2-(cinnamyloxy)-3-hydroxysuccinate (121h).

Following general procedure **GPV** using (2*R*,3*R*)-diethyl 2,3-dihydroxysuccinate (2.06 g, 10.0 mmol, 1.00 equiv), CuCl₂ (134 mg, 1.00 mmol, 0.100 equiv), K₂CO₃ (2.07 g, 15.0 mmol, 1.50 equiv), DMF (20.0 mL, 0.5 M) and (*E*)-(3-chloroprop-1-en-1-yl)benzene (2.79 mL, 3.05 g, 20.0 mmol, 2.00 equiv) gave 682 mg (2.12 mmol, 21%) of (2*R*,3*R*)-diethyl 2-(cinnamyloxy)-3-hydroxysuccinate (**5j**) as a colorless oil after flash silica gel chromatography purification (hexanes / EtOAc, 10:1). R_f (hexanes / EtOAc 3:1) = 0.26; IR (neat): 3497, 2982, 2196, 2014, 1963, 1741, 1449, 1394, 1369, 1261, 1196, 1138, 1103, 1024, 969, 912, 862, 804, 732, 693, 591 cm⁻¹; ¹H NMR (E - Isomer, 400 MHz, CDCl₃): 7.40 – 7.22 (m, 5H), 6.56 (d, J = 15.9 Hz, 1H), 6.19 (ddd, J = 15.9, 6.9, 5.8 Hz, 1H), 4.62 (dd, J = 8.2, 2.1 Hz, 1H), 4.45 (ddd, J = 12.6, 5.8, 1.4 Hz, 1H), 4.37 (d, J = 2.4 Hz, 1H), 4.34 – 4.21 (m, 4H), 4.11 (ddd, J = 12.5, 7.0, 1.2 Hz, 1H), 3.11 (d, J = 8.6 Hz, 1H), 1.31 (t, J = 7.1 Hz, 3H), 1.24 (t, J = 7.1 Hz, 3H); ¹H NMR (Z - Isomer, 400 MHz, CDCl₃): 7.40 – 7.22 (m, 5H), 6.62 (d, J = 15.9 Hz, 1H), 6.37 (dt, J = 15.9, 5.7 Hz, 1H), 4.62 (dd, J = 8.2, 2.1 Hz, 1H), 4.45 (ddd, J = 12.6, 5.8, 1.4 Hz, 1H), 4.37 (d, J = 2.4 Hz, 1H), 4.34 – 4.21 (m, 4H), 4.11 (ddd, J = 12.5, 7.0, 1.2 Hz, 1H), 3.11 (d, J = 8.6 Hz, 1H), 1.31 (t, J = 7.1 Hz, 3H), 1.24 (t, J = 7.1 Hz, 3H); ¹³C NMR (101 MHz, CDCl₃): 171.31, 169.56, 136.45, 133.94, 128.74, 128.13, 126.67, 124.65, 78.35, 77.48, 77.16, 76.84, 72.53, 72.03, 62.27, 61.73, 14.35, 14.29; ¹³C NMR (DEPT-135, 101 MHz, CDCl₃): 133.82, 128.62, 128.00, 126.54, 124.52, 78.22, 72.40, 71.91, 62.15, 61.61, 14.22, 14.16; HRMS (ESI) m/z calculated for C₁₇H₂₃O₆ ([M+H]⁺) 323.1489, found 323.1476.

3.8 Synthesis of 3,5-bis(trifluoromethyl)benzoate esters for cyclizations

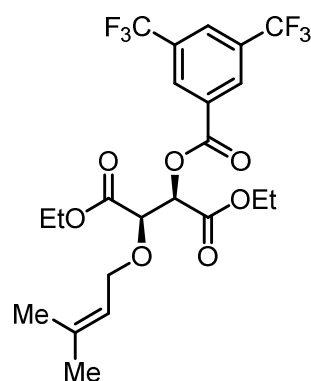
General procedure for the synthesis *via* benzoylation with 3,5-bis(trifluoromethyl)benzoic anhydride (GPVI)

A 25 mL Schlenk flask equipped with a magnetic stir bar was charged with monoalkylated substrate (3.00 mmol, 1.00 equiv) and dissolved in DCM (15 mL, 0.5 M). Triethylamine or *N,N*-diisopropylethylamine (6.00 mmol, 2.00 equiv) was added followed by 3,5-bis(trifluoromethyl)benzoic anhydride⁷⁷ (1.64 g, 3.30 mmol, 1.10 equiv). After stirring for one hour, the mixture was evaporated under reduced pressure. The obtained residue was purified by flash silica gel column chromatography.



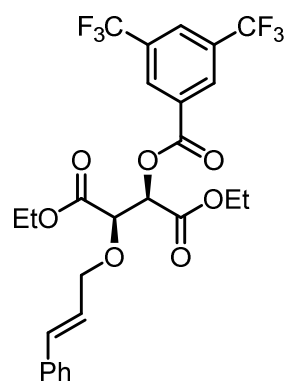
Diethyl (2R,3R)-2-(allyloxy)-3-((3,5-bis(trifluoromethyl)benzoyl)oxy)succinate (**116a**).

Following general procedure *GPVI* using (2R,3R)-diethyl 2-(allyloxy)-3-hydroxysuccinate (**121a**, 739 mg, 3.00 mmol, 1.00 equiv), DCM (15 mL, 0.5 M), *N,N*-diisopropylethylamine (1.04 mL, 775 mg, 6.00 mmol, 2.00 equiv), and 3,5-bis(trifluoromethyl)benzoic anhydride (1.64 g, 3.30 mmol, 1.10 equiv) gave 812 mg (1.67 mmol, 55.7%) of diethyl (2R,3R)-2-(allyloxy)-3-((3,5-bis(trifluoromethyl)benzoyl)oxy)succinate (**116a**) as a colorless oil after column purification (hexanes / EtOAc, 6:1). R_f (hexanes / EtOAc, 6:1) = 0.32; IR (neat): 2987, 1741, 1625, 1460, 1372, 1278, 1242, 1179, 1132, 1069, 1021, 914, 846, 766, 700, 682, 571, 438 cm^{-1} ; ^1H NMR (300 MHz, CDCl_3): 8.50 (s, 2H), 8.09 (s, 1H), 5.95 – 5.82 (m, 1H), 5.81 (d, J = 3.2 Hz, 1H), 5.36 – 5.22 (m, 2H), 4.66 (d, J = 3.2 Hz), 4.38 (ddt, J = 12.7, 5.3, 1.4, 1H), 4.29 (q, J = 7.1 Hz, 2H), 4.27 – 4.16 (m, 2H), 4.04 (ddt, J = 12.7, 6.7, 1.2), 1.31 (t, J = 7.2 Hz, 3H), 1.23 (t, J = 7.2 Hz, 3H); ^{13}C NMR (75 MHz, CDCl_3): 168.47, 165.99, 163.09, 133.17; 132.79 (q, J = 34 Hz), 131.17, 130.12 (m), 126.98 (m), 122.76 (q, J = 273 Hz), 119.01, 76.29, 74.12, 72.75, 62.37, 61.81, 14.12; HRMS (ESI) m/z calculated for $\text{C}_{20}\text{H}_{21}\text{F}_6\text{O}_7$ ($[\text{M}+\text{H}]^+$) 487.1186, found 487.1188.



Diethyl (2R,3R)-2-((3,5-bis(trifluoromethyl)benzoyl)oxy)-3-((3-methylbut-2-en-1-yl)oxy)succinate (116c).

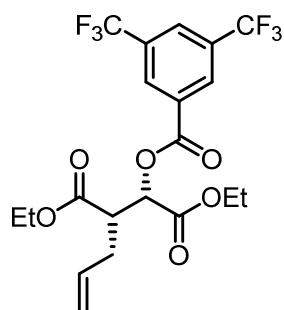
Following general procedure *GPVI* using (2R,3R)-diethyl 2-hydroxy-3-((3-methylbut-2-en-1-yl)oxy)succinate (**121c**, 823 mg, 3.00 mmol, 1.00 equiv), DCM (30 mL, 0.1 M), triethylamine (836 μ L, 607 mg, 6.00 mmol, 2.00 equiv), and 3,5-bis(trifluoromethyl)benzoic anhydride (1.64 g, 3.30 mmol, 1.10 equiv) gave 1.37 g (2.66 mmol, 88.8%) of diethyl (2R,3R)-2-((3,5-bis(trifluoromethyl)benzoyl)oxy)-3-((3-methylbut-2-en-1-yl)oxy)succinate (**121c**) as a colorless oil after column purification (hexanes / EtOAc, 10:1). R_f (hexanes / EtOAc, 6:1) = 0.47; IR (neat): 2985, 1741, 1325, 1448, 1372, 1278, 1242, 1180, 1132, 1070, 1020, 914, 846, 765, 700, 591 cm^{-1} ; ^1H NMR (400 MHz, CDCl_3): 8.50 (s, 2H), 8.08 (s, 1H), 5.78 (d, J = 3.3 Hz, 1H), 5.34 – 5.26 (m, 1H), 4.62 – 4.61 (d, J = 3.3 Hz, 1H), 4.34 – 4.26 (m, 3H), 4.25 – 4.17 (m, 2H), 4.11 (dd, J = 11.8, 7.8 Hz, 1H), 1.77 (s, 3H), 1.68 (s, 3H), 1.31 (t, J = 7.1 Hz, 3H), 1.24 (t, J = 7.2 Hz, 3H); ^{13}C NMR (101 MHz, CDCl_3): 168.78, 166.05, 163.15, 139.32, 132.33 (q, J = 34 Hz), 131.28, 130.12 (m), 126.92 (m), 122.78 (q, J = 273 Hz), 119.49, 75.83, 74.26, 67.76, 62.28, 61.69, 25.84, 17.95, 14.15, 14.10; HRMS (ESI) m/z calculated for $\text{C}_{22}\text{H}_{24}\text{F}_6\text{NaO}_7$ ($[\text{M}+\text{Na}]^+$) 537.1318, found 537.1323.



Diethyl (2R,3R)-2-((3,5-bis(trifluoromethyl)benzoyl)oxy)-3-(cinnamyloxy)succinate (116h).

Following general procedure *GPVI* using (2R,3R)-diethyl 2-(cinnamyloxy)-3-hydroxysuccinate (**121h**, 200 mg, 0.620 mmol, 1.00 equiv), DCM (6 mL, 0.1 M), triethylamine (173 μ L, 125 mg, 1.24 mmol, 2.00 equiv), and 3,5-bis(trifluoromethyl)benzoic anhydride (340 mg, 0.680 mmol, 1.10 equiv) gave 275 mg (0.490 mmol, 78.9%) of diethyl (2R,3R)-2-((3,5-bis(trifluoromethyl)benzoyl)oxy)-3-(cinnamyloxy)succinate (**116h**) as a colorless oil after column purification (hexanes / EtOAc, 10:1). R_f (hexanes / EtOAc, 4:1) = 0.48; IR (neat): 2986, 1740, 1626, 1450, 1371, 1278, 1240, 1181, 1133, 1063, 1063, 1021, 969, 913, 846, 765, 744, 696, 541 cm^{-1} ; ^1H NMR (300 MHz, CDCl_3): 8.53 (s, 2H), 8.10 (s, 1H), 7.43 – 7.20 (m, 5H), 6.62 (d, J = 15.9 Hz, 1H), 6.25 (ddd, J = 15.9, 7.0, 6.0 Hz, 1H), 5.86 (d, J = 3.1 Hz, 1H), 4.74 (d, J = 3.1 Hz, 1H), 4.55 (ddd, J = 12.6, 6.0, 1.2 Hz, 1H), 4.36 – 4.14 (m, 5H), 1.28 – 1.19 (m, 4H); ^{13}C NMR (75 MHz, CDCl_3): 168.55, 166.02, 163.09, 136.17, 134.34, 132.31 (q, J = 34 Hz), 131.24, 130.12 (m), 128.97, 128.08, 126.96 (m), 126.56, 124.20, 122.79 (q, J =

273 Hz), 76.23, 74.17, 72.47, 62.39, 61.81, 14.07, 14.01; HRMS (ESI) m/z calculated for $C_{26}H_{28}F_6NO_7$ ($[M+NH_4]^+$) 580.1764, found 580.1768.

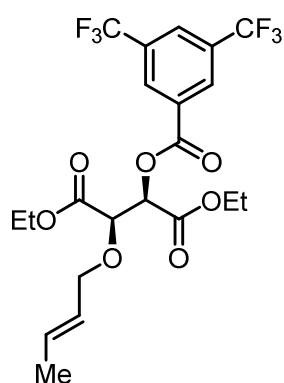


Diethyl (2S,3S)-2-allyl-3-((3,5-bis(trifluoromethyl)benzoyl)oxy)succinate (**116i**).

Following general procedure *GPVI* using diethyl (2S,3S)-2-allyl-3-hydroxysuccinate⁷⁸ (691 mg, 3.00 mmol, 1.00 equiv, dr = 10:1), DCM (15 mL, 0.5 M), *N,N*-diisopropylethylamine (1.04 mL, 775 mg, 6.00 mmol, 2.00 equiv), and 3,5-bis(trifluoromethyl)benzoic anhydride (1.64 g, 3.30 mmol, 1.10 equiv) gave 1.25 g (2.66 mmol, 88.7%) of diethyl (2S,3S)-2-allyl-3-((3,5-bis(trifluoromethyl)benzoyl)oxy)succinate (**116i**, dr = 10:1) as a colorless oil after column purification (hexanes / EtOAc, 12:1). R_f (hexanes / EtOAc, 10:1) = 0.47; IR (neat): 2986, 1739, 1447, 1373, 1278, 1241, 1177, 1131, 1031, 913, 846, 765, 700, 682, 556, 438 cm^{-1} ; 1H NMR (300 MHz, $CDCl_3$, major diastereomer): 8.48 (s, 2H), 8.10 (s, 1H), 5.89 – 5.74 (m, 1H), 5.53 (d, J = 4.6 Hz, 1H), 5.19 – 5.08 (m, 2H), 4.37 – 4.11 (m, 4H), 3.28 (td, J = 7.5, 4.6, 1H), 2.73 – 2.61 (m, 1H), 2.42 – 2.30 (m, 1H), 1.33 – 1.25 (m, 6H); ^{13}C NMR (75 MHz, $CDCl_3$, major diastereomer): 170.42, 167.93, 162.94, 133.83, 132.37 (q, J = 34 Hz), 131.35, 129.95 (m), 122.77 (q, J = 274 Hz), 118.53, 72.82, 62.11, 61.37, 46.24, 32.09, 14.07; HRMS (ESI) m/z calculated for $C_{20}H_{21}F_6O_6$ ($[M+H]^+$) 471.1237, found 471.1246.

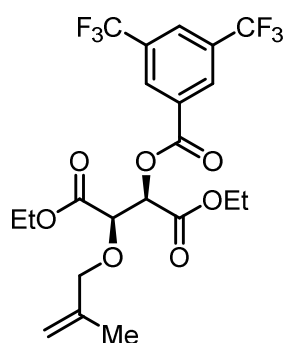
General procedure for the synthesis *via* allylation with silver(I) oxide (*GPVII*)

A 50 mL Schlenk flask equipped with a magnetic stir bar was charged with (*2R,3R*)-diethyl 2-(3,5-bis(trifluoromethyl)benzoyloxy)-3-hydroxysuccinate⁷⁷ (1.33 g, 3.00 mmol, 1.00 equiv) and dissolved in dry Et₂O (20 mL, 0.15 M) under N₂ atmosphere. Ag₂O (1.39 g, 6.00 mmol, 2.00 equiv) was added followed by an allyl bromide derivative (4.50 mmol, 1.50 equiv).⁴⁸ The reaction mixture was stirred for 2 days at room temperature in the dark. The mixture was filtered through a short plug of celite and washed sparingly with Et₂O. The filtrate was evaporated under reduced pressure and the obtained residue was purified by flash silica gel column chromatography.



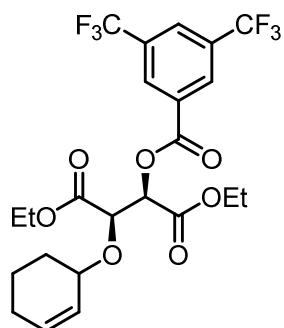
Diethyl (*2R,3R*)-2-(((*E*)-but-2-en-1-yl)oxy)-3-((3-methyl-5-(trifluoromethyl)benzoyl)oxy)succinate (**116b**).

Following general procedure *GPVII* using (*2R,3R*)-diethyl 2-(3,5-bis(trifluoromethyl)benzoyloxy)-3-hydroxysuccinate (**63f**, 1.33 g, 3.00 mmol, 1.00 equiv), Et₂O (20 mL, 0.15 M), Ag₂O (1.39 g, 6.00 mmol, 2.00 equiv), and (*E*)-1-bromobut-2-ene (462 μ L, 606 mg, 4.50 mmol, 1.50 equiv) gave 770 mg (1.54 mmol, 51.3%) of diethyl (*2R,3R*)-2-(((*E*)-but-2-en-1-yl)oxy)-3-((3-methyl-5-(trifluoromethyl)benzoyl)oxy)succinate (**116b**, *E/Z* = 5.6:1) as a colorless oil after column purification (hexanes / EtOAc, 10:1 to 2:1). *R*_f(hexanes / EtOAc, 6:1) = 0.46; IR (neat): 2985, 1742, 1626, 1455, 1371, 1278, 1242, 1180, 1133, 1065, 1021, 969, 914, 846, 766, 700, 542, 502 cm⁻¹; ¹H NMR (300 MHz, CDCl₃, *E* isomer): 8.50 (s, 2H), 8.08 (s, 1H), 5.82 – 5.66 (m, 2H), 5.59 – 5.44 (m, 1H), 4.64 (d, *J* = 3.3 Hz, 1H), 4.42 – 4.13 (m, 5H), 3.99 (ddt, *J* = 12.1, 7.3, 1.0 Hz, 1H), 1.72 (dq, *J* = 6.5, 1.0 Hz, 3H), 1.31 (t, *J* = 7.2 Hz, 3H), 1.22 (t, *J* = 7.2 Hz, 3H); ¹³C NMR (75 MHz, CDCl₃): 168.66, 166.02, 163.13, 132.31 (q, *J* = 34 Hz), 131.76, 131.20, 130.12 (m), 126.99 (m), 126.06, 122.76 (q, *J* = 273 Hz), 75.72, 74.20, 72.42, 17.78, 14.13, 14.10; HRMS (ESI) *m/z* calculated for C₂₁H₂₆F₆NO₇ ([M+NH₄]⁺) 518.1608, found 518.1619.



Diethyl (2*R*,3*R*)-2-((3,5-bis(trifluoromethyl)benzoyl)oxy)-3-((2-methylallyl)oxy)succinate (116d).

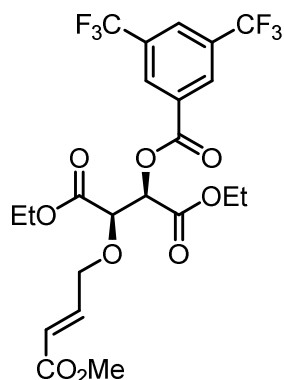
Following general procedure *GPVII* using (2*R*,3*R*)-diethyl 2-(3,5-bis(trifluoromethyl)benzoyloxy)-3-hydroxysuccinate (**63f**, 1.33 g, 3.00 mmol, 1.00 equiv), Et₂O (20 mL, 0.15 M), Ag₂O (1.39 g, 6.00 mmol, 2.00 equiv), and 3-bromo-2-methylprop-1-ene (453 μ L, 606 mg, 4.50 mmol, 1.50 equiv) gave 897 mg (1.79 mmol, 59.8%) of diethyl (2*R*,3*R*)-2-((3,5-bis(trifluoromethyl)benzoyl)oxy)-3-((2-methylallyl)oxy)succinate (**116d**) as a colorless oil after column purification (hexanes / EtOAc, 10:1 to 2:1). *R_f* (hexanes / EtOAc, 6:1) = 0.50; IR (neat): 2986, 1741, 1623, 1457, 1372, 1278, 1241, 1180, 1133, 1077, 1024, 913, 846, 765, 700, 534 cm⁻¹; ¹H NMR (300 MHz, CDCl₃): 8.50 (s, 2H), 8.08 (s, 1H), 5.79 (d, *J* = 3.3 Hz, 1H), 5.00 – 4.92 (m, 2H), 4.63 (d, *J* = 3.3 Hz, 1H), 4.37 – 4.13 (m, 5H), 3.93 (d, *J* = 12.1 Hz, 1H), 1.74 (s, 3H), 1.29 (t, *J* = 7.1 Hz, 3H), 1.23 (t, *J* = 7.1 Hz, 3H); ¹³C NMR (75 MHz, CDCl₃): 168.39, 166.02, 163.09, 140.64, 132.32 (q, *J* = 34 Hz), 131.20, 130.12 (m), 126.96 (m), 122.76 (q, *J* = 273 Hz), 114.36, 76.46, 75.64, 74.11, 62.36, 61.75, 19.38, 14.09, 14.03; HRMS (ESI) *m/z* calculated for C₂₁H₂₂F₆NaO₇ ([*M*+Na]⁺) 523.1167, found 523.1164.



Diethyl (2*R*,3*R*)-2-((3,5-bis(trifluoromethyl)benzoyl)oxy)-3-(cyclohex-2-en-1-yloxy)succinate (116e).

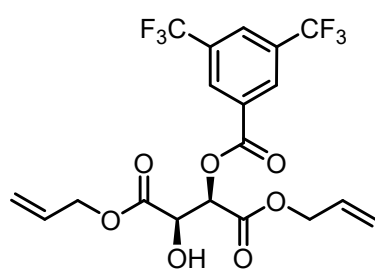
Following general procedure *GPVII* using (2*R*,3*R*)-diethyl 2-(3,5-bis(trifluoromethyl)benzoyloxy)-3-hydroxysuccinate (**63f**, 1.11 g, 2.50 mmol, 1.00 equiv), Et₂O (15 mL, 0.17 M), Ag₂O (1.16 g, 5.00 mmol, 2.00 equiv), and 3-bromocyclohex-1-ene (0.43 mL, 0.60 g, 3.8 mmol, 1.50 equiv) gave 218 mg (0.414 mmol, 16.2%) of diethyl (2*R*,3*R*)-2-((3,5-bis(trifluoromethyl)benzoyl)oxy)-3-(cyclohex-2-en-1-yloxy)succinate (**116e**, dr = 1:1) as a colorless oil after column purification (hexanes / EtOAc, 10:1 to 2:1). *R_f* (hexanes / EtOAc, 6:1) = 0.50; IR (neat): 2941, 1741, 1626, 1449, 1278, 1243, 1179, 1132, 1060, 1022, 969, 914, 846, 766, 700, 681, 590, 539 cm⁻¹; ¹H NMR (300 MHz, CDCl₃, 2 diastereomers): 8.48 (s, 2H), 8.06 (s, 1H), 5.93 – 5.66 (m, 3H), 4.73 (dd, *J* = 8.7, 3.6 Hz, 1H), 4.33 – 4.13 (m, 4H), 4.10 – 3.93 (m, 1H), 2.09 – 1.41 (m, 6H), 1.29 (t, *J* = 7.1, 1.5H), 1.28 (t, *J* = 7.1 Hz, 1.5H), 1.21 (t, *J* = 7.1, 3H); ¹³C NMR (75 MHz, CDCl₃, 2 diastereomers): 168.16, 165.10, 162.16, 162.12, 131.54, 131.28 (q, *J* = 34 Hz), 130.74, 130.37, 130.31, 129.14 (m), 126.02, 125.90 (m), 124.55, 121.80 (q, *J* = 273 Hz), 74.74, 74.55, 73.53, 73.27, 72.87, 61.35, 61.28, 60.72, 60.68, 27.89, 26.23, 24.17, 24.05,

17.83, 17.60, 17.83, 17.60, 13.05, 13.02; HRMS (ESI) m/z calculated for $C_{23}H_{24}F_6NaO_7$ ($[M+Na]^+$) 549.1318, found 549.1322.

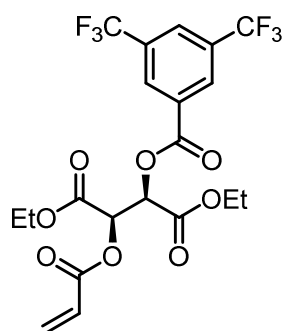


Diethyl (*2R,3R*)-2-((3,5-bis(trifluoromethyl)benzoyl)oxy)-3-(((*E*)-4-methoxy-4-oxobut-2-en-1-yl)oxy)succinate (**116f**).

Following general procedure *GPVII* using (*2R,3R*)-diethyl 2-(3,5-bis(trifluoromethyl)benzoyloxy)-3-hydroxysuccinate (**63f**, 1.10 g, 2.50 mmol, 1.00 equiv), Et_2O (15 mL, 0.17 M), Ag_2O (1.16 g, 5.00 mmol, 2.00 equiv), and methyl (*E*)-4-bromobut-2-enoate (462 μ L, 671 mg, 3.75 mmol, 1.50 equiv) gave 416 mg (0.765 mmol, 30.6%) of diethyl (*2R,3R*)-2-((3,5-bis(trifluoromethyl)benzoyl)oxy)-3-(((*E*)-4-methoxy-4-oxobut-2-en-1-yl)oxy)succinate (**116f**) as a colorless oil after column purification (hexanes / EtOAc, 10:1 to 2:1). R_f (hexanes / EtOAc, 6:1) = 0.38; IR (neat): 2988, 1733, 1666, 1439, 1372, 1278, 1241, 1176, 1132, 1067, 1020, 914, 846, 766, 700, 682, 438 cm^{-1} ; 1H NMR (300 MHz, $CDCl_3$): 8.50 (s, 2H), 8.10 (s, 1H), 6.92 (dt, J = 15.9, 4.6 Hz, 1H), 6.09 (dt, J = 15.9, 1.9 Hz, 1H), 5.85 (d, J = 3.0 Hz, 1H), 4.67 (d, J = 3.0 Hz, 1H), 4.60 (ddd, J = 15.6, 4.3, 2.1, 1H), 4.31 (q, J = 7.1 Hz, 2H), 4.27 – 4.13 (m, 3H), 3.75 (s, 3H), 1.30 (t, J = 7.1 Hz, 3H), 1.23 (t, J = 7.1 Hz, 3H); HRMS (ESI) m/z calculated for $C_{22}H_{26}F_6NO_9$ ($[M+NH_4]^+$) 562.1506, found 562.1507.

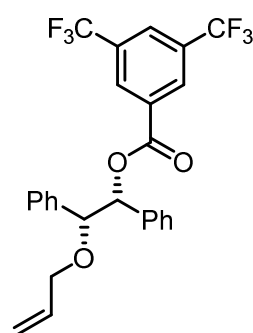
Synthesis of other 3,5-bis(trifluoromethyl)benzoate esters**(2*R*,3*R*)-Diallyl 2-(3,5-bis(trifluoromethyl)benzoyloxy)-3-hydroxysuccinate (114).**

A 50 mL Schlenk flask equipped with a magnetic stir bar was charged with CuCl₂ (40 mg, 0.30 mmol, 10 mol%), sealed with a glass stopper, evacuated, and heated to 550 °C with a heat gun for 2 min. After the flask cooled to room temperature, it was charged with diallyl (2*R*,3*R*)-2,3-dihydroxysuccinate (691 mg, 3.00 mmol, 1.00 equiv), DCM (15 mL, 0.5 M), and *N,N*-diisopropylethylamine (1.04 mL, 775 mg, 6.00 mmol, 2.00 equiv). The mixture was cooled to 0 °C and 3,5-bis(trifluoromethyl)benzoic anhydride⁷⁷ (1.64 g, 3.30 mmol, 1.10 equiv) was added portionwise over 5 min. The reaction was magnetically stirred for 1 h after which the solvent was evaporated under reduced pressure and the obtained residue purified by automatic flash silica gel column chromatography (0 – 20% EtOAc in hexanes) to give 1.01 g (2.15 mmol, 71.7%) of (2*R*,3*R*)-diallyl 2-(3,5-bis(trifluoromethyl)benzoyloxy)-3-hydroxysuccinate (**114**) as a white solid. mp: 97 °C; *R*_f (hexanes / EtOAc, 4:1) = 0.35; IR (neat): 3360, 3087, 2960, 1739.6, 1705, 1411, 1279, 1237, 1184, 1124, 1048, 930, 913, 809, 766, 701 cm⁻¹; ¹H NMR (300 MHz, CDCl₃): 8.46 (s, 2H), 8.11 (s, 1H), 6.00 – 5.72 (m, 3H), 5.44 – 5.24 (m, 3H), 5.20 – 5.12 (m, 1H), 4.98 – 4.91 (m, 1H), 4.81 – 4.62 (m, 4H), 3.33 (bs, 1H); ¹³C NMR (75 MHz, CDCl₃): 170.28, 165.60, 162.82, 132.31 (q, *J* = 34 Hz), 130.94, 130.53, 130.05 (m), 127.10 (m), 122.42 (q, *J* = 273 Hz), 120.32, 119.32, 74.23, 70.50, 67.23, 66.90; HRMS (ESI) *m/z* calculated for C₁₉H₁₇F₆O₇ ([*M*+*H*]⁺) 471.0873, found 471.0878.

**Diethyl (2*R*,3*R*)-2-(acryloyloxy)-3-((3,5-bis(trifluoromethyl)benzoyl)oxy)succinate (116g).**

A 50 mL Schlenk flask equipped with a magnetic stir bar was charged with (2*R*,3*R*)-diethyl 2-(3,5-bis(trifluoromethyl)benzoyloxy)-3-hydroxysuccinate (**63f**, 1.33 g, 3.00 mmol, 1.00 equiv), dissolved in DCM (30 mL, 0.1 M), and cooled to 0 °C. Triethylamine (836 µL, 607 mg, 6.00 mmol, 2.00 equiv) was added followed by dropwise addition of acryloyl chloride (366 µL, 407 mg, 4.50 mmol, 1.50 equiv). The reaction mixture was allowed to reach room temperature over one hour and subsequently evaporated under reduced pressure. The obtained residue was purified by flash silica gel column chromatography (hexanes / EtOAc, 10:1) to give 1.28 g (2.55 mmol, 85.1%) diethyl (2*R*,3*R*)-2-(acryloyloxy)-3-((3,5-bis(trifluoromethyl)benzoyl)oxy)succinate (**116g**) as a colorless oil. *R*_f (hexanes / EtOAc, 6:1) = 0.41; IR

(neat): 2988, 1741, 1625, 1467, 1408, 1278, 1233, 1170, 1132, 1060, 1026, 984, 914, 546, 806, 765, 700, 682, 527, 438 cm^{-1} ; ^1H NMR (300 MHz, CDCl_3): 8.50 (s, 2H), 8.11 (s, 1H), 6.56 (dd, $J = 17.2, 1.1$ Hz, 1H), 6.26 (dd, $J = 17.2, 10.5$ Hz, 1H), 6.04 – 5.97 (m, 2H), 5.91 (d, $J = 2.7$ Hz, 1H), 4.36 – 4.17 (m, 4H), 1.26 (t, $J = 7.1$ Hz, 3H), 1.22 (t, $J = 7.2$ Hz, 3H); ^{13}C NMR (75 MHz, CDCl_3): 165.66, 165.16, 164.59, 162.72, 133.27, 132.47 (q, $J = 34$ Hz), 130.90, 130.08 (m), 127.17 (m), 126.76, 122.72 (q, $J = 273$ Hz), 72.27, 70.85, 62.73, 62.53, 14.07, 14.01; HRMS (ESI) m/z calculated for $\text{C}_{20}\text{H}_{19}\text{F}_6\text{O}_8$ ($[\text{M}+\text{H}]^+$) 501.0979, found 501.0982.

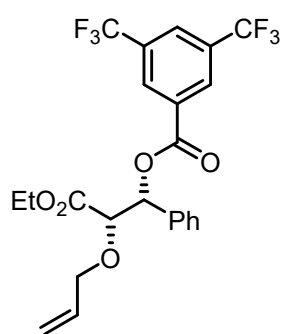


(1*R*,2*R*)-2-(allyloxy)-1,2-diphenylethyl 3,5-bis(trifluoromethyl)benzoate (126a).

A 250 mL Schlenk flask equipped with a magnetic stir bar was charged with (*R,R*)-hydrobenzoin (**124a**, 1.71 g, 8.00 mmol, 1.00 equiv), CuCl_2 (108 mg, 0.80 mmol, 10 mol%), DCM (60 mL), and Pr_2NEt (2.79 mL, 16.0 mmol, 2.00 equiv). The mixture was cooled to 0 °C and a solution of 3,5-bis(trifluoromethyl)benzoic anhydride (**67**, 4.38 g, 8.80 mmol, 1.10 equiv) in DCM (40 mL) was added. The mixture was allowed to reach room temperature and stirred for 24 h. The solvent was evaporated under reduced pressure and the obtained residue was purified by flash silica gel column chromatography (hexanes / EtOAc, 15:1 to 2:1) to give 3.03 g (6.67 mmol, 83.4%) of (*1R,2R*)-2-hydroxy-1,2-diphenylethyl 3,5-bis(trifluoromethyl)benzoate (**125a**) as a white solid. mp: 90 °C; R_f (hexanes / EtOAc, 10:1) = 0.29; IR (neat): 3486, 3036, 1719, 1620, 1455, 1387, 1352, 1269, 1120, 1063, 976, 907, 763, 697, 574 cm^{-1} ; ^1H NMR (300 MHz, CDCl_3): 8.57 (s, 2H), 8.13 (s, 1H), 7.39 – 7.10 (m, 10H), 6.22 (d, $J = 7.4$ Hz, 1H), 5.11 (d, $J = 7.4$ Hz, 1H), 3.18 (s, 1H); ^{13}C NMR (101 MHz, CDCl_3): 163.41, 138.99, 136.11, 132.46, 132.18 (q, $J = 34$ Hz), 129.89 (m), 128.63, 128.41, 128.30, 127.42, 127.08, 126.57 (m), 122.94 (q, $J = 273$ Hz), 81.71, 76.88; HRMS (ESI) m/z calculated for $\text{C}_{23}\text{H}_{16}\text{F}_6\text{NaO}_3$ ($[\text{M}+\text{Na}]^+$) 477.0896, found 477.0894.

A 50 mL Schlenk flask equipped with a magnetic stir bar was charged with (*1R,2R*)-2-hydroxy-1,2-diphenylethyl 3,5-bis(trifluoromethyl)benzoate (**125a**, 2.27 g, 5.00 mmol, 1.00 equiv) and dissolved in dry Et_2O (35 mL, 0.14 M) under N_2 atmosphere. Ag_2O (2.31 g, 10.0 mmol, 2.00 equiv) was added followed by allyl bromide (649 μL , 907 mg, 7.50 mmol, 1.50 equiv). The reaction mixture was stirred for 48 hours at room temperature in the dark after which TLC control indicated incomplete transformation. Subsequently additional Ag_2O (2.31 g, 10.0 mmol, 2.00 equiv) and allyl bromide (649 μL , 907 mg, 7.50 mmol, 1.50 equiv) was added and the reaction was stirred for 48 hours. Again, TLC control indicated incomplete

transformation and additional Ag₂O (2.31 g, 10.0 mmol, 2.00 equiv) and allyl bromide (649 μ L, 907 mg, 7.50 mmol, 1.50 equiv) was added and the reaction was stirred for 48 hours. The mixture was filtered through a short plug of celite and washed sparingly with Et₂O. The filtrate was evaporated under reduced pressure and the obtained residue was purified by flash silica gel column chromatography (hexanes / EtOAc, 40:1) to give 600 mg (1.21 mmol, 24.2%) of (*1R,2R*)-2-(allyloxy)-1,2-diphenylethyl 3,5-bis(trifluoromethyl)benzoate (**126a**, *note: material is only 90% pure*) as a colorless oil. *R*_f (hexanes / EtOAc, 6:1) = 0.67; IR (neat): 2866, 1733, 1626, 1454, 1277, 1241, 1179, 1131, 973, 912, 845, 763, 697, 681, 620, 587; ¹H NMR (300 MHz, CDCl₃): 8.53 (s, 2H), 8.08 (s, 1H), 7.32 – 7.07 (m, 10H), 6.18 (d, *J* = 7.6 Hz, 1H), 5.89 – 5.74 (m, 1H), 5.26 – 5.11 (m, 2H), 4.78 (d, *J* = 7.6 Hz, 1H), 4.03 (ddt, *J* = 13.2, 4.7, 1.6, 1H), 3.81 (ddt, *J* = 13.2, 6.1, 1.3, 1H); ¹³C NMR (75 MHz, CDCl₃): 163.05, 137.11, 136.24, 134.32, 132.20 (q, *J* = 34 Hz), 129.84 (m), 128.21, 128.15, 127.92, 127.60, 126.31 (m), 122.94 (q, *J* = 273 Hz), 116.98, 83.11, 80.43, 69.77; HRMS (ESI) *m/z* calculated for C₂₆H₂₀F₆NaO₃ ([M+Na]⁺) 517.1209, found 517.1209.



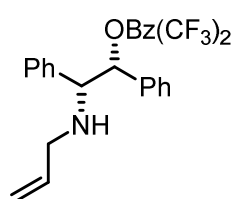
(*1R,2S*)-2-(allyloxy)-3-ethoxy-3-oxo-1-phenylpropyl 3,5-bis(trifluoro-methyl)benzoate (**126b**).

A 250 mL Schlenk flask equipped with a magnetic stir bar was charged with ethyl (*2R,3S*)-2,3-dihydroxy-3-phenylpropanoate⁷⁹ (**124b**, 1.62 g, 7.70 mmol, 1.00 equiv), CuCl₂ (103 mg, 0.77 mmol, 10 mol%), DCM (60 mL), and *Pr*₂NEt (2.70 mL, 15.4 mmol, 2.00 equiv).

The mixture was cooled to 0 °C and a solution of 3,5-bis(trifluoromethyl)benzoic anhydride (**67**, 4.02 g, 8.10 mmol, 1.10 equiv) in DCM (40 mL) was added. The mixture was allowed to reach room temperature and stirred for 19 h. The solvent was evaporated under reduced pressure and the obtained residue was purified by flash silica gel column chromatography (hexanes / EtOAc, 8:1) to give 2.90 g (6.40 mmol, 84%) of an inseparable mixture of (*1S,2R*)-3-ethoxy-2-hydroxy-3-oxo-1-phenylpropyl 3,5-bis(trifluoromethyl)benzoate and (*2R,3S*)-1-ethoxy-3-hydroxy-1-oxo-3-phenylpropan-2-yl 3,5-bis(trifluoromethyl) benzoate (4:1) as a white solid. mp: 83 °C; *R*_f (hexanes / EtOAc, 8:1) = 0.29; IR (neat): 3416, 1735, 1703, 1451, 1390, 1278, 1237, 1175, 1125, 1033, 1008, 969, 912, 845, 760, 698 cm⁻¹; ¹H NMR (400 MHz, CDCl₃, major isomer): 8.51 (s, 2H), 8.09 (s, 1H), 7.48 (m, 2H), 7.44 – 7.26 (m, 3H), 6.33 (d, *J* = 3.3 Hz, 1H), 4.57 (dd, *J* = 6.8, 3.4 Hz, 1H), 4.24 (q, *J* = 7.1 Hz, 2H), 3.16 (d, *J* = 6.8 Hz, 1H), 1.24 (t, *J* = 7.1, 3H); ¹H NMR (400 MHz, CDCl₃, minor isomer): 8.43 (s, 2H), 8.07 (s, 1H), 7.48 (m, 2H), 7.44 – 7.26 (m, 3H), 5.47 (d, *J* = 3.9 Hz, 1H), 5.43 (m, 1H), 4.24 (q, *J* = 7.1 Hz, 2H), 2.64 (d, *J* = 5.3 Hz, 1H), 1.23 (t, *J* = 7.1, 3H); ¹³C NMR (101 MHz, CDCl₃, both isomers):

171.78, 167.38, 163.25, 162.75, 138.55, 135.42, 132.41 (q, $J = 34$ Hz), 132.29 (q, $J = 34$ Hz), 131.88, 131.38, 129.83 (m), 129.00, 128.67, 127.02, 126.78 (m), 126.15, 122.80 (q, $J = 273$ Hz), 77.40, 73.39, 73.30, 62.55, 62.17, 14.01, 13.98; HRMS (ESI) m/z calculated for $C_{20}H_{16}F_6NaO_5$ ($[M+Na]^+$) 473.0794, found 473.0797.

A 100 mL Schlenk flask equipped with a magnetic stir bar was charged with a mixture of (*1S,2R*)-3-ethoxy-2-hydroxy-3-oxo-1-phenylpropyl 3,5-bis(trifluoromethyl)benzoate and (*2R,3S*)-1-ethoxy-3-hydroxy-1-oxo-3-phenylpropan-2-yl 3,5-bis(trifluoromethyl) benzoate (4:1, 2.56 g, 5.68 mmol, 1.00 equiv) and dissolved in dry Et_2O (40 mL, 0.14 M) under N_2 atmosphere. Ag_2O (2.63 g, 11.4 mmol, 2.00 equiv) was added followed by allyl bromide (737 μL , 1.03 g, 8.52 mmol, 1.50 equiv). The reaction mixture was stirred for 24 hours at room temperature in the dark. The mixture was filtered through a short plug of celite and washed sparingly with Et_2O . The filtrate was evaporated under reduced pressure and the obtained residue was purified by automatic flash silica gel column chromatography (0 – 6% EtOAc in hexanes) to give 2.20 g (4.48 mmol, 78.9%) of (*1R,2S*)-2-(allyloxy)-3-ethoxy-3-oxo-1-phenylpropyl 3,5-bis(trifluoromethyl)benzoate (**126b**) as a colorless oil. R_f (hexanes / EtOAc, 6:1) = 0.51; IR (neat): 2997, 1736, 1277, 1240, 1177, 1130, 1026, 912, 845, 763, 698, 681 cm^{-1} ; 1H NMR (400 MHz, $CDCl_3$): 8.53 (s, 2H), 8.08 (s, 1H), 7.53 – 7.45 (m, 2H), 7.42 – 7.31 (m, 3H), 6.36 (d, $J = 5.5$ Hz, 1H), 5.81 – 5.69 (m, 1H), 5.25 – 5.15 (m, 2H), 4.37 (d, $J = 5.5$ Hz, 1H), 4.20 (ddt, $J = 13.0, 5.3, 1.3$ Hz, 1H), 4.10 (q, $J = 7.1$ Hz, 2H), 3.96 (ddt, $J = 13.0, 6.3, 1.3$, 1H), 1.12 (t, $J = 7.1$ Hz, 3H); ^{13}C NMR (101 MHz, $CDCl_3$): 169.26, 162.85, 135.35, 133.37, 132.28 (q, $J = 34$ Hz), 132.23, 129.88 (m), 129.02, 128.53, 127.46, 126.55 (m), 122.86 (q, $J = 273$ Hz), 118.32, 80.37, 77.39, 72.13, 61.35, 13.90; HRMS (ESI) m/z calculated for $C_{23}H_{20}F_6NaO_5$ ($[M+Na]^+$) 513.1107, found 513.1110.

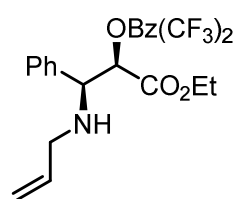


(1*R,2R*)-2-(allylamino)-1,2-diphenylethyl 3,5-bis(trifluoromethyl)benzoate (129**).**⁸⁰

A pressure tube was charged with rac. (*2S,3R*)-2,3-diphenyloxirane⁸¹ (**127**, 1.57 g, 8.00 mmol, 1.00 equiv), $LiClO_4$ (1.70 g, 16.0 mmol, 2.00 equiv), and allylamine (6.00 mL, 4.57 g, 80.0 mmol, 10.0 equiv). The tube was sealed and stirred for 48 h at room temperature followed by 5 h at 120 °C. The solvent was evaporated under reduced pressure, the residue dissolved in 20 mL DCM and washed thrice with 20 mL brine each. The organic layer was dried over Na_2SO_4 and concentrated under reduced pressure to give 1.88 g (7.42 mmol, 93%) of (*1R,2R*)-2-(allylamino)-1,2-diphenylethan-1-ol (**128**) as a slowly solidifying, white solid. mp: 48 °C; R_f (hexanes / EtOAc, 2:1) = 0.25; IR (neat):

3296, 3079, 3032, 2850, 1493, 1453, 1422, 1140, 1077, 1055, 1020, 995, 949, 931, 896, 829, 765, 697, 638, 605, 567 cm^{-1} ; ^1H NMR (400 MHz, CDCl_3): 7.25 – 7.13 (m, 6H), 7.11 – 7.00 (m, 4H), 5.94 – 5.82 (m, 1H), 5.17 – 5.05 (m, 2H), 4.62 (d, $J = 8.7$ Hz, 1H), 3.66 (d, $J = 8.7$ Hz, 1H), 3.31 – 2.96 (m, 4H); ^{13}C NMR (101 MHz, CDCl_3): 141.13, 139.57, 136.16, 128.34, 127.90, 127.83, 127.53, 127.46, 126.87, 116.50, 77.54, 69.54, 49.79; HRMS (ESI) m/z calculated for $\text{C}_{17}\text{H}_{20}\text{NO}$ ($[\text{M}+\text{H}]^+$) 254.1539, found 254.1542.

A Schlenk flask equipped with a magnetic stir bar was charged with (1*R*,2*R*)-2-(allylamino)-1,2-diphenylethan-1-ol (**128**, 476 mg, 1.88 mmol, 1.00 equiv), DCM (18 mL, 0.5 M), and cooled to 0 °C. Triethylamine (513 μL , 3.80 mmol, 2.00 equiv) was added followed by 3,5-bis(trifluoromethyl)benzoic anhydride (**67**, 937 mg, 1.88 mmol, 1.00 equiv). After stirring for 30 min at 0 °C the mixture was evaporated under reduced pressure. The obtained residue was purified by flash silica gel column chromatography (hexanes / EtOAc, 6:1 to 4:1) to give 201 mg (0.410 mmol, 22%) of the title compound as a colorless oil. R_f (hexanes / EtOAc, 4:1) = 0.60; IR (neat): 3071, 3035, 1733, 1639, 1455, 1277, 1244, 1177, 1131, 911, 846, 763, 696, 681, 583 cm^{-1} ; ^1H NMR (300 MHz, CDCl_3): 8.59 (s, 2H), 8.14 (s, 1H), 7.33 – 7.15 (m, 10H), 6.22 (d, $J = 8.0$ Hz, 1H), 5.97 – 5.80 (m, 1H), 5.22 – 5.07 (m, 2H), 4.36 (d, $J = 8.0$ Hz, 1H), 3.26 (ddt, $J = 14.4, 5.2, 1.6$ Hz, 1H), 3.11 (dd, $J = 14.3, 6.6$ Hz, 1H), 1.90 (bs, 1H); ^{13}C NMR (75 MHz, CDCl_3): 163.13, 138.46, 136.87, 136.56, 132.61, 132.32 (q, $J = 34$ Hz), 129.82 (m), 128.71, 128.51, 128.37, 128.25, 128.19, 127.86, 127.37, 126.51 (m), 122.95 (q, $J = 273$ Hz), 116.02, 81.43, 66.16, 49.58; HRMS (ESI) m/z calculated for $\text{C}_{26}\text{H}_{22}\text{F}_6\text{NO}_2$ ($[\text{M}+\text{H}]^+$) 494.1549, found 494.1555.



(1*S*,2*R*)-1-(allylamino)-3-ethoxy-3-oxo-1-phenylpropan-2-yl 3,5-bis(trifluoromethyl)benzoate (135).

A round bottom flask was charged with ethyl (2*R*,3*S*)-3-acetamido-2-hydroxy-3-phenylpropanoate⁸² (**132**, 1.56 g, 6.21 mmol, 1.00 equiv), 60 mL 10% HCl (aq), and refluxed for 4 h. All volatile compounds were evaporated under reduced pressure, 60 mL EtOH, 60 mL cyclohexane, and 0.3 mL conc. H_2SO_4 were added and the resulting mixture refluxed over night using a Dean-Stark water trap. Again all volatiles were evaporated under reduced pressure, the residue neutralized with 10 mL 10% Na_2CO_3 (aq), and the mixture extracted thrice with 10 mL EtOAc each. The combined organic layers were dried over Na_2SO_4 and evaporated under reduced pressure. The obtained white solid was purified by flash silica gel chromatography (EtOAc / Et_3N , 99:1) to give 803 mg (3.84 mmol, 62%) of ethyl (2*R*,3*S*)-3-amino-2-hydroxy-3-phenylpropanoate (**133**) as a colorless oil. R_f

(hexanes / EtOAc, 2:1) = 0.09; IR (neat): 3362, 3284, 3062, 2977, 1729, 1654, 1520, 1452, 1395, 1261, 1210, 1093, 1026, 876, 766, 698 cm^{-1} ; ^1H NMR (400 MHz, CDCl_3): 7.35 – 7.19 (m, 5H), 4.19 (q, J = 4.0 Hz, 2H), 4.16 – 4.07 (m, 2H), 2.67 (bs, 3H), 1.16 (t, J = 7.2 Hz, 3H); ^{13}C NMR (101 MHz, CDCl_3): 173.27, 124.04, 128.40, 127.52, 126.90, 75.26, 61.50, 58.21, 14.05; HRMS (ESI) m/z calculated for $\text{C}_{11}\text{H}_{16}\text{NO}_3$ ($[\text{M}+\text{H}]^+$) 210.1125, found 210.1125.

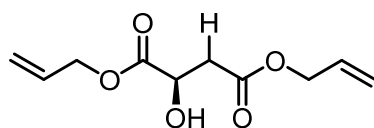
A Schlenk flask was charged with ethyl (2*R*,3*S*)-3-amino-2-hydroxy-3-phenylpropanoate (**133**, 643 mg, 3.08 mmol, 1.00 equiv), THF (6 mL), and Et_3N (442 μL , 321 mg, 3.17 mmol, 1.03 equiv). Allyl bromide (267 μL , 373 mg, 3.08 mmol, 1.00 equiv) was added dropwise over 5 min and the reaction mixture was stirred over night at room temperature. Again, Et_3N (442 μL , 321 mg, 3.17 mmol, 1.03 equiv) and Allyl bromide (267 μL , 373 mg, 3.08 mmol, 1.00 equiv) was added and the reaction mixture was stirred over night at room temperature. This procedure was repeated once more before the solvent was evaporated under reduced pressure and the residue was purified by flash silica gel chromatography (hexanes / EtOAc, 2:1 to 0:1) to give 368 mg (1.48 mmol, 74%) of ethyl (2*R*,3*S*)-3-(allylamino)-2-hydroxy-3-phenylpropanoate (**134**) as a colorless oil. R_f (hexanes / EtOAc, 2:1) = 0.09; IR (neat): 3445, 3338, 3063, 2981, 1732, 1454, 1369, 1260, 1186, 1096, 1026, 918, 868, 763, 700, 632 cm^{-1} ; ^1H NMR (300 MHz, CDCl_3): 7.42 – 7.27 (m, 5H), 5.94 – 5.76 (m, 1H), 5.18 – 5.06 (m, 2H), 4.33 (d, J = 5.0 Hz, 1H), 4.16 (qd, J = 7.2, 1.7 Hz, 2H), 4.04 (d, J = 5.0 Hz, 1H), 3.28 (dd, J = 14.9, 7.3 Hz, 1H), 3.02 (ddt, J = 14.1, 6.9, 1.4 Hz, 1H), 1.17 (t, J = 7.2 Hz, 3H); HRMS (ESI) m/z calculated for $\text{C}_{14}\text{H}_{20}\text{NO}_3$ ($[\text{M}+\text{H}]^+$) 250.1438, found 250.1440.

A Schlenk flask equipped with a magnetic stir bar was charged ethyl (2*R*,3*S*)-3-(allylamino)-2-hydroxy-3-phenylpropanoate (**134**, 217 mg, 0.870 mmol, 1.00 equiv), DCM (9 mL), and cooled to 0 $^\circ\text{C}$. Et_3N (242 μL , 176 mg, 1.74 mmol, 2.00 equiv) was added followed by 3,5-bis(trifluoromethyl)benzoic anhydride (**67**, 455 mg, 0.914 mmol, 1.05 equiv). After stirring for 30 min at 0 $^\circ\text{C}$ the mixture was evaporated under reduced pressure. The obtained residue was purified by flash silica gel column chromatography (hexanes / EtOAc, 6:1) to give 114 mg (0.233 mmol, 27%) of the title compound as a colorless oil. R_f (hexanes / EtOAc, 4:1) = 0.52; IR (neat): 3386, 3084, 2986, 2361, 1739, 1641, 1453, 1372, 1279, 1177, 1135, 1028, 906, 849, 760, 701 cm^{-1} ; ^1H NMR (300 MHz, CDCl_3): 8.46 (s, 2H), 8.09 (s, 1H), 7.42 – 7.25 (m, 5H), 5.93 – 5.76 (m, 1H), 5.39 (d, J = 4.7 Hz, 1H), 5.20 – 5.08 (m, 2H), 4.43 (d, J = 4.8 Hz, 1H), 4.19 (q, J = 7.2 Hz, 2H), 3.32 (ddt, J = 14.2, 5.2, 1.4 Hz, 1H), 3.06 (ddt, J = 14.2, 6.6, 1.2 Hz, 1H), 2.04 (bs, 1H), 1.20 (t, J = 7.2 Hz, 3H); ^{13}C NMR (75 MHz, CDCl_3): 167.75, 163.27, 137.85, 136.18, 132.29 (q, J = 34 Hz), 131.59, 129.89 (m), 128.71, 128.22, 127.57, 126.76 (m), 122.80 (q, J = 273 Hz), 116.53, 78.10, 61.77, 61.68, 49.51, 13.97; HRMS (ESI) m/z calculated for $\text{C}_{23}\text{H}_{22}\text{F}_6\text{NO}_4$ ($[\text{M}+\text{H}]^+$) 490.1448, found 490.1460.

3.9 Photochemical deoxygenative cyclizations

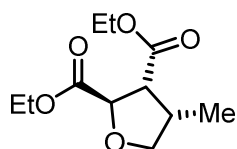
General procedure for deoxygenative cyclizations (*GPVIII*)

A Schlenk tube equipped with a magnetic stir bar was charged with 3,5-bis(trifluoromethyl)benzoate ester (0.500 mmol, 1.00 equiv), *fac*-Ir(ppy)₃^{65,83} (6.6 mg, 10 μmol, 2.0 mol%), sealed with a screw-cap and subsequently evacuated and backfilled with N₂ (3x). MeCN (12.5 ml), Et₃N (0.35 mL, 0.25 g, 2.5 mmol, 5.0 equiv), and degassed water (0.90 mL, 0.90 g, 50 mmol, 100 equiv) was added and the reaction mixture was magnetically stirred until a homogeneous solution was obtained. The reaction mixture was degassed by freeze-pump-thaw (5x) and the screw-cap was replaced with a Teflon sealed inlet for a glass rod, through which irradiation with a 455 nm high power LED took place from above while the reaction was magnetically stirred and heated to 80 °C in an aluminum block from below. After completion of the reaction as judged by TLC (typically 1 h), the mixture was evaporated under reduced pressure and the residue purified by flash silica gel column chromatography.



Diallyl (*R*)-2-hydroxysuccinate (**117**).⁸⁴

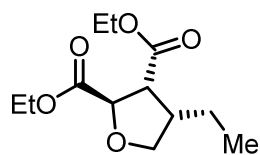
Following general procedure *GPVIII* using (*2R,3R*)-diallyl 2-(3,5-bis(trifluoromethyl)benzoyloxy)-3-hydroxysuccinate (**114**, 94.1 mg, 200 μmol, 1.00 equiv), *fac*-Ir(ppy)₃ (2.7 mg, 4.1 μmol, 2.0 mol%), MeCN (5.0 mL, 0.04 M), Et₃N (0.14 mL, 0.10 g, 1.0 mmol, 5.0 equiv), and degassed water (0.36 mL, 0.36 g, 20 mmol, 100 equiv) gave 23.1 mg (108 μmol, 54%) of diallyl (*R*)-2-hydroxysuccinate (**117**) as a colorless oil after column purification (hexanes / EtOAc, 2:1). *R_f* (hexanes / EtOAc 1:1) = 0.47; ¹H NMR (300 MHz, CDCl₃): 5.98 – 5.81 (m, 2H), 5.39 – 5.20 (m, 4H), 4.96 (dt, *J* = 5.9, 1.2 Hz, 2H), 4.61 (dt, *J* = 5.8, 1.3 Hz, 2H), 4.53 (dd, *J* = 5.8, 4.7 Hz, 1H), 3.25 (bs, 1H), 2.92 (dd, *J* = 16.5, 4.7 Hz, 1H), 2.83 (dd, *J* = 16.5, 5.9 Hz, 1H).



Diethyl (*2R,3R,4S*)-4-methyltetrahydrofuran-2,3-dicarboxylate (**119a**).

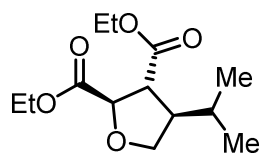
Following general procedure *GPVIII* using diethyl (*2R,3R*)-2-(allyloxy)-3-((3,5-bis(trifluoromethyl)benzoyl)oxy)succinate (**116a**, 243 mg, 500 μmol, 1.00 equiv), *fac*-Ir(ppy)₃ (6.6 mg, 10 μmol, 2.0 mol%), MeCN (12.5 mL, 0.04 M), Et₃N (0.35 mL, 0.25 g, 2.5 mmol, 5.0 equiv), and degassed water (0.90 mL, 0.90 g, 50 mmol, 100 equiv) gave 45.0 mg

(195 μmol , 39%) of diethyl 4-methyltetrahydrofuran-2,3-dicarboxylate (**119a**, dr = 61:30:9) as a colorless oil after column purification (hexanes / EtOAc, 6:1).



Diethyl (2*R*,3*R*,4*S*)-4-ethyltetrahydrofuran-2,3-dicarboxylate (119b).

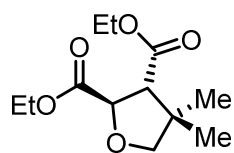
Following general procedure **GPVIII** using diethyl (2*R*,3*R*)-2-(((*E*)-but-2-en-1-yl)oxy)-3-((3-methyl-5-(trifluoromethyl)benzoyl)oxy)succinate (**116b**, 150 mg, 300 μmol , 1.00 equiv), *fac*-Ir(ppy)₃ (4.0 mg, 6.0 μmol , 2.0 mol%), MeCN (7.5 mL, 0.04 M), Et₃N (0.20 mL, 0.15 g, 1.5 mmol, 5.0 equiv), and degassed water (0.54 mL, 0.54 g, 30 mmol, 100 equiv) gave 28.2 mg (115 μmol , 38%) of diethyl (2*R*,3*R*,4*S*)-4-ethyltetrahydrofuran-2,3-dicarboxylate (**119b**, dr = 65:21:14) as a colorless oil after column purification (hexanes / EtOAc, 6:1 to 2:1). *R_f* (hexanes / EtOAc 1:1) = 0.92; IR (neat): 2970, 2938, 2878, 1729, 1464, 1372, 1266, 1179, 1135, 1095, 1028, 943, 857, 433 cm⁻¹; ¹H NMR (Major Diastereomer, 300 MHz, CDCl₃): 4.71 (d, *J* = 5.0 Hz, 1H), 4.18 – 4.08 (m, 5H), 3.64 (dt, *J* = 13.8, 8.2 Hz, 1H), 3.21 (dd, *J* = 8.4, 5.0 Hz, 1H), 2.48 – 2.32 (m, 1H), 1.66 – 1.28 (m, 2H), 1.27 – 1.20 (m, 6H), 0.88 (ddd, *J* = 7.5, 6.1, 3.9 Hz, 3H); ¹³C NMR (Major Diastereomer 1, 75 MHz, CDCl₃): 171.87, 171.37, 79.11, 73.29, 61.36, 61.00, 51.55, 44.06, 21.00, 14.28, 14.18, 12.75; ¹³C NMR (Major Diastereomer 2, 75 MHz, CDCl₃): 172.51, 171.63, 79.93, 74.32, 61.33, 61.26, 54.16, 46.48, 25.09, 14.28, 14.18, 12.37; ¹³C NMR (Major Diastereomer 1, DEPT-135, 75 MHz, CDCl₃): 79.06, 73.23, 61.31, 61.08, 60.94, 51.49, 44.01, 20.94, 14.22, 14.13, 12.70; ¹³C NMR (Major Diastereomer 2, DEPT-135, 75 MHz, CDCl₃): 79.88, 74.26, 61.27, 61.21, 60.94, 54.11, 46.43, 25.03, 14.22, 14.13, 12.32; HRMS (ESI) *m/z* calculated for C₁₂H₂₁O₅ ([M+H]⁺) 245.1384, found 245.1388.



Diethyl (2*R*,3*R*,4*R*)-4-isopropyltetrahydrofuran-2,3-dicarboxylate (119c).

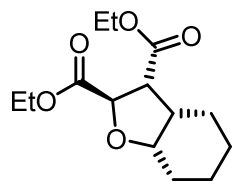
Following general procedure **GPVIII** using diethyl (2*R*,3*R*)-2-((3,5-bis(trifluoromethyl)benzoyl)oxy)-3-((3-methylbut-2-en-1-yl)oxy)succinate (**116c**, 257 mg, 500 μmol , 1.00 equiv), *fac*-Ir(ppy)₃ (6.7 mg, 10 μmol , 2.0 mol%), MeCN (12.5 mL, 0.04 M), Et₃N (0.35 mL, 0.25 g, 2.5 mmol, 5.0 equiv), and degassed water (0.90 mL, 0.90 g, 50 mmol, 100 equiv) gave 39.1 mg (151 μmol , 31%) of diethyl (2*R*,3*R*,4*S*)-4-ethyltetrahydrofuran-2,3-dicarboxylate (**4c**, dr = 65:21:14) as a colorless oil after column purification (hexanes / EtOAc, 6:1 to 2:1). *R_f* (hexanes / EtOAc 3:1) = 0.48; IR (neat): 2963, 2876, 1732, 1468, 1447, 1372, 1263, 1221, 1192, 1106, 1026, 969, 861, 715, 575 cm⁻¹; ¹H NMR (400 MHz, CDCl₃): 4.62 (d, *J* = 7.2

Hz, 1H), 4.28 – 4.16 (m, 4H), 4.13 (t, J = 8.2 Hz, 1H), 3.76 (t, J = 8.7 Hz, 1H), 2.90 (t, J = 7.8 Hz, 1H), 2.40 (q, J = 8.2 Hz, 1H), 1.73 – 1.61 (m, 1H), 1.28 (t, J = 7.1 Hz, 6H), 0.94 (d, J = 6.7 Hz, 3H), 0.89 (d, J = 6.7 Hz, 3H); ^{13}C NMR (101 MHz, CDCl_3): 173.06, 171.43, 80.73, 72.97, 61.30, 61.23, 52.62, 51.56, 30.65, 20.92, 20.72, 14.17, 14.13; HRMS (ESI) m/z calculated for $\text{C}_{13}\text{H}_{23}\text{O}_5$ ($[\text{M}+\text{H}]^+$) 259.1540, found 259.1548.



Diethyl (2*R*,3*R*)-4,4-dimethyltetrahydrofuran-2,3-dicarboxylate (119d).

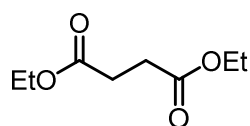
Following general procedure **GPVIII** using diethyl (2*R*,3*R*)-2-((3,5-bis(trifluoromethyl)benzoyl)oxy)-3-((2-methylallyl)oxy)succinate (**116d**, 250 mg, 500 μmol , 1.00 equiv), *fac*-Ir(ppy)₃ (6.6 mg, 10 μmol , 2.0 mol%), MeCN (12.5 mL, 0.04 M), Et₃N (0.35 mL, 0.25 g, 2.5 mmol, 5.0 equiv), and degassed water (0.90 mL, 0.90 g, 50 mmol, 100 equiv) gave 55.9 mg (229 μmol , 46%) of diethyl (2*R*,3*R*)-4,4-dimethyltetrahydrofuran-2,3-dicarboxylate (**119d**, dr > 95:5) as a colorless oil after column purification (hexanes / EtOAc, 5:1 to 2:1). R_f (hexanes / EtOAc 1:1) = 0.8, IR (neat): 2978, 2874, 1729, 1466, 1371, 1337, 1264, 109, 1179, 1093, 1028, 968, 940, 860, 716, 441 cm^{-1} . ^1H NMR (300 MHz, CDCl_3): 4.89 (d, J = 8.0 Hz, 1H), 4.27 – 4.12 (m, 4H), 3.69 (s, 2H), 2.89 (d, J = 8.0 Hz, 1H), 1.31 – 1.23 (m, 6H), 1.20 (s, J = 3.9 Hz, 3H), 1.02 (s, 3H); ^{13}C NMR (75 MHz, CDCl_3): 172.26, 170.64, 81.59, 78.79, 61.38, 61.10, 58.11, 43.68, 24.90, 21.99, 14.43, 14.26; ^{13}C NMR (DEPT-135, 75 MHz, CDCl_3): 81.48, 78.69, 61.28, 61.01, 58.01, 24.80, 21.89, 14.33, 14.16; HRMS (ESI) m/z calculated for $\text{C}_{12}\text{H}_{21}\text{O}_5$ ($[\text{M}+\text{H}]^+$) 245.1384, found 245.1388.



Diethyl (2*R*,3*R*,3*aS*,7*aS*)-octahydrobenzofuran-2,3-dicarboxylate (119e).

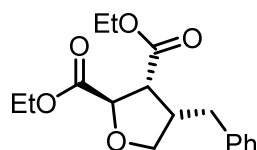
Following general procedure **GPVIII** using diethyl (2*R*,3*R*)-2-((3,5-bis(trifluoromethyl)benzoyl)oxy)-3-(cyclohex-2-en-1-yloxy)succinate (**116e**, 207 mg, 395 μmol , 1.00 equiv), *fac*-Ir(ppy)₃ (5.3 mg, 8.0 μmol , 2.0 mol%), MeCN (10 mL, 0.04 M), Et₃N (0.28 mL, 0.20 g, 2.0 mmol, 5.0 equiv), and degassed water (0.71 mL, 0.71 g, 39 mmol, 100 equiv) gave 34.5 mg (127 μmol , 32%) of diethyl (2*R*,3*R*,3*aS*,7*aS*)-octahydrobenzofuran-2,3-dicarboxylate (**119e**, dr = 53:47) as a colorless oil after flash column purification (hexanes / EtOAc, 6:1). R_f (hexanes / EtOAc 3:1) = 0.6; IR (neat): 2970, 2938, 2878, 1729, 1464, 1372, 1266, 1179, 1135, 1095, 1028, 943, 857, 433 cm^{-1} ; ^1H NMR (Major Diastereomer, 300 MHz, CDCl_3): 4.91 (d, J = 8.4 Hz, 1H), 4.23 – 4.14 (m, 4H), 3.36 (dd, J = 8.3, 6.5 Hz, 1H),

2.37 – 2.27 (m, 1H), 2.15 – 2.05 (m, 1H), 1.75 – 1.29 (m, 7H), 1.28 – 1.22 (m, 6H); ^1H NMR (Minor Diastereomer, 300 MHz, CDCl_3): 4.72 (d, $J = 5.9$ Hz, 1H), 4.23 – 4.14 (m, 4H), 3.01 (dd, $J = 5.7, 4.9$ Hz, 1H), 2.37 – 2.27 (m, 1H), 1.91 – 1.79 (m, 1H), 1.75 – 1.29 (m, 7H), 1.28 – 1.22 (m, 6H); ^{13}C NMR (Major Diastereomer, 75 MHz, CDCl_3): 172.98, 170.31, 79.15, 76.39, 61.31, 61.07, 53.33, 41.29, 27.71, 24.18, 23.24, 19.77, 14.38, 14.28; ^{13}C NMR (Minor Diastereomer, 75 MHz, CDCl_3): 172.94, 171.96, 78.66, 78.34, 61.41, 61.31, 53.22, 42.72, 28.13, 26.97, 23.30, 21.04, 14.31, 14.28; ^{13}C NMR (Major Diastereomer, DEPT-135, 75 MHz, CDCl_3): 79.05, 76.30, 61.22, 60.98, 53.24, 41.19, 27.62, 24.09, 23.14, 19.68, 14.29, 14.19; ^{13}C NMR (Minor Diastereomer, DEPT-135, 75 MHz, CDCl_3): 78.56, 78.25, 61.32, 61.22, 53.13, 42.63, 28.04, 26.88, 23.20, 20.95, 14.22, 14.19; HRMS (ESI) m/z calculated for $\text{C}_{14}\text{H}_{23}\text{O}_5$ ($[\text{M}+\text{H}]^+$) 271.1540, found 271.1543.



Diethyl succinate (119g).⁶⁸

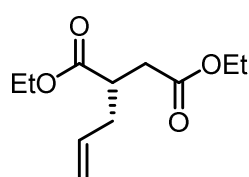
Following general procedure **GPVIII** using diethyl (2*R*,3*R*)-2-(acryloyloxy)-3-((3,5-bis(trifluoromethyl)benzoyl)oxy)succinate (**116g**, 100 mg, 200 μmol , 1.00 equiv), *fac*-Ir(ppy)₃ (2.7 mg, 4.1 μmol , 2.0 mol%), MeCN (5.0 mL, 0.04 M), Et₃N (0.14 mL, 0.10 g, 1.0 mmol, 5.0 equiv), and degassed water (0.36 mL, 0.36 g, 20 mmol, 100 equiv) gave 14.3 mg (97.4 μmol , 49%) of diethyl succinate (**119g**) as a colorless oil after column purification (hexanes / EtOAc, 8:1). R_f (hexanes / EtOAc, 6:1) = 0.37; ^1H NMR (300 MHz, CDCl_3): 4.07 (q, $J = 7.1$ Hz, 4H), 2.55 (s, 4H), 1.19 (t, $J = 7.1$ Hz, 6H).



Diethyl (2*R*,3*S*,4*S*)-4-benzyltetrahydrofuran-2,3-dicarboxylate (119h).

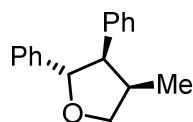
Following general procedure **GPVIII** using diethyl (2*R*,3*R*)-2-((3,5-bis(trifluoromethyl)benzoyl)oxy)-3-(cinnamyloxy)succinate (**116h**, 270 mg, 480 μmol , 1.00 equiv), *fac*-Ir(ppy)₃ (6.5 mg, 9.8 μmol , 2.0 mol%), MeCN (12 mL, 0.04 M), Et₃N (335 μL , 243 mg, 2.4 mmol, 5.0 equiv), and degassed water (0.86 mL, 0.86 g, 48 mmol, 100 equiv) gave 70.3 mg (229 μmol , 48%) of diethyl (2*R*,3*S*,4*S*)-4-benzyltetrahydrofuran-2,3-dicarboxylate (**119h**, dr = 78:22) as a colorless oil after automatic flash silica gel column chromatography (0 – 20% EtOAc in hexanes). R_f (hexanes / EtOAc, 4:1) = 0.27; IR (neat): 2983, 2942, 1729, 1455, 1372, 1262, 1178, 1097, 1027, 951, 860, 746, 700, 493 cm^{-1} ; ^1H NMR (Major Diastereomer, 400 MHz, CDCl_3): 7.34 – 7.10 (m, 5H), 4.84 (d, $J = 5.9$ Hz, 1H), 4.28 – 4.15 (m, 4H), 3.95 (dd, $J = 8.5, 6.1$ Hz, 1H), 3.78 (dd, $J = 8.5, 6.2$ Hz, 1H), 3.35 (dd, $J = 8.0, 5.8$ Hz, 1H), 2.84 – 2.76 (m,

2H), 2.53 (dd, $J = 13.5, 10.3$ Hz, 1H), 1.29 (t, $J = 7.1$ Hz, 3H), 1.27 (t, $J = 7.1$ Hz, 3H); ^1H NMR (Minor Diastereomer, 400 MHz, CDCl_3): 7.34 – 7.10 (m, 5H), 4.69 (d, $J = 6.9$ Hz, 1H), 4.28 – 4.15 (m, 2H), 4.15 – 4.00 (m, 3H), 3.78 – 3.71 (m, 1H), 2.84 – 2.76 (m, 4H), 1.28 (t, $J = 7.2$ Hz, 3H), 1.21 (t, $J = 7.0$ Hz, 3H); ^{13}C NMR (Major Diastereomer, 101 MHz, CDCl_3): 171.69, 171.03, 139.30, 128.69, 128.61, 126.50, 78.93, 73.12, 61.40, 61.16, 51.48, 43.66, 34.09, 14.27, 14.16; ^{13}C NMR (Minor Diastereomer, 101 MHz, CDCl_3): 172.04, 171.48, 138.93, 128.75, 128.56, 126.54, 79.90, 74.06, 61.38, 61.26, 53.75, 46.03, 37.94, 14.16, 14.11; HRMS (ESI) m/z calculated for $\text{C}_{17}\text{H}_{23}\text{O}_5$ ($[\text{M}+\text{H}]^+$) 307.1540, found 307.1543.



Diethyl (*S*)-2-allylsuccinate (119i).

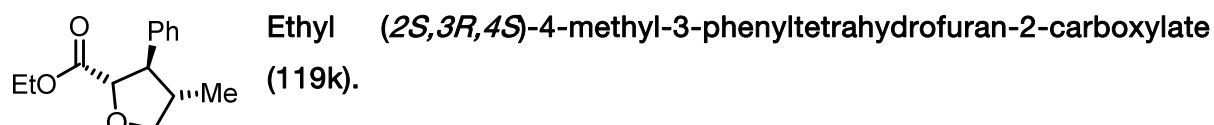
Following general procedure **GPVIII** using diethyl (*2S,3S*)-2-allyl-3-((3,5-bis(trifluoromethyl)benzoyl)oxy)succinate (**116i**, 235 mg, 500 μmol , 1.00 equiv), *fac*-Ir(ppy)₃ (6.6 mg, 10 μmol , 2.0 mol%), MeCN (12.5 mL, 0.04 M), Et₃N (0.35 mL, 0.25 g, 2.5 mmol, 5.0 equiv), and degassed water (0.90 mL, 0.90 g, 50 mmol, 100 equiv) gave 64.9 mg (303 μmol , 61%) of diethyl (*S*)-2-allylsuccinate (**119i**) as a colorless oil after column purification (hexanes / EtOAc, 4:1). R_f (hexanes / EtOAc, 4:1) = 0.51; IR (neat): 2982, 1730, 1440, 1372, 1301, 1159, 1096, 1030, 919, 858, 793, 628 cm^{-1} ; ^1H NMR (400 MHz, CDCl_3): 5.76 – 5.55 (m, 1H), 5.05 – 4.96 (m, 2H), 4.13 – 3.99 (m, 4H), 2.89 – 2.79 (m, 1H), 2.61 (dd, $J = 16.5, 9.0$ Hz, 1H), 2.43 – 2.30 (m, 2H), 2.27 – 2.17 (m, 1H), 1.18 (t, $J = 7.2$ Hz, 3H), 1.17 (t, $J = 7.2$ Hz, 3H); ^{13}C NMR (101 MHz, CDCl_3): 174.12, 171.86, 134.44, 117.71, 60.60, 60.51, 40.82, 35.92, 35.21, 14.16, 14.12; HRMS (ESI) m/z calculated for $\text{C}_{11}\text{H}_{19}\text{O}_4$ ($[\text{M}+\text{H}]^+$) 215.1278, found 215.1281.



(*2S,3R,4R*)-4-methyl-2,3-diphenyltetrahydrofuran (119j).

Following general procedure **GPVIII** using (*1R,2R*)-2-(allyloxy)-1,2-diphenylethyl 3,5-bis(trifluoromethyl)benzoate (**126a**, 98.9 mg, 200 μmol , 1.00 equiv), *fac*-Ir(ppy)₃ (2.7 mg, 4.1 μmol , 2.0 mol%), MeCN (5.0 mL, 0.04 M), Et₃N (139 μL , 101 mg, 1.00 mmol, 5.0 equiv), and degassed water (0.36 mL, 0.36 g, 20 mmol, 100 equiv) gave 20.0 mg (83.8 μmol , 42%) of (*2S,3R,4R*)-4-methyl-2,3-diphenyltetrahydrofuran (**119j**, dr = 49:42:9) as a colorless oil after flash silica gel column chromatography (hexanes / EtOAc, 25:1). An additional column chromatography gave 9.2 mg (38 μmol , 19%) of (*2S,3R,4R*)-4-methyl-2,3-diphenyltetrahydrofuran as a single diastereomer. R_f (hexanes / EtOAc, 6:1) = 0.55; IR (neat): 2968, 2930, 2874, 1742, 1603, 1495, 1453, 1382, 1279, 1245, 1182, 1140, 1069, 1047, 1027, 925, 803,

748, 698, 611, 580, 528 cm^{-1} ; ^1H NMR (Major Diastereomer, 400 MHz, CDCl_3): 7.38 – 7.20 (m, 10H), 5.34 (d, J = 5.4 Hz, 1H), 4.36 (dd, J = 8.3, 7.1 Hz, 1H), 3.75 (t, J = 8.0 Hz, 1H), 3.34 (dd, J = 7.6, 5.3 Hz, 1H), 2.68 (sept, J = 7.3 Hz, 1H), 0.72 (d, J = 7 Hz, 3H); ^{13}C NMR (Major Diastereomer, 101 MHz, CDCl_3): 143.58, 139.72, 128.88, 128.35, 128.25, 127.12, 126.58, 125.41, 85.12, 74.81, 57.43, 37.41, 13.50; HRMS (ESI) m/z calculated for $\text{C}_{17}\text{H}_{18}\text{O}$ ($[\text{M}+\text{H}]^+$) 238.1352, found 238.1352.

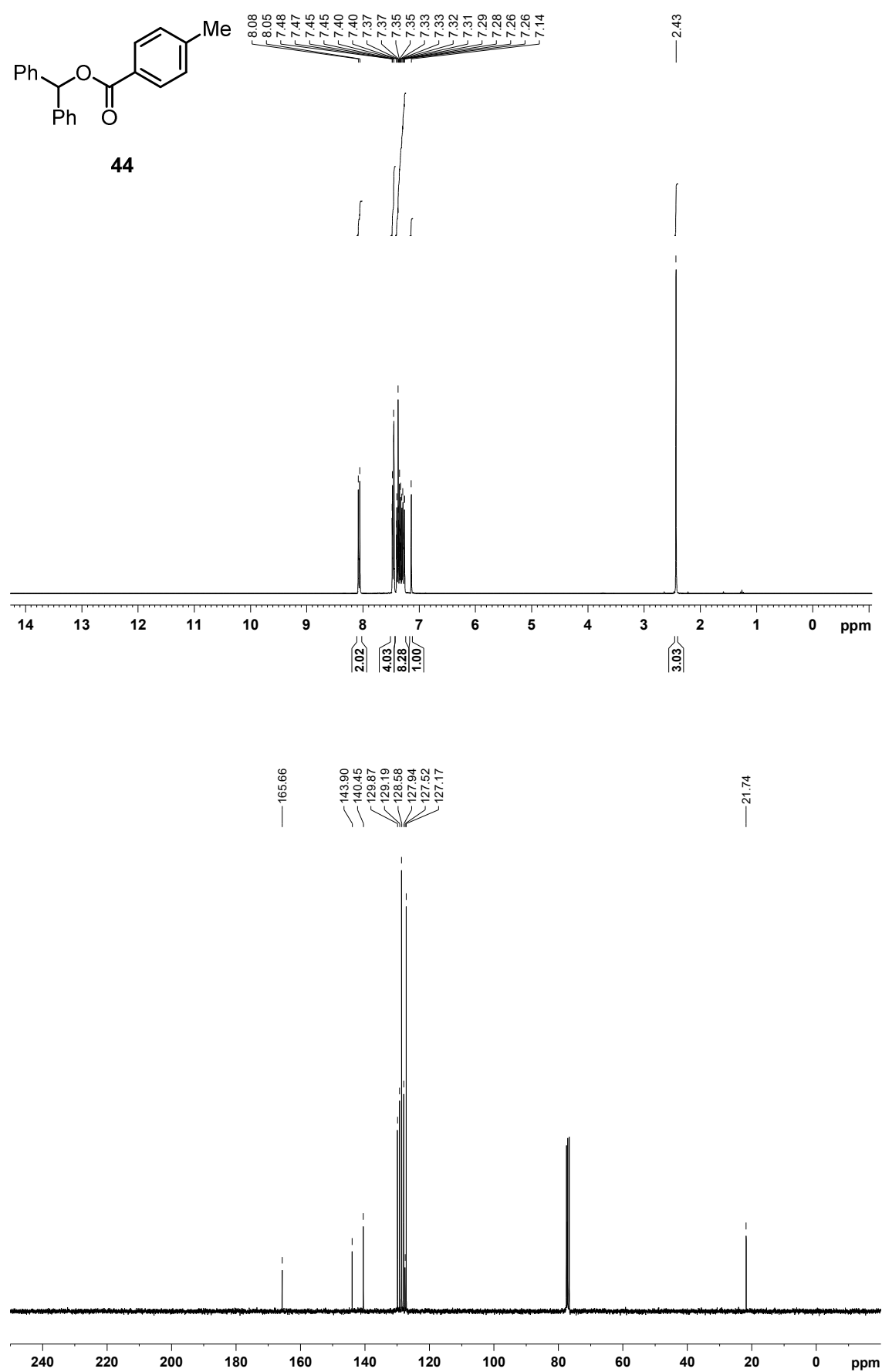


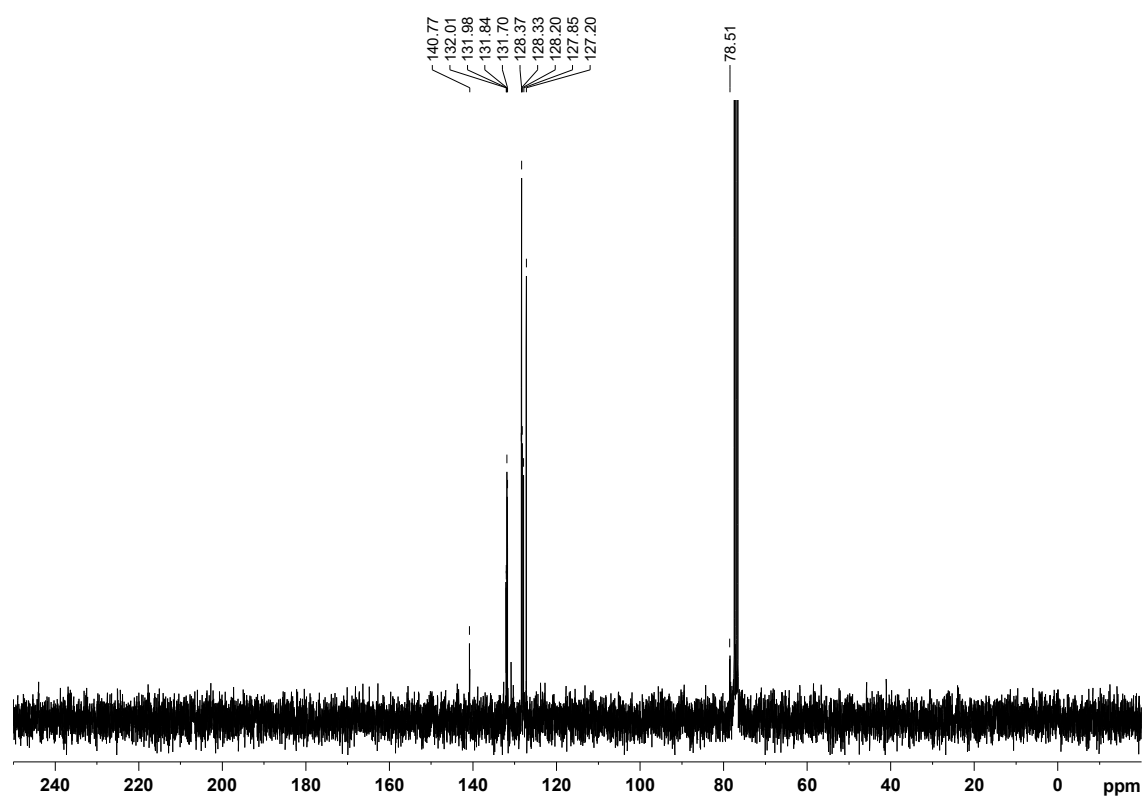
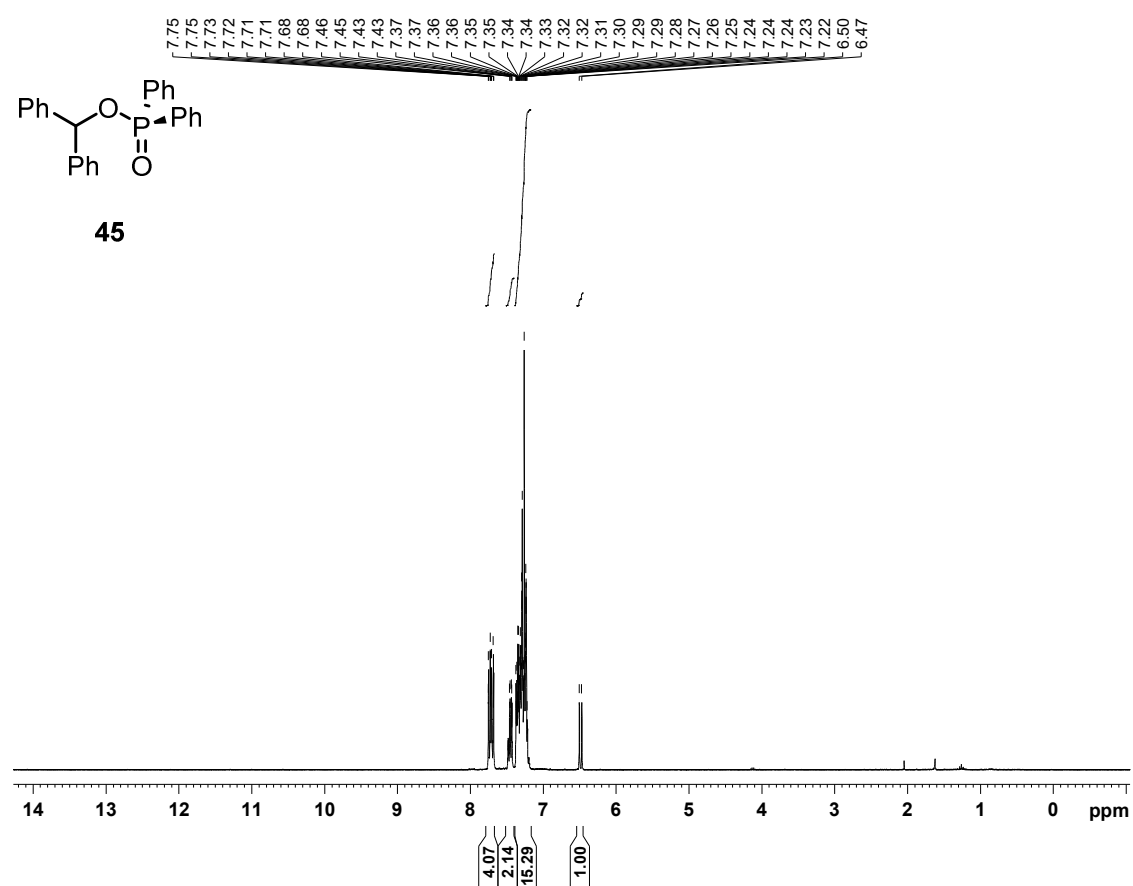
Following general procedure **GPVIII** using (1*R*,2*S*)-2-(allyloxy)-3-ethoxy-3-oxo-1-phenylpropyl 3,5-bis(trifluoromethyl)benzoate (**126b**, 98.0 mg, 200 μmol , 1.00 equiv), *fac*-Ir(ppy)₃ (2.7 mg, 4.1 μmol , 2.0 mol%), MeCN (5.0 mL, 0.04 M), Et₃N (139 μL , 101 mg, 1.00 mmol, 5.0 equiv), and degassed water (0.36 mL, 0.36 g, 20 mmol, 100 equiv) gave 26.1 mg (111 μmol , 56%) of ethyl (2*S*,3*R*,4*S*)-4-methyl-3-phenyltetrahydrofuran-2-carboxylate (**119k**, dr = 67:19:14) as a colorless oil after flash silica gel column chromatography (hexanes / EtOAc, 10:1). R_f (hexanes / EtOAc, 6:1) = 0.25; IR (neat): 2962, 2873, 1745, 1603, 1456, 1377, 1270, 1187, 1108, 1083, 1029, 965, 939, 864, 754, 700, 520 cm^{-1} ; ^1H NMR (Major Diastereomer, 300 MHz, CDCl_3): 7.41 – 7.14 (m, 5H), 4.46 (d, J = 8.5 Hz, 1H), 4.32 – 4.25 (m, 1H), 4.23 – 4.09 (m, 2H), 3.72 (dd, J = 10.1, 8.4 Hz, 1H), 2.93 (dd, J = 10.1, 8.5 Hz, 1H), 2.57 – 2.39 (m, 1H), 1.18 (t, J = 7.2 Hz, 3H), 0.99 (d, J = 6.5 Hz, 3H); ^{13}C NMR (Major Diastereomer, 75 MHz, CDCl_3): 172.72, 139.56, 128.75, 127.78, 127.20, 84.11, 76.29, 60.92, 58.28, 43.47, 14.21, 14.19; ^{13}C NMR (Minor Diastereomer 1, 75 MHz, CDCl_3): 172.47, 142.37, 128.42, 127.23, 125.03, 83.55, 75.53, 61.19, 55.80, 36.54, 15.48, 14.33; ^{13}C NMR (Minor Diastereomer 2, 75 MHz, CDCl_3): 171.39, 137.37, 128.32, 127.67, 124.72, 82.02, 75.99, 60.37, 56.37, 42.38, 38.19, 13.61; HRMS (ESI) m/z calculated for $\text{C}_{14}\text{H}_{19}\text{O}_3$ ($[\text{M}+\text{H}]^+$) 235.1329, found 235.1331.

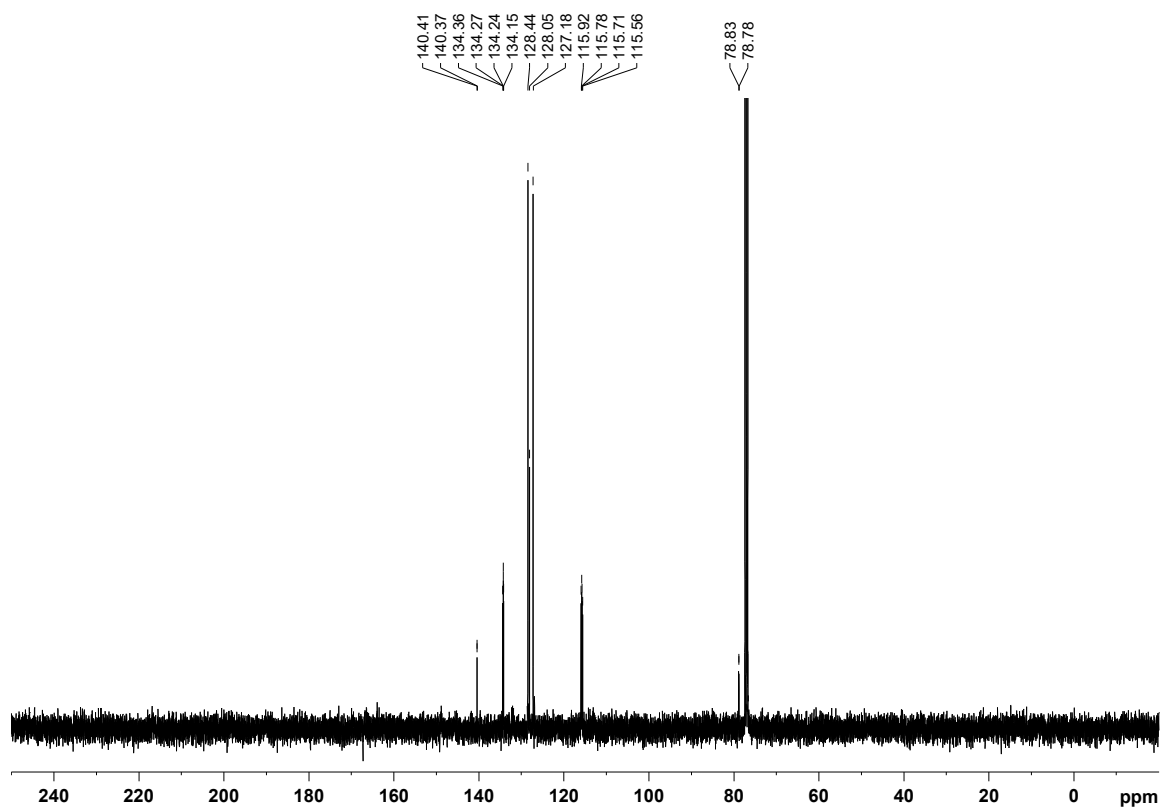
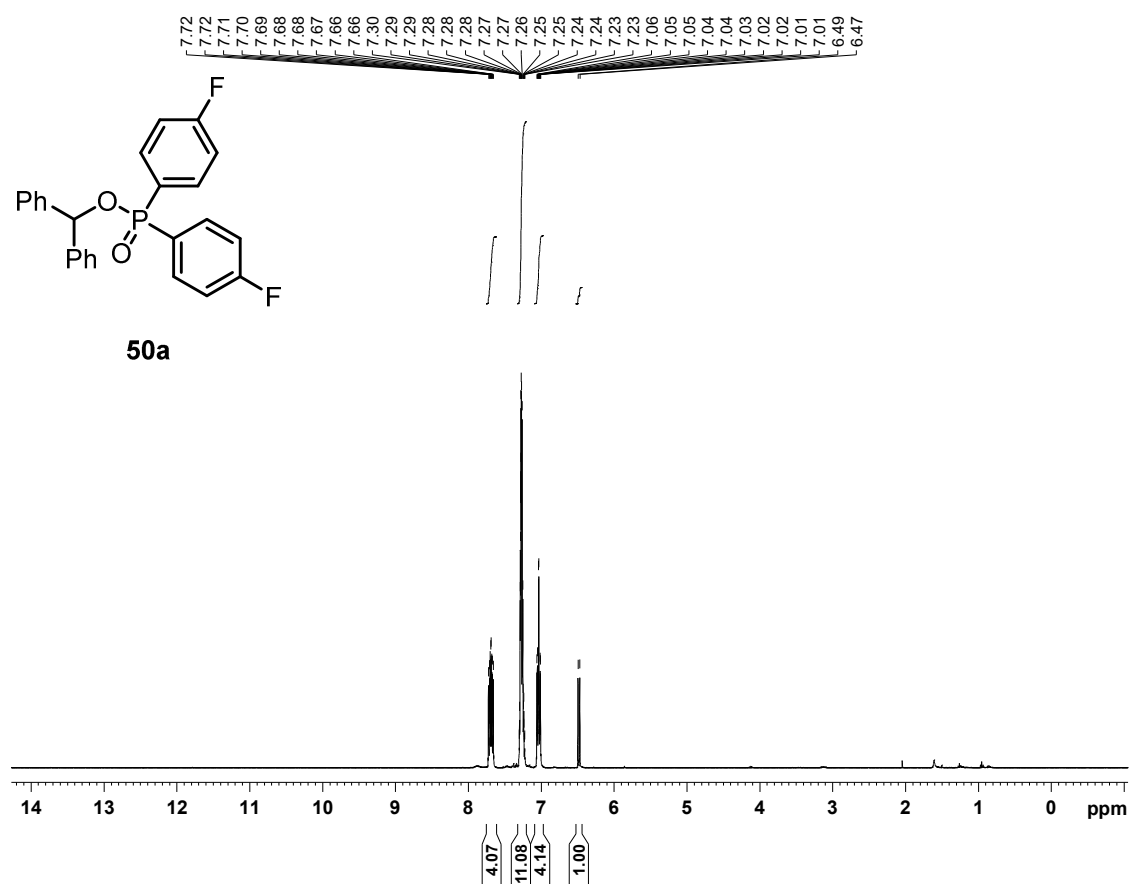
3.10 NMR spectra of new compounds

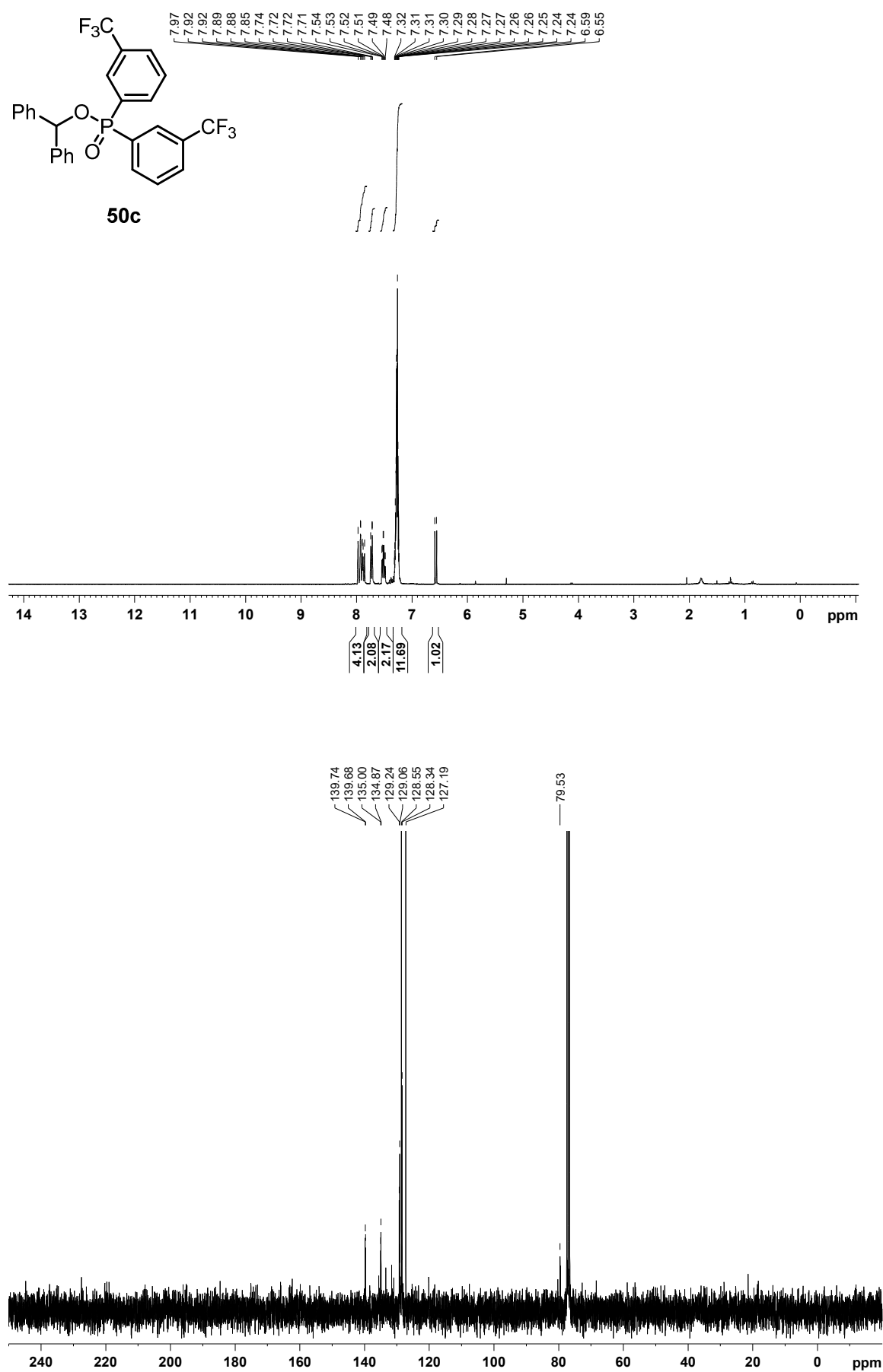
Typically, ^1H -NMR followed by ^{13}C -NMR spectra are depicted. Where the identity of the material might be in question, ^{19}F -NMR (decoupled), ^{31}P -NMR (decoupled), COSY, NOESY, HSQC, and / or HMBC spectra are supplied.

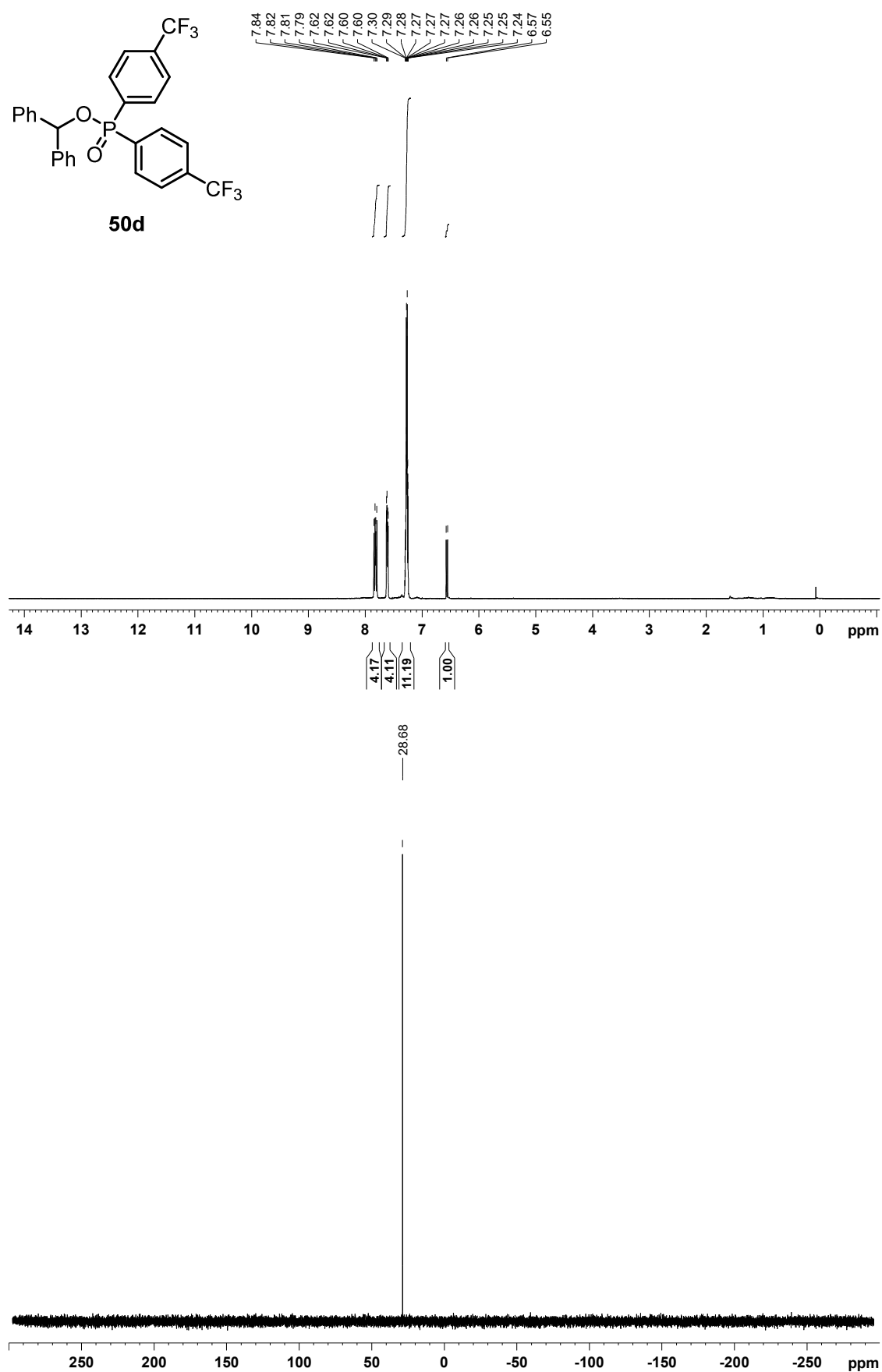
Note: All spectra of new compounds that were already included in any Supporting Information are not part of the printed edition of this work. However, spectra are available in the digital edition.

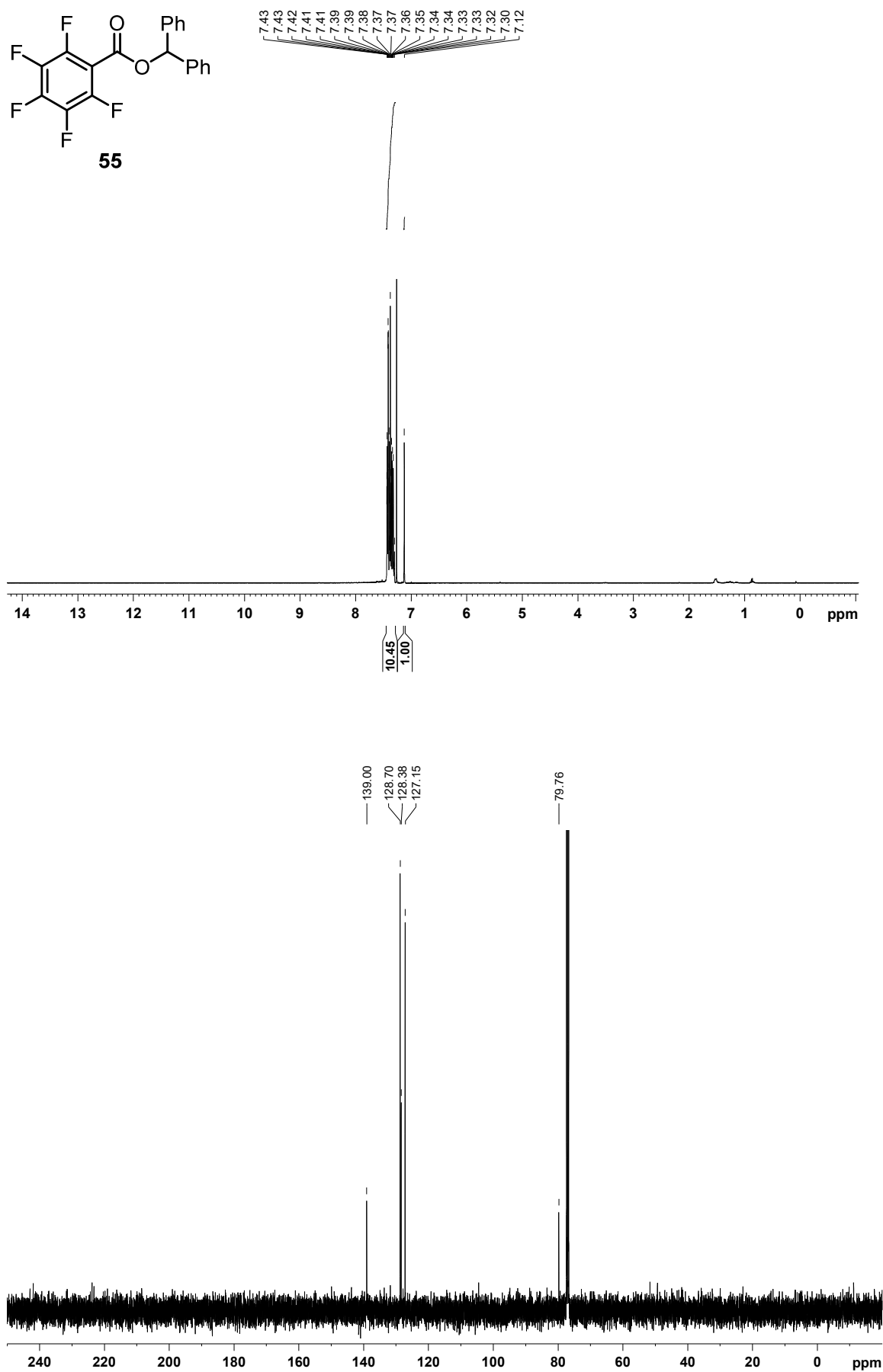


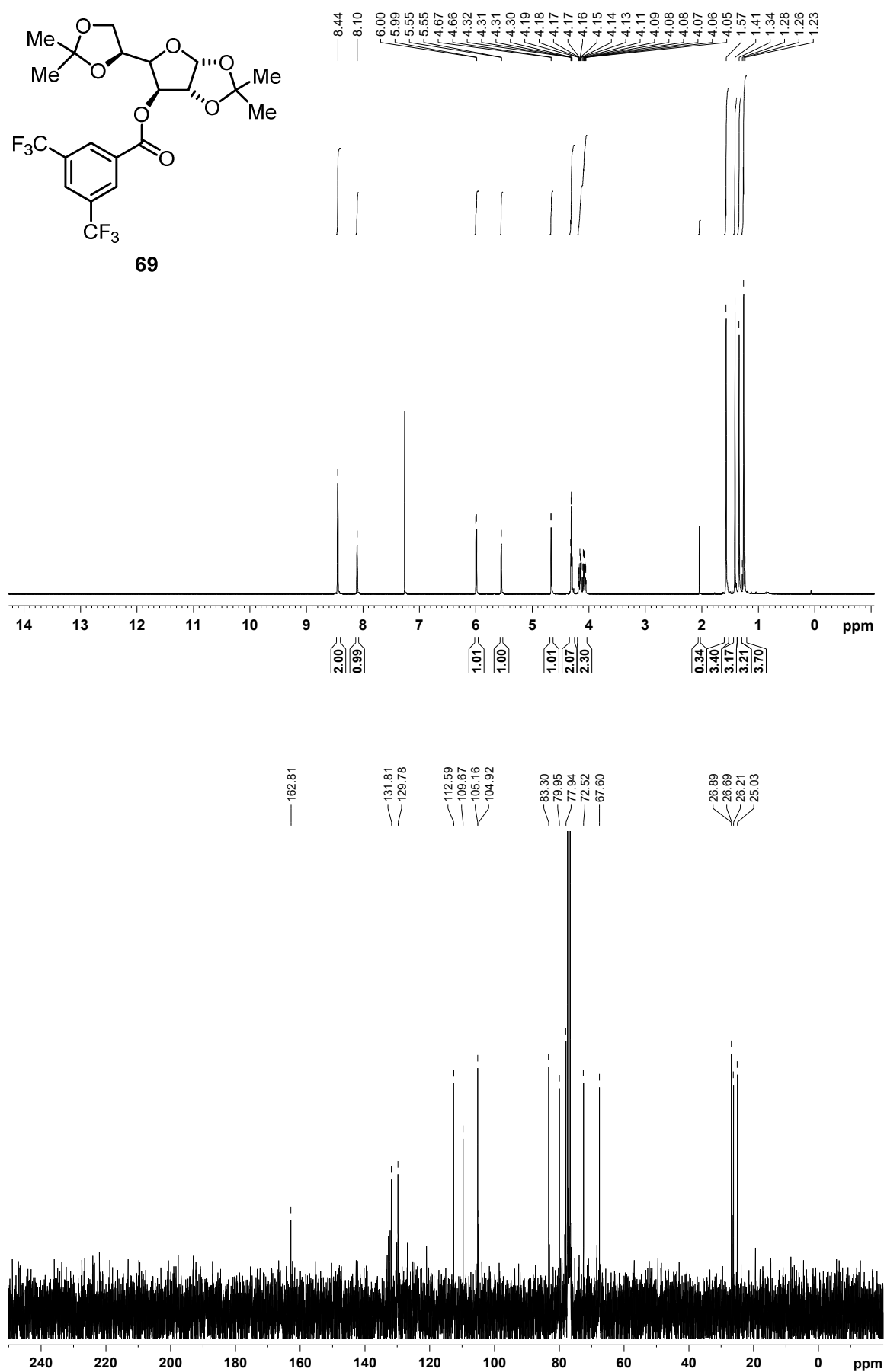


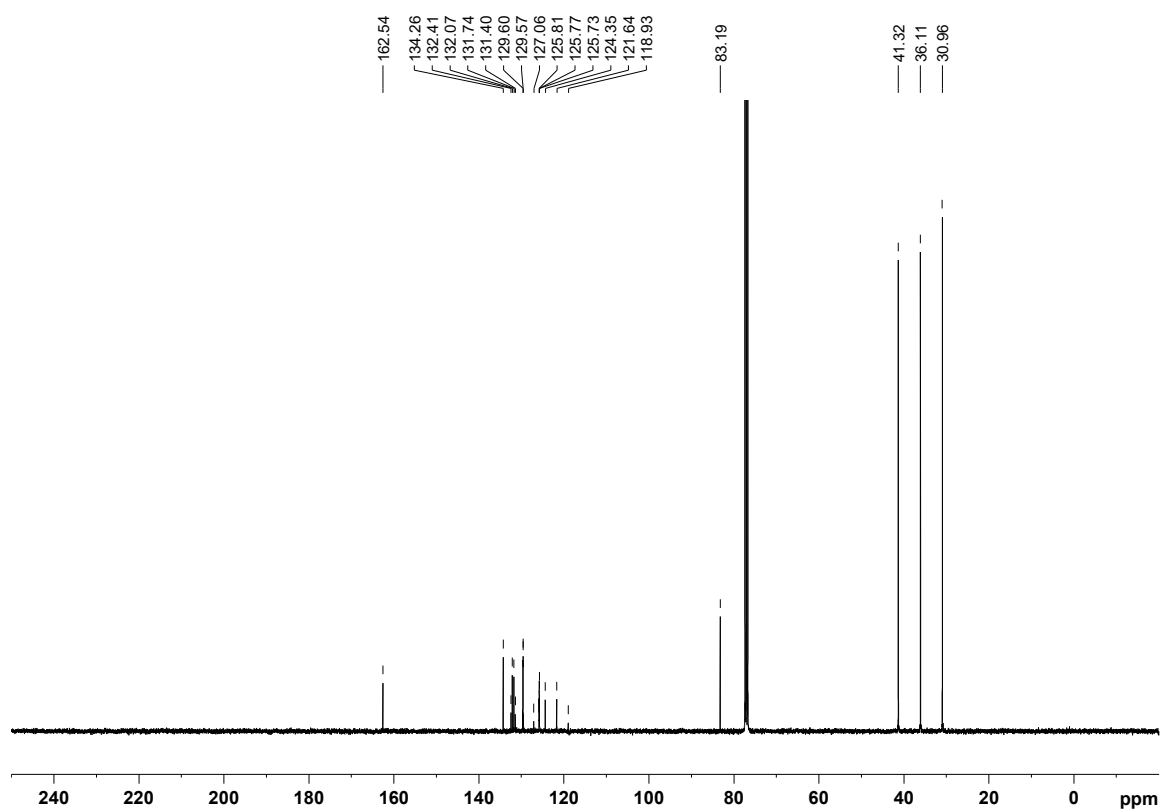
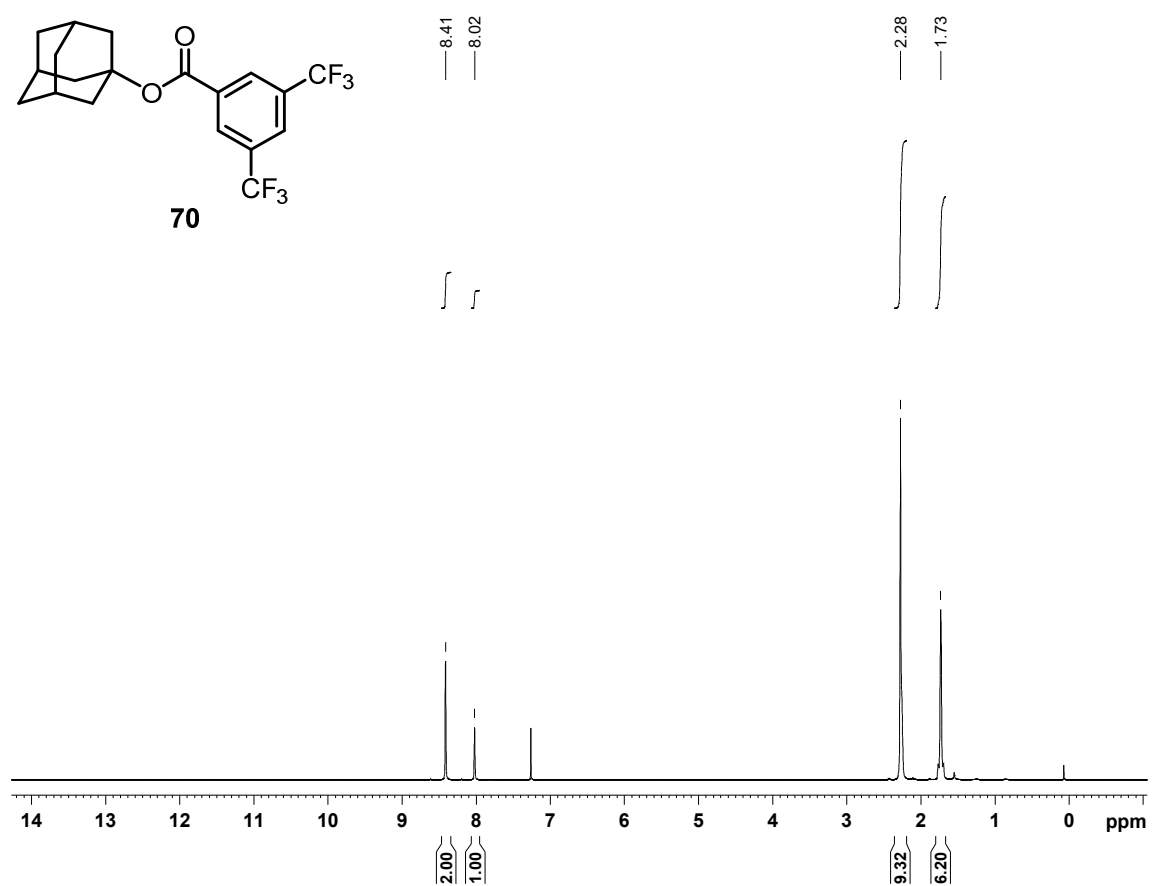


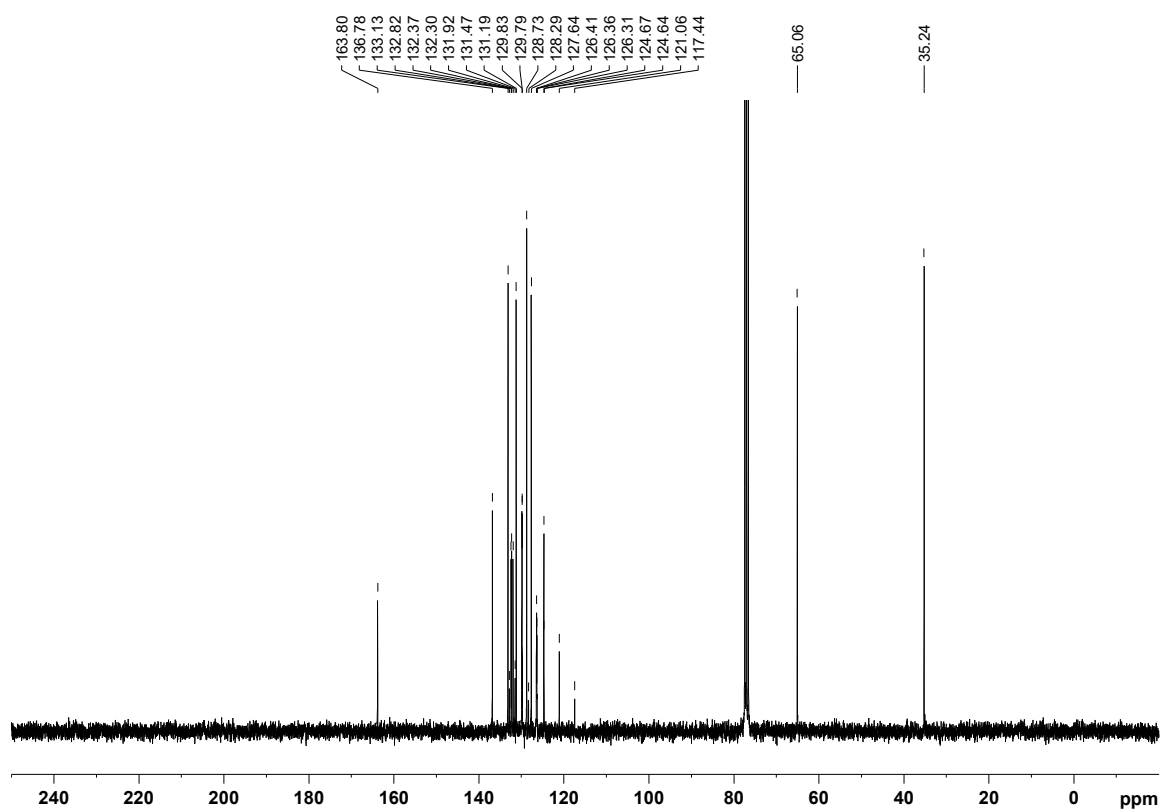
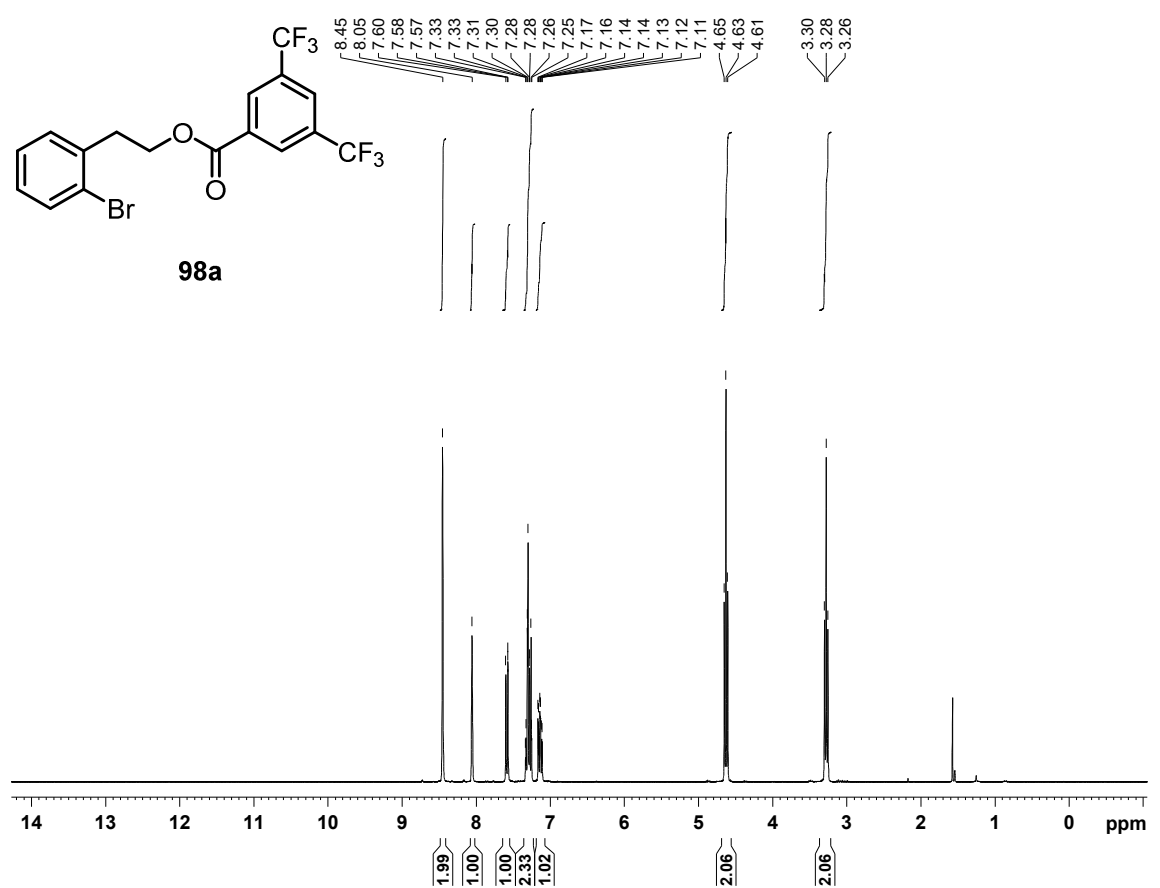


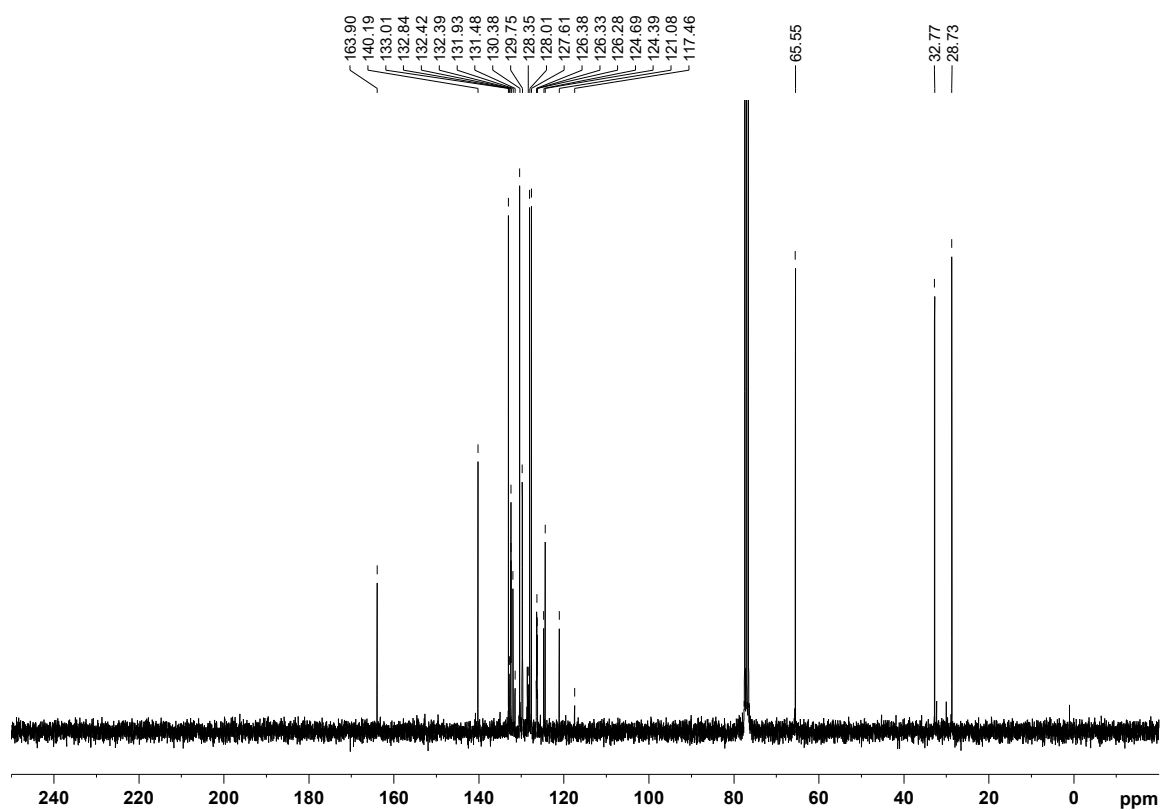
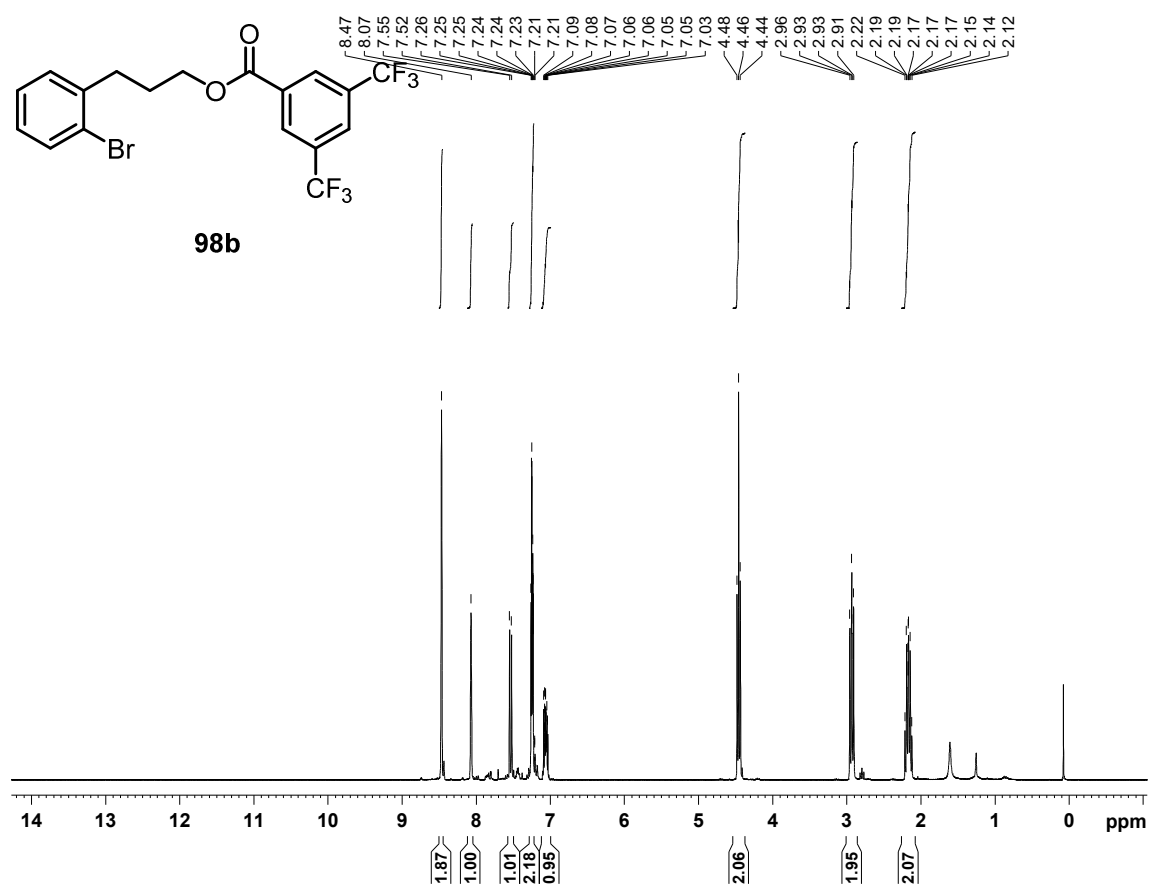


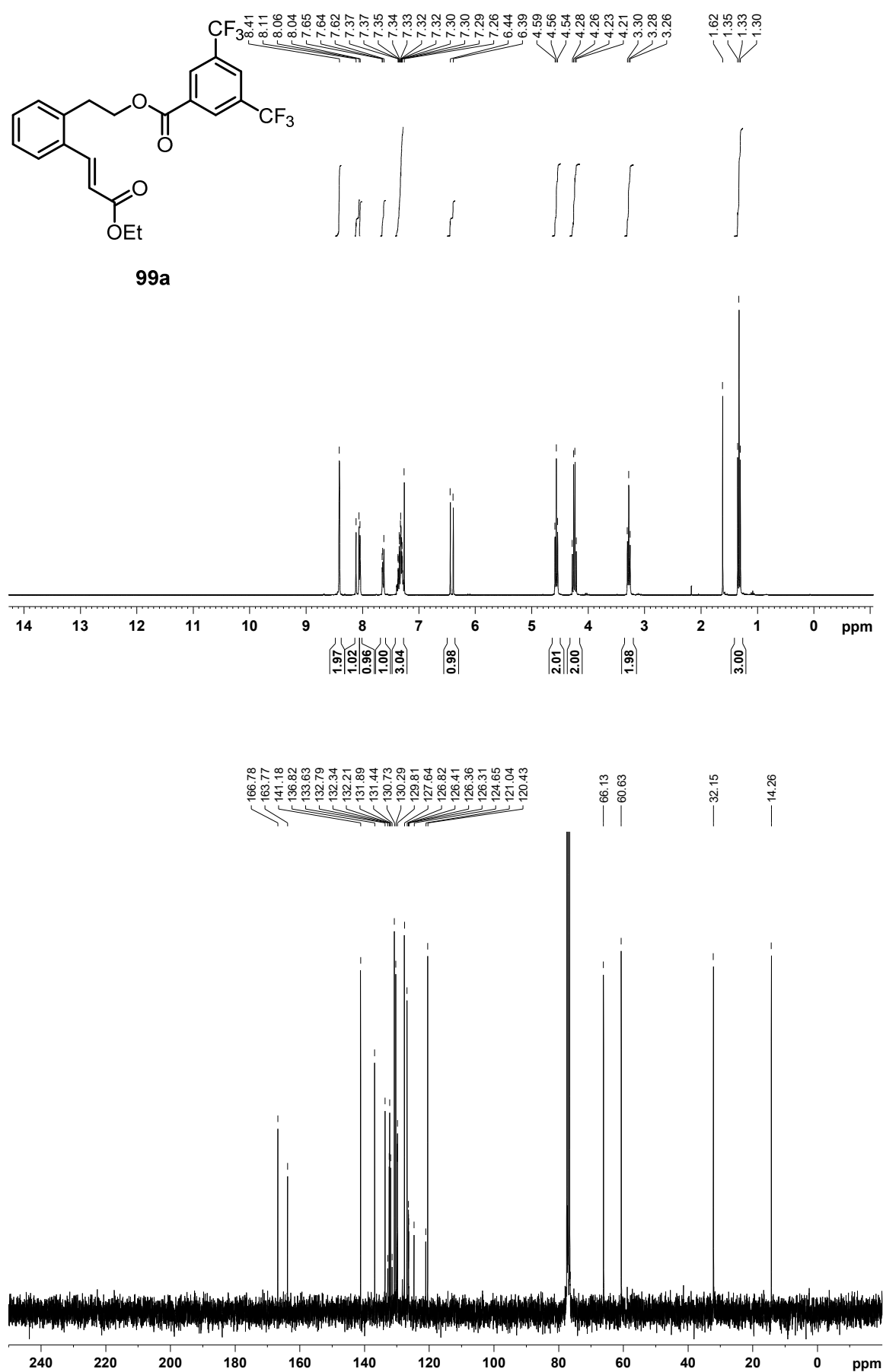


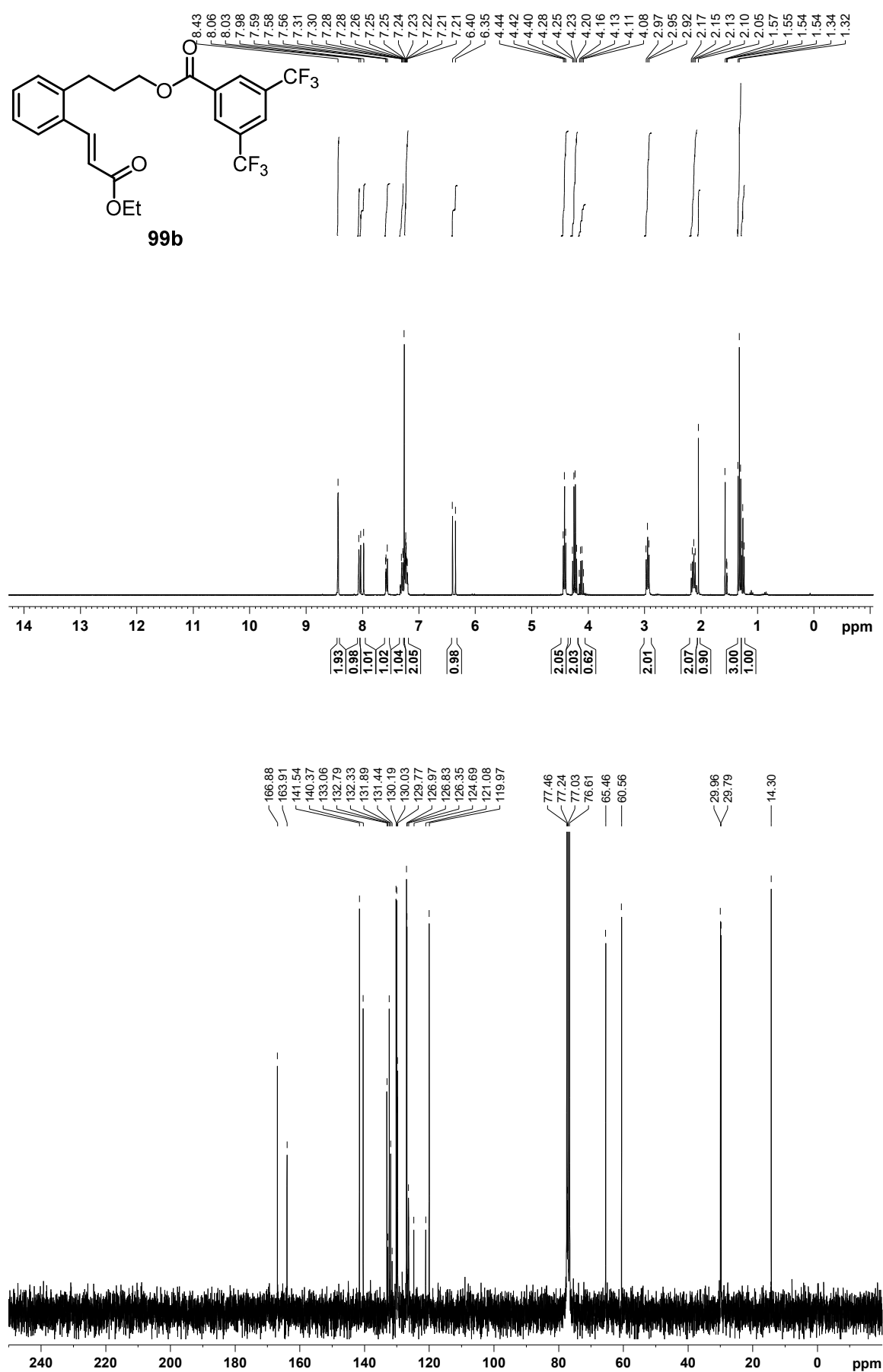


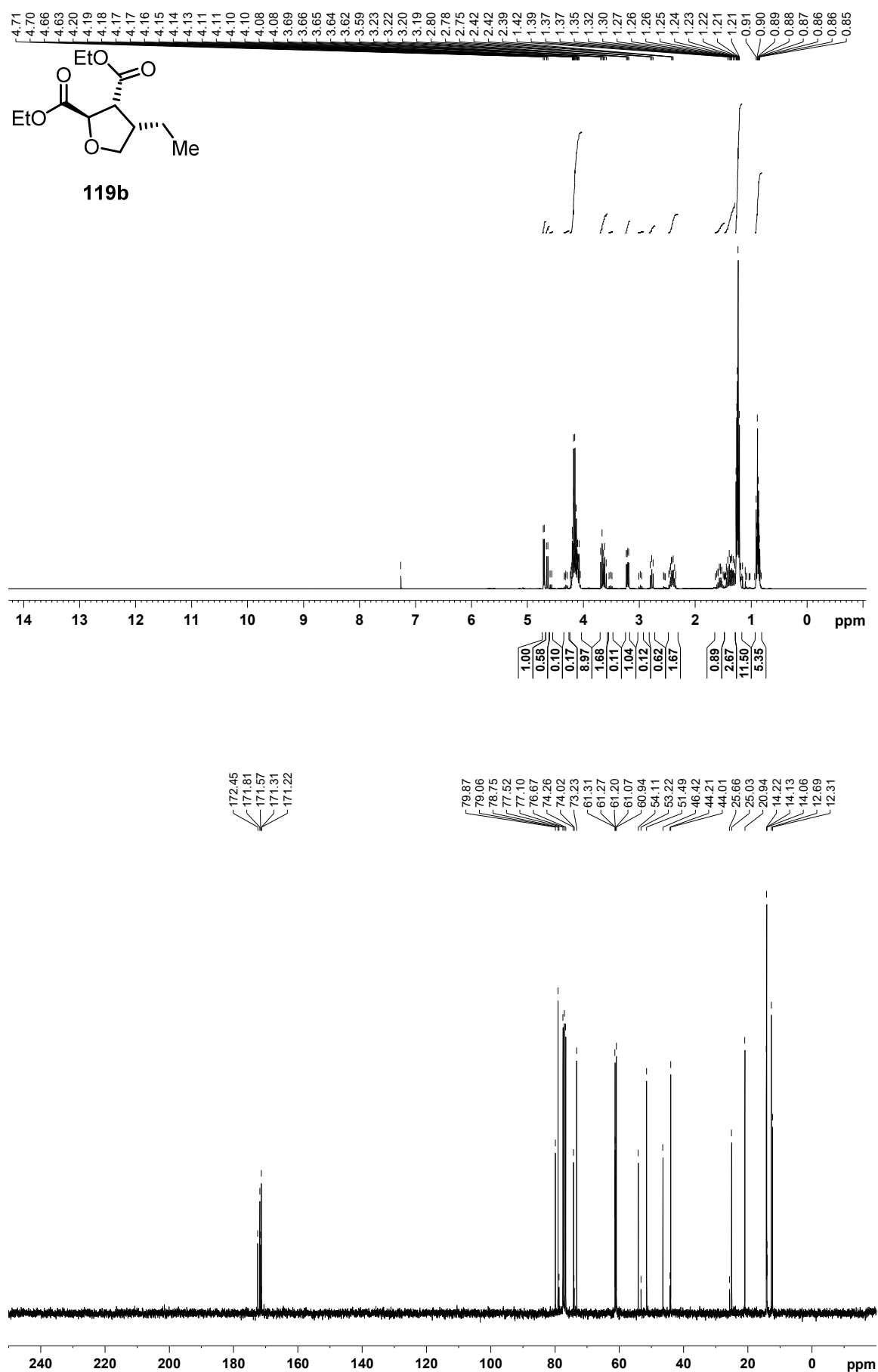


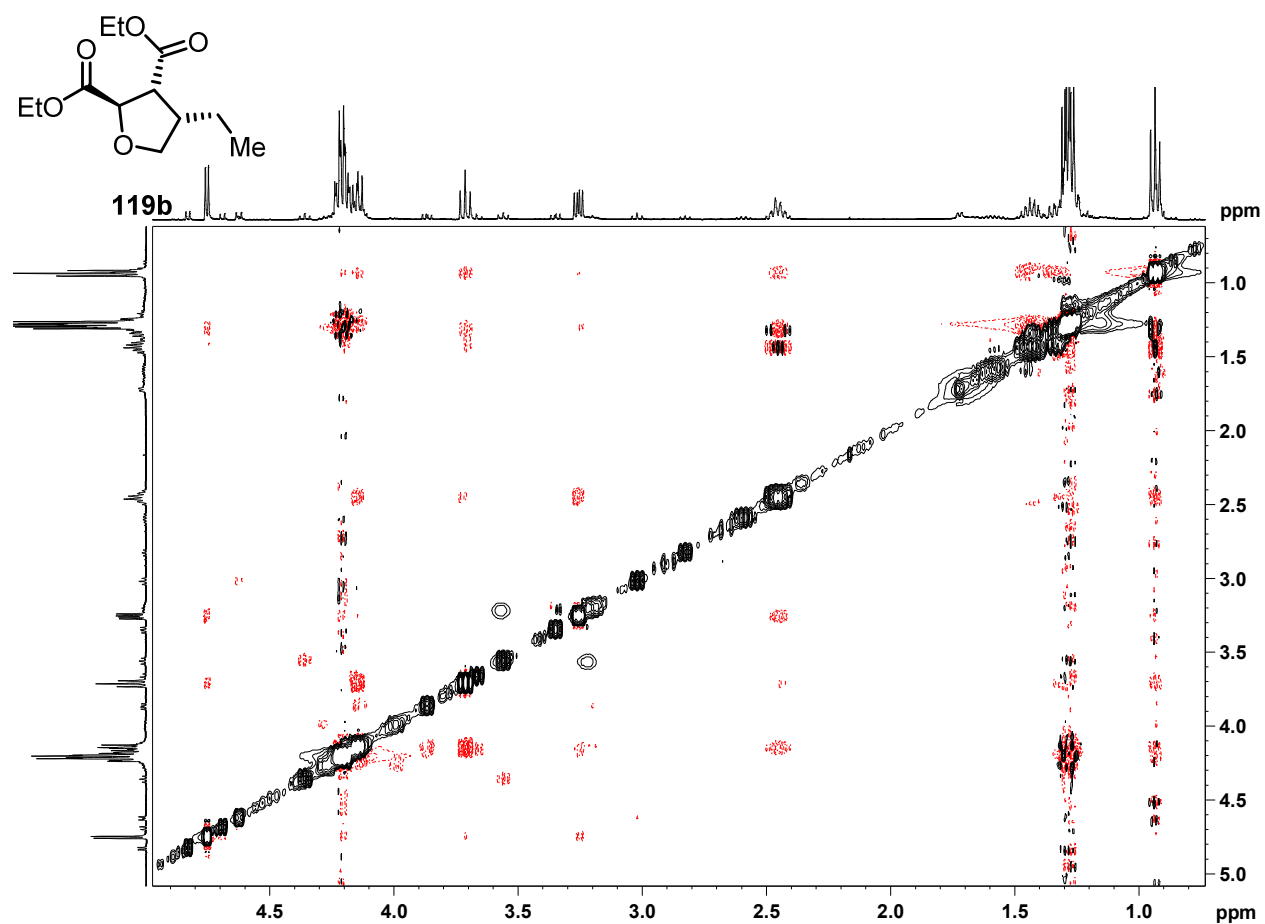


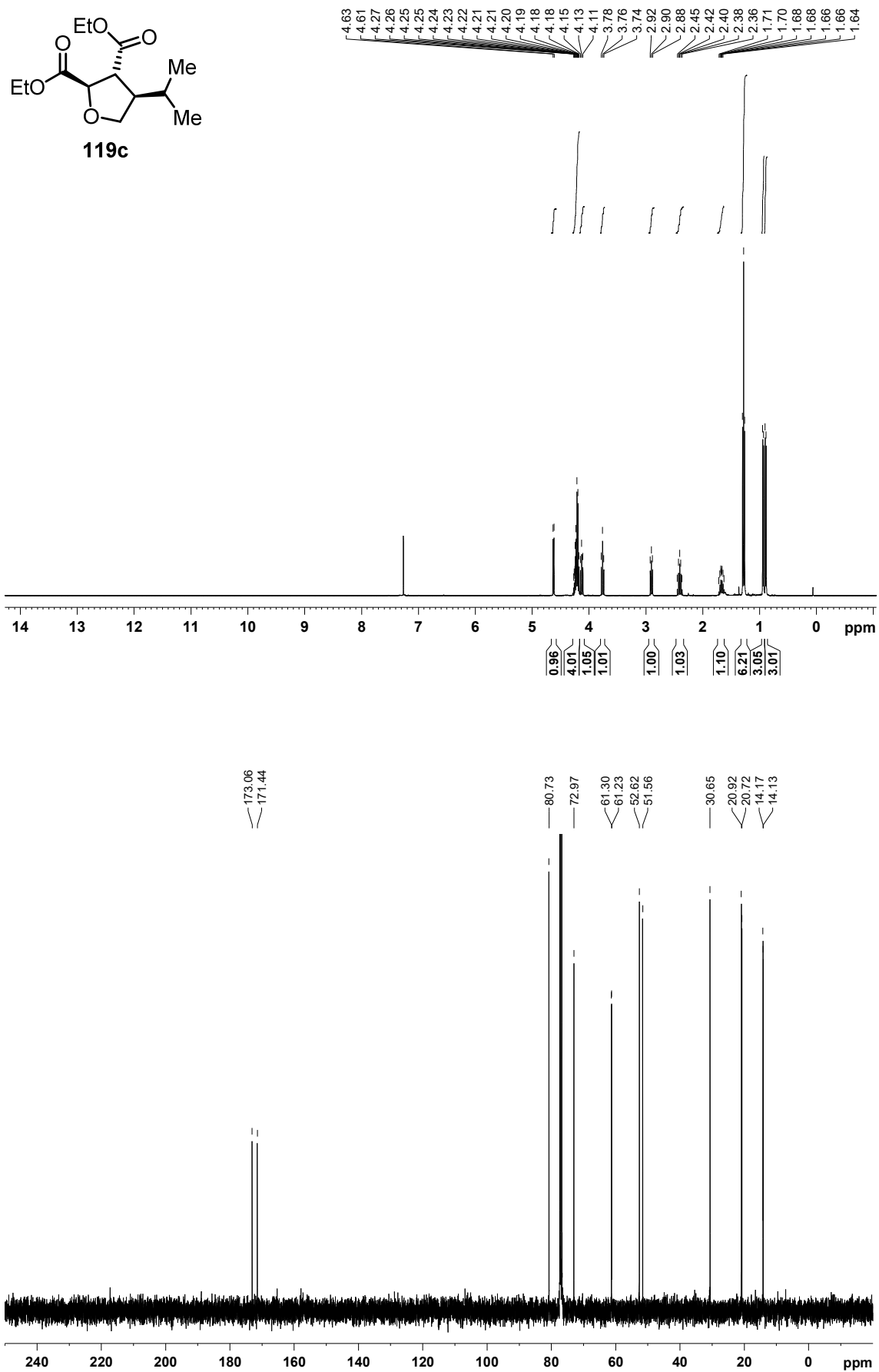


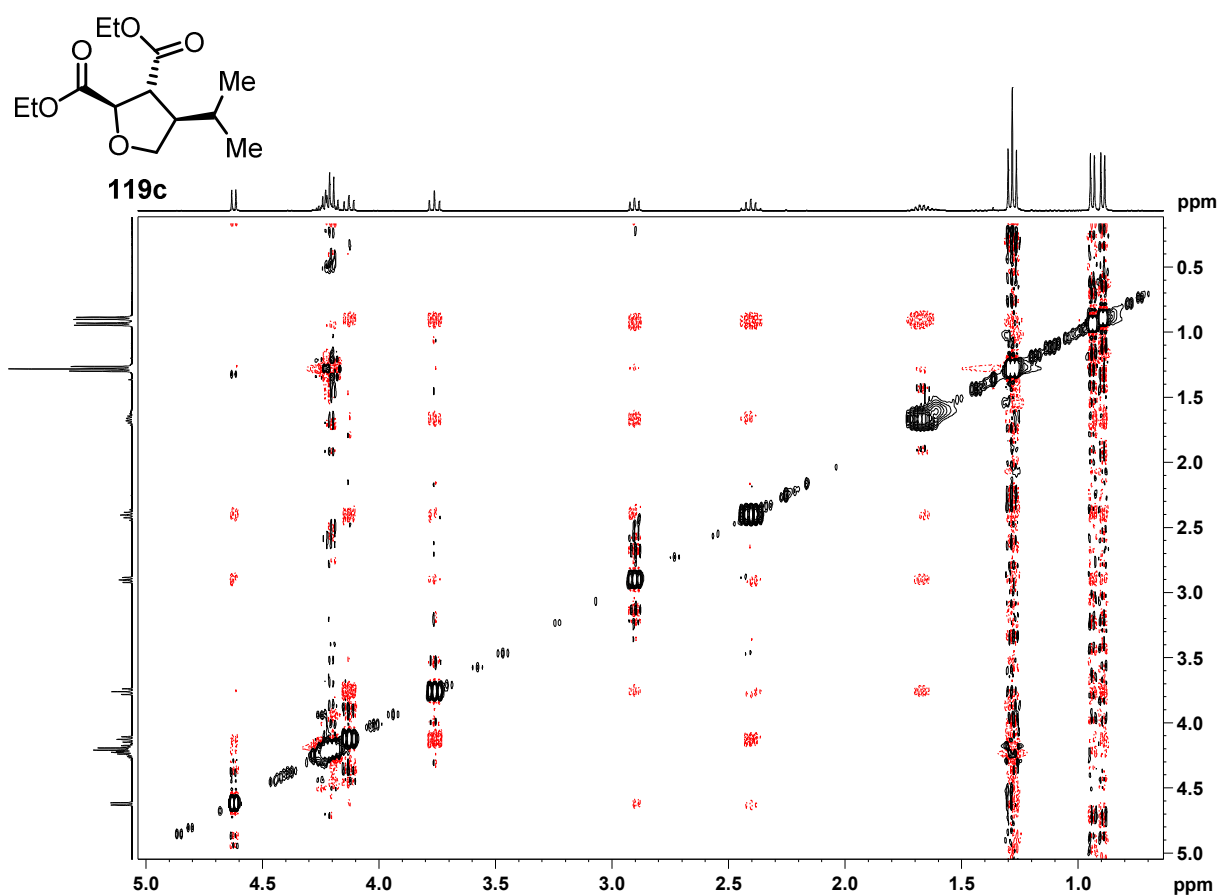


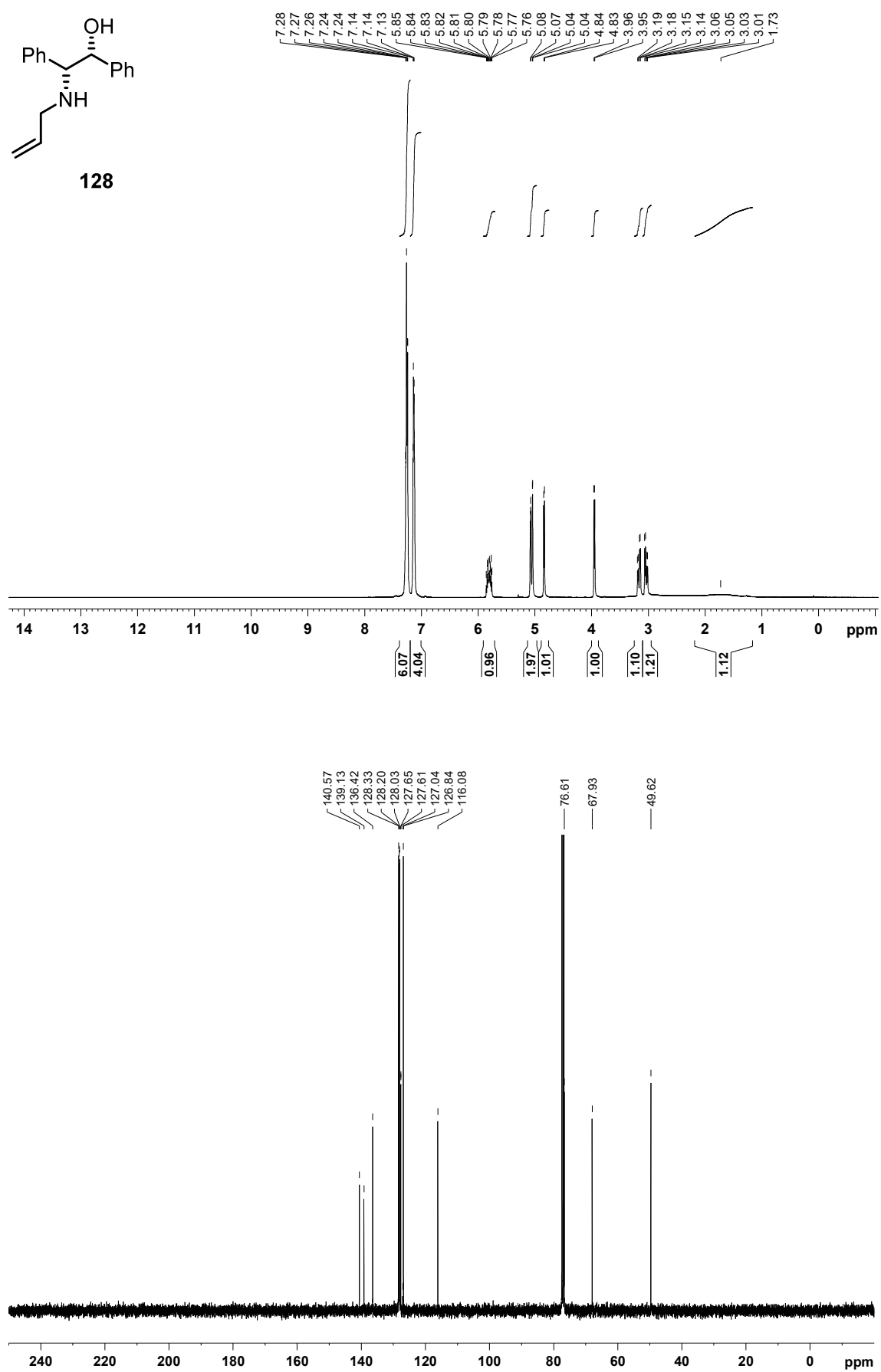












4 Literature

- (1) Dodds, D. R.; Gross, R. A. Chemicals from Biomass. *Science* **2007**, *318*, 1250–1251.
- (2) Arpe, H.-J. *Industrielle Organische Chemie*, 6th ed.; Wiley-VCH: Weinheim, 2007.
- (3) Barton, D. H. R.; McCombie, S. W. A New Method for the Deoxygenation of Secondary Alcohols. *J. Chem. Soc., Perkin Trans. 1* **1975**.
- (4) Studer, A.; Amrein, S. Silylated Cyclohexadienes: New Alternatives to Tributyltin Hydride in Free Radical Chemistry. *Angew. Chem. Int. Ed.* **2000**, *39*, 3080–3082.
- (5) Sopher, D. W.; Utley, J. H. P. Alkene Formation in the Cathodic Reduction of Oxalates. *J. Chem. Soc. Chem. Commun.* **1981**, 134.
- (6) Islam, N.; Sopher, D. W.; Utley, J. H. P. Electro-Organic Reactions. Part 28. Preparative Applications of the Oxalate Cathodic Cleavage Reaction Including One-Pot Conversions of Aldehydes and Ketones. *Tetrahedron* **1987**, *43*, 2741–2748.
- (7) Utley, J. H. P.; Ramesh, S. Electroorganic Reactions. Part 58. Revisiting the Cleavage of Oxalate Ester Radical-Anions. *Arkivoc* **2003**, 18–26.
- (8) Lam, K.; Markó, I. E. Organic Electrosynthesis Using Toluates as Simple and Versatile Radical Precursors. *Chem. Commun.* **2009**, 95–97.
- (9) Lam, K.; Marko, E. Novel Electrochemical Deoxygenation Reaction Using Diphenylphosphinates. *Org. Lett.* **2011**, *13*, 406–409.
- (10) Saito, I.; Ikehira, H.; Kasatani, R.; Watanabe, M.; Matsuura, T. Selective Deoxygenation of Secondary Alcohols by Photosensitized Electron-Transfer Reaction. A General Procedure for Deoxygenation of Ribonucleosides. *J. Am. Chem. Soc.* **1986**, *108*, 3115–3117.
- (11) Prudhomme, D. R.; Wang, Z.; Rizzo, C. J. An Improved Photosensitizer for the Deoxygenation of Benzoates and M-(Trifluoromethyl) Benzoates. *J. Org. Chem.* **1997**, *62*, 8257–8260.
- (12) Wang, Z.; Prudhomme, D. R.; Buck, J. R.; Park, M.; Rizzo, C. J. Stereocontrolled Syntheses of Deoxyribonucleosides via Photoinduced Electron-Transfer Deoxygenation of Benzoyl-Protected Ribo- and Arabinonucleosides. *J. Org. Chem.* **2000**, *65*, 5969–5985.
- (13) Wang, Z.; Rizzo, C. J. Stereocontrolled Synthesis of 2'-Deoxyribonucleosides. *Tetrahedron Lett.* **1997**, *38*, 8177–8180.
- (14) Shen, B.; Jamison, T. F. Continuous Flow Photochemistry for the Rapid and Selective Synthesis of 2'-Deoxy and 2,3-Dideoxynucleosides. *Aust. J. Chem.* **2013**, *66*, 157–164.
- (15) Bordoni, A.; de Lederkremer, R. M.; Marino, C. Photoinduced Electron-Transfer Alpha-Deoxygenation of Aldonolactones. Efficient Synthesis of 2-Deoxy-D-Arabinohexono-1,4-Lactone. *Carbohydr. Res.* **2006**, *341*, 1788–1795.
- (16) Bordoni, A.; de Lederkremer, R. M.; Marino, C. 5-Deoxy Glycofuranosides by Carboxyl Group Assisted Photoinduced Electron-Transfer Deoxygenation. *Tetrahedron* **2008**, *64*, 1703–1710.

- (17) Garegg, P. J.; Samuelsson, B. Novel Reagent System for Converting a Hydroxy-Group into an Iodo-Group in Carbohydrates with Inversion of Configuration. *J. Chem. Soc., Perkin Trans. 1* **1979**, 978–980.
- (18) Nguyen, J. D.; Reiß, B.; Dai, C.; Stephenson, C. R. J. Batch to Flow Deoxygenation Using Visible Light Photoredox Catalysis. *Chem. Commun.* **2013**, 49, 4352–4354.
- (19) Nguyen, J. D.; D'Amato, E. M.; Narayanam, J. M. R.; Stephenson, C. R. J. Engaging Unactivated Alkyl, Alkenyl and Aryl Iodides in Visible-Light-Mediated Free Radical Reactions. *Nat. Chem.* **2012**, 4, 854–859.
- (20) Flamigni, L.; Barbieri, A.; Sabatini, C.; Ventura, B.; Barigelletti, F. Photochemistry and Photophysics of Coordination Compounds: Iridium. *Top. Curr. Chem.* **2007**, 143–203.
- (21) Hill, H. A. O.; Pratt, J. M.; O'Riordan, M. P.; Williams, F. R.; Williams, R. J. P. The Chemistry of Vitamin B12: Part XV. Catalysis of Alkyl Halide Reduction by Vitamin B12: Studies Using Controlled Potential Reduction. *J. Chem. Soc. A* **1971**, 1859–1862.
- (22) Clark, T. J.; Rodezno, J. M.; Clendenning, S. B.; Aouba, S.; Brodersen, P. M.; Lough, A. J.; Ruda, H. E.; Manners, I. Rhodium-Catalyzed Dehydrocoupling of Fluorinated Phosphine-Borane Adducts: Synthesis, Characterization, and Properties of Cyclic and Polymeric Phosphinoboranes with Electron-Withdrawing Substituents at Phosphorus. *Chem. Eur. J.* **2005**, 11, 4526–4534.
- (23) Caminade, A.-M.; Khatib, F. El; Baceiredo, A.; Koenig, M. Phosphorous and Sulfur and the Related Elements Ozonization: An Efficient Method for the Oxidation of Halophosphines Ozonization: An Efficient Method for the Oxidation of Halophosphines. *Phosphorus, Sulfur Silicon Relat. Elem.* **1987**, 29, 365–367.
- (24) King, R. B.; Sadanani, N. D. Dialkylaminodichlorophosphines. *Synth. React. Inorg. Met.-Org. Chem.* **1985**, 15, 149–153.
- (25) Wu, H.-C.; Yu, J.-Q.; Spencer, J. B. Stereospecific Deoxygenation of Phosphine Oxides with Retention of Configuration Using Triphenylphosphine or Triethyl Phosphite as an Oxygen Acceptor. *Org. Lett.* **2004**, 6, 4675–4678.
- (26) Abarbri, M.; Dehmel, F.; Knochel, P. Bromine-Magnesium-Exchange as a General Tool for the Preparation of Polyfunctional Aryl and Heteroaryl. *Tetrahedron Lett.* **1999**, 40, 7449–7453.
- (27) Leazer, J. L.; Cvetovich, R.; Tsay, F.; Dolling, U.; Vickery, T.; Bachert, D. An Improved Preparation of 3,5-Bis(trifluoromethyl)acetophenone and Safety Considerations in the Preparation of 3,5-Bis(trifluoromethyl)phenyl Grignard Reagent. *J. Org. Chem.* **2003**, 68, 3695–3698.
- (28) Giencke, A.; Lackner, H. Desmethyl(trifluoromethyl)actinomycin. *Liebigs Ann. Chem.* **1990**, 6, 569–579.
- (29) Clarke, P. A.; Holton, R. A.; Kayaleh, N. E. Direct One Step Mono-Functionalisation of Symmetrical 1,2-Diols. *Tetrahedron Lett.* **2000**, 41, 2687–2690.
- (30) Clarke, P. A.; Kayaleh, N. E.; Smith, M. A.; Baker, J. R.; Bird, S. J.; Chan, C. A One-Step Procedure for the Monoacylation of Symmetrical 1,2-Diols. *J. Org. Chem.* **2002**, 67, 5226–5231.
- (31) Senaweera, S. M.; Singh, A.; Weaver, J. D. Photocatalytic Hydrodefluorination: Facile Access to Partially Fluorinated Aromatics. *J. Am. Chem. Soc.* **2014**, 136, 3002–3005.

- (32) Bou-Hamdan, F. R.; Seeberger, P. H. Visible-Light-Mediated Photochemistry: Accelerating [Ru(bpy)₃]²⁺-Catalyzed Reactions in Continuous Flow. *Chem. Sci.* **2012**, *3*, 1612.
- (33) Neumann, M.; Zeitler, K. Application of Microflow Conditions to Visible Light Photoredox Catalysis. *Org. Lett.* **2012**, *14*, 2658–2661.
- (34) Garlets, Z. J.; Nguyen, J. D.; Stephenson, C. R. J. The Development of Visible-Light Photoredox Catalysis in Flow. *Isr. J. Chem.* **2014**, *48109*, 351–360.
- (35) Herrmann, J. M.; König, B. Reductive Deoxygenation of Alcohols: Catalytic Methods beyond Barton-McCombie Deoxygenation. *European J. Org. Chem.* **2013**, 7017–7027.
- (36) Barton, D. H. R.; Crich, D. Formation of Quaternary Carbon Centers from Tertiary Alcohols by Free Radical Methods. *Tetrahedron Lett.* **1985**, *26*, 757–760.
- (37) Barton, D. H. R.; Crich, D.; Kretzschmar, G. The Invention of New Radical Chain Reaction. Part 9. Further Radical Chemistry of Thiohydroxamic Esters; Formation of Carbon-Carbon Bonds. *J. Chem. Soc. Perkin Trans. 1* **1986**, 39–53.
- (38) Togo, H.; Fujii, M.; Yokoyama, M. Conversion of Hydroxyl Groups in Alcohols to Other Functional Groups with N-Hydroxy-2-Thiopyridone, and Its Application to Dialkylamines and Thiols. *Bull. Chem. Soc. Jpn.* **1991**, *64*, 57–67.
- (39) Togo, H.; Matsubayashi, S.; Yamazaki, O.; Yokoyama, M. Deoxygenative Functionalization of Hydroxy Groups via Xanthates with Tetraphenyldisilane. *J. Org. Chem.* **2000**, *65*, 2816–2819.
- (40) Blazejewski, J. C.; Diter, P.; Warchol, T.; Wakselman, C. Radical Allylation of Trifluoromethylated Xanthates: Use of DEAD for Removing the Allyltributyltin Excess. *Tetrahedron Lett.* **2001**, *42*, 859–861.
- (41) Sunazuka, T.; Yoshida, K.; Kojima, N.; Shirahata, T.; Hirose, T.; Handa, M.; Yamamoto, D.; Harigaya, Y.; Kuwajima, I.; Omura, S. Total Synthesis of (-)-Physovenine from (-)-3a-Hydroxyfuroindoline. *Tetrahedron Lett.* **2005**, *46*, 1459–1461.
- (42) Rowlands, G. J. Radicals in Organic Synthesis. Part 1. *Tetrahedron* **2009**, *65*, 8603–8655.
- (43) Srikanth, G. S. C.; Castle, S. L. Advances in Radical Conjugate Additions. *Tetrahedron* **2005**, *61*, 10377–10441.
- (44) Lackner, G. L.; Quasdorf, K. W.; Overman, L. E. Direct Construction of Quaternary Carbons from Tertiary Alcohols via Photoredox-Catalyzed Fragmentation of Tert-Alkyl N-Phthalimidoyl Oxalates. *J. Am. Chem. Soc.* **2013**, 15342–15345.
- (45) Chyongjin Pac; Ihama, M.; Yasuda, M.; Miyauchi, Y.; Sakurai, H. [Ru(bpy)₃]²⁺-Mediated Photoreduction of Olefins with 1-Benzyl-1,4-Dihydronicotinamide: A Mechanistic Probe for Electron-Transfer Reactions of NAD(P)H-Model Compounds. *J. Am. Chem. Soc.* **1981**, *103*, 6495–6497.
- (46) Kirby, A. J. *The Anomeric Effect and Related Stereoelectronic Effects at Oxygen*; Hafner, K., Lehn, J.-M., Rees, C. W., Ragué Schleyer, von P., Zahradnik, R., Eds.; Springer: Berlin, 1983.
- (47) Mast, C. A.; Eissler, S.; Stoncius, A.; Stammler, H.-G.; Neumann, B.; Sewald, N. Efficient and Versatile Stereoselective Synthesis of Cryptophycins. *Chem. Eur. J.* **2005**, *11*, 4667–4677.
- (48) Schmidt, B.; Wildemann, H. Diastereoselective Ring-Closing Metathesis in the Synthesis of Dihydropyrans. *J. Org. Chem.* **2000**, *65*, 5817–5822.

- (49) Baldwin, J. E. Rules for Ring Closure. *J. Chem. Soc., Chem. Commun.* **1976**, 734–736.
- (50) Love, B. E.; Jones, E. G.; Carolina, N. The Use of Salicylaldehyde Phenylhydrazones as an Indicator for the Titration of Organometallic Reagents. *J. Org. Chem.* **1999**, *64*, 3755–3756.
- (51) Sedelmeier, J.; Bolm, C. Application of Beta-Hydroxysulfoximines in Catalytic Asymmetric Phenyl Transfer Reactions for the Synthesis of Diarylmethanols. *J. Org. Chem.* **2007**, *72*, 8859–8862.
- (52) Kodama, S.; Hashidate, S.; Nomoto, A.; Yano, S.; Ueshima, M.; Ogawa, A. Vanadium-Catalyzed Atmospheric Oxidation of Benzyl Alcohols Using Water as Solvent. *Chem. Lett.* **2011**, *40*, 495–497.
- (53) Boymond, L.; Rottländer, M.; Knochel, P. Preparation of Highly Functionalized Grignard Reagents by an Iodine - Magnesium Exchange Reaction and Its Application in Solid-Phase Synthesis. *Angew. Chem. Int. Ed.* **1998**, *37*, 1701–1703.
- (54) Padmanaban, M.; Biju, A. T.; Glorius, F. N-Heterocyclic Carbene-Catalyzed Hydroxymethylation of Aldehydes. *Org. Lett.* **2011**, *13*, 98–101.
- (55) Cheng, M.; Bakac, A. Kinetics and Mechanism of the Reaction of Cr(II) Aqua Ions with Benzoylpyridine N-Oxide. *Dalton Trans.* **2007**, *56*, 2077–2082.
- (56) Kim, J.; De Castro, K. A.; Lim, M.; Rhee, H. Reduction of Aromatic and Aliphatic Keto Esters Using Sodium borohydride/MeOH at Room Temperature: A Thorough Investigation. *Tetrahedron* **2010**, *66*, 3995–4001.
- (57) Ohta, S.; Hayakawa, S.; Moriwaki, H.; Harada, S.; Okamoto, M. Synthesis and Application of Imidazole Derivatives. Synthesis and Acyl Activation of 2-Acyl-1-Methyl-1H-Imidazoles. *Chem. Pharm. Bull.* **1986**, *34*, 4916–4926.
- (58) Young, I. S.; Kerr, M. A. Total Synthesis of (+)-Nakadomarin A. *J. Am. Chem. Soc.* **2007**, *129*, 1465–1469.
- (59) Marshall, L. J.; Roydhouse, M. D.; Slawin, A. M. Z.; Walton, J. C. Effect of Chain Length on Radical to Carbanion Cyclo-Coupling of Bromoaryl Alkyl-Linked Oxazolines: 1,3-Areneotropic Migration of Oxazolines. *J. Org. Chem.* **2007**, *72*, 898–911.
- (60) Rendler, S.; Fröhlich, R.; Keller, M.; Oestreich, M. Enantio- and Diastereotopos Differentiation in the Palladium(II)-Catalyzed Hydrosilylation of Bicyclo[2.2.1]alkene Scaffolds with Silicon-Stereogenic Silanes. *European J. Org. Chem.* **2008**, *2008*, 2582–2591.
- (61) Adamczyk, M.; Watt, D. S. Synthesis of Biological Markers in Fossil Fuels. 2. Synthesis and ¹³C NMR Studies of Substituted Indans and Tetralins. *J. Org. Chem.* **1984**, *49*, 4226–4237.
- (62) Deleuze-Masquéfa, C.; Gerebtzoff, G.; Subra, G.; Fabreguettes, J.-R.; Ovens, A.; Carraz, M.; Strub, M.-P.; Bompard, J.; George, P.; Bonnet, P.-A. Design and Synthesis of Novel Imidazo[1,2-A]quinoxalines as PDE4 Inhibitors. *Bioorg. Med. Chem.* **2004**, *12*, 1129–1139.
- (63) Rauter, A. P.; Fernandes, A. C.; Czernecki, S.; Valery, J.-M. Deoxygenation at C-4 and Stereospecific Branched-Chain Construction at C-3 of a Methyl Hexopyranuloside . Synthetic Approach to the Amipurimycin Sugar Moiety. *J. Org. Chem.* **1996**, *61*, 3594–3598.
- (64) Bashyal, B. P.; Chow, H.-F.; Fellows, L. E.; Fleet, G. W. J. The Synthesis of Polyhydroxylated Amino Acids from Glucuronolactone. *Tetrahedron* **1987**, *43*, 415–422.

- (65) Sprouse, S.; King, K. A.; Spellane, P. J.; Watts, R. J. Photophysical Effects of Metal-Carbon σ Bonds in Ortho-Metalated Complexes of Ir(III) and Rh(III). *J. Am. Chem. Soc.* **1984**, *106*, 6647–6653.
- (66) Slinker, J. D.; Gorodetsky, A. A.; Lowry, M. S.; Wang, J.; Parker, S.; Rohl, R.; Bernhard, S.; Malliaras, G. G. Efficient Yellow Electroluminescence from a Single Layer of a Cyclometalated Iridium Complex. *J. Am. Chem. Soc.* **2004**, *126*, 2763–2767.
- (67) Haberberger, M.; Someya, C. I.; Company, A.; Irran, E.; Enthaler, S. Application of a Nickel-Bispidine Complex as Pre-Catalyst for C(sp²)-C(sp³) Bond Formations. *Catal. Lett.* **2012**, *142*, 557–565.
- (68) Identical with an Authentic Sample. Material was identical with an authentic sample.
- (69) Henry, N.; Enguehard-Gueiffier, C.; Thery, I.; Gueiffier, A. One-Pot Dual Substitutions of Bromobenzyl Chloride, 2-Chloromethyl-6-halogenoimidazo[1,2a]pyridine and -[1,2b]pyridazine by Suzuki-Miyaura Cross-Coupling Reactions. *Eur. J. Org. Chem.* **2008**, 4824–4827.
- (70) Inés, B.; SanMartin, R.; Moure, M. J.; Domínguez, E. Insights into the Role of New Palladium Pincer Complexes as Robust and Recyclable Precatalysts for Suzuki-Miyaura Couplings in Neat Water. *Adv. Synth. Catal.* **2009**, *351*, 2124–2132.
- (71) Endo, K.; Ishioka, T.; Ohkubo, T.; Shibata, T. One-Pot Synthesis of Symmetrical and Unsymmetrical Diarylmethanes via Diborylmethane. *J. Org. Chem.* **2012**, *77*, 7223–7231.
- (72) Harker, W. R. R.; Carswell, E. L.; Carbery, D. R. A Practical Protocol for the Highly E-Selective Formation of Aryl-Substituted Silylketene Acetals. *Org. Lett.* **2010**, *12*, 3712–3715.
- (73) Li, L.; Cai, P.; Guo, Q.; Xue, S. Et₂Zn-Mediated Rearrangement of Bromohydrins. *J. Org. Chem.* **2008**, *73*, 3516–3522.
- (74) Yin, W.; Wang, C.; Huang, Y. Highly Practical Synthesis of Nitriles and Heterocycles from Alcohols under Mild Conditions by Aerobic Double Dehydrogenative Catalysis. *Org. Lett.* **2013**, *15*, 1850–1853.
- (75) Rauter, A. P.; Fernandes, A. C.; Figueiredo, J. A. A Novel Deoxygenation of Hydroxy Groups Activated by a Vicinal Carbonyl Group via Reaction with Ph₃P/I₂/Imidazole. *J. Carbohydr. Chem.* **1998**, *17*, 1037–1045.
- (76) Maki, T.; Ushijima, N.; Matsumura, Y.; Onomura, O. Catalytic Monoalkylation of 1,2-Diols. *Tetrahedron Lett.* **2009**, *50*, 1466–1468.
- (77) Rackl, D.; Kais, V.; Kreitmeier, P.; Reiser, O. Visible Light Photoredox-Catalyzed Deoxygenation of Alcohols. *Beilstein J. Org. Chem.* **2014**, *10*, 2157–2165.
- (78) Seebach, D.; Aebi, J.; Wasmuth, D. Diastereoselective α -Alkylation of β -Hydroxycarboxylic Esters through Alkoxyide Enolates: Diethyl (2S,3R)-(+)-3-Allyl-2-Hydroxysuccinate from Diethyl (S)-(-)-Malate. *Org. Synth.* **1985**, *63*, 109.
- (79) Sharpless, K. B.; Amberg, W.; Bennani, Y. L.; Crispino, G. A.; Hartung, J.; Jeong, K.-S.; Kwong, H.-L.; Morikawa, H.; Wang, Z.-M.; Xu, D.; Zhang, X.-L. The Osmium-Catalyzed Asymmetric Dihydroxylation: A New Ligand Class and a Process Improvement. *J. Org. Chem.* **1992**, *57*, 2768–2771.
- (80) Reddy, K. S.; Riera, A.; Perica, M. A.; Verdaguer, X. Synthesis of Heavily Substituted 1,2-Amino Alcohols in Enantiomerically Pure Form. *J. Org. Chem.* **2005**, *70*, 7426–7428.
-

- (81) Yang, D.; Yip, Y.-C.; Jiao, G.-S.; Wong, M.-K. In Situ Catalytic Epoxidation of Olefins with Tetrahydrothiopyran-4-One and Oxone: Trans-2-Methyl-2,3-Diphenyloxirane. *Org. Synth.* **2002**, *78*, 225.
- (82) Bruncko, M.; Schlingloff, G.; Sharpless, K. B. N-Bromacetamide - A New Nitrogen Source for the Catalytic Asymmetric Aminohydroxylation of Olefins. *Angew. Chem. Int. Ed.* **1997**, 1483–1486.
- (83) Sun, J.; Wu, W.; Zhao, J. Long-Lived Room-Temperature Deep-Red-Emissive Intraligand Triplet Excited State of Naphthalimide in Cyclometalated Ir(III) Complexes and Its Application in Triplet-Triplet Annihilation-Based Upconversion. *Chem. – A Eur. J.* **2012**, *18*, 8100–8112.
- (84) Sharma, S. V.; Jothivasan, V. K.; Newton, G. L.; Upton, H.; Wakabayashi, J. I.; Kane, M. G.; Roberts, A. A.; Rawat, M.; La Clair, J. J.; Hamilton, C. J. Chemical and Chemoenzymatic Syntheses of Bacillithiol: A Unique Low-Molecular-Weight Thiol amongst Low G + C Gram-Positive Bacteria. *Angew. Chem. Int. Ed.* **2011**, *50*, 7101–7104.
- (85) Kais, V.; Rackl, D.; Reiser, O. Photocatalytic Deoxygenation of Alcohols with Ethyl Oxalates. *manuscript in preparation*.
- (86) Kais, V. Visible Light Photoredox Catalysis – Applications in Synthesis Mediating New Bond Formations, 2015.

E Polymer-tagged Photocatalysts

1 Introduction

The principle to run artificial chemical reactions in a catalytic fashion only emerged at the beginning of the 20th century.¹ A catalyst accelerates the rate of a chemical reaction and is itself left unchanged by the reaction.² Catalysis is a key feature of modern chemistry: sub-stoichiometric amounts of a compound are used to produce large quantities of other substances.³ About 90% of all modern chemical plants operate with catalytic processes.

Chemical catalysis can in principle be divided into two categories: heterogeneous catalysis and homogeneous catalysis. In heterogeneous catalysis the catalyst is located in a different phase than the substrate. Mostly a solid catalyst acts as reaction surface for liquid or gaseous reagents. In contrast, in homogeneous catalysis both catalyst and reagent share the same, usually liquid, phase. Despite the fact that higher reaction rates under milder conditions are achievable with homogeneous catalysis, heterogeneous catalysis is by far predominant in industrial applications. Even in pharmaceutical companies, where rather small quantities of products are produced compared to the petrochemical industry, only 5 – 10% of the steps in drug production are catalyzed in a homogeneous fashion.⁴ This can be attributed to the fact that in homogeneous catalysis separation of the catalyst from the products demands complicated setups and is therefore too expensive on an industrial scale.

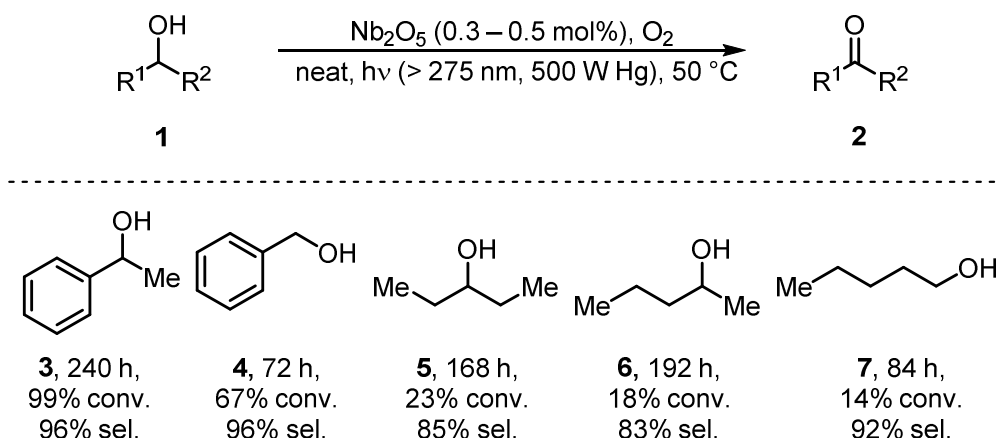
Facile catalyst recovery and reuse is key in many industrial processes as the costs for catalysts usually accounts for a considerable portion of the total process costs. Beside the classic strategy to have the catalyst in a different state than the products and recover it by some sort of filtration process, there are also different approaches to achieve facile catalyst recovery in homogeneous reactions. The following sections will describe different strategies that have been used to recycle photocatalysts in organic synthesis. Unselective decomposition reactions and other, non-synthetic systems are not discussed.^{5,6} Likewise, catalysts variants that were only used for oxygenation reactions² will mostly be exempt as they were already showcased on a number of earlier reviews^{7–13}. The following sections are arranged by the type of the active photocatalyst. Their respective applications as well as the employed immobilization and recycling methods are herein described.

1.1 Inorganic semi-conductors

The employment of inorganic semi-conductors as recyclable catalysts is self-evident as they are solid materials that can usually easily be recovered after heterogeneous reaction by a filtration process. However, for a truly recyclable catalyst it is crucial that the recovered material shows significant catalytic activity when resubjected to a subsequent reaction run. Heterogeneity alone is therefore not a sufficient criterion for a recyclable catalyst.

As a prototypical example of earlier, simple oxidation reactions the photochemical oxidation of primary and secondary alcohols to aldehydes, carboxylic acids, and ketones by Nb_2O_5 is presented (Scheme 1). While this process can give high oxidation yields and selectivities for simple substrates like 1-phenylethanol (**3**), more challenging, aliphatic alcohols (**5** – **7**) required very long irradiation times to achieve synthetically useful selectivities at very low conversions. The authors claim that the catalyst could be reused without any decline in activity or selectivity, however, no experimental details were reported in this regard.

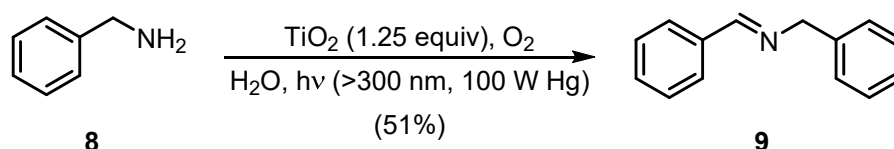
Scheme 1. Photochemical oxidation by Nb_2O_5 . Reaction times, conversion rates and corresponding selectivities for the carbonyl compound are given for representative examples.



Overoxidation is always a concern when inorganic semi-conductors are irradiated in H_2O in the presence of O_2 as the highly active oxygen species $\cdot\text{OH}$ and $\text{O}_2\cdot^-/\text{HO}_2\cdot$ can be formed. While this aspect is used for photochemical degradation reactions and in disinfection applications, it is detrimental when selective organic transformations are desired.^{5,6} A way to gain selectivity is to decrease the adsorption capabilities of the organic materials to the surface of the photocatalytically active semi-conductor, *e.g.* by using a different crystal modification or partial coating of the catalysts surface.^{14,15} For example, WO_3 -coated TiO_2 could be used as recyclable catalyst for photo-oxidation of benzylic alcohols to carbonyls.¹⁵ However, such alterations are unfortunately connected with a loss of activity. Nevertheless, Chen *et al.* could use commercially available, highly active Degussa P25 TiO_2 for the selective oxidation

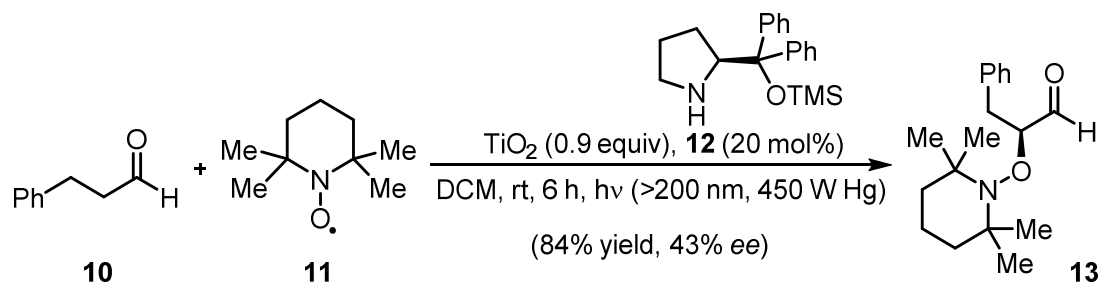
of amines to imines in water (Scheme 2).¹⁶ This is possible as the to-be-oxidized amines are soluble in water unlike the product imines which precipitate from the solution. Adsorption to the TiO₂ and resulting overoxidation is thus limited. Filtration of the reaction solution after a certain irradiation period gave product imine **9** and TiO₂. Imine **9** could be separated by washing and TiO₂ reused to achieve further conversion of the starting material solution. This procedure was repeated once more to furnish 51% overall yield of imine **9**.

Scheme 2. Synthesis of imine **9** through selective oxidation of benzylamine (**8**) by TiO₂.



Jang and co-workers demonstrated the enantioselective α -oxyamination of aldehydes catalyzed by TiO₂ (Scheme 3).¹⁷ The stereochemical induction was realized by the employment of prolinol **12** as chiral co-catalyst. The initial activity of the recovered TiO₂ photocatalyst declined in subsequent reaction runs: while a new batch gave α -oxyaminated product **13** in 84% yield, a second and a third run only gave 71% and 48%, respectively. As reason for the loss in activity, a structural change of the catalyst was excluded: X-ray powder diffraction pattern of TiO₂ was unchanged. Instead, the reduced yield was attributed to contamination of the semi-conductor surface by organic compounds.

Scheme 3. Enantioselective α -oxyamination of aldehydes catalyzed by TiO₂ and prolinol **3**.



Also in the photocatalytic reductions of nitrobenzenes with PbBiO₂Br of König *et al.*, a rapid decline in catalyst performance was observed.¹⁸ While full conversion of nitrobenzene (**14**) was initially observed after 20 h of irradiation, only 80 % were obtained in a subsequent reaction run. During the photochemical reaction the catalyst turned gray, however, the catalysts crystal structure after the reaction was unchanged as was confirmed by XRD analysis. The initial good catalytic activity could be retained for multiple runs when the catalyst was treated in an ultrasonic bath after the reaction. Thereby the grey color was partially removed and the catalyst still yielded full conversion after four recycling cycles. König *et al.* could use

PbBiO₂Br also in the enantioselective alkylation of aldehydes.¹⁹ However, recycling capabilities were poor as significantly lower conversions were obtained after reuse. For these reactions also TiO₂ was employed as catalyst: while it led to lower product yields and enantiomeric excesses than PbBiO₂Br, it could be reused at least once with constant catalytic properties.

Scheme 4. Photocatalytic reduction of nitrobenzene (**14**) with PbBiO₂Br.

Recycling experiments with (depicted in blue) and without sonication of the catalyst.¹⁸

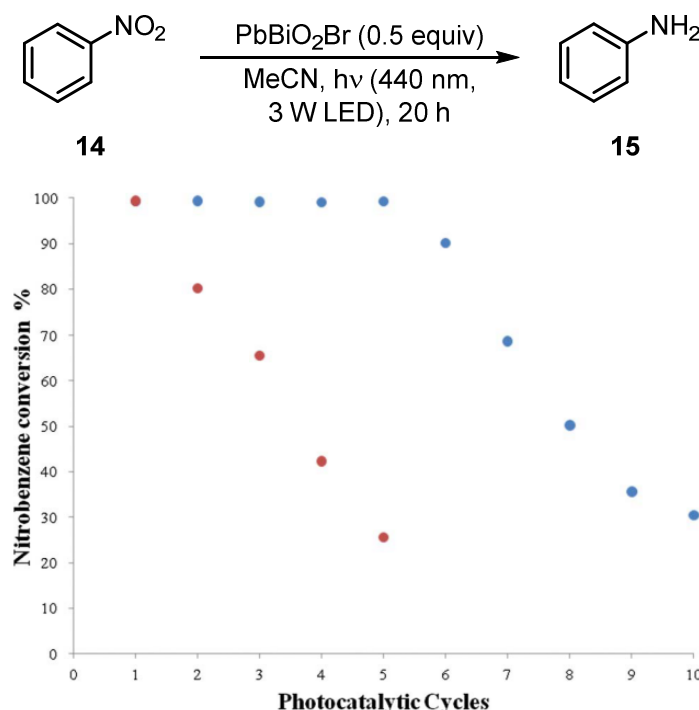
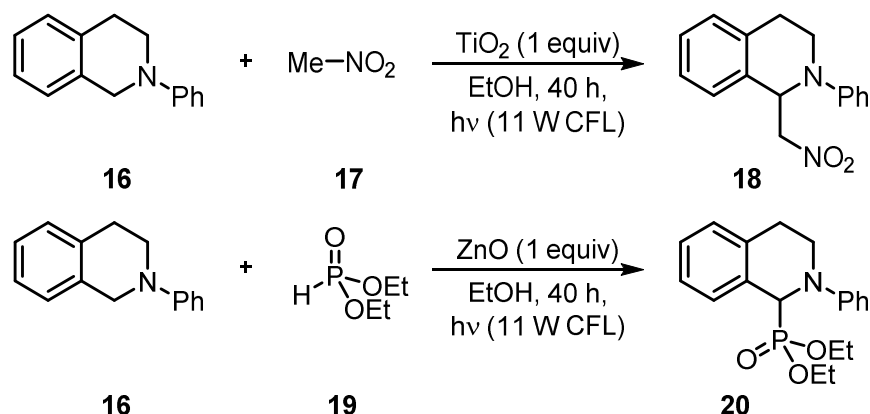


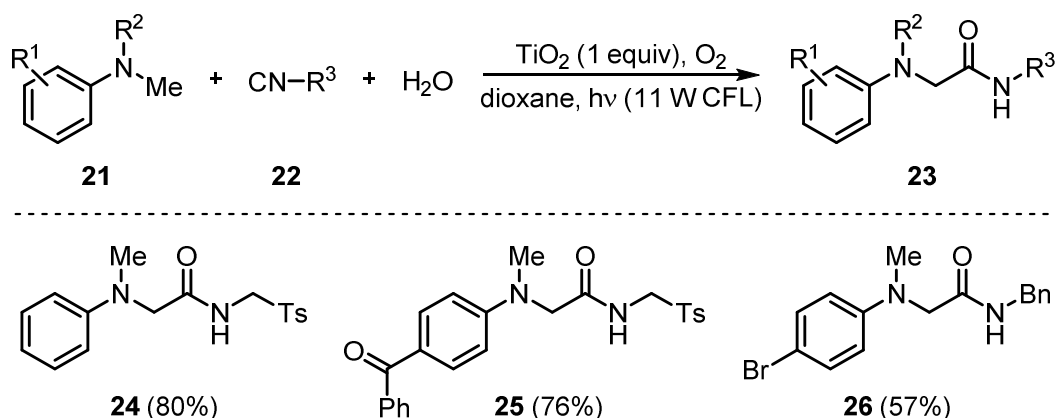
Figure reproduced with courtesy of The Royal Society of Chemistry.

Rueping and co-workers successfully used TiO₂ and ZnO in a series of oxidative cross dehydrogenative coupling reactions (Table 1).²⁰ TiO₂ proved optimal for the oxidative aza-Henry reaction between *N*-phenyl-tetrahydroisoquinoline (**16**) and nitromethane (**17**), ZnO for the phosphorylation of **16** with diethyl phosphite (**19**). After centrifugal separation of the reaction solution, the heterogeneous catalysts could be reused at least four times without an evident decline in activity. While both catalysts are cheap, readily available, and recyclable, they are hopelessly ineffective compared to organic transition metal complexes.²¹ The reaction time till full conversion of 0.1 mmol of tetrahydroisoquinoline (**16**) with one equivalent (*sic*) of TiO₂ took 40 h; the homogeneously operating photocatalyst [Ir(ppy)₂(dtb-bpy)](PF₆) required only 10 h to convert 1.0 mmol of **16** with a comparable light source. [Ir(ppy)₂(dtb-bpy)](PF₆) thus used the light more effectively than TiO₂ by a factor of 4x10⁴.

Table 1. Recycling results of TiO₂ and ZnO in an aza-Henry and a phosphonylation reaction.

Cycle	1	2	3	4	5
TiO ₂ in aza-Henry reaction	85%	83%	87%	92%	87%
ZnO in phosphonylation	86%	94%	86%	88%	-

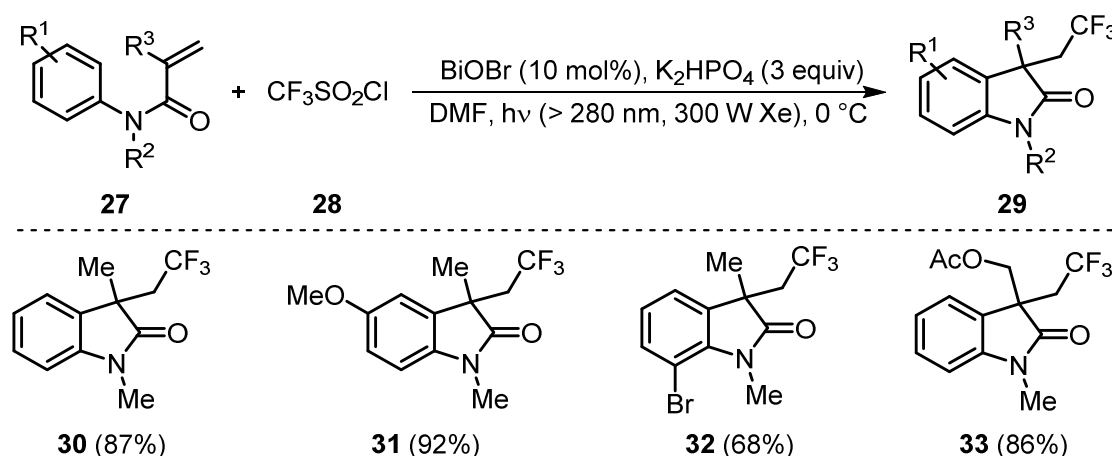
An oxidative Ugi-type reaction with TiO₂ as recyclable photocatalyst was realized by Rueping *et al.*²² A variety of different *N*-methyl-*N*-alkylanilines (**21**) could be coupled with a multitude of isocyanides (**22**, Scheme 5). The recyclability of TiO₂ in this reaction was probed through centrifugal separation of the catalyst after the reaction and reusal for 4 subsequent experiments. Indeed, the catalytic activity of TiO₂ was not impaired and constant product yields were obtained throughout the recycling series.

Scheme 5. Synthesis of α -aminamides *via* an oxidative Ugi-type reaction by TiO₂ catalysis.

BiOBr nanosheets could catalyze the light-mediated, intermolecular trifluoromethylation/arylation of alkenes as was demonstrated by Zhang *et al.* (Scheme 6).²³ A multitude of different substitution patterns on the aryl group was well tolerated as well as modification of

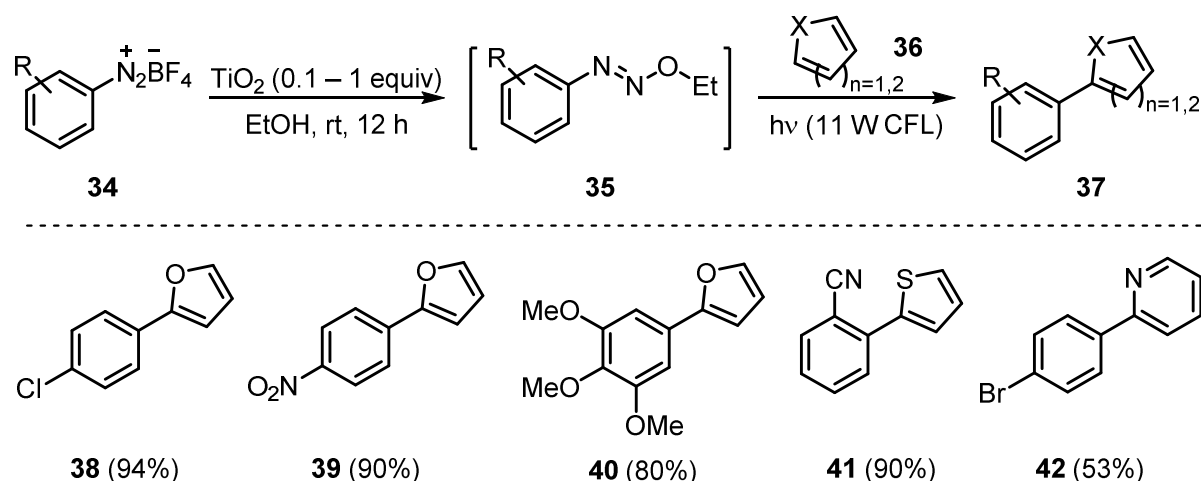
the acrylamide moiety. The photocatalyst could be recovered through centrifugation. However, catalytic activity was reduced significantly. While the first run yielded 87% of oxindole **30**, two subsequent runs only gave 79% and 65%, respectively (background reaction without catalyst already gave 29% yield). TEM analysis of the used catalyst showed a structural change: BiOBr nanosheets were transformed into less active nanoparticles. The authors proposed that the comparably instable BiOBr nanosheets could be replaced by more stable TiO₂ nanosheets to allow better recyclability.

Scheme 6. Oxindole synthesis through a trifluoromethylation arylation cascade catalyzed by BiOBr.



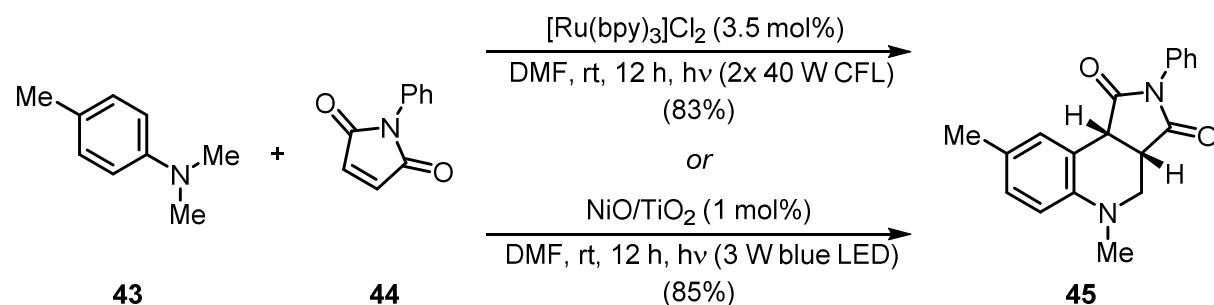
The direct arylation of heteroarenes by TiO₂ (Evonik-Degussa P25) was very demonstrated by Rueping *et al.*²⁴ In this reaction TiO₂ not only acts as the heterogeneous and recyclable photocatalyst but also catalyzes the formation of the active azoether intermediate **35** (Scheme 7). With this method the synthesis of electronically distinct arylated pyrroles, thiophenes, and pyridines was possible in excellent yields. After performance of the photoreaction TiO₂ could easily be separated by centrifugation. It was demonstrated that the material can be reused for at least five runs to produce arylated furan **38** in constant yields of 90±2%.

Scheme 7. Photochemical C–H arylation of heteroarenes **36** by TiO₂.



Typically, semi-conductor photocatalysts are used in high loadings of up to over-stoichiometric amounts. The rutile modification of TiO₂ has a band gap of 3.0 eV corresponding to an excitation wavelength of 415 nm; the anatase modification even has a band gap of 3.2 eV (387 nm).¹⁷ Therefore, excitation is usually carried out by UV light (< 400 nm) irradiation to surmount this large band gap. High loading and UV light irradiation can be eluded through metal oxide surface modification of the semi-conductor, as was demonstrated by Tada *et al.*²⁵ Additionally, this procedure slowed down the hole–electron pair recombination. Shen and co-workers could exploit this in their cyclization of tertiary anilines with maleimides catalyzed by NiO surface-modified TiO₂.²⁶ The activity of this catalyst even surpassed earlier results with the homogeneously operating photocatalyst [Ru(bpy)₃]²⁺ (Table 2). After the photochemical reaction, NiO/TiO₂ can be recovered by centrifugal separation. Transmission electron microscopy (TEM) revealed no morphological change of the material, therefore reusal in further catalytic runs was examined. Indeed, the NiO/TiO₂ catalyst could be used without further treatment for at least 9 consecutive runs without an observable decline in activity, giving product **45** in 79±4% yield.

Table 2. Comparison of [Ru(bpy)₃]Cl₂ with NiO/TiO₂ for the synthesis of **45** and recycling studies.

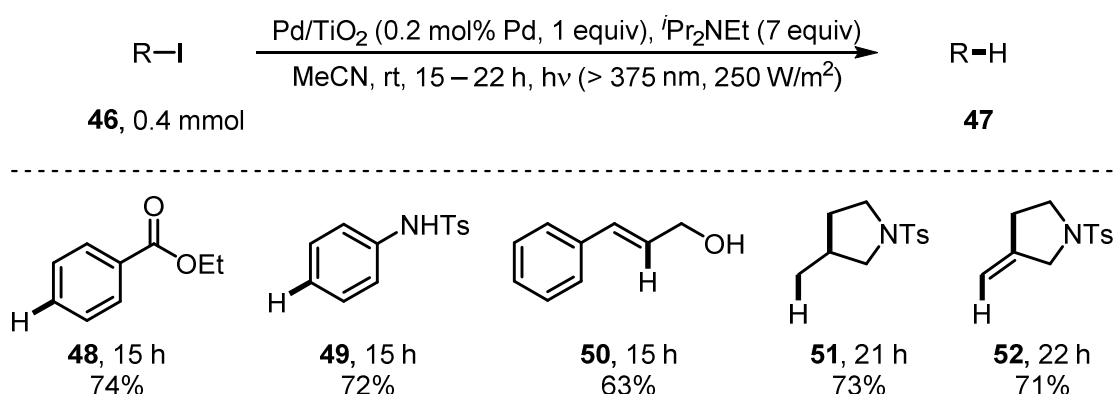


Recycling run of NiO/TiO ₂	1	2	3	4	5	6	7	8	9
Yield of 45 [%]	80	83	82	79	81	78	75	79	78

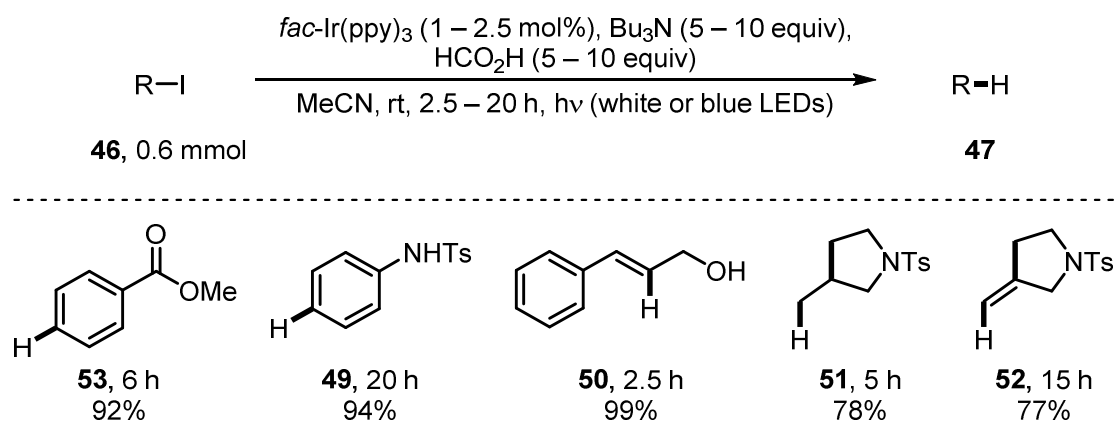
The surfaces of inorganic semi-conductors can also be modified with organic molecules in order to improve photocatalytic performance. Yamashita *et al.* used dihydroxynaphthalene-modified TiO₂ in this regard for the photochemical reduction of nitrobenzene (**14**) to aniline (**15**).²⁷ This surface-modified TiO₂ catalyst could be recovered *via* filtration and reused at least three times.

Also in the work of Scaiano *et al.* surface decorated TiO_2 was used to promote organic reactions. More specifically, platinum nanoparticles on TiO_2 were used for photochemical hydrodeiodations and intramolecular deiodative cyclizations (Scheme 8).²⁸ Again, the absorption band of the semi-conductor was shifted closer into the visible region and catalytic activity was enhanced through Pt incorporation. Upon photoexcitation, electrons in the conduction band of the semi-conductor can reduce alkyl, alkenyl, and aryl halides. Resulting carbon-centered radicals can either directly abstract a hydrogen atom or only after intramolecular cyclization to deliver hydrodeiodated products **47**. The hole in the valence band of the semi-conductor is refilled through electrons of *N,N*-diisopropylethylamine, which thus acts as a sacrificial electron donor. After the reaction, Pt/ TiO_2 could be recovered by centrifugation. The reusability was examined for the deiodation leading to **48**. In the second and third usage of the same catalyst, 54% and 58% yield of **48** were obtained, respectively. A fourth run only gave trace amounts of product. The limited recycling capabilities were attributed to aggregation of Pt nanoparticles which thus lost their catalytic activity.

Scheme 8. Photochemical deiodation reaction catalyzed by Pd/ TiO_2 with selected products.

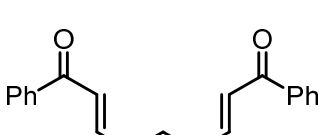
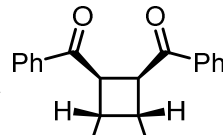
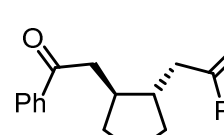
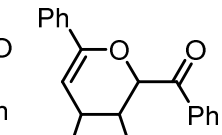


Conveniently, the same organohalides **46** were deiodated earlier by Stephenson *et al.* with homogeneously operating *fac*-Ir(ppy)₃ as photocatalyst so that the activities of both catalysts can be compared (Scheme 9).²⁹ However, as the light sources and the setup aren't identical in the two literature precedents, only general trends can be extracted from the available data. The transition metal complex-based catalyst *fac*-Ir(ppy)₃ could be used at significantly lower loadings and generally gave higher product yield after shorter irradiation times. Also no dangerous UVA light needed to be employed, LED irradiation with visible light was sufficient.

Scheme 9. Similar deiodination reactions with homogeneously operating *fac*-Ir(ppy)₃ as photocatalyst.

Similar observations are true for enone cycloadditions catalyzed by Pt/TiO₂ (Table 3). Such reactions were previously performed with transition metal complex [Ru(bpy)₃]Cl₂ in the group of Yoon.^{30,31} While in the case of [Ru(bpy)₃]Cl₂ the reaction product can be chosen by either employing Lewis or Brønsted acid activation of the substrates, Pt/TiO₂ catalysis only delivered mixtures of both. Additionally, TiO₂ presumably acted as Lewis acid and catalyzed a further Diels Alder reaction to **57**. Despite the many advantages of transition metal catalysis, no facile catalyst recovery is possible. At best, the catalyst can be recovered by column chromatography.³² However, this is highly impractical compared to (centrifugal) filtration.

Table 3. Enone cycloadditions catalyzed by either Pd/TiO₂ or [Ru(bpy)₃]Cl₂.

 <p>54</p>	 <p>55</p>	 <p>56</p>	 <p>57</p>
Pd/TiO ₂ , ⁱ Pr ₂ NEt, 15 h, <i>hν</i> (> 375 nm)	51%	18%	25%
Ru(bpy) ₃ ²⁺ , LiBF ₄ , ⁱ Pr ₂ NEt, 50 min, <i>hν</i> (275 W halogen lamp)	89%	-	-
Ru(bpy) ₃ ²⁺ , HCO ₂ H, ⁱ Pr ₂ NEt, 2.5 h, <i>hν</i> (23 W CFL)	-	82%	-

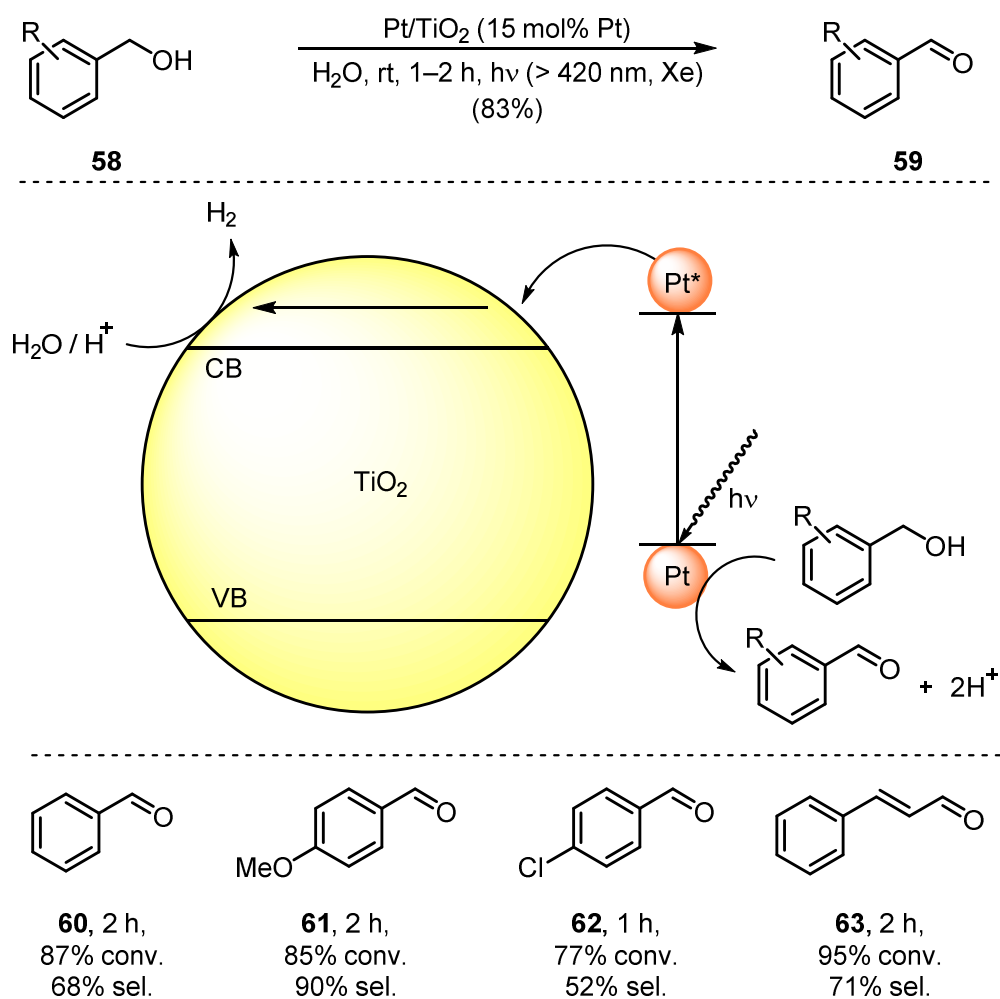
1.2 Surface plasmonic resonators

Metallic nanoparticles of noble metals can be intensively colored due to strong absorption of light in the visible range of the electromagnetic spectrum which arises from a resonant oscillation of surface electrons (surface plasmon band, SPB). As a support for those noble metal nanoparticles often inorganic semiconductors like TiO_2 or ZnO are used. Those supports themselves can absorb light and thus synergize in catalytic processes. Due to the heterogeneous nature of those inorganic semiconductors recovery after catalysis can be realized as before by (centrifugal) filtration.

Tian *et al.* used platinum nanoparticles on a TiO_2 film for the selective oxidation of benzylic and allylic alcohols to aldehydes (Scheme 10).³³ In this work the influence of the metallic nanoparticle size was systematically investigated: the smaller the size of the particles, the higher the conversion but the lower the selectivity. The optimized size of Pt was 33 nm on 25 nm anatase- TiO_2 particles. The reaction mechanism is proposed to go through photoexcitation of the Pt nanoparticles. The excited electrons are injected into the conduction band of TiO_2 where they reduce protons to H_2 which was detected by online GC measurements. Oxidized platinum nanoparticles take up electrons from benzylic alcohol **58** and thus oxidize it to aldehyde **59**. This proposed plasmon-driven mechanism was verified by transient absorption spectroscopy. As the Pt/ TiO_2 is coated on an ITO-glass plate recycling is trivial. The film showed only a very small (<5%) decline in efficiency upon usage for 1000 h. Interestingly the lost activity could be regenerated when the catalyst film was irradiated for ten hours with UV light.

Very similar oxidation results were obtained with an Au/ TiO_2 plasmonic system.³⁴ In this work O_2 was used as electron acceptor instead of H^+ . As the Au/ TiO_2 was not coated onto a glass plate, catalyst recovery was achieved by centrifugal separation. Unfortunately, no data on the stability of this system is available.

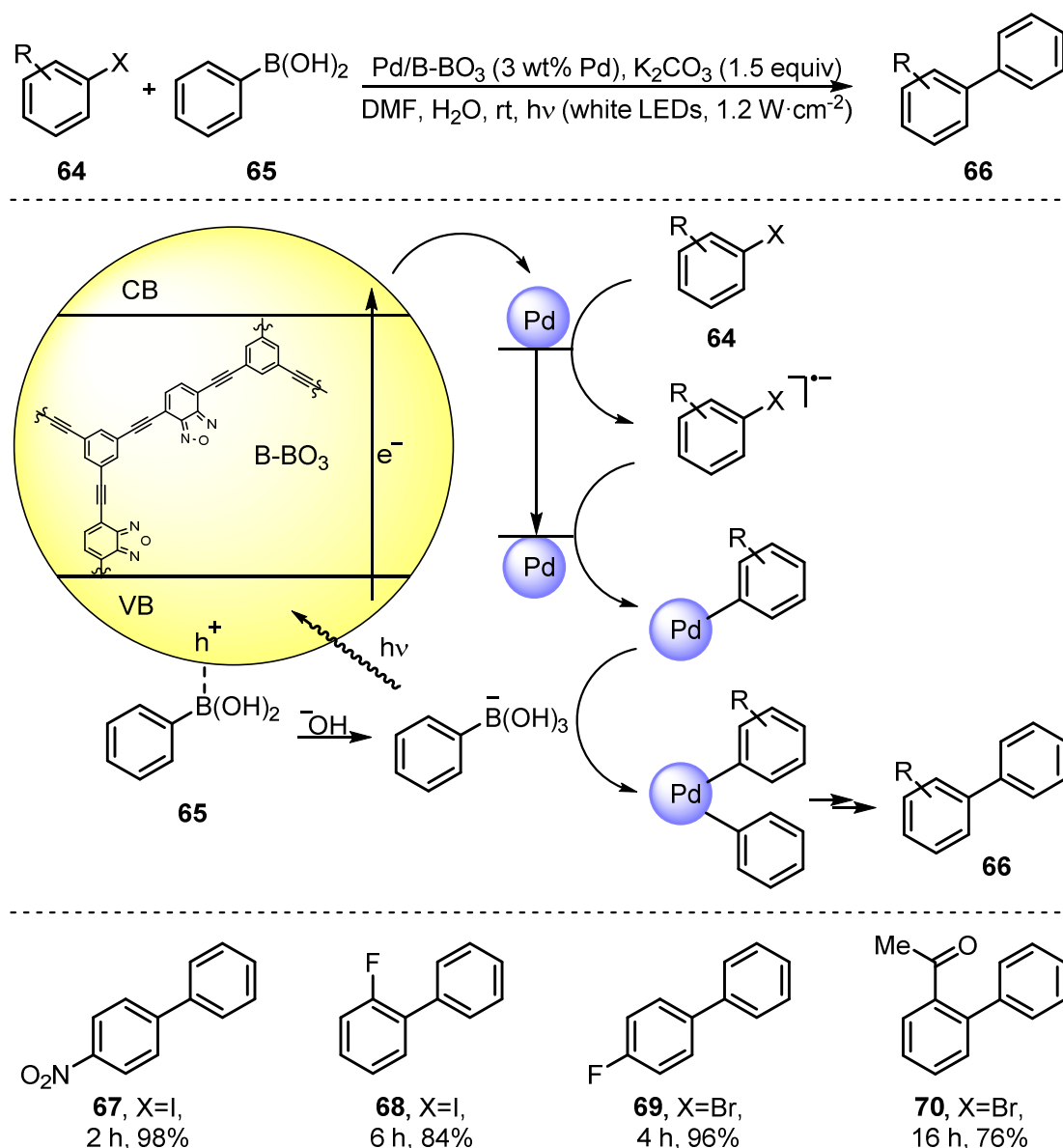
The group of Luque also used Au/ TiO_2 nanoparticles for amide formation between benzaldehyde and morpholine under laser light excitation in the presence of H_2O_2 and catalytic amounts of KOH at room temperature.³⁵ Hereby Au/ TiO_2 particles act as nanoscale-heat sinks that allow the thermal formation of product amides without actually heating the reaction mixture macroscopically. Control experiments confirmed that the surface plasmon resonance absorption of the Au nanoparticles is only used to locally generate heat as an experiment without laser irradiation but conventional heating to 60 °C gave identical results. It was shown that the particles can be separated by filtration and reused once more for the purpose of localized heat generation.

Scheme 10. Photooxidation of benzylic alcohols by Pt/TiO₂, mechanism, and substrate scope.

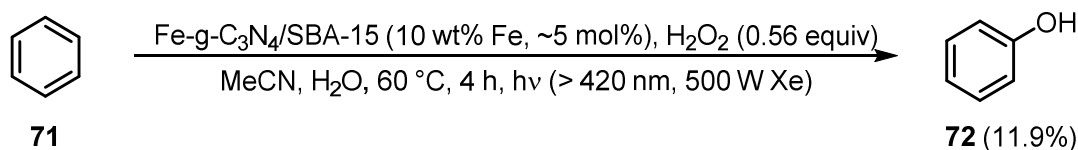
1.3 Organic semi-conductors

Very recently palladium nanoparticles were immobilized within a conjugated microporous poly(benzoxadiazole) network (B-BO₃).³⁶ Through the incorporation of Pd the visible light absorption capabilities of the material were significantly increased. The band gap of the organic semi-conductor B-BO₃ was slightly decreased to 2.38 eV (522 nm) and the electron-hole pair lifetime was increased. Pd/B-BO₃ was successfully used for photocatalytic Suzuki coupling reactions between halobenzenes **64** and phenylboronic acid (**65**) (Scheme 11). It was proposed that light absorption by the material produces electron-hole pairs within the semi-conductive polymer B-BO₃. Electrons migrate to the Pd centers where they are injected into halobenzenes and thereby weaken the carbon – halogen bonds. Transient radical anions form an aryl complex with Pd. Simultaneously the hole in B-BO₃ activates phenylboronic acid towards formation of the negatively charged B(OH)₃⁻ species which can then add to the aryl palladium complex. The remaining steps towards the products are identical to the regular Suzuki coupling. After the photochemical cross coupling reaction Pd/B-BO₃ could be filtered and reused. While in the first two runs full conversion of arylhalide **64** was observed, a steady decline to 90% conversion took place over five reaction runs. TEM images of Pd/B-BO₃ revealed no structural change after photoreactions, however, small Pd leaching (< 0.5%) was detected each run by ICP.

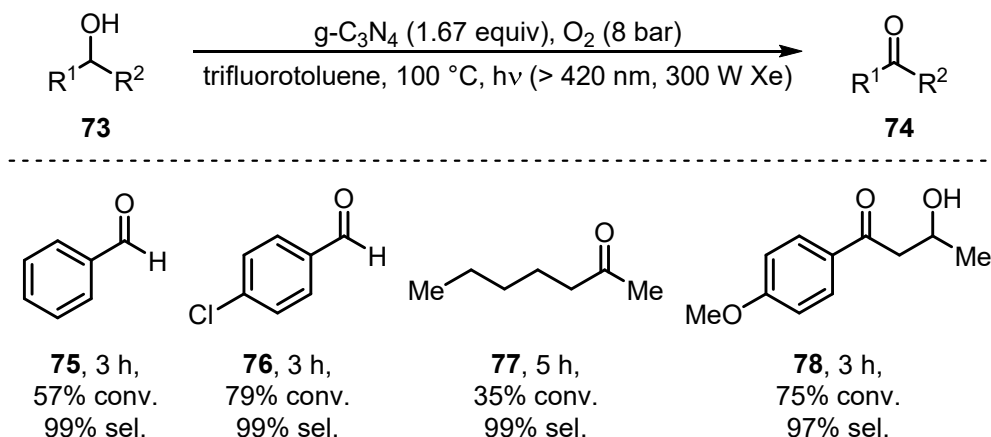
Similarly to this process, Suzuki reactions can also be catalyzed by palladium nanoparticles on mesoporous carbon nitrides (g-C₃N₄) which is an all organic semi-conductor.³⁷ Catalytic performance and recycling capabilities of Pd/g-C₃N₄ were comparable to those of Pd/B-BO₃.

Scheme 11. Visible light mediated Suzuki coupling with reaction mechanism and substrate scope.

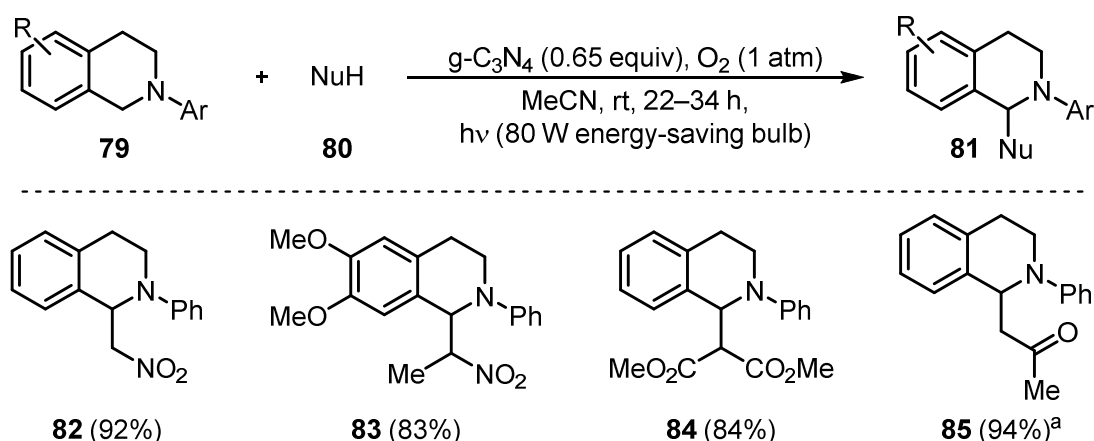
Iron containing mesoporous carbon nitride (Fe-g-C₃N₄) coated on the surface of mesoporous silica (SBA-15) proved to selectively oxidize benzene (**71**) to phenol (**72**) under visible light irradiation in the presence of H₂O₂ (Scheme 12).³⁸ While the reaction could also take place without light, significantly higher turn over frequencies (14.8 h⁻¹) were achieved when the reaction was irradiated by a 500 W Xe lamp (420 nm cut-off filter). Fe-g-C₃N₄ thereby acts as an all-organic, solid semi-conductor photocatalyst with an excitation maximum at 460 nm. Compared to classical (photo-)Fenton processes no strong acids are required and the catalyst Fe-g-C₃N₄/SBA-15 can easily be recovered by filtration and reused at least three times without a decline in efficiency.

Scheme 12. Fe-g-C₃N₄/SBA-15 catalyzed oxidation of benzene (**71**) to phenol (**72**).

Mesoporous carbon nitrides can also be used for the selective oxidation of alcohols to carbonyl compounds with visible light (Scheme 13).³⁹ Superoxide radical anion O₂^{•-} is formed by reduction of molecular oxygen by the photoexcited g-C₃N₄. O₂^{•-} can then abstract a hydrogen atom from the alcohol substrate. Followed by yet another hydrogen atom and an electron abstraction, target carbonyl compounds are formed in high selectivities. Catalyst recovery could be performed by filtration. The material lost one third of its activity after four reaction runs, however, full catalytic performance of g-C₃N₄ could be restored after washing with diluted NaOH solution. Similar oxidation protocols were realized for allylic alcohols,⁴⁰ α-hydroxy carbonyl,³⁹ sulfides,⁴¹ and amines.⁴² In all cases g-C₃N₄ exhibited very good recycling capabilities.

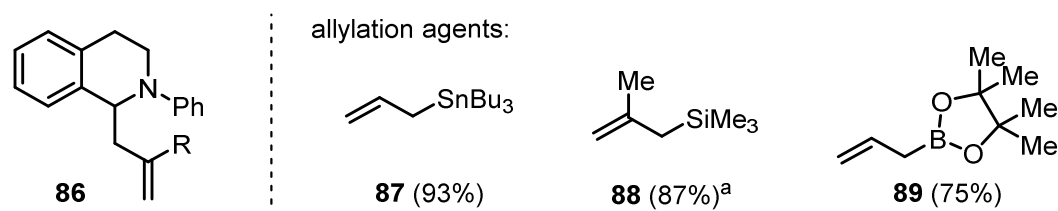
Scheme 13. Photocatalytic oxidation of alcohols **72** to carbonyl compounds **73** by g-C₃N₄.

Apart from oxidation reactions, g-C₃N₄ proved to be an excellent working, easily recyclable photocatalyst in C–C bond formation reactions as was described by Blechert *et al.*⁴³ In their studies g-C₃N₄ could be used for Mannich-type reactions with *N*-aryltetrahydroisoquinolines (**79**, Scheme 14). The quantum yield for the reaction to form **82** was determined to be 17.6%, confirming that g-C₃N₄ is an efficient photocatalyst. After the photoreactions g-C₃N₄ could be separated by either filtration or centrifugation. The catalytic activity remained at a very high level and quantitative starting material consumption was observed for at least five consecutive runs. Again, washing of the solid catalyst material with a diluted sodium hydroxide solution before reusal was essential to reactivate the catalyst.

Scheme 14. Mannich-type C–C bond formations catalyzed by g-C₃N₄.

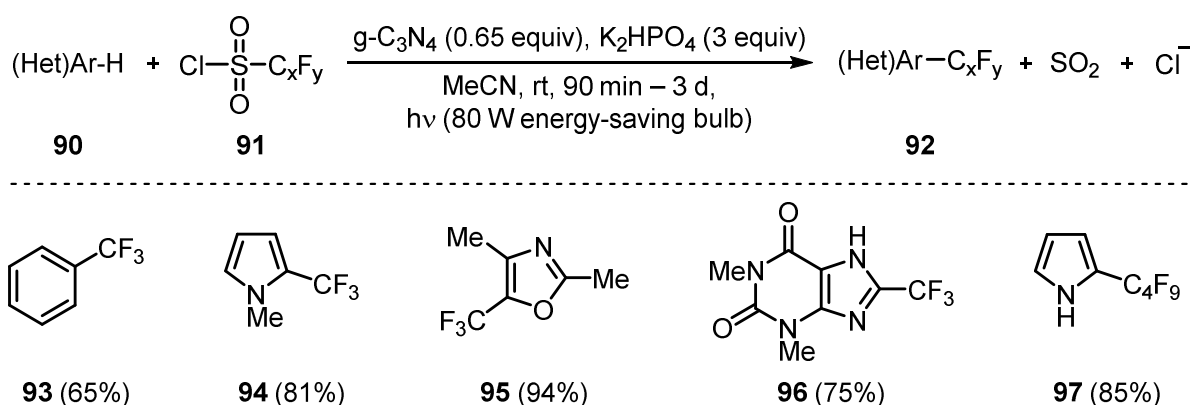
^a20 mol% proline was used as co-catalyst.

The scope of this C–C bond formation reaction was further expanded to weaker nucleophiles: allyl tributylstannanes, allyl trimethylsilanes, allyl boranes could be used to achieve allylation of *N*-phenyltetrahydroisoquinoline (**79**, R = H) to **83** in excellent yields (Figure 1).⁴⁴ As oxygen was used as terminal oxidant, amide formation through intermediary hydroperoxide anions was a challenge. However, amide formation could be suppressed when the reaction was slowed down by using lower amounts of catalyst, employing air instead of pure oxygen atmosphere, and a switch of solvent to methanol.

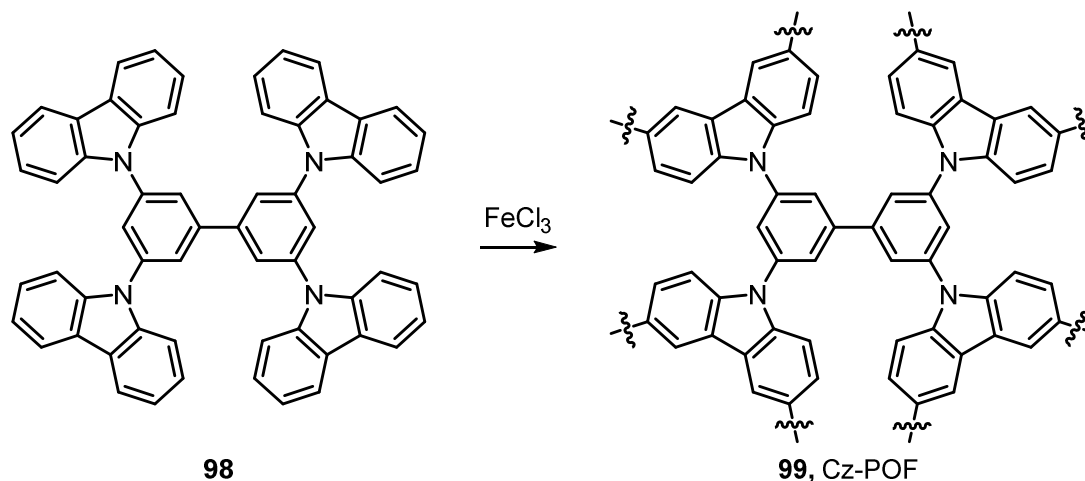
Figure 1. Allylation agents for the photochemical synthesis of **83** with recyclable g-C₃N₄.

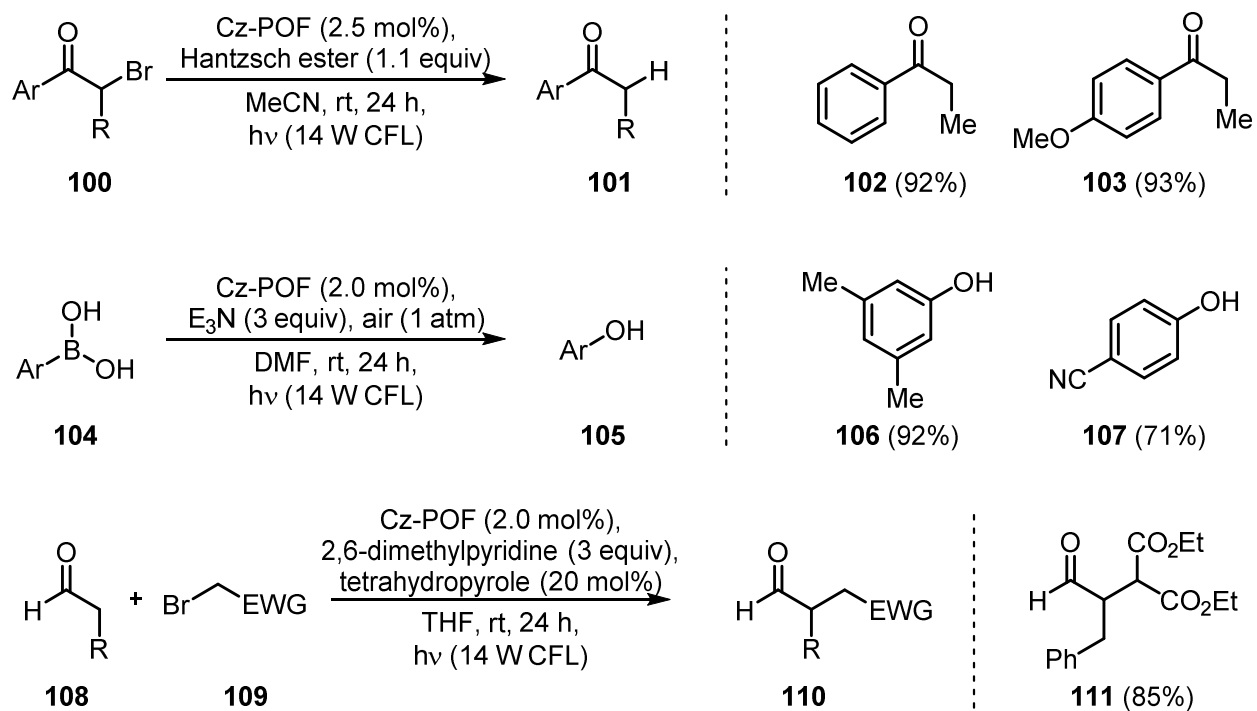
^a5 mol% of CuI was added as co-catalyst.

Easily recyclable photocatalyst g-C₃N₄ proved to be efficient in the perfluoroalkylation of arenes (Scheme 15).⁴⁵ The reactions had to be performed in the absence of oxygen as perfluoroalkylsulfonyl chlorides served as terminal oxidants to generate perfluoroalkyl radicals upon extrusion of SO₂. Ionic side reactions caused by perfluoroalkylsulfonyl chlorides could be suppressed when higher loadings of photocatalyst were used. Perfluoroalkylation yields were generally very good and regioselectivities high (>7:1). The recyclability was tested for the reaction leading to **94**. After separation of solid g-C₃N₄ and washing with water and acetonitrile, the catalyst could be used for at least three additional reaction runs without any decline in yield or selectivity.

Scheme 15. Perfluoroalkylation of (hetero-)aromatics by g-C₃N₄ under visible light Photocatalysis.

A highly porous carbazolic organic framework (Cz-POF) was introduced as homogeneous, recyclable photocatalyst by Zhang *et al.*⁴⁶ Through integration of carbazole into a π -conjugated porous organic framework (POF) its absorption band was shifted into the visible region of the electromagnetic spectrum (Scheme 16). Also the material was insoluble and therefore easily recovered by filtration after the reaction. It was easily prepared by polymerization of monomeric carbazole derivative **98**. Cz-POF exhibits a surface area of 2065 m²·g⁻¹ and a pore volume of 1.57 mL·g⁻¹. A band gap of 2.91 eV corresponds to an absorption at 426 nm. This material facilitated the hydrodebromination of phenacyl bromides, oxidative hydroxylation of arylboronic acids, and α -alkylation of aldehydes (Scheme 17).

Scheme 16. Synthesis of a porous carbazolic organic framework (Cz-POF) as photocatalyst.

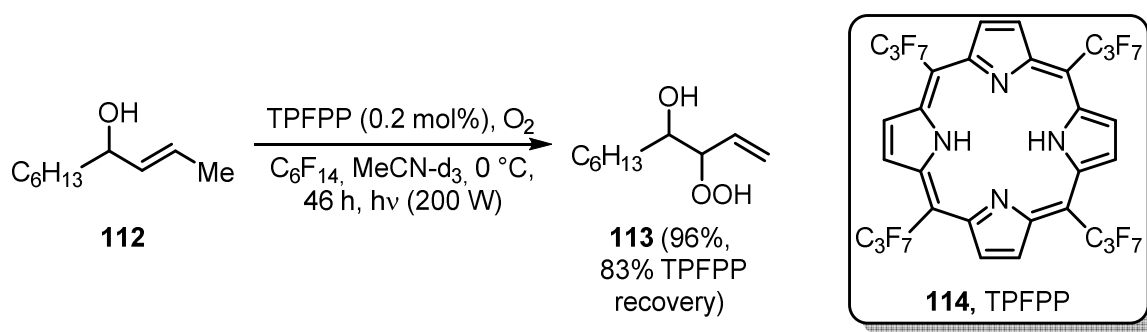
Scheme 17. Application of Cz-POF in photoredox catalysis by Zhang *et al.*⁴⁶

1.4 Organic dyes and sensitizers

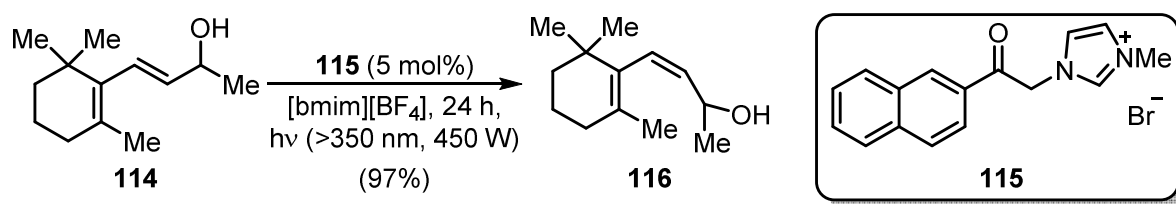
The first organic dye to be immobilized on a heterogeneous support was Rose Bengal on polystyrene, as was invented by Schaap *et al.*^{47,48} Many very similar works have been published with Rose Bengal being immobilized for example on polystyrene,^{49,50} PVC and cellulose acetate,⁵¹ silica gel,⁵² ion exchange resins,⁵³ and ionic liquids.⁵⁴ However, Rose Bengal and other organic dyes were mostly used for simple oxygenation reactions which are not focused in this review. Also, in earlier works the main goal was to achieve easy catalyst separation rather than a reuse of catalyst as organic dyes are typically inexpensive. Other reasons to bind photosensitizers to supports included the suppression of side reactions⁵⁵ and increased excited life times which are beneficial for photochemical reaction.⁵⁶ Recyclability was seldomly investigated in those works. A variety of other organic dyes have been immobilized in an innovative way, which are very briefly described here. In all those cases oxygenation reactions involving singlet oxygen were performed and the catalysts could be reused to a certain extent.

Methylene blue doped zeolite Y was used for such oxygenation reactions.⁵⁷ Recycling was realized by simple filtration and some washing steps. In a similar way, dicyanoanthracene on silica was used.⁵⁸ Phthalocyanines on ion exchange resin also proved efficient in oxygenation reactions. After filtration the dye could be reused five times with only a slight decrease in efficiency.⁵³ Also phthalocyanines tagged with long alkyl chains were used for the same purpose. After homogeneous catalysis they were precipitated out of the reaction solution and reused four times, albeit the irradiation times had to be prolonged.⁵⁹ Porphyrins embedded in dendrimers,⁶⁰ polysiloxane matrices,⁶¹ PVC,⁶² polymeric divinylbenzenes,⁶³ and porphyrin derivatives covalently bound to polystyrene^{64–66} or a Merrifield resin⁶⁷ catalyzed photochemical oxygenations and were reused after filtration. Also polyethyleneglycol-supported porphyrins were active oxygenation catalysts. Their recovery was achieved through precipitation and the material could be reused six times without a loss in efficiency.⁶⁸

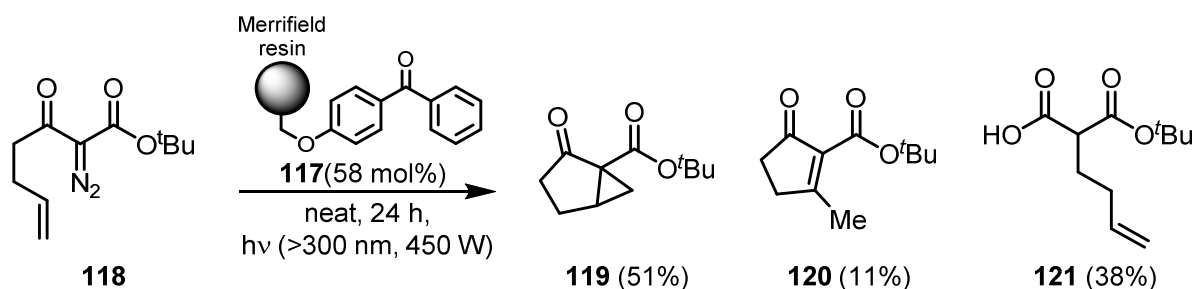
Most of those oxygenation catalysts were immobilized on heterogeneous supports, thereby mass transport problems can become an issue. Beside soluble polymer-tagged catalysts that were recovered after precipitation, also porphyrins tagged with perfluoroalkyl chains were realized (Scheme 18).^{69–71} In this case, photochemical oxygenations were performed in a biphasic system consisting of perfluorohexane and deuterated acetonitrile. After the reaction, phases were separated and the perfluorinated phase could be reused in further oxygenation reactions. Through this technique photobleaching of the catalytically active porphyrin could be drastically reduced.

Scheme 18. Perfluoroalkyl-tagged porphyrin **114** and its application in the oxygenation of **112**.

In addition to oxygenation reaction through singlet oxygen generated by recyclable organic molecules, also sensitization processes were realized. Jones *et al.* successfully used ionic liquid bound triplet sensitizer **115** for the sensitization of trans- β -ionole (**114**, Scheme 19).⁷² Thereby photochemical *E/Z* isomerization was triggered and cis- β -ionole (**116**) could be isolated in yields up to 97%. Reactions were performed in an ionic liquid ($[\text{bmim}][\text{BF}_4]$) and product could be extracted with diethyl ether while the remaining ionic liquid material was used for further transformations.

Scheme 19. Photochemical isomerization catalyzed by recyclable sensitizer **115**.

Also Merrifield resin-bound benzophenone **117** could act as triplet sensitizer and trigger photochemical reactions of α -diazocarbonyl compound **118** (Scheme 20).⁷³ Thereby three different reaction products were obtained: while cyclopropane **119** and elimination-cyclization product **120** originate from triplet energy transfer by excited photocatalyst **117**, Wolff rearrangement product **121** is formed through direct irradiation of **118** into its singlet state. As the reactions were conducted under solvent-free conditions, products were released from resin **117** by washing with solvent. After coating with new α -diazocarbonyl compound **118**, again triplet sensitization was catalyzed by **117**, albeit the previously observed product distribution varied in favor of Wolff rearrangement product **121**. In a direct comparison of resin-bound **117** with homogeneously operating 4-methoxybenzophenone, the achieved product selectivities of **117** are poor: a product ratio of 51:11:38 was obtained with the recyclable **117**, while a ratio of 80:15:5 was produced by the homogeneous derivative.

Scheme 20. Application of Merrifield resin-bound benzophenone **117** for the sensitization of **118**.

Also enantioselective photoreactions can be conducted with polymer bound sensitizers as demonstrated by Bach *et al.*⁷⁴ In this study the previously explored chiral photosensitizer template **122**⁷⁵ was covalently bound to a Wang resin and a methoxypolyethylene glycol (MPEG) polymer with an average molecular mass of 2000 Da (Scheme 21). Both methods led to easily recoverable catalysts: Wang resin-bound **123** could be separated by filtration and MPEG-tagged **124** was filtered after precipitation with diethyl ether. The catalysts retained their initial activities for at least five reaction runs with typically catalyst recovery rates of >95% (Table 4). However, catalytic activities of both catalysts significantly differed: Wang resin-bound sensitizer **123** was considerably less active than **124**, presumably because the Wang resin is intransparent and thus light penetration of the reaction solution was severely inhibited. The transparent MPEG-supported **124** doesn't face this drawback and gave comparable yields as the original template sensitizer **122**. However, in direct comparison of **122** with **124** it has to be noted that recyclability is dearly bought with significantly higher sensitizer loadings (26.8 equiv instead of 2.6 equiv, *sic*), higher dilutions (by a factor of three), and slightly lower enantiomeric excesses (90% *ee* instead of 93%) even at reduced temperatures (-74 °C instead of -60 °C).

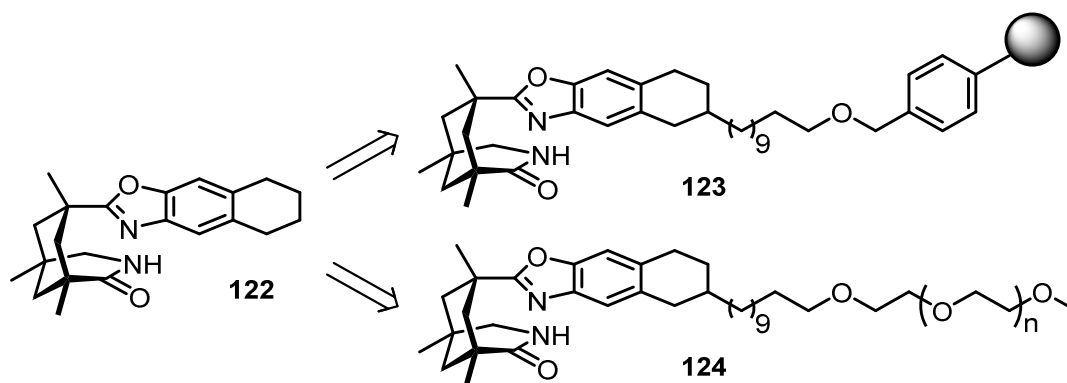
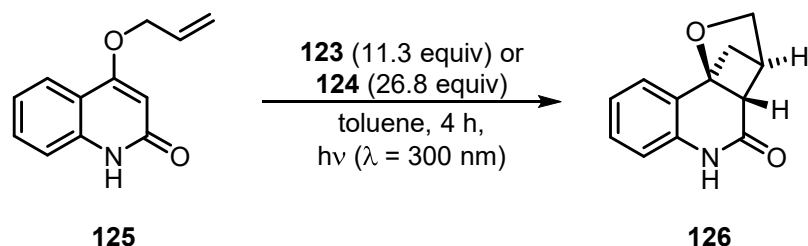
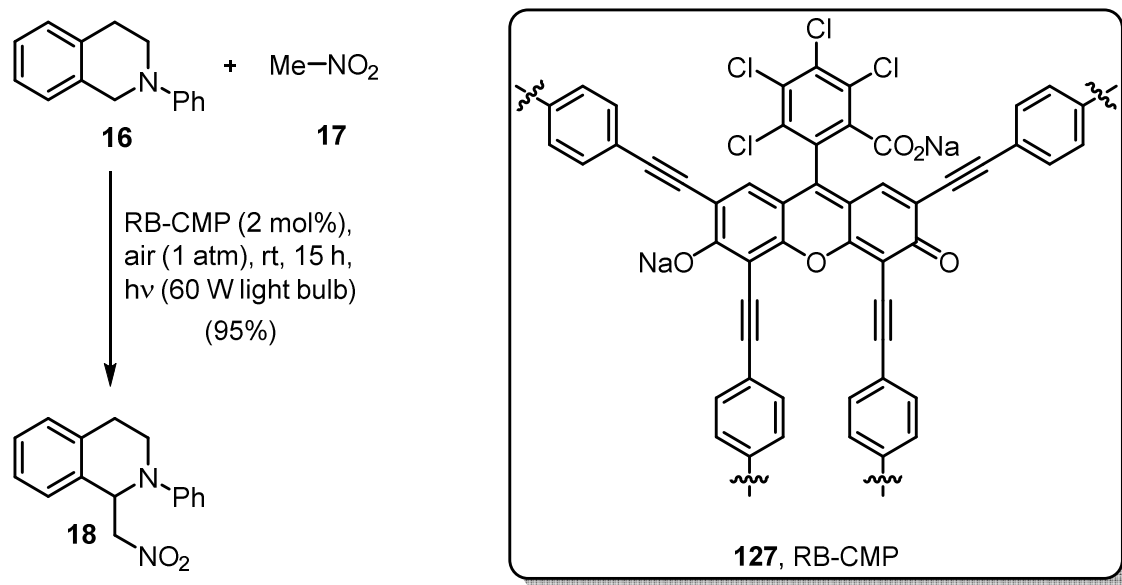
Scheme 21. Immobilization of chiral photosensitizer template **122** on a Wang resin (**123**) and a MPEG polymer (**124**).

Table 4. Comparison of Wang resin-supported sensitizer **123** and MPEG-bound **124** in the photocatalytic [2+2] addition of **125**.

Sensitizer 123				124		
Run	e.r.	Sens. Recovery [%]	Conv. [%]	e.r.	Sens. Recovery [%]	Conv. [%]
1	93:7	99	31	95:5	99	96
2	93:7	91	25	95:5	99	98
3	93:7	96	27	96:4	97	97
4	92:8	96	24	96:4	98	99
5	93:7	96	27	96:4	97	96

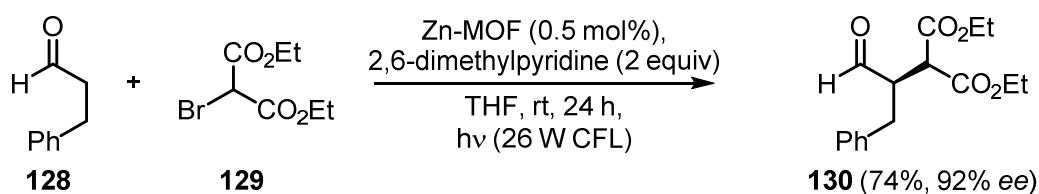
The organic dye Rose Bengal was incorporated into the main chain of conjugated microporous polymers (CMP) by Sonogashira–Hagihara cross-coupling polycondensation with 1,4-diethylbenzene.⁷⁶ This procedure gave a highly porous ($> 830 \text{ m}^2\cdot\text{g}^{-1}$), solid photocatalyst RB-CMP that could catalyze aza-Henry reactions (Scheme 22). After the photochemical transformation the material could be recovered by filtration and after washing and drying steps reused ten times for the same reaction. During those recycling runs the activity of the catalyst decreased slightly as only 90% starting material conversion was observed in the last recycling experiment. Nevertheless, the recycling results are remarkable as the catalyst activity was even slightly higher than in comparison with homogeneously operating Rose Bengal at a loading of 2 mol%:⁷⁷ 99% starting material (**16**) conversion was observed with RB-CMP after 12 h while homogeneous Rose Bengal only converted 73% in this time span under identical conditions.

Scheme 22. Conjugated microporous polymer with Rose Bengal (**127**, RB-CMP) as catalyst for aza-Henry reactions.



A metal organic framework (MOF) was constructed from Zn(NO₃)₂·6H₂O, (*L*)-*N*-*tert*-butoxycarbonyl-2-(imidazole)-1-pyrrolidine (*L*-BCIP), and 4,4',4''-tricarboxyltriphenylamine by Duan *et al.*⁷⁸ This material was catalytically active in the asymmetric α -alkylation of aldehydes by diethyl bromomalonate (Scheme 23). While chirality is induced though enamine formation between aldehyde and *L*-BCIP, the excited state of the triphenylamine moiety within the MOF can act as potent reductant.⁷⁸ The catalyst material was isolated after successful photoreaction by centrifugation and could be reused two consecutive times with a slight decrease in activity and selectivity: the yield dropped from 74% to 70% and the *ee* from 92% to 88%.

Scheme 23. Photochemical chiral alkylation of aldehydes **128** by diethyl bromomalonate (**129**).

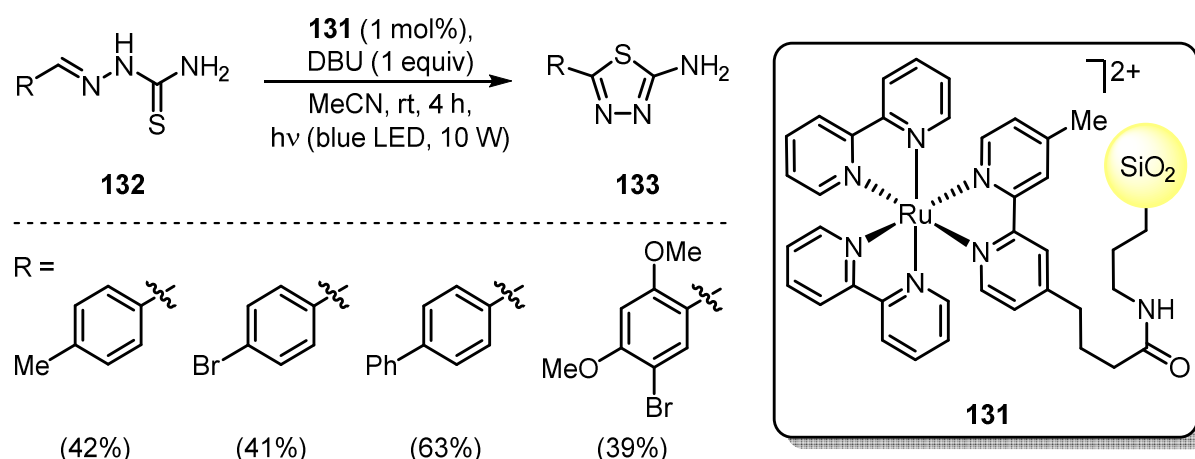


1.5 Transition metal complexes

As for organic dyes and sensitizers, a lot of effort was earlier directed to the immobilization of (transition) metal complexes for oxygenation reactions. Important examples are briefly summarized: Sn^{4+} porphyrins were embedded in metal organic frameworks (MOF) and could be filtered after oxygenation reaction and reused.^{79,80} A Pt^{2+} quaterpyridine complex was incorporated into a Nafion membrane which could be filtered and reused without a loss in efficiency.⁸¹ Homogeneously operating polyvinylimidazole bound Ru^{2+} complex could be precipitate from the reaction solution and reused again.⁸² Heterogeneous, silica-bound Ru^{2+} complex could be recycled through filtration and reapplied to the synthesis of alcohols, epoxides, and carbonyls.^{83,84} Ru^{2+} complexes were also covalently bound to insoluble polyamide polymers that were active in oxygenation reactions.⁸⁵

The by far most predominant method to obtain recyclable transition metal complexes for photocatalytic applications other than oxygenations, is the attachment to insoluble supports. A prototypical example is the covalent attachment of $\text{Ru}(\text{bpy})_3^{2+}$ onto commercially available amino-functionalized silica by Francis *et al.*⁸⁶ In this study, the catalyst was used to synthesize 5-substituted-1,3,4-thiadiazol-2-amines (**133**, Scheme 24). After the photochemical reaction, a simple vacuum filtration gave back the catalyst which could be reused in at least eight consecutive reactions. No decline of efficiency was evident, likewise no UV-Vis absorption of the filtered product solutions was detected that could be ascribed residual catalyst amounts. The immobilized $\text{Ru}(\text{bpy})_3^{2+}$ derivative gave almost identical yields as its homogeneously operating parent complex.

Scheme 24. Intramolecular cyclizations catalyzed by reusable silica-bound $\text{Ru}(\text{bpy})_3^{2+}$ **131**.



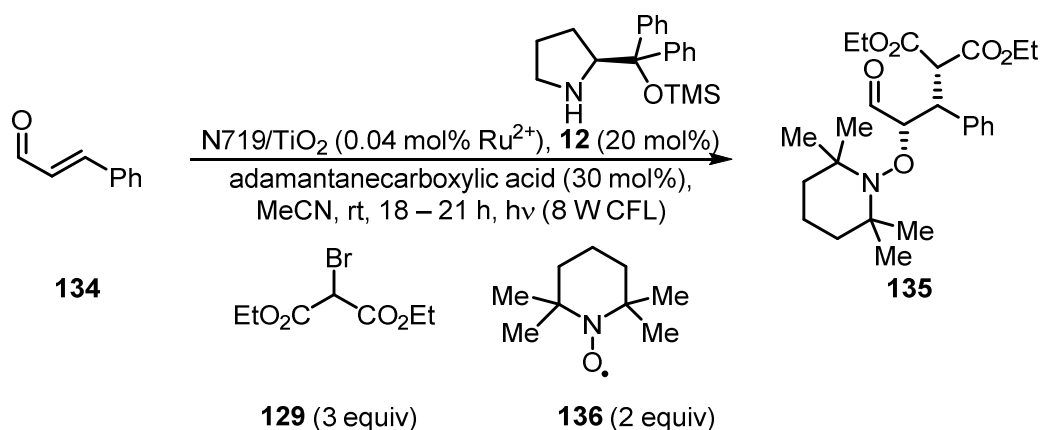
$\text{Ru}(\text{bpy})_3^{2+}$ could also be immobilized on Nafion-coated silica solely by electrostatic interactions by the group of Choi.⁸⁷ Also naked silica was used in this study, however only

minor amounts of $\text{Ru}(\text{bpy})_3^{2+}$ were adsorbed. The coating of $\text{Ru}(\text{bpy})_3^{2+}$ on Nafion-modified silica was stable in almost all common organic solvents, only in DMF minor leaching was observed. The catalyst was then used for free radical polymerizations of various acrylates. Recovery was facilitated by centrifugation while the polymeric product was still in solution. In this way the immobilized $\text{Ru}(\text{bpy})_3^{2+}$ could be reused at least five times.

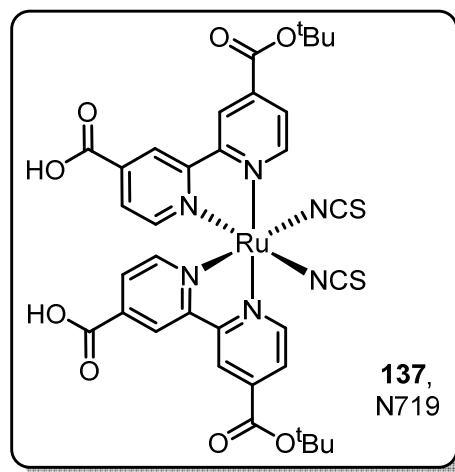
Yet another Ru^{2+} -based photocatalyst (N719, **137**) was attached to silica by electrostatic interactions in the work of Jang *et al.*⁸⁸ The group could successfully employ this catalyst for novel tandem Michael / oxyamination reactions of α,β -unsaturated aldehydes **134** (Table 5). It is worth to note that the transition metal complex N719 and the inorganic semiconductor support TiO_2 synergize as photocatalysts as control experiments with either only homogeneous N719 (entry 2) or heterogeneous TiO_2 (entry 3) delivered lower yields than their combination (entry 1). Catalyst recovery was realized by simple filtration of the solid material after catalysis. It could be reused twice (entry 4 and 5), however the catalytic activity declined with every run.

Table 5. Photochemical tandem Michael / oxyamination reactions catalyzed by N719/ TiO_2 .

Catalyst structure and recycling results.



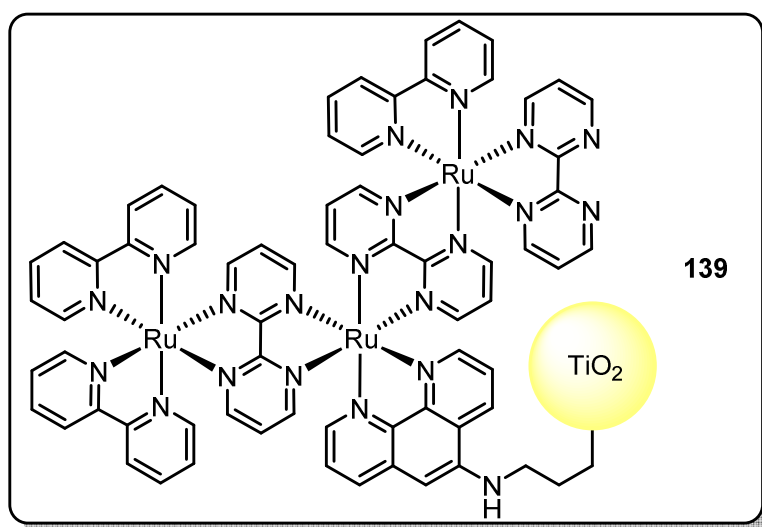
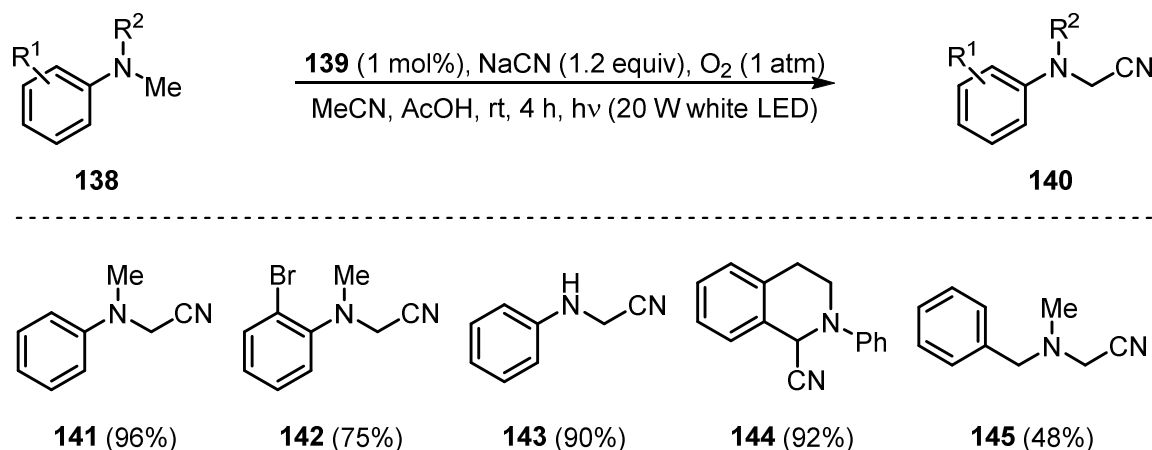
Entry	Modification	Yield [%]
1	-	80 ^a
2	N719 (0.05 mol%)	62
3	TiO_2	11
4	1 st recycling	63
5	2 nd recycling	37



^a96% *ee*, >95% *de*.

A slight synergistic effect of Ru^{2+} complex **139** with its covalently bound TiO_2 support is also evident in the oxidative cyanation of tertiary amines **138** as demonstrated by Jain *et al.* (Scheme 25).⁸⁹ A homogeneous derivative of the photocatalyst **139** delivered cyanated product **140** only in 90% yield instead of 96% yield with attached TiO_2 . The tethered catalyst exhibited very good catalytic properties in the photochemical synthesis of a variety of electronically and sterically distinct tertiary amines **138**. Through its TiO_2 support, facile catalyst separation was possible by filtration. Recycling was feasible for at least eight consecutive cyanation reactions leading to **141**. The isolated yield of **141** only insignificantly dropped by 2% to still furnish **141** in 94% yield after the eight catalytic runs. In ICP-OES analyses of the obtained products no contamination with leached ruthenium was detected, demonstrating the high stability of this Ru^{2+} complex.

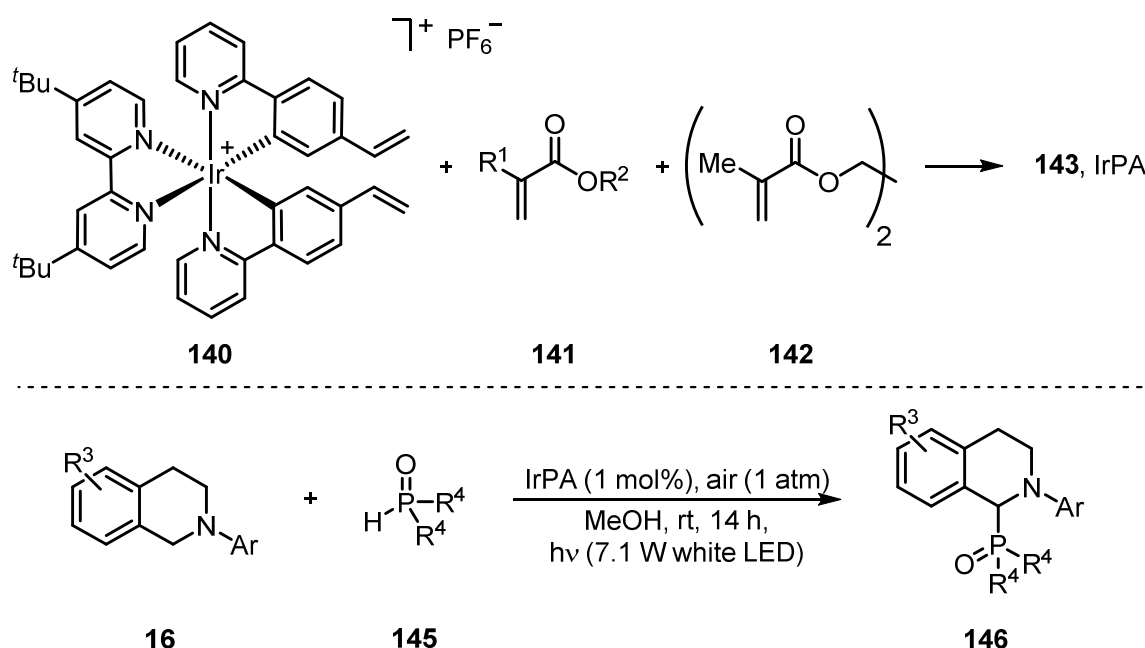
Scheme 25. Application of covalently to SiO_2 bound Ru^{2+} catalyst **139** in the oxidative cyanation of secondary and tertiary amines **138**.



Kobayashi *et al.* polymerized vinyl-substituted Ir^{3+} complex **140** in the presence of acrylates **141** and cross-linker **142** (Scheme 26).⁹⁰ As preliminary experiments indicated a

rather high leaching of over 2% in a photochemical test reaction, the material was resubjected to polymerization conditions to coat it with an additional polyacrylate layer. Iridium leaching could be lowered under 0.3%. The obtained insoluble, polymeric material had an iridium chromophore loading of 2 wt%. It was used in photochemical coupling reactions of *N*-aryl tetrahydroisoquinolines **16** with P-H nucleophiles **145**. After the reaction, the polymeric catalyst could be recovered by filtration and reused four times. In course of the recycling runs the catalytic activity of the material suffered slightly as the conversion rate of **16** decreased from >95% to 88%.

Scheme 26. Synthesis of polyacrylate (PA) supported photocatalyst IrPA (**143**) and its application in the oxidative coupling of *N*-aryl tetrahydroisoquinolines **16** with P-H nucleophiles **145**.



Another approach to obtain recyclable photocatalysts was realized by Lin *et al.* They integrated Ru^{2+} and Ir^{3+} complexes as core structural element of porous cross-linked polymers (PCP) through a trimerization of alkyne-functionalized building blocks (Scheme 27).⁹¹ Thereby the transition metal phosphor acts not only as the catalytically active center but also as heterogeneous support at the same time. The polymeric catalysts exhibited surface areas of $1500\text{ m}^2\cdot\text{g}^{-1}$. RuPCP could be used for photochemical α -arylations of bromomalonate and an oxyamination of an aldehyde. Both IrPCP and RuPCP were also successfully applied in aza-Henry reactions of *N*-phenyltetrahydroisoquinoline (**16**) with nitromethane (**17**). The immobilized photocatalysts either gave similar or even slightly higher conversions than their homogeneous counterparts in all experiments. Catalyst recycling was performed by filtration and only slight deterioration of substrate conversion was observed over five recycling runs (Table 6). UV-Vis and ICP measurements of the reaction products indicate no leaching of

metal species. However, a disadvantage of IrPCP and RuPCP is the relative low loading of photosensitizer (2.2 – 4.5 wt%) relative to the total mass of polymer.

Scheme 27. Synthesis of porous cross-linked polymers containing Ru^{2+} and Ir^{3+} complexes.

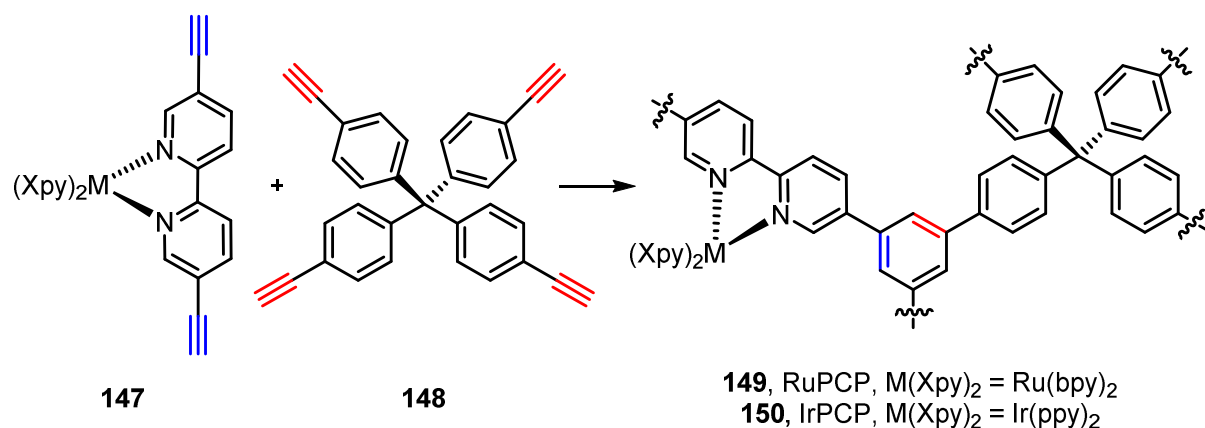


Table 6. Recycling results of RuPCP (**149**) in the aza-Henry reaction of *N*-phenyltetrahydroisoquinoline (**16**) with nitromethane (**17**).

Entry / Run	1	2	3	4	5
Conversion [%]	94	94	93	90	90

To overcome the low catalyst loading, Lin *et al.* later modified the structure of the cross-linked porous polymer.⁹² Tetraalkyne **148** was omitted, the alkyne substituents on the ligands of the Ru^{2+} complex were moved from 5,5' to 4,4' position, and an oxidative Eglinton coupling was performed to deliver porous cross-linked porous polymer RuPCP2. The $[\text{Ru}(\text{bpy})_3]^{2+}$ content in this new material was 91 wt% and the surface area $198 \text{ m}^2\cdot\text{g}^{-1}$. Catalytic activities in aza-Henry reactions were slightly higher than before with original RuPCP and again recyclability was proven. Excited state life times of RuPCP2 were slightly inferior to its homogeneous analogon $[\text{Ru}(\text{bpy})_3]^{2+}$.^{93,94} The excellent catalytic performance of RuPCP2 (even though its surface area was almost ten times smaller than RuPCP) was rationalized by migration of excited states through the polymer: Dexter triplet to triplet energy transfer from excited inner chromophores to outer Ru^{2+} units enables redox reactions on the surface of the polymeric material even though light is absorbed on the inside. Through such a remarkable core-to-surface excited state transport also other, entirely nonporous (surface areas $< 3 \text{ m}^2\cdot\text{g}^{-1}$), cross-linked Ru^{2+} and Ir^{3+} catalytic materials were realized.⁹⁵

Lin *et al.* also immobilized Ru²⁺ and Ir³⁺ complexes in an insoluble metal organic framework (MOF, Zr₆O₄(OH)₄(bpdc)₆ / UiO-67).⁹⁶ Application of Ru²⁺/UiO-67 and Ir³⁺/UiO-67 in photochemical aza-Henry, aerobic amine coupling, and thioanisole oxidation reactions were demonstrated. After separation by centrifugation the catalytic materials could be reused three times with only a slight decay in conversion (Table 7).

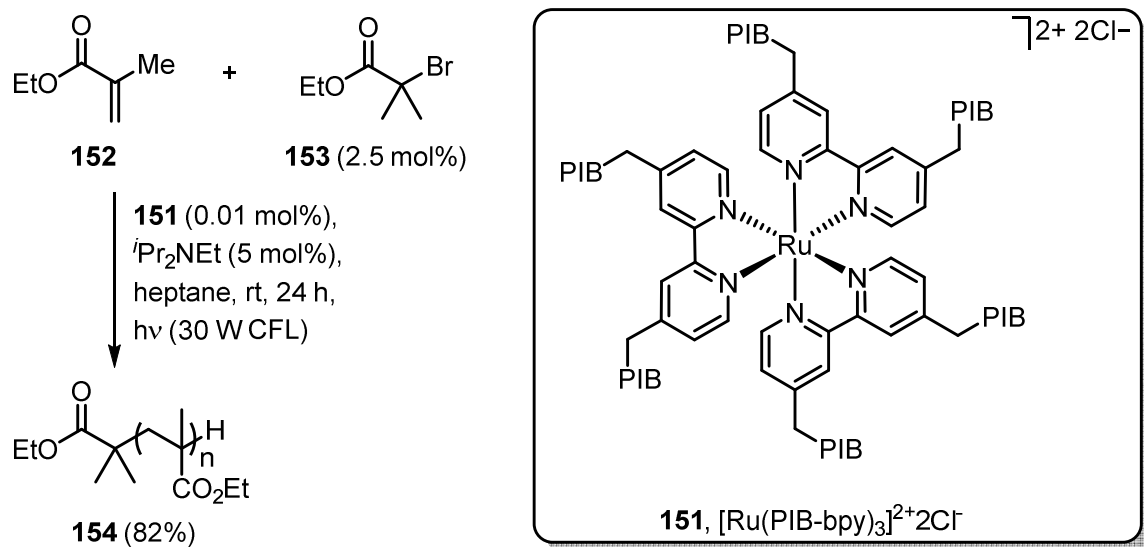
Table 7. Recycling results of Ru²⁺/UiO-67 and Ir³⁺/UiO-67 in the aza-Henry reaction of *N*-phenyltetrahydroisoquinoline (**16**) with nitromethane (**17**).

Entry / Run	1	2	3
Ru ²⁺ /UiO-67	59%	57%	59%
Ir ³⁺ /UiO-67	86%	69%	62%

In contrast to all previously presented, heterogeneous recyclable transition metal complexes Bergbreiter *et al.* developed a homogeneously operating Ru²⁺ photocatalyst.⁹⁷ This was achieved by the introduction of multiple polyisobutylene (PIB) chains onto the bipyridine ligands of [Ru(bpy)₃]²⁺.^{†††} PIB was previously used as support for both reagents and catalysts.⁹⁸ It is transparent, soluble in a variety of organic solvents, and tagged molecules can be analyzed by common analytical techniques such as IR, NMR, and MS. Recovery can typically be achieved by precipitation or liquid/liquid extractions due to PIBs highly hydrophobic nature. PIB-bound photocatalyst [Ru(PIB-bpy)₃]Cl₂ (**151**) was used in this work for the free radical polymerization of acrylate **152** (Scheme 28). Polymeric product **154** precipitated from the irradiated solution and could be separated after reaction by filtration. To the remaining solution of photocatalyst **151** in hexane new reagents were added and polymerization was restarted to give polyacrylate **154** in identical yield. When this procedure was repeated, product yield dropped to 70%. The loss in activity was attributed to partial catalyst decomposition. Precipitated polymeric product **154** was investigated by ICP-MS for leached heavy metals. The ruthenium content was below 2 ppm, while when homogeneous [Ru(bpy)₃]²⁺ was used 48 ppm Ru was detectable in the product. These results show that through attachment of as much as six PIB chains onto the catalyst, separation of Ru from the polymer product was significantly enhanced. However, an disadvantage is the resulting low chromophore content in [Ru(PIB-bpy)₃]Cl₂ of only around 4 wt% due to the high molecular weight of each PIB chain of 2300 Da.

^{†††} The introduction of PIB chains was unselective. However, fully PIB-substituted complex [Ru(PIB-bpy)₃]Cl₂ (**151**) behaved identically to only partially PIB-substituted one. For clarity, no differentiation is made in regard of the degree of catalyst substitution.

Scheme 28. Application of homogeneously operating photocatalyst $[\text{Ru}(\text{PIB-bpy})_3]\text{Cl}_2$ (**151**) in free radical polymerizations.



1.6 Summary^{†††}

A multitude of recyclable photocatalyst was developed for oxygenation reactions in the past. The excited photocatalysts were mainly used to produce singlet oxygen. However, new photocatalytical processes, especially photoredox reactions, had different requirements, *e.g.* a direct contact of the excited catalyst with organic substrate molecules.

Within the last couple of years, all photocatalyst classes have been explored in search for efficient, recyclable catalysts. Investigated inorganic semi-conductors typically were easily recoverable by filtration. However, surface depositions often limited a further use. Efficiencies of semi-conductors with unmodified surfaces are often low compared to the other photocatalyst classes. Studies with surface-modified semi-conductors gave promising results.

Organic semi-conductors, especially mesoporous carbon nitride emerged as an easily recyclable, heterogeneous photocatalyst class. Many transformations that previously required expensive transition metal complexes, could also be performed with organic semi-conductors. Separation of the catalytic material again was performed by filtration processes and the recovered catalysts could usually be used for additional reactions. Classical organic dyes play a minor role as recyclable catalysts as their low costs usually do not justify recycling efforts.

Transition metal complexes have been heterogenized by either attachment to a solid support or by integrating them into the backbone of an insoluble matrix. While catalytic activities can be typically be held over some consecutive recycling experiments, low chromophore contents were often an issue. Only one example is available for homogeneously operating, recyclable transition metal catalysts. Its separability process (precipitation of polymeric product) is not general. Also the used solvent (heptane) is not expected to be compatible with more typical organic transformations.

It is therefore highly desirable to develop homogeneously operating photocatalysts that can be used in common solvents. Through a homogeneous operation mode, the long excited state life times and catalytic actives of the unmodified parent complexes might presumably be maintained. Specifically, a recyclable derivative of highly reductive *fac*-Ir(ppy)₃ is highly desirable as more and more papers are published based on this catalysts marvelous performance.

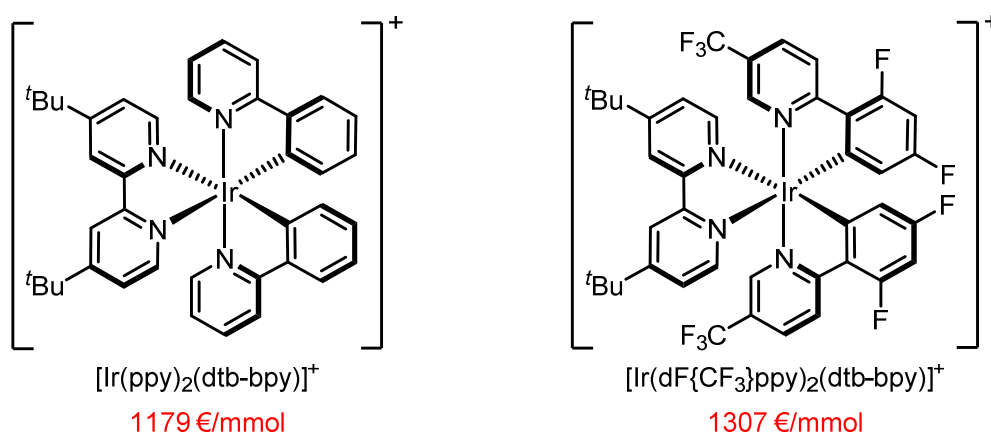
^{†††} All numberings of schemes, figures, tables, and structures are reset after this section.

2 Bis-Cyclometalated Iridium(III) Complexes

2.1 Introduction

Biscyclometalated iridium(III) complexes like $[\text{Ir}(\text{ppy})_2(\text{dtb-bpy})]^+$ and $[\text{Ir}(\text{dF}(\text{CF}_3)\text{ppy})_2(\text{dtb-bpy})]^+$ represent a heavily used class of homogeneously operating, visible light photoredox catalysts (Figure 1). Both are commercially available but their extremely high price in combination with catalyst loadings of typically around 1 mol% in a synthetic reaction severely impedes reactions on larger scales. Also the homogeneous operation mode complicates separation of products which further increases the reaction costs. Efficient and simple recycling strategies for this catalyst class are therefore highly desirable.

Figure 1. Commonly employed biscyclometalated iridium(III) complexes and their retail prices.⁹⁹



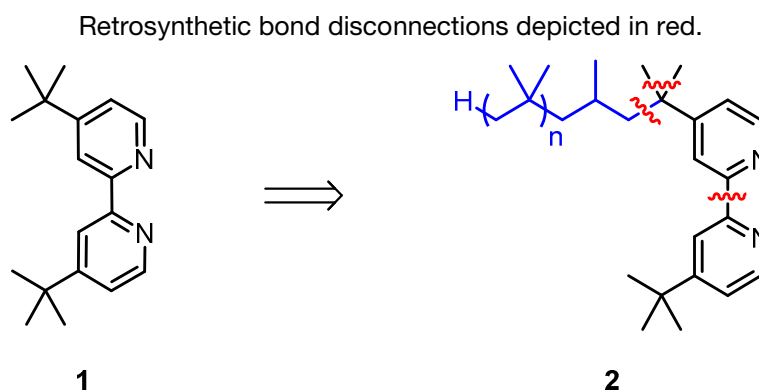
To avoid any mass transportation issues employment of a homogeneously operating catalyst is potentially superior. Also unproductive light scattering and absorption processes by an intransparent support are eliminated in this way.

Recyclability should be achievable by tagging one of the ligands with a polyisobutylene (PIB) chain. This polymeric support is transparent and dissolves in a variety of organic solvents. Tethered compounds can be purified by standard column chromatography when necessary and be well characterized with common analytical techniques as IR, NMR, and MS. Both catalyst and reagents have been covalently bond to this support by Bergbreiter *et al.*^{97,98,100–121} Separation of the polyisobutylene tagged agent is typically achieved by extraction with a non-polar solvent like heptane or precipitation of the reaction products.

2.2 Ligand synthesis

No changes of the catalysts' electronic properties should be made as the catalysts have been optimized and selected for specific reactions in this regard. As site for the introduction of the polyisobutylene chain, one of the *tert*-butyl groups of 4,4'-di-*tert*-butyl-2,2'-bipyridine (**1**) seemed ideal: a substitution of a methyl group by a PIB chain should have no or only very little influence on the electronic nature of the catalyst (Scheme 1). In this way, it should be possible to use the catalysts for their originally published reactions without modifications that originate from altered electronics. As ligand **1** is contained in both of the most heavily used iridium(III) complexes $[\text{Ir}(\text{ppy})_2(\text{dtb-bpy})]^+$ and $[\text{Ir}(\text{dF}(\text{CF}_3)\text{ppy})_2(\text{dtb-bpy})]^+$, polyisobutylene tagging of it could give access to recyclable variants of both catalysts.

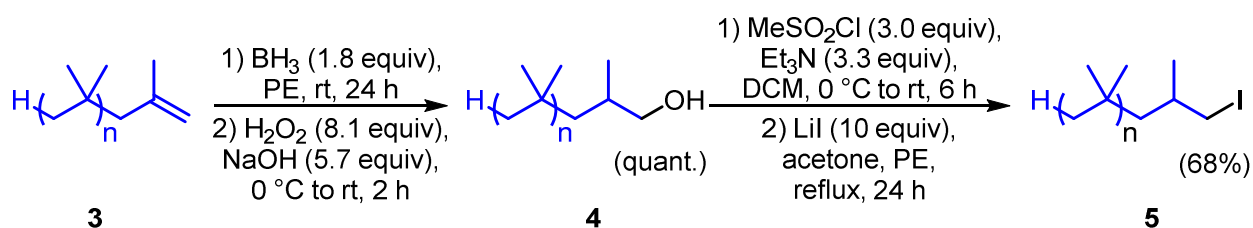
Scheme 1. Replacement of a methyl group by a PIB chain of dtb-bpy (**1**). PIB chain depicted in blue.



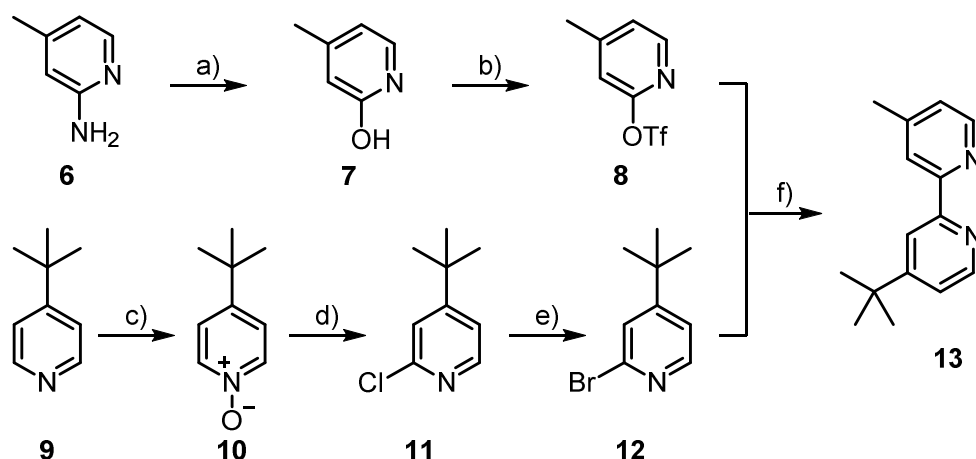
The synthesis of polyisobutylene tagged bipyridine ligand **2** was envisioned to be accomplished by initial preparation of an asymmetrical bipyridine followed by three alkylation steps: one alkylation to introduce the polyisobutylene chain and two more methylations to quaternize the benzylic position (Scheme 1). A quaternary carbon center lacking any carbon – hydrogen bonds was viewed crucial as the otherwise secondary or tertiary benzylic position might be an origin for catalyst instability.

Access to a suitable polyisobutylene alkylation agent was provided by BASF SE in form of alkene-terminated Glissopal® 1000 (**3**) (Scheme 2).^{§§§} Derived from a literature synthesis for polyisobutylene bromide, hydroboration, followed by mesylation and substitution gave polyisobutylene iodide (**5**) in good yield.¹²⁰

^{§§§} The number 1000 refers to the average molecular weight of the polymer in Da. This corresponds to an average chain length of 18 isobutylene units.

Scheme 2. Synthesis of polyisobutylene iodide (**5**) from BASF Glissopal® 1000 (**3**).

Having key alkylation agent **5** in hand, unsymmetrical bipyridine **13** was prepared (Scheme 3). Literature procedures gave triflate-modified pyridine **8** and bromo-substituted pyridine **12** in acceptable yields.^{122–125} A palladium-mediated coupling of *in situ* prepared zinc organyl of **12** with triflate-modified pyridine **8** yielded bipyridine **13** in 55% yield in analogy to similar other previously reported unsymmetrical bipyridines.¹²⁵

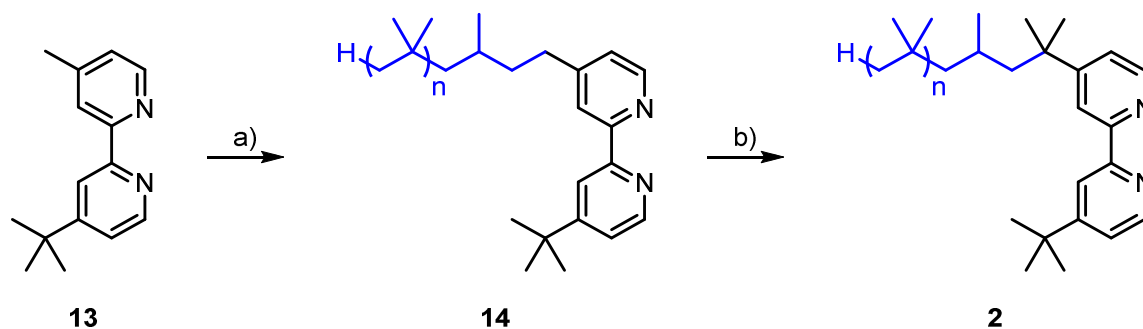
Scheme 3. Preparation of unsymmetrical bipyridine **13**.

Reagents and conditions: a) NaNO_2 (1.1 equiv), H_2SO_4 (2.1 equiv), H_2O , 0°C to reflux, 15 min, 60%; b) Tf_2O (1.1 equiv), pyridine, 0°C , 40 min, 87%; c) H_2O_2 (1.2 equiv), HOAc, 70°C , 72 h, 89%; d) POCl_3 (5.9 equiv), reflux, 2 d, 40%; e) HBr (1.2 equiv), HOAc, reflux, 2 d, 38%; f) 1. $^t\text{BuLi}$ (2.4 equiv), THF, -78°C , 30 min; 2. R-Br **12** (1.2 equiv) 3. ZnCl_2 (2.7 equiv), rt, 2 h; 4. LiCl (2.2 equiv), R-OTf **8** (1.0 equiv), Pd(PPh)_4 (3.5 mol%), reflux, 16 h, 55%.

Bipyridine **13** was then tagged with a PIB chain by deprotonation with lithium di/*iso*-propylamide followed by treatment with PIB-I (**5**) (Scheme 4). To achieve quaternization of the secondary benzylic position two more alkylations with methyl iodide were required. As it turned out during preliminary studies with 4-polyisobutylpyridine, LDA was not capable to deprotonate the secondary benzylic position in a clean fashion: a mixture of various products was obtained upon treatment with methyl iodide. The +I effect from the additional alkyl group in comparison to **13** presumably disfavors further deprotonation. Similar problems were encountered during the metalation of 2-isopropylpyridine by Rocca *et al.*¹²⁶ They conveniently solved the challenge by employment of a superbasic mixture of di/*iso*propylamine, potassium

tert-butylate, and $^n\text{BuLi}$. Indeed, usage of this superbases with methyl iodide two times in a row furnished target ligand PIB-dtb-bpy (**2**) in reasonable yield of 65% over two steps.

Scheme 4. Synthesis of PIB-dtb-bpy (**2**) through three subsequent alkylations.

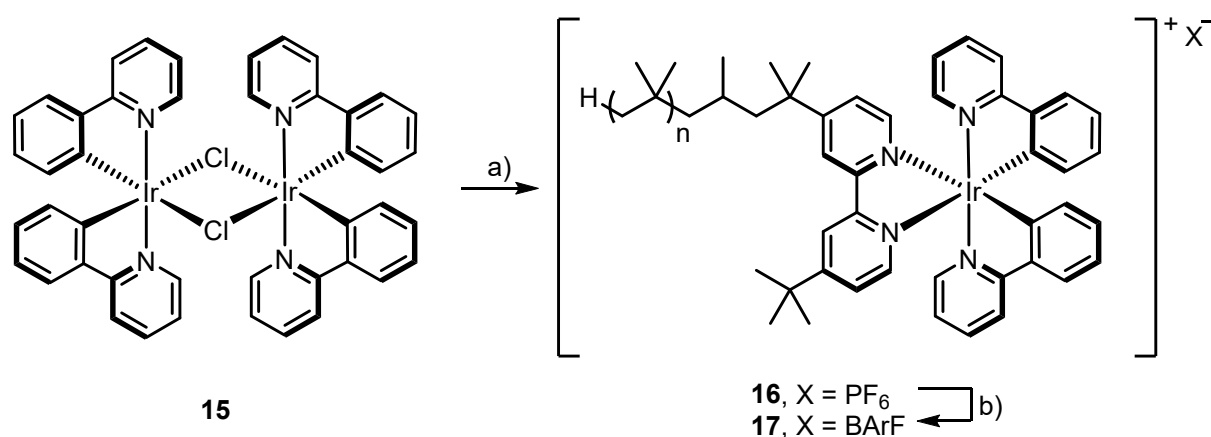


Reagents and conditions: a) 1. LDA (1.15 equiv), THF, $-78\text{ }^{\circ}\text{C}$ to $0\text{ }^{\circ}\text{C}$, 5 min; 2. PIB-I (**5**, 1.0 equiv), $-78\text{ }^{\circ}\text{C}$ to rt, on; b) 1. KO t Bu (14 equiv), $^i\text{Pr}_2\text{NH}$ (14 equiv), $^n\text{BuLi}$ (14 equiv), THF, $-78\text{ }^{\circ}\text{C}$ to $-50\text{ }^{\circ}\text{C}$, 30 min; 2. MeI (40 equiv), $-78\text{ }^{\circ}\text{C}$ to rt, on, two subsequent experiments, 65%.

2.3 Catalyst synthesis

The polyisobutylene-tagged ligand **2** was reacted with μ -chloro-bridged iridium dimer **15** to give $[\text{Ir}(\text{ppy})_2(\text{PIB-dtb-bpy})](\text{PF}_6)$ (**16**) in analogy to the synthesis of the unsubstituted complex $[\text{Ir}(\text{ppy})_2(\text{dtb-bpy})]^+$ (Scheme 5).¹²⁷ $[\text{Ir}(\text{ppy})_2(\text{PIB-dtb-bpy})](\text{PF}_6)$ (**16**) was soluble in both acetonitrile and heptane to the same extent. This is disadvantageous for the isolation in subsequent photoreactions: while on the one hand a certain residual solubility in acetonitrile of the polyisobutylene-tagged photocatalyst **16** was desired to be able to perform photoreactions in their original solvent, a too high solubility will drastically increase the number of extraction steps needed to recover the catalyst after the reaction. At a distribution coefficient K_D of 1, meaning that a compound dissolves equally between two solvents, five consecutive equivoluminal extraction steps are necessary to recover 95% of the compound. To lower the solubility in acetonitrile two approaches are conceivable: either redesign the catalyst core structure *e.g.* by introduction of a second polyisobutylene chain (*vide infra*) or more easily conducted by the exchange of the counter ion. Hexafluorophosphate which is already comparably nonpolar was therefore exchanged by the far less coordinating counterion tetrakis(3,5-bis(trifluoromethyl)phenyl)borate (BARF). Gratifyingly $[\text{Ir}(\text{ppy})_2(\text{PIB-dtb-bpy})](\text{BARF})$ (**17**) showed only very little solubility in acetonitrile. When **17** was partitioned between acetonitrile and heptane, no yellow color could be seen in the acetonitrile phase indicating that catalyst **17** can be easily recovered from a photoreaction performed in acetonitrile.

Scheme 5. Synthesis of $[\text{Ir}(\text{ppy})_2(\text{PIB-dtb-bpy})](\text{PF}_6)$ (**16**) and exchange of the counterion to BARF[−].

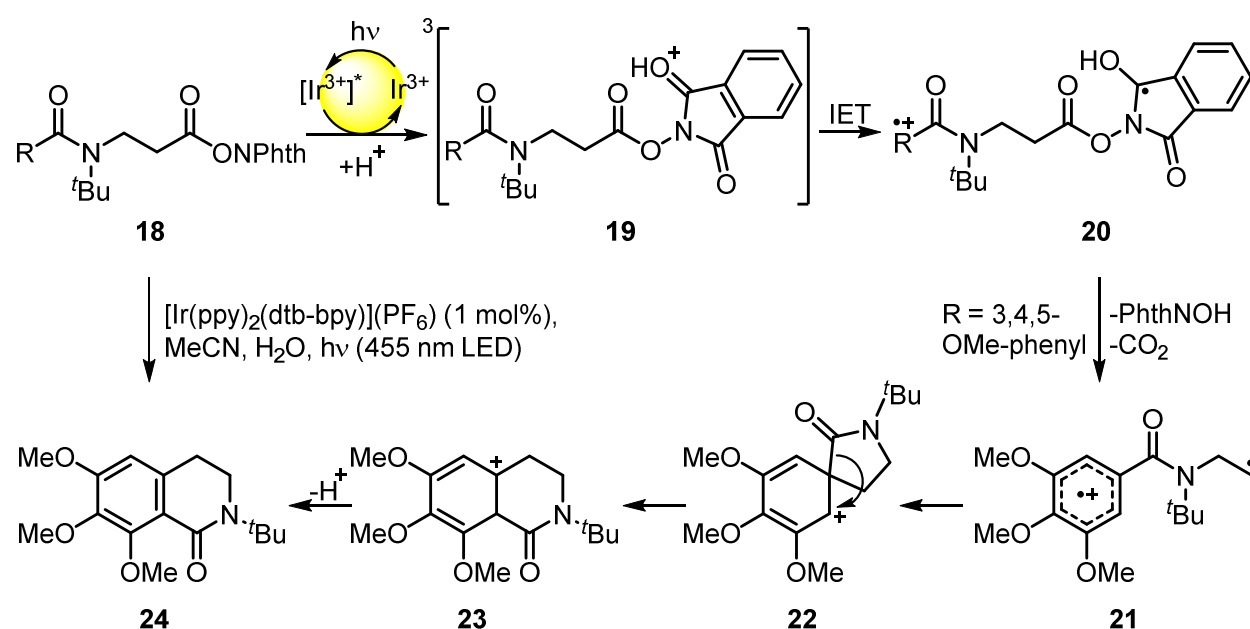


Reagents and conditions: a) 1. PIB-dtb-bpy (**2**, 2.1 equiv), ethylene glycol, 150 °C, 20 h 2. NH_4PF_6 (10 equiv), H_2O , rt, 15 min, 82% b) NaBARF (3.3 equiv), MeCN, rt, 30 min, 64%.

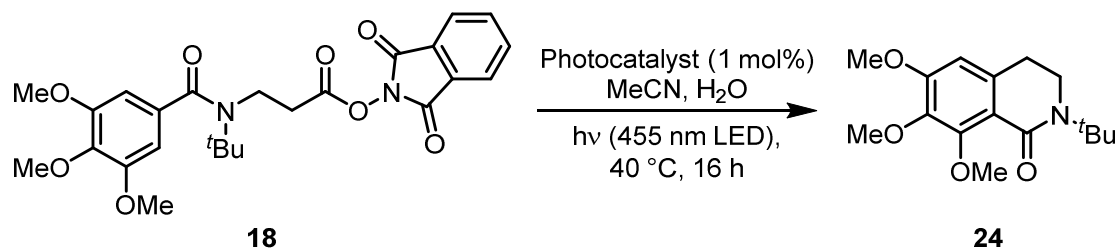
2.4 Application in photochemical reactions

As a test reaction for the applicability of $[\text{Ir}(\text{ppy})_2(\text{PIB-dtb-bpy})](\text{BARf})$ (**17**) a decarboxylative isoquinolinone synthesis developed by Christian Faderl was chosen. The proposed mechanism of this reaction is depicted in Scheme 6. Energy transfer from the excited photocatalyst $[\text{Ir}(\text{ppy})_2(\text{dtb-bpy})]^+$ to *N*-acyloxypthalimide **18** followed by protonation gives **19** in its triplet state. Intramolecular electron transfer (IET) from the electron rich aryl substituent to the electron deficient phthalimide moiety gives **20**. N–O bond mesolysis liberates *N*-hydroxypthalimide and furnishes a carboxyl radical that quickly decarboxylates to give the carbon-centered diradical cation **21**. Spirocyclization, bond migration, followed by deprotonation finally leads to isoquinolinone **24**.

Scheme 6. Proposed mechanism for the isoquinolinone synthesis developed by Christian Faderl.



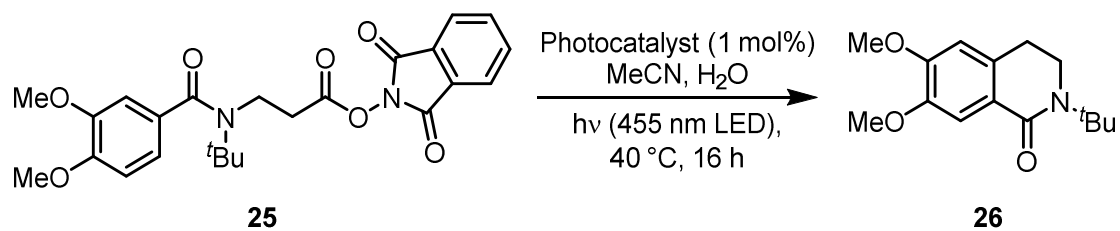
$[\text{Ir}(\text{ppy})_2(\text{PIB-dtb-bpy})](\text{BARf})$ (**17**) was well soluble in acetonitrile. However, when water was added which is needed for the protonation step, the reaction mixture seemed inhomogeneous. Performance of the reaction at slightly elevated temperatures of 40 °C led to a homogeneous reaction mixture and gave identical product yield as the original catalyst $[\text{Ir}(\text{ppy})_2(\text{dtb-bpy})](\text{PF}_6)$ (Table 1).

Table 1. Comparison of original photocatalyst [Ir(ppy)₂(dtb-bpy)](PF₆) and PIB-tagged derivative [Ir(ppy)₂(PIB-dtb-bpy)](BArF) (**17**) in the photochemical synthesis of isoquinolinone **24**.

Entry	Photocatalyst	Yield [%] ^a
1	[Ir(ppy) ₂ (dtb-bpy)](PF ₆)	66
2	[Ir(ppy) ₂ (PIB-dtb-bpy)](BArF) (17)	65

^aIsolated yield.

Having ensured that both catalysts give similar synthetical results, recycling of the PIB-tagged derivative **17** after successful reaction was investigated (Table 2). After full conversion of the starting material **25** as judged by TLC control, the reaction mixture was extracted once with heptane. While the heptane phase was evaporated and used in subsequent reaction runs without further treatment, product **26** could be isolated from the acetonitrile phase by column chromatography. The reaction time had to be slightly increased at the second run (entry 3) to achieve full conversion. This trend continued in the subsequent reaction runs: the reaction time needed to be prolonged each cycle. Nevertheless it was possible to obtain virtually identical isoquinolinone yields through the experiments. The evident decay of the catalytic activity can be attributed to both, incomplete catalyst recovery through extraction and catalyst decomposition. PIB-tagged bipyridine ligand **2** is potentially labile in the complex as it is only attached to the iridium center by coordinative bonds in comparison to the two other ligands which are held by a covalent iridium – carbon bond.⁹³ While the issue of incomplete catalyst recovery could be tackled by the introduction of either more or longer PIB chains into the catalyst structure, the labile nature of the bipyridine ligand is an inherent problem of the biscyclometalated iridium(III) complex class.

Table 2. Photochemical decarboxylation of **25** and recycling of [Ir(ppy)₂(PIB-dtb-bpy)](BArF) (**17**).

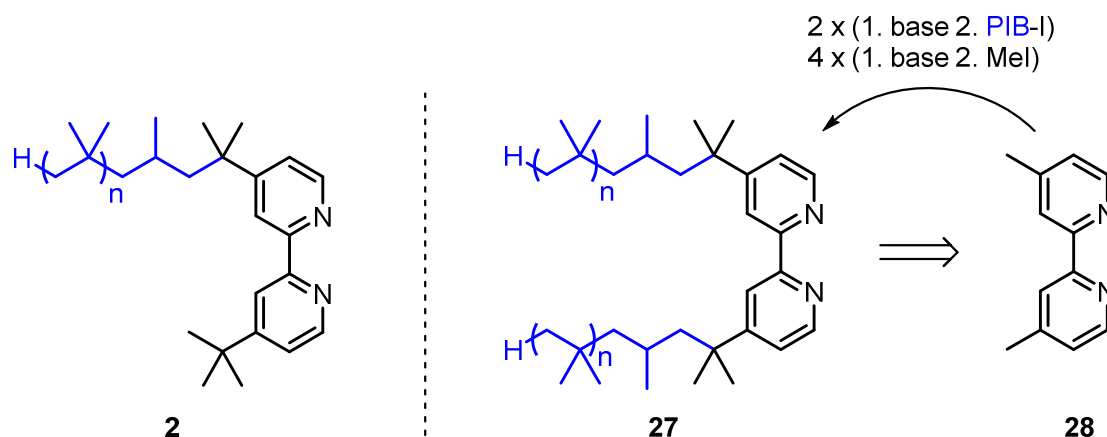
Entry	Photocatalyst	Run	Time [h] ^a	Yield [%] ^b
1	[Ir(ppy) ₂ (dtb-bpy)](PF ₆)	-	16	67
2	[Ir(ppy) ₂ (PIB-dtb-bpy)](BArF) (17)	1	16	64
3	[Ir(ppy) ₂ (PIB-dtb-bpy)](BArF) (17)	2	24	66
4	[Ir(ppy) ₂ (PIB-dtb-bpy)](BArF) (17)	3	40	62
5	[Ir(ppy) ₂ (PIB-dtb-bpy)](BArF) (17)	4	64	59
6	[Ir(ppy) ₂ (PIB-dtb-bpy)](BArF) (17)	5	96	61

^aIrradiation time till full consumption of starting material as judged by TLC control. ^bIsolated yield.

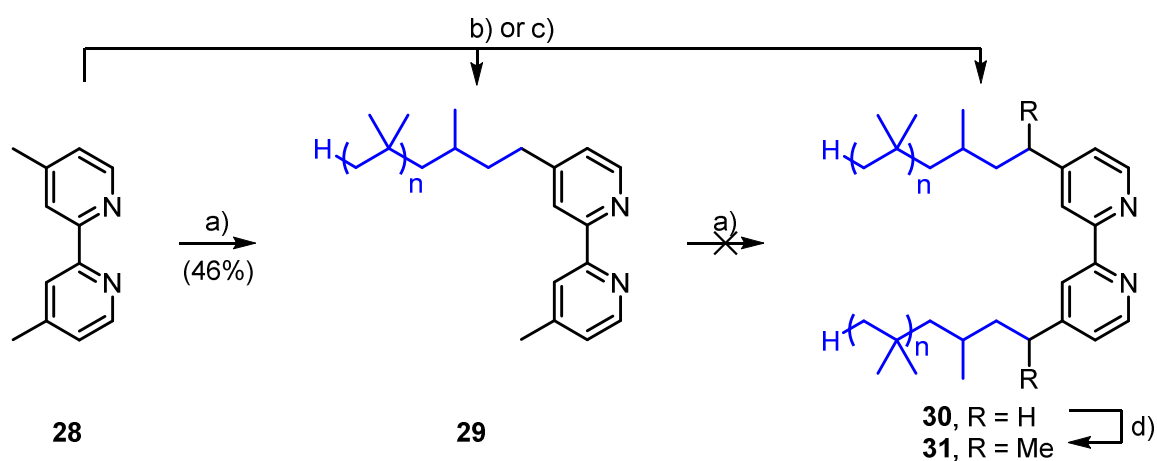
2.5 Streamlined ligand synthesis

To introduce more PIB-chains into the catalyst structure and thus facilitate its recovery the ligand synthesis was revised. Another aspect was to streamline the synthetic route: as much as seven linear steps (nine in total) were required for the synthesis of unsymmetrical PIB-tagged bipyridine ligand **2**. In comparison, a synthesis starting from commercially available 4,4'-dimethyl-2,2'-bipyridine (**28**) would only require six simple alkylation steps in total (Scheme 7).

Scheme 7. Unsymmetrical bipyridine ligand **2** in comparison to symmetrical ligand **27**.



Mono PIB-tagged bipyridine **29** could be synthesized in analogy to the previous introduction of the PIB chain through deprotonation with LDA and treatment with PIB-I (**5**) in moderate yield (Scheme 8). However, when **29** was subjected to identical reaction conditions only starting material and no bis-PIB-tagged **30** could be isolated. Interestingly, treatment of dimethylbipyridine **28** with superbasic KDA resulted not only in the formation of monoalkylation product **29** but also minor amounts of dialkylated bipyridine **30** were observed. Incensement of the stoichiometry of the base and the alkylation agent directly gave bis-PIB-tagged **30** in only one reaction step. Intrigued by the observation that two alkylation steps can be performed in one reaction, final ligand **27** should be possible to prepare in only 3 total steps from commercial **28**. Indeed, one step double methylation gave **31** in good yield, proving that this is a viable route to **28** and thus can give access to more hydrophobic biscyclometalated iridium(III) complexes. At this point it was nevertheless refrained from proceeding with the synthetic efforts in favor of triscyclometalated iridium(III) complexes as those complexes exhibit a higher photostability and are thus potentially more suitable for recycling purposes.

Scheme 8. Synthesis of symmetrical PIB-tagged bipyridine ligands **30** and **31**.

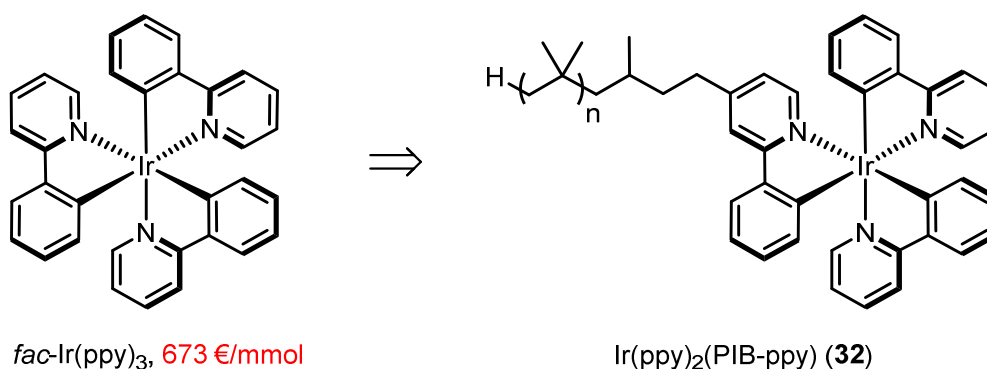
Reagents and conditions: a) 1. LDA (1.6 equiv), THF, -78 °C to rt, 5 min; 2. PIB-I (**5**, 1.0 equiv), PE, 0 °C to rt, 2 d; b) 1. KO^tBu (1.3 equiv), ⁱPr₂NH (1.3 equiv), ⁿBuLi (1.3 equiv), THF, -78 °C to -50 °C, 30 min; 2. PIB-I (**5**, 1.3 equiv), -78 °C to rt, on, 22% **29**, 7% **30**; c) 1. KO^tBu (3.0 equiv), ⁱPr₂NH (3.0 equiv), ⁿBuLi (3.0 equiv), THF, -78 °C to -50 °C, 30 min; 2. PIB-I (**5**, 3.0 equiv), -78 °C to rt, on, 45% **30**; d) 1. KO^tBu (14 equiv), ⁱPr₂NH (14 equiv), ⁿBuLi (14 equiv), THF, -78 °C to -50 °C, 30 min; 2. MeI (40 equiv), -78 °C to rt, on, 71%

3 Tris-Cyclometalated Iridium(III) Complexes

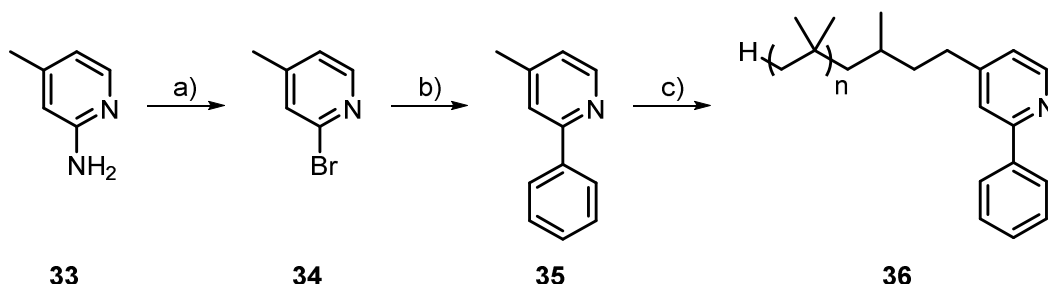
3.1 Preliminary studies

The most prominent tris cyclometalated iridium(III) complex in photoredox chemistry is by far *fac*-Ir(ppy)₃. More and more studies are published making use of its very high reduction potential *e.g.* in the direct arylation of sp³ C–H bonds,¹²⁸ trifluoromethylation of alkynes,¹²⁹ or decarboxylative coupling reactions.¹³⁰ To obtain a recyclable derivative of *fac*-Ir(ppy)₃ the same strategy was applied as with earlier investigations with biscyclometalated iridium(III) complex [Ir(ppy)₂(PIB-dtb-bpy)]⁺(BArF)[–] (**17**), namely the introduction of a polyisobutylene chain as a nonpolar, homogeneously soluble polymeric support.

Scheme 9. Triscyclometalated iridium(III) complex *fac*-Ir(ppy)₃ with its PIB-tagged counterpart **32**.⁹⁹

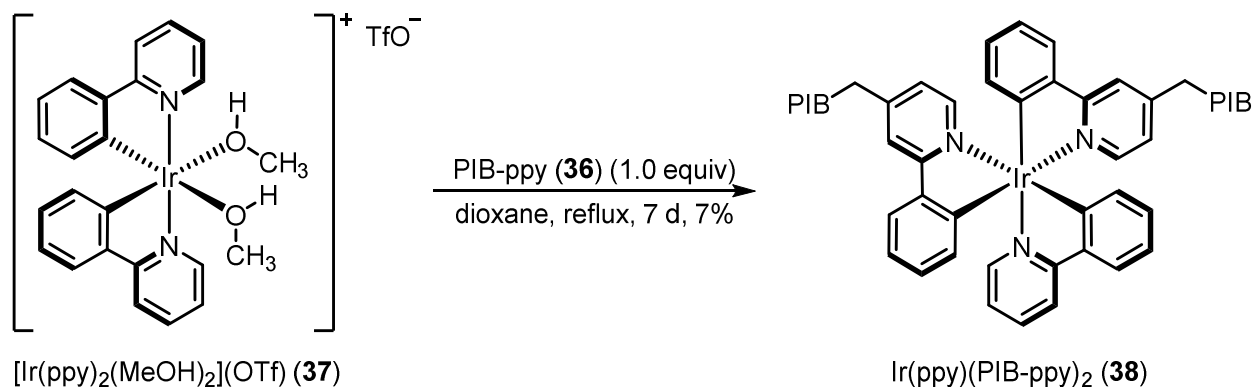


The initial synthesis route for **32** relied on the polyisobutylene tagged 2-phenylpyridine ligand **36**. Its synthesis was accomplished in good yield by preparation of literature-known 4-methyl-2-phenylpyridine (**33**) *via* a Suzuki coupling followed by alkylation with PIB-I (**5**) (Scheme 10).¹³¹

Scheme 10. Synthesis of PIB-tagged 2-phenylpyridine ligand **36**.

Reagents and conditions: a) 1. HBr (4.8 equiv), rt; 2. Br₂ (2.8 equiv), -20 °C, 90 min; 3. NaNO₂ (2.7 equiv), H₂O, -20 °C to rt, 2 h; 4. NaOH (18 equiv), H₂O, -20 °C to rt, 1 h, 61%; b) PhB(OH)₂ (1.5 equiv), Pd(OAc)₂ (1.5 mol%), K₂CO₃ (2.0 equiv), H₂O, EtOH, 80 °C, 18 h, 77%; c) 1. LDA (1.1 equiv), THF, -78 °C, 30 min; 2. PIB-I (**5**, 0.95 equiv), hexanes, -78 °C to rt, on, 83%.

Reaction of PIB-tagged 2-phenylpyridine ligand **36** with literature-known precursor **37** for the formation of triscyclometalated iridium(III) complex however gave none of the desired complex **32** (Scheme 11). Another complex **38** was instead isolated in poor yield after the reaction mixture was reflux for prolonged times. This complex stems from a formal double substitution with PIB-tagged 2-phenylpyridine ligand **36**.^{****} Efforts to optimize this synthesis were fruitless: neither adjustment of the reagent stoichiometry, microwave irradiation, nor addition of amine base to facilitate the C–H bond cleavage yielded **38** (or the initially desired Ir(ppy)₂(PIB-ppy) (**32**)), only inseparable mixtures were obtained.

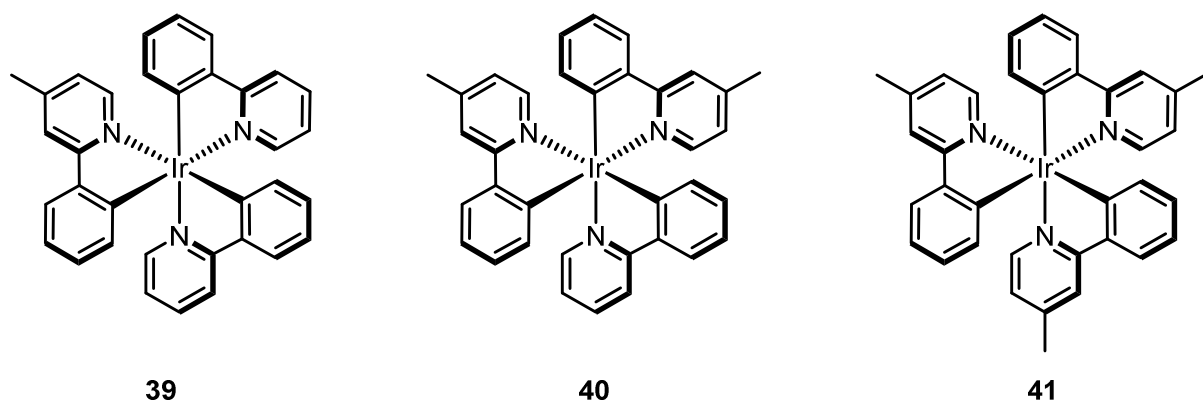
Scheme 11. Synthesis of double substituted photocatalyst Ir(ppy)(PIB-ppy)₂ (**38**).

^{****}Ir(ppy)(PIB-ppy)₂ (**38**) was investigated in the Bachelor theses of Alexander Wimmer and Markus Tautz. It successfully performed as visible light photoredox catalyst in deiodation reactions. Facile recycling was possible after at least three consecutive reaction runs without diminished product yields.

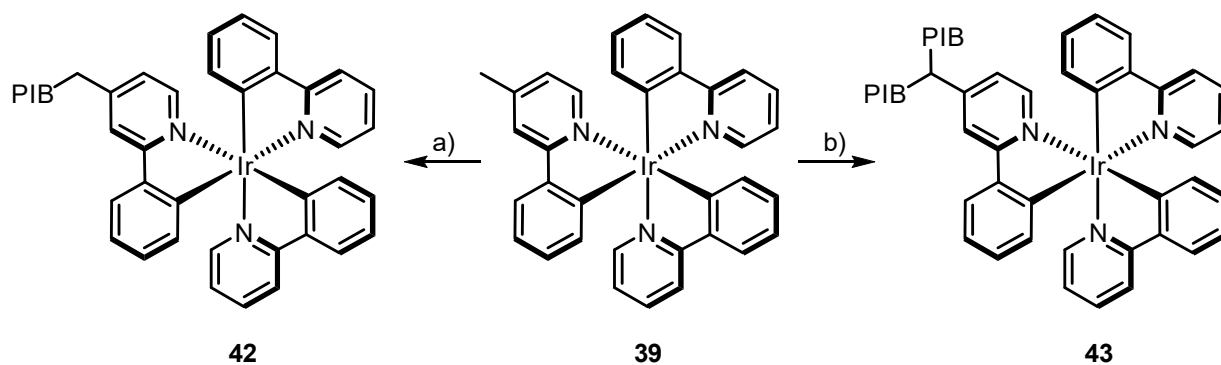
3.2 On-complex modifications

As the complexation of precursor **37** with the PIB-tagged 2-phenylpyridine ligand **36** failed to give the desired triscyclometalated iridium(III) complex **32**, the synthetic strategy was revised. Instead of preassembly of the tagged ligand followed by formation of a triscyclometalated iridium(III) complex the order of steps was inverted: first methyl-substituted tris 2-phenylpyridyl iridium(III) complexes **39** – **41** were synthesized and then tagged with a PIB chain on-complex (Figure 2).

Figure 2. Prepared triscyclometalated iridium(III) complex **39** – **41** for alkylation reactions.

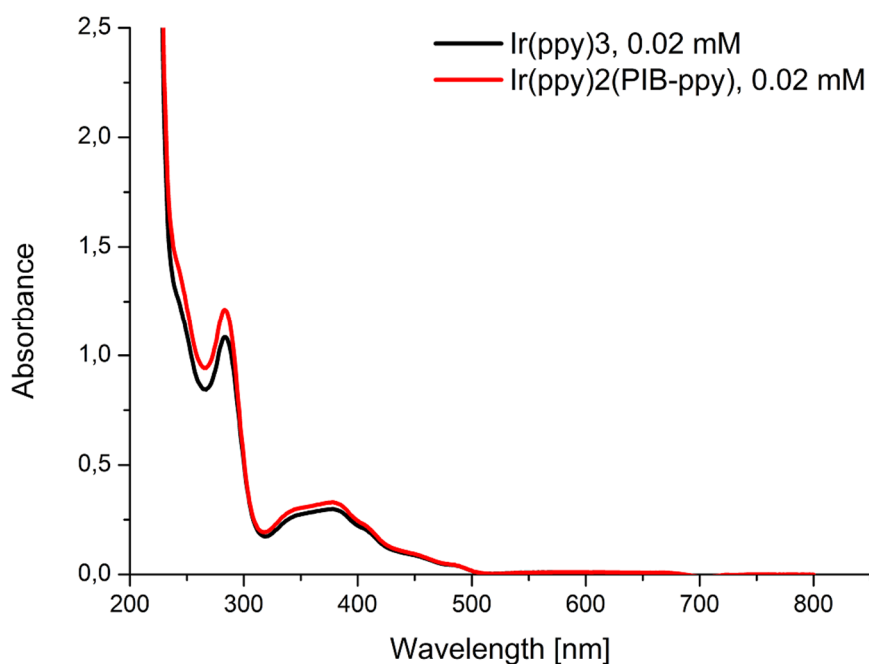


Polyisobutylene-tagging of all compounds was possible by using LDA as metalation agent and PIB-I (**5**) as alkylation reagent. With bi- and tri-methyl substituted complexes **40** and **41** unselective polyfunctionalization was observed that led to hardly separable mixtures. However, poly-PIB-tagged derivatives of **40** and **41** could in theory also be used as photocatalyst as shown by Bergbreiter who also employed unspecified poly-PIB-tagged $[\text{Ru}(\text{bpy})_3]^{2+}$ derivatives in catalysis.⁹⁷ To get a more defined catalyst structure synthetic efforts were directed to the selective alkylation of mono-methyl substituted $\text{Ir}(\text{ppy})_2(4\text{-Me-ppy})$ (**39**). Optimized reaction conditions to either obtain single or dual PIB-tagging are depicted in Scheme 12. Since the tertiary, benzylic position in $\text{Ir}(\text{ppy})_2(\text{PIB}_2\text{-ppy})$ (**43**) might have adversary properties due to the potentially very activated C–H bond, following investigations were focused on the mono-alkylated $\text{Ir}(\text{ppy})_2(\text{PIB-ppy})$ (**42**).

Scheme 12. Optimized procedures to obtain either Ir(ppy)₂(PIB-ppy) (**42**) or Ir(ppy)₂(PIB₂-ppy) (**43**).

Reagents and conditions: a) 1. LDA (1.3 equiv), THF, -78 °C, 15 min; 2. PIB-I (**5**, 1.4 equiv), hexanes, -78 °C to rt, on, 54%; b) 1. LDA (14 equiv), THF, -78 °C, 15 min; 2. PIB-I (**5**, 15 equiv), hexanes, -78 °C to rt, on, 84%.

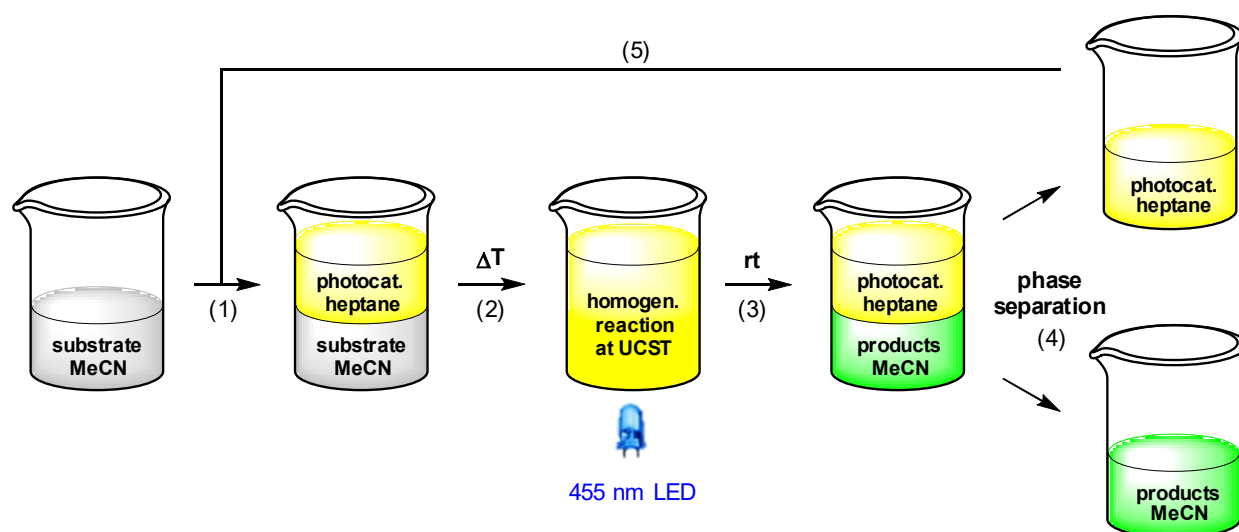
Polymer-bound Ir(ppy)₂(PIB-ppy) (**42**) exhibits an almost identical UV-Vis spectrum as its parent complex *fac*-Ir(ppy)₃ (Figure 3). Photochemical reactions can therefore be carried out without the need of adjusting the excitation wavelength.

Figure 3. Comparison of the UV-Vis absorption spectra of *fac*-Ir(ppy)₃ with Ir(ppy)₂(PIB-ppy) (**42**).

3.3 Recycling strategy

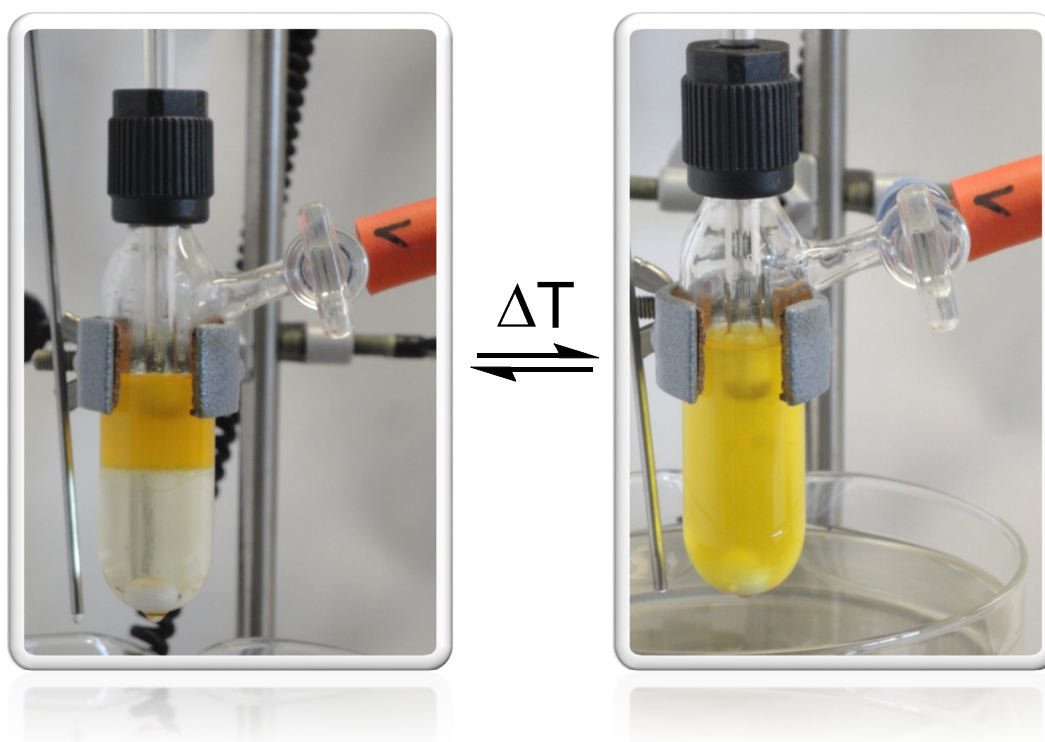
It was planned to perform photochemical reactions under their originally published conditions and recover PIB-tagged catalyst **42** by a subsequent liquid / liquid extraction with heptane (as earlier with $[\text{Ir}(\text{ppy})_2(\text{PIB-dtb-bpy})]^+(\text{BArF})^-$ (**17**)). Typical solvents for photochemical transformations with *fac*- $\text{Ir}(\text{ppy})_3$ are DMF and acetonitrile. As it turned out $\text{Ir}(\text{ppy})_2(\text{PIB-ppy})$ (**42**) is soluble in neither, even at elevated temperatures. This solubility profile appeared to be ideal to carry out homogenous photo-chemical transformations using a thermomorphic solvent system (TMS).^{98,132,133} Such a system comprises of a polar solvent that has a huge miscibility gap with a nonpolar solvent. At elevated temperatures the miscibility gap disappears and the former biphasic system becomes homogeneous. After cooling the former two phases reappear, making the process fully reversible. Acetonitrile and heptane form such a TMS with an upper critical solution temperature (UCST), the temperature where full miscibility is achieved, of 84.6 °C.¹³⁴ Thus, for the photochemical reactions investigated, substrates and reagents were dissolved in acetonitrile at room temperature and heptane, containing catalyst **42**, was added (Scheme 13, (1)), forming a biphasic solution. Heating the reaction mixture to 85 °C led to a homogeneous mixture which was then irradiated with blue LED light (455 nm) until the transformation was completed (2). Cooling to room temperature (3) and phase separation (4) gave back an acetonitrile phase containing the photochemical products and a heptane phase with catalyst $\text{Ir}(\text{ppy})_2(\text{PIB-ppy})$ (**42**) that could be added to the next reaction run (5).

Scheme 13. Photoreactions with $\text{Ir}(\text{ppy})_2(\text{PIB-ppy})$ (**42**) in a thermomorphic solvent system consisting of acetonitrile and heptane.



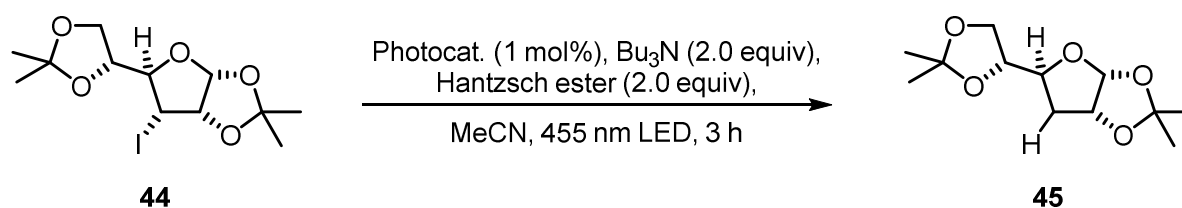
A photographic representation of this recycling process is shown in Figure 4. Polyisobutylene-tagged photocatalyst $\text{Ir}(\text{ppy})_2(\text{PIB-ppy})$ (**42**) is exclusively dissolved in the upper heptane phase as can be seen due to its typical yellow color (left picture). After the reaction mixture was heated in an oil bath to 85 °C the former biphasic mixture became homogeneous (right picture). This process is fully reversible. The depicted reaction vessels are the actual Schlenk tubes with a glass rod as light transmitter that were employed for the synthetic reactions.

Figure 4. Photocatalyst $\text{Ir}(\text{ppy})_2(\text{PIB-ppy})$ (**42**) in a mixture of heptane and acetonitrile at room temperature and after heating to 85 °C in an oil bath.



3.4 Application in photochemical batch reactions

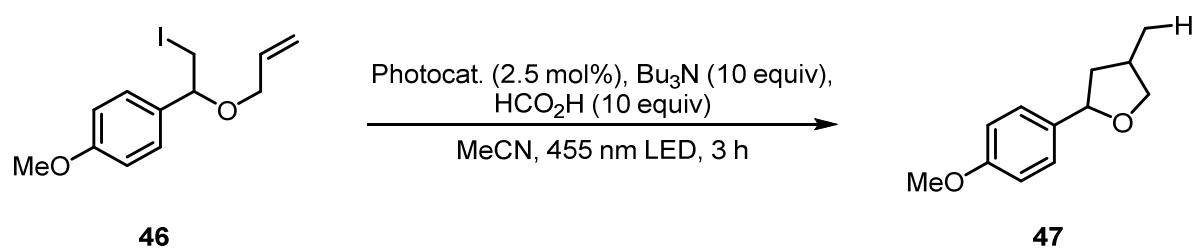
To demonstrate the feasibility of above mentioned concept, polyisobutylene-tagged Ir(ppy)₂(PIB-ppy) (**42**) was applied to a photochemical deiodation reaction of **44** developed by Stephenson *et al.* (Table 3, entry 1).²⁹ Using a mixture of acetonitrile and heptane at 85 °C instead of acetonitrile at room temperature had little influence on the reaction outcome (entry 2). Polymer-supported Ir(ppy)₂(PIB-ppy) (**42**) was able to catalyze the reaction of **44** (entry 3). The catalyst was recycled as described above and resubjected to a new reaction run. In the next run an increase of product yield from 78 to 96% was observed (entry 4). This rise can be explained by the residual solubility of product **45** in the heptane phase after performed photoreaction. As the heptane phase is then added to the next reaction run, also partially extracted product from the last reaction run is added, leading to a steady state of extracted and added product after the second catalyst run. The catalyst containing heptane phase was thoroughly extracted with additional acetonitrile after all recycling runs, giving 12% of **45** (relative to one run). This corresponds to the amount of extracted product after the first recycling run (entry 3). In the following runs deiodation yield stayed constantly high and it was possible to perform the reaction for at least 10 times with the same batch of catalyst without an evident decline in efficiency (entry 4 – 12).

Table 3. Deiodation of **44** with recyclable Ir(ppy)₂(PIB-ppy) (**42**).

Entry	Catalyst	Conditions	Run	Yield [%] ^a
1	<i>fac</i> -Ir(ppy) ₃	MeCN, room temperature ²⁹	-	60 ^b , 83 ^c
2	<i>fac</i> -Ir(ppy) ₃	MeCN/heptane at 85 °C	-	73
3	Ir(ppy) ₂ (PIB-ppy) (42)	MeCN/heptane at 85 °C	1	78+12 ^d
4	Ir(ppy) ₂ (PIB-ppy) (42)	MeCN/heptane at 85 °C	2	96
5	Ir(ppy) ₂ (PIB-ppy) (42)	MeCN/heptane at 85 °C	3	88
6	Ir(ppy) ₂ (PIB-ppy) (42)	MeCN/heptane at 85 °C	4	90
7	Ir(ppy) ₂ (PIB-ppy) (42)	MeCN/heptane at 85 °C	5	86
8	Ir(ppy) ₂ (PIB-ppy) (42)	MeCN/heptane at 85 °C	6	94
9	Ir(ppy) ₂ (PIB-ppy) (42)	MeCN/heptane at 85 °C	7	94
10	Ir(ppy) ₂ (PIB-ppy) (42)	MeCN/heptane at 85 °C	8	90
11	Ir(ppy) ₂ (PIB-ppy) (42)	MeCN/heptane at 85 °C	9	87
12	Ir(ppy) ₂ (PIB-ppy) (42)	MeCN/heptane at 85 °C	10	92

^aDetermined by GC-FID with diphenylmethane as internal standard. ^bIsolated yield. ^cPublished product yield.²⁹ ^dAdditional amount of product extracted from heptane phase after all catalysis runs.

In addition to a simple deiodation, also the catalytic performance and recycling capabilities of Ir(ppy)₂(PIB-ppy) (**42**) in the deiodation/cyclization of **46** were examined (Table 4).²⁹ Also here the reusable catalyst variant **42** gave excellent results (entry 3 – 12). The amount of extracted cyclization product **47** is higher due to its less polar nature, nevertheless the recycling behavior of **42** was not impaired.

Table 4. Deiodination/cyclization of **46** with reusable Ir(ppy)₂(PIB-ppy) (**42**).

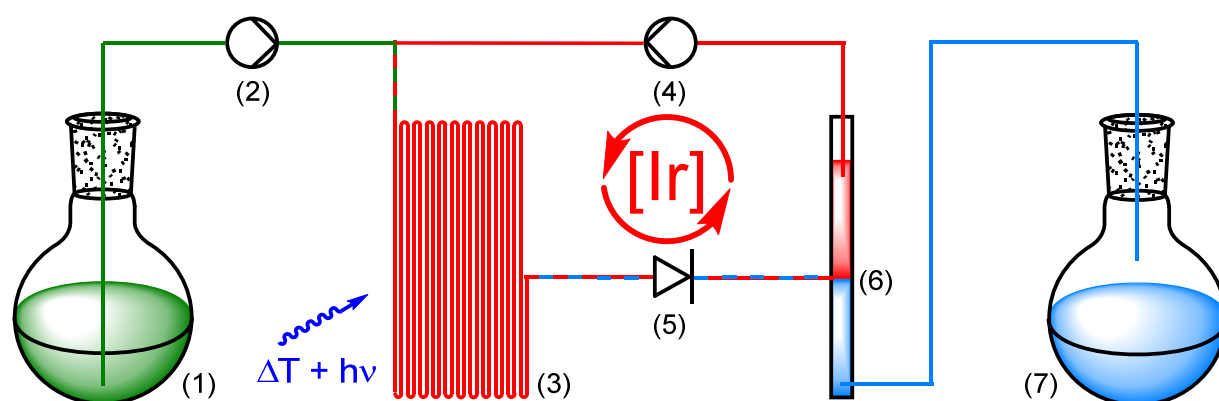
Entry	Catalyst	Conditions	Run	Yield [%] ^a
1	<i>fac</i> -Ir(ppy) ₃	MeCN, room temperature ²⁹	-	57 ^b
2	<i>fac</i> -Ir(ppy) ₃	MeCN/heptane at 85 °C	-	37
3	Ir(ppy) ₂ (PIB-ppy) (42)	MeCN/heptane at 85 °C	1	47+17 ^c
4	Ir(ppy) ₂ (PIB-ppy) (42)	MeCN/heptane at 85 °C	2	67
5	Ir(ppy) ₂ (PIB-ppy) (42)	MeCN/heptane at 85 °C	3	60
6	Ir(ppy) ₂ (PIB-ppy) (42)	MeCN/heptane at 85 °C	4	64
7	Ir(ppy) ₂ (PIB-ppy) (42)	MeCN/heptane at 85 °C	5	68
8	Ir(ppy) ₂ (PIB-ppy) (42)	MeCN/heptane at 85 °C	6	74
9	Ir(ppy) ₂ (PIB-ppy) (42)	MeCN/heptane at 85 °C	7	74
10	Ir(ppy) ₂ (PIB-ppy) (42)	MeCN/heptane at 85 °C	8	76
11	Ir(ppy) ₂ (PIB-ppy) (42)	MeCN/heptane at 85 °C	9	63
12	Ir(ppy) ₂ (PIB-ppy) (42)	MeCN/heptane at 85 °C	10	66

^aDetermined by GC-FID with diphenylmethane as internal standard. ^bIsolated yield. ^cPublished product yield.²⁹ ^dAdditional amount of product extracted from heptane phase after all catalysis runs.

3.5 Setup for photoreaction in continuous flow

Encouraged by the outstanding catalytic performance and excellent recyclability of PIB-tagged **42** in previous batch reactions, a continuously operating process in which the catalyst is constantly recycled and reused was envisioned. For hydroformylations conceptually related flow systems with continuous catalyst recycling have already been developed.^{135–137} In those studies a polar rhodium catalyst is retained in a DMF phase while the product (long-chained aldehydes) dissolves in decane. For this study photochemical transformations in a thermomorphic solvent system were ran in a transparent, heatable micro reactor that enable visible light irradiation of the reaction mixture while it is homogeneous (Scheme 14).^{†††,138} Substrate and reagents dissolved in acetonitrile (1) are pumped (2) into a microreactor (3) along with a solution of Ir(ppy)₂(PIB-ppy) (**42**) in heptane (4). Through heating to 90 °C the biphasic system becomes a homogeneous solution which is then irradiated with visible light. A throttle valve (5) ensures that the solvents are not boiling. After the photoreaction is completed the mixture reaches a cooled phase separator unit (6). While the catalyst containing phase is recycled (4), the product-containing acetonitrile is collected (7).

Scheme 14. Continuously operating, catalyst recycling, photoreaction setup.



An actual representation of the setup is depicted in Figure 5 (upper part). The assigned numbers to each element are identical to the schematic representation in Scheme 14. In the lower part of Figure 5 the pump unit for the photocatalyst solution (4), the tubing connecting to the reactor (3), and the phase separatory unit (6) are detailed.

^{†††} The reaction setup was designed and set up with the help of Dr. Peter Kreitmeier.

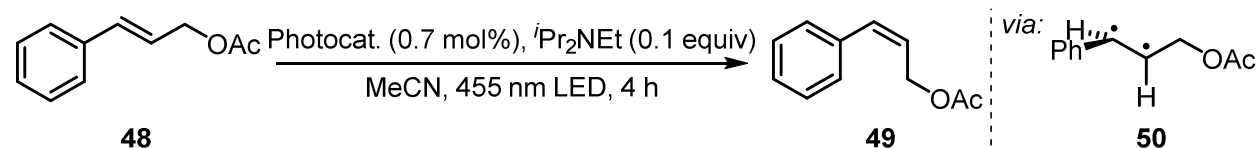
Figure 5. Upper part: setup overview. Lower part: detailed photographs of selected components.



3.6 Application in photochemical flow reactions

This flow setup was applied in the photochemical generation of *Z*-alkenes from readily available *E*-alkenes through uphill catalysis as demonstrated by Weaver *et al.*¹³⁹ The double bond in **48** is presumably broken through energy transfer from the excited photocatalyst forming a biradical species **50** that rapidly undergoes intersystem crossing to give the isomerized compound **49** (Table 5). Control experiments in a batch process showed that this reaction can be carried out at elevated temperatures without a detrimental effect on the *E/Z* ratio (entry 2). Also, neither a switch of solvent to a acetonitrile / heptane mixture nor the employment of Ir(ppy)₂(PIB-ppy) (**3**) deteriorated the reaction outcome (entry 3), prompting us to set up this reaction in a continuous process.

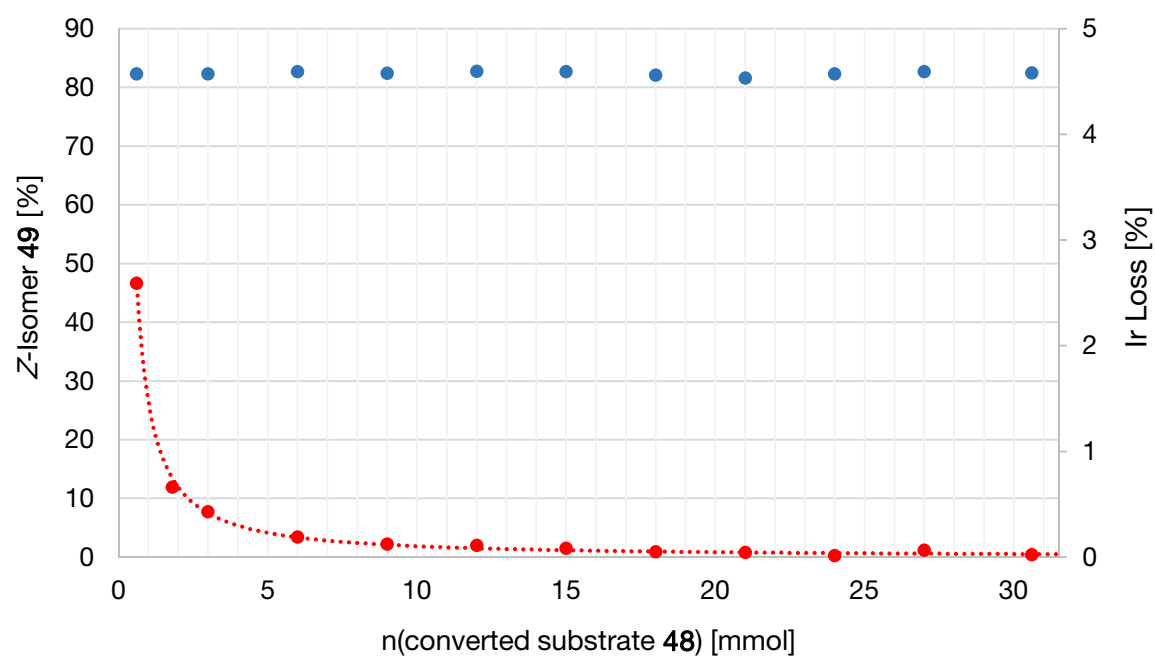
Table 5. Test reactions towards the *E/Z* isomerization in a continuous process.



Entry	Catalyst	Conditions	<i>Z/E</i> ratio ^a
1	<i>fac</i> -Ir(ppy) ₃	MeCN, room temp.	82:18
2	<i>fac</i> -Ir(ppy) ₃	MeCN, 90 °C	82:18
3	Ir(ppy) ₂ (PIB-ppy) (42)	MeCN/heptane, 90 °C	82:18

^aRatio determined by ¹H-NMR / GC-FID integration of the crude reaction mixture.

The results of the isomerization of **48** in a flow process with continuous catalyst recycling are depicted in Figure 6. As can be seen the *Z/E* ratio remains at constant high levels throughout the whole reaction process. The amount of catalyst employed corresponds to the amount used in a 1 mmol batch reaction setup,¹³⁹ demonstrating that this setup can effectively decrease the catalyst loading by a factor of at least 30. Catalyst leaching is comparably high at the beginning of the reaction with 2.6% of the totally employed iridium lost relative to the first mmol of converted substrate **48** as determined by ICP-OES. Gratifyingly, the iridium loss severely declines in course of the further reaction, reaching levels well below 0.1% iridium lost per mmol of converted substrate **49**. ¹H-NMR analysis performed for the catalyst after the reaction suggests that mainly catalyst molecules that were connected to shorter PIB chains, i.e. having higher polarity, were lost.

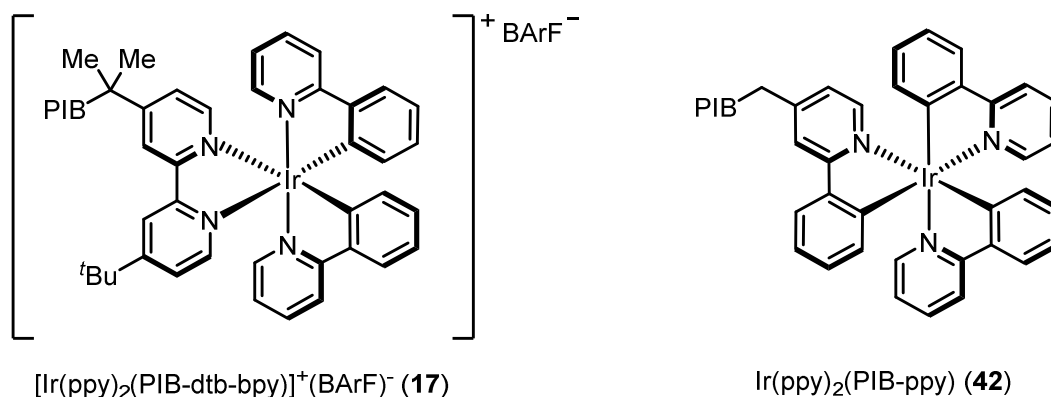
Figure 6. Photochemical E/Z isomerization in a flow process with continuous catalyst recycling.

Z-isomer ratio depicted in blue (determined by GC-FID), iridium content lost normalized for 1 mmol substrate depicted in red (determined by ICP-OES). Reaction parameters: 30 mmol *E*-alkene **48** (1.0 equiv), 3 mmol Pr_2NEt (0.1 equiv), 7 μmol $\text{Ir}(\text{ppy})_2(\text{PIB}_2\text{-ppy})$ (**42**) (0.023 mol%), MeCN, heptane, 90 °C, flowrate 20 μmol **48**/min.

4 Conclusion and Outlook

Two polyisobutylene-tagged photocatalyst were synthesized and applied to photocatalytic reactions (Figure 7). Their catalytic performance is in no way inferior to their parent complexes while they could be successfully recovered and reused after performed photo reactions.

Figure 7. Synthesized and applied PIB-tagged photocatalysts **17** and **42**.



Especially $\text{Ir}(\text{ppy})_2(\text{PIB-ppy})$ (**42**) showed excellent catalytic performance as well as recyclability in batch and in flow reactions. A process could be developed where the photocatalyst **42** was constantly recycled, allowing to use drastically lower amounts of high priced iridium compared to the batch process. Catalyst **42** therefore provides an alternative to *fac*- $\text{Ir}(\text{ppy})_3$ when large-scale reaction setups are required.

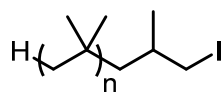
Not only is an easy catalyst recovery conceivable using $\text{Ir}(\text{ppy})_2(\text{PIB-ppy})$ (**42**) but through its solubility profile also other applications are conceivable. It might find use as bi-phasic catalyst in photochemical reactions when during the reaction highly colored compounds i.e. light absorbing molecules are generated that would impede further excitation of the photocatalyst. Those molecules might be either unwanted decomposition products or the actual generated photoproduct. By having the PIB-tagged photocatalysts in another phase than the reagents and colored products excitation of the photocatalyst and thus further reaction progress might still be available. Investigations in this regard are currently underway by Thomas Föll and Santosh Pagire within the Reiser group.

5 Experimental Part

5.1 General information

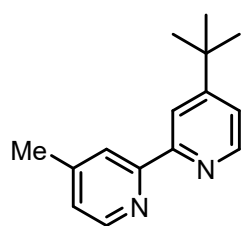
All chemicals were used as received or purified according to Purification of Common Laboratory Chemicals if necessary.¹⁴⁰ Glassware was dried in an oven at 110 °C or flame dried and cooled under a dry atmosphere prior to use. All reactions were performed using Schlenk techniques. The blue light irradiation in batch processes was performed using a CREE XLamp XP-E D5-15 LED (λ = 450-465 nm). In micro reactor processes 8 OSRAM OSOLON Black Series LD H9GP LEDs (λ = 455 \pm 10 nm) were employed. Analytical thin layer chromatography was performed on Merck TLC aluminium sheets silica gel 60 F 254. Reactions were monitored by TLC and visualized by a short wave UV lamp and stained with a solution of potassium permanganate, p-anisaldehyde, or Seebach's stain. Flash column chromatography was performed using Merck flash silica gel 60 (0.040-0.063 mm). The melting points were measured on a Büchi SMP-20 apparatus in a silicon oil bath. Values thus obtained were not corrected. ATR-IR spectroscopy was carried out on a Biorad Excalibur FTS 3000 spectrometer, equipped with a Specac Golden Gate Diamond Single Reflection ATR-System. NMR spectra were recorded on Bruker Avance 300 and Bruker Avance 400 spectrometers. Chemical shifts for ^1H NMR were reported as δ , parts per million, relative to the signal of CHCl_3 at 7.26 ppm. Chemical shifts for ^{13}C NMR were reported as δ , parts per million, relative to the center line signal of the CDCl_3 triplet at 77 ppm. Coupling constants J are given in Hertz (Hz). The following notations indicate the multiplicity of the signals: s = singlet, brs = broad singlet, d = doublet, t = triplet, q = quartet, quint = quintet, sept = septet, and m = multiplet. Mass spectra were recorded at the Central Analytical Laboratory at the Department of Chemistry of the University of Regensburg on a Varian MAT 311A, Finnigan MAT 95, Thermoquest Finnigan TSQ 7000 or Agilent Technologies 6540 UHD Accurate-Mass Q-TOF LC/MS. Gas chromatographic analyses were performed on a Fisons Instruments gas chromatograph equipped with a capillary column (30 m \times 250 μm \times 0.25 μm) and a flame ionisation detector. The yields reported are referred to the isolated compounds unless otherwise stated.

5.2 Synthesis of biscyclometalated iridium(III) complexes



Polyisobutylene iodide (5).

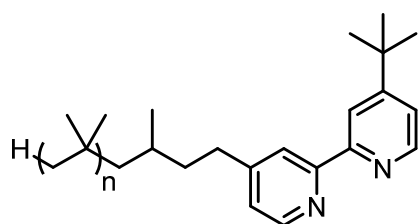
In a 2 L Schlenk flask polyisobutylene hydroxide¹²⁰ (102 g, 100 mmol, 1.00 equiv) was dissolved in 1.00 L DCM and the mixture was cooled to 0 °C. Et₃N (46.0 mL, 33.4 g, 330 mmol, 3.30 equiv) followed by MeSO₂Cl (23.2 mL, 33.4 g, 300 mmol, 3.00 equiv) were added dropwise over 15 min each. The reaction mixture was stirred for 6 h at room temperature after which the solvent was evaporated under reduced pressure and the residue was redissolved in mixture of 750 mL hexanes and 750 mL acetone. LiI (134 g, 1.00 mol, 10.0 equiv) was added and the suspension was refluxed for 7 d. After cooling, reaction mixture was transferred to a separatory flask with the help of 1.5 L of hexanes, the lower acetone phase was discarded and the upper hexanes phase was washed with 1.0 L water, 2x 200 mL DMF, 2x 500 mL water, and dried over Na₂SO₄. The solvent was evaporated under reduced pressure to give 86.0 g (76.2 mmol, 76.2%) of polyisobutylene iodide (5) as a viscous, colorless oil. IR (neat): 2949, 2893, 1470, 1389, 1365, 1230, 952, 921 cm⁻¹; ¹H NMR (300 MHz, CDCl₃): 3.21 (dd, *J* = 9.4, 4.3 Hz, 1H), 3.07 (dd, *J* = 9.4, 6.7 Hz, 1H), 1.45 – 0.90 (m, PIB, 190H); ¹³C NMR (75 MHz, CDCl₃): 60 – 56 (multiple PIB peaks), 52.66 (PIB-CH₂CH(CH₃)CH₂-I), 39 – 29 (multiple PIB peaks), 23.93 (PIB-CH₂CH(CH₃)CH₂-I), 20.97 (PIB-CH₂CH(CH₃)CH₂-I).



4-(*tert*-butyl)-4'-methyl-2,2'-bipyridine (13).¹²⁵

To 20 mL THF in a 100 mL Schlenk flask at -78 °C was added ^tBuLi (1.6 M in hexane, 8.3 mL, 13 mmol, 2.4 equiv) followed by dropwise addition of 2-bromo-4-(*tert*-butyl)pyridine¹²⁴ (1.42 g, 6.64 mmol, 1.20 equiv). The reaction mixture turned dark red / brown while it was stirred at -78 °C for 30 min. Dried ZnCl₂ (2.04 g, 14.9 mmol, 2.70 equiv) was added and the suspension was stirred for 2 h at room temperature after which 4-methylpyridin-2-yl trifluoromethanesulfonate¹²⁵ (1.34 g, 5.53 mmol, 1.00 equiv), dried LiCl (516 mg, 12.2 mmol, 2.20 equiv), and solution of Pd(PPh₃)₄ [prepared by stirring Pd₂(dba)₃ (177 mg, 193 μmol, 3.5 mol%) and PPh₃ (406 mg, 1.55 mmol, 28.0 mol%) in 5 mL THF for 1 h] was added. The resulting mixture turned yellow while it was refluxed for 16 h. After cooling, the mixture was treated with a solution of 18 g Na₂H₂EDTA in 150 mL water and stirred for 5 min. The pH was adjusted to 9 with the help of sat NaHCO₃ (aq) and

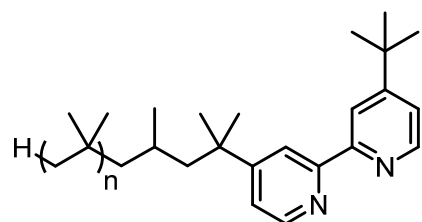
NaOH (2 M) and the mixture was transferred to a separatory funnel with the help of 75 mL DCM. After phase separation, the aqueous phase was extracted two more times with 75 mL DCM each. The combined organic phases were washed with 100 mL brine, dried over Na_2SO_4 , and evaporated under reduced pressure. The obtained orange oil was purified by flash chromatography (hexanes / EtOAc, 6:1 to 4:1) on deactivated silica (pretreated with 10% Et_3N in hexanes) to give 690 mg (3.05 mmol, 55.1%) of 4-(*tert*-butyl)-4'-methyl-2,2'-bipyridine (**XX**) as a slightly yellow oil. R_f (hexanes / EtOAc, 2:1) = 0.50; IR (neat): 3057, 2964, 2870, 1593, 1546, 1458, 1374, 1258, 1201, 1109, 1076, 993, 901, 840, 826, 768, 710, 671, 659, 556, 524, 470 cm^{-1} ; ^1H NMR (400 MHz, CDCl_3): 8.58 (dd, J = 5.3, 0.4 Hz, 1H), 8.55 (d, J = 5.0 Hz, 1H), 8.41 (dd, J = 2.0, 0.5 Hz, 1H), 8.22 (t, J = 0.7 Hz, 1H), 7.30 (dd, J = 5.3, 2.0 Hz, 1H), 7.12 (dd, J = 4.9, 1.0 Hz, 1H), 2.43 (s, 3H), 1.39 (s, 9H); ^{13}C NMR (101 MHz, CDCl_3): 161.08, 156.39, 156.22, 149.02, 148.97, 148.04, 124.53, 122.08, 120.86, 118.19, 35.02, 30.63, 21.19; HRMS (ESI) m/z calculated for $\text{C}_{15}\text{H}_{19}\text{N}_2$ ($[\text{M}+\text{H}]^+$) 227.1543, found 227.1544.



4-(*tert*-butyl)-4'-(methylpolyisobutyl)-2,2'-bipyridine (PIB-tb-bpy, **14**).

To 3 mL THF in a 25 mL Schlenk flask was added Pr_2NH (217 μL , 157 mg, 1.55 mmol, 1.15 equiv) and the solution was cooled to -78°C . $n\text{-BuLi}$ (1.6 M in hexane, 0.97 mL, 1.55 mmol, 1.15 equiv) was added dropwise, the mixture was warmed to 0°C for 5 min, and cooled back to -78°C . A solution of 4-(*tert*-butyl)-4'-methyl-2,2'-bipyridine (**13**, 320 mg, 1.41 mmol, 1.05 equiv) in 1 mL THF was added dropwise, the mixture was warmed to 0°C and stirred for 5 min upon which a solution of polyisobutylene iodide (**5**, 1.52 g, 1.35 mmol, 1.00 equiv) in 5 mL hexanes was added dropwise. The resulting reaction mixture was stirred for 3 d after which the solvent was evaporated under reduced pressure, the obtained material redissolved in 30 mL DCM, washed twice with 10 mL water each, dried over Na_2SO_4 , and evaporated under reduced pressure. The obtained orange oil was purified by flash chromatography (hexanes / EtOAc, 100:0 to 10:1) on deactivated silica (pretreated with 10% Et_3N in hexanes) to give 700 mg (0.571 mmol, 42.2%) of 4-(*tert*-butyl)-4'-(methylpolyisobutyl)-2,2'-bipyridine (PIB-tb-bpy, **14**) as a slightly yellow, viscous oil. R_f (hexanes / EtOAc, 20:1) = 0.25; IR (neat): 2951, 2904, 2217, 1732, 1594, 1465, 1389, 1365, 1229, 907, 834, 733 cm^{-1} ; ^1H NMR (300 MHz, CDCl_3): 8.59 (d, J = 5.3 Hz, 1H), 8.56 (d, J = 5.0 Hz, 1H), 8.42 (d, J = 1.7 Hz, 1H), 8.23 (s, 1H), 7.31 (dd, J = 5.24, 1.9 Hz, 1H), 7.13 (dd, J = 5.0, 1.3 Hz, 1H), 2.77 – 2.59 (m, 2H), 1.60 – 0.90 (m, 190H); ^{13}C NMR (75 MHz, CDCl_3): 149.00, 123.80, 121.42, 120.85, 118.22, 60 – 56 (multiple PIB

peaks), 38 – 22 (multiple PIB peaks); LRMS (ESI) m/z calculated for $C_{83}H_{155}N_2$ ($[M+H]^+$) 1180.2, found 1180.5.

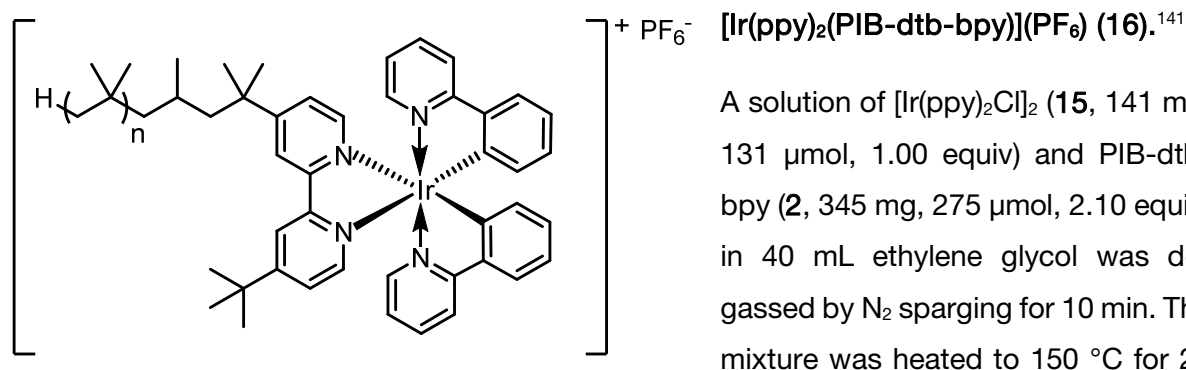


4-(*tert*-butyl)-4'-(2-polyisobutylpropan-2-yl)-2,2'-bipyridine (PIB-dtb-bpy, 2).¹²⁶

KO^tBu (786 mg, 7.00 mmol, 14.0 equiv) was weighted into a 50 mL Schlenk flask. 10 mL THF and ⁱPr₂NH (0.98 mL, 0.71 g, 7.0 mmol, 14 equiv) were added and the mixture was cooled to -78 °C upon which ⁿBuLi (1.6 M in hexanes, 4.4 mL, 7.0 mmol, 14 equiv) was added dropwise. The mixture was stirred at -50 °C for 30 min after which a solution of PIB-tb-bpy (**14**, 600 mg, 0.500 mmol, 1.00 equiv) in 10 mL hexanes was added dropwise and the mixture was stirred for another 30 min at -50 °C. The dark red / brown solution was cooled to -78 °C and a solution of MeI (1.25 mL, 2.84 g, 20.0 mmol, 40 equiv) was added dropwise. The reaction mixture was allowed to reach room temperature over night, quenched with 10 mL water, stripped from organic solvents by evaporation under reduced pressure, and extracted trice with 10 mL DCM each. The combined organic phases were dried over Na₂SO₄ and evaporated under reduced pressure. The resulting brown, viscous oil, mainly containing 4-(*tert*-butyl)-4'-(2-polyisobutylethan-2-yl)-2,2'-bipyridine, was used without further purification in the next step.

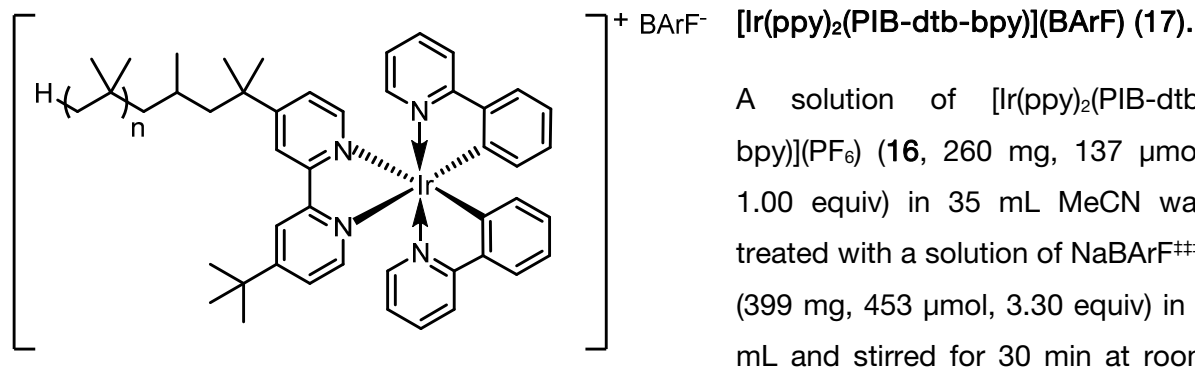
KO^tBu (786 mg, 7.00 mmol, 14.0 equiv) was weighted into a 50 mL Schlenk flask. 10 mL THF and ⁱPr₂NH (0.98 mL, 0.71 g, 7.0 mmol, 14 equiv) were added and the mixture was cooled to -78 °C upon which ⁿBuLi (1.6 M in hexanes, 4.4 mL, 7.0 mmol, 14 equiv) was added dropwise. The mixture was stirred at -50 °C for 30 min after which a solution of 4-(*tert*-butyl)-4'-(2-polyisobutylethan-2-yl)-2,2'-bipyridine (0.500 mmol) in 10 mL hexanes was added dropwise and the mixture was stirred for another 30 min at -50 °C. The dark red / brown solution was cooled to -78 °C and a solution of MeI (1.25 mL, 2.84 g, 20.0 mmol, 40 equiv) was added dropwise. The reaction mixture was allowed to reach room temperature over night, quenched with 10 mL water, stripped from organic solvents by evaporation under reduced pressure, and extracted trice with 10 mL DCM each. The combined organic phases were dried over Na₂SO₄ and evaporated under reduced pressure. The resulting dark orange oil was purified by flash chromatography (hexanes / EtOAc, 50:1 to 10:1) on neutral alumina to give 409 mg (0.326 mmol, 65.2% over 2 steps) of 4-(*tert*-butyl)-4'-(2-polyisobutylpropan-2-yl)-2,2'-bipyridine (PIB-dtb-bpy, **2**) as a slightly yellow, viscous oil. R_f (neutral alumina, hexanes / EtOAc, 50:1) = 0.32; IR (neat): 2952, 2897, 2761, 2720, 2489, 1587, 1546, 1468, 1389, 1366, 1231, 1154, 1105, 952, 924, 837, 731, 671, 614 cm⁻¹; ¹H NMR (300 MHz, CDCl₃): 8.59 (t, J = 5.4 Hz, 2H), 8.42 (dd, J = 5.2, 1.5 Hz, 2H), 7.29 (td, J = 5.2, 1.9 Hz, 2H), 1.75 – 0.60 (m, 200H); ¹³C NMR (75 MHz, CDCl₃): 160.89, 160.38, 156.46, 156.32, 149.04, 148.78, 121.56, 120.73,

118.90, 118.19, 60 – 53 (multiple PIB peaks), 39 – 24 (multiple PIB peaks) ; LRMS (ESI) m/z calculated for $C_{85}H_{159}N_2$ ($[M+H]^+$) 1208.2, found 1208.4.



A solution of $[Ir(ppy)_2Cl]_2$ (**15**, 141 mg, 131 μ mol, 1.00 equiv) and PIB-dtb-bpy (**2**, 345 mg, 275 μ mol, 2.10 equiv) in 40 mL ethylene glycol was de-gassed by N_2 sparging for 10 min. The mixture was heated to 150 $^{\circ}C$ for 20

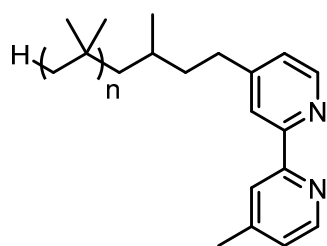
h. After cooling, the dark brown reaction solution was diluted with 300 mL water and a solution of NH_4PF_6 (2.1 g, 13 mmol, 10 equiv) in 10 mL water was added. The olive green precipitate was filtered off, washed with water, and purified by flash chromatography (hexanes / EtOAc, 1:1 to 0:1) on neutral alumina to give 410 mg (215 μ mol, 82.1%) of $[Ir(ppy)_2(PIB-dtb-bpy)](PF_6)$ (**16**) as a yellow solid. R_f (neutral alumina, EtOAc) = 0.67; IR (neat): 2951, 2896, 1608, 1584, 1477, 1439, 1416, 1389, 1366, 1305, 1269, 1229, 1163, 1063, 1032, 952, 924, 836, 759, 738, 631, 613, 557 cm^{-1} ; 1H NMR (300 MHz, $CDCl_3$): 8.32 (d, J = 8.6 Hz, 2H), 7.94 – 7.80 (m, 4H), 7.79 – 7.70 (m, 2H), 7.66 (d, J = 7.7 Hz, 2H), 7.61 – 7.50 (m, 2H), 7.44 – 7.33 (m, 2H), 7.13 – 6.95 (m, 4H), 6.93 – 6.82 (m, 2H), 1.80 – 0.50 (m, 190H); ^{13}C NMR (101 MHz, $CDCl_3$): 167.77, 167.70, 167.52, 163.87, 163.71, 155.72, 155.55, 150.69, 149.90, 149.54, 149.01, 148.64, 143.68, 143.58, 138.10, 131.82, 131.71, 130.69, 125.88, 125.57, 124.68, 123.61, 123.53, 123.40, 122.44, 121.86, 121.39, 119.55, 119.37; 60 – 53 (multiple PIB peaks), 40 – 24 (multiple PIB peaks); ^{19}F NMR (282 MHz, $CDCl_3$): -73.47 (d, J = 713 Hz); LRMS (ESI) m/z calculated for $C_{111}H_{182}IrN_4$ ($[M]^+$) 1764.4, found 1764.8.



A solution of $[Ir(ppy)_2(PIB-dtb-bpy)](PF_6)$ (**16**, 260 mg, 137 μ mol, 1.00 equiv) in 35 mL MeCN was treated with a solution of $NaBARF^{+++}$ (399 mg, 453 μ mol, 3.30 equiv) in 5 mL and stirred for 30 min at room

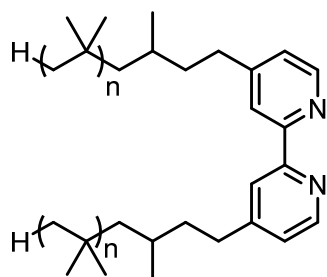
⁺⁺⁺ NaBARF was provided by Dr. Andreas Kreuzer.

temperature. The mixture was transferred to a separatory funnel with the help of 50 mL heptane, the phase separated, and the MeCN phase was extracted twice more with 50 mL heptane each. The combined heptane phases were evaporated under reduced pressure to give 231 mg (88.2 μ mol, 64.4%) of $[\text{Ir}(\text{ppy})_2(\text{PIB-dtb-bpy})](\text{BARf})$ (**17**) as a yellow oil. IR (neat): 2952, 2898, 1610, 1479, 1389, 1366, 1354, 1276, 1230, 1162, 1124, 945, 927, 887, 839, 756, 743, 713, 682, 670 cm^{-1} ; ^1H NMR (300 MHz, CDCl_3): 8.21 (s, 2H), 7.95 – 7.83 (m, 4H), 7.75 – 7.55 (m, 12H), 7.51 – 7.35 (m, 8H), 7.05 (t, J = 7.4 Hz, 2H), 6.93 (t, J = 7.3 Hz, 2H), 6.79 (q, J = 5.9 Hz, 2H), 6.28 (t, J = 6.6 Hz, 2H), 1.90 – 0.40 (m, 280H); ^{13}C NMR (101 MHz, CDCl_3): 168.26, 168.23, 168.14, 164.24, 164.08, 164.05, 162.79, 161.99, 161.49, 161.00, 150.48, 149.91, 147.99, 147.91, 147.84, 143.27, 143.24, 138.01, 134.78, 131.63, 131.05, 129.04, 128.76, 128.59, 125.88, 125.75, 124.97, 123.17, 122.89, 122.85, 122.77, 122.75, 120.96, 120.83, 120.46, 120.30, 119.80, 119.70, 117.42, 60 – 58 (multiple PIB peaks), 40 – 24 (multiple PIB peaks); LRMS (ESI) m/z calculated for $\text{C}_{95}\text{H}_{150}\text{IrN}_4$ ($[\text{M}]^+$) 1540.1, found 1540.4.

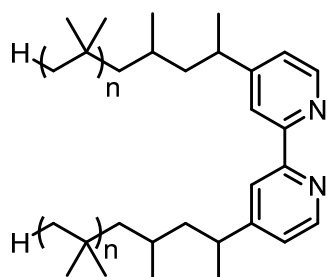


4-methyl-4'-(methylpolyisobutyl)-2,2'-bipyridine (PIB-Me-bpy, 29).

To 10 mL THF in a 25 mL Schlenk flask was added Pr_2NH (336 μL , 243 mg, 2.40 mmol, 1.2 equiv) and the solution was cooled to -78°C . $n\text{-BuLi}$ (1.6 M in hexane, 1.4 mL, 2.2 mmol, 1.1 equiv) was added dropwise, the mixture was warmed to 0°C for 5 min, and cooled back to -78°C . A solution of 4,4'-dimethyl-2,2'-bipyridine (**28**, 369 mg, 2.00 mmol, 1.00 equiv) in 2 mL THF was added dropwise, the mixture was warmed to 0°C and stirred for 5 min upon which a solution of polyisobutylene iodide (**5**, 2.26 g, 2.00 mmol, 1.00 equiv) in 10 mL hexanes was added dropwise. The resulting reaction mixture was stirred for 2 d after which the solvent was evaporated under reduced pressure, the obtained material redissolved in 30 mL DCM, washed twice with 10 mL water each, dried over Na_2SO_4 , and evaporated under reduced pressure. The obtained oil was purified by flash chromatography (hexanes / EtOAc, 100:0 to 20:1) on deactivated silica (pretreated with 10% Et_3N in hexanes) to give 1.09 g (0.916 mmol, 46%) of 4-methyl-4'-(methylpolyisobutyl)-2,2'-bipyridine (PIB-Me-bpy, **29**) as a colorless, viscous oil. R_f (hexanes / EtOAc, 10:1) = 0.22; IR (neat): 2949, 2893, 1595, 1555, 1464, 1389, 1365, 1229, 991, 949, 923, 822 cm^{-1} ; ^1H NMR (300 MHz, CDCl_3): 8.54 (d, J = 4.9 Hz, 1H), 8.53 (d, J = 4.9 Hz, 1H), 8.23 (s, 1H), 8.23 (s, 1H), 7.15 – 7.10 (m, 2H), 2.79 – 2.57 (m, 2H), 2.43 (s, 3H), 1.75 – 0.70 (m, 190H); ^{13}C NMR (75 MHz, CDCl_3): 155.61, 155.58, 153.72, 148.77, 148.67, 148.50, 124.79, 124.05, 122.27, 121.52, 60 – 53 (multiple PIB peaks), 40 – 28 (multiple PIB peaks), 22.75, 21.25; LRMS (ESI) m/z calculated for $\text{C}_{83}\text{H}_{155}\text{N}_2$ ($[\text{M}+\text{H}]^+$) xxx, found xxx.

**4,4'-bis(methylpolyisobutyl)-2,2'-bipyridine (PIB-PIB-bpy, 30).**

KO^tBu (337 mg, 3.00 mmol, 3.00 equiv) was weighted into a 50 mL Schlenk flask. 10 mL THF and ⁱPr₂NH (0.42 mL, 0.30 g, 3.0 mmol, 3.0 equiv) were added and the mixture was cooled to -78 °C upon which ⁿBuLi (1.6 M in hexanes, 1.9 mL, 3.0 mmol, 3.0 equiv) was added dropwise. The mixture was stirred at -50 °C for 30 min after which 4,4'-dimethyl-2,2'-bipyridine (**28**, 184 mg, 1.00 mmol, 1.00 equiv) added and the mixture was stirred for another 60 min at -50 °C. The dark red / brown solution was cooled to -78 °C and a solution of PIB-I (**5**, 3.4 g, 3.0 mmol, 3.0 equiv) in 10 mL hexanes was added dropwise. The reaction mixture was allowed to reach room temperature over night, quenched with 10 mL water, stripped from organic solvents by evaporation under reduced pressure, and extracted trice with 10 mL DCM each. The combined organic phases were dried over Na₂SO₄ and evaporated under reduced pressure. The resulting dark orange oil was purified by flash chromatography (hexanes / EtOAc, 100:0 to 10:1) on deactivated silica (pretreated with 10% Et₃N in hexanes) to give 975 mg (0.446 mmol, 45%) of 4,4'-bis(methylpolyisobutyl)-2,2'-bipyridine (PIB-PIB-bpy, **30**) as a colorless, viscous oil. *R_f* (hexanes / EtOAc, 10:1) = 0.73; IR (neat): 2950, 2893, 1594, 1469, 1389, 1365, 1229, 950, 923, 831, 760 cm⁻¹; ¹H NMR (300 MHz, CDCl₃): 8.55 (d, *J* = 5.0 Hz, 2H), 8.24 (s, 2H), 7.13 (dd, *J* = 5.0, 1.4 Hz, 2H), 2.78 – 2.60 (m, 4H), 1.80 – 0.70 (m, 300H); ¹³C NMR (75 MHz, CDCl₃): 156.18, 153.17, 148.98, 123.88, 121.29, 60 – 53 (multiple PIB peaks), 41 – 22 (multiple PIB peaks); LRMS (EI) *m/z* calculated for C₁₅₆H₃₀₁N₂ ([M+H]⁺) 2203.3, found 2203.3.

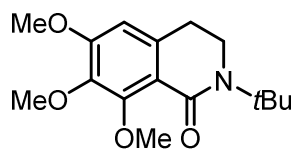
**4,4'-di(2-polyisobutylethan-2-yl)-2,2'-bipyridine (31).**

KO^tBu (333 mg, 2.97 mmol, 14.0 equiv) was weighted into a 25 mL Schlenk flask. 4.2 mL THF and ⁱPr₂NH (0.42 mL, 0.30 g, 3.0 mmol, 14 equiv) were added and the mixture was cooled to -78 °C upon which ⁿBuLi (1.6 M in hexanes, 1.9 mL, 3.0 mmol, 14 equiv) was added dropwise. The mixture was stirred at -50 °C for 30 min after which a solution of PIB-PIB-bpy (**30**, 462 mg, 212 μmol, 1.00 equiv) in 4.2 mL hexanes was added and the mixture was stirred for another 3 h at -50 °C. The dark red / brown solution was cooled to -78 °C and MeI (0.53 mL, 1.2 g, 8.5 mmol, 40 equiv) was added dropwise. The reaction mixture was allowed to reach room temperature over night, quenched with 10 mL water, stripped from organic solvents by evaporation under reduced pressure, and extracted trice with 10

mL DCM each. The combined organic phases were dried over Na_2SO_4 and evaporated under reduced pressure. The resulting dark orange oil was purified by flash chromatography (hexanes / EtOAc, 10:1) on deactivated silica (pretreated with 10% Et_3N in hexanes) to give 333 mg (0.151 mmol, 71%) of 4,4'-di(2-polyisobutylethan-2-yl)-2,2'-bipyridine (**31**) as a colorless, viscous oil. R_f (hexanes / EtOAc, 10:1) = 0.75; ^1H NMR (300 MHz, CDCl_3): 8.57 (s, 2H), 8.27 (s, 2H), 7.13 (s, 2H), 2.88 (bs, 2H), 1.90 – 0.70 (m, 330H); ^{13}C NMR (75 MHz, CDCl_3): 158.39, 157.48, 156.37, 156.32, 149.06, 122.34, 120.36, 119.98, 60 – 54 (multiple PIB peaks), 47.94, 47.67, 39 – 20 (multiple PIB peak).

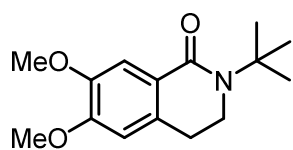
5.3 Photoreactions in a batch setup with [Ir(ppy)₂(PIB-dtb-bpy)](BArF)

Literature conditions



2-(*tert*-butyl)-6,7,8-trimethoxy-3,4-dihydroisoquinolin-1(2*H*)-one (24).

A Schlenk tube was charged with 1,3-dioxoisindolin-2-yl 3-(*N*-(*tert*-butyl)-3,4,5-trimethoxybenzamido)propanoate^{§§§§} (**18**, 96.7 mg, 200 μmol, 1.00 equiv) and [Ir(ppy)₂(dtb-bpy)](PF₆) (1.8 mg, 2.0 μmol, 1.0 mol%), sealed with a screw-cap, evacuated and backfilled with N₂ (three cycles), and 3 mL of a mixture of MeCN and water (40/1, v/v) was added. The reaction was degassed by freeze-pump-thaw (three cycles) and the screw-cap was replaced with a Teflon sealed inlet for a glass rod, through which irradiation with a 455 nm high power LED took place from above while the reaction was magnetically stirred and heated to 40 °C in an aluminum block from below. After 16 h of irradiation the LED was switched off, the reaction mixture was evaporated under reduced pressure, and the obtained residue purified by flash silica gel chromatography (hexanes / EtOAc, 2:1 to 1:1) to give 39.0 mg (133 μmol, 66%) of 2-(*tert*-butyl)-6,7,8-trimethoxy-3,4-dihydroisoquinolin-1(2*H*)-one (**24**) as a slightly yellow solid. ¹H NMR (300 MHz, CDCl₃): 6.40 (s, 1H), 3.92 (s, 3H), 3.85 (s, 3H), 3.83 (s, 3H), 3.50 – 3.43 (m, 2H), 2.77 – 2.70 (m, 2H), 1.52 (s, 9H).



2-(*tert*-butyl)-6,7-dimethoxy-3,4-dihydroisoquinolin-1(2*H*)-one (26).

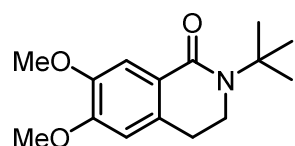
A Schlenk tube was charged with 1,3-dioxoisindolin-2-yl 3-(*N*-(*tert*-butyl)-3,4-dimethoxybenzamido)propanoate^{*****} (**25**, 227 mg, 500 μmol, 1.00 equiv) and [Ir(ppy)₂(dtb-bpy)](PF₆) (4.6 mg, 5.0 μmol, 1.0 mol%), sealed with a screw-cap, evacuated and backfilled with N₂ (three cycles), and 10 mL of a mixture of MeCN and water (40/1, v/v) was added. The reaction was degassed by freeze-pump-thaw (three cycles) and the screw-cap was replaced with a Teflon sealed inlet for a glass rod, through which irradiation with a 455 nm high power LED took place from above while the reaction was magnetically stirred and heated to 40 °C in an aluminum block from below. After 16 h of irradiation the LED was

^{§§§§} Material was provided by Christian Faderl

^{*****} Material was provided by Christian Faderl

switched off, the reaction mixture was evaporated under reduced pressure, and the obtained residue purified by flash silica gel chromatography (hexanes / EtOAc, 2:1 to 1:1) to give 88.2 mg (335 μmol , 67.0%) of 2-(*tert*-butyl)-6,7-dimethoxy-3,4-dihydroisoquinolin-1(2*H*)-one (**26**) as a slightly yellow solid. ^1H NMR (300 MHz, CDCl_3): 7.60 (s, 1H), 6.60 (s, 1H), 3.91 (s, 3H), 3.90 (s, 3H), 3.56 (dd, $J = 7.2, 6.4$ Hz, 2H), 2.84 (t, $J = 6.7$ Hz, 2H), 1.53 (s, 9H); ^{13}C NMR (75 MHz, CDCl_3): 165.77, 151.44, 147.84, 131.78, 124.08, 110.48, 108.55, 57.29, 55.98, 55.01, 42.61, 29.00, 28.95

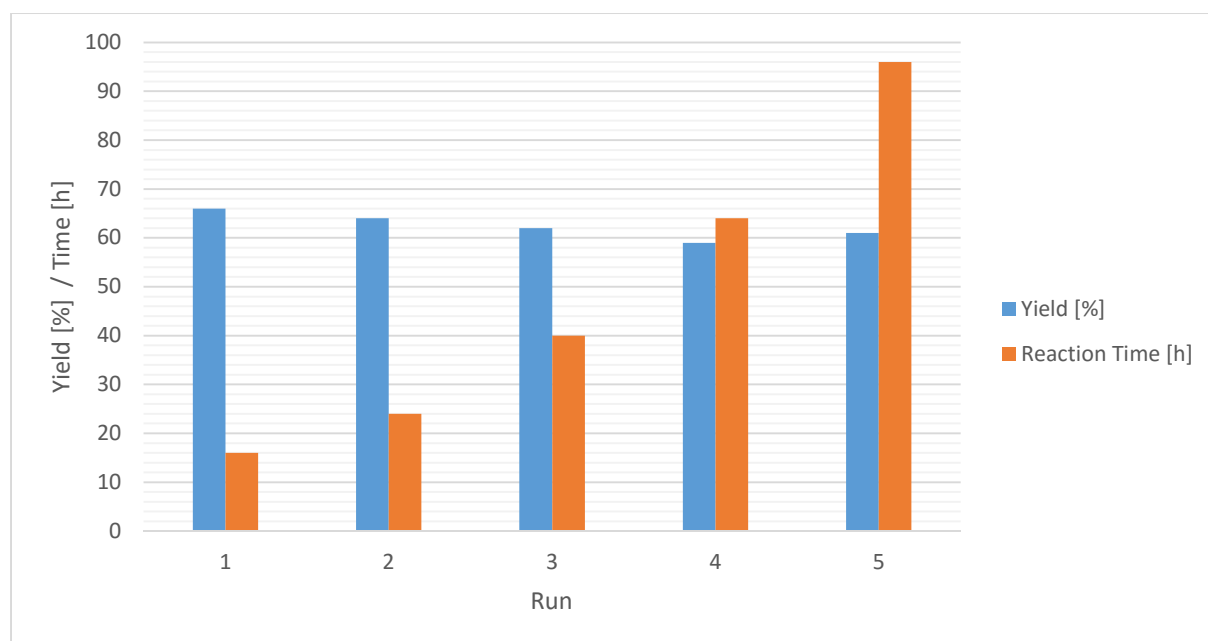
Recycling conditions



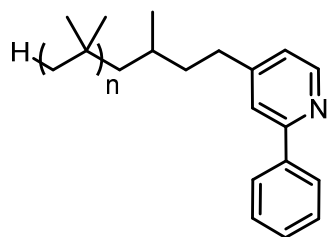
2-(*tert*-butyl)-6,7-dimethoxy-3,4-dihydroisoquinolin-1(2*H*)-one (**26**).

A Schlenk tube was charged with 1,3-dioxoisindolin-2-yl 3-(*N*-(*tert*-butyl)-3,4-dimethoxybenzamido)propanoate (**25**, 227 mg, 500 μmol , 1.00 equiv) and $[\text{Ir}(\text{ppy})_2(\text{PIB-dtb-bpy})](\text{BArF})$ (**17**, 13.1 mg, 5.0 μmol , 1.0 mol%), sealed with a screw-cap, evacuated and backfilled with N_2 (three cycles), and 10 mL of a mixture of MeCN and water (40/1, v/v) was added. The reaction was degassed by freeze-pump-thaw (three cycles) and the screw-cap was replaced with a Teflon sealed inlet for a glass rod, through which irradiation with a 455 nm high power LED took place from above while the reaction was magnetically stirred and heated to 40 $^\circ\text{C}$ in an aluminum block from below. After 16 h of irradiation the LED was switched off, the reaction mixture was washed into a separatory flask with the help of 10 mL heptane. The phases were separated and evaporated under reduced pressure. The obtained residue of the acetonitrile phase was purified by flash silica gel chromatography (hexanes / EtOAc, 2:1 to 1:1) to give 86.7 mg (329 μmol , 65.8%) of 2-(*tert*-butyl)-6,7-dimethoxy-3,4-dihydroisoquinolin-1(2*H*)-one (**26**) as a slightly yellow solid.

All following catalyst runs were set up equally to the first run using all of the yellow, oily, heptane phase residue of the previous run instead of $[\text{Ir}(\text{ppy})_2(\text{PIB-dtb-bpy})](\text{BArF})$ (**17**). The reaction times were prolonged to achieve full starting material conversion as judged by TLC control.

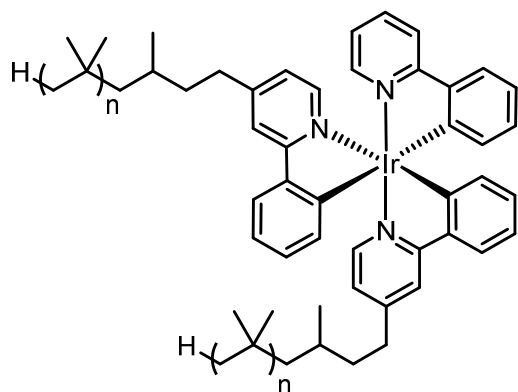


5.4 Synthesis of triscyclometalated iridium(III) complexes



4-(methylpolyisobutyl)-2-phenylpyridine (PIB-ppy, **36**).

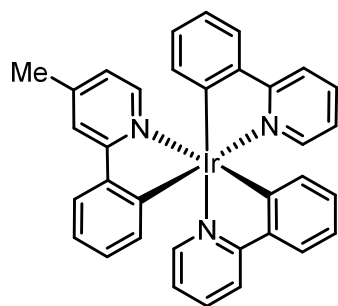
A Schlenk flask was charged with 4-methyl-2-phenylpyridine¹³¹ (**35**, 355 mg, 2.10 mmol, 1.05 equiv), 10 mL THF and cooled to -78 °C. A solution of LDA, prepared *in situ* by treating a solution of Pr_2NH (336 μL , 243 mg, 2.40 mmol, 1.20 equiv) in 5 mL THF with $n\text{BuLi}$ (1.6 M in hexanes, 1.10 mL, 2.20 mmol, 1.10 equiv), was added dropwise. The solution was stirred for 30 min at -78 °C during which it turned intense red. A solution of polyisobutylene iodide (**5**, 2.26 g, 2.00 mmol, 1.00 equiv) in 10 mL hexanes was added dropwise and the reaction mixture was allowed to reach room temperature over night. After evaporation of the solvents under reduced pressure, purification was achieved by flash silica gel chromatography (hexanes / EtOAc, 10:1 to 5:1 with 2% Et_3N) to give 1.96 g (1.66 mmol, 83.0%) of PIB-ppy (**36**) as a viscous slightly yellow oil. R_f (hexanes / EtOAc, 6:1 with 2% Et_3N) = 0.60; IR (neat): 2950, 2896, 1741, 1600, 1558, 1471, 1389, 1366, 1231, 951, 923, 933, 774, 693, 637 cm^{-1} ; ^1H NMR (300 MHz, CDCl_3): 8.60 (d, J = 5.2 Hz, 1H), 8.04 – 7.96 (m, 2H), 7.58 (s, 1H), 7.53 – 7.40 (m, 3H), 7.14 (d, J = 5.1 Hz), 2.80 – 2.58 (m, 2H), 1.80 – 0.70 (m, 200H); ^{13}C NMR (75 MHz, CDCl_3): 156.71, 148.38, 129.37, 128.88, 127.18, 122.65, 121.33, 60 – 53 (multiple PIB peaks), 41 – 20 (multiple PIB peaks); LRMS (ESI) m/z calculated for $\text{C}_{84}\text{H}_{155}\text{IrN}_2$ ($[\text{M}+\text{H}]^+$) 1179.2, found 1179.3.



$\text{Ir}(\text{ppy})_2(\text{PIB-ppy})_2$ (**38**).

A Schlenk flask was charged with $[\text{Ir}(\text{ppy})_2(\text{MeOH})_2](\text{OTf})$ (**37**, 429 mg, 600 μmol , 1.00 equiv), PIB-ppy (**36**, 707 mg, 600 μmol , 1.00 equiv), and 18 mL dioxane. The mixture was degassed by N_2 sparging for 5 min and subsequently refluxed for 7 d after which the reaction mixture was transferred to a separatory funnel with 100 mL Et_2O . The mixture was washed twice with 50 mL water each, back washed twice with 50 mL Et_2O each, dried over Na_2SO_4 and evaporated under reduced pressure. The remaining brown oil was pu-

rified by flash chromatography (hexanes / Et₂O, 10:1 to 1:1) on basic Al₂O₃. Fractions containing mixtures of the complex and the free ligand were united, evaporated under reduced pressure, redissolved in 20 mL heptane, washed with a solution of 1 mL AcOH in 20 mL MeCN, and again evaporated under reduced pressure to give 54.9 mg (20.3 μmol, 6.8%) of Ir(ppy)(PIB-ppy)₂ (**38**) as a yellow oil. *R_f* (Al₂O₃, hexanes / Et₂O, 5:1) = 0.86; IR (neat): 2951, 2897, 1600, 1580, 1556, 1471, 1389, 1366, 1261, 1231, 1158, 1093, 1058, 1026, 952, 923, 800, 776, 753, 733, 693, 638 cm⁻¹; ¹H NMR (400 MHz, CD₂Cl₂): 8.55 (d, *J* = 5.1 Hz, 1H), 8.02 (d, *J* = 7.4 Hz, 2H), 7.92 (dd, *J* = 8.1, 3.1, 1H), 7.76 (s, 1H), 7.72 – 7.56 (m, 5H), 7.53 – 7.39 (m, 4H), 7.11 (d, *J* = 4.7 Hz, 1H), 6.96 – 6.86 (m, 3H), 6.83 – 6.72 (m, 5H), 2.79 – 2.60 (m, 4H), 1.75 – 0.75 (m, 320H); ¹³C NMR (101 MHz, CD₂Cl₂): 166.96, 166.45, 161.76, 161.61, 149.55, 147.61, 147.56, 147.07, 144.41, 144.29, 137.25, 137.15, 136.56, 130.08, 129.87, 129.28, 129.05, 127.32, 124.44, 124.20, 122.94, 122.45, 121.13, 120.24, 120.19, 120.13, 119.22, 59 – 57 (multiple PIB peaks), 41 – 22 (multiple PIB peaks).

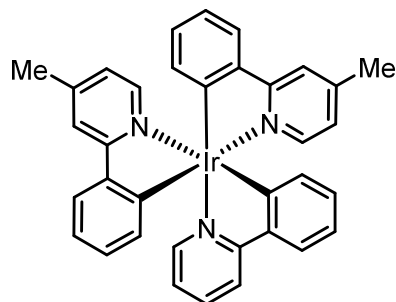


Ir(ppy)₂(4-Me-ppy) (39**).**¹⁴²

To a solution of [Ir(ppy)₂Cl]₂ (793 mg, 740 μmol, 1.00 equiv) in 74 mL DCM a solution of AgOTf (399 mg, 1.55 mmol, 2.09 equiv) in 37 mL MeOH was dropwise added. The mixture was stirred at room temperature over night in the dark and subsequently filter through a short plug of Celite® with the help of 100 mL DCM. The solvent was evaporated under reduced pressure to give 1.06 g (1.48 mmol, 100%) of [Ir(ppy)₂(MeOH)₂](OTf) (**37**) as a green solid which was used without further purification.

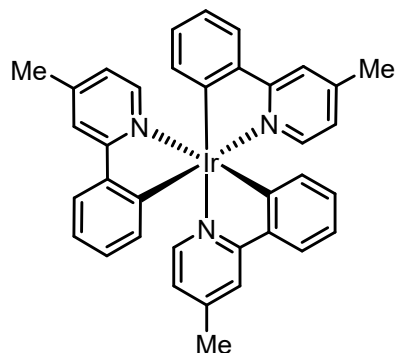
A Schlenk flask was charged with [Ir(ppy)₂(MeOH)₂](OTf) (**37**, 1.06 g, 1.48 mmol, 1.00 equiv), 4-methyl-2-phenylpyridine¹³¹ (751 mg, 4.44 mmol, 3.00 equiv), 30 mL EtOH, and 30 mL MeOH. The mixture was degassed by N₂ sparging for 5 min and subsequently refluxed for 24 h after which 6 g of Celite® was added to reaction mixture stirred for another 5 min. This suspension was filtered through a plug of Celite®, which was then washed with 100 mL MeOH and 100 mL hexanes. The filtrates were discarded and the complex was eluted with 200 mL DCM. Evaporation under reduced pressure and drying of the residue *in vacuo* gave 563 mg (842 μmol, 56.9% over two steps) of Ir(ppy)₂(4-Me-ppy) (**39**) as a bright yellow powder. *R_f* (hexanes / EtOAc, 1:1) = 0.23; IR (neat): 3034, 1613, 1598, 1578, 1469, 1411, 1299, 1261, 1157, 1058, 1026, 876, 816, 752, 730 cm⁻¹; ¹H NMR (400 MHz, CD₂Cl₂): 7.92 (dd, *J* = 8.4, 2.9 Hz, 2H), 7.75 (s, 1H), 7.70 – 7.62 (m, 5H), 7.60 (d, *J* = 5.6 Hz, 1H), 7.57 (d, *J* = 5.3 Hz, 1H), 7.41 (d, *J* = 5.8 Hz, 1H), 6.96 – 6.85 (m, 5H), 6.82 – 6.70 (m, 7H), 2.43 (s, 3H); ¹³C NMR

(101 MHz, CD_2Cl_2): 166.92, 166.30, 161.76, 161.71, 161.33, 148.36, 147.62, 147.60, 169.99, 144.35, 144.31, 144.27, 137.24, 137.21, 137.07, 136.58, 136.56, 130.04, 129.89, 124.43, 124.19, 123.70, 122.48, 120.23, 120.17, 120.02, 119.24, 21.50; HRMS (ESI) m/z calculated for $\text{C}_{34}\text{H}_{27}\text{IrN}_3$ ($[\text{M}+\text{H}]^+$) 670.1830, found 670.1811.



Ir(ppy)(4-Me-ppy)₂ (40).¹⁴²

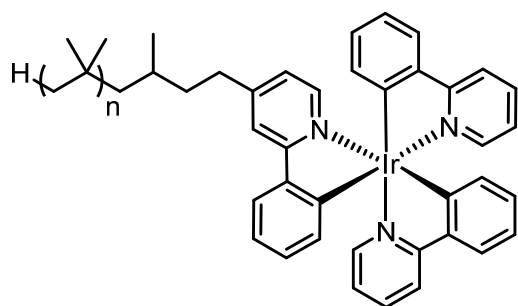
A Schlenk flask was charged with $[\text{Ir}(\text{4-Me-ppy})_2(\text{MeOH})_2](\text{OTf})$ ¹⁴² (223 mg, 300 μmol , 1.00 equiv), 2-phenylpyridine (140 mg, 900 μmol , 3.00 equiv), 5.0 mL EtOH, and 5.0 mL MeOH. The mixture was degassed by N_2 sparging for 5 min and subsequently refluxed for 24 h after which 1 g of Celite® was added to reaction mixture stirred for another 5 min. This suspension was filtered through a plug of Celite®, which was then washed with 20 mL MeOH and 20 mL hexanes. The filtrates were discarded and the complex was eluted with 50 mL DCM. Evaporation under reduced pressure, drying of the residue *in vacuo*, and purification by flash silica gel chromatography (hexanes / DCM, 1:1 to 0:1) gave 105 mg (153 μmol , 51.2% of Ir(ppy)(4-Me-ppy)₂ (40) as a bright yellow powder. R_f (hexanes / DCM, 1:1) = 0.34; IR (neat): 3035, 1600, 1578, 1469, 1416, 1409, 1308, 1157, 1024, 875, 818, 778, 753, 729, 644 cm^{-1} ; ^1H NMR (400 MHz, CD_2Cl_2): 7.91 (d, J = 8.2 Hz, 1H), 7.74 (bs, 2H), 7.70 – 7.57 (m, 5H), 7.44 (d, J = 5.7 Hz, 1H), 7.40 (d, J = 5.7, 1H), 6.95 – 6.85 (m, 4H), 6.82 – 6.71 (m, 8H), 2.42 (d, J = 2.0 Hz, 6H); ^{13}C NMR (101 MHz, CD_2Cl_2): 166.95, 166.34, 166.33, 162.05, 161.67, 161.62, 148.28, 148.27, 147.62, 147.01, 144.41, 144.36, 144.33, 137.28, 137.14, 137.11, 136.49, 130.00, 129.85, 124.42, 124.18, 123.66, 122.43, 120.14, 120.08, 119.98, 119.18, 21.50; HRMS (ESI) m/z calculated for $\text{C}_{35}\text{H}_{29}\text{IrN}_3$ ($[\text{M}+\text{H}]^+$) 684.1987, found 684.1970.



Ir(4-Me-ppy)₃ (41).¹⁴²

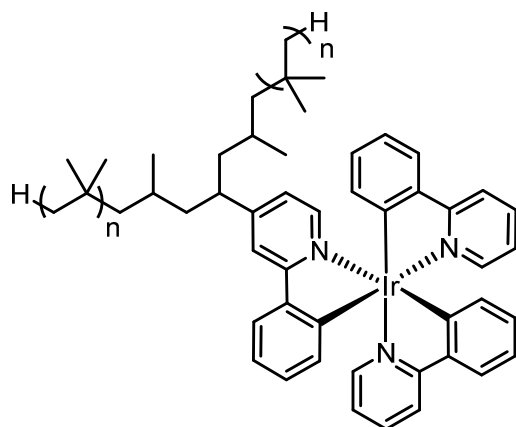
A Schlenk flask was charged with $[\text{Ir}(\text{4-Me-ppy})_2(\text{MeOH})_2](\text{OTf})$ ¹⁴² (223 mg, 300 μmol , 1.00 equiv), 4-methyl-2-phenylpyridine¹³¹ (152 mg, 900 μmol , 3.00 equiv), 5.0 mL EtOH, and 5.0 mL MeOH. The mixture was degassed by N_2 sparging for 5 min and subsequently refluxed for 24 h after which 1 g of Celite® was added to reaction mixture stirred for another 5 min. This suspension was filtered through a plug of Celite®, which was then

washed with 20 mL MeOH and 20 mL hexanes. The filtrates were discarded and the complex was eluted with 50 mL DCM. Evaporation under reduced pressure, drying of the residue *in vacuo*, and purification by flash silica gel chromatography (hexanes / DCM, 1:1 to 0:1) gave 161 mg (231 μ mol, 77.0%) of Ir(4-Me-ppy)₃ (**41**) as a bright yellow powder. R_f (hexanes / DCM, 1:1) = 0.36; IR (neat): 3038, 1610, 1577, 1551, 1464, 1424, 1402, 1263, 1231, 1153, 1057, 1021, 875, 829, 779, 736 cm^{-1} ; ^1H NMR (400 MHz, CD_2Cl_2): 7.73 (s, 3H), 7.65 (d, J = 7.8 Hz, 3H), 7.42 (d, J = 5.5 Hz, 3H), 6.91 – 6.63 (m, 12H), 2.43 (s, 9H); ^{13}C NMR (101 MHz, CD_2Cl_2): 166.35, 161.83, 148.17, 147.01, 144.46, 137.20, 129.76, 124.10, 123.60, 120.10, 119.93; HRMS (ESI) m/z calculated for $\text{C}_{36}\text{H}_{30}\text{IrN}_3$ (M^+) 697.2065, found 697.2079.



Ir(ppy)₂(PIB-ppy) (**42**).

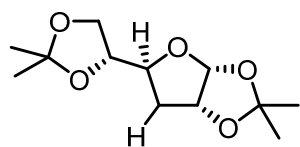
A Schlenk flask was charged with Ir(ppy)₂(4-Me-ppy) (**39**, 268 mg, 400 μ mol, 1.00 equiv), 8 mL THF and cooled to -78°C . A solution of LDA, prepared *in situ* by treating a solution of Pr_2NH (79 μL , 57 mg, 0.56 mmol, 1.4 equiv) in 6 mL THF with $n\text{BuLi}$ (1.6 M in hexanes, 0.33 mL, 0.52 mmol, 1.3 equiv), was added dropwise. The solution was stirred for 15 min at -78°C during which it turned dark red / brown. A solution of polyisobutylene iodide (**5**, 0.63 g, 0.56 mmol, 1.4 equiv) in 6 mL hexanes was added dropwise and the reaction mixture was allowed to reach room temperature over night. After evaporation of the solvents under reduced pressure, purification was achieved by flash silica gel chromatography (hexanes / DCM, 1:0 to 1:1) to give 363 mg (216 μ mol, 54.0%) of Ir(ppy)₂(PIB-ppy) (**3**) as a bright yellow solid. R_f (hexanes / DCM, 2:1) = 0.50; mp: $>190^\circ\text{C}$; IR (neat): 2948, 1891, 1600, 1570, 1469, 1411, 1388, 1364, 1261, 1227, 1156, 1056, 1027, 950, 831, 779, 752, 732, 649 cm^{-1} ; ^1H NMR (400 MHz, CD_2Cl_2): 7.94 – 7.88 (m, 2H), 7.55 (s, 1H), 7.70 – 7.60 (m, 5H), 7.57 (t, J = 5.1 Hz, 2H), 7.42 (d, J = 5.8 Hz, 1H), 6.95 – 6.85 (m, 5H), 6.82 – 6.71 (m, 7H), 2.78 – 2.58 (m, 2H), 1.75 – 0.70 (m, 150H); ^{13}C NMR (101 MHz, CDCl_3): 165.76, 165.20, 151.11, 151.08, 146.05, 145.53, 142.79, 142.69, 142.63, 136.14, 136.10, 136.01, 134.78, 128.80, 128.63, 122.82, 122.60, 121.28, 120.76, 118.66, 118.63, 117.66, 59 – 52 (multiple PIB peaks), 40 – 20 (multiple PIB peaks); LRMS (ESI) m/z calculated for $\text{C}_{106}\text{H}_{170}\text{IrN}_3$ ($[\text{M}+\text{H}]^+$) 1679.3, found 1679.7.

**Ir(ppy)₂(PIB₂-ppy) (43).**

A Schlenk flask was charged with Ir(ppy)₂(4-Me-ppy) (**39**, 27 mg, 39 μ mol, 1.0 equiv), 1 mL THF and cooled to -78 °C. A solution of LDA, prepared *in situ* by treating a solution of Pr_2NH (79 μ L, 57 mg, 0.56 mmol, 14 equiv) in 6 mL THF with $n\text{BuLi}$ (1.6 M in hexanes, 0.33 mL, 0.52 mmol, 13 equiv), was added dropwise. The solution was stirred for 15 min at -78 °C during which it turned dark red / brown. A solution of polyisobutylene iodide (**5**, 0.63 g, 0.56 mmol, 14 equiv) in 6 mL hexanes was added dropwise and the reaction mixture was allowed to reach room temperature over night. After evaporation of the solvents under reduced pressure, purification was achieved by flash silica gel chromatography (hexanes / DCM, 1:0 to 1:1) to give 89 mg (33 μ mol, 84%) of Ir(ppy)₂(PIB₂-ppy) (**43**) as a yellow oil. R_f (hexanes / DCM, 2:1) = 0.71; IR (neat): 2950, 2895, 1601, 1580, 1471, 1389, 1366, 1261, 1230, 1158, 1058, 1025, 952, 923, 753, 734, 666, 630 cm^{-1} ; ^1H NMR (400 MHz, CDCl_3): 7.91 – 7.82 (m, 2H), 7.70 – 7.60 (m, 4H), 7.69 – 7.35 (m, 5H), 6.95 – 6.32 (m, 12H), 2.77 – 2.63 (m, 1H), 1.60 – 0.70 (m, 360H); ^{13}C NMR (101 MHz, CD_2Cl_2): 167.03, 166.53, 166.49, 161.84, 161.63, 161.26, 157.57, 157.02, 147.62, 147.32, 147.17, 144.46, 144.27, 144.15, 137.27, 136.55, 130.13, 129.92, 124.46, 124.34, 124.22, 122.59, 122.43, 122.35, 120.24, 119.24, 118.94, 118.43, 60 – 52 (multiple PIB peaks), 42 – 22 (multiple PIB peaks); LRMS (ESI) m/z calculated for $\text{C}_{122}\text{H}_{203}\text{IrN}_3$ ($[\text{M}+\text{H}]^+$) 1903.6, found 1904.0.

5.5 Photoreactions in a batch setup with Ir(ppy)₂(PIB-ppy)

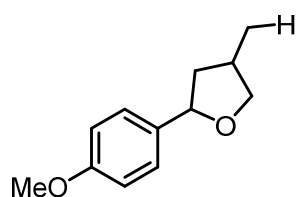
Literature conditions



(*3aR,5S,6aR*)-5-((*R*)-2,2-dimethyl-1,3-dioxolan-4-yl)-2,2-dimethyltetrahydrofuro[2,3-*d*][1,3]dioxole (**45**).²⁹

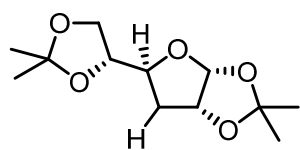
A Schlenk tube was charged with (*3aR,5R,6R,6aS*)-5-((*R*)-2,2-dimethyl-1,3-dioxolan-4-yl)-6-iodo-2,2-dimethyltetrahydrofuro[2,3-*d*][1,3]dioxole¹⁴³ (**44**, 368 mg, 1.00 mmol, 1.00 equiv) and *fac*-Ir(ppy)₃ (6.6 mg, 10 μmol, 1.0 mol%), Hantzsch ester (507 mg, 2.00 mmol, 2.00 equiv) sealed with a screw-cap, evacuated and backfilled with N₂ (three cycles), and 10 mL MeCN and Bu₃N (0.48 mL, 0.37 g, 2.0 mmol, 2.0 equiv) were added. The reaction was degassed by N₂ sparging for 10 min and the screw-cap was replaced with a Teflon sealed inlet for a glass rod, through which irradiation with a 455 nm high power LED took place from above while the reaction was magnetically stirred below. After 16 h of irradiation the LED was switched off, the reaction mixture was evaporated under reduced pressure, and the obtained residue was redissolved in 25 mL EtOAc. After washing with 25 mL 1 M HCl (aq), back extraction with 25 mL EtOAc (twice), washing with 25 mL sat NaHCO₃ (aq) and 25 mL brine, the organic layers were dried over Na₂SO₄ and evaporated under reduced pressure. The residue was purified by flash silica gel chromatography (hexanes / EtOAc, 6:1) to give 145 mg (598 μmol, 59.8%) of (*3aR,5S,6aR*)-5-((*R*)-2,2-dimethyl-1,3-dioxolan-4-yl)-2,2-dimethyltetrahydrofuro[2,3-*d*][1,3]dioxole (**45**) as white solid. ¹H NMR (300 MHz, CDCl₃): 5.74 (d, *J* = 3.6 Hz, 1H), 4.69 (t, *J* = 4.2 Hz, 1H), 4.14 – 3.98 (m, 3H), 3.81 – 3.69 (m, 1H), 2.11 (dd, *J* = 12.9, 3.3 Hz, 1H), 1.76 – 1.62 (m, 1H), 1.44 (s, 3H), 1.35 (s, 3H), 1.28 (s, 3H), 1.25 (s, 3H).

The reaction was repeated as above on a 0.3 mmol scale at 85 °C with 3 mL of heptane as co-solvent and an irradiation time of 3 h after which all starting material was consumed as judged by TLC control. The reaction mixture was transferred to a separatory funnel with the help of 3 mL MeCN and 3 mL heptane and phases were separated. Diphenylmethane was added to the MeCN and an aliquot was analyzed by GC-FID showing full starting material conversion and 73% yield of (*3aR,5S,6aR*)-5-((*R*)-2,2-dimethyl-1,3-dioxolan-4-yl)-2,2-dimethyltetrahydrofuro[2,3-*d*][1,3]dioxole (**45**) in the MeCN phase.

**2-(4-methoxyphenyl)-4-methyltetrahydrofuran (47).**²⁹

A Schlenk tube was charged with 1-(1-(allyloxy)-2-iodoethyl)-4-methoxybenzene¹⁴⁴ (**46**, 318 mg, 1.00 mmol, 1.00 equiv) and *fac*-Ir(ppy)₃ (16 mg, 25 μmol, 2.5 mol%), sealed with a screw-cap, evacuated and backfilled with N₂ (three cycles), and 10 mL MeCN, Bu₃N (2.38 mL, 1.85 g, 10.0 mmol, 10.0 equiv), and HCOOH (377 μL, 460 mg, 10.0 mmol, 10.0 equiv) were added. The reaction was degassed by N₂ sparging for 10 min and the screw-cap was replaced with a Teflon sealed inlet for a glass rod, through which irradiation with a 455 nm high power LED took place from above while the reaction was magnetically stirred below. After 16 h of irradiation the LED was switched off, the reaction mixture was evaporated under reduced pressure, and the obtained residue was redissolved in 25 mL EtOAc. After washing with 25 mL 1 M HCl (aq), back extraction with 25 mL EtOAc (twice), washing with 25 mL sat NaHCO₃ (aq) and 25 mL brine, the organic layers were dried over Na₂SO₄ and evaporated under reduced pressure. The residue was purified by flash silica gel chromatography (hexanes / EtOAc, 50:1 to 6:1) to give 110 mg (573 μmol, 57.3%) of 2-(4-methoxyphenyl)-4-methyltetrahydrofuran (**47**, dr = 5.3:1) as a slightly yellow oil. ¹H NMR (major diastereomer, 300 MHz, CDCl₃): 7.31 – 7.21 (m, 2H), 6.92 – 6.82 (m, 2H), 4.98 (t, *J* = 7.0 Hz, 1H), 4.21 (dd, *J* = 8.2, 6.9 Hz, 1H), 3.79 (s, 3H), 3.46 (dd, *J* = 8.2, 7.0 Hz, 1H), 2.56 – 2.35 (m, 1H), 2.07 – 1.85 (m, 1H), 1.10 (d, *J* = 6.9 Hz, 3H).

The reaction was repeated as above on a 0.3 mmol scale at 85 °C with 3 mL of heptane as co-solvent and an irradiation time of 3 h after which all starting material was consumed as judged by TLC control. The reaction mixture was transferred to a separatory funnel with the help of 3 mL MeCN and 3 mL heptane and phases were separated. Diphenylmethane was added to the MeCN phase and an aliquot was analyzed by GC-FID showing full starting material conversion and 37% yield of 2-(4-methoxyphenyl)-4-methyltetrahydrofuran (**47**) in the MeCN phase.

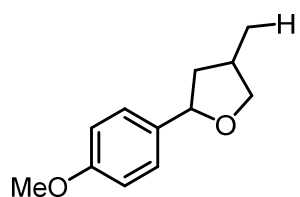
Recycling conditions

(3aR,5S,6aR)-5-((R)-2,2-dimethyl-1,3-dioxolan-4-yl)-2,2-dimethyltetrahydrofuro[2,3-d][1,3]dioxole (45).²⁹

A Schlenk tube was charged with Hantzsch ester (152 mg, 0.60 mmol, 2.0 equiv), (3aR,5R,6R,6aS)-5-((R)-2,2-dimethyl-1,3-dioxolan-4-yl)-6-iodo-2,2-dimethyltetrahydrofuro[2,3-d][1,3]dioxole¹⁴³ (**44**, 0.10 M solution in MeCN, 3.0 mL, 0.30 mmol, 1.0 equiv) and Ir(ppy)₂(PIB-ppy) (**42**, 5.0 mg, 3.0 μmol, 1.0 mol%), sealed with a screw-cap, and Bu₃N (143 μL, 111 mg, 0.60 mmol, 2.0 equiv) was added. The reaction was degassed by N₂ sparging for 10 min and the screw-cap was replaced with a Teflon sealed inlet for a glass rod, through which irradiation with a 455 nm high power LED took place from above while the reaction was magnetically stirred and heated in an aluminum block below. After 3 h of irradiation at 85 °C the LED was switched off, the reaction mixture was washed into a separatory flask with the help of 3 mL MeCN and 3 mL heptane, and the phases were separated. Diphenylmethane was added to the MeCN phase and an aliquot was analyzed by GC-FID to determine the yield of (3aR,5S,6aR)-5-((R)-2,2-dimethyl-1,3-dioxolan-4-yl)-2,2-dimethyltetrahydrofuro[2,3-d][1,3]dioxole (**45**). The heptane phase was evaporated under reduced pressure and the residue used as catalyst in the next run.

All following catalyst runs were set up equally to the first run using all of the yellow, oily, heptane phase residue of the previous run instead of Ir(ppy)₂(PIB-ppy) (**42**). All reaction parameters were kept constant for the following runs.

Results of the single reaction runs are given in the main part.



2-(4-methoxyphenyl)-4-methyltetrahydrofuran (47).²⁹

A Schlenk tube was charged with 1-(1-(allyloxy)-2-iodoethyl)-4-methoxybenzene¹⁴⁴ (**46**, 0.10 M solution in MeCN, 3.0 mL, 0.30 mmol, 1.0 equiv) and Ir(ppy)₂(PIB-ppy) (**42**, 12.6 mg, 7.5 μmol, 2.5 mol%), sealed with a screw-cap, and Bu₃N (0.71 mL, 0.56 g, 3.0 mmol, 10 equiv) and HCOOH (113 μL, 138 mg, 10.0 mmol, 10.0 equiv) were added. The reaction was degassed by N₂ sparging for 10 min and the screw-cap was replaced with a Teflon sealed inlet for a glass rod, through which irradiation with a 455 nm high power LED took place from above while the reaction was magnetically stirred and heated in an aluminum block below. After 3 h of

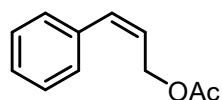
irradiation at 85 °C the LED was switched off, the reaction mixture was washed into a separatory flask with the help of 3 mL MeCN and 3 mL heptane, and the phases were separated. Diphenylmethane was added to the MeCN phase and an aliquot was analyzed by GC-FID to determine the yield of 2-(4-methoxyphenyl)-4-methyltetrahydrofuran (**47**). The heptane phase was evaporated under reduced pressure and residue used as catalyst in the next run.

All following catalyst runs were set up equally to the first run using all of the yellow, oily, heptane phase residue of the previous run instead of Ir(ppy)₂(PIB-ppy) (**42**). All reaction parameters were kept constant for the following runs.

Results of the single reaction runs are given in the main part.

5.6 Photoreactions in continuous flow

Literature conditions



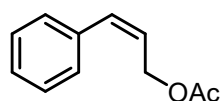
(*Z*)-3-phenylallyl acetate (**49**).

A Schlenk tube was charged with (*E*)-3-phenylallyl acetate (**48**, 176 mg, 1.00 mmol, 1.00 equiv), *fac*-Ir(ppy)₃ (4.6 mg, 7.0 μmol, 0.7 mol%), 5 mL MeCN, and ^tPr₂NEt (17 μL, 13 mg, 0.10 mmol, 0.10 equiv), and sealed with a screw-cap. The reaction was degassed by N₂ sparging for 10 min and the screw-cap was replaced with a Teflon sealed inlet for a glass rod, through which irradiation with a 455 nm high power LED took place from above while the reaction was magnetically stirred below. After 4 h of irradiation the LED was switched off, the reaction mixture was analyzed by GC-FID and ¹H-NMR showing a *Z*:*E* ratio of 82:18 with both analysis techniques. ¹H NMR (*Z* isomer, 300 MHz, CDCl₃): 7.24 – 6.98 (m, 5H), 6.47 (d, *J* = 11.7 Hz, 1H), 5.66 – 5.55 (m, 1H), 4.65 – 4.58 (m, 2H), 1.85 (s, 3H).

The reaction was repeated as above at 90 °C. GC-FID of the reaction mixture again showed a *Z*:*E* ratio of 82:18.

The reaction was repeated as above at 90 °C with with 2.5 mL MeCN as solvent and 2.5 mL heptane as co-solvent. Ir(ppy)₂(PIB-ppy) (**42**, 11.8 mg, 7.0 μmol, 0.7 mol%) was used instead of *fac*-Ir(ppy)₃. Phases were separated after the reaction. GC-FID of the MeCN phase again showed a *Z*:*E* ratio of 82:18.

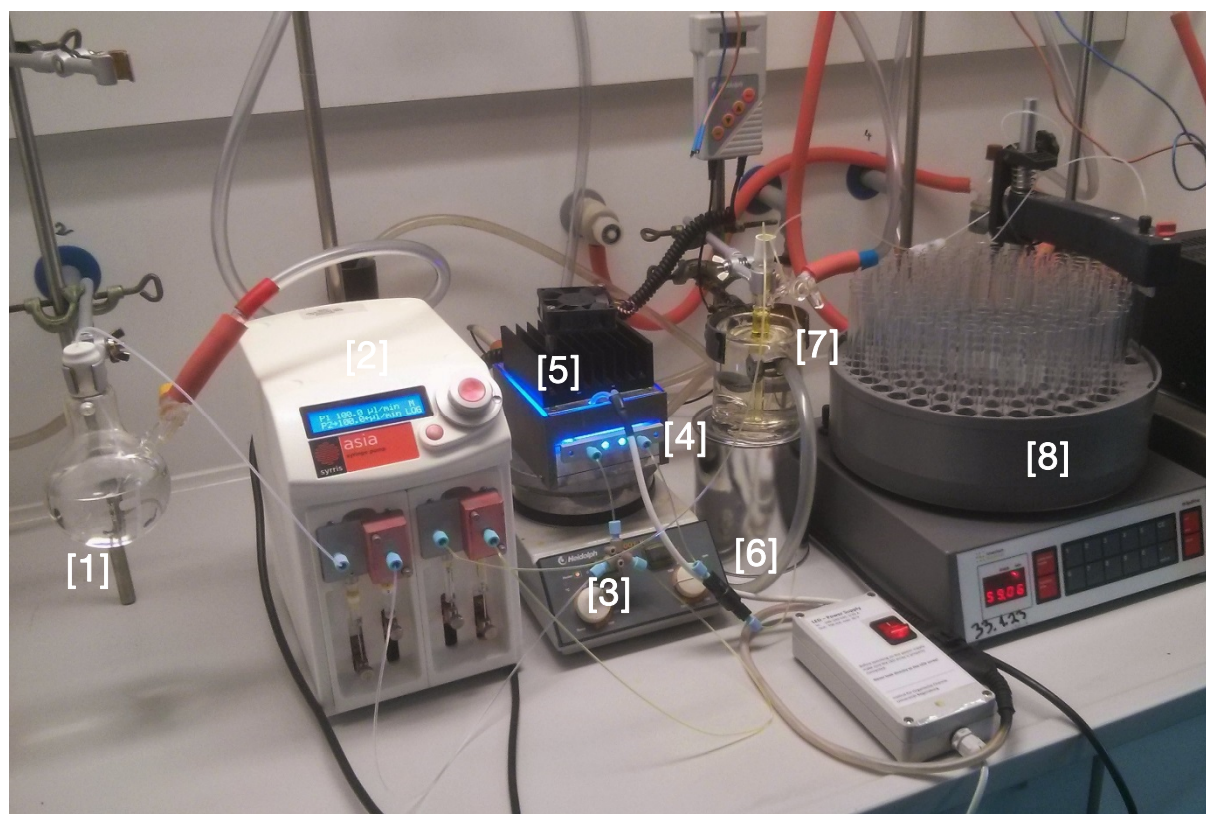
Recycling conditions



(*Z*)-3-phenylallyl acetate (**49**).

Note: Numbers in brackets represent the corresponding device in the picture.

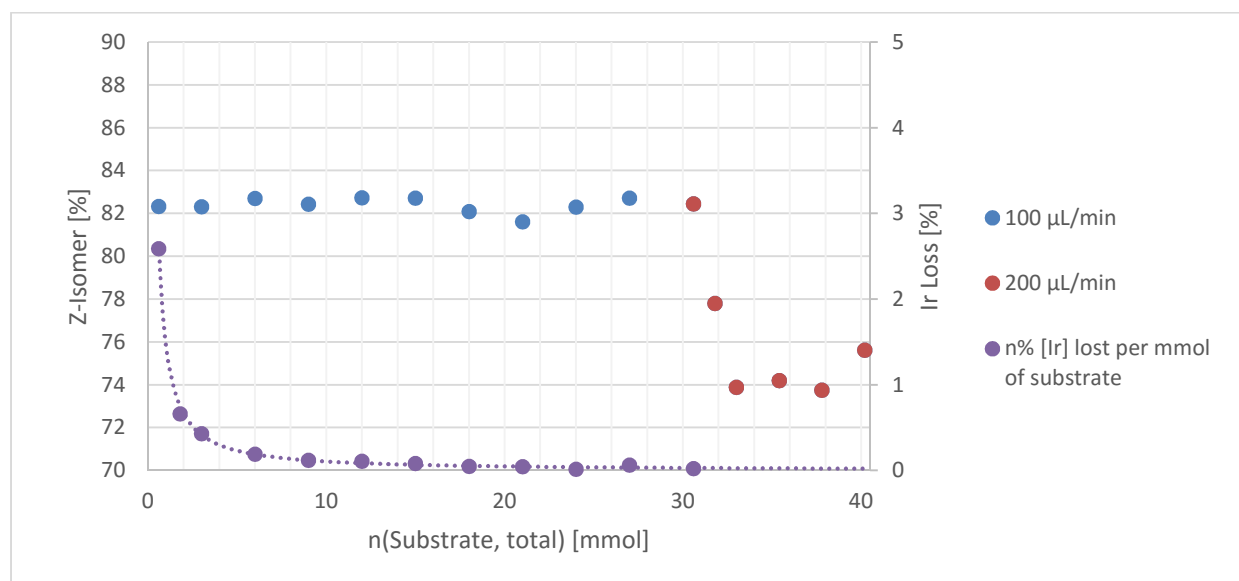
A Schlenk flask [1] was charged with (*E*)-3-phenylallyl acetate (**48**, 7.04 g, 40.0 mmol, 1.00 equiv), 190 mL MeCN (heptane saturated)*, 10 mL heptane**, and ^tPr₂NEt (0.70 mL, 0.52 g, 4.0 mmol, 0.10 equiv). The reaction was degassed by N₂ sparging for 15 min. A Schlenk tube was charged with Ir(ppy)₂(PIB-ppy) (**42**, 11.8 mg, 7.0 μmol, 0.018 mol%) and 5 mL heptane and the mixture was degassed by N₂ sparging for 5 min. The complete microreactor setup was purged with N₂ for 15 min.



The substrate solution [1] was connected to the Asia dual syringe pump system [2] and the photocatalyst solution was transferred to the phase separator unit [7]. The heptane syringe pump was started (100 $\mu\text{L}/\text{min}$) and thus the microreactor unit [4] was filled with catalyst solution. The microreactor unit [4] was heated and once it reached 90 $^{\circ}\text{C}$, the LED array [5] and the MeCN syringe pump were turned on (100 $\mu\text{L}/\text{min}$), heptane and MeCN stream mixed [3] and were subsequently pumped through the hot microreactor unit [4]. In there, the heptane / MeCN reached the upper critical solution temperature (UCST) and thus the mixture became homogeneous. To avoid boiling of the solvent mixture a 60 psi pressure valve [6] was connected to the output of the microreactor unit. After about 3 mL of product-containing MeCN were collected in the phase separator unit [7], the N_2 valve of the phase separator unit was closed which triggered collection of the product-containing MeCN phase in the fraction collector [8]. The collected fractions (pooling rate 30 min, 3.0 mL MeCN, 0.60 mmol product) were analyzed by GC-FID to determine the *Z:E* ratio and afterwards by ICP-OES to determine the iridium content.

For the ICP-OES analysis (*properly working fume hood, full protection gear!*) the solvent of each sample was evaporated in a stream of N_2 and the residue was treated with 2 mL conc HNO_3 (aq), boiled for about 1 min till the evolution of nitrous gases stopped. Afterwards the sample was treated with 2 mL conc H_2SO_4 and again boiled till the evolution of nitrous gases stopped (about 1 min). The sample was then treated with another 2 mL conc HNO_3 (aq) and

boiled till it was a fully homogeneous yellow to orange liquid (about 2 min). After cooling to room temperature, the sample was diluted with water to a total volume of 8.0 mL, filtered through a 0.2 μm syringe filter, and measured in the ICP-OES apparatus.

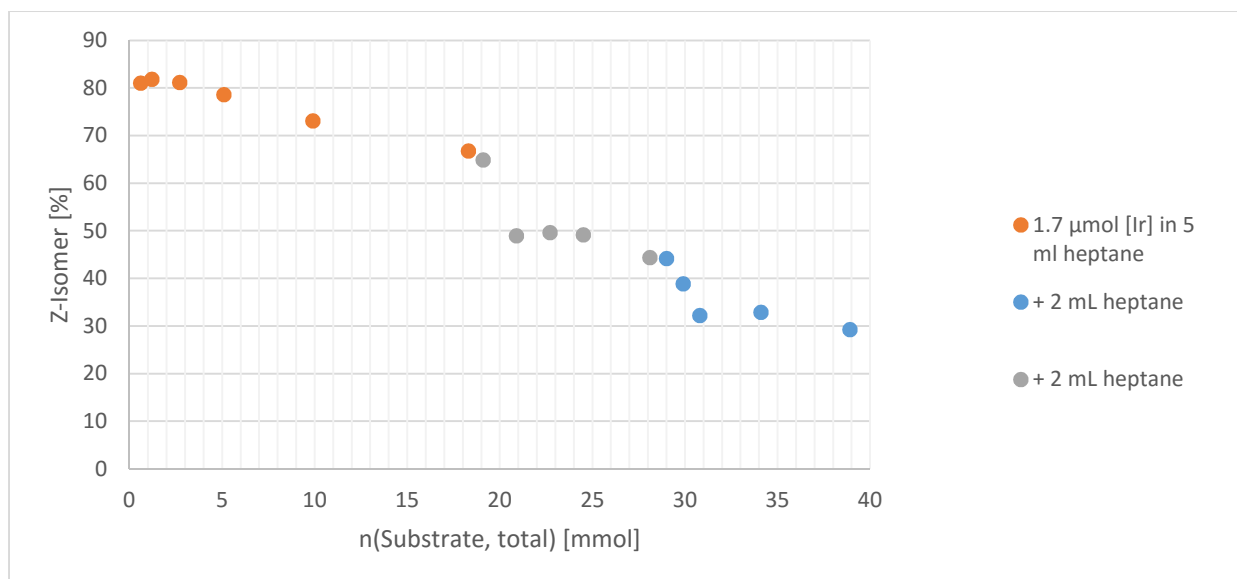


*Heptane saturated MeCN has to be used in order to avoid unnecessary leaching of heptane into the collected MeCN fractions, caused by minimal solubility of heptane in MeCN.

Additionally, the addition of (*E*)-3-phenylallyl acetate (48**, 0.2 M) and Pr_2NEt (0.02 M) to already heptane saturated MeCN leads to an increased solubility of heptane which has to be addressed by the addition of further quantities of heptane to the substrate solution before starting the reaction.

When the reaction setup was run as above with only 2.9 mg $\text{Ir}(\text{ppy})_2(\text{PIB-ppy})$ (**42**, 1.7 μmol) instead of with 11.8 mg $\text{Ir}(\text{ppy})_2(\text{PIB-ppy})$ (**42**, 7.0 μmol), a relative severe decline of the *Z*:*E* ratio can be observed after already 3 mmol of converted substrate.

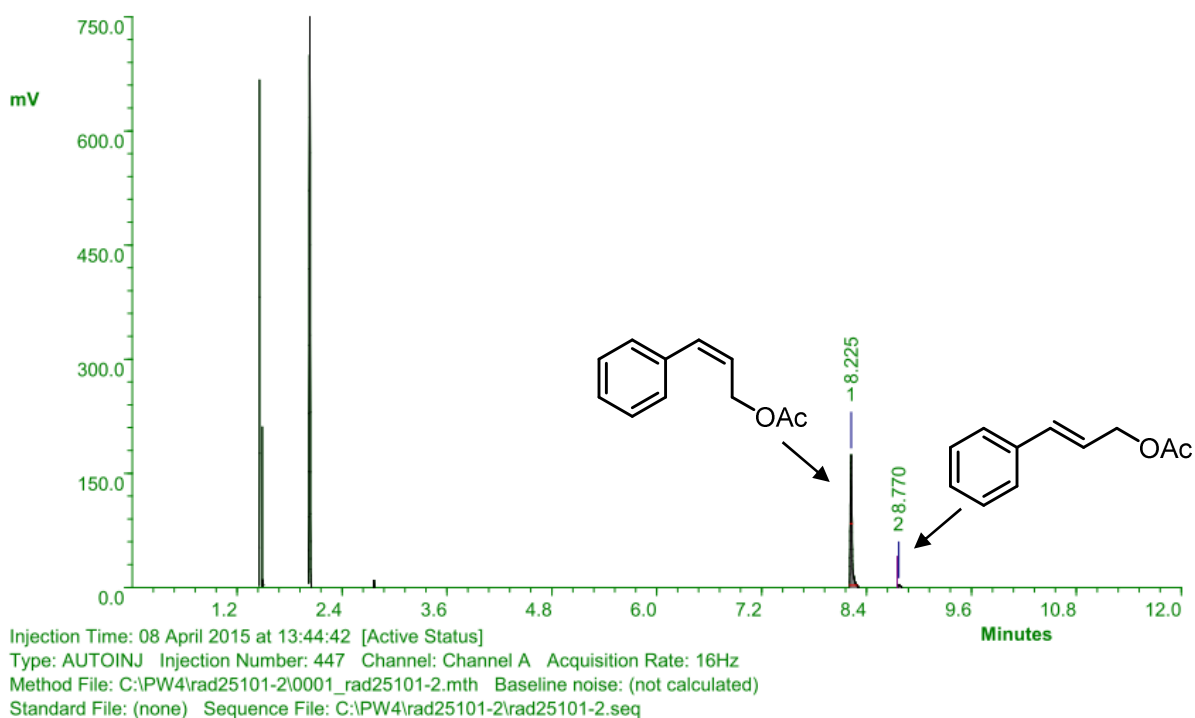
Also, in this experiment the increased solubility of heptane in the reaction solution was not addressed. The lost heptane had to be replaced two times during the experiments with 2 mL heptane each. The so-caused dilution of the catalyst solution lead to two erratic drops in *Z*:*E* ratio.



5.7 GC-FID analysis

An example GC-FID spectrum of the reaction mixture of the photochemical *E/Z* isomerization of (*Z*)-3-phenylallyl acetate (**49**) is depicted below.

PC/Chrom [version 4.6.0.gs] - FILE: C:\PW4\rad25101-2\0447_rad25101-2.pw4
Name: (unnamed)
Description:



Peak	RT	Area	%Ar	Conc.(Ar)	Height	M	Units	Name
1	8.225	305.439	82.12	Not Calculated	180.090	1		
2	8.770	66.497	17.88	Not Calculated	9.806	1		

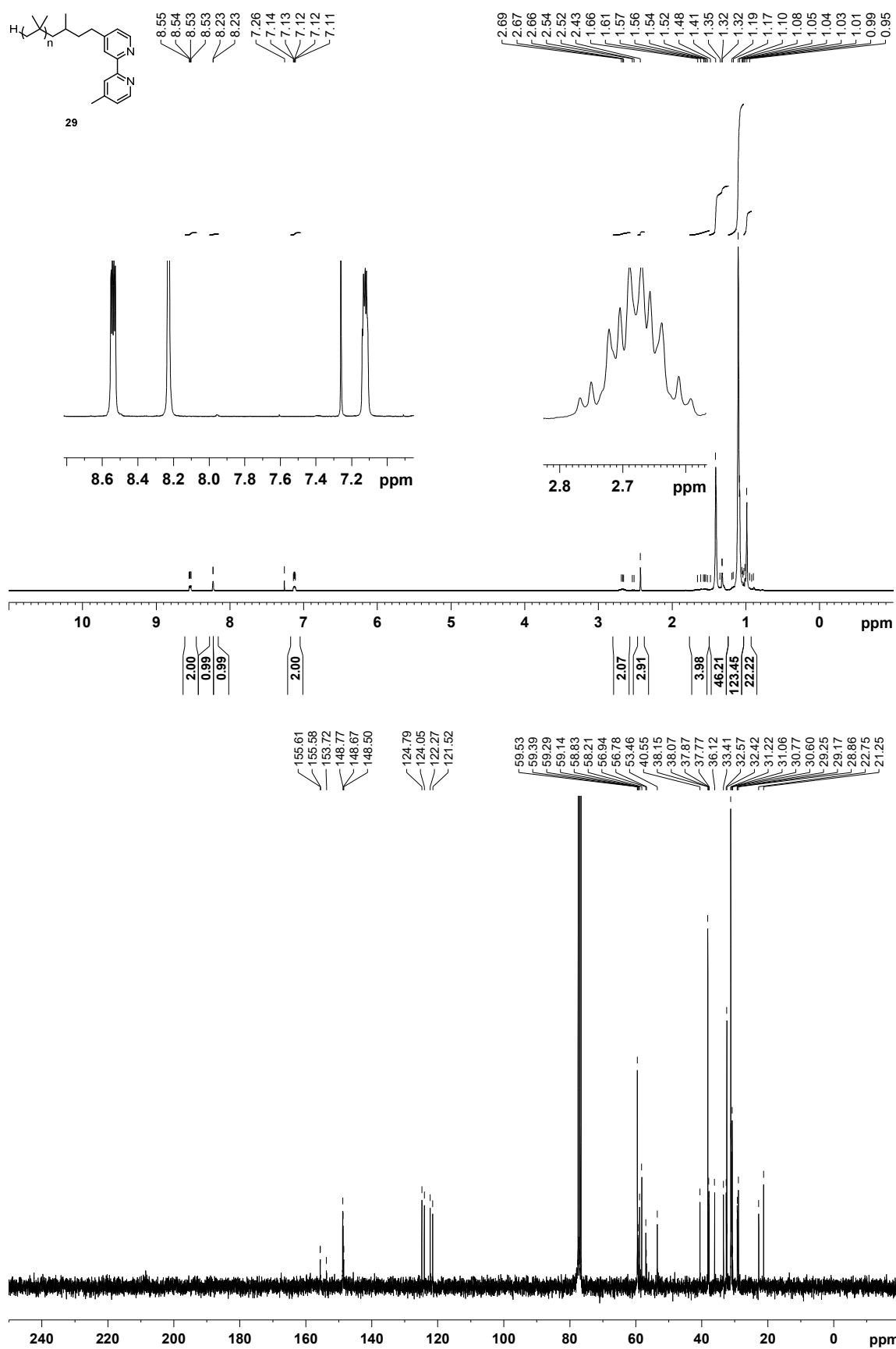
Analyses were carried out using following temperature program:

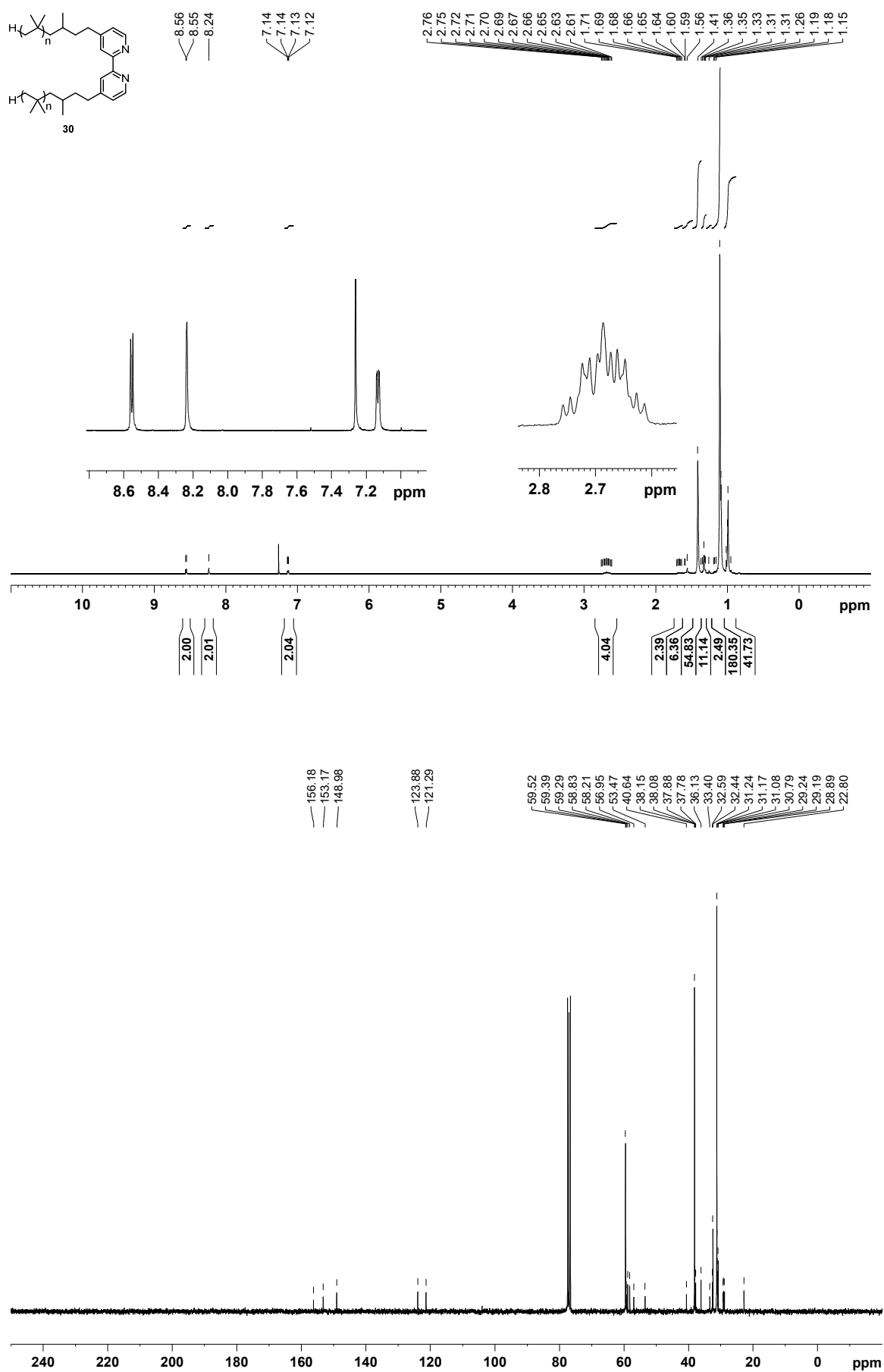
Starting temperature: 75 °C
Hold: 1 min
Heating rate: 15 °C/min
End temperature: 240 °C

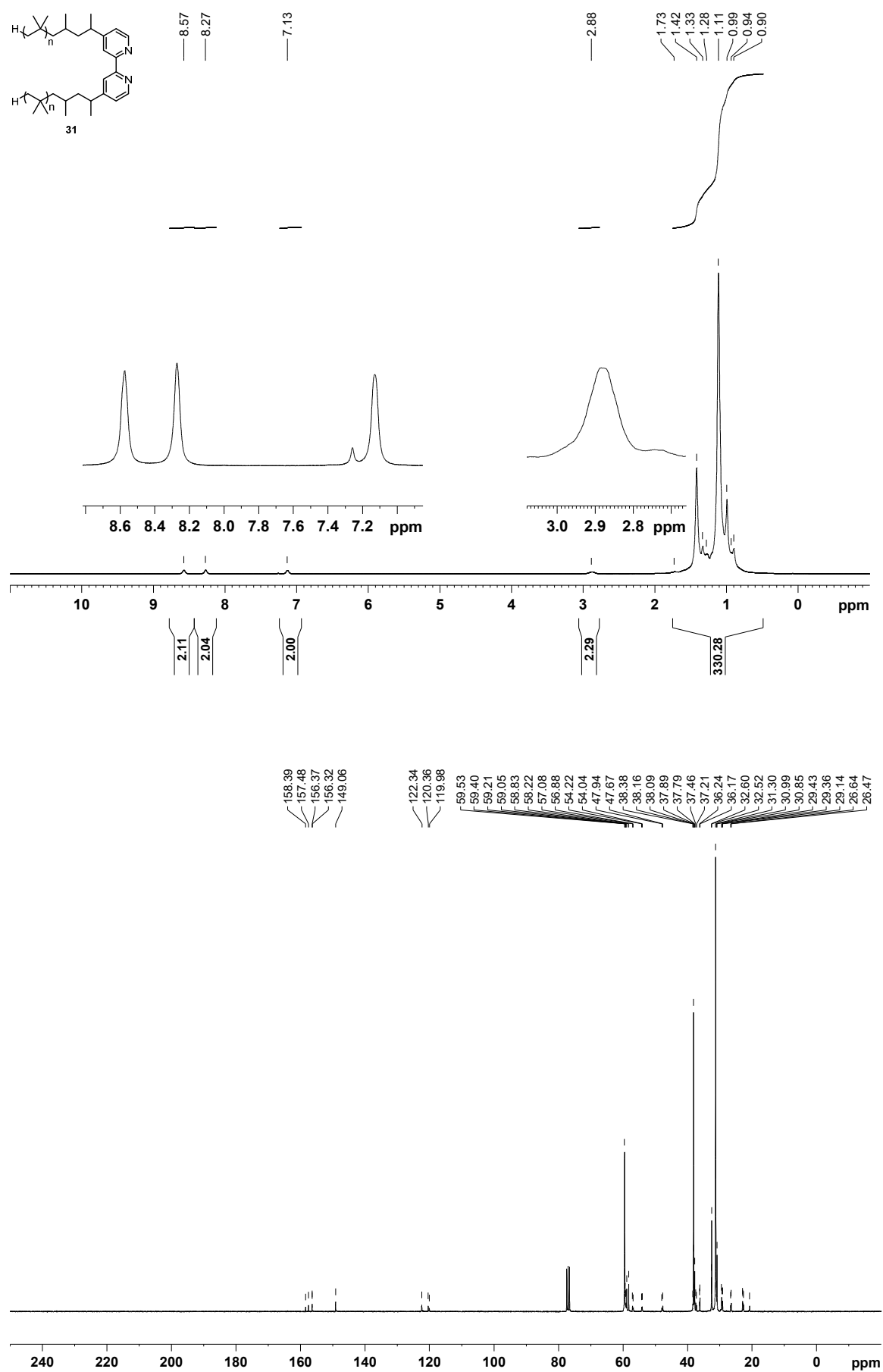
5.8 NMR spectra of new compounds

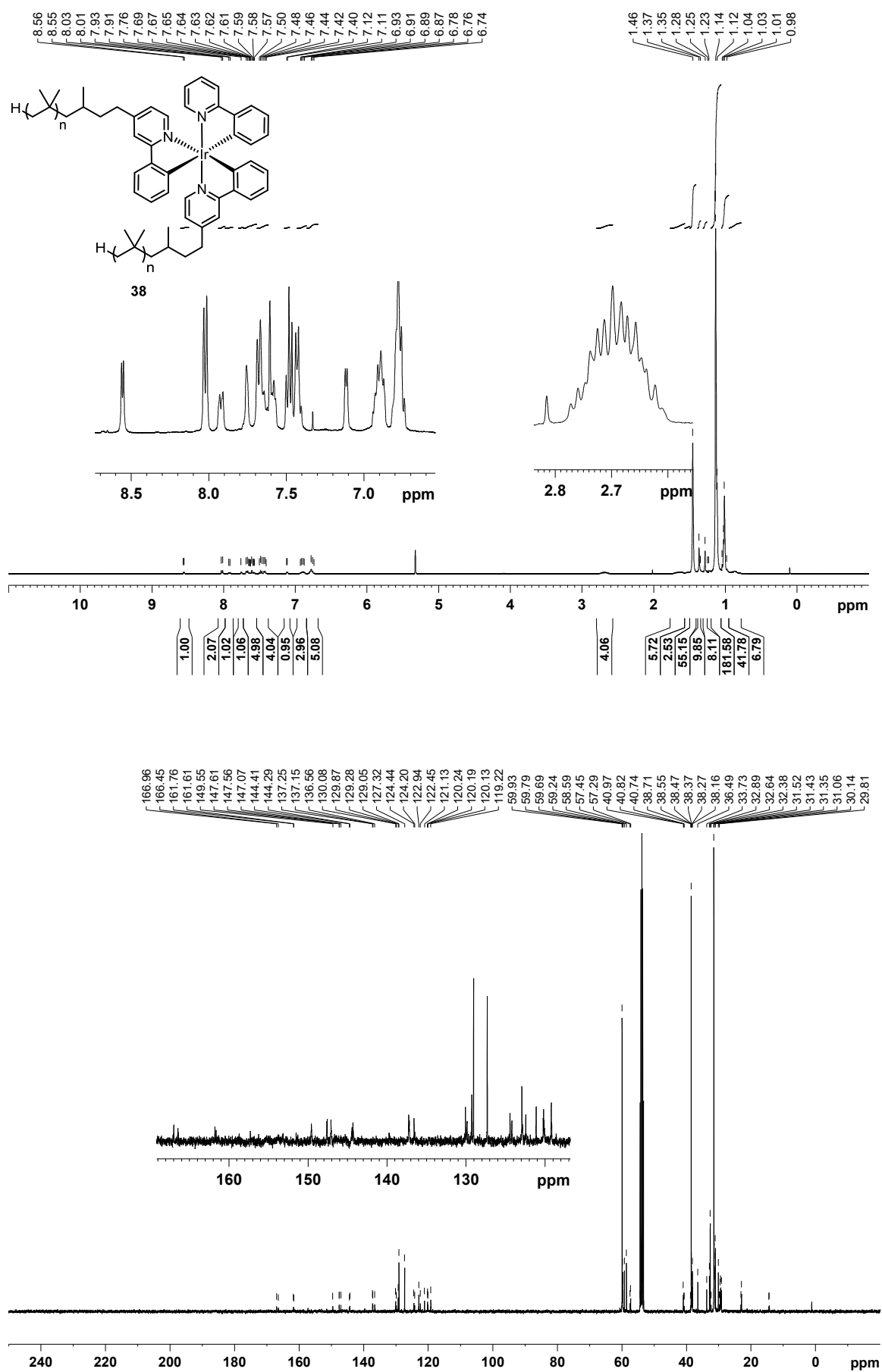
Typically, ^1H -NMR followed by ^{13}C -NMR spectra are depicted. Where the identity of the material might be in question, ^{19}F -NMR (decoupled), ^{31}P -NMR (decoupled), COSY, NOESY, HSQC, and / or HMBC spectra are supplied.

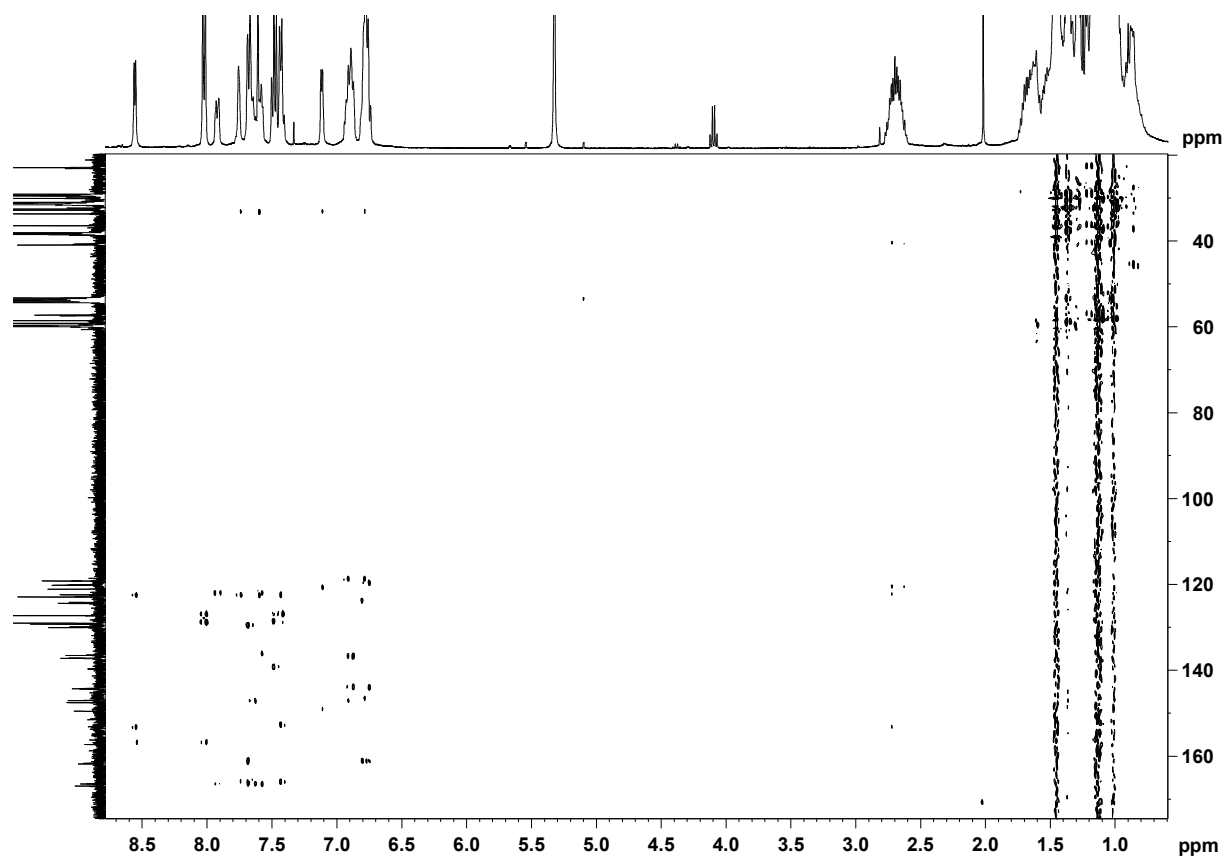
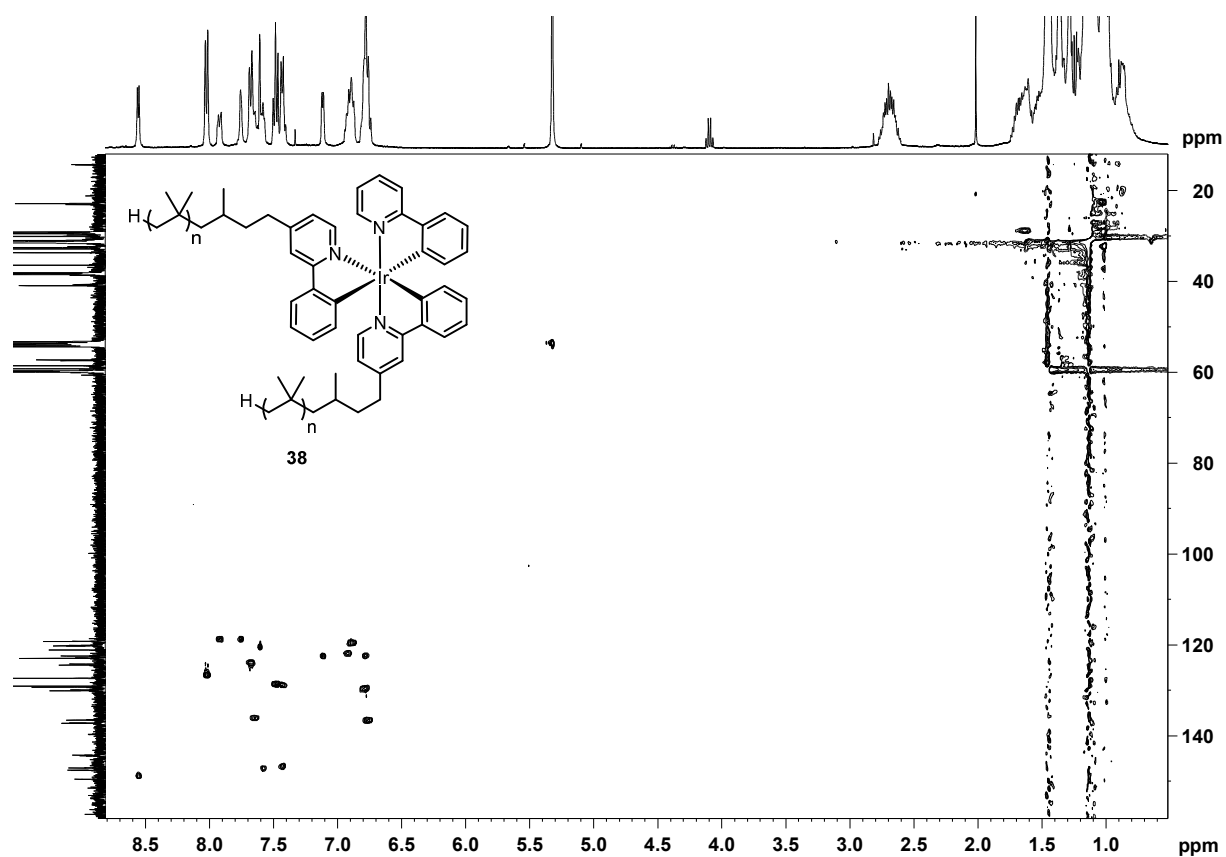
Note: All spectra of new compounds that were already included in any Supporting Information are not part of this printed edition of this work. However, spectra are available in the digital edition.

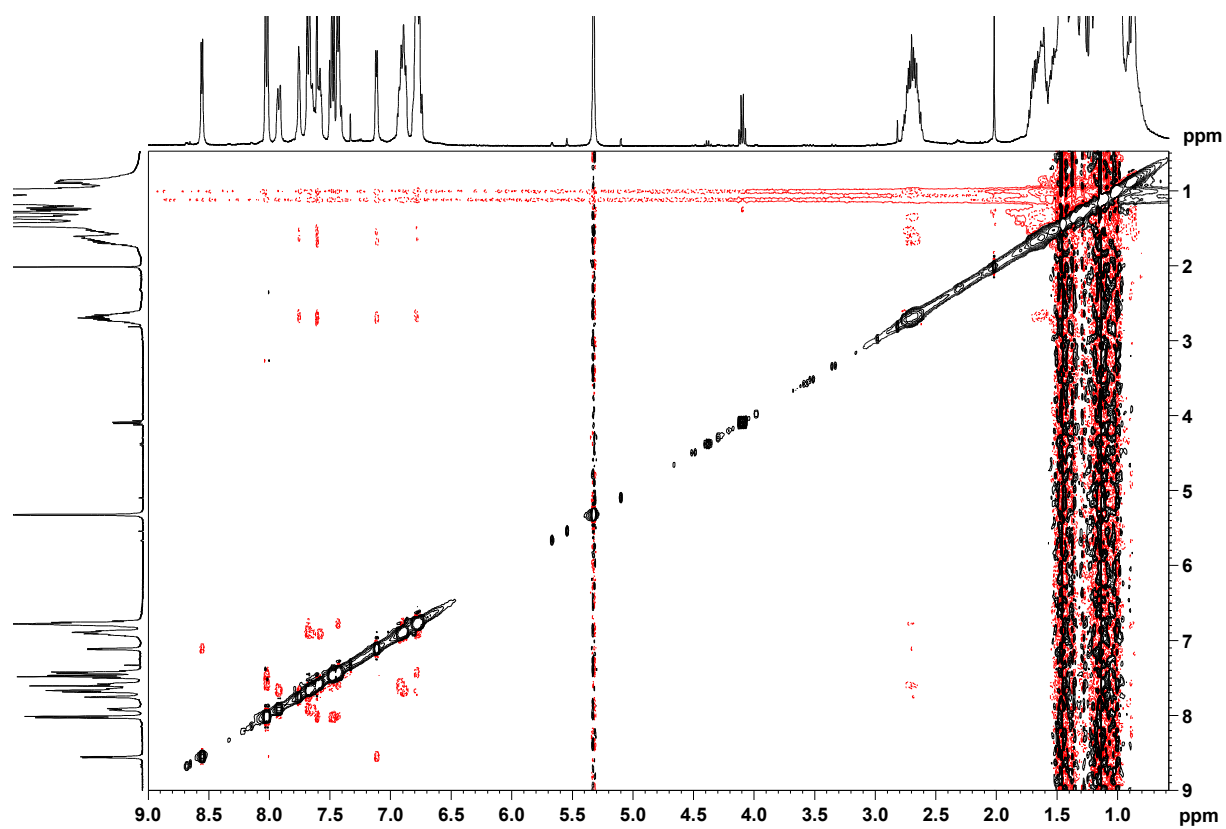
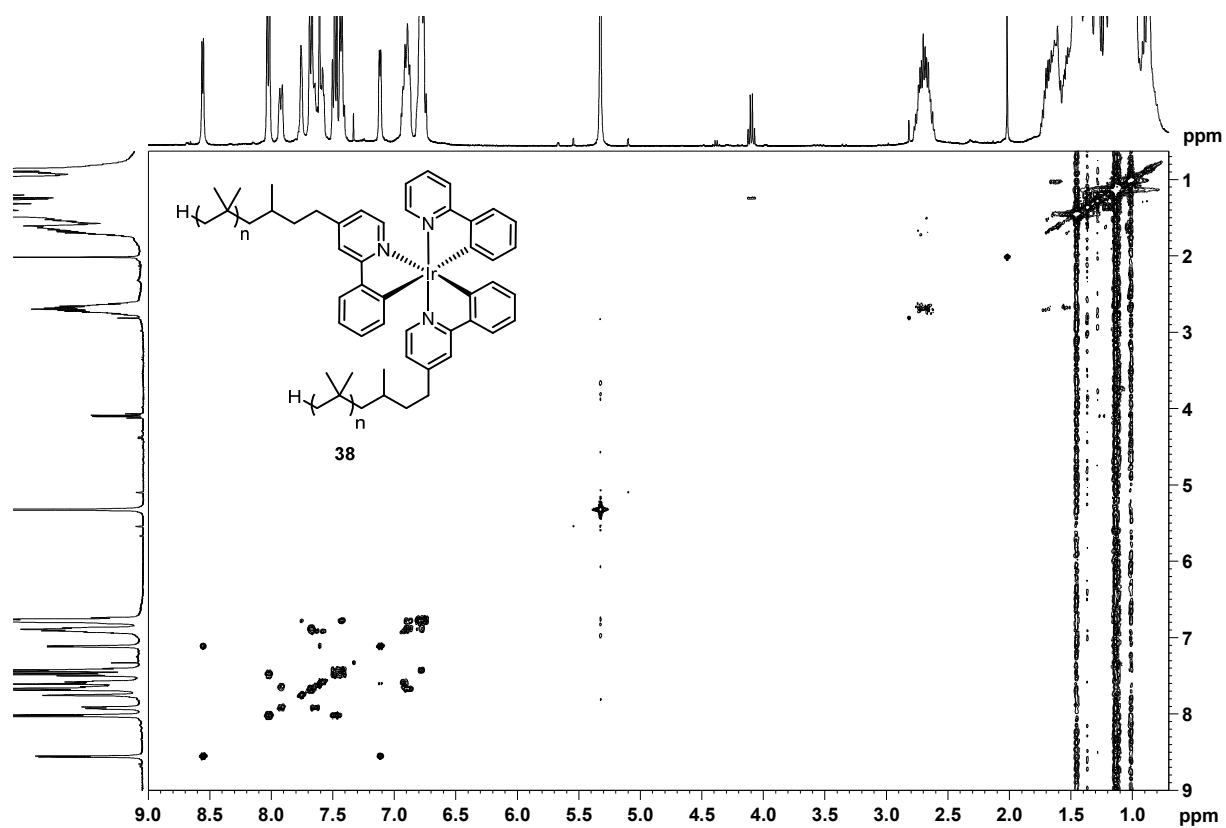


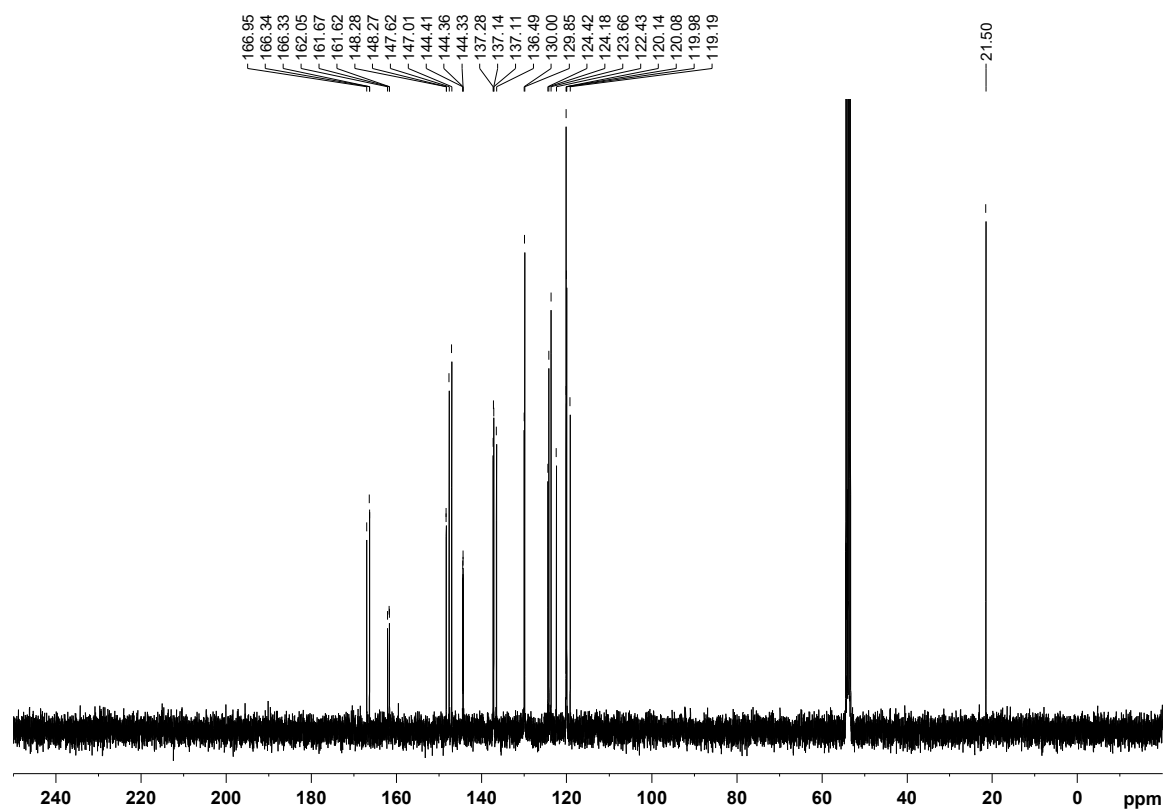
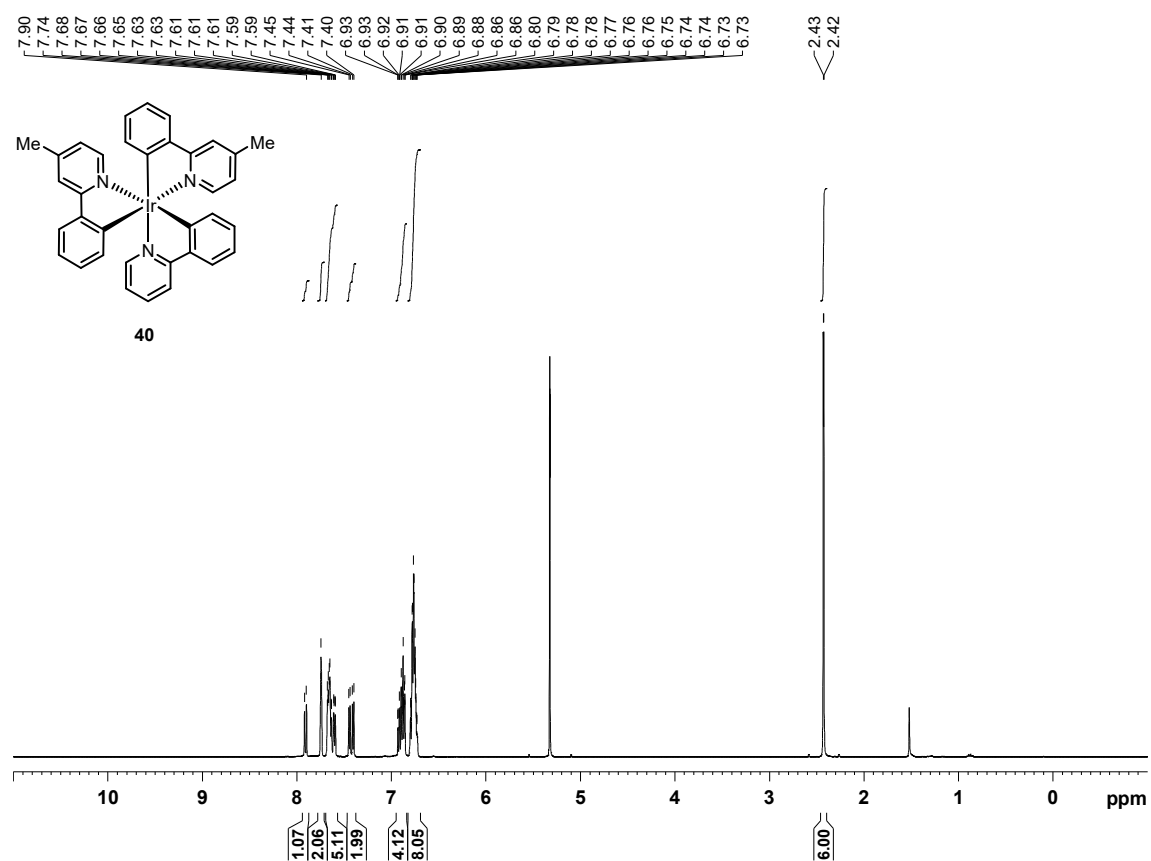


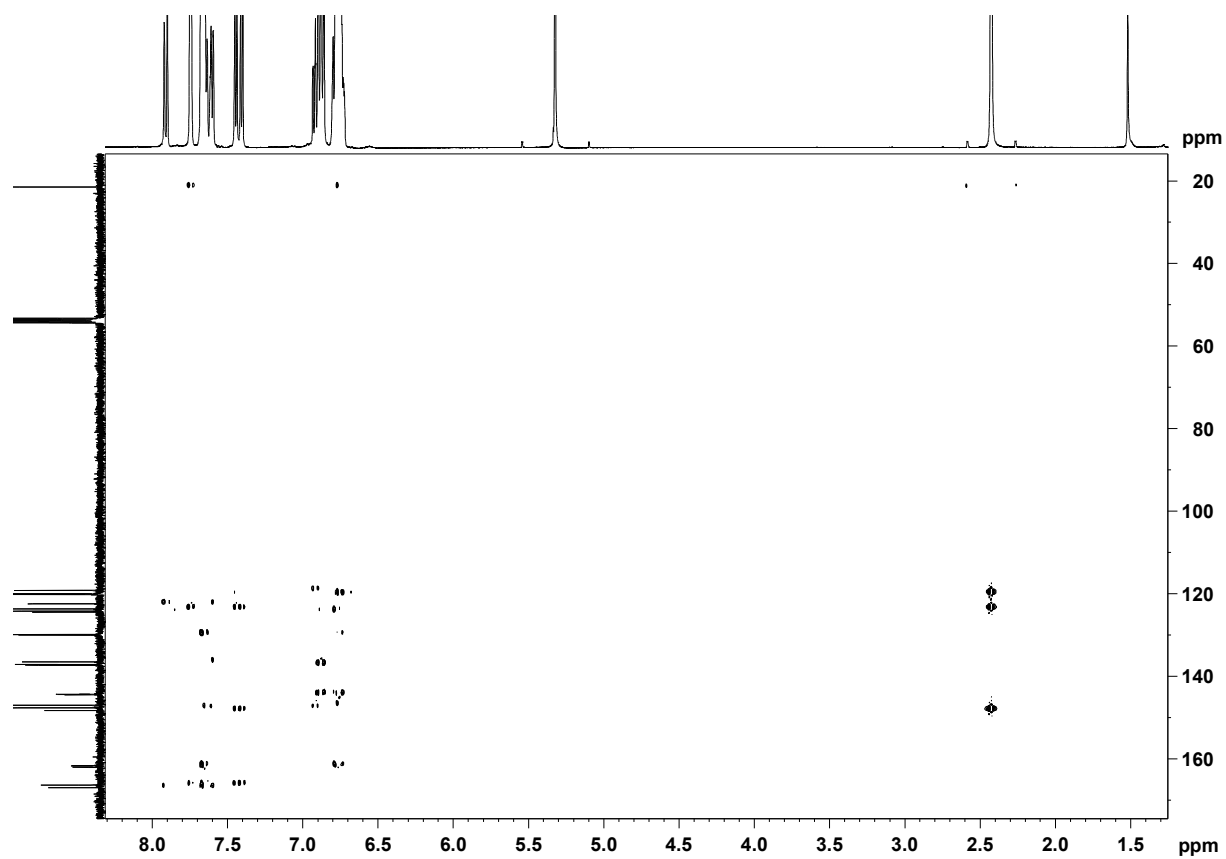
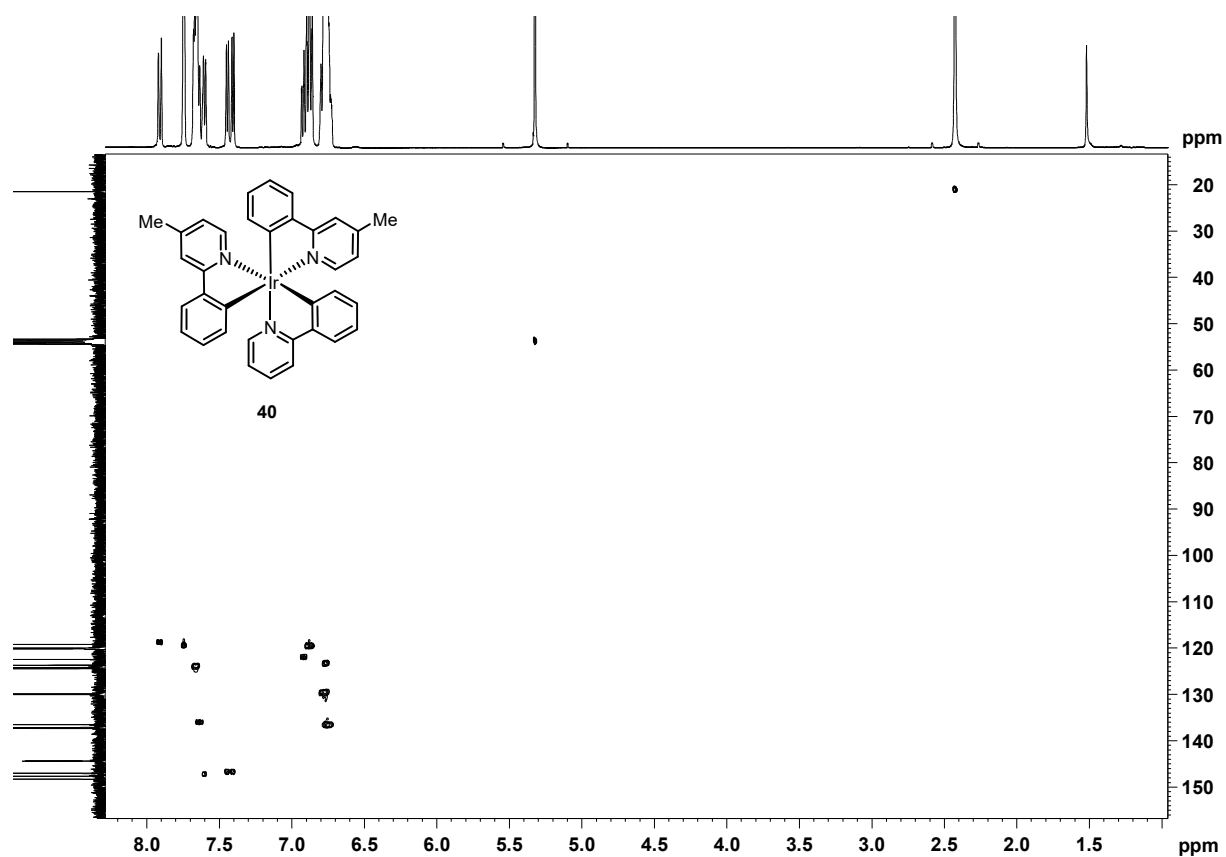


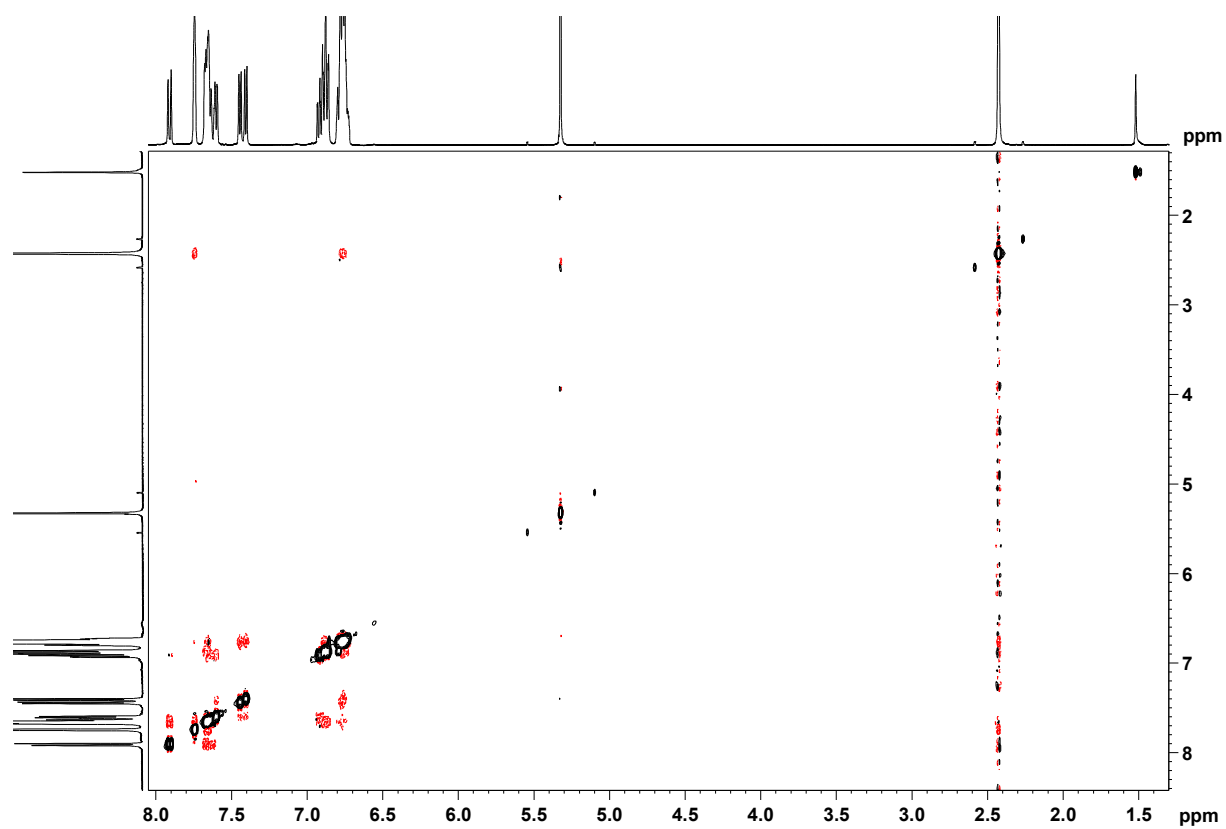
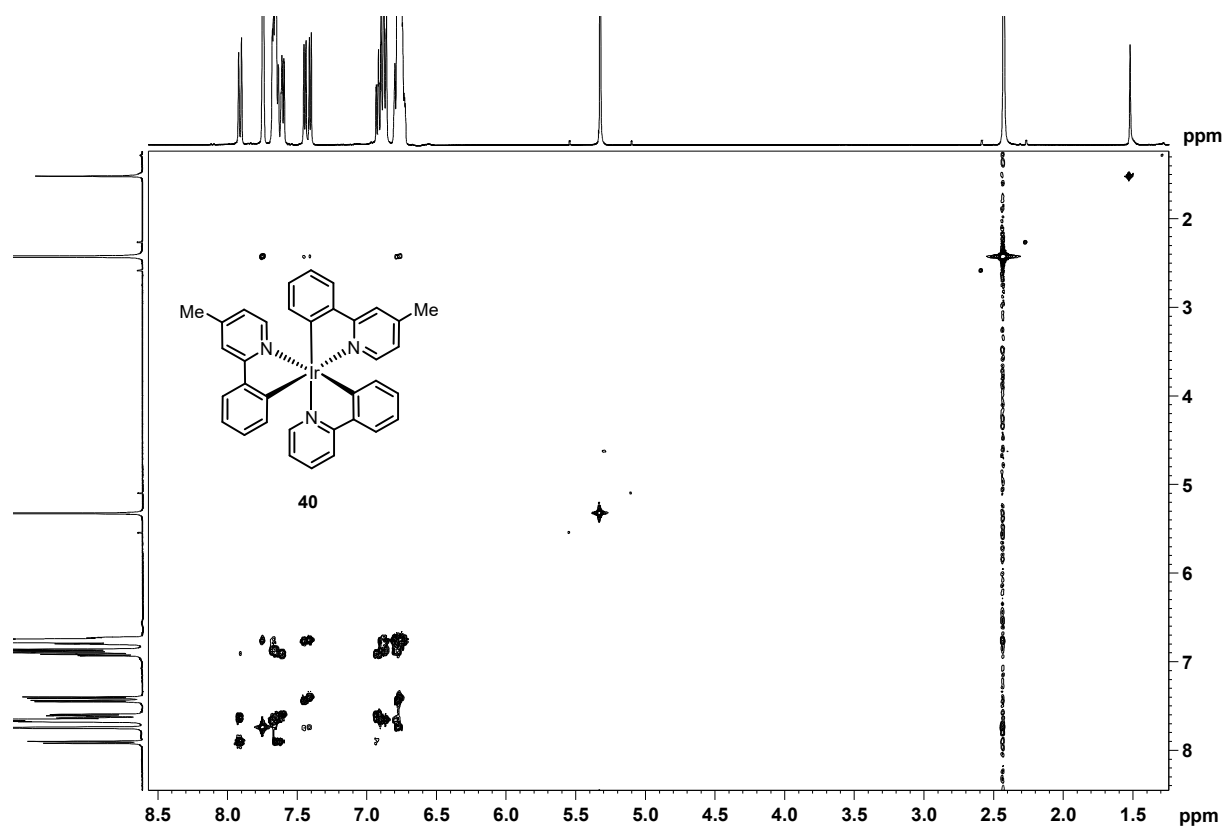


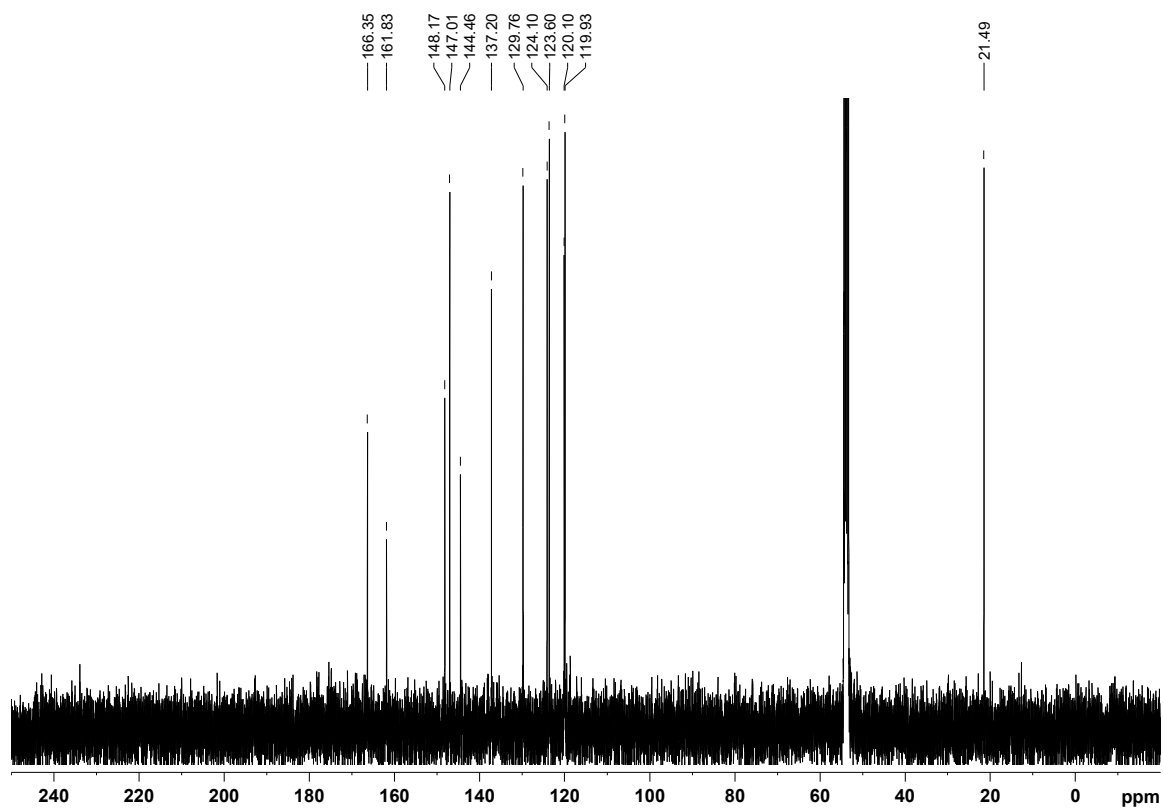
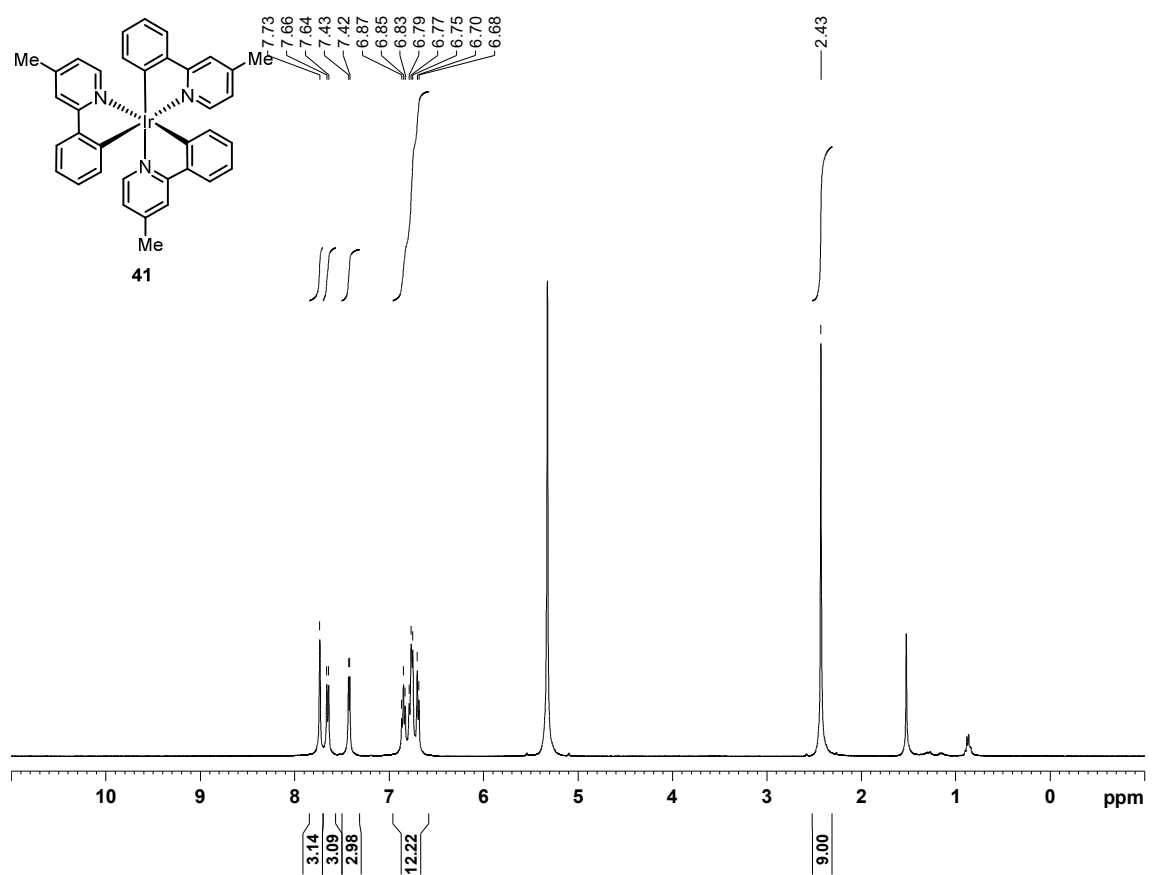


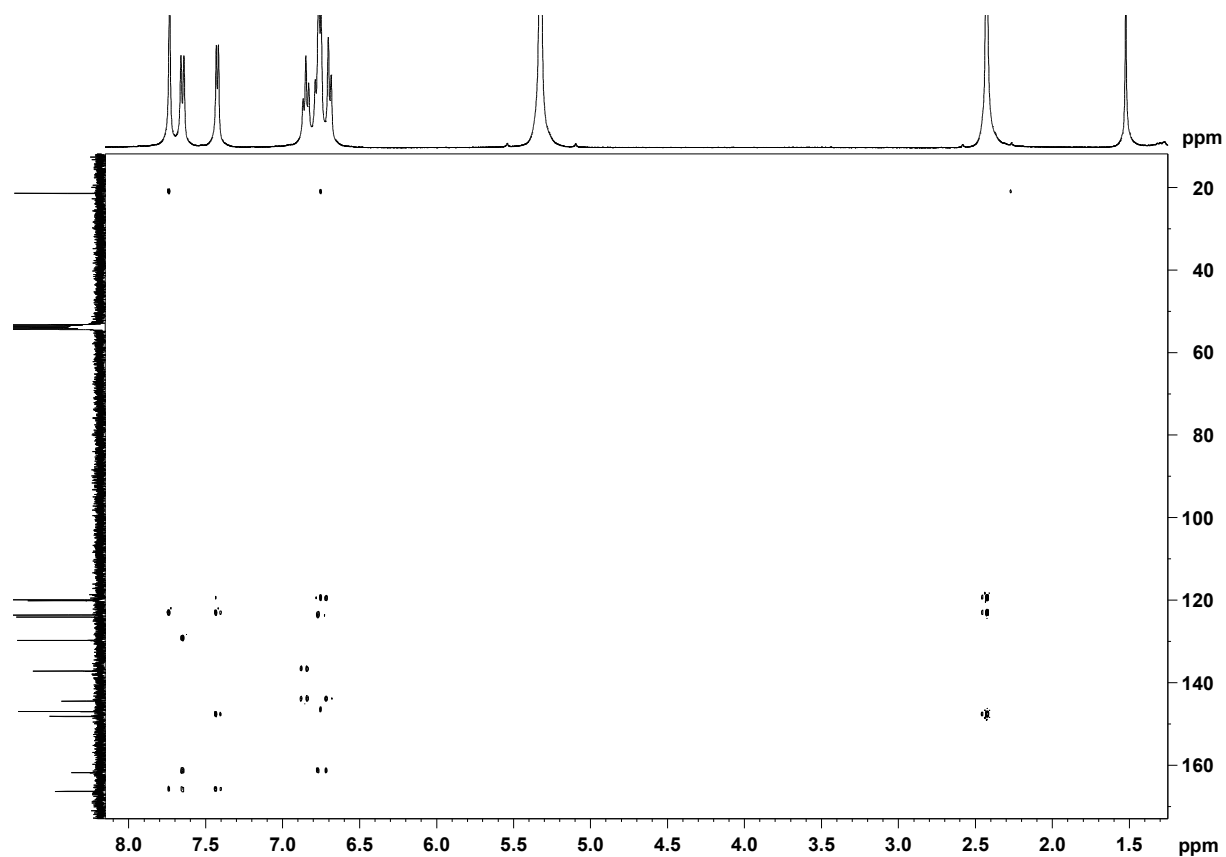
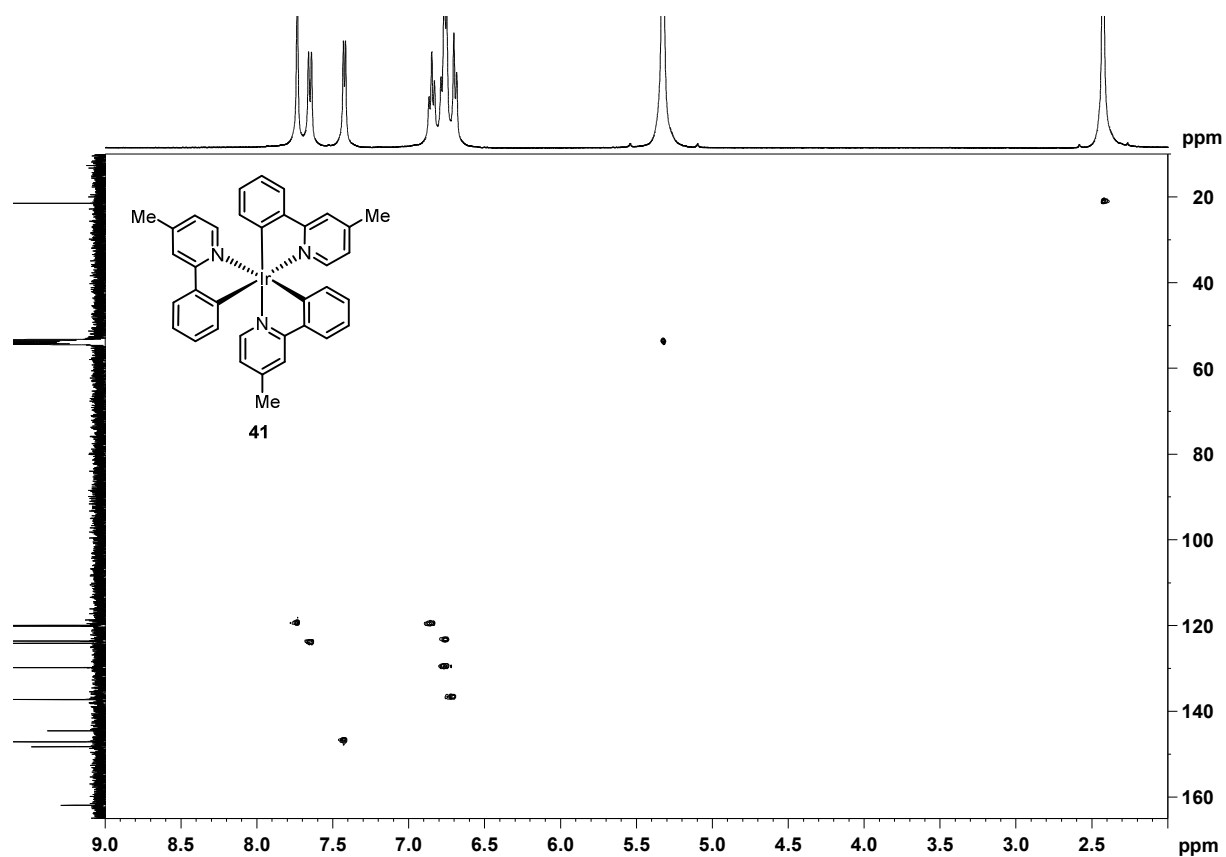


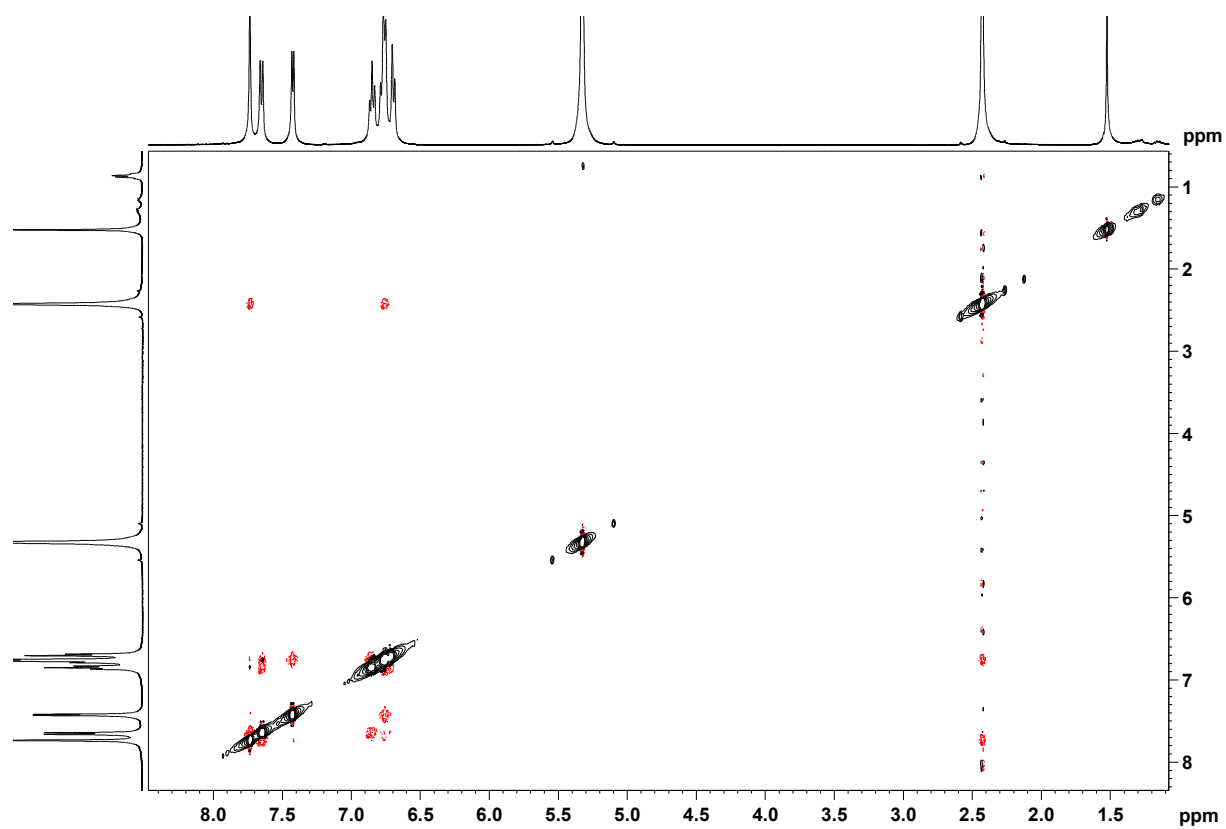
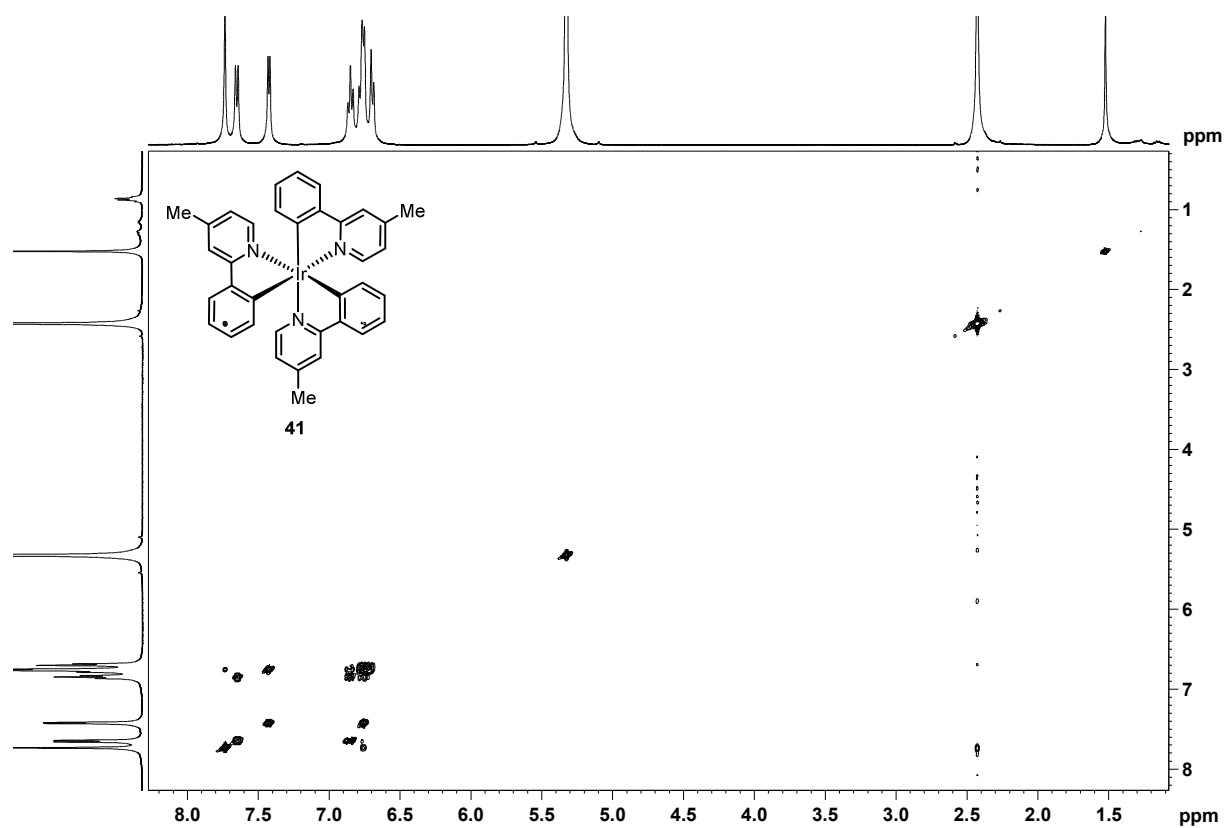












6 Literature

- (1) Van Santen, R. *Catalysis*, 1st ed.; Beller, M., Renken, A., Santen, R. A., Eds.; Wiley-VCH: Weinheim, 2012.
- (2) McNaught, A. D.; Wilkinson, A. *International Union of Pure and Applied Chemistry Compendium of Chemical Terminology*, 2nd ed.; Blackwell Scientific Publications: Oxford, 1997.
- (3) Rothenberg, G. *Catalysis*, 1st ed.; Wiley-VCH: Weinheim, 2008.
- (4) Beller, M. Applying Homogeneous Catalysis for the Synthesis of Pharmaceuticals. In *Ernst Schering Foundation Symposium Proceedings*; Seeberger, P. H., Blume, T., Eds.; Springer: Heidelberg, 2006; pp 99–116.
- (5) Spagnul, C.; Turner, L. C.; Boyle, R. W. Immobilized Photosensitizers for Antimicrobial Applications. *J. Photochem. Photobiol. B Biol.* **2015**.
- (6) Chen, C.; Ma, W.; Zhao, J. Semiconductor-Mediated Photodegradation of Pollutants under Visible-Light Irradiation. *Chem. Soc. Rev.* **2010**, *39*, 4206–4219.
- (7) Wahlen, J.; De Vos, D. E.; Jacobs, P. A.; Alsters, P. L. Solid Materials as Sources for Synthetically Useful Singlet Oxygen. *Adv. Synth. Catal.* **2004**, *346*, 152–164.
- (8) DeRosa, M. C.; Crutchley, R. J. Photosensitized Singlet Oxygen and Its Applications. *Coord. Chem. Rev.* **2002**, *233–234*, 351–371.
- (9) Faust, D.; Funken, K.-H.; Horneck, G.; Milow, B.; Ortner, J.; Sattlegger, M.; Schäfer, M.; Schmitz, C. Immobilized Photosensitizers for Solar Photochemical Applications. *Sol. Energy* **1999**, *65*, 71–74.
- (10) Cherevatskaya, M.; König, B. Heterogeneous Photocatalysts in Organic Synthesis. *Russ. Chem. Rev.* **2014**, *83*, 183–195.
- (11) Palmisano, G.; García-López, E.; Marcì, G.; Loddo, V.; Yurdakal, S.; Augugliaro, V.; Palmisano, L. Advances in Selective Conversions by Heterogeneous Photocatalysis. *Chem. Commun.* **2010**, *46*, 7074–7089.
- (12) Augugliaro, V.; Palmisano, L. Green Oxidation of Alcohols to Carbonyl Compounds by Heterogeneous Photocatalysis. *ChemSusChem* **2010**, *3*, 1135–1138.
- (13) Lang, X.; Chen, X.; Zhao, J. Heterogeneous Visible Light Photocatalysis for Selective Organic Transformations. *Chem. Soc. Rev.* **2014**, *43*, 473–486.
- (14) Yurdakal, S.; Palmisano, G.; Loddo, V.; Alagöz, O.; Augugliaro, V.; Palmisano, L. Selective Photocatalytic Oxidation of 4-Substituted Aromatic Alcohols in Water with Rutile TiO₂ Prepared at Room Temperature. *Green Chem.* **2009**, *11*, 510.
- (15) Tsukamoto, D.; Ikeda, M.; Shiraishi, Y.; Hara, T.; Ichikuni, N.; Tanaka, S.; Hirai, T. Selective Photocatalytic Oxidation of Alcohols to Aldehydes in Water by TiO₂ Partially Coated with WO₃. *Chem. Eur. J.* **2011**, *17*, 9816–9824.
- (16) Li, N.; Lang, X.; Ma, W.; Ji, H.; Chen, C.; Zhao, J. Selective Aerobic Oxidation of Amines to Imines by TiO₂ Photocatalysis in Water. *Chem. Commun.* **2013**, *49*, 5034–5036.

- (17) Ho, X.-H.; Kang, M.-J.; Kim, S.-J.; Park, E. D.; Jang, H.-Y. Green Organophotocatalysis. TiO₂-Induced Enantioselective Alpha-Oxyamination of Aldehydes. *Catal. Sci. Technol.* **2011**, *1*, 923.
- (18) Földner, S.; Pohla, P.; Bartling, H.; Dankesreiter, S.; Stadler, R.; Gruber, M.; Pfitzner, A.; König, B. Selective Photocatalytic Reductions of Nitrobenzene Derivatives Using PbBiO₂X and Blue Light. *Green Chem.* **2011**, *13*, 640.
- (19) Cherevatskaya, M.; Neumann, M.; Földner, S.; Harlander, C.; Kümmel, S.; Dankesreiter, S.; Pfitzner, A.; Zeitler, K.; König, B. Visible-Light-Promoted Stereoselective Alkylation by Combining Heterogeneous Photocatalysis with Organocatalysis. *Angew. Chem. Int. Ed.* **2012**, *51*, 4062–4066.
- (20) Rueping, M.; Zoller, J.; Fabry, D. C.; Poscharny, K.; Koenigs, R. M.; Weirich, T. E.; Mayer, J. Light-Mediated Heterogeneous Cross Dehydrogenative Coupling Reactions: Metal Oxides as Efficient, Recyclable, Photoredox Catalysts in C-C Bond-Forming Reactions. *Chem. Eur. J.* **2012**, *18*, 3478–3481.
- (21) Condie, A. G.; González-Gómez, J. C.; Stephenson, C. R. J. Visible-Light Photoredox Catalysis: Aza-Henry Reactions via C-H Functionalization. *J. Am. Chem. Soc.* **2010**, *132*, 1464–1465.
- (22) Vila, C.; Rueping, M. Visible-Light Mediated Heterogeneous C-H Functionalization: Oxidative Multi-Component Reactions Using a Recyclable Titanium Dioxide (TiO₂) Catalyst. *Green Chem.* **2013**, *15*, 2056.
- (23) Liu, C.; Zhao, W.; Huang, Y.; Wang, H.; Zhang, B. Light-Induced BiOBr Nanosheets Accelerated Highly Regioselective Intermolecular Trifluoromethylation/arylation of Alkenes to Synthesize CF₃-Containing Aza-Heterocycles. *Tetrahedron* **2015**, *71*, 4344–4351.
- (24) Zoller, J.; Fabry, D. C.; Rueping, M. Unexpected Dual Role of Titanium Dioxide in the Visible Light Heterogeneous Catalyzed C-H Arylation of Heteroarenes. *ACS Catal.* **2015**, 3900–3904.
- (25) Tada, H.; Jin, Q.; Nishijima, H.; Yamamoto, H.; Fujishima, M.; Okuoka, S. I.; Hattori, T.; Sumida, Y.; Kobayashi, H. Titanium(IV) Dioxide Surface-Modified with Iron Oxide as a Visible Light Photocatalyst. *Angew. Chem. Int. Ed.* **2011**, *50*, 3501–3505.
- (26) Tang, J.; Grampp, G.; Liu, Y.; Wang, B.-X.; Tao, F.-F.; Wang, L.-J.; Liang, X.-Z.; Xiao, H.-Q.; Shen, Y.-M. Visible Light Mediated Cyclization of Tertiary Anilines with Maleimides Using Nickel(II) Oxide Surface-Modified Titanium Dioxide Catalyst. *J. Org. Chem.* **2015**, *80*, 2724–2732.
- (27) Kamegawa, T.; Seto, H.; Matsuura, S.; Yamashita, H. Preparation of Hydroxynaphthalene-Modified TiO₂ via Formation of Surface Complexes and Their Applications in the Photocatalytic Reduction of Nitrobenzene under Visible-Light Irradiation. *ACS Appl. Mater. Interfaces* **2012**, *4*, 6635–6639.
- (28) McTiernan, C. D.; Pitre, S. P.; Ismaili, H.; Scaiano, J. C. Heterogeneous Light-Mediated Reductive Dehalogenations and Cyclizations Utilizing Platinum Nanoparticles on Titania (PtNP@TiO₂). *Adv. Synth. Catal.* **2014**, *356*, 2819–2824.
- (29) Nguyen, J. D.; D'Amato, E. M.; Narayanam, J. M. R.; Stephenson, C. R. J. Engaging Unactivated Alkyl, Alkenyl and Aryl Iodides in Visible-Light-Mediated Free Radical Reactions. *Nat. Chem.* **2012**, *4*, 854–859.
- (30) Ischay, M. A.; Anzovino, M. E.; Du, J.; Yoon, T. P. Efficient Visible Light Photocatalysis of [2+2] Enone Cycloadditions. *J. Am. Chem. Soc.* **2008**, *130*, 12886–12887.
-

- (31) Du, J.; Espelt, L. R.; Guzei, I. A.; Yoon, T. P. Photocatalytic Reductive Cyclizations of Enones: Divergent Reactivity of Photogenerated Radical and Radical Anion Intermediates. *Chem. Sci.* **2011**, *2*, 2115–2119.
- (32) Sun, Q.; Dai, Z.; Liu, X.; Sheng, N.; Deng, F.; Meng, X.; Xiao, F.-S. Highly Efficient Heterogeneous Hydroformylation over Rh-Metalated Porous Organic Polymers: Synergistic Effect of High Ligand Concentration and Flexible Framework. *J. Am. Chem. Soc.* **2015**, *137*, 5204–5209.
- (33) Zhai, W.; Xue, S.; Zhu, A.; Luo, Y.; Tian, Y. Plasmon-Driven Selective Oxidation of Aromatic Alcohols to Aldehydes in Water with Recyclable Pt/TiO₂ Nanocomposites. *ChemCatChem* **2011**, *3*, 127–130.
- (34) Tsukamoto, D.; Shiraishi, Y.; Sugano, Y.; Ichikawa, S.; Tanaka, S.; Hirai, T. Gold Nanoparticles Located at the Interface of Anatase/Rutile TiO₂ Particles as Active Plasmonic Photocatalysts for Aerobic Oxidation. *J. Am. Chem. Soc.* **2012**, *134*, 6309–6315.
- (35) Pineda, A.; Gomez, L.; Balu, A. M.; Sebastian, V.; Ojeda, M.; Arruebo, M.; Romero, A. A.; Santamaria, J.; Luque, R. Laser-Driven Heterogeneous Catalysis: Efficient Amide Formation Catalysed by Au/SiO₂ Systems. *Green Chem.* **2013**, *15*, 2043–2049.
- (36) Wang, Z. J.; Ghasimi, S.; Landfester, K.; Zhang, K. a. I. Photocatalytic Suzuki Coupling Reaction Using Conjugated Microporous Polymer with Immobilized Palladium Nanoparticles under Visible Light. *Chem. Mater.* **2015**, 1921–1924.
- (37) Li, X.-H.; Baar, M.; Blechert, S.; Antonietti, M. Facilitating Room-Temperature Suzuki Coupling Reaction with Light: Mott-Schottky Photocatalyst for C-C-Coupling. *Sci. Rep.* **2013**, *3*, 1743.
- (38) Chen; Xiufang; Zhang; Jinshui; Fu; Xianzhi; Antonietti; Markus; Wang; Xinchun. Fe-G-C₃N₄-Catalyzed Oxidation of Benzene to Phenol Using Hydrogen Peroxide and Visible Light. *J. Am. Chem. Soc.* **2010**, *131*, 11658–11659.
- (39) Zheng, Z.; Zhou, X. Metal-Free Oxidation of Alpha-Hydroxy Ketones to 1,2-Diketones Catalyzed by Mesoporous Carbon Nitride with Visible Light. *Chinese J. Chem.* **2012**, *30*, 1683–1686.
- (40) Zhang, P.; Wang, Y.; Yao, J.; Wang, C.; Yan, C.; Antonietti, M.; Li, H. Visible-Light-Induced Metal-Free Allylic Oxidation Utilizing a Coupled Photocatalytic System of G-C₃N₄ and N-Hydroxy Compounds. *Adv. Synth. Catal.* **2011**, *353*, 1447–1451.
- (41) Zhang, P.; Wang, Y.; Li, H.; Antonietti, M. Metal-Free Oxidation of Sulfides by Carbon Nitride with Visible Light Illumination at Room Temperature. *Green Chem.* **2012**, *14*, 1904.
- (42) Su, F.; Mathew, S. C.; Möhlmann, L.; Antonietti, M.; Wang, X.; Blechert, S. Aerobic Oxidative Coupling of Amines by Carbon Nitride Photocatalysis with Visible Light. *Angew. Chem. Int. Ed.* **2011**, *50*, 657–660.
- (43) Möhlmann, L.; Baar, M.; Rieß, J.; Antonietti, M.; Wang, X.; Blechert, S. Carbon Nitride-Catalyzed Photoredox C-C Bond Formation with N-Aryltetrahydroisoquinolines. *Adv. Synth. Catal.* **2012**, *354*, 1909–1913.
- (44) Möhlmann, L.; Blechert, S. Carbon Nitride-Catalyzed Photoredox Sakurai Reactions and Allylboration. *Adv. Synth. Catal.* **2014**, *356*, 2825–2829.
- (45) Baar, M.; Blechert, S. Graphitic Carbon Nitride Polymer as a Recyclable Photoredox Catalyst for Fluoroalkylation of Arenes. *Chem. Eur. J.* **2015**, *21*, 526–530.
-

- (46) Luo, J.; Zhang, X.; Zhang, J. Carbazolic Porous Organic Framework as an Efficient, Metal-Free Visible-Light Photocatalyst for Organic Synthesis. *ACS Catal.* **2015**, 2250–2254.
- (47) Schaap, A. P.; Thayer, A. L.; Zaklika, K. A.; Valenti, P. C. Photooxygenations in Aqueous Solution with a Hydrophilic Polymer-Immobilized Photosensitizer. *J. Am. Chem. Soc.* **1979**, 101, 4016–4017.
- (48) Neckers, D. C.; Blossey, E. C.; Schaap, A. P. Polymer-Bound Photosensitizing Catalysts. US4315998, 1982.
- (49) Burguete, M. I.; Gavara, R.; Galindo, F.; Luis, S. V. New Polymer-Supported Photocatalyst with Improved Compatibility with Polar Solvents. Synthetic Application Using Solar Light as Energy Source. *Catal. Commun.* **2010**, 11, 1081–1084.
- (50) Tamagaki, S.; Liesner, C. E.; Neckers, D. C. Polymer-Based Sensitizers for Photochemical Reactions. Silica Gel as a Support. *J. Org. Chem.* **1980**, 45, 1573–1576.
- (51) Kenley, R. A.; Kirshen, N. A.; Mill, T. Photooxidation of Di-N-Butyl Sulfide Using Sensitizers Immobilized in Polymer Films. *Macromolecules* **1980**, 13, 808–815.
- (52) Guarini, A.; Tundo, P. Rose Bengal Functionalized Phase-Transfer Catalysts Promoting Photooxidations with Singlet Oxygen. Nucleophilic Displacements on Dioxetanic and Endoperoxidic Intermediates. *J. Org. Chem.* **1987**, 52, 3501–3508.
- (53) Gerdes, R.; Bartels, O.; Schneider, G.; Wöhrle, D.; Schulz-Ekloff, G. Photooxidations of Phenol, Cyclopentadiene and Citronellol with Photosensitizers Ionically Bound at a Polymeric Ion Exchanger. *Polym. Adv. Technol.* **2001**, 12, 152–160.
- (54) Fall, A. Synthesis and Use of Imidazolium Bound Rose Bengal Derivatives for Singlet Oxygen Generation. *Open Org. Chem. J.* **2012**, 6, 21–26.
- (55) Rabek, J. F. Applications of Polymers in Solar Energy Utilization. *Prog. Polym. Sci.* **1988**, 13, 83–188.
- (56) Oxidations, O.; Maldotti, A.; Andreotti, L.; Molinari, A.; Borisov, S.; Vasil, V. Photoinitiated Catalysis in Nafion Membranes Containing Palladium(II) Meso-Tetrakis(N-Methyl-4-Pyridyl)porphyrin and Iron(III) Meso-Tetrakis(2,6-Dichlorophenyl)porphyrin for O₂-Mediated Oxidations of Alkenes. *Chem. Eur. J.* **2001**, 7, 3564–3571.
- (57) Pace, A.; Clennan, E. L. A New Experimental Protocol for Intrazeolite Photooxidations. The First Product-Based Estimate of an Upper Limit for the Intrazeolite Singlet Oxygen Lifetime. *J. Am. Chem. Soc.* **2002**, 124, 11236–11237.
- (58) Soggiu, N.; Cardy, H.; Habib Jiwan, J. L.; Leray, I.; Soumilion, J. P.; Lacombe, S. Organic Sulfides Photooxidation Using Sensitizers Covalently Grafted on Silica: Towards a More Efficient and Selective Solar Photochemistry. *J. Photochem. Photobiol. A Chem.* **1999**, 124, 1–8.
- (59) Xu, H.; Chan, W. K.; Ng, D. K. P. Efficient and Recyclable Phthalocyanine-Based Sensitizers for Photooxygenation Reactions. *Synthesis* **2009**, 1791–1796.
- (60) Chavan, S. A.; Maes, W.; Gevers, L. E. M.; Wahlen, J.; Vankelecom, I. F. J.; Jacobs, P. A.; Dehaen, W.; De Vos, D. E. Porphyrin-Functionalized Dendrimers: Synthesis and Application as Recyclable Photocatalysts in a Nanofiltration Membrane Reactor. *Chem. Eur. J.* **2005**, 11, 6754–6762.

- (61) Van Laar, F. M. P. R.; Holsteyns, F.; Vankelecom, I. F. J.; Smeets, S.; Dehaen, W.; Jacobs, P. A. Singlet Oxygen Generation Using PDMS Occluded Dyes. *J. Photochem. Photobiol. A Chem.* **2001**, *144*, 141–151.
- (62) Han, X.; Bourne, R. A.; Poliakoff, M.; George, M. W. Immobilised Photosensitisers for Continuous Flow Reactions of Singlet Oxygen in Supercritical Carbon Dioxide. *Chem. Sci.* **2011**, *2*, 1059.
- (63) Griesbeck, A. G.; El-Idreesy, T. T. Solvent-Free Photooxygenation of 5-Methoxyoxazoles in Polystyrene Nanocontainers Doped with Tetrastyrilporphyrine and Protoporphyrine-IX. *Photochem. Photobiol. Sci.* **2005**, *4*, 205–209.
- (64) Griesbeck, A. G.; El-Idreesy, T. T.; Bartoschek, A. Photooxygenation in Polystyrene Beads with Covalently and Non-Covalently Bound Tetraarylporphyrin Sensitizers. *Adv. Synth. Catal.* **2004**, *346*, 245–251.
- (65) Griesbeck, A. G.; Bartoschek, A. Sustainable Photochemistry: Solvent-Free Singlet Oxygen-Photooxygenation of Organic Substrates Embedded in Porphyrin-Loaded Polystyrene Beads. *Chem. Commun.* **2002**, 1594–1595.
- (66) Prat, F.; Foote, C. S. Technical Note A Resin-Bound Photosensitizer for Aqueous Photooxidations. *Photochemistry* **1998**, *67*, 626–627.
- (67) Ribeiro, S. M.; Serra, A. C.; Rocha Gonsalves, A. M. d'A. Covalently Immobilized Porphyrins on Silica Modified Structures as Photooxidation Catalysts. *J. Mol. Catal. A Chem.* **2010**, *326*, 121–127.
- (68) Benaglia, M.; Danelli, T.; Fabris, F.; Sperandio, D.; Pozzi, G. Poly(ethylene Glycol)-Supported Tetrahydroxyphenyl Porphyrin: A Convenient, Recyclable Catalyst for Photooxidation Reactions. *Org. Lett.* **2002**, *4*, 4229–4232.
- (69) DiMagno, S. G.; Dussault, P. H.; Schultz, J. a. Fluorous Biphasic Singlet Oxygenation with a Perfluoroalkylated Photosensitizer. *J. Am. Chem. Soc.* **1996**, *118*, 5312–5313.
- (70) Pozzi, G.; Mercks, L.; Holczknecht, O.; Martimbianco, F.; Fabris, F. Straightforward Synthesis of a Fluorous Tetraarylporphyrin: An Efficient and Recyclable Sensitizer for Photooxygenation Reactions. *Adv. Synth. Catal.* **2006**, *348*, 1611–1620.
- (71) Pozzi, G.; Montanari, F.; Quici, S. Cobalt Tetraarylporphyrin-Catalysed Epoxidation of Alkenes by Dioxxygen and 2-Methylpropanal under Fluorous Biphasic Conditions. *Chem. Commun.* **1997**, 69–70.
- (72) Hubbard, S. C.; Jones, P. B. Ionic Liquid Soluble Photosensitizers. *Tetrahedron* **2005**, *61*, 7425–7430.
- (73) Pastor-Perez, L.; Lloret-Fernandez, C.; Anane, H.; El Idrissi Moubtassim, M. L.; Julve, M.; Stiriba, S.-E. An Approach to Polymer-Supported Triplet Benzophenone Photocatalysts. Application to Sustainable Photocatalysis of an Alpha-Diazocarbonyl Compound. *RSC Adv.* **2013**, *3*, 25652–25656.
- (74) Breitenlechner, S.; Bach, T. A Polymer-Bound Chiral Template for Enantioselective Photochemical Reactions. *Angew. Chem. Int. Ed.* **2008**, *47*, 7957–7959.
- (75) Bach, T.; Bergmann, H.; Grosch, B.; Harms, K. Highly Enantioselective Intra- and Intermolecular [2+2] Photocycloaddition Reactions of 2-Quinolones Mediated by a Chiral Lactam Host: Host - Guest Interactions, Product Configuration, and the Origin of the Stereoselectivity in Solution. *J. Am. Chem. Soc.* **2002**, *124*, 7982–7990.
-

- (76) Jiang, J. X.; Li, Y.; Wu, X.; Xiao, J.; Adams, D. J.; Cooper, A. I. Conjugated Microporous Polymers with Rose Bengal Dye for Highly Efficient Heterogeneous Organo-Photocatalysis. *Macromolecules* **2013**, *46*, 8779–8783.
- (77) Pan, Y.; Kee, C. W.; Chen, L.; Tan, C.-H. Dehydrogenative Coupling Reactions Catalysed by Rose Bengal Using Visible Light Irradiation. *Green Chem.* **2011**, *13*, 2682.
- (78) Wu, P.; He, C.; Wang, J.; Peng, X.; Li, X.; An, Y.; Duan, C. Photoactive Chiral Metal-Organic Frameworks for Light-Driven Asymmetric Alpha-Alkylation of Aldehydes. *J. Am. Chem. Soc.* **2012**, *134*, 14991–14999.
- (79) Xie, M. H.; Yang, X. L.; Zou, C.; Wu, C. De. A Sn IV-Porphyrin-Based Metal-Organic Framework for the Selective Photo-Oxygenation of Phenol and Sulfides. *Inorg. Chem.* **2011**, *50*, 5318–5320.
- (80) Zhang, T.; Lin, W. Metal-Organic Frameworks for Artificial Photosynthesis and Photocatalysis. *Chem. Soc. Rev.* **2014**, 5982–5993.
- (81) Li, X.-H.; Wu, L.-Z.; Zhang, L.-P.; Tung, C.-H.; Che, C.-M. Luminescence and Photocatalytic Properties of a platinum(II)-Quaterpyridine Complex Incorporated in Nafion Membrane. *Chem. Commun.* **2001**, 2280–2281.
- (82) Suzuki, M.; Bartels, O.; Gerdes, R.; Schneider, G.; Wo, D.; Li, N. W. Photo-Oxidation of 1,3-Cyclopentadiene Using Partially Quaternized Poly (1-Vinylimidazole)-Bound Ruthenium(II) Complexes. *Phys. Chem. Chem. Phys.* **2000**, *2*, 109–114.
- (83) Papafotiou, F.; Karidi, K.; Garoufis, a.; Louloudi, M. Covalent Attachment of a Biomimetic Ru-(terpy)(bpy) Complex on Silica Surface: Catalytic Potential. *Polyhedron* **2013**, *52*, 634–638.
- (84) He, H.; Li, W.; Xie, Z.; Jing, X.; Huang, Y. Ruthenium Complex Immobilized on Mesoporous Silica as Recyclable Heterogeneous Catalyst for Visible Light Photocatalysis. *Chem. Res. Chinese Univ.* **2014**, *30*, 310–314.
- (85) Lin, W.; Sun, T.; Zheng, M.; Xie, Z.; Huang, Y.; Jing, X. Synthesis of Cross-Linked Polymers via Multi-Component Passerini Reaction and Their Application as Efficient Photocatalysts. *RSC Adv.* **2014**, *4*, 25114.
- (86) Barbante, G. J.; Ashton, T. D.; Doeven, E. H.; Pfeffer, F. M.; Wilson, D. J. D.; Henderson, L. C.; Francis, P. S. Photoredox Catalysis of Intramolecular Cyclizations with a Reusable Silica-Bound Ruthenium Complex. *ChemCatChem* **2015**, *7*, 1655–1658.
- (87) Zhang, G.; Song, I. Y.; Park, T.; Choi, W. Recyclable and Stable Ruthenium Catalyst for Free Radical Polymerization at Ambient Temperature Initiated by Visible Light Photocatalysis. *Green Chem.* **2012**, *14*, 618.
- (88) Yoon, H. S.; Ho, X. H.; Jang, J.; Lee, H. J.; Kim, S. J.; Jang, H. Y. N719 Dye-Sensitized Organophotocatalysis: Enantioselective Tandem Michael Addition/oxyamination of Aldehydes. *Org. Lett.* **2012**, *14*, 3272–3275.
- (89) Kumar, P.; Varma, S.; Jain, S. L. A TiO₂ Immobilized Ru(II) Polyazine Complex: A Visible-Light Active Photoredox Catalyst for Oxidative Cyanation of Tertiary Amines. *J. Mater. Chem. A* **2014**, *2*, 4514.
- (90) Yoo, W.-J.; Kobayashi, S. Efficient Visible Light-Mediated Cross-Dehydrogenative Coupling Reactions of Tertiary Amines Catalyzed by a Polymer-Immobilized Iridium-Based Photocatalyst. *Green Chem.* **2014**, *16*, 2438–2442.

- (91) Xie, Z.; Wang, C.; DeKrafft, K. E.; Lin, W. Highly Stable and Porous Cross-Linked Polymers for Efficient Photocatalysis. *J. Am. Chem. Soc.* **2011**, *133*, 2056–2059.
- (92) Wang, J. L.; Wang, C.; Dekrafft, K. E.; Lin, W. Cross-Linked Polymers with Exceptionally High [Ru(bipy)₃]²⁺ Loadings for Efficient Heterogeneous Photocatalysis. *ACS Catal.* **2012**, *2*, 417–424.
- (93) Kalyanasundaram, K. Photophysics, Photochemistry and Solar Energy Conversion with tris(bipyridyl)ruthenium(II) and Its Analogues. *Coord. Chem. Rev.* **1982**, *46*, 159–244.
- (94) Juris, A.; Balzani, V. 211. Characterization of the Excited State Properties of Some New Photosensitizers of the Ruthenium (Polypyridine) Family. *Helv. Chim. Acta* **1981**, *64*, 2175.
- (95) Wang, C.; Xie, Z. G.; deKrafft, K. E.; Lin, W. B. Light-Harvesting Cross-Linked Polymers for Efficient Heterogeneous Photocatalysis. *ACS Appl. Mater. Interfaces* **2012**, *4*, 2288–2294.
- (96) Wang, C.; Xie, Z.; deKrafft, K. E.; Lin, W. Doping Metal Organic Frameworks for Water Oxidation, Carbon Dioxide Reduction, and Organic Photocatalysis. *J. Am. Chem. Soc.* **2011**, *133*, 13445–13454.
- (97) Priyadarshani, N.; Liang, Y.; Suriboot, J.; Bazzi, H. S.; Bergbreiter, D. E. Recoverable Reusable Polyisobutylene (PIB)-Bound Ruthenium Bipyridine (Ru(PIB-bpy)₃Cl₂) Photoredox Polymerization Catalysts. *ACS Macro Lett.* **2013**, *2*, 571–574.
- (98) Bergbreiter, D. E. Soluble Polymers as Tools in Catalysis. *ACS Macro Lett.* **2014**, *3*, 260–265.
- (99) *Sigma-Aldrich Prices (May 2015)*.
- (100) Su, H.-L.; Hongfa, C.; Bazzi, H. S.; Bergbreiter, D. E. Polyisobutylene Phase-Anchored Ruthenium Complexes. *Macromol. Symp.* **2010**, *297*, 25–32.
- (101) Priyadarshani, N.; Benzine, C. W.; Cassidy, B.; Suriboot, J.; Liu, P.; Sue, H.-J.; Bergbreiter, D. E. Polyolefin Soluble Polyisobutylene Oligomer-Bound Metallophthalocyanine and Azo Dye Additives. *J. Polym. Sci. Part A Polym. Chem.* **2014**, *52*, 545–551.
- (102) Bergbreiter, D. E.; Su, H.-L.; Koizumi, H.; Tian, J. Polyisobutylene-Supported N-Heterocyclic Carbene Palladium Catalysts. *J. Organomet. Chem.* **2011**, *696*, 1272–1279.
- (103) Bergbreiter, D. E.; Hobbs, C.; Tian, J.; Koizumi, H.; Su, H.-L.; Hongfa, C. Synthesis of Aryl-Substituted Polyisobutylenes as Precursors for Ligands for Greener, Phase-selectively Soluble Catalysts. *Pure Appl. Chem.* **2009**, *81*, 1981–1990.
- (104) Priyadarshani, N.; Liang, Y.; Suriboot, J.; Bazzi, H. S.; Bergbreiter, D. E. Recoverable Reusable Polyisobutylene (PIB)-Bound Ruthenium Bipyridine [Ru(PIB-bpy)₃Cl₂] Photoredox Polymerization Catalysts. *ACS Macro Lett.* **2013**, *2*, 571–574.
- (105) Hongfa, C.; Tian, J.; Andreatta, J.; Darensbourg, D. J.; Bergbreiter, D. E. A Phase Separable Polycarbonate Polymerization Catalyst. *Chem. Commun.* **2008**, 975–977.
- (106) Bergbreiter, D. E.; Li, J. Terminally Functionalized Polyisobutylene Oligomers as Soluble Supports in Catalysis. *Chem. Commun.* **2004**, 42–43.
- (107) Liang, Y.; Harrell, M. L.; Bergbreiter, D. E. Using Soluble Polymers to Enforce Catalyst-Phase-Selective Solubility and as Antileaching Agents to Facilitate Homogeneous Catalysis. *Angew. Chem. Int. Ed.* **2014**, *53*, 8084–8087.

- (108) Bergbreiter, D. E.; Hobbs, C.; Hongfa, C. Polyolefin-Supported Recoverable/Reusable Cr(III)-Salen Catalysts. *J. Org. Chem.* **2011**, *76*, 523–533.
- (109) Bergbreiter, D. E.; Priyadarshani, N. Syntheses of Terminally Functionalized Polyisobutylene Derivatives Using Diazonium Salts. *J. Polym. Sci. Part A Polym. Chem.* **2011**, *49*, 1772–1783.
- (110) Yahya, R.; Craven, M.; Kozhevnikova, E. F.; Steiner, A.; Samunual, P.; Kozhevnikov, I. V.; Bergbreiter, D. E. Polyisobutylene Oligomer-Bound Polyoxometalates as Efficient and Recyclable Catalysts for Biphasic Oxidations with Hydrogen Peroxide. *Catal. Sci. Technol.* **2015**, *5*, 818–821.
- (111) Bergbreiter, D. E.; Yang, Y. C. Variable-Temperature NMR Studies of Soluble Polymer-Supported Phosphine-Silver Complexes. *J. Org. Chem.* **2010**, *75*, 873–878.
- (112) Bergbreiter, D. E.; Yang, Y.-C.; Hobbs, C. E. Polyisobutylene-Supported Phosphines as Recyclable and Regenerable Catalysts and Reagents. *J. Org. Chem.* **2011**, *76*, 6912–6917.
- (113) Khamaturova, T. V.; Zhang, D.; Suriboot, J.; Bazzi, H. S.; Bergbreiter, D. E. Soluble Polymer-Supported Hindered Phosphine Ligands for Palladium-Catalyzed Aryl Amination. *Catal. Sci. Technol.* **2015**, *5*, 2378–2383.
- (114) Bergbreiter, D. E.; Ortiz-Acosta, D. Recyclable Polyisobutylene-Supported Pyridyl N-Oxide Allylation Catalysts. *Tetrahedron Lett.* **2008**, *49*, 5608–5610.
- (115) Priyadarshani, N.; Suriboot, J.; Bergbreiter, D. E. Recycling Pd Colloidal Catalysts Using Polymeric Phosphine Ligands and Polyethylene as a Solvent. *Green Chem.* **2013**, *15*, 1361.
- (116) Al-Hashimi, M.; Bakar, M. D. A.; Elsaid, K.; Bergbreiter, D. E.; Bazzi, H. S. Ring-Opening Metathesis Polymerization Using Polyisobutylene Supported Grubbs Second-Generation Catalyst. *RSC Adv.* **2014**, *4*, 43766–43771.
- (117) Al-Hashimi, M.; Hongfa, C.; George, B.; Bazzi, H. S.; Bergbreiter, D. E. A Phase-Separable Second-Generation Hoveyda-Grubbs Catalyst for Ring-Opening Metathesis Polymerization. *J. Polym. Sci. Part A Polym. Chem.* **2012**, *50*, 3954–3959.
- (118) Khamaturova, T. V.; Zhang, D.; Suriboot, J.; Bazzi, H. S.; Bergbreiter, D. E. Soluble Polymer-Supported Hindered Phosphine Ligands for Palladium-Catalyzed Aryl Amination. *Catal. Sci. Technol.* **2015**, *5*, 2378–2383.
- (119) Hongfa, C.; Tian, J.; Bazzi, H. S.; Bergbreiter, D. E. Heptane-Soluble Ring-Closing Metathesis Catalysts. *Org. Lett.* **2007**, *9*, 3259–3261.
- (120) Li, J.; Sung, S.; Tian, J.; Bergbreiter, D. E. Polyisobutylene Supports - a Non-Polar Hydrocarbon Analog of PEG Supports. *Tetrahedron* **2005**, *61*, 12081–12092.
- (121) Bergbreiter, D. E.; Tian, J. Soluble Polyisobutylene-Supported Reusable Catalysts for Olefin Cyclopropanation. *Tetrahedron Lett.* **2007**, *48*, 4499–4503.
- (122) Adger, B. M.; Ayrey, P.; Bannister, R.; Forth, M. A.; Hajikarimian, Y.; Lewis, N. J.; O'Farrell, C.; Owens, N.; Shamji, A. Synthesis of 2-Substituted 4-Pyridylpropionates. Part 2. Alkylation Approach. *J. Chem. Soc. Perkin Trans. I* **1988**, 2791–2796.
- (123) Duric, S.; Tzschucke, C. C. Synthesis of Unsymmetrically Substituted Bipyridines by Palladium-Catalyzed Direct C-H Arylation of Pyridine N-Oxides. *Org. Lett.* **2011**, *13*, 2310–2313.

- (124) Barolo, C.; Nazeeruddin, M. K.; Fantacci, S.; Di Censo, D.; Comte, P.; Liska, P.; Viscardi, G.; Quagliotto, P.; De Angelis, F.; Ito, S.; Grätzel, M. Synthesis, Characterization, and DFT-TDDFT Computational Study of a Ruthenium Complex Containing a Functionalized Tetradentate Ligand. *Inorg. Chem.* **2006**, *45*, 4642–4653.
- (125) Savage, S. A.; Smith, A. P.; Fraser, C. L. Efficient Synthesis of 4-, 5-, and 6-Methyl-2,2'-Bipyridine by a Negishi Cross-Coupling Strategy Followed by High-Yield Conversion to Bromo- and Chloromethyl-2,2'-Bipyridines. *J. Org. Chem.* **1998**, *63*, 10048–10051.
- (126) Pasquinet, E.; Rocca, P.; Marsais, F.; Godard, A.; Queguiner, G. On the Metallation of 2-Isopropylpyridine. *Tetrahedron* **1998**, *54*, 8771–8782.
- (127) Lowry, M. S.; Goldsmith, J. I.; Slinker, J. D.; Rohl, R.; Pascal, R. A.; Malliaras, G. G.; Bernhard, S. Single-Layer Electroluminescent Devices and Photoinduced Hydrogen Production from an Ionic Iridium(III) Complex. *Chem. Mater.* **2005**, *17*, 5712–5719.
- (128) Cuthbertson, J. D.; MacMillan, D. W. C. The Direct Arylation of Allylic sp³ C–H Bonds via Organic and Photoredox Catalysis. *Nature* **2015**, *519*, 74–77.
- (129) Iqbal, N.; Jung, J.; Park, S.; Cho, E. J. Controlled Trifluoromethylation Reactions of Alkynes through Visible-Light Photoredox Catalysis. *Angew. Chem. Int. Ed.* **2014**, *53*, 539–542.
- (130) He, Z.; Bae, M.; Wu, J.; Jamison, T. F. Synthesis of Highly Functionalized Polycyclic Quinoxaline Derivatives Using Visible-Light Photoredox Catalysis. *Angew. Chem. Int. Ed.* **2014**, *53*, 14451–14455.
- (131) Rao, X.; Liu, C.; Qiu, J.; Jin, Z. A Highly Efficient and Aerobic Protocol for the Synthesis of N-Heteroaryl Substituted 9-Arylcarbazolyl Derivatives via a Palladium-Catalyzed Ligand-Free Suzuki Reaction. *Org. Biomol. Chem.* **2012**, *10*, 7875–7883.
- (132) Behr, A.; Henze, G.; Schomäcker, R. Thermoregulated Liquid/Liquid Catalyst Separation and Recycling. *Adv. Synth. Catal.* **2006**, *348*, 1485–1495.
- (133) Bergbreiter, D. E.; Sung, S. D. Liquid/liquid Biphasic Recovery/Reuse of Soluble Polymer-Supported Catalysts. *Adv. Synth. Catal.* **2006**, *348*, 1352–1366.
- (134) Francis, A. W. *Critical Solution Temperatures*, 31st ed.; American Chemical Society: Washington, DC, 1961.
- (135) Zagajewski, M.; Dreimann, J.; Behr, A. Verfahrensentwicklung Vom Labor Zur Miniplant: Hydroformylierung von 1-Dodecen in Thermomorphen Lösungsmittelsystemen. *Chem. Ing. Tech.* **2014**, *86*, 449–457.
- (136) Zagajewski, M.; Behr, a.; Sasse, P.; Wittmann, J. Continuously Operated Miniplant for the Rhodium Catalyzed Hydroformylation of 1-Dodecene in a Thermomorphic Multicomponent Solvent System (TMS). *Chem. Eng. Sci.* **2014**, *115*, 88–94.
- (137) Dietz, S. D.; Ohman, C. M.; Scholten, T. A.; Gebhard, S. Biphasic Hydroformylation of Higher Olefins. In *Organic Reactions Catalysis Society*; Richmond, VA, 2008.
- (138) Rackl, D.; Kais, V.; Kreitmeier, P.; Reiser, O. Visible Light Photoredox-Catalyzed Deoxygenation of Alcohols. *Beilstein J. Org. Chem.* **2014**, *10*, 2157–2165.
- (139) Singh, K.; Staig, S. J.; Weaver, J. D. Facile Synthesis of Z-Alkenes via Uphill Catalysis. *J. Am. Chem. Soc.* **2014**, *136*, 5275–5278.

- (140) Armarego, W. L. F.; Chai, C. L. L. *Purification of Laboratory Chemicals*, 6th ed.; Butterworth-Heinemann: Oxford, 2009.
- (141) Slinker, J. D.; Gorodetsky, A. A.; Lowry, M. S.; Wang, J.; Parker, S.; Rohl, R.; Bernhard, S.; Malliaras, G. G. Efficient Yellow Electroluminescence from a Single Layer of a Cyclometalated Iridium Complex. *J. Am. Chem. Soc.* **2004**, *126*, 2763–2767.
- (142) Kottas, G.; Ansari, N.; Elshenawy, Z.; Deangelis, A.; Xia, C. Heteroleptic Iridium Complexes as Dopants. EP2551933A1, 2013.
- (143) Ueng, S.-H.; Fensterbank, L.; Lacôte, E.; Malacria, M.; Curran, D. P. Radical Reductions of Alkyl Halides Bearing Electron Withdrawing Groups with N-Heterocyclic Carbene Boranes. *Org. Biomol. Chem.* **2011**, *9*, 3415–3420.
- (144) Murphy, J. A.; Khan, T. A.; Zhou, S.-Z.; Thomson, D. W.; Mahesh, M. Highly Efficient Reduction of Unactivated Aryl and Alkyl Iodides by a Ground-State Neutral Organic Electron Donor. *Angew. Chem. Int. Ed.* **2005**, *44*, 1356–1360.

F List of Abbreviations

Å	angstrom	°C	degrees Celsius
abs	absolute	C	catalyst
Ac	acetyl	¹³ C-NMR	carbon NMR
AcOH	acetic acid	calcd.	calculated (for MS analysis)
Ac ₂ O	acetic anhydride	cat.	catalytic, catalyst
AIBN	azobisisobutyronitrile	CB	conduction band
Alk	alkyl	Cbz	carboxybenzyl
All	allyl	CI	chemical ionization
anhyd.	anhydrous	cm	centimeter
aq	aqueous	cm ⁻¹	wavenumbers(s)
Ar	aryl	CMP	conjugated microporous polymer
atm	atmosphere	conv	conversion
		COSY	correlation spectroscopy
BARf	tetrakis(3,5-bis(trifluoromethyl)phenyl)borate	CT	charge transfer
B-BO ₃	conjugated microporous poly(benzoxadiazole) network	CV	cyclic voltammetry
BCIP	N- <i>tert</i> -butoxycarbonyl-2-(imidazole)-1-pyrrolidine	δ	chemical shift (ppm) downfield from TMS
bpy	2,2'-bipyridine, 2,2'-bipyridyl	d	days; doublet (spectral)
bmim	1-butyl-3-methylimidazolium	DCC	<i>N,N'</i> -dicyclohexylcarbodiimide
Bn	benzyl (PhCH ₂)	DCE	1,2-dichloroethane
Boc	<i>tert</i> -butoxycarbonyl	DCM	dichloromethane
bp	boiling point	DEAD	diethyl azodicarboxylate
br	broad (spectral peak)	DET	diethyl tartrate
Bu	butyl	dF(CF ₃)ppy	2-(2,4-difluorophenyl)-5-(trifluoromethyl)pyridine
BuLi	butyl lithium	DHQD	hydroquinidine
Bz	benzoyl (PhCO)	DIPEA	<i>N,N</i> -diisopropylethylamine
Bz(CF ₃) ₂	3,5-bis(trifluoromethyl)benzoyl		

DMAP	4-(<i>N,N</i> -dimethylamino)pyridine	h	hour(s)
DME	1,2-dimethoxyethane	HE	Hantsch ester, diethyl 1,4-dihydro-2,6-dimethyl-3,5-yrinedicarboxylate
DMECZ	3,6-dimethyl-9-ethylcarbazole	HMBC	heteronuclear multiple bond correlation
DMF	<i>N,N</i> -dimethylformamide	HMDS	hexamethyldisilazane
DMSO	dimethylsulfoxide	¹ H-NMR	proton NMR
dr	diastereomeric ratio	hν	light
ΔT	heat	HOMO	highest occupied molecular orbital
dtb-bpy	4,4'-di- <i>tert</i> -butyl-2,2'-bipyridine	HP	high pressure
ε	molar absorptivity	HPLC	high-performance liquid chromatography
E _{1/2}	standard reduction potential	HRMS	high-resolution mass spectrometry
ed.	edition	HSQC	heteronuclear single quantum coherence
Ed.	editor(s)	Hz	Hertz
ee	enantiomeric excess	i.e.	that is
EDTA	ethylenediaminetetraacetic acid	ICP-OES	inductively coupled plasma optical emission spectrometry
<i>e.g.</i>	<i>exempli gratia</i> , for example	IET	intramolecular electron transfer
eq	equation	IR	infrared
equiv	equivalent(s)	ISC	intersystem crossing
ESI	electrospray ionization	J	Joule
Et	ethyl	<i>J</i>	coupling constant (in NMR analysis)
<i>et al.</i>	and others (co-authors)	k	kilo
etc.	and so forth	K	Kelvin
Et ₃ N	trimethylamine	K _D	distribution coefficient
eV	electron volt	KDA	suberbasic mixture of potassium <i>tert</i> -butoxide, diisopropylamine and ⁴ BuLi
EWG	electron withdrawing group	L	liter; ligand
F	Faraday		
FT	Fourier transform		
g	gram(s); gaseous		
g-C ₃ N ₄	mesoporous carbon nitride		
GC-FID	gas chromatography with a flame ionization detector		

F List of Abbreviations

LAH	lithium aluminum hydride	N719	di-tetrabutylammonium cis-bis(<i>is</i> thiocyanato)bis(2,2'-bipyridyl-4,4'-dicarboxylato) ruthenium(II)
LDA	lithium diisopropylamide		
LED	light emitting diode	ⁿ Bu	normal butyl (primary)
LHMDS	lithium hexamethyldisilazane	NBS	<i>N</i> -bromosuccinimide
lit.	literature value	nm	nanometer
λ_{max}	max UV-vis wavelength	NMO	<i>N</i> -methylmorpholine <i>N</i> -oxide
LUMO	lowest unoccupied molecular orbital	NMR	nuclear magnetic resonance
		NOE	nuclear Overhauser effect
m	meter; milli; multiplet (spectral)	ns	nanosecond(s)
M	molar (moles per liter)	Nu	nucleophile
M ⁺	parent molecular ion (in MS)		
μ	micro	on	over night
max	maximum	oxdn	oxidation
MCZ	9-methylcarbazole		
Me	methyl	PA	polyacrylate
MeCN	acetonitrile	PCP	porous cross-linked polymers
Mes	mesityl (2,4,6-trimethylphenyl)	PEG	polyethylene glycol
MHz	megahertz	PET	photoinduced electron transfer
min	minute(s); minimum	pH	proton log units
mL	milliliter	Ph	phenyl
MLCT	metal to ligand charge transfer	PHAL	1,4-phthalazinediyl
mm	millimeter	Phth	phthaloyl
mM	millimolar	PIB	poly/ <i>is</i> obutylene
mmHg	millimeter of mercury	POF	porous organic framework
mmol	millimole(s)	pp	pages
MOF	metal organic framework	ppm	part per million
mol	mole(s)	ppy	2-phenylpyridine
mp	melting point	ⁱ Pr	propyl
MP	medium pressure	PTSA	<i>p</i> -toluenesulfonic acid
MS	mass spectrometry; molecular sieves	Pv	pivaloyl
Ms	mesyl (methanesulfonyl)	PWh	peta watt hour(s)
<i>m/z</i>	mass to charge ratio (in MS)	py	pyridine

q	quartet (spectral)	TLC	thin-layer chromatography
quin	quintet (spectral)	TMS	trimethylsilyl, tetramethylsilane, thermomorphic solvent system
R	arbitrary moiety	Tol	toluene
rac.	racemic	tosyl	<i>p</i> -toluenesulfonyl
recryst	recrystallized	<i>t</i> _R	retention time (in chromatography)
red	reduction	Ts	<i>p</i> -toluenesulfonyl (tosyl)
redox	reduction-oxidation	TS	transition state
R _f	retention factor (in chromatography)	UCST	upper critical solution temperature
rt	room temperature	UiO-67	zinc-based metal organic framework
rxn	reaction	UV	ultraviolet (light)
s	seconds; singlet (spectral)	UV-Vis	ultraviolet-visible absorption spectroscopy
sat.	saturated	VB	valence band
SBA-15	mesoporous silica	vis	visible
SCE	saturated calomel electrode	vol	volume
sept	septet (spectral)	vs	versus
SET	single electron transfer	v/v	volume to volume ratio
sext	sextet (spectral)	w/o	without
t	triplet (spectral)	wt%	weight percent
T	temperature in Kelvin	w/w	weight to weight ratio
TBAB	tetra- <i>n</i> -butylammonium bromide	X	arbitrary reagent 1; halogen
<i>t</i> Bu	<i>tert</i> -butyl	Y	arbitrary reagent 2
temp	temperature		
TEMPO	2,2,6,6-tetramethylpiperidine 1-oxyl		
Tf	trifluoromethanesulfonyl (triflyl)		
TFA	trifluoroacetic acid		
THF	tetrahydrofuran		

G Curriculum Vitae

Daniel Rackl

*21.01.1987 in Neumarkt i. d. OPf., Germany

Hauptstr. 12

92334 Berching

Tel: +49 8462 2276

Email: daniel.rackl@gmail.com

Education

10/2011 – 09/2015	PhD Studies, Chemistry, University of Regensburg, Germany
<i>Thesis:</i>	Visible Light Photoredox Catalyzed Deoxygenations and Polymer-tagged Photocatalysts
<i>Supervisor:</i>	Oliver Reiser
10/2010 – 09/2011	Master Studies, Chemistry, University of Regensburg, Germany
<i>Major Subject:</i>	Organic Chemistry
<i>Minor Subjects:</i>	Physical Chemistry, Biochemistry
<i>Degree:</i>	Master of Science (1,2)
07/2009 – 07/2010	ATLANTIS Dual Degree Bachelor Program, Chemistry, University of Arkansas, United States of America
<i>Thesis:</i>	Synthesis of 2,3-Disubstituted Indoles via α -Amino Carbon Radicals; 2 <i>H</i> - Azirines and Their FeCl ₂ Catalyzed Transformations
<i>Supervisor:</i>	Nan Zheng

Degree: Bachelor of Science (GPA 4.0)

08/2008 – 12/2008

ERASMUS Semester, University College Dublin, Ireland

Topic: An Approach for the Synthesis of Several Metabolism Products of 4-Bromo-2,5-dimethoxyphenethylamine (2C-B)

Supervisor: Pat Guiry

10/2006 – 09/2010

Bachelor Studies, Chemistry, University of Regensburg, Germany

Thesis: Synthesis of 2,3-Disubstituted Indoles via α -Amino Carbon Radicals Generated under Visible Light Photocatalysis (1,0)

Supervisor: Oliver Reiser

Degree: Bachelor of Science (1,5)

1997 – 2006

Willibald Gluck Gymnasium, Neumarkt i. d. OPf., Germany

Degree: Abitur (2,0)

Professional Experience

10/2011 – 04/2015

Research Assistant, Institute of Organic Chemistry, University of Regensburg, Germany

04/2009 – 05/2009

Student Assistant, Institute of Analytical Chemistry, Chemo- and Biosensors, University of Regensburg, Germany

List of Publications

- Kachkovskyi, G.; Kais, V.; Kohls, P.; Paria, S.; Pirtsch, M.; Rackl, D.; Seo, H.; Reiser, O. Homogeneous Visible Light-Mediated Transition Metal Photoredox Catalysis Other than Ruthenium and Iridium. In *Chemical Photocatalysis*; König, B., Ed.; De Gruyter: Berlin, 2013; pp 139–150.
- Rackl, D.; Kais, V.; Kreitmeier, P.; Reiser, O. Visible Light Photoredox-Catalyzed Deoxygenation of Alcohols. *Beilstein J. Org. Chem.* **2014**, *10*, 2157–2165.
- Rackl, D.; Kreitmeier, P.; Reiser, O. Synthesis of Polyisobutylene-Tagged *fac*-Ir(ppy)₃ Complexes and their Application as Recyclable Visible-Light Photocatalysts in a Continuous Flow Process. *Green Chem.* **2015**. DOI: 10.1039/C5GC01792K.
- Kais, V.; Rackl, D.; Reiser, O. **2015**. Photocatalytic Deoxygenation of Alcohols with Ethyl Oxalates. *Manuscript in preparation*.
- Rackl, D.; Kais, V.; Lutscher, E.; Reiser, O. Synthesis of Chiral Tetrahydrofuran and Pyrrolidine Derivatives *via* Visible Light-Mediated Deoxygenations. **2015**. *Manuscript in preparation*.
- Faderl, C.; Rackl, D.; Kachkovskyi, G.; Reiser, O. Photosensitized Decarboxylation and Rearrangement to Phenylethylamine and Isoquinolinone Derivatives. **2015**. *Manuscript in preparation*.
- Rackl, D.; Reiser, O. Recyclable Photocatalysts in Organic Synthesis. **2015**. *Manuscript in preparation*.

H Acknowledgements

Bedanken möchte ich mich zunächst sehr herzlich bei Prof. Dr. Oliver Reiser der mir die Teilnahme am ATLANTIS Programm ermöglichte, mich in seiner Arbeitsgruppe aufnahm, während der Bearbeitung des Themas wertvolle Unterstützung und Kritik lieferte und mich zur Aufnahme von weiteren Studien im Rahmen einer PostDoc Position animierte.

Für die technische Unterstützung danke ich allen voran Dr. Peter Kreitmeier der mit seiner Expertise praktische Arbeiten erleichterte bzw. gar erst möglich gemacht hat. Mein Dank gilt auch unseren Technikern Georg Adolin, Klaus Döring, Helena Konkel, Roxane Harteis und Brigitte Eichenseher.

Den Mitarbeitern der zentralen Analytik Fritz Kastner, Annette Schramm und Georgine Stühler danke ich für die Hilfe bei der Aufnahme von NMR Spektren aller Art und Wolfgang Söllner, Josef Kiermaier und Carol Prockl für die Durchführung der Massenspektroskopien.

Für die Hilfe bei den Messungen der CV-Spektren bedanke ich mich bei Regina Hoheisel (AK König) und für ICP-OES Messungen bei Joachim Rewitzer (AK Bäumner).

Für die Integration in die Arbeitsgruppe, die sehr heimatliche Atmosphäre und alle außer-universitären Aktivitäten in den vergangenen Jahren möchte ich mich sehr gern bei allen damaligen und heutigen Freunden und Kollegen bedanken. Ganz besonderen Dank gilt dabei Andreas Okun, Viktor Kais, Matthias Knorn, Dr. Ludwig Pilsl, Christian Faderl, Dr. Klaus Harrar, Dr. Paul Kohls, Martin Hofmann, Matthias Gnahn, Benjamin Kastl, Soraia Fernandes, Francesca Besostri, Dr. Roland Linhard, Dr. Quirin Kainz, Dr. Andreas Kreuzer und der Hedi.

Viktor Kais danke ich für die Zusammenarbeit und Diskussionen im Gebiet der Deoxygenierungen. Dr. Paul Kohls schulde ich großen Dank für die Besprechungen über recycelbare Photokatalysatoren und seine anfängliche Hilfe bei der Durchführung von Photoreaktionen.

Für die Bereitstellung diverser Reagenzien, Katalysatoren und Lösungsmitteln danke ich Viktor Kais, Christian Faderl, Sabine Möhle, Dr. Paul Kohls, Dr. Andreas Kreuzer, Martin Hofmann und Daniel Dobler.

Thomas Broja gebührt mein Dank für seine Konstruktion des Chromatotrons RIOT, für seine stete Diskussionsbereitschaft über chemische Sachverhalte aller Art und seine jahrelange Freundschaft. Auch bei Michael Haindl möchte ich mich gerne in diesem Zusammenhang bedanken.

Meinen ehemaligen Bachelorstudenten und Forschungspraktikanten Martin Hofmann, Marleen Häring, Matthias Gnahn, Philipp Büschelberger, Marco Peteranderl, Patrick Bayer, Alexander Wimmer, Daniel Bindl und Markus Tautz danke ich für ihre engagierte Mitarbeit.

Meinen Laborkollegen Dr. Klaus Harrar, Dr. Ludwig Pils, Andreas Okun, Sabine Möhle, Silvia Panzeri, und Thomas Föll gilt ganz besonderer Dank für die Schaffung einer entspannten, produktiven Arbeitsatmosphäre und die Diskussion alltäglicher chemischer Angelegenheiten.

Für das sehr gewissenhafte Korrekturlesen dieser Arbeit bedanke ich mich herzlich bei Martin Hofmann, Christian Faderl und Matthias Knorn.

Abschließend bedanke ich mich von ganzen Herzen bei meiner Familie von der ich seit jeher bedingungslose Unterstützung und Rückhalt erfahren habe. Allen Dank!

I Declaration

Herewith I declare that this present thesis is a presentation of my original work prepared single-handed. Wherever contributions from others are involved, all of them are marked clearly, with reference to the literature, license and acknowledgement of collaborative research.

A handwritten signature in black ink, reading "Daniel Rackl". The script is cursive and fluid, with the first name "Daniel" and the last name "Rackl" clearly distinguishable.

Daniel Rackl

Regensburg, 16.07.2015